INQUA - IGCP 567 MORELIA (MEXICO), 2012

Proceedings

INQUA - IGCP567 Proceedings Vol. 3, 2012

Earthquake Geology and Archaeology: Science, Society and Sesimic hazaard

PALEOSEISMOLOGY & ARCHAEOSEISMOLOGY

MORELIA • MEXICO 2012

Editors

R. Pérez-López, P.G. Silva, M.A. Rodríguez Pascua
V.H. Garduño Monroy, G.Suarez and K. Reicherter

PROCEEDINGS

3rd INQUA-IGCP 567 International Workshop on EarthquakeGeology, Palaeoseismology and Archaeoseismology

19-24 November 2012
Morelia (Mexico)

ISBN: 000-000-000-000-0

PALEOSEISMOLOGY &
ARCHAEOSEISMOLOGY
MORELIA • MEXICO 2012

***Editors*:**

R. Pérez-López, P.G. Silva, M.A. Rodríguez Pascua, V.H. Garduño-Monroy, G. Suarez and K. Reicherter

This abstract volume has been produced for the 3rd INQUA-IGCP 567 International Workshop on Palaeoseismology and Archaeoseismology, held in Morelia (MEXICO) in 2012. This workshop commemorates also the 100th Anniversary of the Acambay Earthquake of 1912.

The event has been organized together by the INQUA Focus Area on Paleoseismology and Active Tectonics and the IGCP - 567: Earthquake Archaeology.

ISBN: in progress. (00-0000-0000-00)

Paleoseismology &
Archaeoseismology
MORELIA • MEXICO 2012

INDEX

COMBINING PAST-ARCHAEOLOGICAL EXPEDITION AND GEOLOGICAL DATA AT TELL ES-SULTAN (JERICHO, DEAD SEA): EVIDENCE OF TWO NEOLITHIC (7500-6000 B.C.) EARTHQUAKES

Laura Alfonsi(1), Francesca R. Cinti(1), Shmuel Marco(2), Domenico Di Mauro(1)

(1) Istituto Nazionale di Geofisica e Vulcanologia, Via di Vigna Murata, 605, Roma (laura.alfonsi@ingv.it)
(2) Department of Geophysics and Planetary Sciences, Tel Aviv University, Israel

Abstract (Combining past-archaeological expedition and geological data at Tell es-Sultan (Jericho, Dead Sea): evidence of two Neolithic (7500-6000 B.C.) earthquakes)

Tell es-Sultan (Jericho, Dead Sea) was affected by destructive earthquakes since 11,000 B.C. We analyse and correlate available archaeological reports from expeditions back to the XIX century. The convergence of the collected data pointed to two specific subsequent earthquakes for the damage reported at Tell es-Sultan. The youngest event occurred around 6000 B.C., and the previous one at about 7000 B.C. Considering an older event documented around 7500 B.C., we infer a rough average recurrence interval for damaging earthquakes of 750 yr. This value is comparable with other estimates from palaeo-seismites, paleoseismological, archaeological and seismological studies in the Dead Sea area. We suggest the Nuweime fault that bounds the Tell as a plausible source for local seismic shaking. This case study highlights the role of archaeological documentations of past expeditions for filling gaps of information on the pre-history of seismically-prone areas, particularly when original data are vanished with time.

***Key words**: Archaeoseismology, Dead Sea Fault, Tell es-Sultan, pre-historical earthquakes*

INTRODUCTION

The present work aims at recovering the earthquake record from the ancient settlement of Jericho (Palestine), known as Tell es-Sultan, inhabited in a period of which we have no local geological information. Tell es-Sultan is suitable for archaeoseismic investigations because of, its location in a seismically active area, its continuous occupation since the last 11,000 years, and its settlement reconstruction made by archaeologists providing abundant documentation. Starting from early XIX century to the modern expeditions, archaeologists have associated peculiar damaging, fracturing and human remains discovered at the ancient Jericho site to repeated seismic shaking events during the Neolithic history. Among the fundamental researches are those leaded by Prof. J. Garstang and Dame K. Kenyon, the two main archaeological teams that considered earthquake effects in the 11000-6000 B.C. period (Garstang et al., 1935; Garstang and Garstang, 1948; Kenyon, 1957; Kenyon, 1981). The analysis in this work descends from their observations. Damages were recognized as the result of strong ground shaking by Kenyon (1981) based on findings in the layers referred to the interval 8500-6000 B.C. The earlier archaeological expedition by Prof. J. Garstang (Garstang et al., 1935; Garstang and Garstang, 1948) revealed the presence of surface fracturing affecting the layers of 7500-6000 B.C. In particular, this latter interval bears distinct traces of seismic effects. The map in *Fig. 1* shows the distribution of the damages in the site during the 7500-6000 B.C. This map locates elements of different age, not connected in time and space to date, within the same frame. Earthquakes effects are inferred from the

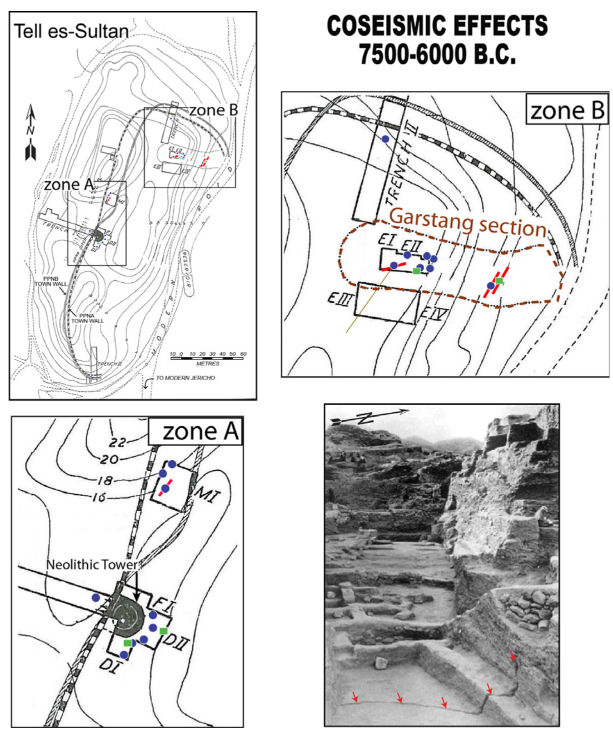

Fig. 1: Map of coseismic effects at Tell es-Sultan between 7500-6000 B.C. The locations of the effects are marked by dots: blue collapse and damage, green human skeleton, red line fracture and faulting. Original Plan of the Tell modified from Kenyon (1981). Photo to the lower right: east view of the Garstang excavation (Garstang & Garstang, 1948). In the foreground is visible a fracture crossing the floor and the adjacent wall.

position, orientation, and analysis of the original pictures and the archaeological stratigraphic sections within the Tell. In order to define the age of the evidence found at different parts of the site, we use the archaeological stratigraphy and relative periodization for correlation between damaged strata (Kenyon, 1981; Nigro, 2006).

DISCUSSION

The merging of archeological and geological data in the area of Tell es-Sultan allowed us to discriminate on the occurrence and on the characteristics of two subsequent seismic events, the youngest around 6000 B.C., and the previous one at about 7000 B.C., separated by a ~ 1000 years interval.

The earthquakes timing defined in this work represent an independent check for the earthquakes occurrence reconstructed with different approaches and for correlation among different records. As comes from the evidence for seismic events from damaged speleothems, nearly 40 km west of Tell es-Sultan (Soreq and Har-Tuv caves), where earthquake evidence at ~8.6 ka has been found (Kagan et al., 2005; Braun et al., 2009).

Information on past earthquakes in the Dead Sea Basin and adjacent region was recovered from seismites and faults in lake sediments. Seismites are found in the 70-15-ka Lisan Formation (Marco et al., 1996) and in the subsequent Dead Sea deposits (Ken-Tor et al., 2001; Migowski et al., 2004; Kagan et al., 2011).

For what concern the earthquake shaking recurrence at the site, we infer a rough average recurrence interval for damaging earthquakes at Tell es-Sultan of 750 yr, considering an older event documented around 7500 B.C. (Kenyon, 1981; 1957; Bar-Yosef, 1986). This value falls in the range of previously published recurrence values in a comparable time window for the Dead Sea area. Migowsky et al. (2004) defined an earthquake recurrence interval of 500 yrs for the period 8000-5500 B.C. from paleo-seismites. Our value is also similar to the average repeat time for strong earthquakes (~500 yr) derived for a larger time window (last 60,000 yr) from paleoseismological, archaeological and seismological studies in the Dead Sea fault system (Hamiel et al., 2009 and references therein).

Earthquakes source implications have been derived from a reconstruction of the active fault system of the DST in the area of Tell es-Sultan, reporting the NE-SW-trending Nuweime fault at the east border of Tell es-Sultan (Begin, 1974; Shamir et al., 2005). A morphological step is observed along the southeastern margin of the Tell (picture in *Fig. 2*), its southern and northern extension traces the position of the Nuweime fault. Paleoseismic investigation could impose tighter constraints on the activity of the Nuweime fault. In a seismic context, the activity of the Nuweime fault would contribute to the vulnerability of the Tell area being one of the possible faults responsible for the seismic shaking damages at the Tell and surrounding region. Among the major site of great cultural interest of the area is the Hisham palace (Fig. 2), just few km north of ancient Jericho. This site, an beautiful example of Umayyad architecture (661-750 A.D.) is well known for being severely damaged by earthquakes. We are currently carrying on archaeoseismic investigation at Hisham with the main purposes of discriminating the age of seismic events, the possible sources, and the intensity of the shaking effect at the site.

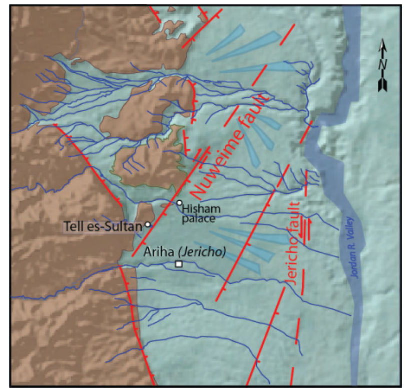

Fig. 2: Geological sketch of the Tell es-Sultan surrounding area. Fault traces (i.e. Begin, 1974; Shamir et al., 2005), location of the Tell and another major site of great cultural interest, Hisham Palace.

Finally, the Jericho case study highlights the possibility to fill the gap of information on the pre-history of a seismically-prone area through the analysis of archaeological documentations of past expeditions, as precious source for archaeoseismic investigators, especially when original data vanish with time. Hisham Palace instead still preserves the effects of seismic shaking, attracting the investigators for deeper analysis.

Acknowledgements: The Italian archaeological mission to Jericho (University La Sapienza, Rome) is credited for logistic on site and discussions.

References

Bar-Yosef, O. (1986). The walls of Jericho- an alternative interpretation. *Current Anthropology* 27, 157-162.

Begin, Z. B. (1974). The geological map of Israel, Jericho sheet. Scale 1:50,000. *Geological Survey of Israel*, Jerusalem.

Braun, Y., E. Kagan, M. Bar-Matthews, A. Ayalon, and A. Agnon (2009). Dating spleleoseismites near the Dead Sea Transorm and the Carmel Fault: clues to coupling a plate boundary and its branch. *Israel Journal of Earth Sciences* 58, 257-273.

Garstang, J., J. P. Droop, and J. Crowfoot (1935). “Jericho: City and Necropolis (Fifth Report)”, *Annals of Archaeology and Anthropology* 22, 143-184.

Garstang J., and J.B.E. Garstang (1948). *The Story of Jericho*, London.

Hamiel, Y., R., Amit, and Z. B. Begin (2009). The Seismicity along the Dead Sea Fault during the Last 60,000 Years, *Bulletin of the Seismological Society of America* 99 (3), 2020-2026.

Kagan, E. J., A. Agnon, M. Bar-Matthews and A. Ayalon (2005). Dating large infrequent earthquakes by damaged cave deposits. *Geology* 33, 261–264.

Kagan, E., M. Stein, A. Agnon, and F. Neumann (2011). Intrabasin paleoearthquakes and quiescence correlation of the late Holocene Dead Sea. *Journal of Geophysical Research* 116 (B0), 4311.

Ken-Tor, R., A. Agnon, Y. Enzel, S. Marco, J. F. W. Negendank, and M. Stein (2001). High-resolution geological record of historic earthquakes in the Dead Sea basin: *Journal of Geophysical Research* 106 (B2), 2221-2234.

Kenyon, K.M. (1957). *Digging Up Jericho*, London, Ernest Benn. 261–62.

Kenyon, K.M. (1981). *Excavations at Jericho, III. The Architecture and Stratigraphy of the Tell*, London.

Marco, S., M. Stein, A. Agnon, and H. Ron (1996). Long term earthquake clustering: a 50,000 year paleoseismic record in the Dead Sea Graben. *Journal of Geophysical Research* 101, 6179-6192.

Migowski, C., A., Agnon, R., Bookman, J.F.W. Negendank,. and M. Stein (2004). Recurrence pattern of Holocene earthquakes along the Dead Sea transform revealed by varve-counting and radiocarbon dating of lacustrine sediments. *Earth and Planetary Science Letters* 222, 301-314.

Nigro, L. and H. Taha (eds.), (2006). Tell es-Sultan/Jericho in the Context of the Jordan Valley: Site Management, Conservation and Sustainable Development. Proceedings of the International Workshop Held in *Ariha 7th - 11th February 2005 by the Palestinian Department of Antiquities and Cultural Heritage - Ministry of Tourism and Antiquities*, UNESCO Office - Ramallah, Rome “La Sapienza” University (Rome «La Sapienza» Studies on the Archaeology of Palestine & Transjordan 02), Rome.

Shamir, G., Y. Eyal, and I. Bruner (2005). Localized versus distributed shear in transform plate boundary zones: The case of the Dead Sea Transform in the Jericho Valley, *Geochemistry Geophysics Geosystems* 6 (5), doi:10.1029/2004GC000751.

PALEOSEISMOLOGY & ARCHAEOSEISMOLOGY
MORELIA • MEXICO 2012
INQUA-TERPRO PALEOSEISMOLOGY
EARTHQUAKE ARCHAEOLOGY

OVER 4 DECADES OF PALEOSEISMIC STUDIES IN VENEZUELA: ACHIEVEMENTS AND CHALLENGES

Audemard M., Franck A.

Venezuelan Foundation for Seismological Research –FUNVISIS-, Final Prolongación Calle Mara, Quinta Funvisis, El Llanito, Caracas. faudemard@funvisis.gob.ve

Abstract: *Venezuela surprisingly has a very long tradition of paleoseismic research, which is not the case of other Latin American countries. National efforts on Seismic Hazard Assessments (SHA) were devoted very soon after the Caracas july 1967 earthquake. This event, renouned worldwide jointly with the Niigata 1964 earthquake for launching the study of earthquake site effects, is not only responsible for the official foundation of FUNVISIS in 1972, as the result of one of the major conclusions arisen form the study of that earthquake delivered by the Caracas Earthquake Presidential Commission, but for the need of applying SHA to the Venezuelan oil industry infrastructure at an early stage; reason by which Woodward-Clyde & Associates conducted a regional study in Northwestern Venezuela as early as 1968, where the super giant Maracaibo oil field lies. This contribution tries to give a brief summary of the paleoseismic work done in Venezuela since that first American study, for over 40 years now, as well as to current and future lines of research being applied to the study of past earthquakes and seismogenic faults in Venezuela.*

Key words: *Paleoseismology, Paleolimnology, site effects, trenching*

Some 57 trenches for paleoseismic studies have been excavated and studied in Venezuela since a pioneering 2-trench study carried out by the American company *Woodward-Clyde & Associates*, as early as 1968, at the request of a former foreign oil company, for the seismic hazard assessment (SHA) of a protective earth embankment system. It was constructed along the eastern shore of lake Maracaibo to avoid inundation of increasing subsiding areas due to oil extraction. That was the only evaluation not performed by *la Fundación Venezolana de Investigaciones Sismológicas –FUNVISIS-* (Venezuelan Foundation for Seismological Research). Results from all these studies have been progressively incorporated in specific SHA for essential infrastructure, and simultaneously in the national seismic building codes. More recently, they have become a cornerstone for the microzoning studies of several major cities, which were essentially started from 2005. It is worth mentioning that most of the Venezuelan large cities sits on sedimentary basins of significant fill thickness.

The above-mentioned paleoseismic studies were performed across Quaternary or active faults. Success of trenching across faults in Venezuela deeply relied on a thorough and detailed mapping of fault-related landforms. Not until very recently, Venezuela did not count with the help provided by indirect geophysical methods, such as GPR or electrical resistivity tomography. Experience developed in the Pacific US on tectonic geomorphology of strike-slip faults was transferred and applied to our major right-lateral strike-slip faults, such as the Boconó, el Pilar and Oca-Ancón faults, since the late 70's. However, Venezuela lies on a complex transpressional (compressive-transcurrent) plate boundary zone. This fact led us to develop in house the geomorphic evaluation of thrust faults since the early 90's, and more particularly on active blind thrusting bounding uplifting orogens such as the Mérida Andes.

Onshore, the future of paleoseismology in Venezuela as a discipline heads to multiplying the existing number of trenches, either on partly-evaluated faults or on previously non-studied faults, and very particularly on very slow faults, in order to establish from direct seismic deformations: (1) seismogenic potential of each fault or fault segment (repeat time of maximum likely earthquakes); (2) seismogenic fault segmentation; (3) fault interaction due to stress changes after an earthquake; (4) time-space distribution of major earthquakes along a given fault or fault segment; (5) seismotectonic association of historical earthquakes; (6) occurrence of last event on a fault; and (7) likelihood of occurrence of the forthcoming event on a given fault. Moreover, it can also bring additional light on: average slip rate of active faults, seismic slip per event, vertical and horizontal components of slip on a fault relying on actual striation observed on fault plane. This is of vital importance in the estimation of permanent deformations on the man-made environment of any type or any relevance, at the crossing with active faults. Not only the evaluation of on-fault deformation has been assessed through trenching, seismically induced effects have also been investigated with the same techniques. However, genetic relationships (cause-effect relations) derived from the second set of features are more time and effort consuming. As to this, the Earth Sciences Department of FUNVISIS since late 2000, in collaboration with the Laboratoire of Géodynamique des Chaînes Alpines –LGCA- of the University of Chambery (current ISTerre) –Bourget du Lac, Savoie, France- have targeted peri-glacial lakes and paleo-lakes of the Santo Domingo-Apartaderos region, in the central Venezuelan Andes, recovering long cores and determining a combined seismic history for the Boconó fault by correlating and integrating on-fault and off-fault earthquake chronologies.

In recent years, we have been using a sort of advertising slogan that reflects a major tendency of where we are now looking at. I quote: "*I have turned my back to onshore Venezuela and stare now at offshore Venezuela and Caribbean coastal areas*". Since 2006, we have launched and carried out an aggressive program of single-channel high-resolution shallow seismic reflection acquisition in collaboration with the Renard Centre of Marine Geology –RCMG- of the University of Ghent, a more modest campaign of core recovery offshore so far and a growing interest on paleo- and historical tsunami recognition along our exposed low-lying inhabited seashores. The cataloguing of tsunami prone areas started with an investigation of historical first-hand accounts and testimonies that guided the geologic exploration (by coring and trenching) of a set of coastal lagoon in eastern Venezuela. This has been luckily boosted by the interest of UNESCO of implementing an Early Tsunami Warning System for the Caribbean and adjacent regions –Caribbean ETWS-, which is a benevolent consequence of the disastrous Sumatra 2004 tsunami. We still have to elucidate whether these local tsunamis are triggered by earthquake-induced submarine sliding or sea bottom deformation produced by right-lateral strike-slip faulting; being this author inclined for the second cause, at least during some of the major offshore events (e.g., San Narciso 1900 event).

We have definitely not abandoned onshore exploration!! In parallel, we have been trenching very slow faults (e.g. El Ávila fault) but also fast ones (2 new trenches in the southernmost sector of the Boconó Fault in the Mérida Andes and 2 others on the Bruscas segment of the San Sebastián Fault), cataloguing prone areas to liquefaction nationwide, determining liquefaction potential and mass wasting susceptibility of certain regions (particularly for city microzoning projects), establishing the time-space distribution of major –both historical and prehistorical- earthquakes at regional scale, mapping spatial distribution of liquefaction features during certain modern large earthquakes. Some of these products have led to building a magnitude-to-feature size relationship from either a national or international catalogue of earthquakes triggering liquefaction. These served as input for the development of the ***INQUA*** **E**nvironmental **S**eismic **I**ntensity Scale as to 2007. In the same way, to refine geologically/geomorphologically derived fault slip rates, from the beginning of this XXI century, local benchmark networks have been installed and measured with GPS in eastern (since 2003) and western (since 2011) Venezuela. This is also being improved by the current installation of cGPS stations, with a multi-parameter goal (tectonic slip, tsunami detection and weather watching and forecasting). Other features, such as seismically induced deep-seated landslides, have been targeted since late year 2000. During the reconnaissance of potential GPS sites, very large mass movements of the type of Deep-Seated Gravitational Slope Deformations –DSGSD- have been identified and mapped, bringing new insights on the current evolution of high relief areas of the Mérida Andes.

PALEOSEISMOLOGY & ARCHAEOSEISMOLOGY
MORELIA • MEXICO 2012
INQUA-TERPRO PALEOSEISMOLOGY
EARTHQUAKE ARCHAEOLOGY

HAZARDS OF GEOLOGICAL FAULTS IN MORELIA

Ávila-Olivera, Jorge A. (1), Salmerón-Díaz, José E. (2), Garduño-Monroy, Víctor H. (3), Hernández-Madrigal, Víctor M. (3)

(1) Dpto. Ciencias de la Tierra, Instituto de Investigaciones sobre los Recursos Naturales, Universidad Michoacana de San Nicolás de Hidalgo, Michoacán, MEXICO. ja.avilaolivera@gmail.com
(2) Centro de Investigaciones en Geografía Ambiental, Universidad Nacional Autónoma de México, Michoacán, MEXICO. edmundods@hotmail.com
(3) Dpto. Geología y Mineralogía, Instituto de Investigaciones Metalúrgicas, Universidad Michoacana de San Nicolás de Hidalgo, Michoacán, MEXICO. vhgardunom@gmail.com, vitorio_manuel@yahoo.it

Abstract (Hazards of geological faults in Morelia): *Morelia is the capital of Michoacán State, and is located in the central western of Mexico, in the geological province of Mexican Volcanic Belt (MVB). The city is being affected by fourteen geological faults of ENE-WSW and E-W direction that belong to the Morelia-Acambay Faults System (MAFS), which has generated important earthquakes like the Acambay in 1912 and Maravatío in 1979, with magnitudes of M6.7 and M5.4 respectively. These faults represent three different kinds of hazard: a). Sinkings, crackings and faults at the surface caused by Subsidence-Creep-Fault Processes (SCFP); b).Lateral movement of faults triggered by the regional active stress field and;c). Potencial seismicity of faults. In order to monitoring and analysis these hazards it was employed the interferometric technique and also measuring with geodetic GPS, which reveal rates of subsidence and lateral displacements up to 35 mm/year and 30 mm/year, respectively.*

Key words: *subsidence, stress field, potential seismicity, GPS monitoring*

Introduction

Morelia is the capital of Michoacán State, and is located in the central western of Mexico, in the geological province of the Mexican Volcanic Belt (MVB). At the beginning of 80's population noted that some constructions of the city were damaged by differential sinkings, crackings and faults at the surface that followed a preferential direction. At the present time is known that these discontinuities are a result of the Subsidence-Creep-Fault Processes (SCFP), which origin resides at geological synsedimentary faults (Ávila-Olivera and Garduño-Monroy, 2010).

The geological faults that are present in Morelia have ENE-WSW and E-W direction (Garduño-Monroy et al., 1998, 1999, 2001), and belong to the Morelia-Acambay fault system (MAFS), which in turns is part of the Tula-Chapala fault zone (TCFZ) at its central portion (Johnson, 1986; Johnson and Harrison, 1989; Martínez-Reyes and Nieto-Samaniego, 1990; Pasquaré et al., 1991; Suter et al., 1992, 1995, 2001; Silva-Mora, 1995). The ENE-WSW structures are normal faults with downthrown blocks to NW and have scarp heights or 20 to 60 cm; while E-W discontinuities are also normal faults with its hanging wall toward north and have a surface throw which reach 200 m in some parts of the city. (Garduño-Monroy et al., 2009a).

In recent years, aside from the vertical rupture that is observed in constructions of the city that were placed above geological faults, also is noted a horizontal motion, which is an indication that faults are developing a lateral movement (*Fig. 1*). Is presumed that this displacement is due to activity of the regional stress field of the MAFS, in function of a focal mechanisms analysis of earthquake historically occurred (Ávila-Olivera et al., 2009; Díaz-Salmerón et al., 2011).

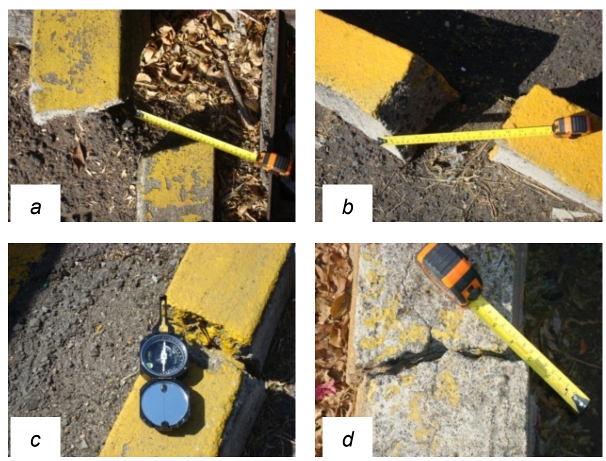

Fig. 1: Evidences of lateral movement of geological faults in Morelia. a). Nocupétaro fault; b). La Colina fault; c). El Realito fault; d). La Paloma fault.

In relation to seismicity, in the north portion of Michoacán State have occurred some of the historical events more violent in central Mexico, (Garduño-Monroy et al., 1998). In 1845 and 1858 Morelia was affected by two earthquakes with magnitude around M6.0 (Jara et al., 1994; Singh at al., 1996). Previous studies report that the E-W structures of the MAFS are seismically active (Quintero-Legorreta et al., 1988; Suter et al., 1992, 1995, 2001). Important earthquakes related to MAFS were generated like the Acambay in 1912 with a magnitude of M6.7 (Urbina and Camacho, 1913), and the Maravatío in 1979 with a magnitude of M5.3 (Astiz-Delgado, 1980; Suter et al., 1992, 1996). In Morelia four small events were occurred on October 17, 2007, with magnitudes varying from M3.5 to M3.8 (Garduño-Monroy et al., 2009a).

Evolution of geological faults

Geological faults began to be noted in Morelia since 1983, when some damage was observed at La Colina and Tres Puentes neighborhoods and also on the Héroes de Nocupétaro Avenue. These harms were caused by La Colina and Nocupétaro faults respectively. In 1988 a third fault was detected, it was named Chapultepec. All the faults were termed in function of the places where their effects were noted for the first time. By 1993 the number of structures increased to six with the emergence of Torremolinos, El Realito and La Soledad faults. Two more faults occurred in 1999, Cuautla and Ventura Puente (Garduño-Monroy et al., 2001; Ávila-Olivera, 2004). Nowadays the infrastructure of Morelia is being damaged by fourteen discontinuities with the addition of La Paloma, Cerritos, Girasoles, Viveros, Lago, Puerta del Sol faults (Díaz-Salmerón, pers. Com.) (*Fig. 2*).

Monitoring of geological faults

In order to monitoring and analysis the hazards related to geological faults in Morelia it was carried out a couple of geodetic studies. The first one is applying the InSAR (Interferometric Synthetic Aperture Radar) technique, while the other one is through the use of geodetic GPS sensors (Ávila-Olivera et al., 2010).

The InSAR technique requires a minimum of two ASAR scenes of the study area in order to be applicable. The analysis was performed using a set of nine scenes taken by ENVISAT satellite, which spanning the period from July 2003 to May 2006 (Farina et al., 2007). After to process all the possible combinations of interferometric pairs, it was obtained a set of interferograms through the method of two pass interferometry. The interferograms with a good correlation signal, were subjected a process of phase unwrapping in order to transform the interferograms into ground displacements along the satellite l.o.s. (line of sight). In function of the incident angle of the ENVISAT antenna (23° from the vertical), the determined displacements with this technique are related to sinkings (*Fig. 2*).

For the second geodetic study, it set up a monitoring net of control points in Morelia since 2005 (Ávila-Olivera, 2009). At the present time the net is integrated by 45 control points. Annually the net is occupied by geodetic GPS sensors applying the measure technique fast-static, which is characterized by short observation times to geopositioning the interest points. In order to reach the milimetric accuracy that allows this equipment, it was used the differential GPS method (DGPS), which consists in observe and calculate a base line between two GPS sensors that observe the same number of satellites simultaneously.

The annually measurement campaigns allow to determinate the position change of control points through time, and given that GPS sensors provide the location through coordinates X, Y, Z, is possible to decompose the displacement into components horizontal (*Fig. 2)* and vertical.

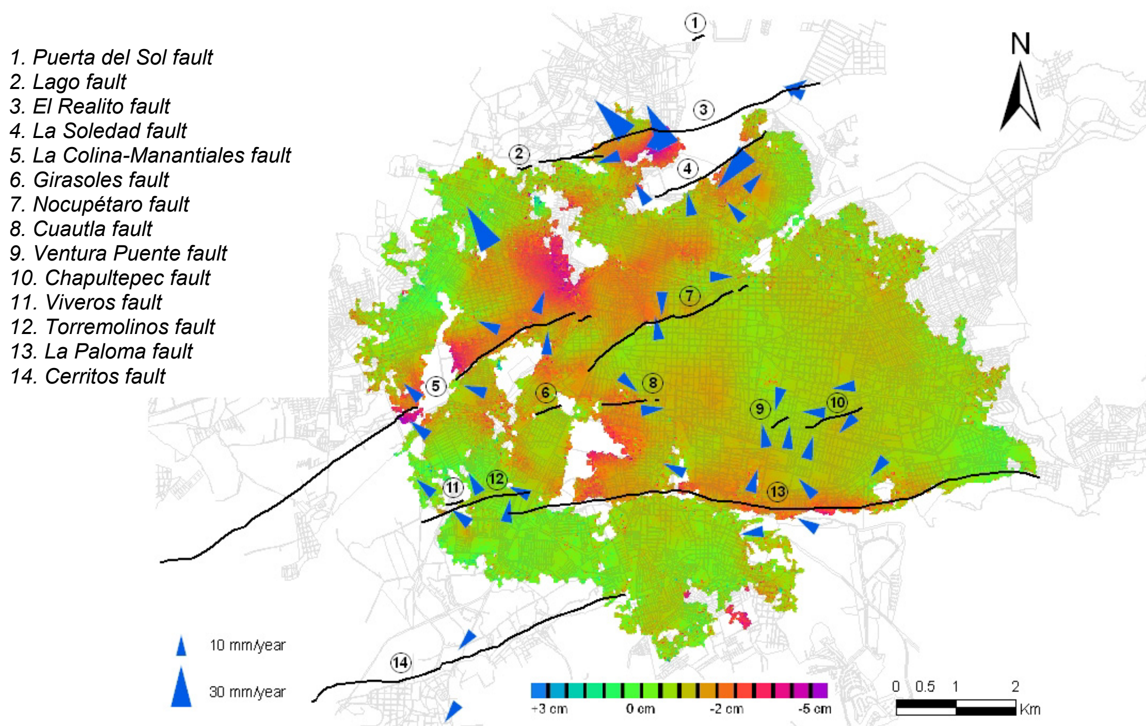

Fig. 2: Monitoring of the terrestrial surface deformation in Morelia. Color bar indicates the subsidence annual rate determinated by interferometry. Blue triangles show the lateral displacement direction of control points measured with geodetic GPS.

Seismic potential

Morelia may be affected by two types of seismicity:
a). Interplate earthquakes, generated by the Cocos plate subduction under North America plate along Pacific margin, like the earthquake of September 25, 1985, and; b). Intraplate earthquakes, which can be related to intermediate-depth structures of subduction plate (depths greater than 30 km), or also can be associated a geological faults that are generated in the crustal of top plate (Singh et al., 1996; Garduño-Monroy et al., 2001). This last seismicity can be felt with more intensity than the others mentioned and its recurrence time is higher than 1,000 years (Suter et al., 1995). The MAFS is related to these kinds of earthquakes (Pasquaré et al., 1991; Suter et al., 1992, 1995; Johnson, 1986; Martínez-Reyes and Nieto-Samaniego, 1990).

The historical record reports two intermediate-depth intraplate earthquakes that affected Morelia, one was occurred on April 7, 1845 and other on June 19, 1858 (Singh et al., 1996), with intensities on the Modified Mercalli scale of VIII and IX (Figueroa, 1963; Sánchez-Garcilazo, 2000), and magnitudes of M6.0 and M6.4, respectively (Garduño et al., 2009b).

In relation to shallow intraplate earthquakes associated with the MAFS, two are the most important. The Acambay earthquake of November 19, 1912 had a magnitude of M6.7. The event occurred along the Acambay-Tixmadejé fault, generating a coseismic rupture of 41 km long (Suter et al., 1995). The focal mechanism indicates a minimum but consistent left-lateral strike-slip component (Suter et al., 1992).

The other one is the Maravatío earthquake of February 22, 1979, with a magnitude of M5.3, which was generated on the Venta de Bravo fault – a structure of 45 km long – to a depth of 8.2 km. The focal mechanism also indicates a left-lateral strike-slip component (Astiz-Delgado, 1980). In June 1998 the same fault produced nine events with magnitudes about M3.0 and epicenters at depths between 3 and 11 km (Garduño et al., 2009b). The focal mechanisms consist of an extension N-S oriented with a small left lateral component (Lermo-Samaniego, 1998, pers. com.).

In Morelia the Nocupétaro fault generated four events on October 17, 2007, with magnitudes varying from M3.5 to M3.8 and epicenters depths between 1 and 6 km (Garduño-Monroy et al., 2009a).

Discussion

The hazard of subsidence that occurs in Morelia can be classified into two types: a). Subsidence at the fault, these sinkings takes place into the influence zone of geological faults, specifically on hanging wall, with annual rates of up to 40 mm (e.g. La Colina Fault); b). Subsidence intra block, which is the result of the consolidation process of lacustrine and fluviolacustrine sediments which conform the subsoil of the city. In Accordance with a DInSAR analysis, the second type of subsidence presents a magnitude which varying from 0 to 35 mm/year. The maximum rate is observed toward northern, western and northwestern portion of the city (Farina et al., 2008), where the sediments thickness is bigger, reaching values up to 160 m (Ávila-Olivera et al., 2010).

The hazard of horizontal movement of geological faults in Morelia, have a left-lateral component, which is identified in the stress mechanisms of historical shallow intraplate earthquakes related to the MAFS. All the focal mechanisms show a left transtension NW-SE (Ávila-Olivera et al., 2009). The GPS monitoring indicates that the magnitude of this lateral movement reach values up to 30 mm/year toward western (Ávila-Olivera et al., 2007).

The hazard of seismic activity of geological faults in Morelia, it was detected in the focal mechanisms of historical shallow intraplate earthquakes which indicated that they are related to the MAFS. In addition, on October 17, 2007, were occurred four seismic events with epicenters along the Nocupétaro fault which crosses the city with a direction ENE-WSW (Garduño-Monroy et al., 2009a).

A paleoseismology study realized previously reveals that assuming a total coseismic rupture of La Colina and Nocupétaro faults, it can be estimated an earthquake with a moment magnitude (Mw) between 5.8 and 6.5. In regard to La Paloma fault – with a surface rupture length of 12 km – the same study estimates an earthquake with a moment magnitude (Mw) between 6.3 and 6.7 (Garduño-Monroy et al., 2009a).

An additional hazard related to La Paloma fault is due to its particular morphology – with a surface throw of 200 m in some sectors – and due to the presences of loose rock blocks of different sizes, some with volume of $10m^3$. This combination of factors can make than during an earthquake the blocks move downward reaching velocities up to 8 m/s and getting to the urban area (Arreygue-Rocha et al., 2002).

Conclusions

Morelia is being affected by three kinds of hazards related to geological faults: a). Sinkings, crackings and faults at the surface caused by SCFP; b). Lateral movement of faults triggered by the regional active stress field and; c). Seismic activity that can develop these faults .One single discontinuity can experiment the three types of hazard as happens with the Nocupétaro and La Colina faults.

References

Arreygue-Rocha, E., Garduño-Monroy, V.H., Canuti, P., Casagli, N., Iotti, A., Chiesa, S. 2002. Análsis geomecánico de la inestabilidad del escarpe La Paloma en la Ciudad de Morelia, Michoacán, México, *Revista Mexicana de Ciencias Geológicas*, 19 (2), 91-106.

Astiz-Delgado, L.M. 1980. Sismicidad en Acambay, Estado de México: el temblor del 22 de febrero de 1979. *Tesis de* *licenciatura, Facultad de Ingeniería, Universidad Nacional Autónoma de México*, 130 p.

Ávila-Olivera, J.A. 2004. Contribución a los estudios geotécnicos y geofísicos en zonas urbanas con Procesos de Subsidencia-Creep-Falla, caso: la Ciudad de Morelia, Michoacán, México. *Tesis de Maestría, Universidad Autónoma de Querétaro*, 234 p.

Ávila-Olivera, J.A., Calderón-Muñoz, J., Garduño-Monroy, V.H. 2007. Monitoreo de los Procesos de Subsidencia-Creep-Falla que afectan a la Ciudad de Morelia, Michoacán, empleando DGPS geodésico, *Geos, Unión Geofísica Mexicana*, 27 (1), 157.

Ávila-Olivera, J.A. 2009. Evolución de los Procesos de Subsidencia-Creep-Falla, casos: Morelia, Mich. Y Celaya, Gto. *Tesis Doctoral, Instituto de Geofísica, Universidad Nacional Autónoma de México*, 233 p.

Ávila-Olivera, J.A., Garduño-Monroy, V.H., Hernández-Madrigal, V.M., Cabral-Cano, E., Remy, D., Díaz-Molina, O. 2009. Relación de los Procesos de Subsidencia-Creep-Falla de la Ciudad de Morelia con el campo de esfuerzos trasntensional izquierdo del Cinturón Volcánico Mexicano, *Geos, Unión Geofísica Mexicana*, 29 (1), 183.

Ávila-Olivera, J.A., Garduño-Monroy, V.H., Farina, P. 2010. Integrated study of land subsidence in Morelia, Michoacán, Mexico. In: *Land Subsidence, Associated Hazards and the role of Natural Resources Development* (Carreón-Freyre, D., Cerca, M., Galloway, D.L. eds.). Querétaro, Mexico, 185-190.

Ávila-Olivera, J.A., Garduño-Monroy, V.H. 2010. Conceptual model of land subsidence with a structural control. In: *Land Subsidence, Associated Hazards and the role of Natural Resources Development* (Carreón-Freyre, D., Cerca, M., Galloway, D.L. eds.). Querétaro, Mexico, 195-197.

Díaz-Salmerón, J.E., Garduño-Monroy, V.H., Ávila-Olivera, J.A., Hernández-Madrigal, V.M. 2011. Relación entre el estado de esfuerzos regional activo y los Procesos de Subsidencia-Creep-Falla (PSCF), en la Ciudad de Morelia, Michoacán, México, *Geos, Unión Geofísica Mexicana*, 31 (1), 52.

Farina, P., Ávila-Olivera, J.A., Garduño-Monroy, V.H. 2007. Structurally-controlled urban subsidence along the Mexican Volcanic Belt (MVB) monitored by InSAR. In: *Proceedings of Envisat Symposium 2007*. Montreux, Switzerland, 23-27.

Farina, P., Ávila-Olivera, J.A., Garduño-Monroy, V.H., Catani, F. 2008. DInSAR analysis of differential ground subsidence affecting urban areas along the Mexican Volcanic Belt (MVB), *Rivista Italiana di Telerilevamento*, 40 (2), 103-113.

Figueroa, J. 1963. Isosistas de macrosismos mexicanos, *Facultad de Ingeniería, Universidad Nacional Autónoma de México*, Reporte 67.

Garduño-Monroy, V.H., Arreygue-Rocha, E., Chiesa, S., Israde-Alcántara, I., Rodríguez-Torres, G.M., Ayala, G.M. 1998. Las fallas geológicas y sísmicas de la ciudad de Morelia y su influencia en la planificación del territorio, *Ingeniería Civil*, 1 (5), 3-12.

Garduño-Monroy, V.H., Rodríguez-Torres, G.M., Israde-Alcántara, I., Arreygue-Rocha, E., Canuti, P., Chiesa, S. 1999. Efectos del clima (El Niño) en los fenómenos de fluencia de las fallas geológicas de la ciudad de Morelia, *Geos, Unión Geofísica Mexicana*, 9 (2), 84-93.

Garduño-Monroy, V.H., Arreygue-Rocha, E., Israde-Alcántara, I., Rodríguez-Torres, G.M. 2001. Efectos de las fallas asociadas a sobreexplotación de acuíferos y la presencia de fallas potencialmente sísmicas en Morelia, Michoacán, México, *Revista Mexicana de Ciencias Geológicas*, 18 (1), 37-54.

Garduño-Monroy, V.H., Pérez-López, E., Israde-Alcántara, I., Rodríguez-Pascua, M.A., Szynka-ruk, E., Hernández-Madrigal, V.M., García-Zepeda, M.L., Corona-Chávez, P., Ostroumov, M., Medina-Vega, V.H., García-Estrada, G., Carranza, O., López-Granados, E., Mora-Chaparro, J.C. 2009a. Paleoseismology of the southwstern Morelia-Acambay fault system, central Mexico, *Geofísica Internacional*, 48 (3), 319-335.

Garduño-Monroy, V.H., Chávez-Hernández, J., Aguirre-González, J., Vázquez-Rosas, R., Mijares-Arellano, H., Israde-Alcántara, I., Hernández-Madrigal, V.M., Rodríguez-Pascua, M.A., Pérez-López, R. 2009b. Zonificación de los periodos naturales de oscilación superficial en la ciudad de Pátzcuaro, Mich., México, con base en microtemores y estudios de paleosismología, *Revista Mexicana de Ciencias Geológicas*, 26 (3), 623-637.

Jara, M., Hurtado, F., Jara, J.M., Suárez, R. 1994. Zonificación sísmica de la Ciudad de Morelia, *Universidad Michoacana de San Nicolás de Hidalgo, Escuela de Ingeniería Civil, Boletín Informativo*, 5.

Johnson, C.A. 1986. A study of neotectonics in central Mexico from a LANDSAT Tematic Mapper imagery. *Master Thesis, Rosentiel School of Marine and Atmospheric Science, University of Miami*, 112 p.

Johnson, C.A., Harrison, C.G.A. 1989. Tectonics and Volcanism in Central Mexico: A Landsat Thematic Mapper Perspective. *Remote Sensing of Environment*, 28, 273-286.

Martínez-Reyes, J., Nieto-Samaniego, A.F. 1990. Efectos geológicos de la tectónica reciente en la parte central de México, *Universidad Nacional Autónoma de México, Instituto de Geología, Revista*, 9(1), 33-50.

Pasquaré, G., Ferrari, L., Garduño, V.H., Tibaldi, A., Vezzoli, L. 1991. Geology of the central sector of the Mexican Volcanic Belt, states of Guanajuato and Michoacán: Boulder, Geological Society of America, Map and Chart series, MCH072, 1 map and text, 22 p.

Quintero-Legorreta, O., Mota-Palomino, R., Suter, M. 1988. Esfuerzos y deformación contemporáneos en la parte central de la Faja Volcánica Transmexicana; y geometría, distribución y sismicidad de las fallas activas, *Geos, Unión Geofísica Mexicana*, época II, 8 (extraordinario), p. 33.

Sánchez-Garcilazo, V. 2000. Estudio de la microsismicidad del Estado de Michoacán, *Tesis de Maestría, Universidad Michoacana de San Nicolás de Hidalgo*, 133 p.

Singh, S.K., Ordaz, M., Pérez-Rocha, L. 1996. The great mexican earthquake of 19th June 1958; expected ground motion and damage in Mexico City from a similar future event, *Seismological Society of America, Bulletin*, 86(6), 1655-1666.

Silva-Mora, L. 1995. Hoja Morelia 14Q-g(2) con resumen de la geología de la hoja Morelia, estados de Michoacán y Guanajuato: México, D.F., Universidad Nacional Autónoma de México, Instituto de Geología, Cartas Geológicas de México, serie de 1:100.000, 1 mapa con texto, 25 p.

Suter, M., Quintero-Legorreta, O., Johnson, C.A. 1992. Active faults and state of stress in the central part of the trans-Mexican volcanic belt, 1, The Venta de Bravo Fault, *Journal of Geophysical Research*, 97, 11983-11994.

Suter, M., Quintero-Legorreta, O., López-Martínez, M., Aguirre-Díaz, G., Farrar, E. 1995. The Acambay graben; active intraarc extension in the Trans-Mexican Volcanic Belt, Mexico, *Tectonics*, 14 (5), 1245-1262.

Suter, M., Carrillo-Martínez, M., Quintero-Legorreta, O. 1996. Macroseismic study of shallow earthquakes in the central and eastern parts of the Trans-Mexican Volcanic Belt, Mexico, *Seismological Society of America, Bulletin*, 86(6), 1952-1963.

Suter, M., López-Martínez, M., Quintero-Legorreta, O., Carrillo-Martínez, M. 2001. Quaternary intra-arc extension in the central Trans-Mexican volcanic belt, *GSA bull*. 113 (6), 693-703.

Urbina, F., Camacho, H. 1913. La zona megaseismica Acambay-Tixmadeje, Estado de México, conmovida el 19 de noviembre de 1912, *Boletín del Instituto Geológico de México*, *32*, p. 125.

MACROSEISMIC DATA IN MICHOACAN, MEXICO, DURING THE 19TH CENTURY

Arzola Cristóbal, Grecia S. (1) y Garduño-Monroy, Victor H. (2)

(1) Facultad de Historia. Universidad Michoacana de San Nicolás de Hidalgo. Morelia, Michoacán, México. isishat@hotmail.com
(2) Instituto de Investigaciones Metalúrgicas. Universidad Michoacana de San Nicolás de Hidalgo. Morelia. MEXICO. vhgardunom@gmail.com

Abstract (Macroseismic data in Michoacán, Mexico, during the 19th century): *it is well-known that the state of Michoacán is a major seismic area in the Mexican Republic. Seismic movements have been daily bread to the population. This paper intends to reconstruct the 19th century regional seismic history of Michoacán. Whereas the information stems form already published catalogues, the history will be enriched by extensive research in the periodical publications of the state's capital, Morelia, thereby expanding the catalogues, notably by the inclusion of already registered seismic data, and new data yielded by the research, including a number of events which had remained unknown by the researchers.*

Key words*: Seismicity, Michoacán. 19th century, Periodic press.*

Introduction

In the course of history, societies have had to cope up with many different natural phenomena. The relationship between these and populations have been a source of interest for men, as natural phenomenon also involve what we call "disasters", which designate the impact of a geological hydrometeorological, technological or biological phenomenon upon a given population, entailing damage at social, cultural, economical, infrastructural and environmental levels (Maskrey [comp.], 1993).
Certain conditions must nonetheless be fulfilled for this disaster to occur, as mentioned by Garcia Acosta (2004): the event must take place "in the context of a historic model of vulnerability" (free translation). We thereby understand that the socio-environmental conditions of the community at the very moment of the event are utterly important. Additionally, the short and long term responses to a disaster, the possible transformation and growing processes it entails, or conversely the ignorance of it by the authorities and the civilians must be added to the eventual results.
Social sciences began to take interest in studies about disasters brought about by nature in the 1920s. Only in the last decades of the past century the study of disasters in Mexico began to take a social perspective, most importantly after the earthquake of September 1985. Sociology and anthropology were the two disciplines most impacted by the study of these events (Garcia Acosta, 1994). This does not, however, mean that before this date the theme had not been tackled from a historic perspective, yet its importance was relegated to its relationship with other economical and social processes.

After the 1985 earthquake, a group of researchers, among which Teresa Rojas Rabiela and Virginia Garcia Acosta, decided to embark upon the theme of disasters, and to focus mainly on earthquakes. Their intention was to describe disasters with a historical and social turn, with special emphasis on seismic phenomena.

This paper is a segment of a larger research carried out with the intention of obtaining a License in History. The research includes a historic compilation of earthquakes occurred in Michoacán since the 16th Century, culminating in the 19th Century. The work by Garcia Acosta and Suarez Reynoso, *Los Sismos en la Historia de México*(1996) is of crucial importance for this research.
The present paper is therefore a review of the local press. The idea was to relist the earthquakes occurred in the State of Michoacán during the 19th century. This means that we retain the seismic activity, including those earthquakes whose epicenters were situated in or outside the cited territory.
The state of Michoacán, situated in the central-western part of the Mexican Republic, has three potential seismic sources: a) the pacific subduction; b)the Mexican Volcanic Belt; c) the Infiernillo-Balzas-Tepalcatepec seismic zone. This means that Michoacan may be considered as a high seismic risk zone (Garduño Monroy et al., 2011). We must underline the importance of Michoacán's seismic history in order to understand clearly how these events took place in the past and how they possibly will occur again, as well as to obtain a better comprehension of their impact on society. Similarly, this study intends to enrich the INQUA seismic catalogue.

Methodology

As already mentioned, our research stemmed mainly from the seismic catalogue gathered by Garcia Acosta (1996). The first step was to select the information, retaining only that which regarded the state of Michoacán. The next was to refer to the university newspaper library "Mariano Jesus Torres" to search for newspapers and carry out what Rodriguez de la Torre (1993) called "busqueda *extensivista*". We therefore started seeking out seismic phenomena as if we were unaware of their occurrence in determined month or year. We revised the local press, that is we sorted out all the publications which could enlarge the seismic historical catalog, adding of new seismic data of already registered earthquakes and "new" earthquakes which had passed undetected. We did not distinguish them by their intensity.

Sin embargo, debemos advertir que la clasificación de sismos aquí presentada no es la totalidad de eventos sísmicos registrados en la obra *Los sismos en la historia de México* (García Acosta, 1996), para el Estado de Michoacán; sino que corresponden a aquellos encontrados en nuestra revisión de la prensa michoacana y que fueron ampliados con nuevos datos y sismos que no estaban registrados en la misma.

Again, we must advert that the seism classification presented hereunder does not include the totality of seismic events registered in *Los Sismos en la Historia de México* (Garcia Acosta, 1996) for the state of Michoacán. We only included those encountered in the local press, amplified by new data, and earthquakes not previously registered in the book.
Accordingly, we tackle the subject form a perspective that is set in a large temporality, for as mentioned by Suarez Reynoso (1996): "seismic phenomena are of long periodicities: the repetition of an earthquake of a certain magnitude in one fault can occur in a time span of several decades or centuries". From hence the importance of a catalogue that covers a long period, so as to establish a significant characterization of seismic activity in our State. In the same vein, social reactions to the latter also appear to differ in the course of time.
Among the resources of the "Mariano de Jesus Torres" newspaper library in Morelia, we have consulted the so-called "Publicaciones periodicas antiguas locales", which reviews most newspapers of the 19th century. Until today, those who have been of considerable importance for our research are:

- *Boletín del Observatorio Meteorológico del Colegio Seminario de Morelia* (1897, 1899)
- *Boletín de la Sociedad Michoacana de Geografía y Estadística* (1905-1906)
- *El Centinela* (1899)
- *El Constitucionalista* (1868)
- *Gaceta Oficial del Gobierno del Estado Libre y Soberano de Michoacán* (1885-1887, 1889-1892)
- *La Lealtad* (1893)
- *La Libertad* (1894-1896, 1899)

Conclusions
The events we found were textually transcribed and chronologically classified, starting by year of occurrence. The data referring to the year of publication are registered in a table preceding the news transcription.
We found a totality of 35 notices referring to a seismic phenomenon occurred in the state of Michoacan, 14 of which came from the *Gaceta Oficial del Gobierno del Estado Libre y Soberano de Michoacán*; 10 from *La Libertad*; 4 from the *Boletín de la Sociedad Michoacana de Geografía y Estadística*; 3 from the *Boletín del Observatorio Meteorológico del Colegio Seminario de Morelia*; 2 from *La Lealtad*; one from *El Constitucionalista* and the last from *El Centinela*.

The sizes of the descriptions vary greatly, the smallest having only 18 words, and the most detailed, describins a series of earthquakes felt between October and November 1872 in Agua Fria and Jaripeo has 4646 words. We therefore can establish an average of 50 to 70 words per news.
As to the content of the information, many but not all (17) exclusively describe the seism, 7 briefly inform the hour of the event, the direction and the duration of the earthquakes, but the rest of the text focuses on social reaction and physical damages on buildings. 6 of them do not describe the seism in itself, but rather explain how it was perceived, what kind of damage the buildings suffered, and the perspective of their future reconstruction. 4 of the news were transcriptions of reports made by experts about the volcanoes and the earthquakes of Agua Fria and Jaripeo. There was also a very interesting article related to a "scientific prediction" by Don Juan N Contreras from Guanajuato, who appeared to be a kind of meteorologist, who was also capable of predicting earthquakes, storms and other natural phenomena.
According to the seismic sources to which they correspond, we could classify the earthquakes as follows:

a) subduction earthquakes:
   - 9 April 1889
   - 1 August 1889
   - 13 January 1899
b) intraplate earthquakes:
   - 16 September 1885
   - 30 August 1890
   - 19 July 1891
   - 30 October 1893
   - 11 January 1895
   - 31 October 1897
   - 19 November 1897
   - 24 January 1899
   - 4 February 1899

However, as Rodriguez de la Torre (1993) mentions, one of the tasks of the researcher in seismic history is "to know and to define as much earthquakes as possible, in order to always enrich the catalogues". Therefore we can highlight certain events which are already included in Garcia-Acosta's study by adding new data, and also include "new" earthquakes which are not part of it:

New data for already listed earthquakes
As mentioned before, the information hereunder does not correspond to the entire number of earthquakes which took place in the state of Michoacán, which is the reason why we do not mention two of the most important earthquakes of the 19th century, namely those occurred on 7 April 1845 and 19 June 1858. They are nonetheless present in our broader research, since we found important information linked to these events in the archives of the city of Morelia, notably a complete house-by-house review of the damage caused upon the buildings of the capital, listed in 1845.

The following catalog contains the information found in *Los Sismos en la Historia de México* (Garcia Acosta 1996), to which we added the information obtained by our search in the 19th century periodical press of Morelia; the blue frames correspond to the new data.

•16 September 1885 earthquake:

HOUR	**Between 10:30 y 11:00 AM**
PLACE	Morelia, Tacámbaro
TYPE	Oscillatory
INTENSITY	Strong
DURATION	
CARDINAL DIRECCION	
SOURCE	*G. O.* Mich. N° 2 and 7. García A., 1996; 419

-1 August 1889 earthquake:

HOUR	**7:15 AM**
PLACE	Tacámbaro, Ario, Santa Clara, Apatzingán
TYPE	Oscillatory
INTENSITY	Strong
DURATION	2 or 3 seconds
CARDINAL DIRECCION	Northeast to Southeast. In Apatzingán from East to West
SOURCE	*G. O.* Mich. N° 396. García A., 1996; 443

- 19 November 1897 earthquake:

HOUR	**10:36 AM**
PLACE	Morelia
TYPE	Oscillatory
INTENSITY	low
DURATION	1 second
CARDINAL DIRECCION	East to West
SOURCE	*B. del O. M.* Morelia, Mich. N° 35. García A., 1996; 518

- 13 January 1899 earthquake :

HOUR	**between 7:50 and 7:57 PM**
PLACE	Morelia, Aguililla, Carrizal, Coalcomán
TYPE	Trepidatory and Oscillatory
INTENSITY	Strong
DURATION	From 15 to 45 seconds
CARDINAL DIRECCION	North to South and East to West
SOURCE	*La Libertad*. Morelia, Mich. Año 7°. N° 3. García A., 1996; 522-523

- 24 January 1899 earthquake:

HOUR	**Between 5:00 and 5:10 PM**
PLACE	Ocampo, Morelia
TYPE	Oscillatory
INTENSITY	Strong
DURATION	45 seconds
CARDINAL DIRECCION	Northeast to Southeast
SOURCE	*La Libertad*. Morelia, Mich. Año 7°. N° 4. García A., 1996; 525

Non -listed earthquakes

These are the earthquakes found during the research carried out in the 19th century periodic press of the city of Morelia, and which are not to be found in another catalogue.

- 9 April 1889 earthquake:

HOUR	**7:45 AM**
PLACE	Coalcomán, Apatzingán
TYPE	Oscillatory
INTENSITY	strong
DURATION	10 to12 seconds. In Apatzingán 6 seconds
CARDINAL DIRECCION	
SOURCE	*G. O.* Mich. N°365

- 30 August 1890 eartquake:

HOUR	**9:10 PM**
PLACE	Tlalpujahua
TYPE	Trepidatory
INTENSITY	Strong
DURATION	5 seconds
CARDINAL DIRECCION	North to South
SOURCE	*G. O.* Mich. N°487

- 19 July 1891 earthquake:

HOUR	**4:00 AM**
PLACE	Zinapécuaro
TYPE	Trepidatory
INTENSITY	Strong
DURATION	
CARDINAL DIRECCION	
SOURCE	*G. O.* Mich. N° 577

- 30 October 1893 earthquake:

HOUR	**0:15 AM**
PLACE	Morelia
TYPE	Trepidatory
INTENSITY	
DURATION	
CARDINAL DIRECCION	
SOURCE	*La Lealtad*. Morelia, Mich. N°52

- 11 January 1895 earthquake:

HOUR	**Between 3:00 and 4:00 AM**
PLACE	Morelia
TYPE	

INTENSITY	Strong
DURATION	
CARDINAL DIRECCION	
SOURCE	*La Libertad*. Morelia, Mich. Año 3°. N° 3

- 31 October 1897 earthquake:

HOUR	**11:30 PM**
PLACE	Morelia
TYPE	Oscillatory and trepidatory
INTENSITY	Low
DURATION	
CARDINAL DIRECCION	Northeast to Southeast and West to East
SOURCE	*B. del O. M.* Morelia, Mich. Tomo I. N° 34

- 4 February 1899 earthquake:

HOUR	**Night**
PLACE	Morelia
TYPE	
INTENSITY	Low
DURATION	
CARDINAL DIRECCION	
SOURCE	*B. del O. M.* Morelia, Mich. Tomo I. N° 50

Finally, it is important to underline that our revision does not pretend to be an exhaustive study of all earthquakes occurred in Michoacán, for being this a study extending on a very large time span, there is a considerable amount of information to be revised. On the contrary, our interest relies in relating the seismic history of our state and make space for new and more complete studies.

Acknowledgements: firstly, we wish to thank D. Victor Hugo Garduño Monroy for his constant support and for his confidence in the realization of our research. We also wish to thank M.C. Laura Eugenia Solis Chavez and the Seminario de Historia Ambiental y Desarrollo Regional for its help and suggestions in the improvement of the text.

References

Boletín del Observatorio Meteorológico del Colegio Seminario de Morelia. 1897. 34 (1). Noviembre 4. 133-134.
Boletín del Observatorio Meteorológico del Colegio Seminario de Morelia. 1897. 35 (1). Diciembre 4. 137-139.
Boletín del Observatorio Meteorológico del Colegio Seminario de Morelia. 1899. 50 (1). Marzo 4. 197-198.
El Centinela. 1899. 29 (6). Enero 29. Michoacán. 4.
Gaceta Oficial del Gobierno del Estado Libre y Soberano de Michoacán. 1885. 2 (I). Septiembre 24. 3.
Gaceta Oficial del Gobierno del Estado Libre y Soberano de Michoacán. 1885. 7 (I). Octubre 11. 2.
Gaceta Oficial del Gobierno del Estado Libre y Soberano de Michoacán. 1889. 365 (IV). Abril 11. 3.
Gaceta Oficial del Gobierno del Estado Libre y Soberano de Michoacán. 1889. 396 (IV). Agosto 8. 3.
Gaceta Oficial del Gobierno del Estado Libre y Soberano de Michoacán de Ocampo. 1891. 577 (VI). Julio 23. 3.
García Acosta, V. 1992. Enfoques teóricos para el estudio histórico de los "desastres naturales". En: *Estudios históricos sobre desastres naturales en México: balance y perspectivas*. CIESAS. México. 19-31.
García Acosta, V. 1996. *Los sismos en la historia de México*. UAM/CIESAS/FCE. México. Tomo 1. 718 p.
García Acosta, V. 2004. La perspectiva histórica en la antropología del riesgo y del desastre, acercamientos metodológicos. *Relaciones*. 97 (XXV). 125-142.
La Lealtad. 1893. 52 (1). Octubre 31. Michoacán. 4.
La Libertad. 1895. 3 (3). Enero 15. Michoacán. 4.
La Libertad. 1899. 3 (7). Enero 17. Michoacán. 5.
La Libertad. 1899. 4 (7). Enero 24. Michoacán. 5.
La Libertad. 1899. 5 (7). Enero 31. Michoacán. 3.
Maskrey, A. (comp.). 1993. *Los desastres no son naturales*. Red de Estudios Sociales en Prevención de Desastres en América Latina. Lima, Perú. 45.
Rodríguez de la Torre, F. 1993. Lecturas sistemáticas de prensa periódica: Hacia una revisión de la sismicidad europea durante los siglos XVII y XVIII. En: *EC project "Review of Historical Seismicity in Europe" (RHISE). Consultado en: http://emidius.mi.ingv.it/RHISE/i_18del/i_18del.html.*
Suárez Reynoso, G. 1996. Presentación ¿Por qué estudiar la historia sísmica de México? En: García Acosta, V. *Los sismos en la historia de México*. UAM/CIESAS/FCE. México. Tomo 1. 11.

PALEOSEISMOLOGY & ARCHAEOSEISMOLOGY
MORELIA • MEXICO 2012
INQUA-TERPRO PALEOSEISMOLOGY
EARTHQUAKE ARCHAEOLOGY

ACTIVE FAULTINGS TRIGGERED BY THE LARGE SUBDUCTION EARTHQUAKES IN JAPAN

Takashi Azuma (1)

(1) Active Fault and Earthquake Research Center, AIST. Tsukuba, JAPAN. t-azuma@aist.go.jp

Abstract : *The source of the activities of the active faults is the shear stress accumulated on the fault plane caused by the plate motion. But some of active faults near the plate boundary may react and generate large earthquakes soon after the larger earthquakes on the plate boundary. The 2011 Fukushima-Hamadori earthquake (M 7.0) was a typical case of the triggered earthquake, and the 1896 Rikuu (M 7.2) and the 1945 Mikawa (M 6.8) earthquakes were also similar type earthquakes.*

Key words*: active fault, subduction earthquake, triggered earthquake*

INTRODUCTION

The source of the activities of the active faults is the shear stress accumulated on the fault plane caused by the plate motion. But some of active faults near the plate boundary may react and generate large earthquakes soon after the larger earthquakes on the plate boundary. This presentation shows three examples of the inland earthquakes with significant surface faulting triggered by the large subduction earthquakes (Fig. 1).

TRIGGERD EARTHQUAKES IN JAPAN

The 2011 Fukushima-Hamadori earthquake
One month after the 2011 Tohoku earthquake (M 9.0) along the Japan Trench, M 7.0 of the Fukushi-Hamadori earthquake occurred. This inland earthquake generated on the two traces of normal faults, the Idosawa fault (N-S trending) and Yunodake fault (NW-SE trending) (Fig. 2) that were recognized as active faults before the occurrence of this earthquake (The Research Group for Active Faults of Japan, 1991). The Idosawa fault had a large amount of displacement up to 2.1 m (Fig. 3), whereas that along the Yunodake fault was less than 0.6 m, although the length of the surface faults were almost same (ca. 15 km) along both faults (Awata et al., 2011). These faults have long recurrence intervals (ca. 12 kyr for the Idosawa fault: Tsutsumi and Toda, 2011) of their activities.

They were seemed to have reacted by the occurrence of the tensional stress caused by the crustal movement of the overridden plate of the Japan Trench, where the compressional stress are dominant in usual.

The 1945 Mikawa earthquake
Along the Nankai Trough, the 1944 Tonankai earthquake of M 7.9 was accompanied by the 1945 Mikawa earthquake of M 6.8. The Mikawa earthquake generated surface faults with 28 km in length along the Yokosuka fault and the Fukouzu fault (Sugito and Okada, 2004). Trenching studies on these faults shows that the intervals of faulting were longer than 4 kyr for the Fukozu fault (Sone and Ueta, 1993a) and 54 kyr for the connecting fault (Sone and Ueta, 1993b).

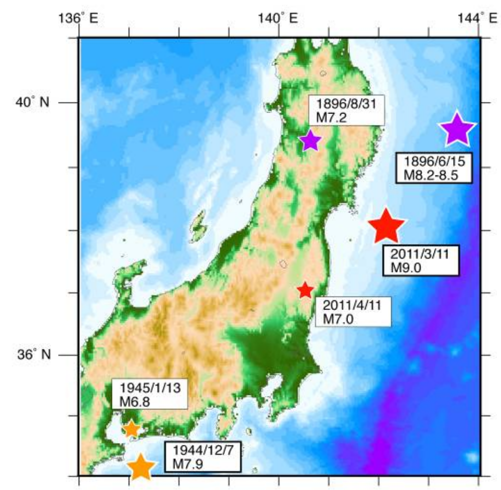

Fig. 1: Location of the epicenters of the subduction earthquakes and triggered inland earthquakes in Japan. Red: The 2011 Off the Pacific Coast of northeast Japan earthquake (M9.0) and the 2011 Fukushima-Hamadori earthquake (M7.0). Orange: The 1944 Showa Tonankai earthquake (M7.9) and the Mikawa earthquake (M6.8). Purple: the 1896 Meiji Sanriku earthquake (M8.2-8.5) and the 1896 Rikuu earthquake.

The 1896 Rikuu earthquake
The 1896 Rikuu earthquake occurred at eastside of the Yokote inland basin in Akita Prefecture at a half and two month after of 1896 Meiji Sanriku earthquake of M 8.2-8.5 along the Japan Trench, which is considered as a tsunami earthquake. The 1896 Rikuu earthquake generated surface ruptures along the eastern margin of the northern part of the Yokote Basin (the Senya fault) and another side of the Mahiru Mountain (the Kawafune fault). Both faults are N-S trending reverse faults. Length of surface ruptures were 36 km along the Senya fault and 6 km along the Kawafune fault (Matsuda et al, 1886). From the trenching studies, the recurrence interval of the Senya fault is 3.5 kyr. (Research Group for the Senya Fault, 1986).

References

Awata, Y., T. Maruyama, T. Azuma, E. Saito, K. Kagohara, Y. Sugiyama, T. Yoshioka, K. Taniguchi, R. Ando, M. Yoshimi and T. Hayashida. 2011. Surface ruptures along the Shionohira and Yunodake faults associated with Mw 6.7 earthqauke in 2011, southeastern Fukushima Prefecture. In: *Program and Abstract: Symposium on behaviour of inland active faults and seismicity/crustal movements associated with the 2011 Off the Pacific Coast of Tohoku Earthquake*. Chiba, Japan, 3-6. (in Japanese)

Matsuda, T., H. Yamazaki, T. Nakata and T. Imaizumi. 1980. The surface faults associated with the Rikuu earthquake of 1896. *Bulletin of the Earthquake Research Center of the University of Tokyo.* 55, 795-855. (in Japanese with English abstract)

Research Group for the Senya Fault. 1986. Holocene activities and near-surface features of the Senya fault, Akita Prefecture, Japan – excavation study at Komori, Senhata-cho-. *Bulletin of the Earthquake Research Center of the University of Tokyo.* 61, 339-402. (in Japanese with English abstract)

Sone, K. and K. Ueta. 1993a. Trenching study of the Fukozu fault at Tokoji, Aichi Prefecture in 1988. *Active Fault Research* (11), 43-46. (in Japanese)

Sone, K. and K. Ueta. 1993b. Trenching study of the Fukozu fault at Nishi-Fukozu, Aichi Prefecture in 1988. *Active Fault Research* (11), 47-50. (in Japanese)

Sugito, N. and A. Okada. 2004. Surface rupture associated with the 1945 Mikawa earthquake. *Active Fault Research* (24), 103-127. (in Japanese with English abstract)

The Research Group for Active Faults of Japan. 1991. Active faults of Japan – sheet maps and inventories. *University of Tokyo Press*. 439 p.

Tsutsumi, H. and S. Toda. 2011. Tectonic geomorphology and paleoseismology of the Itozawa and Yunodake faults reactivated during the Aipril 11, 2011 earthquake at Iwaki City, Fukushima Prefecture. In: *Program and Abstract: Symposium on behaviour of inland active faults and seismicity/crustal movements associated with the 2011 Off the Pacific Coast of Tohoku Earthquake*. Chiba, Japan, 1-2. (in Japanese)

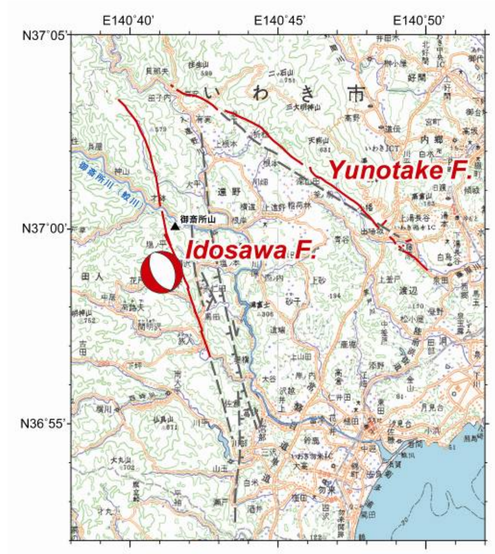

Fig. 2: Traces of surface ruptures of the Idosawa fault and the Yunotake fault associated with the 2011 Fukushima-Hamadori earthquake (M7.0). Red lines and grey lines show surface ruptures and active fault traces recognized before the earthquake (The Research Group for Active Fault of Japan, 1991, Nakata and Imaizumi, 2002). Focal mechanism shows this earthquake occurred on the normal fault and started on the Idosawa fault.

Fig. 3: Photo of the fault scarp on the Idosawa fault at Betto, Tabito town in Iwaki City, associated with the 2011 Fukushima-Hamadori earthquake (M7.0). The fault cut the paved road. Height of the fault scarp was 1.8 m at this site. The right lateral component of the faulting can be seen from the displacement of the concrete blocks.

SEISMITES AND PALEOTSUNAMIS DEPOSITS, ASSESSING FOR PALEOSEISMICITY IN PERU

Benavente, Carlos (1), Delgado, Fabrizio (1), Spiske, Michaela (2), Audin, Laurence (3)

(1) Instituto Geológico Minero y Metalúrgico-INGEMMET. Av. Canadá 1470, Lima, Perú. cbenavente@ingemmet.gob.pe
(2) Westfälische Wilhelms-Universität, Institut für Geologie und Paläontologie, Corrensstrasse 24, 48149 Münster, Germany
(3) Institut de recherche pour le développement IRD, Francia

Abstract: *Human occupation records in Perú provide historical record of large earthquakes prior to the 20th century. In this study, we extend our knowledge of major events by evaluating the stratigraphy and chronology of sediments exposed in various sectors of the Central Andes. These observations suggests that strong seismic activity occurred during the Quaternary, either along the subduction megathrust or on crustal faults. Indeed in Cusco and Colca regions, ,active faults affect fluvio-glacial and alluvial Holocene to Pliocene deposits. High in the topography, lacustrine deposits as well as Quaternary moraines display multiple geomorphic evidences of displacements ans seismites attesting for regional seismotectonic activity. Similarly along the Peruvian coast, 90 excavations succeeded in identifying for the first time paleo-tsunami deposits in southern Peru. Among them, the most impressive are encountered in Puerto Casma and Boca Rio and sign the historic 1619 subduction event and former unknown events (1641 ± 26 years B.P. ie 1668, as well as 2.26 ± 0.37 ka and 1.98 ± 0.23 ka respectively) .*

Key words*: Peruvian Andes, paleoseismology, seismites, tsunami deposits.*

INTRODUCTION

Peru is located on the western rim of South America, and most of the territory is subject to high seismic hazard both within the Andes and along the Pacific coast (Fig. 1).

The instrumental and historical seismic catalog in our country is insufficient for risk assessment. Therefore we studied active faults and Quaternary outcrops according to their tectonic and sedimentary structures in order to extend the knowledge on paleoseismology and related tsunami risk.

In this paper, we present the most prominent results of multiple studies realized in Peru aiming to identify deposits with seismic background and Quaternary tectonic structures. The first part deals with deformed sedimentary structures associated with intra-continental earthquakes (seismites) and crustal active faults, while the second part is related to the identification of paleo-tsunami deposits in the Quaternary stratigraphic record along the active subduction on the Peruvian margin.

The identification and characterization of seismites were conducted in two Quaternary lake basins.

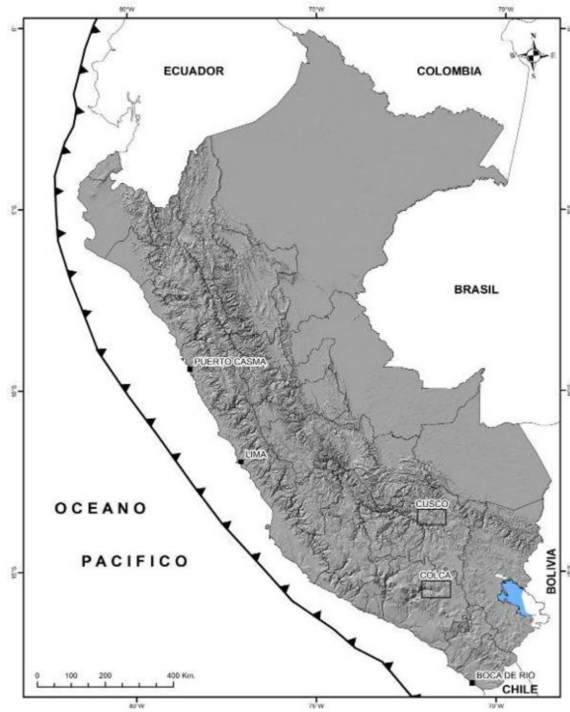

Fig. 1: Location of study area

RESULTS

Continental Peru

The identification and characterization of seismites were conducted in two Quaternary lake basins of Southern Peru.

The first basin is located between the Altiplano and Eastern Cordillera of the Peruvian Andes. The Cusco Basin is installed in a tectonic controlled area and is bordered by active fault systems (Cabrera, 1988; Benavente et al., 2010). Lacustrine deposits in the Cusco Basin are related to the occurrence of shoshonitic lavas (volcanic rocks of the Rumicolca Formation) with an age of 0.6 Ma (Carlier, G. & Lorand, 2008). The analysis of nine stratigraphic columns indicates that two lakes formed during the Quaternary in Cusco Basin (Fig. 2, see last page), damned in the SE sector of the basin, where the volcanic rocks of the Rumicolca Formation outcrop. A total of 36 levels of distinct seismites were identified, including slump-like, flame and ball, and pillow structures.

We propose that, in the early Pleistocene (Fig. 2A and 2D), the dam broke and subsequently a river system developed. During this period, several seismic events being occurred as observed on column 2I (Fig. 2; see ball and pillow structures in 20 thick meters sandbars. According to Rodriguez et al. (1998) table of seismites characterization; this event corresponds to a magnitude > 7. Subsequently a floodplain developed. An earthquake recorded in 6 different sites around the lake triggered landslides and liquefaction (Fig. 2A, 2B, 2E, 2F, 2G, 2I). The volume and geographic extention of the material affected by this event traduces an earthquake of magnitude > 7 (Rodriguez et al., 1998). In the late Pleistocene, a slump showing similar characteristics (Fig. 2A, 2FY 2H), possibly traduces a more recent lake discharge.

Tectonic activity fossilized in the deformation of lacustrine deposits is supposed to be related to seismic events on Tambomachay, Qoricocha, Chincheros Pachatusan or Chincheros fault systems, among others. These neotectonic faults are extending 50 km-long NWwards and affect fluvial to glacial deposits (10,000 BP) as well as recent alluvial sediments. These structures are 3 to 10 km away from Cusco basin and currently show seismic activity.

The second basin is located west of the first one, in the world deepest canyons: the Colca Canyon on the western flank of the Andes. Colca lacustrine deposits formed between 1.8 Ma and 0.6 Ma. Indeed K-Ar dating of lavas overlying the lacustrine deposits sequence (IV) contrains this chronology west of the town of Achoma (Klinck et al., 1986).

We propose here, based on field surveys and stratigraphic analysis that the lake was formed by a dam of Colca River. Damming was caused by an debris flow originated on the northeastern flank of the Hualca Hualca volcano, on the left bank of the river Colca. The dam lithology comprises subangular andesitic clasts fractured by rapid cooling. Gomez et al. (2004) propose a minimum volume of 1.3 km3 for the debris flow, after detailed surveying.

The dam induced a temporal lake (~ 150 m deep), evidenced by the deposition of thin white deposits with parallel lamination at the base of the basin (sequence I on Fig.2).

The consistent stratification and symmetrical sequence I, indicates that the lake was mainly stable during the Pleistocene (Fig. 2I). Later the stratification becomes asymmetric throughout the whole basin during the Lower-Middle Pleistocene? This is resulting from seismic activity, recorded in the stratigraphy by slumps (at the base of sequence II), ball and pillow and flame structures (Fig. 2A, 2B and 2C). According to Rodriguez (1998) and the nine seismic events identified in sequence II, the first two earthquakes were the largest in magnitude. These seismic events weakened the dam of the lake and induced the rupture.

Progressively a river system (sequence III) developed, associated with erosion and consequent incision of the lacustrine deposits, abandoning alluvial terraces. In sequence III, we identified only one seismite ball of pillow type, probably because in this dynamic environment, this type of sediments structures is difficult to preserve.

Overlying the fluvial sequence is another lacustrine sequence (sequence IV), which indicates another damming the river, being registered within the top of the sequence III and signs of a minor eruption of volcanic ash, which were deposited within the lake at the basal part of the sequence IV. In the upper part of the observed sequence IV ball and pillow type structures, flame and slumps, can be associated with structures generated by seismic events possibly weakening the dam and progressive development of a river system (Sequence V).

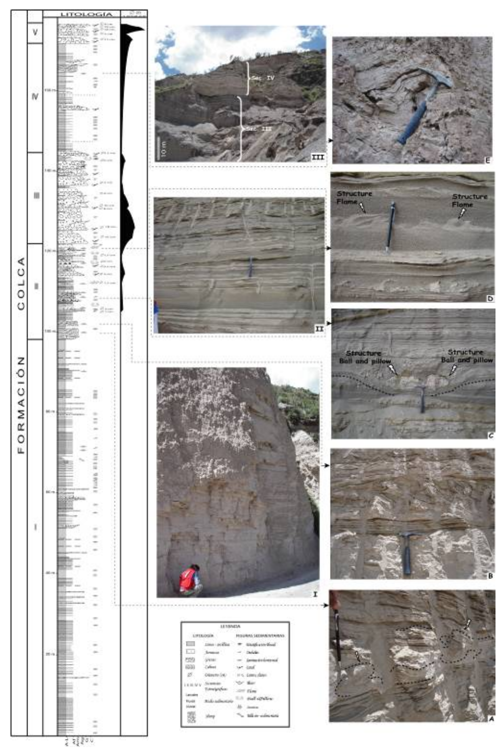

Fig. 3: Stratigraphic column type of lake deposits Colca Valley.

Finally, we present our results of newly identified paleotsunami deposits along the Peruvian margin based on new OSL dating, that notably implement Peru tsunami catalog and attest the need of further studies to constrain coastal risks.

Coastal Peru

We present two examples of tsunami deposits, located in northern and southern Peru. Presented results are largely taken Spiske et al., (In review) and Benavente et al., (2012).

Peru-Chile trench is one of the world's most active subduction zone, with high frequency of Mw>8 earthquakes and tsunami generation. We here conducted systematic exploration for deposits and / or traces of historical tsunamis performing 90 excavations and boreholes along 2400 km of the Peruvian coast.

We present two examples of tsunami deposits, located in northern and southern Peru (Spiske et al., subm and Benavente et al., 2012).

The beach of Puerto Casma is located 45 km south of Chimbote (northern Peru). In this 3 km wide bay, we identified at a depth of 0.60 m below the surface, a unusual level of sand (3-6 cm thick) within different beach sediments. This level is abnormal both in its composition and coloring (coarser, enriched in heavy minerals, plagioclase and quartz grains), in regard to beach sediments. Additionally this level contains fragments of shells, rocks and presents an erosional contact. The OSL dating (optically stimulated luminescence) reveals an age of 1641 ± 26 years B.P. Therefore, these deposits could be associated with the 1619 earthquake; previously described as non-tsunamigenic. Hence contributing another event to the tsunami catalog upgrade of Peru.

In Boca de Rio (southern Peru), we identified at 0.50 m depth, two tsunami deposits with thickness of about 4 cm. These consist of coarse sands found within fine grained marsh deposits. Both deposits show fragments of shells and towards the base have undulating contacts. The lower unit is located 0.40 m below the surface, while the upper is located 0.30 m below the surface. Both deposits interpreted as a result of two historical tsunamis that flooded the coastal plain. The dates for the deposition of the two levels by the OSL method suggest an age of 2.26 ± 0.37 ka for the lower level and 1.98 ±

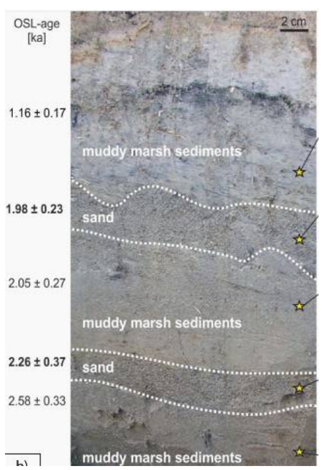

Fig. 4: Tsunami deposits located in Boca de Rio-southern Peru

0.23 ka for the top. Consequently their ages are beyond the limits of the historical of tsunamis. The mean time lapse between the two levels is approximately 272 years.

T The largest earthquakes in Southern Peru occurred in 1604 and 1868, and the lapse of time between these major events is 264 years. Furthermore it is documented that the earthquake of 1604 and 1868 had similar parameters (Dorbath et al. 1990). This is also to the case for the two levels of Boca Rio, where the modeled flow parameters are similar, as evidenced Spiske et al. (in review). These observations suggest that the levels identified in Boca Rio were produced by an earthquake sequence similar to 1604 and 1868 events.

CONCLUSIONS AND DISCUSSIONS

Paleoseismicity studies are an essential tool for determining seismic risk, especially in areas of deformation in which major earthquakes that can be separated by greater of times than the instrumental and historical records.

The regions of Cusco and Colca constitute an active tectonic zone where deformed structures (seismites) are related to reactivation of faults system failures as in the Huambo-Cabanaconde Cusco to Colca Basin cases. In addition to the long recurrences intervals of these crustal earthquakes, we can propose that these events were of magnitude greater than 7, from characterizations of seismically deformed structures.

Regarding tsunamis deposits, we can conclude that major earthquakes and tsunamis occurred frequently in the past, thus contributing to the expansion of the national catalog of tsunamis. Finally, this work should be useful in making decisions related to the plan of geological hazards and risk maps.

Acknowledgements:
These works were developed in cooperation with the Institut de Recherche pour le Développement IRD, France and Universität, Institut für Geologie und Paläontologie, Münster, Germany.

References

Benavente, C., Cárdenas, J., Concha R., García, B., & Morales, M. 2010. Evidencias de paleosismos en la estratigrafía de la cuenca cuaternaria Cusco. XV Congreso Peruano de Geología, Cusco,. Resúmenes extendidos pp. 1280-1283, Sociedad Geológica del Perú.

Benavente, C., Spiske, M., Piepenbreier, J., Kunz, A., Bahlburg, H. & Steffahn, J. 2012. Sedimentología y dataciones por Luminiscencia Estimulada Ópticamente (osl) de depósitos de paleotsunamis a lo largo de la costa peruana. XVI Congreso Peruano de Geología, Resúmenes extendidos. Sociedad Geológica del Perú.

Cabrera J. (1988). Néotectonique et sismotectonique dans la cordillere Andine au niveau du changement de géométrie de la subduction: La Région de Cuzco (Pérou). Thesis, pp. 268., Univ. Paris-Sud, Orsay, 1988.

Carlier, G. & Lorand, J. P. (2008). Zr-rich accessory minerals (titanite, perrierite, zirconolite, baddeleyite) record strong oxidation associated with magma mixing in the south Peruvian potassic province. Lithos, vol. 104, pp. 54-70.

Dorbath, L., Cisternas, A., Dorbath, C., 1990. Assessment of the size of large and great historical earthquakes of Peru. Bulletin of the Seismological Society of America 80 (3), 551–576.

Gómez, J. C., Macías, J. L., Siebe, C., & Ocola, L. 2004. Delimitación y análisis sedimentológico de la avalancha de escombros del volcán Hualca Hualca, valle del Colca, Arequipa-Perú. XII Congreso Peruano de Geología, Resúmenes extendidos. Sociedad Geológica del Perú, p.575-577.

Klinck, B.A., Ellison, R.A., Hawkins, M.P., 1986. The geology of the Cordillera Occidental and Altiplano, west of Lake

Titicaca southern Peru. INGEMMET, Preliminary Report Lima.

Rodriguez, M.A. (1998). Paleosismicidad y sismotectónica de las cuencas lacustres neógenas del Prebético d Albacete. Tesis para optar el Grado de Ciencias Geológicas pp.360. Universidad Complutense de Madrid.

Spiske, M., Piepenbreier, J., Benavente, C., Bahlburg, H., in review. The onshore preservation potential of siliciclastic tsunami deposits in arid climate regions. Earth-Science Reviews, in review.

Fig.2: Columns Cusco Basin stratigraphy

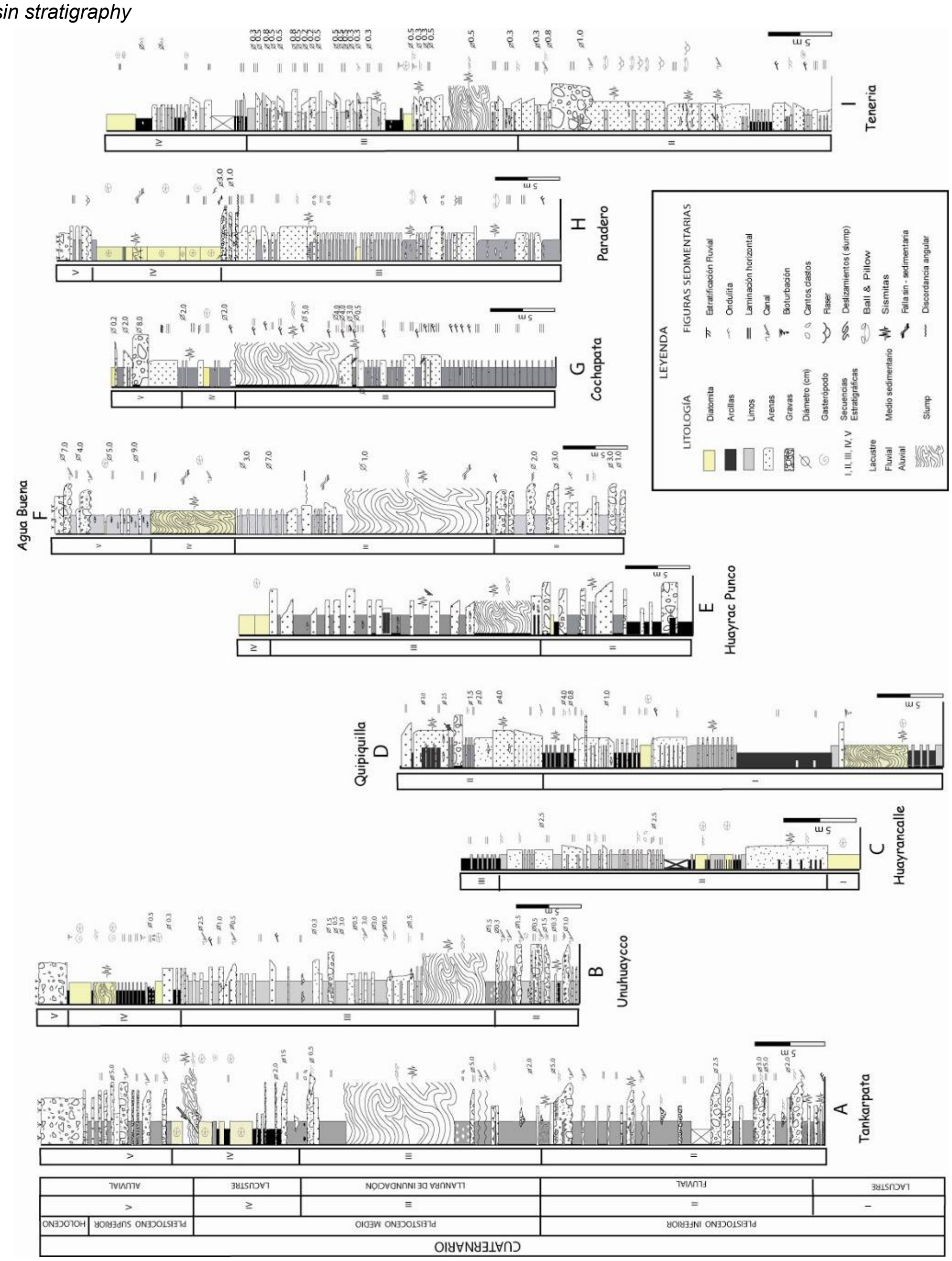

PALEOSEISMOLOGY & ARCHAEOSEISMOLOGY
MORELIA • MEXICO 2012
INQUA-TERPRO PALEOSEISMOLOGY
EARTHQUAKE ARCHAEOLOGY

LATE JURASSIC REACTIVATION OF THE ST. LAWRENCE RIFT SYSTEM, QUEBEC, CANADA: EVIDENCE FROM APATITE (U-TH)/HE DATING

Laura Bouvier. (1), Daniele Pinti (2), Alain Tremblay (3), William G. Minarik (4), Mary K. Roden-Tice (5)

(1) GEOTOP-UQAM, Montréal, QC, Canada. bouvier.laura@courrier.uqam.ca
(2) GEOTOP-UQAM, Montréal, QC, Canada. pinti.daniele@uqam.ca
(3) GEOTOP-UQAM, Montréal, QC, Canada. tremblay.a@uqam.ca
(4) GEOTOP-McGill University, Montréal, QC, Canada. william.minarik@mcgill.ca
(5) Plattsburgh State University of New York, Plattsburgh, USA. rodentmk@plattsburgh.edue

Abstract: *The St. Lawrence rift system (SLRS), eastern Canada, is a seismically active zone delimited by crustal-scale faults. Reactivation of the SLRS is believed to have occurred since Late Proterozoic. The lack of isotopic chronological constraints and the absence of strata younger than the Ordovician make it difficult to determine the timing of fault increments. However, recent AFT dating suggests a reactivation during the Mesozoic. (U-Th)/He thermochronometry on apatite was thus performed along three transects across the SLRS in order to verify the occurrence of younger episodes of faulting. The footwall rocks yielded He ages ranging from 123 ± 10 to 188 ± 16 Ma whereas hanging wall samples yielded He ages ranging from 138 ± 18 to 162 ± 14 Ma confirming the existence of a Late Jurassic episode of fault reactivation.*

Key words: *(U-Th)/He, apatite, fault, Saint-Laurent Rift System*

INTRODUCTION

Situated on the eastern edge of the Canadian Shield, the St. Lawrence Rift System (SLRS) is a NE-trending half-graben, extending for more than 500 km along the St. Lawrence River valley. This is a seismically active zone which produced five earthquakes of magnitude larger than 6.0 in the last 350 years, in Charlevoix area (*Fig. 1*). The rift-related faults fringe the contact between the Proterozoic granite-gneiss Grenvillian basement to the NW and the Cambrian–Ordovician sedimentary rock of the St. Lawrence Lowlands Group to the SE (*Fig. 1*). These structures have been traditionally described as normal faults (Rondot, 1989). Field observations suggest the reactivation of brittle faults bordering the SRLS since Late Proterozoic (Cawood et al., 2011). The absence of rock strata younger than Ordovician along the SLRS and the lack of precise isotopic age constraints hamper the recognition of post-Ordovician faulting episodes. Field relations in Québec, Charlevoix and Saguenay River regions (*Fig. 1*) suggest faulting event(s) younger than the Devonian, the supposed age of Charlevoix crater.

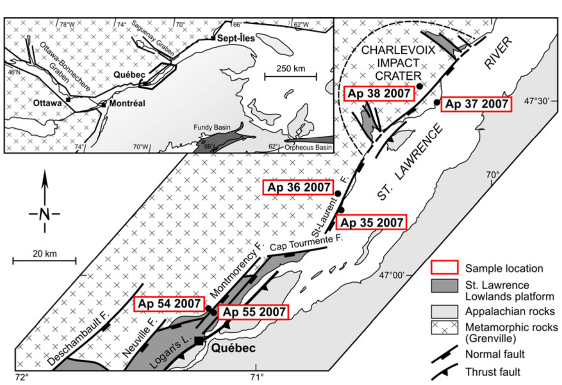

Fig. 1: Schematic map of the St. Lawrence Rift System.

Recent apatite fission track (AFT) ages determined for Grenvillian basement rocks from the hanging wall and footwall of typical SLRS rift faults indicate localized Mesozoic reactivation of the rift (Tremblay et al., 2012). In the frame of these recent results we decided to measure apatite (U-Th)/He ages for Grenvillian basement rocks from the hanging wall and footwall of the Montmorency and Saint-Laurent faults at three different locations along the SLRS (*Fig. 1*).

GEOLOGICAL SETTING

The studied segment of the SLRS is located along the St. Lawrence River and extends for 100 km, from Québec to Charlevoix (*Fig. 1*). The bedrock consists of high-grade metamorphic rocks, charnockite, anorthosite and granite of the Grenville Province (Rivers et al., 1989). Their uplift and cooling below 300°C occurred 850 Ma ago (Anderson, 1988). Down-faulted Cambrian-Ordovician rocks of the St. Lawrence Lowlands platform overlie the Grenvillian basement (Lavoie, 1994). The St. Lawrence Lowlands Group is constituted of non-metamorphosed and slightly deformed Cambrian to Early Ordovician sandstones and dolostones deposited in a rift and a passive margin setting. They are overlain by Middle to Late Ordovician shallow to deep marine foreland basin shale and molasse deposits (Lavoie, 1994). There are no sedimentary rocks younger than Late Ordovician in the area. The Charlevoix area hosts an impact structure of Devonian age formed by two NW-SE trending valleys that are part of the impact-related annular graben (Rondot, 1968). The rift faults to crosscut older structures and fault rocks attributed to the crater formation (Lemieux et al., 2003), therefore, suggesting a faulting increment along the rift system postdating Late Devonian–Early Carboniferous.

The faults of the SLRS are separated into NE-trending longitudinal faults sub-parallel to the rift axis (Montmorency and Saint-Laurent faults), and NW- to EW-trending transfer faults (Cap-Tourmente fault; *Fig. 1*; Tremblay et al., 2003). The longitudinal faults extend for tens of km along strike and usually abut against transverse faults of more limited extent (≤10 km). Both sets of structures are high-angle dip-slip faults with south- to southeast-dipping angles averaging 70-85° (*Fig. 2*). The faults show mutual crosscutting relations and were interpreted as conjugate structures related to a single tectonic event (Tremblay et al., 2003).

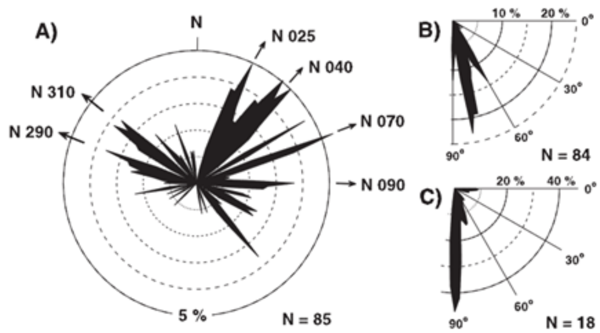

Fig. 2: Rose diagrams for faults of the St. Lawrence Rift System in the studied area. (A) Strike orientations for the rift faults. (B)Dip angle values for the rift faults. (C) Pitch angle values of fault striations (N = number of data) columns wide (After Tremblay et al., 2003).

All faults are marked by cohesive cataclasite. The typical fault zones are ≥ 10 to 20 m thick, and consist of fault breccia, cataclasites, ultracataclasites and foliated fault gouges. The core zone of faults is, however, marked by lenses of non-cohesive gouge and fault breccia (Tremblay et al., 2012). The coexistence of non-cohesive and cohesive fault rocks can be tentatively attributed to fault reactivation, the non-cohesive fault rocks being possibly related to a younger faulting increment compared to cohesive rocks (*Fig. 3*; Tremblay et al., 2012).

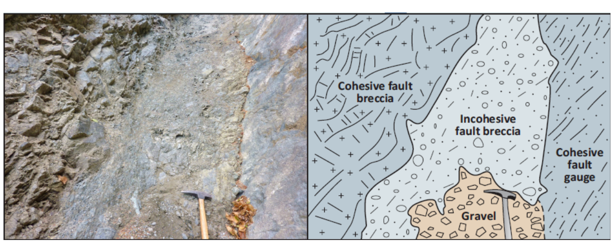

Fig. 3: Field photograph and sketch of coexisting cohesive and non-cohesive fault rocks along the Saint-Laurent fault. This feature can be tentatively attributed to fault reactivation, the non-cohesive fault rocks being possibly related to a younger faulting increment compared to cohesive fault rocks.

ANALYTICAL METHODS

The (U-Th)/He thermochronology method is based on the production of radiogenic ^{4}He from decay of ^{238}U, ^{235}U and ^{232}Th (an in minor amount from ^{147}Sm) in apatite. Main application of (U-Th)/He thermochronology is the assessment of cooling histories of rocks as they pass through the upper 1-3 km of the crust. This demands accurate, quantitative knowledge of He diffusion. Helium diffusion in apatite can be described as a function of temperature (*Fig. 4*): helium is retained only below 60-75°C, the closure temperature (T_c) assuming a cooling rate of 10°C/Myr (Ehlers and Farley, 2002). At higher temperatures, ^{4}He is lost by diffusion as fast as it is produced by α-decay, resetting the chronometer. Thus helium age corresponds to a cooling age (*Fig. 4*). However, the accumulation of He within a crystal occurs gradually: the partial retention zone (PRZ; *Fig. 4*) is the temperature range or depth where the radiogenic He is only partially retained (Reiners et Brandon, 2006).

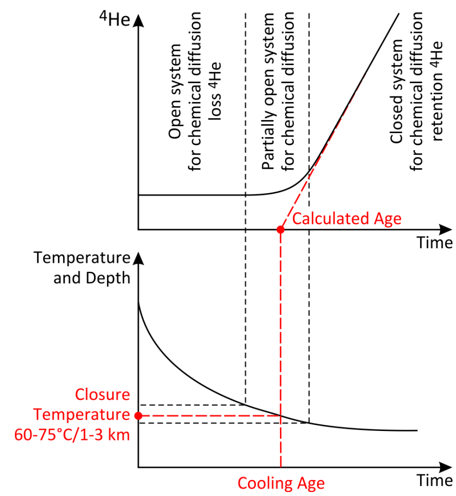

Fig.4: Time evolution of 4He signal during cooling of a rock. Closure temperature (Tc) is associated with the cooling age. The partial retention zone, PRZ, is the area where the system is partially open to the diffusion.

Apatite grains were obtained from six Grenvillian granitic to tonalitic gneisses. Apatites were isolated with heavy liquid and magnetic separation from 2-3 kg of rock. Samples were selected under binocular and then optical microscope. Apatite dimensions were obtained to apply the parameter F_T of Farley et al. (1996) to the calculated ages (*Fig. 5*) to take into account the α-particle ejection.

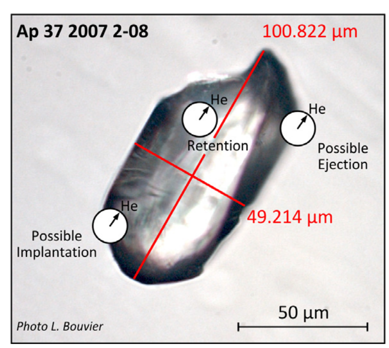

*Fig. 5: Microscope image of a hexagonal apatite (L*l=dimensions of apatite) (Photo L. Bouvier).*

Selected apatites must have hexagonal prism shapes, proper dimensions (75-170 µm), and show no mineral or fluid inclusions. However, most of apatite extracted from gneiss was rich in mineral inclusions, as monazite (*Fig. 6*) and some of them showed shapes different than a hexagonal prism shape (*Fig. 7*).

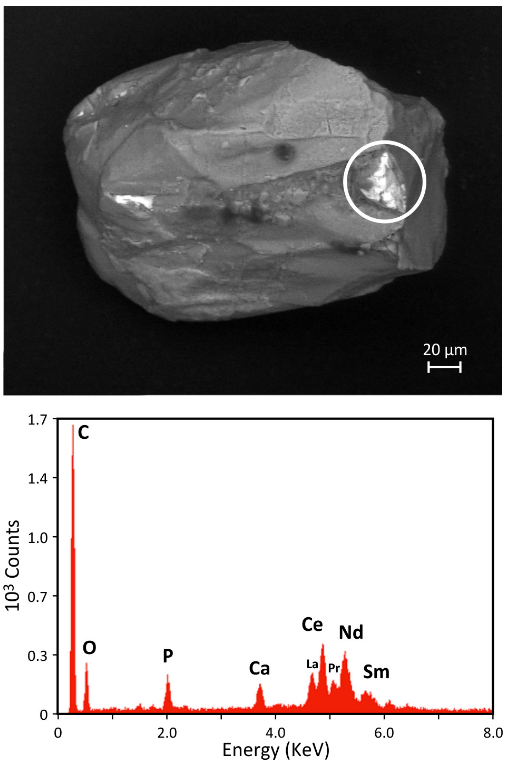

Fig.6: backscattered image of a monazite inclusion within an apatite crystal (A) as revealed by its chemical analysis (B).

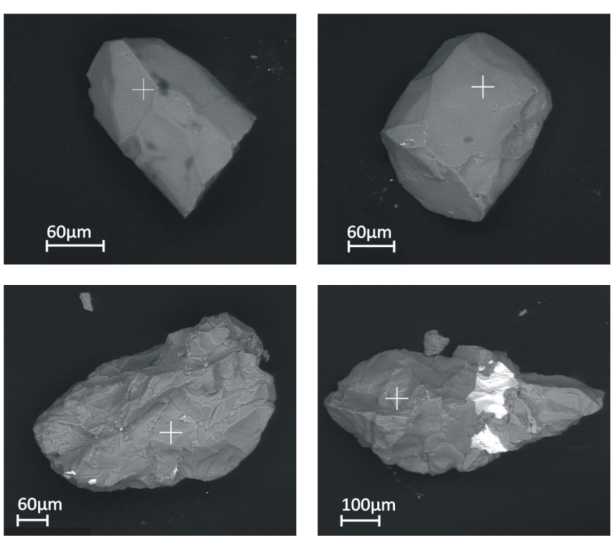

Fig.7: Examples of apatite shapes observed in our samples.

After selection, few tens of apatite crystals were inserted in Pt foils and charged in a resistance furnace (*Fig. 8*). Apatite were heated in vacuo at ~950°C for 20 mn to degas He (*Fig. 8*). After purification, He was quantified by comparison to a manometrically-calibrated He standards on a quadrupole mass spectrometer (Balzers Prisma C-200) (*Fig. 8*). For each sample, the international standard Durango apatite was analyzed ((U-Th)/He age of 31.02 ± 1.01 Ma, Mc Dowell et al., 2005). Analytical precision is 1.5% (2σ) and accuracy better than 1%. Analyses were performed at the GEOTOP Noble Gas Laboratory in Montréal.

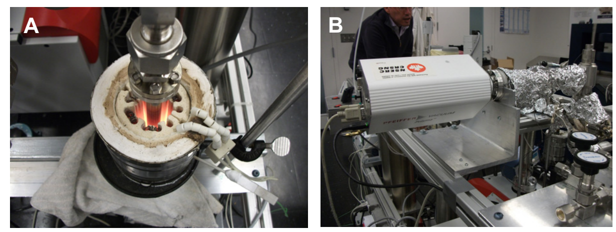

Fig. 8: A: System vacuum extraction (furnace) and purification (gettering), B: Quadrupole mass spectrometer (Balzers Prisma C-200).

Measurement of U and Th by ICP-MS was carried out at McGill University using the technique developed by Reiners and Nicolescu (2006). Pt foils were directly immersed in nitric acid and the grains dissolved for U-Th-Sm analysis to avoid the difficult task of transferring the degassed apatite crystals from the foil to another vial. Each batch of analyses was accompanied by three sets of routine standards and blanks, used to check cleanliness of reagents and Teflon, and procedural blanks.

RESULTS AND DISCUSSION

Figure 10 shows AFT ages obtained by Tremblay et al. (2012). (U-Th)/He ages are weighted averages (Fig. 10). Montmorency fault shows inversed (U-Th)/He ages between the footwall and the hanging wall compared to AFT ages. Saint-Laurent fault shows younger (U-Th)/He ages for the hanging wall than the footwall. Most of the (U-Th)/He ages are slightly younger than AFT ages as expected, because of the lower closure temperature of helium (60-70˚C) than that of AFT (100˚C).
AFT ages discontinuities (and consequently (U-Th)/ He ages) were interpreted as the result of normal faulting at ca. 200 Ma, followed by tectonic inversion at ca. 150 Ma or younger (Tremblay et al., 2012).

Acknowledgements: This project was supported by NSERC Discovery grants of DLP and AT. We wish to thank M. Laithier for the artwork. We would also like to thank Victor Hugo (University Michoacana, Mexico) for invite this paper to the 3rd INQUA-IGCP-567 International Workshop on Active Tectonics.

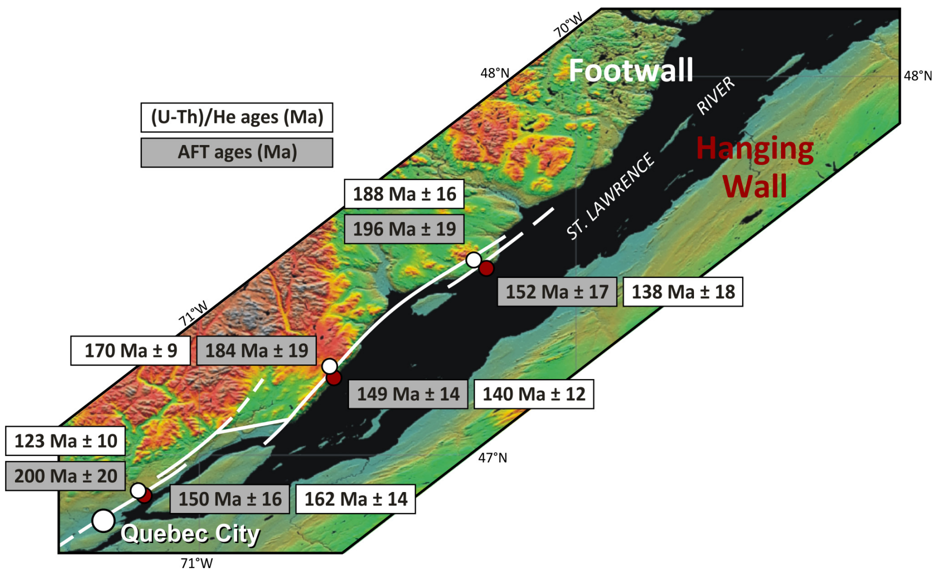

Fig. 10: Comparison of AFT ages and (U-Th)/He ages obtained along the SLRS faults.

References

Anderson, S.L. 1988. Interpretation of K–Ar mineral dates from the Grenville orogenic belt. *American Journal of Science* (288), 701-734.

Cawood, P.A., McCausland, P.J.A. & Dunning, G.R. 2011. Opening Iapetus: constraints from the Laurentian margin in Newfoundland. *Geological Society of America Bulletin* (113), 443-453.

Ehlers, T. A., and Farley, K. A. 2002. Apatite (U-Th)/He thermochronology: methods and applications to problems in tectonics and surface processes. *Earth and Planetary Science Letters* (206), 1-14.

Farley, K.A., Wolf, R.A., Silver, L.T. 1996. The effects of long alpha-stopping distances on (U-Th)/He ages. Geochimica et Cosmochimica Acta (60), 4223-4229.

Lavoie, D. 1994. Diachronous tectonic collapse of the Ordovician continental margin, eastern Canada: comparison between the Quebec Reentrant and St. Lawrence Promontory. *Canadian Journal of Earth Science* (31), 1309-1319.

Lemieux, Y., Tremblay, A. and Lavoie, D. 2003. Structural analysis of supracrustal faults in the Charlevoiz area, Québec: relation to impact cratering. *Canadian Journal of Earth Sciences* (40), 221-235.

McDowell, F.W., McIntosh, W.C. and Farley, K.A., 2005. A precise ^{40}Ar-^{39}Ar reference age for the Durango apatite (U-Th)/He and fission-track dating standard. *Chemical Geology* 214 (3-4), 249-263.

Reiners, P.W., Brandon, M.T. 2006. Using thermochronology to understand orogenic erosion. *Annual Review of Earth and Planetary Sciences* (34), 419-66.

Reiners, P.W., Nicolescu, S. 2006. Measurement of parent nuclides for (U-Th)/He chronometry by solution sector ICP-MS. *http://www.geo.arizona.edu/~reiners/arhdl/arhdl.htm*

Rivers, C.T., Martignole, J., Gower, C.F., Davidson, A. 1989. New tectonic divisions of the Grenville Province, southeast Canadian shield. *Tectonics* (8), 63-84.

Rondot, J. 1968. Nouvel impact météoritique fossile? La structure semi-circulaire de Charlevoix. *Canadian Journal of Earth Sciences* (5), 1305-1317.

Rondot, J. 1989. Géologie de Charlevoix. *Ministère de l'Énergie et des Ressources du Québec, Rapport MB 89-21*, 606.

Tremblay, A., Long, B. and Massé, M. 2003. Supracrustal faults of the St. Lawrence rift system, Quebec: kinematics and geometry as revealed by field mapping and marine seismic reflection data. *Tectonophysics* (369), 231-252.

Tremblay, A., Roden-Tice, M., Brandt, J. A., Megan, T. (2012). Mesozoic fault reactivation along the St. Lawrence rift system, Eastern Canada: thermochronologic evidence from apatite fission. *Geological Society of America Bulletin* in press.

POSIBLES DEFORMACIONES SISMICAS SEDIMENTARIAS EN EL MAAR LA ALBERCA, VALLE DE SANTIAGO, GUANAJUATO

Castro López, V. (1), Soria-Caballero, D.C. (2), Domínguez Vázquez, G. (3) y Garduño-Monroy, V.H. (4).

(1) Maestría en Geociencias y Planificación del Territorio, IIM-UMSNH. México. salix@live.com.mx
(2) Posgrado en Ciencias de la Tierra, Instituto de Geología-UNAM. México. dianscc@hotmail.com
(3) Facultad de Biología, UMSNH. México. gdoguez@yahoo.com.mx
(4) Departamento de Geología y Mineralogía, IIM-UMSNH. México. vhgardunom@gmail.com

Resumen (Posibles Deformaciones Sísmicas sedimentarias en el Maar La Alberca, Valle de Santiago, Guanajuato): En el presente trabajo se muestra un estudio litoestratigráfico de núcleos extraídos del lago cráter conocido como la Hoya La Alberca, localizado en Valle Santiago Guanajuato, en México. En la mayor parte de los núcleos las estructuras dominantes fueron secuencias laminares y en menor proporción masivas. Las láminas milimétricas arcillosas eran de color ocre a obscuro, alternadas generalmente con estratos de limos y limo-arcillosos, se observaron claramente en algunas partes del núcleo, posibles estructuras sísmicas entre las profundidades de 40 cm y 190 cm expresadas como un microfallamiento aparente, así como en las secciones de 120 cm, 300 a 350 cm, 570 a 594 cm, 600 a 635 cm y a 710 cm expresada como laminas arcillosas con pequeñas deformaciones e inclinaciones.

Key words: *Deformación sinsedimentaria, maar, CVVS.*

INTRODUCCION

El campo volcánico de Valle de Santiago (CVVS), Guanajuato, es parte del campo volcánico Michoacán-Guanajuato (CVMG), el cual se ubica en la parte central del Cinturón Volcánico Transmexicano (CVTM). El CVVS comprende numerosos conos cineríticos, conos de lava (Cano-Cruz y Carrasco-Núñez, 2008) y 13 lagos maares, que se encuentran alineados y orientados con dirección NNW-SSE (Murphy, 1982) (Fig.1). Dichos maares se formaron como el resultado de la actividad explosiva freatomagmática, a ellos se encuentran asociadas coladas de lavas, depósitos piroclásticos (oleadas) y de caída (tefras) (Uribe-Cinfuentes y Urrutia Fucugauchi, 2006).

El vulcanismo del CVVS es principalmente de composición basáltico-andesítica, con edades que varían del Plioceno al Reciente (Uribe-Cinfuentes y Urrutia Fucugauchi, 2006). Siendo el cerro Guates la más antigua (6.88 Ma), y una de la hoya más joven: San Nicolás 1.2 Ma (Ban et al., 1992).

En el presente trabajo se analizaron las secuencias sedimentarias del maar actualmente seco conocida localmente como Hoya La Alberca ubicado al oeste del CVVS. La Alberca posee una edad de 0.073 Ma. (Ban et al., 1992), su cráter es casi circular y tiene un diámetro de 500 m en dirección E-W, con una altura de 60 m sobre el nivel del valle y una profundidad total de 110 m. Las paredes internas del cráter son casi verticales. La secuencia estratigráfica a partir del nivel del lago se conforma de base a cima por: una lava andesítica masiva, afanítica de color gris claro a medio, depositada en el cuello del cráter, se considera una secuencia volcánica pre-maar. Sobreyaciendo esta secuencia, se encuentra una capa de paleosuelo de color claro, el cual está cubierto por un derrame de lava escoreácea de

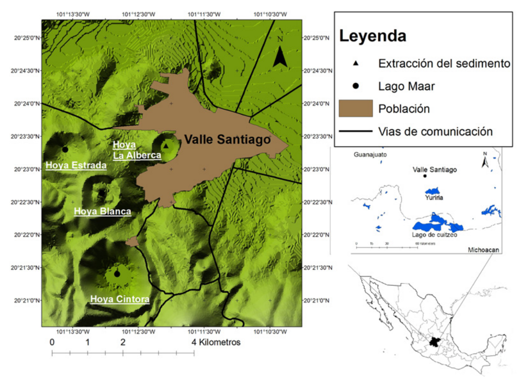

Fig. 1: Ubicación geográfica de la extracción del núcleo La Alberca, Valle Santiago Guanajuato.

composición basáltica y de espesor irregular. En la parte norte, esta unidad está ligada a un pequeño cono volcánico de tipo estromboliano que generó derrames muy pequeños de poco espesor (escoria de caída). Por último y cubriendo los depósitos previos encontramos la secuencia volcanoclástica, principalmente en el lado suroeste del cráter (Uribe-Cifuentes y Urrutia Fucugauchi, 2006).

El volcanismo de Valle de Santiago está condicionado por la influencia de la estructura regional Tzitzio-Valle de Santiago de dirección NNW-SSE la cual presenta un movimiento normal sumado a un componente lateral derecho, esta estructura se encuentra al oeste del Sistema de Fallas Taxco-Querétaro (SFTQ) y controla fuertemente la distribución del volcanismo causando un desplazamiento hacia el SE. Aparentemente, esta estructura ha sido reactivada por la formación y desarrollo del CVTM (Garduño-Monroy et al., 2009)

METODOLOGÍA

Se extrajeron una serie de núcleos en la parte distal y proximal de la Cuenca, usando un nucleador de sedimentos manual tipo ruso que permite extraer secciones de 50 cm de longitud, alcanzando profundidades dependientes de la compactación de los sedimentos. Con este equipo se obtuvieron un total de 16 segmentos los cuales formaron una secuencia sedimentaria continua de 8 m de profundidad en la porción distal de la cuenca. Los núcleos fueron fotografiados, descritos y muestreados a cada 5cm para análisis de polen, análisis elemental mediante FRX, contenido de carbono, susceptibilidad magnética y macropartículas de carbón.

RESULTADOS

La columna estratigráfica descrita para la zona proximal de La Alberca tuvo una profundidad de 8 m y fue dividida en cuatro unidades principales de la base a cima:

Unidad D (800 - 680 cm): Secuencia de láminas muy finas (milimétricas) de colores café claro y oscuro intercalados, de 120 cm de espesor total. Presenta hacia su base algunas bandas centimétricas de arcillas color café oscuro. Aproximadamente a los 7 m de profundidad se observa una estructura casi circular de limos color café oscuro que deforma las capas arcillosas a su alrededor (Fig.2).

Unidad C (680 - 560 cm): Secuencia heterogénea de 30 cm de espesor, caracterizada por la presencia de un conjunto de láminas arcillosas de color ocre, alternadas en la base con algunos estratos de limos y limo-arcillosos. En la cima predomina la secuencia arcillosa laminada la cual presenta pequeñas deformaciones a profundidades de 560 cm a 640 cm.

Unidad B (560 - 250 cm): Secuencia heterogénea de capas masivas seguidas de secuencias laminares. En la base se observa un estrato limoso color café oscuro masivo, seguido por una estrato de <10cm de espesor de arcillas laminadas color ocre cubierta por una banda de limos de <5cm de espesor color café oscuro. Hacia la cima predomina una serie de laminaciones arcillosas de colores ocre claro y oscuro intercaladas con algunos estratos de sedimentos limosos color café oscuro.

Unidad A (250 - 0 cm): Secuencia de sedimentos laminares arcillosos colores café claro y oscuro dispuestos de forma alternada, con un espesor de 150 cm, cambiando de manera transicional hacia la cima a sedimentos limo-arcillosos y limosos menos sin disposición laminar definida. En esta unidad se aprecia una ligera inclinación de los estratos limitada por capas inferiores y superiores horizontales.

Las estructuras sedimentarias relacionadas posiblemente a eventos sísmicos se refieren a estratos limosos y arcillosos de espesores milimétricos los cuales se encuentran deformados y/o inclinados, estas estructuras se encuentran confinadas por secuencias laminares horizontales arcillosas o capas masivas de

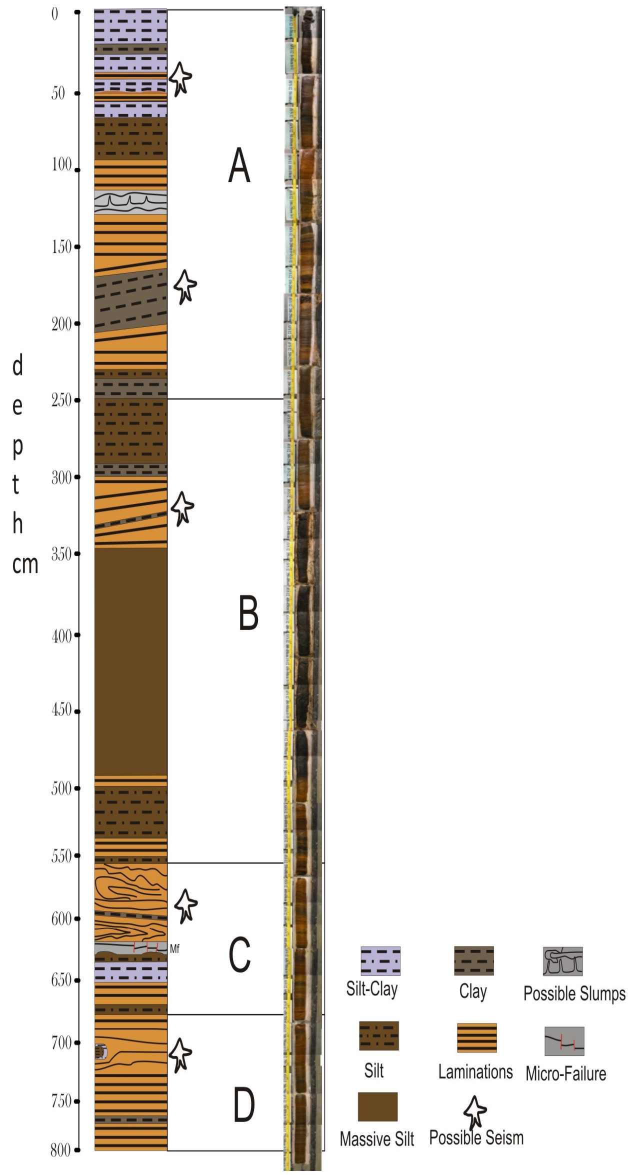

Fig. 2: columna estratigráfica descrita para la zona proximal de la Hoya La Alberca de Valle de Santiago.

sedimento limo-arcilloso, lo cual sugiere que la deformación de estratos sucedió poco después de la sedimentación de partículas en el lago durante un evento puntual en el tiempo, después del cual la sedimentación continuo de manera normal generando laminaciones horizontales o capas masivas. Esta clase de estructuras sedimentarias probablemente sísmicas fueron observadas a profundidades de 40 cm y 190 cm manifestándose como un microfallamiento aparente, en la secciones de 120 cm, 300 a 350 cm, 570 a 594 cm, 600 a 635 cm y a 710 cm expresada como láminas deformadas e inclinadas (Fig. 3).

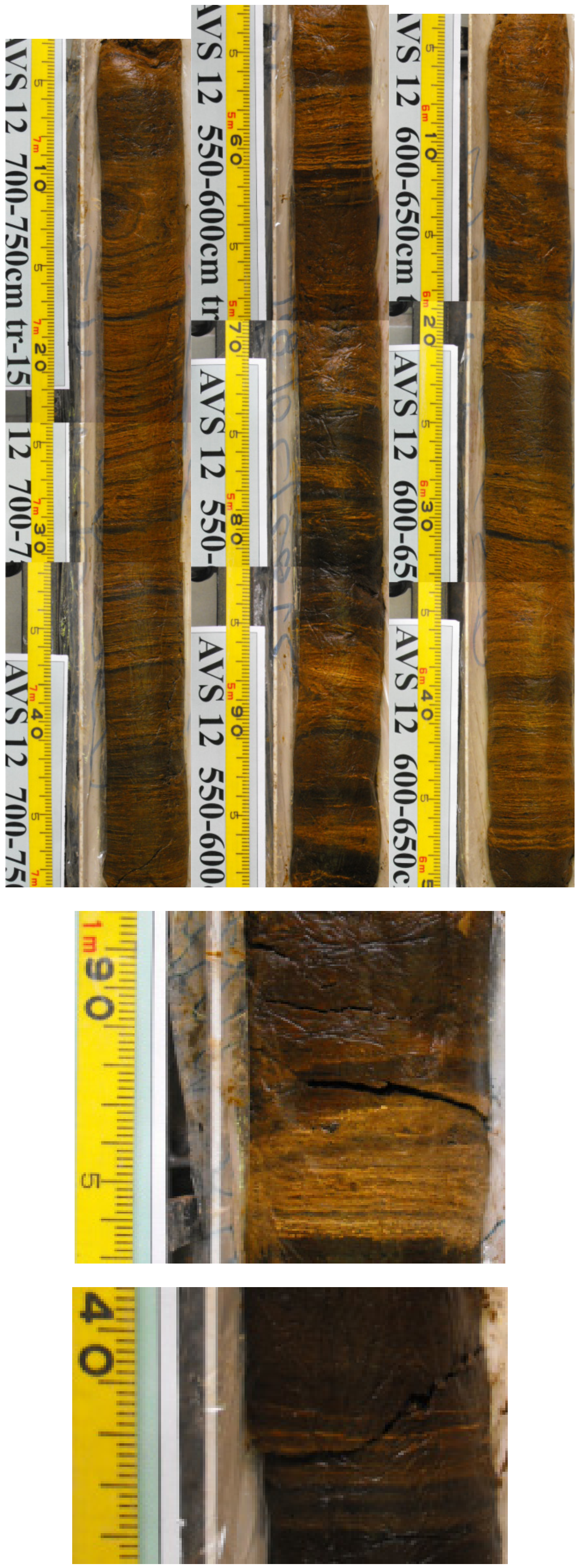

Fig. 3: Sismitas en segmentos de núcleo extraído de La Alberca de Valle de Santiago.

DISCUSIONES

La revisión de los primeros núcleos obtenidos para el lago cráter conocido como Hoya La Alberca, sugieren la presencia de deformaciones sinsedimentarias que podrían ser asociadas a actividad sísmica antigua, debido a la influencia que ejerce la falla Tzitzio – Querétaro la cual se encuentra subyaciendo dicho lago y cuyos movimientos (tipo normal-lateral derecho) durante la historia de la cuenca pudieron haber quedado registrados en los sedimentos, de manera similar a lo reportado por Rodríguez-Pascua et al. (2012) para la falla de Pozohondo al SE de España. La extracción de núcleos adicionales en diferentes puntos dentro de la cuenca, el muestreo y los fechamientos de sedimentos, así como la realización de estudios estratigráficos y paleosismológicos más detallados son necesarios para clarificar el origen de dichas deformaciones sedimentarias así como para comprender la historia sísmica del Campo Volcánico de Valle de Santiago, ubicado en Guanajuato, México.

Agradecimientos: agradecemos al laboratorio de paleoambientes del IIM, UMSNH que facilitaron para el muestreo y análisis de sedimento, a la Doc. Gabriela por la ayuda al muestreo en campo, al Dr. Víctor Garduño, Dra. Isabel Israde y al M.C. Neftalí Razo Pérez por su colaboración en el laboratorio.

References

Ban, M., T.Hasenaka, H. Delgado-Granados y Takaoka. 1992. Ages of lavas from shield volcanoes in Michoacán Guanajuato, Mexico. Geofis. Int., 31: 467-473

Cano-Cruz, M. y G. Carrasco-Núñez. 2008. Evolución de un cráter de explosión (maar) riolítico: Hoya de Estrada, Campo Volcánico Valle de Santiago, Guanajuato, México. *Revista Mexicana de Ciencias Geológicas. 25 (3):.* 549-564.

Garduño-Monroy VH, Pérez-López R, Israde-Alcántara I, Rodríguez-Pascua MA, Szynkaruk E, Hernández-Madrigal VM, García-Zepeda ML, Corona-Chávez P, Ostroumov M, Medina-Vega VH, García-Estrada G, Carranza O, López-Granados ME, Mora-Chaparro JC. 2009. Paleoseismology of the southwestern Morelia-Acambay fault system, central Mexico. Geofísica Internacional 48 (3): 319-335.

Murphy, G.P., 1982. The Chronology, Pyroclastic Stratigraphy, and Petrology of the Valle de Santiago Maar Field, Central Mexico. M. A. Thesis, University of California, Berkeley.

Rodríguez-Pascua MA, R Pérez-López, VH Garduño-Monroy, JL Giner-Robles, PG Silva, MA Perucha-Atienza, VM Hernández-Madrigal, J Bischoff. 2012. Paleoseismic and geomorphologic evidence of recent tectonic activity of the Pozohondo Fault (Betic Cordillera, SE Spain). Journal of Iberian Geology 38 (1): 239-252.

Uribe-Cinfuentes, R. M. y J. Urrutia-Fucugauchi, 2006. Xenolitos y vulcanismo en la región de valle Santiago, Guanajuato-estudios paleomagneticos y magneticos de rocas. Tesis doctoral en ciencias, sismología y física del interior de la tierra. UNAM, pp. 192.

NEOTECTONICS STUDIES OF HAZARDOUS FAULTS IN THE CENTRAL ANDES: ISSUES AND CHALLENGES

Costa, Carlos H.

Departamento de Geología, Universidad Nacional de San Luis, Ejército de los Andes 950, Bloque II, 5700 San Luis, Argentina
costa@unsl.edu.ar

Abstract (Neotectonic and hazardous faults in the Central Andes: issues and challenges): *Neotectonic and paleoseismological studies constitute a basic requirement for seismic hazard assessment. At the Central Andes, as in many other regions, most seismic hazard assessments rely on the seismic catalog data. In other cases, neotectonic and paleoseismological data, when available, are often partly used or their results could be even misleading for users. This contribution aims to briefly address some current issues and challenges posed by the current state of the art and recent advances on the neotectonics of the Central Andes and adjacent regions, as regards to its contribution to seismic hazard analyses.*

Key words*: Central Andes, Neotectonics, Seismic hazard*

INTRODUCTION

It is widely accepted that geologic analysis of recent deformation is a necessary input data in seismic hazard assessment, allowing the recognition of pre-historic earthquakes that have deformed the earth surface. This approach allows sometimes to avoid the underestimation of the seismogenic potential posed by neotectonic structures. Such information is very relevant particularly at intraplate regions, where the seismogenic capability of fault sources is not well illuminated by current crustal seismicity, mostly because the return period for damaging earthquakes is beyond the short time spam covered by the historical and instrumental seismicity.
There is a general agreement to consider that in the Andean and sorrounding areas, the Quaternary period provides a conservative time framework to include structures that have produced earthquakes in the past and have the capability for generating damaging earthquakes in the future, thus posing a threat in terms of seismic hazard. (Costa et al. 2006; Multi Andean Project, 2009). Therefore, structures with evidences of Quaternary deformation (here also named as neotectonic structures) are considered potentially hazardous as for seismic hazard purposes. Hundreds of these structures have been inventoried along the Central Andes in South America, particularly during the last two decades (Audemard et al., 2000, Costa et al., 2000, Paris et al., 2000; Egüez et al., 2003; Lavenu et al.2000; Macharé et al., 2003; Saadi et al., 2002; PMA, 2009; Veloza et al., 2012). However, only a few of these structures have been studied under neotectonic or paleoseismic methods. Data compilation used for developing cartography and inventories with the available knowledge of Quaternary deformation, have relied on the existing information derived in many cases from regional geologic studies and/or general terrain analysis. Accordingly, their characterization as seismogenic sources under a suitable format for seismic hazard models is commonly inadequate or imply considerable epistemic uncertainties. Key data as for the Seismic Hazard Models requirements, such as slip rate and the 3D geometry of outcropping structures, are not available for the majority of them.
A significant amount of the inventoried Quaternary deformation along the Central Andes and sorrounding regions lie within the plate interior, where slip rates are considered to be lower than those characterizing major structures at the Northern Andes. Only a few of these faults have experienced historic primary surface ruptures onshore. Also, because a few of these structures have not yet been studied under paleoseismological techniques (i.e detailed trench logs, key horizons dating, etc), parameters that best capture the source capability and hazard are poorly constrained or unknown for most structures (i.e., slip rate, recurrence interval, and age of last movement).
The few known historic coseismic primary surface ruptures onshore, limit the comparison of basic parameters (surface rupture length, coseismic displacement) at the different Andean crustal settings with world-wide historical relationship.
In some areas, like at the Pampean flat-slab, (27°-33°S) the South American plate foreland has been involved in the Andean building orogenesis. As a result, a series of faulted blocks known as the Sierras Pampeanas have evolved during the Neogene and characterized by bounding reverse faults with Quaternary activity, even at distances up to 600 km away of the trench.
The Sierras Pampeanas have traditionally been considered as an area with a capability for large earthquakes considerably lower than the Andean belt. However, many earthquake-related evidences have been found along several neotectonic structures in this region during the last years. They include primary surface coseismic ruptures, large rock-avalanches and paleoliquefaction features. These phenomena have no historical analogs in the region, but they testify for the occurrence of large crustal earthquakes since the late Pleistocene.
Historical seismicity suggests that threshold magnitude for crustal earthquakes to produce surface rupture at the Andean front and these foreland regions is considered to be Ms > 7.0 (Costa, 2005). However, when estimating

the Maximum Credible Earthquake (MCE) based on the most common empirical relationships used worldwide, such as rupture length, rupture area and coseismic slip, most results fall below such threshold magnitude.

The interpretations of this situation may range from: a. The basic data for estimating the MCE were wrong; b. New proxies for the Sierras Pampeanas region should be developed/adapted ; c. Both.

Although the "threshold earthquake" cannot be properly contrasted with historic data, it is considered that evidences of coseismic surface ruptures account for prehistoric crustal earthquakes with magnitudes larger than those recorded in the seismic catalog, so all these issues may lead to underestimates of seismic hazard in some regions.

In addition, fault hazard or seismogenic potential estimation solely based on proxies commonly used for plate boundary structures (such as age of last movement) may be inappropriate and even misleading for intraplate structures.

Consequently, many seismic hazard assessments usually do not consider neotectonic data, or do so partly. This situation often creates a gap in seismic hazard assessments, where geologic data are not well suited or not properly formatted for the SHA requirements and accordingly they are not suitably represented in the body of data.

For bridging this gap a close collaboration and teamwork development among earth scientists is fully necessary, where neotectonic practitioners could learn how to upgrade the existing data (even incorporating wide ranges of epistemic uncertainties) in order to make them to be considered as seismogenic sources. Training and experiences exchange among geologists is required in order to upgrade a classic map of neotectonic deformation into a 3D fault source.

Based on the current state of knowledge of Quaternary deformation in the Central Andes, this presentation aims to encourage discussions on the role of neotectonic data in seismic hazard assessment as well as on future research directions.

Acknowledgements: This is a contribution for TERPRO Focus Area Group on Quaternary Geology of South America, which has partly sponsored this presentation.

References

Audemard, F. Machette, M., Cox, J., Dart, R. and Haller, K. 2000. Map and Database of Quaternary Faults in Venezuela and its Offshore Regions. *U.S. Geological Survey Open-File Report 00-018,* 82 p.

Costa, C., 2005. The seismogenic potential for large earthquakes at the southernmost Pampean flat-slab (Argentina) from a geologic perspective. *Proceedings V International Symposium on Andean Geodynamics:* 211-214, Barcelona.

Costa, C., Machette, M., Dart, R., Bastías, H., Paredes, J., Perucca, L., Tello, G. and Haller, K. 2000a. Map and Database of Quaternary Faults and Folds in Argentina. *U. S. Geological Survey Open-File Report 00-0108*, 75 p.

Costa, C.H., Audemard, F.H.R., Becerra, M.F.A., Lavenu, A., Machette, M.N., París, G., 2006a. An overview of the main quaternary deformation of South America. *Revista de la Asociación Geológica Argentina* 61 (4), 461–479.

Egüez, A., Alvarado, A., Yepes, H. Machette, M., Costa, C. and Dart, R. 2003. Database and Map of Quaternary Faults and Folds in Ecuador and its Offshore Region. *U.S. Geological Survey Open-File Report 03-289*, 77 p.

Lavenu, A., Thiele, R., Machette, M., Dart, R., Bradley, L. and Haller, K. 2000. Maps and Database of Quaternary Faults in Bolivia and Chile, *U.S. Geological Survey Open-File Report 00-283*, 50 p.

Macharé, J., Fenton, C., Machette, M. Lavenu. A., Costa, C. and Dart, R. 2003. Database and Map of Quaternary Faults and Folds in Perú and its Offshore Region. *U.S. Geological Survey Open-File Report 03-451*, 55 p.

Paris, G., Machette, M., Dart, R., and Haller, K. 2000. Map and Database of Quaternary Faults and Folds in Colombia and its offshore Regions *U.S.Geological Survey Open-File Report 00-284,* 66 p.

Proyecto Multinacional Andino, 2009. Mapa de deformaciones cuaternarias de los países Andinos. *Publicación Geológica Multinacional N° 7. SERNAGEOMIN,* 311p. *Anexo en CD-ROM*, Santiago.

Saadi, A., Machette, M.N., Haller, K.M., Dart, R.L., Bradley, L.-A., de Souza, A.M. 2002. Map and Database of Quaternary Faults and Lineaments in Brazil: U.*S. Geological Survey Open-File Report 02-230*, 58 p.

Veloza, G., Styron, R., Taylor, M. and Mora, A., 20120. Open-source archive of active faults for northwest South America. *GSA Today 22, 10, doi: 10.1130/GSAT-G156A.1.*

GEOLOGICAL SURVEY OF COSEISMIC EFFECTS PRODUCED BY THE 2012 EMILIA EARTHQUAKE SEQUENCE (NORTHERN ITALY)

*EMERGEO Working Group**
Istituto Nazionale di Geofisica e Vulcanologia, Via di Vigna Murata, 605, Roma (francesca.cinti@ingv.it)

**Alessio Giuliana, Alfonsi Laura, Brunori Carlo Alberto, Burrato Pierfrancesco, Casula Giuseppe, Cinti Francesca Romana, Civico Riccardo, Colini Laura, Cucci Luigi, De Martini Paolo Marco, Falcucci Emanuela, Galadini Fabrizio, Gaudiosi Germana, Gori Stefano, Mariucci Maria Teresa, Montone Paola, Moro Marco, Nappi Rosa, Nardi Anna, Nave Rosa, Pantosti Daniela, Patera Antonio, Pesci Arianna, Pignone Maurizio, Pinzi Stefania, Pucci Stefano, Vannoli Paola, Venuti Alessandra,Villani Fabio*

Abstract (Post-seismic geological survey of coseismic effects produced by the 2012 Emilia earthquake sequence (Northern Italy)

In May-June 2012 a seismic sequence struck the Emilia-Romagna region in the southern Po Plain, resulting in 26 deaths and hundreds of injured, 15.000 homeless, severe damage of historical centers and industrial areas, and an economic toll of ~2 billions of euros. The sequence includes two mainshocks, the Mw 5.9 on May 20 and the Mw 5.8 on May 29, occurring on north-verging thrusts. Emergeo promptly surveyed the coseismic geological effects produced by the Emilia sequence that were mainly ground failures caused by intense liquefaction phenomena and cracking. The main approaches used for the reconnaissance are: (i) ground- and aerial- based survey; (ii) reports from local people and through Internet-based data sourcing at the INGV portal. The collected data are then discussed in the light of the i) local geological and geomorphic setting; ii) coseismic displacement defined by InSar interferograms; iii) liquefaction related hazard.

***Key words**: post-earthquake survey, coseismic geological effect, liquefaction, ground failure, 2012 Emilia earthquake, Po Plain*

INTRODUCTION

In May-June 2012 a seismic sequence struck a broad area of the Emilia-Romagna region, in the southern part of the Po plain (Fig.1). The seismic crisis caused 26 deaths and hundreds of injured, 15.000 homeless, severe damage of historical centers and industrial areas, and an estimated economic toll of ~2 billions of euros. The sequence includes two mainshocks. The first on May 20 with a Ml 5.9 and the second, ~12 km southwest, on May 29 with a Ml 5.8 (Fig.1). The whole aftershocks area extends in an E-W direction for more than 50 km, includes five Ml>5.0 events, (Fig. 1), and shows the activation of a seismogenic layer confined to the upper 12 km of crust. The focal mechanisms of the main events (Fig. 1) consistently show a compressional kinematics with E-W oriented reverse nodal planes (TDMT database, *http://cnt.rm.ingv.it/tdmt.html*). These mechanisms are consistent with a horizontal, N-S oriented compression (P-axes) defined by present-day stress indicators in the region (Montone et al., 2012). Although with some differences, seismic, InSar, GPS, and macroseismic data from the May-June 2012 sequence consistently suggest that two south dipping thrusts of the Ferrara arc activated during the 2012.

The seismicity of the past 20 yr (ISIDe database, http://iside.rm.ingv.it/; CSI 1.1, 2006) shows a low seismicity area in coincidence of the area hit by the 2012 sequence and the same appears also for the location of the main historical events (CPTI11 available at http://emidius.mi.ingv.it/CPTI).

This sequence occurred in an area where the official hazard map of Italy assigned a low level of seismic hazard with respect of the whole Peninsula (GdL MPS, 2004).

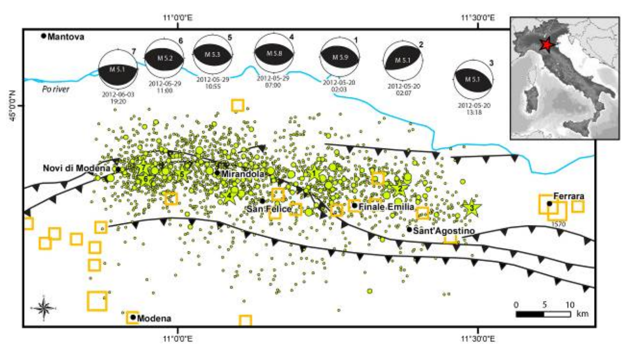

Fig. 1: The Emilia 2012 sequence (ISIDe database, http://iside.rm.ingv.it/): stars stand for Ml≥5.0 earthquakes and numbers refer to focal mechanisms (TDMT database, http://cnt.rm.ingv.it/tdmt.html); circles are scaled by magnitude (Ml=4.1÷4.9, Ml=3.1÷4.0, Ml≤3.0). Main active compressional structures in the area (Boccaletti and Martelli, 2004), as well as historical earthquakes (yellow square) are shown.

Widespread coseismic geological effects were produced by the 2012 Emilia sequence and the most diffuse coseismic feature observed during the survey was related to liquefaction process (Fig. 2). INGV-Emergeo working group promptly surveyed the area to collect the coseismic geological evidences, by coordinating and integrating information to assure the maximum coverage of the affected area. Here, we present the data collected by the through the following approaches: (i) direct field survey; (ii) helicopter and powered hang-glider trike survey; (iii) reports from local people collected locally in the field or through a web based survey opened at the INGV portal named “hai visto effetti geologici del terremoto?” (did you see earthquake geological effects?) at *www.haisentitoilterremoto.it/emergeo.html*. Using a terrestrial Laser scanner, we also initiated a monitoring of the evolution of fractures and associated subsidence induced by the earthquakes within one of the most damaged village (San Carlo).

During the seismic crisis, the Emergeo working group dedicated particular efforts in developing methods for collecting information through the direct contribute of the population hit by the shaking. A self-consistent system for data gathering, processing and delivery was set up, producing the transformation of unprocessed data into information ready to use for the emergency management (Emergeo Informatics System-siE).

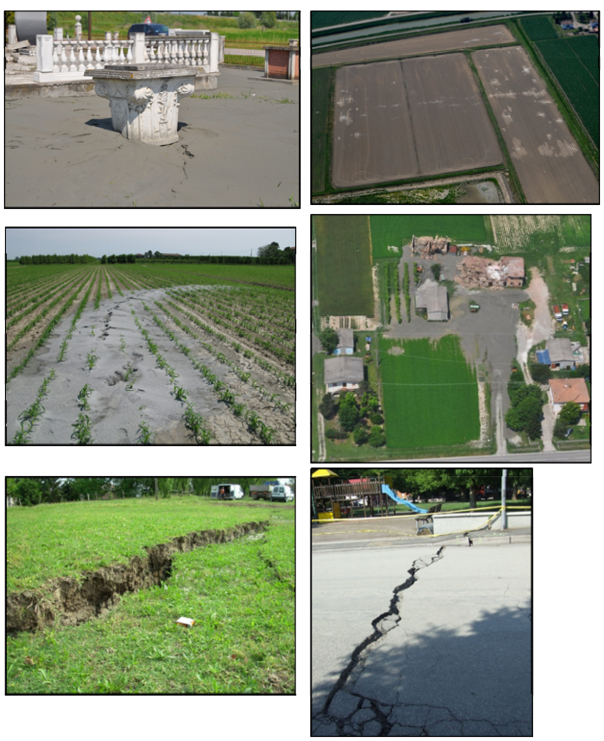

Fig. 2: Photos of the liquefaction phenomena and fractures with and without fine sediment extrusion formed on natural and artificial ground surface. Photo by Emergeo working group

DISCUSSION

Experimental tools employed for data gathering, processing, and delivery accompanied the ground and aerial survey (Fig. 3): - setting up of a WEBGIS (available at www.esriitalia.it/emergeo/); - use of social network for info delivery (es. www.flickr.com/photos/emergeo_ingv/); - Internet and direct alerts data sourcing.

It is worth to note that the involvement of the population via web, although experimental, furnished encouraging results but at the same time revealed a still low level of confidence associated to the earthquake phenomenon.

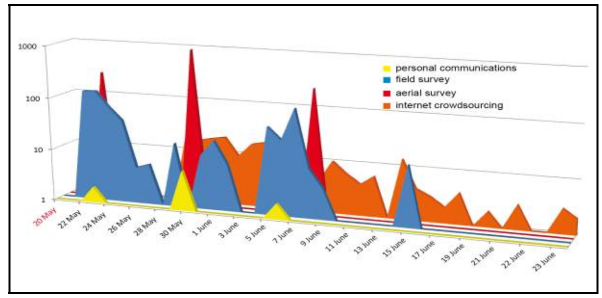

Fig. 3: Graphical illustration of the observation flow vs time for the different investigating tools.

A total net number of 1362 geologic coseismic effects at the surface have been recognized and grouped into three main categories; i) liquefaction; ii) fracture/liquefaction; iii) fracture. Moreover, localized bulges and subsidence related to the extrusion of sediments (categories i) and ii)) were surveyed (Fig. 2).

Under the liquefaction category we classified single spot such as a single sand volcano, several scattered vents and coalescent flat cones, sand infilled water well, fountain and manhole (with and without sand extrusion). Differently the fracture/liquefaction category comprises mainly elongated and aligned multiple sand volcanoes, and sand flows out from coseismic open fracture, occurred both on natural and artificial ground surface. Finally, the fracture category includes newly formed open fracture and crack without liquefaction and evident sand outlet. In particular the measurements were: 1) heights of the sand volcano buildings and area of sand draping for an estimation of the ejected sand volumes; 2) morphologies and diameter of the sand outlets; 3) spacing of the sand outlets and length and strike of their alignments; 4) spacing, length and strike of the fractures; 5) style of the fractures pattern; 6) opening and offset of the fractures; 7) average strike of the fractures pattern or sand outlet alignments. The aerial-based observation were validated by field survey and integrated in the whole dataset. Considering the land use, typology and status of the cultivations covering the flat land, it is possible that part of the phenomena have been missed expecially in coincidence of wheat fields. All the collected observations were stored, manipulated, analysed and managed in a Geographical Information System.

For the majority of the liquefactions and fractures, their alignment and orientation is related to the network of braided paleo-drainages and abandoned meanders and are particularly concentrated at the borders of the epicentres cloud. However, several features were also found within the Po River flood plain in places where no river embankments are present.

Most of the data collected at surface are enclosed within the area of the aftershock epicentres, as well as in the area of significant deformation measured by the InSar data. In particular, the observed ground features are mainly clustered at the borders of the InSar based-deformed area, while very few effects occurred in the area of maximum uplift.

All these considerations converge to suggest that the long-term activity of the Emilia 2012 source would have influenced the drainage pattern with time, and consequently the features observed in 2012 may recur at specific places. Finally, the scenario of liquefaction phenomena induced by the 2012 sequence details a narrow zone of high degree of hazard occurring within the aftershocks area. Then, the Emilia case provides a new perspective on the actual risk on which we have to work.

Acknowledgements:
Special thanks to the local people for their collaboration and direct contribute to the survey of the coseismic geological effects.

References

Boccaletti M., Martelli L. (Coords) 2004. Carta sismo-tettonica della Regione Emilia-Romagna scala 1:250.000 e note illustrative. Selca, Firenze.

CSI Catalogo della sismicità italiana 1981-2002, versione 1.1. INGV-CNT, Roma http://csi.rm.ingv.it/

DISS Working Group (2010). Database of Individual Seismogenic Sources (DISS), Version 3.1.1: A compilation of potential sources for earthquakes larger than M 5.5 in Italy and surrounding areas. http://diss.rm.ingv.it/diss/.

Emergeo Working Group: Preliminary Report on the coseismic geological effects (26.05.2012). available at http://emergeo.ingv.it/it/

GdL MPS, 2004 rif. Ordinanza PCM del 28 Aprile 2005, n. 3519, All. 1b).

Montone P., Mariucci M.T. and Pierdominici S., 2012. The Italian present-day stress map, Geophys. Journ. Int., 189, 2, 705–716, May 2012, doi: 10.1111/j.1365-246X.2012.05391.x.

A. Rovida A., Camassi R., Gasperini P. ,and M. Stucchi (eds.), 2011. CPTI11, the 2011 version of the Parametric Catalogue of Italian Earthquakes. Milano, Bologna, http://emidius.mi.ingv.it/CPTI

APLICACIONES DEL ANÁLISIS DE ANILLOS DE CRECIMIENTO DE LOS ÁRBOLES EN EVENTOS GEOLÓGICOS-AMBIENTALES EN MICHOACAN: DENDROCRONOLOGÍA Y DENDROGEOMORFOLOGÍA

Garduño-Mendoza Erika (1), Garduño-Monroy Víctor H. (1)

(1) Departamento de Geología y Mineralogía, Instituto de Investigaciones Metalúrgicas, UMSNH, egm.ama@gmail.com
Universidad Michoacana de San Nicolás de Hidalgo
(+52) (443) 3 22 35 00, Avenida Francisco J. Mujica S/N Ciudad Universitaria,
C.P. 58030, Morelia, Michoacán, México

Abstract: *Las técnicas dendrogeomorfológicas y dendrocronológicas, ofrecen una alternativa para describir los procesos geodinámicas, incluyendo las condiciones climáticas que influyen en el crecimiento y expresión de los anillos de crecimiento de los arboles. Los anillos de crecimiento de las coníferas principalmente, expresan los eventos atípicos que ocurren en las áreas donde crecen los arboles, influyendo en la anatomía del árbol. Posteriormente para su análisis se realiza un conteo de estos anillos y se define en que año ocurrió dicho fenómeno, como sequia, inundación, incendio, heladas prolongadas, plagas, deslizamientos, actividad volcánica y sismos. Todos estos eventos se registran en el crecimiento y deformación de los anillos de los arboles. Por lo cual se presenta una alternativa de investigación en estas ciencias ya antiguas pero poco exploradas, que contribuirán al entendimiento, descripción y datación de los fenómenos geológicos-ambientales.*

Key words*: Dendrogeomorphology, Dendrochronology, Tree rings, events geodynamics*

INTRODUCCION

El estudio de los anillos de crecimiento de los árboles, tiene sus inicios desde la antigüedad; Teofrasto en Grecia (322 A.C.), fue uno de los primeros naturalistas en observar las deformaciones y crecimiento anormal de los arboles. Ya para el año 1500 D.C., Leonardo Da Vinci en Italia, observo que los anillos de los árboles talados, mostraban el número de años de crecimeinto y de acuerdo a su espesor, los años que eran más o menos seco. Por lo tanto, concluyo que los arboles del norte de Italia eran mas gruesos debido a las lluvias que los del sur de Italia.

Ya para inicios del siglo XIX, aparece en escena Andrew E. Douglass (1867-1962), quien es considerado como el padre de la Dendrocronología. Douglass era alumno del famoso astrónomo Percival Lowell quien, en 1894, envió Douglass a Arizona EUA, para que iniciara la construcción del Observatorio. Durante la construcción del observatorio, se requirió de madera para este objeto, y es ahí donde Douglass noto las semejanzas de los anillo de los arboles, observando los patrones de crecimiento en los tocones de los arboles. Siendo así pionero en la ciencia de la Dendrocronología; uno de los principios mas importantes aportados por Douglass es el *crossdating,* donde se aplica a una variedad de disciplinas de la climatología, astronomía y arqueología, entre otras.

La dendrocronología es una ciencia que estudia el crecimiento anual de los anillos de los arboles, es una herramienta para detectarlos cambios climáticos del pasado; útil para sitios lejanos donde no se cuenta con estaciones climáticas.

Por otro lado la dendrogeomorfología, es una ciencia que estudia las respuestas del crecimiento anormal en respuesta a los procesos geodinámicos que se dan en la superficie terrestre, tales como deslizamientos, erupciones volcánicas, sismos, inundaciones etc.

Y al utilizar estas dos disciplinas se pueden realizar correlaciones para describir eventos y determinar en que año y época del año ocurrió un evento (madera temprana y madera tardía).

En este sentido podemos definir un anillo de crecimiento como la sobre posición sucesiva de las capas de tejido leñosos en el tronco del árbol, en razón del crecimiento periódico del cambium (un año). Por lo cual realizando el conteo de los anillos, podemos correlacionar las fechas de ocurrencia de los eventos registrados (sequias, incendios, actividad volcánica, inundaciones etc.)

Figura 1.- Anillos de crecimiento de pinus sp donde se observan los anillos definidos y las deformaciones por deslizamientos.

Figura 3.- Sección de un árbol en la que se han marcado las cicatrices dejadas por los incendios con la fecha en que ocurrieron.

Fuente: [http://www.rmtrr.org/gallery.html.](http://www.rmtrr.org/gallery.html)

Figure 2. - Cross section of a pine tree marked for counting rings. We observe some sliding

de las coníferas.

Dentro del estudio de los anillos de crecimiento, existen diferentes divisiones, una ellas es la Dendrosismología, donde los efectos de sismos y terremotos que registran los árboles, se evidencian por los daños físicos que producen tales eventos. En los anillos de crecimiento se presentan anillos ausentes, rupturas en la superficie o fraccionamientos. Las dislocaciones que sufren las capas producen daños en la estructura del árbol, como resquebrajamiento de las raíces, regiones de tensión, inclinación del árbol, etc. (EPSOL, 2011).

METODOLOGÍA

Existen dos tipos de muestras que pueden ser utilizadas para llevar a cabo el análisis en dendrocronología. El primero es en muestras de virutas, tomadas con un taladro Pressler; se utiliza principalmente para árboles vivos. Y secciones transversales para arboles ya talados (tocones) o maderas derribadas. Después de la toma de las muestras, estas se dejan secar, evitando la formación de hongos en la madera.

Figura 4.- Muestra de viruta tomada con taladro Pressler, paraanálisis dendrocronológico, Durango.Fuente: Garduño-Mendoza, 2011

Figura 5.- Muestra en sección transversal de Pino, Angangueo Michoacán. Fuente: Garduño-Mendoza, 2012

Posteriormente las virutas se pegan en molduras de madera y se procede al lijado. En secciones transversales solo de dejan secar. Uno de los elementos principales para la observación de las anormalidades o excentricidades de los anillos de crecimiento, es el lijado de las muestras. Se realiza comenzando con lijas de grano mayor a grano mas fino, con el objeto de dejar bien expuestos los anillos y las cicatrices que buscamos.

Figura 6.- Sección transversal de Oyamel, después del lijado para una observación optima de las muestras. Se observa la madera temprana (clara) y la madera tardía (obscura).

RESULTADOS

La metodología para los análisis dendrocronológico y morfológicos están bien estudiada y definida. Existen menos de 15 trabajos de investigación publicados para el estado de Michoacán. La superficie total del estado de Michoacán es de 5, 980,400 ha de las cuales 4, 206,451 ha son zonas forestales (Navia Antezana, 2003). Podemos encontrar arboles de mas de 1000 años como son los Ahuehuetes en el Lago de Camecuaro o Pinos de mas de 180 años en la región oriente de Michoacán. Por lo cual se plantea realizar estudios dendrocronológicos, dendroclimáticas y densdrosismológicos para todo el estado, ya que por el tipo de vegetación y los eventos que se han registrado en el estado es una oportunidad de describir y datar eventos geodinámicas. Mediante estas técnicas dendrocronológicas, se pretende encontrar los registros de los eventos sísmicos de gran magnitud (mayores de 7.0 Escala de Richter) que se han registrados en Michoacán, como los del año 1899 (Oaxaca y Guerrero), 1911 (Costa de Michoacán), 1912 (Acambay), 1985 (Michoacán y Guerrero), 1995 (Jalisco), 2000 (Costa de Guerrero y Michoacán) y 2012 (Michoacán).

CONCLUSIONES

El área de la dendrocronología y dendrogeomorfología, son campos de estudio muy antiguos, que no han sido explorados y explotados al máximo para la obtención de información en Michoacán. Por lo cual se recomienda promover la investigación en estas áreas de conocimiento, recordemos que el índice de tala clandestina en Michoacán es elevado. Existe un registro de pérdida de bosques michoacanos, del año 1976 al 2000 de más de 20 mil hectáreas de bosque y 30 mil hectáreas de selva que fueron desmontadas, lo cual representa tasas de deforestación de 0.47 y 0.65 por año, respectivamente. Por lo cual se recomienda tomar muestras de arboles, antes de que sean derribados estos arboles que brindan información de procesos geodinámicas.

REFERENCES

C. Mendoza Adame. Michoacán, en la zona crítica de tala clandestina en México. La Jornada Michoacán. Viernes 10 de Junio de 2011

EPSOL. Dendrocronología. 2011. www.dspace.espol.edu.ec/.../2/CAPITULO%201%20FINAL.doc

J. A. Ballesteros, A. Díez-Herrero, J. M. Bodoque, M. Stoffel, M. Bollschweiler, O. Hitz.Caracterización de la señal anatómica en la madera de árboles afectados por avenidas torrenciales. Trabajos de Geomorfología en España, 2006 – 2008. X Reunión Nacional de Geomorfología, Cádiz 2008

J. Moya and J. Corominas.2007. Are broad-leaved species useful for dating of events causing tree tilting? A critical analysis from the case of the October 1907 Brallans landslide (Central Pyrenees, Spain).Geophysical Research Abstracts, Vol. 9, 04457, 2007 SRef-ID: 1607-7962/gra/EGU2007-A-04457

J. Navia Antezana, Manejo Forestal en Michoacán. GIRA AC. www.gira.org.mx

J. Villanueva Díaz, J. Cerano Paredes, V. Constante García, L. Motes González, L. Vázquez Selem; Muestreo Dendrocronológico: Colecta, Preparación y Procesamiento de núcleos de crecimiento y secciones transversalesCENID-RASPA; INIFAP, Durango, México 2009

Paul R. Sherppard, Michael H. Ort, Kirk C. Anderson, Mark D. Elson, Lorenzo Vazquez Selem, Angelika W. Clemens, Nicole C. Little, Robert J. Speakman. Multiple Dendrochonological signals indicate the eruption of Paricutin Volcano, Michoacan, Mexico. Research Vol. 64(2), 2008, pp. 97–108

Roig-Fidel A.2000.Dendrocronología en América Latina; Universidad Nacional del Cuyo; Editorial de la Universidad de Cuyo, Argentina. 9-109 pp

V. Constante García, J. Villanueva Díaz, J. Cerano Paredes, J. Estrada Ávalos Parámetros para definir el potencial dendrocronológico. CENID-RASPA; INIFAP, Durango, México 2010.

ACKNOWLEDGEMENTS

Laboratory of Wood Technology, UMSNH, for space for sample processing

PALEOSEISMOLOGY & ARCHAEOSEISMOLOGY
MORELIA • MEXICO 2012
INQUA-TERPRO PALEOSEISMOLOGY
EARTHQUAKE ARCHAEOLOGY

PROGRESS IN SEISMIC AND ARCHEOSEISMIC STUDIES IN THE ZONE OF MITLA, OAXACA

Garduño-Monroy V.H[1]., Macías J.L[2]., Arturo Oliveros M[3]. and Hernández Madrigal V.M[1].

1. UMSNH-IIM Departamento de Geología y Mineralogía, vhgardunom@gmail.com
2. Instituto de Geofísica de la UNAM-Unidad Morelia
3. INAH-Morelia

Abstract (Progress in seismic and archeoseismic studies in the zone of Mitla, Oaxaca, Mexico*)* *This work depicts the results of preliminary studies which are being carried out in the archeological zone of Oaxaca. The seismic activity affecting the state of Oaxaca has allowed prehispanic cultures to acquire a deep knowledge of its consequences. This notwithstanding, current archeological interpretations could be obscuring historical disasters which have been generated by huge seismic events. One of those may be related with the collapse that may have affected the archeological zone of Mitla.*

Keywords: Mitla, historic seism, collapse

Introduction

Despite the richness of archeological centers, few archeoseismic studies have been carried out in Mexico. Garcia-Acosta and Suarez-Reinoso (1996) made the first contribution by highlighting the evidences of seism descriptions in prehispanic periods. All Mesoamerican cultures show a respectful behavior towards these activities of the Earth, which, together with the volcanoes, generated a whole set of "cohabitation" rituals.
Oaxaca is a major seismic activity zone in Mexico and possibly in the world. The seismic activity of the area is due to the Cocos plate subduction underneath Mexico or the North American plate, and to activities taking place inside the plate or intraplate (Fig. 1). According to instrumental statistic data, Oaxaca has more than 300 earthquakes per year, with magnitudes between 3 and 4 (Sociedad de Ingenieria Sismica) (Fig. 1). Three earthquakes with intensities above 7 have taken place since 1998. As reported by the Sociedad de Ingenieria Sismica, a number of earthquakes with magnitudes between 7 and 8 have taken place in the last 320 years. 11 considerable earthquakes have taken place in the same time span (Table 1).

Place	Date	Magnitude
Oaxaca	23 August 1696	7.5
Oaxaca	21 December 1701	
Oaxaca	9 March 1845	8.0
Oaxaca	5 May 1854	8.0
Oaxaca-Chiapas	14 January 1903	8.2
PuertoEscondido (Oaxaca)	9 October 1928	7.6
Oaxaca	23 Augustus 1965	7.5
Oaxaca	29 November 1978	7,6
Huajapan de León	24 October 1980	7.0
Puerto Ángel	30 September 1999	
Pinotepa	20 March 2012	7.4

Table 1. Main Oaxaca earthquakes, as reported by the Sociedad de Ingenieria Sismica

One of the valleys in the hearth of Oaxaca harbored various Prehispanic ceremonial centers, headed by Monte Alban. This zone was the antic Zapotec capital and at its heyday one of Mesoamerica's most populated cities. It was established around 500 BC and flourished until 750 AD. South of Monte Alban, in the valley of Tlacolula lies another important archeological zone: Mitla, from *Mictlan,* or "place of the dead" in Nàhuatl, Lyobaa or "place to rest" in Zapotec, Ñuu Ndiyi or "place of the dead" in Mixtec. Mitla presents evidences of human settlements since the beginning of our era (0-200 AD). The decline of Monte Alban as a power centre turned Mitla into an important settlement, functioning as another point of domination facing the Zapotecs of the valley. It heyday took place between 950 and 1521 AD.
This work exposes evidence of seismic events that could be linked to the Oaxaca fault activity, which in its turn shaped the tectonic frontiers of the area. In the same vein, these seismic movements also influenced the architectural design of pre-Columbian and colonial cultures of southern Mexico.

The seismic activity of Oaxaca stems from two origins: the first and most important is linked to the subduction of the Cocos plate. The second could be related to intraplate faulting. Both are associated with the limits of the terrain and with the main valleys (Tehuacan and Valles Centrales). In a regional framework, the central valleys of Oaxaca are part of the Oaxaca fault system. The latter forms the tectonic limit between Oaxaca and Cuicateco. Beside its normal component, it has been considered to also present a horizontal component, the sense of which remains debatable (Biblio) (Fig.2).

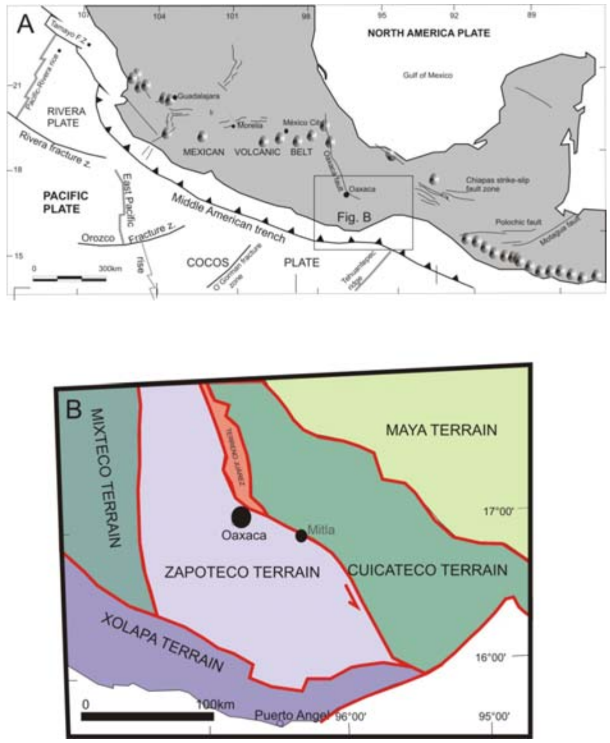

Fig. 1. Mexican Tectonic frame, showing the main elements: (A) the tectonic terrains of southern Mexico and their limits. This scheme highlights the position of Mitla in the southern prolongation of the Oaxaca fault system, with left-lateral component (B).

Regional Geology

From a more local morphological and geological point of view, three main divisions are recognizable: a) to the north, a huge NO-SE oriented sierra, with up to 2300m high tops and parallel and dendritic drainage. This sierra is formed by huge rhyolitic ignimbrite packs, which present layers of different density and color, mainly pink and white, presenting at some points a 500m thickness. The ignimbrites stem from the Miocene, as they have been dated between 14.4+- 0.4 and 15.48+- 0.2 (Ferrusquia-Villafranca (1990), Irondo *et al.* (2004)) respectively. b). Hills formed by slope deposits and huge avalanche deposits run parallel to the sierra. c). The valley presents fluvial and lacustrian deposits from the Pleistocene (Ferrusquia-Villafranca, 1990) (Fig. 2).

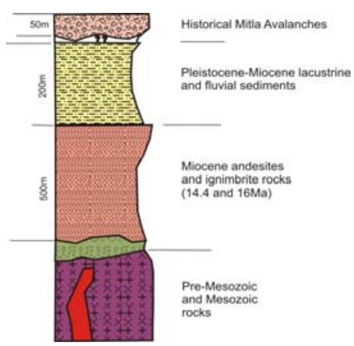

Fig. 2. Scheme of stratigraphic column of the Sierra de Mitla region. (Modification Martinez-Serrano *et al.* 2008 supported by Ferrusquia Villafranca *et al.* (1974)

The main structures to be recognized in the northern Mitla sierra have NO-SE orientation and normal left-lateral movement (Fig3a). The normal component is verified by the level differences between the valleys and the sierras; the left lateral component can be verified in the Mitla sierra by the observance of NE-SW creek courses, displaced with left lateral component by NW-SE oriented structures (Fig. 3A).

The heights of the NO-SE Mitla sierra present huge scars of crowns, the deposits of which have accumulated towards the current settlement of Mitla (Fig 4B and C). These deposits form a tongue, the base of which is composed of highly fractured and fault plane broken ignimbrite rock fragments, denoting erratic blocks with SE movement and puzzle structures (Fig3C).

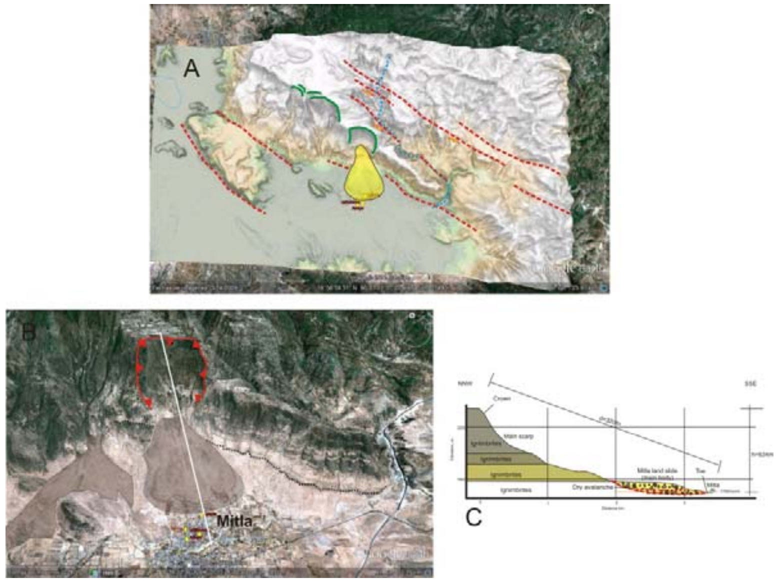

Fig.3. The Mitla Avalanche. A. Main NO-SE structures with recent left displacement movement. B. The Mitla avalanche and its spatial distribution. C. Mitla avalanche section

Within the deposits of the Mitla avalanche lie three unities: the base, formed by avalanche deposits of huge erratic blocks of several meter-diameters and a matrix of the same ignimbrite with monolithic aspect. Its thickness reaches 30m (Fig. 5). Above this avalanche body lies a huge amount of isolated blocks that could be related to the same avalanche. The assumption is that the avalanche had major density, making the huge ignimbrite blocks float during their natural transportation (Fig. 5a). The area of the avalanche would be of 18,583 m3 with a volume of 0.53 Km3. Above these lie cohesive flows with a strong clayey matrix and ignimbrite blocks. Its coefficient of friction (L/H) is 0.53, which corresponds to a dry avalanche.

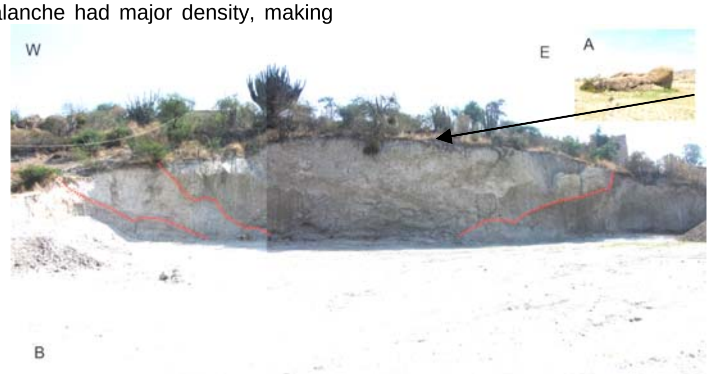

Fig. 5 Picture of the avalanche deposits with erratic ignimbrite blocks and huge NE-running fault discontinuities (B). Huge ignimbrite blocks lie upon the avalanche deposit.

Considering the volume of these elements, their relation with active faults, and using Keefer's relation (1994) we may be able to assume that these avalanches are related with an earthquake whose magnitude could be situated between 7 and 8. The age of this event is still unknown, but it is a fact that the deposits modified the topography of the N-S secondary Mitla valley, which maintained a level of 1700masl.

Archeoseismology

Combining the evidence of this huge seism with the current seismic registers that correspond to the tectonic frame of Oaxaca, we could consider that all prehispanic centers of the central valleys of Oaxaca were touched by this tectonic activity. Therefore, their buildings were designed accounting for the vertical movements (pyramids) and horizontal movements (interlocking). The latter are present in numerous archeological sites of Mitla (Fig 6). In the "Salon de las columnas" there is a beam with interlocking, the collapse of which could be related to a seism. In Zapotec culture, the word Xoò means seism. The codex Talleriano-Remensis relates 13 earthquakes, among which the seism of 1507, described as an extraordinary event in which 1300 warriors died. This type of catastrophe could only happen during an uncommonly heavy rain or a seism-avalanche. Therefore, the significance of "place of the dead" could also be linked to an avalanche, which destroyed part of the prehispanic population of Mitla.

Conclusions

These data on the seismicity of Oaxaca, the characterization of the Oaxaca fault system in Mitla, the avalanches generated by earthquakes and the designs on the codex, should motivate more detailed archeoseismologic studies in the Mitla zone. The word Xoò, which means seism in Mixtec, gathered with the other meanings of Mitla such as "place of the dead" may correspond to the disaster of the avalanche which modified the lacustrian and fluvial plane of Mitla, where another part of the scarcely known Mixtec culture developed.

Bibliografia

Ferrusquía-Villafranca, I., Wilson, J.A., Denison, R.E., McDowell, F.W., Solorio-Munguía, J., 1974, Tres edades radiométricas oligocénicas y miocénicas de rocas volcánicas de las regiones de la Mixteca Alta y Valle de Oaxaca, Estado de Oaxaca: Boletín de la Asociación Mexicana de Geólogos Petroleros, 26, 249-262.

Ferrusquía-Villafranca, I., 1990, Contribución a la diferenciación del Terciario continental de México, Parte 3, Geología Cenozoica del área Suchilquitongo, Estado de Oaxaca, México: Universidad Nacional Autónoma de México, Instituto de Geología, Unpublished report, 91-135.

Keefer D., 1994. The importance of earthquake-induced landslide to longterm slop erosion:Geomorphology, vol. 10, p.265-284.

Martínez-Serrano, R.G., Solís-Pichardo, G Flores-Márquez E.L.,, Macías-Romo, C. and Delgado-Durán, J., 2008. Geochemical and Sr-Nd isotopic characterization of the Miocene volcanic events in the Sierra Madre del Sur, central and southeastern Oaxaca, Mexico. Revista Mexicana de Ciencias Geológicas, v. 25, núm. 1, p. 1-20

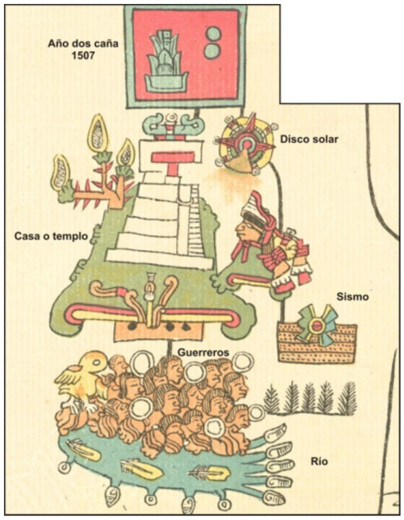

Fig. 6. Part of the Codex Talleriano-Remensis, relating a huge seismic event associated to the tragedy of the death of 1300 warriors in 1507 in the Mixtec region.

EVIDENCE OF PAST SEISMS IN CUSCO (PERU) AND TZINTZUNTZAN (MEXICO): CULTURAL RELATIONS

Víctor Hugo Garduño-Monroy1, Carlos Benavente Escóbar2, Arturo Oliveros3, , Miguel Ángel Rodríguez Pascua4, Raúl Pérez López4 , Jorge Luis Giner5

1. UMSNH-IIM Departamento de Geología y Mineralogía
2. INGEMMET, Instituto Geológico Minero y Metalúrgico
3. INAH-Morelia
4. Departamento de Investigación y Prospectiva Geocientífica, Instituto Geológico y Minero de España. C/ Ríos Rosas, 23.28003-Madrid. SPAIN.
5. Dpto. Geología. Facultad de Ciencias. Universidad Autónoma de Madrid. Cantoblanco. Tres Cantos. Madrid. SPAIN.

*Abstract :(**Evidence of ancient seisms in Cusco, Peru and Tzintzuntzan, Mexico and their cultural relations**) At first sight the ancient pre-Columbian cultures seem to have had no awareness of seisms. Purhepecha and Andean cultures nevertheless not only show awareness of these, but also similitude between their anti seismic building techniques. This work exposes clear evidence of coseismic ruptures found In Cusco and in Tzintzuntzan-Patzcuaro. More profound research could nevertheless be helpful to reveal sceneries which are for their most part unknown to current generations.*

Keywords: Archeoseismology, clamp structures, coseismic ruptures

Introduction

Anthropological studies of American cultures frequently reveal narrow cultural relations in the fields of language, art, building techniques, etc. (Ruiz 1978). The Mexican Purhepecha culture and the Incas of Peru are a clear example of these relationships. Despite the 5000km distance, authors have noticed striking similarities between these peoples (Fig. 1).

This work explains the prehispanic background that yields evidence of the similar tectonic scenery in which Inca and Purhepecha cultures found themselves. Both settled in a Pacific plate segment with strong seismic and volcanic activity. This situation certainly induced these cultures to find similar paraseismic techniques.

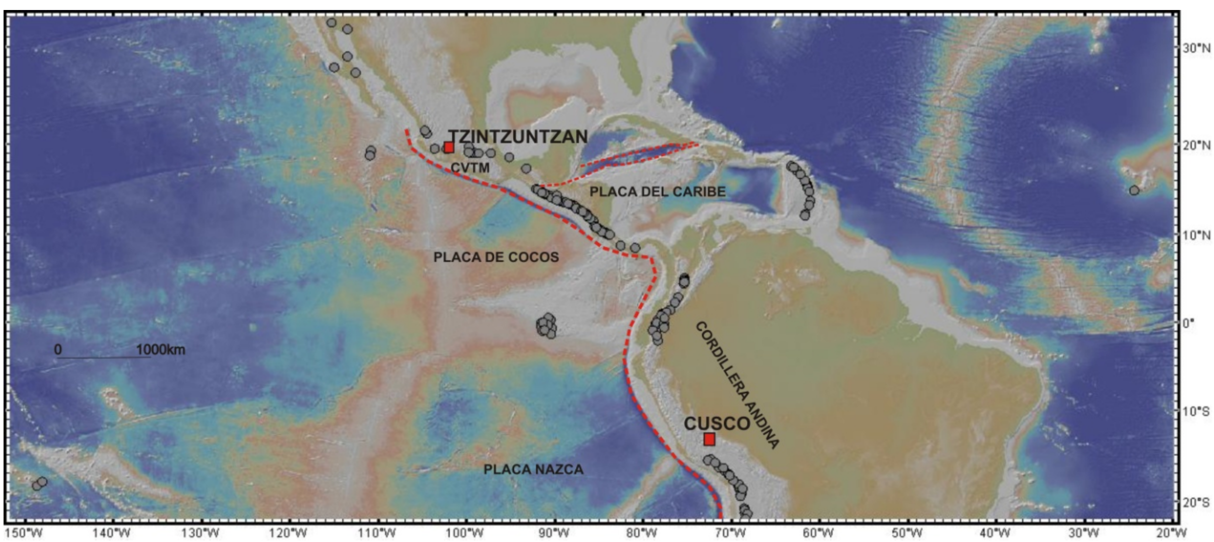

Fig. 1. Location of the Cuzco and Tzintzuntzan sites in a tectonic scheme. The grey circles represent volcanoes. The dotted red line stands for the limits of the plates.

The Inca culture

The Inca Empire extended through the eastern zone of the subcontinent (the Andean region) between the 15th and the 16th centuries. This was the period during which the Inca civilization reached its organization and territorial expansion climax. Their territory was known as Tahuantinsuyo, and its capital was Cusco. The empire covered nearly 2 million square km between the Pacific Ocean and the Amazon rainforest, and between San Juan de Pasto (Colombia) north and the river Maule (Chile) at the south.

The Inca civilization reached its cultural, technological and scientific development throughout a major part of the Andean region, which is characterized by abrupt altitude changes: in less than 100km, the Andes rise from sea level 4,600m asl. The reason for this sudden change is that the western edge of the continent is controlled by the subduction of the Nazca plate, underneath the South-American plate. Peru is therefore the scenery of much seismic activity.

The Purhepecha culture

This culture almost exclusively developed in the current state of Michoacán, between the river Lerma (north) and the river Balsas (south). Loma Alta is one of the most ancient stages of Purhepecha culture. This stage took place in Jaracuaro during the Classical period (500AD), but had its heyday during the Postclassical period (from 900 to 1500AD). Major development was to be found at the oriental shore of the lake of Patzcuaro with the development of the Purhepecha reign. The Purhepechas never submitted to the Mexicas and managed to control zones that reached Jalisco and Colima. They had, and still have, a language which is not related to the languages of central Mexico. Moreover, they developed a particular architectural style consisting of mixed plant pyramids: rectangular and semicircular, called Yacatas. At least two great constructive periods remain of their capital center.

Historical seisms among the Incas

There is evidence that the Incas were many times laid down by earthquakes. This is the reason why they worked with such care and consistency to find and improve building techniques, until reaching their trapezoidal architecture with an antiseismic building system. This architectural technique has allowed the Inca buildings to stand through heavy seismic activity. According to historical data, the reactivation of different faults resulted in earthquakes in 1581, 1590, 1650, 1707, 1744, 1746, 1905, 1928, 1941, 1943, 1950, 1965, 1980 and 1986. The chronicles assert that many of these events heavily damaged and sometimes destroyed the city of Cuzco.

In order to broaden the seismic record of this region, we carried out neotectonics and paleoseimologic studies, because the historical and instrumental sources appeared insufficient to the achievement of research on the seismic dangers presented by the active faults of the Cusco region. Moreover, the main seisms could have been separated by major time lapses than those known by instrumental and historical records.

Seisms among the Purhepechas

The region in which the Purepecha Reign developed is situated in the active fault corridor that streches in E-W direction, called Morelia-Acambay in its oriental part. Geological studies reveal that huge earthquakes took place during the Pleistocene (2 seisms), one during the Recent Holocene, with possible M=6 magnitudes, as indicated by cosesimic ruptures.

Two other important seisms had affected the Patzcuaro area by the middle of the 17th century. Their origin remains uncertain. The 1858 earthquake is associated with intraplate subduction, but the isoseismal lines suggest a relation with the E-W faults of the Morelia-Acambay fault system. Superficial seisms have also occurred on these segments between 1912 and 1979.

Active faults in Cusco

The first results reveal two active fault systems: the Cusco fault system and the Vilcanota fault system. Both are formed by normal faults with evident quaternary and historical activity, similar to the Tambomachay faults (linked to the 1950 earthquake) and the Qoricocha fault (linked to the 1986 earthquake). These systems stretch along almost 100km (Figs. 2 and 3).

Fine stratigraphic studies were also carried out upon quaternary lacustrian deposits, in order to identify deformed sedimentary structures associated to seismic events: “seismites”. The result revealed a total of 37 seismic events. According to their appearance, these were provoked by earthquakes above 6.

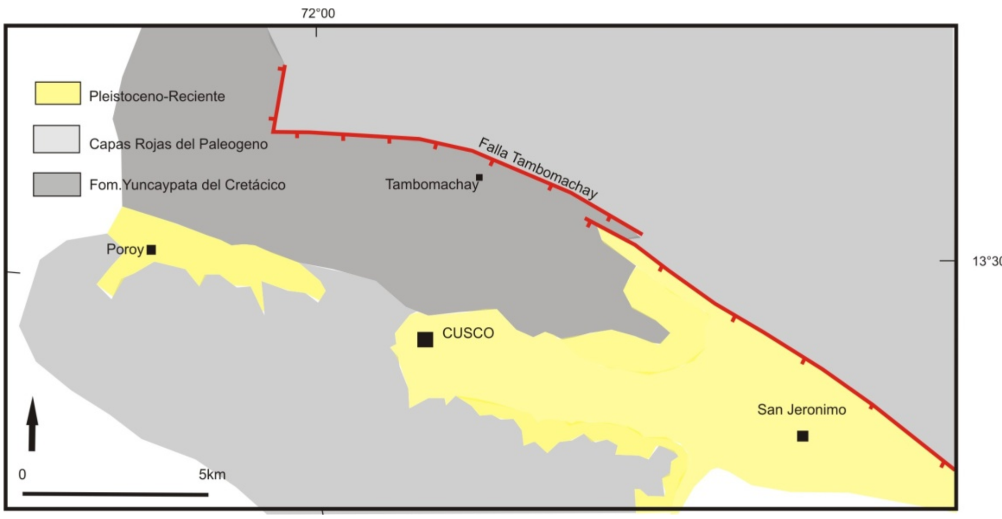

Fig. 2. Structural geology of the Cusco basin (Modified by Sebrier *et al.* 1985)

Fig. 3. Coseismic ruptures in the Cusco region

Active faults in Patzcuaro

The Patzcuaro lake is formed by volcanic and tectonic processes have played their part in its shaping. The tectonic process is more evident in the southern part of the lake, where a E-W normal fault system generates an alignment of volcanoes, avalanches-collapses and normal faults. The Patzcuaro-Jaracuaro graben developed on these active faults, which generated a rise of the bottom of the lake during the Pleistocene-Holocene, and ultimately formed the island of Jaracuaro, which means “place that appears” in Purepecha. Current paleoseismic studies reveal a seism posterior to 28,110, which caused the collapse of a whole sector of the El Estribo volcano. This collapse produced an avalanche due to a seism, the intensity of which was possibly of magnitude 7. On the other hand, coseismic ruptures in the trenches show fault scarps of approximately 70cm, possibly associated with magnitudes M=6 (Fig. 4).

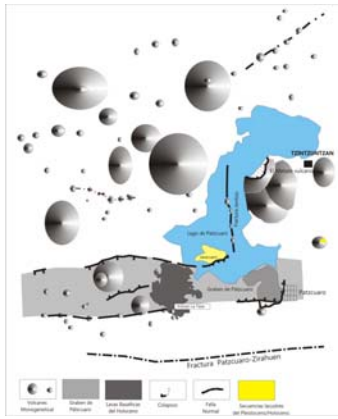

Fig. 4. Structural geology of the Patzcuaro -Tzintzuntzan lake, with visible E-W active faults.

Antiseismic architecture

With such seismic antecedents, both pre-Columbian cultures developed per force an awareness of geologic processes. It is remarkable that both used similar building techniques to protect their constructions from seismic attacks. This technique, called “Interlocking”, or “clamp structures”, has been found mainly at the base of the Yacatas, and here and there in the more recent constructions of Tzintzuntzan. These techniques have also been found in Cusco, yet presenting a different geometry.

A 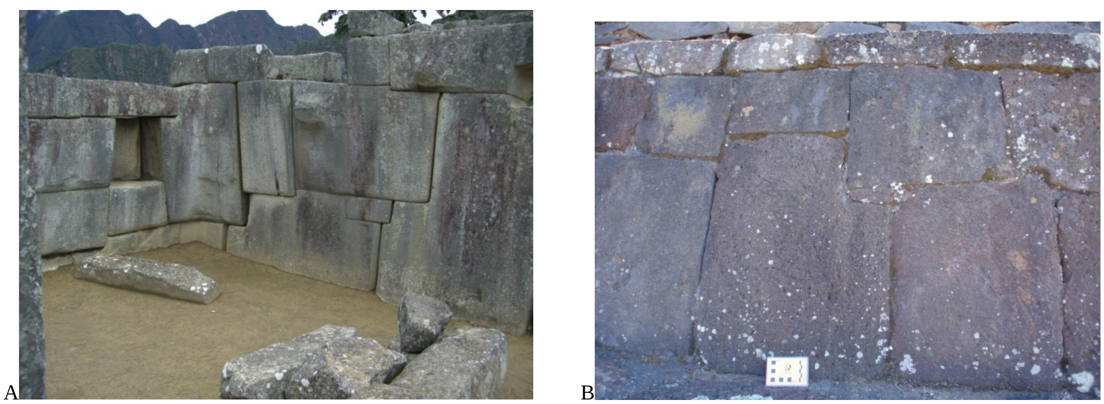 B

Fig 5. Interlocking techniques used in Cusco (picture: Arturo Oliveros) (A) and in Tzintzuntzan (B)

Conclusions

These discoveries reveal the importance of archeoseismic studies both in Mexico (Patzcuaro-Tzintzuntzan) as in Peru (Cusco). These studies allow us to know the historical earthquakes which motivated the development of anti seismic techniques. The results are clearly visible in the structures presenting interlockingThese structures minimize the impact of earthquakes as far as horizontal movements are concerned. Interlocking structures have been found in Mitla, Oaxaca, Teotihuacan, State of Mexico an a few other sites of Maya culture.

Bibliografia

C. Cuadra, M. B. Karkee, J. Ogawa and J. Rojas. (2003) “Preliminary investigation of earthquake risk to Inca’s architectural heritage”. Fourth International Conference on Earthquake Resistant Structures
ERES IV, Ancona, Italy, Set. 2003, pp. 167-176.

Malmstrom V., (1995). Geographical origins of the Tarascans. Geographical Review. Vol. 85, No. 1

Ruiz E. (1978). Michoacán Ed. Cosmos, Mexico, 20-25.

Sebrier M., Mercier J.L., Megar F., Lauhacher G. y Carey-Gailhardis E., (1985). Quaternary Normal and Reverse

Faulting and the state of stress in the Central Andes of South Peru. Tectonics, Vol. 4, No.7, 739-780.

PALEOSEISMOLOGY & ARCHAEOSEISMOLOGY
MORELIA • MEXICO 2012
INQUA-TERPRO PALEOSEISMOLOGY
EARTHQUAKE ARCHAEOLOGY

ORIENTED FALL STRUCTURES (EARTHQUAKE ARCHAEOLOGICAL EFFECT). A REVIEW IN INSTRUMENTAL EARTHQUAKES

Giner-Robles, Jorge L. (1), Martín-González, Fidel (2), Pérez-López, Raúl (3), Rodríguez-Pascua, Miguel A. (3), Silva, Pablo G. (4)

(1) Dpto. Geología y Geoquímica, Facultad de Ciencias, Universidad Autónoma de Madrid. Madrid. SPAIN. jorge.giner@uam.es
(2) Área de Geología, ESCET, Universidad Rey Juan Carlos. Móstoles (Madrid). SPAIN. fidel.martin@urjc.es
(3) Instituto Geológico y Minero de España. Madrid. SPAIN. ma.rodriguez@igme.es, r.perez@igme.es
(4) Dpto. Geología, Escuela Politécnica Superior de Ávila, Universidad Salamanca. Ávila. SPAIN. pgsilva@usal.es

Abstract (Oriented fall structures (Earthquake Archaeological Effect). A review in instrumental earthquakes): *Falling oriented structures (e.g. columns, obelisks) at archaeological sites has been used as an indicator of seismic activity, However it is controversial their interpretation, especially in relation to the orientation dependence of the type of structure (e.g.: construction quality, conservation). In this paper we analyze the structures of this type damaged by three instrumental earthquakes, with seismic intensities above VII:, Lorca earthquake (05/06 / 2011) (Spain); Chrischurch seismic sequences (04/09/2010 and 22/02/2011) (New Zealand) and Emilia Romagna Earthquakes (20/05/2012 and 29/05/2012) (Italy). The quantitative results show the consistency of the orientations of collapse of these structures, non dependent on age, type or structure conservation. The effect of seismic shock on near earthquakes seems to produce consistent orientated falls, although in the analysis of archaeological sites is necessary the analysis combination to determine the possible seismic origin of the structures.*

Key words: *earthquake archaeological effects (EAE), oriented fall structures, ChristChurch earthquakes, Lorca earthquake, Emilia Romagna earthquakes.*

INTRODUCTION

In archaeoseismological analysis, it is very common to consider the oriented fall of columns as a result of seismic activity in the area (Nur & Ron, 1996; Stiros, 1996).

Many authors believe that orientation in columns fall indicates the direction in which the seismic wave arrived, i.e. columns fall in the opposite direction to the way the seismic wave arrives (Fig.1) (Nur & Ron, 1996).

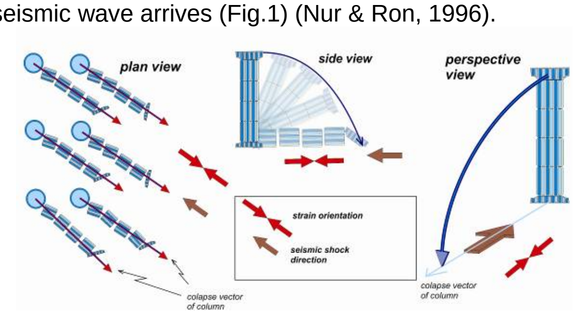

Fig. 1: Analysis of structure deformation in oriented column falls. The direction of maximum strain is parallel to the sense in which the columns fall. Damage directionality is defined by the sense in which the column falls (Giner-Robles et al, 2011).

Other authors elucidate on this statement because they believe it can significantly be affected by other factors, of construction nature (e.g. quality of materials, imperfections), anthropogenic nature (e.g. deliberate destruction) (Ambraseys, 2006; Marco, 2008), or topographic nature (e.g. slopes, escarpments) (Silva et al., 2009). Some authors (Hinzen, 2009; Hinzen et al., 2009) use cyclical movement models of these structures to indicate that small changes in the energy and even duration of the vibration can lead to columns falling in different directions.

Therefore, for the avoidance of doubt when interpreting this type of earthquake effect due to local effects, the analysis should be conditional upon the number of columns involved and the surface area where they appear. A significant number of affected columns has to be analyzed and the greater the extension of the area where these structures appear, the lesser the local effects will be.

To properly quantify the occurrence of these earthquakes archaeological effects (EAE´s, Rodríguez-Pascua et al., 2011), we studied systematically analyzed this type of collapsed structures in instrumental earthquakes. These earthquakes with intensities equal to or greater than VII are the Lorca earthquake (Spain) May 5th, 2011 (M 5.1), the seismic sequences of Chritschurch September 4th, 2010 (M 7.1) and February 22, 2011 (M 6.3) (New Zealand) and the earthquakes of Emilia Romagna (Italy) May 20 (M 5.9) and May 29, 2012 (M 5.8). The methodology used in this work is based on Giner-Robles et al. (2009, 2011).

CHRISTCHURCH SEISMIC SEQUENCES

The Christchurch seismic sequences (New Zealand) of September 2010 and February 2011, generated two destructive events on 09/04/2010 (M 7.1) and 22/02/2010 (M 6.3) and 13/01/2012, (M 6) and produced remarcable damage in the city. After the second sequence the CBD (Central Business District) was closed and no recognition was possible. For this reason we chose to analyze the cemeteries. These facilities had numerous falls oriented structures, given the large number of columnar structures as obelisks and crosses (Fig. 2). These structures showed that the orientation of these falls were very homogeneous, with small dispersion due to the geometry of the affected structure (e.g. round or square bases). In some cases there were two orientations well defined. They have been provisionally interpreted as the result of the two seismic shock related to the second and third seismic sequences that struck the city.

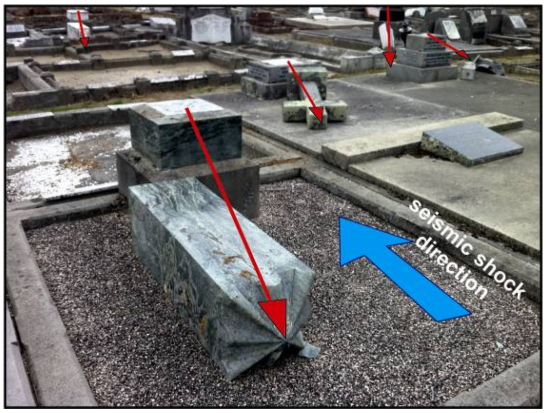

Fig. 2: Fallen crosses and obelisks oriented in the Bromley Cemetery (Chistchurch, New Zealand) as a result of the earthquakes that struck this town in 2011 and 2012. The orientation and azimuth of the falls is the same in the entire cemetery.

LORCA EARTHQUAKE

The Lorca earthquake (Spain) May 5th, 2011 (Mw 5.1) (VII), with hypocenter very close to the city of Lorca (<3 km) caused extensive damage. Among the 140 EAES (Rodríguez-Pascua et al., 2011) recorded, we analyzed 33 oriented falls structures (chimneys, balustrades, etc.) (Fig. 3).

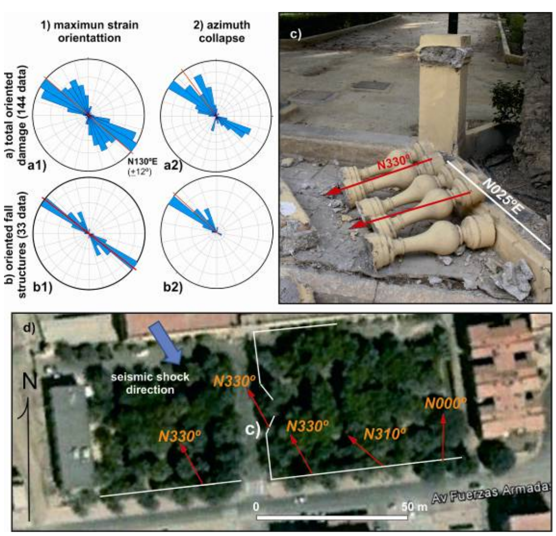

Fig. 3: Comparison of roses of maximum deformation (1) and azimuth of the collapse (2), set of all damages analyzed (a) and falls oriented (b). c) Detail of a fall on the balustrade in a city park. d) Map uniformity is observed in the directions of maximum deformation and in the azimuth of collapse.

Damages are distributed homogeneously throughout the city and they have an orientation with very small dispersion (N130º E) (Fig. 3 b 2), and orientation parallel to the whole damage analysis (Fig. 3 a1). The azimuth of all structures can be group at N310º and at N130º, this bimodality seems to be related to the geographical location of the EAE's possibly related to the trace of the fault (Giner-Robles et al., this volume). However, all of the orientated structures have azimuths oriented towards the NW, consistent with the location of the trace fault.

Although in some cases there is some dispersion (Fig. 3c and d), orientations are subparallel and consistent with the data recorded in the city

EMILIA ROMAGNA EARTHQUAKES

The seismic sequences of Emilia Romagna (Italy) May 2012, produced oriented damage, most of it, collapses and falls oriented. The analysis of the orientation of maximum deformation (Giner-Robles et al., 2011) shows N240º to N330º, two directions that may represent the occurrence of the two earthquake sequences.

Among the investigated sites it is included the cemetery of the town of Mirandola. Oriented structures were observed in single elements (obelisks, tombstone), as well as in complex elements such as columned porches. In the central part of the cemetery is located an obelisk that collapsed (N270º) (Fig. 4).

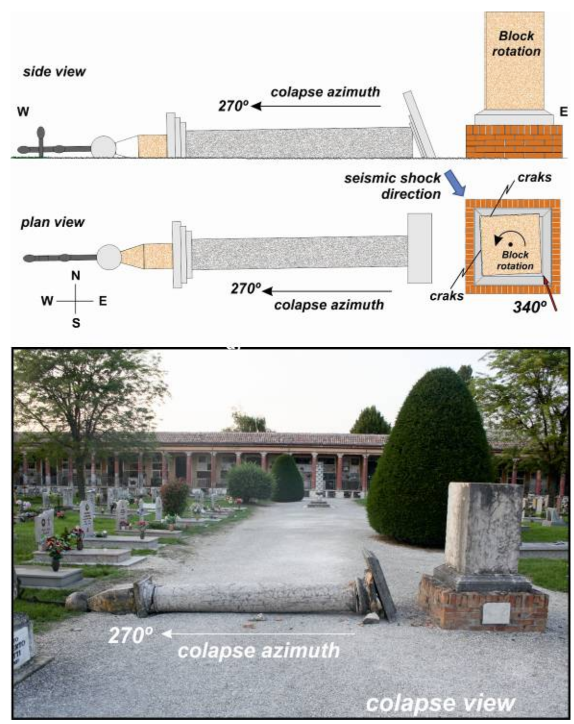

Fig. 4: Structure collapsed in the cemetery of Mirandola city (Emilia Romagna, Italy). Scheme (a) and photograph (b) of the collapsed structure. The obelisk collapses towards the N270º, while the base undergoes rotation and displacement.

A detailed analysis shows that the square base of the obelisk suffered a rotation and a shift towards N340º (Fig. 5a). It is also observed that the upper northwest corner of the base (Fig. 5c) shows breaks. These breaks define a seismic shock towards NW. Cracks are not observed in the SE corner (Fig. 5b) which is consistent with the orientation of the displacement vector of the base (N340º).

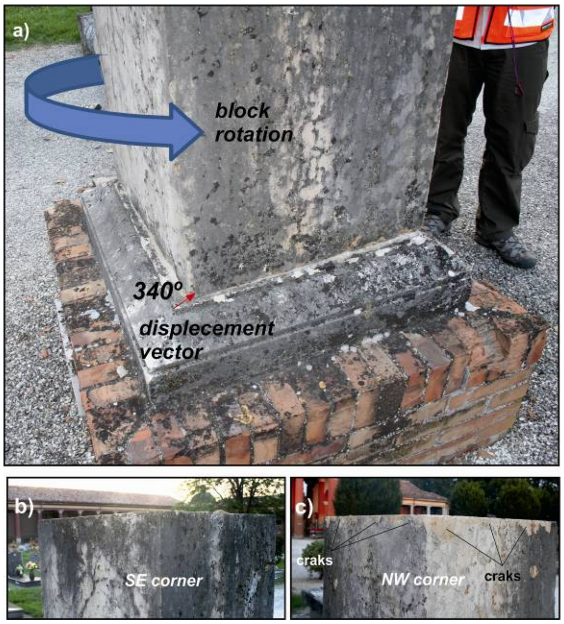

Fig. 5: a) View from the SE of the base of the obelisk, note its rotation and displacement as N340º. Views of the top corners of the obelisk base: the SE corner (b) no damaged, while the NW corner (c) shows cracks as a result of seismic shock oriented along NW, parallel to the displacement of the base.

In the south of the cemetery, the columns fell orientated. The columns collapsed obliquely to the direction of the structure according to N340º (Fig. 6).

Orientated obelisk towards N270º is conditioned by the presence of square slabs between the base of the obelisk and the circular base of the column, but is clearly induced by the seismic shock direction. This orientation (N340º) is clearly observable in the base of the obelisk (Fig. 5a) and in the fall of all the atrium columns in the cemetery (Fig. 6).

In San Giacomo Roncole, very close to Mirandola, it has been recorded another structure associated with an obelisk. In this case, the structure was not collapsed, but it can clearly be seen that the characteristics of the construction can condition the direction of displacement of the obelisk. This obelisk has been displaced towards the only orientation that allows the structure (Fig. 7a and b), but the breaks in the block shows the actual orientation of the movement (N250º), parallel to the collapse of the gable of the church which is south of the obelisk (N240º) (Fig. 7c)

Fig. 6: Series of columns collapsed in the cemetery of Mirandola, the azimuth coincides with the displacement vector of the base of the obelisk (see fig.5).

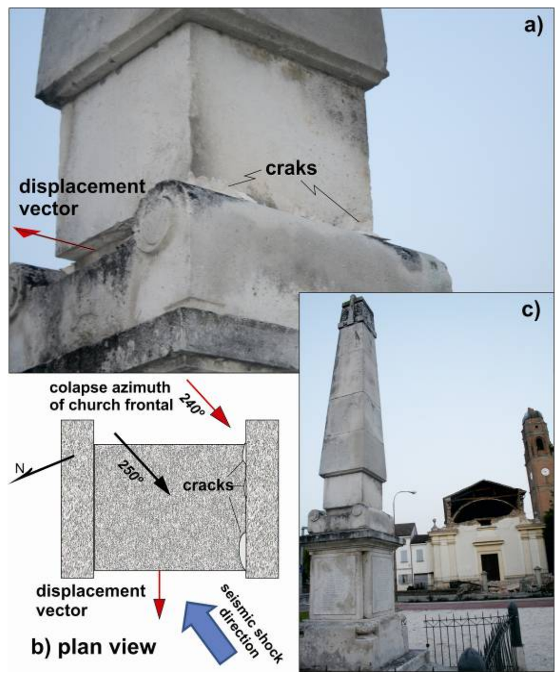

Fig. 7: Obelisk in the village of San Giacomo Roncole. It is noted that displacement has occurred in the only possible direction (a, b), but breaks the block indicate the actual direction of motion, orientation subparallel to the collapse of the facade of the church seen in the background (c) (N240º).

DISCUSSION AND CONCLUSIONS

The oriented collapsed structures in near field effect in the earthquakes of the three instrumental earthquakes studied, show that these structures have very uniform fall orientations. Besides, these orientations do not seem to be conditioned by the characteristics of the structure (e.g. conservation, age, building materials).

Some dispersion is observed in some cases. In most of them, these small variations in orientation are related to the structure which has collapsed. Small variations in shape and / or geometry of the structure can produce dispersions in the orientation of the fall. However, this dispersion is always within the parameters of normal dispersion in a statistical measure. Moreover, the systematic and detailed analysis allows establishing the correct direction seismic shock that caused the collapse.

Both, the field recognizance and analysis of instrumental earthquakes (performed in this work), as well as the modeling of the response of these structures with the seismic waves, can enhance the analysis and interpretation of these oriented fall structures in archaeological sites.

The analysis in this work point out that in an area affected by an near earthquake, oriented fall occurs with a consistent azimuth direction and only present some dispersion due to particular conditions of the structure.

The relationships of these orientations with the earthquake focal parameters (e.g.: epicentral location, strike-slip fault) requires more comprehensive analysis of the distribution of different EAE's around the area affected by the earthquake.

Acknowledgements: This work has been supported by Spanish research projects EDASI (Fundación MAPFRE), RESCATELO (CGL2011-14925-E) and it is a contribution to INQUA Project 1229 (EEE Metrics) and IGCP-567.

References

Ambraseys E. Earthquakes and archaeology. *Journal of Archaeological Science*, 2006, 33: 1008-1016.

Stiros, S. C. Identification of Earthquakes from Archaeological Data: Methodology, Criteria and Limitations.1996. In: *Archaeoseismology* (Stiros, S. and Jones, R. eds). *Fitch* Laboratory Occasional Paper 7. British School at Athens., 129-152.

Giner-Robles, J.L.; Rodríguez-Pascua, M.A.; Pérez-López, R.; Silva, P.G.; Bardají, T.; Grützner C. y Reicherter, K. 2009. *Structural analysis of Earthquake Archaeological Effects (EAE) Baelo Claudia Examples (Cádiz, South Spain)*, 137 pp.

Giner-Robles, J.L.; Silva Barroso, P.G.; Pérez-López, R.; Rodríguez-Pascua, M.A.; Bardají Azcárate, T.; Garduño-Monroy, V.H. y Lario Gómez, J. 2011. *Evaluación del daño sísmico en edificios históricos y yacimientos arqueológicos. Aplicación al estudio del riesgo sísmico*. Proyecto EDASI". Serie Investigación. Fundación MAPFRE, 96 pp.

Giner-Robles, J.L.; Pérez-López, R., Rodríguez-Pascua, M.A.; Silva Barroso, P.G.; Martín-González, F., Cabañas, L. (en este volumen) Oriented damage in buildings due to Lorca Earthquake May 11, 2011: Application to archaeoseismology.

Hinzen, K.G. Dynamic response of simple structures. In: R. Pérez-López, C. Grützner, J. Lario, K. Reicherter and P.G. Silva (eds). Archaeoseismology and Palaeoseismology in the Alpine-Himalayan Collisional Zone. Abstracts Volume of the 1st INQUA-IGCP 567 International Workshop on Earthquake Archaeology and Palaeoseismology, 7th- 13th September. 2009; p. 47. Baelo Claudia, Spain.

Hinzen, K.G., Fleischer, C., Reamer, S.K., Schreiber, S., Schütte, S. and Yerli, B. Quantitative methods in archaeoseismology. In: R. Pérez-López, C. Grützner, J. Lario, K. Reicherter and P.G. Silva (eds). Archaeoseismology and Palaeoseismology in the Alpine-Himalayan Collisional Zone. Abstracts Volume of the 1st INQUA-IGCP 567 International Workshop on Earthquake Archaeology and Palaeoseismology, 7th-13th September. 2009; p. 50. Baelo Claudia, Spain.

Marco, S. (2008). Recognition of earthquake-related damage in archaeological sites: Examples from the Dead Sea fault zone. *Tectonophysics*, 453, 148-156

Nur, A. and Ron, H. And the Walls Came Tumbling Down: Earthquake History in the Holyland. In: Stiros and Jones, Archaeoseismology. British School at Athens. Fitch Laboratory Occasional Paper nº 7.p. 75-86. 1996

Rodríguez-Pascua, M.A., Pérez-López, R., Silva, P.G., Giner-Robles, J.L., Garduño-Monroy, V.H., y Reicherter, K. (2011): "A Comprehensive Classification of Earthquake Archaeological Effects (EAE) for Archaeoseismology", Quaternary International, 242: 20-30.

PALEOSEISMOLOGY & ARCHAEOSEISMOLOGY
MORELIA • MEXICO 2012
INQUA-TERPRO PALEOSEISMOLOGY
EARTHQUAKE ARCHAEOLOGY

POSTSEISMIC EARTHQUAKE ARCHAEOLOGICAL EFFECTS (EAE´S) IN MORELIA AND PATZCUARO CITIES (MICHOACAN, MEXICO)

Giner-Robles, Jorge L. (1), Bardaji Azcárate, Teresa (2), Rodríguez-Pascua, Miguel A (3), Pérez-López, Raúl (3), Silva, Pablo G. (4), Garduño Monroy, Victor H. (5), Lario Gómez, Javier (6)

(1) Dpto. Geología y Geoquímica, Facultad de Ciencias, Universidad Autónoma de Madrid. Madrid. SPAIN. jorge.giner@uam.es
(2) Dpto. Geología, Universidad de Alcalá de Henares. Madrid. SPAIN. teresa.bardaji@uah.es
(3) Instituto Geológico y Minero de España. Madrid. SPAIN. ma.rodriguez@igme.es, r.perez@igme.es
(4) Instituto de Investigaciones Metalúrgicas. Universidad Michoacana de San Nicolás de Hidalgo. Morelia. MEXICO. vhgardunom@gmail.com
(5) Dpto. Geología, Escuela Politécnica Superior de Ávila, Universidad Salamanca. Ávila. SPAIN. pgsilva@usal.es
(6) Facultad de Ciencias. Universidad Nacional de Educación a Distancia. Madrid. SPAIN. javier.lario@ccia.uned.es

Abstract (Postseismic earthquake archaeological effects (EAE´s) in Morelia and Patzcuaro cities, Michoacan, México): *Many earthquake resistant structures are observed in historical colonial buildings constructed during 16th and 17th centuries in the localities of Morelia and Patzcuaro (Michoacan, Mexico). These construction procedures can be classified as postseismic Earthquake Archaeological Effects (EAE's). The best example is the Patzcuaro earthquake occurred in 1858. This earthquake produced numerous damages and different building techniques for reconstruction and reparation can be clearly observed in both cities. This information allows checking the historical documentation about the event and improving the studies related to seismic hazard. Likewise, the identification of similar structures both in pre-Columbian and in colonial buildings from 16th and 17th centuries allows to know and inferring the high seismic occurrence in the area as well as the activities carried out by both civilizations in order to minimize the damages produced by this kind of events.*

Key words: *postseismic earthquake archaeological effects (EAE´s), 1858 Patzcuaro earthquake, interlocked bloks, Michoacan State*

INTRODUCCIÓN

A classification of the earthquakes' effects recorded in an archaeological site or in a historical building (EAE's) has been recently developed by Rodríguez-Pascua et al. (2011). This classification undertakes a whole study of EAE's applying the most suitable methodologies for their analysis in any context, and it is based in the gathering of all the effects inTO two groups: co-seismic effects (simultaneous to the earthquake occurrence) and post-seismic effects (after the earthquake occurrence), (Fig.1). However, in some exceptional cases, both co-seismic and post-seismic effects are recorded in the same archaeological site (Silva et al., 2005; Giner-Robles et al., 2009).

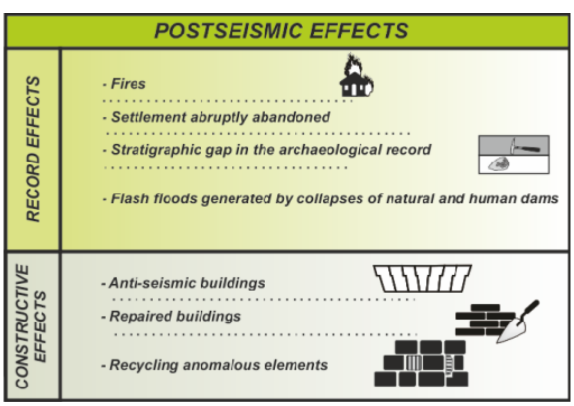

Fig. 1: Post-seismic effects (modificado de Rodríguez-Pascua et al., 2011)

There are many examples of cases in which the co seismic effects of earthquakes disappear almost completely as a result of repairs and / or new constructions, especially in cities that have not been abandoned after the occurrence of a major seismic event. Nevertheless, a large number of post-seismic effects on earlier constructions (reconstruction) or constructions after the earthquake occurred can be found in these types of cities. Such data impede proper analysis of the deformation but can provide a great deal of information about the seismic history of the area.

Clear examples of such behavior are the cities of Morelia (formerly Nueva Valladolid) and Patzcuaro in the Mexican state of Michoacan, where the systematic use of earthquake-resistant construction measures is evident in reconstructed masonry buildings. Documentation exists regarding destructive earthquakes that affected large parts of Michoacan, including the city of Morelia, between the 16th and 19th centuries. The best documented earthquake is the Patzcuaro quake of 1858, with an intensity of IX MSK.

MORELIA CITY

Numerous examples of reconstructions of seismic damage and the use of interlocking (post-seismic effects on buildings) are to be found in the city of Morelia (Giner-Robles et al., 2011). The systematic use of interlocking as a measure of earthquake-resistant construction is visible in more than 120 civic buildings in the city of Morelia dating from the 17th and 18th centuries, a period of great colonial urban development in the city.

Many interlocks can be seen in different buildings, especially on the lower floors and areas associated with the top, middle and bottom parts of doors and windows. The Baroque Government Palace (1760 - 1770) is a clear example of such a construction method (Fig. 2).

Fig. 2: a) Main façade of Government House in the city of Morelia (Michoacan, Mexico) (1760-1770). This Baroque palace shows the systematic use of interlocked stones on doors and windows on the ground floor of the building. b) Detail of the main gate of the palace. c) Detail of a window with interlocking at the top and bottom. This interlocking layout is seen in the same position in virtually all the windows on the ground floor of the building.

Interlocking appears consistently on the doors and windows of the ground floor. However, the systematic use of such stonework is considered by some authors to be a measure that bears no relation to earthquake-resistant construction methods. Nevertheless, there are many examples in this Mexican city that illustrate the real purpose of the use of interlocked stones: to reduce damage to infrastructures from horizontal seismic source-induced loads.

A particular highlight is the repair of the old San Diego convent in the city of Morelia, capital of the state of Michoacan. The building dates from the mid 18th century (1768) and the entire façade reveals the systematic use of interlocked stones to completely break the horizontality of the rows, especially on the ground floor (Fig. 3).

The building was rebuilt in the late 19th century (1895) after the great Patzcuaro earthquake of 1858 (intensity IX MSK), which caused extensive damage to the towns of Patzcuaro and Morelia. The reconstruction is a clear example of the use of such construction methods to reduce damage (Fig. 4).

Some of the interlocked structures are complex, such as those inventoried in the old St. Augustine inn (1550 to 1626) (Fig.5).

This complexity is a clear evidence of a its specific objective: to reduce damage from horizontal seismic source induced loads. It should be noted that many of the buildings with this type of structure in the city of Morelia date from the 16th and 17th centuries, i.e. before the Patzcuaro earthquake, indicating that some of the previous historical earthquakes caused damage enough in the city to justify the adoption of these seismic resistant measures.

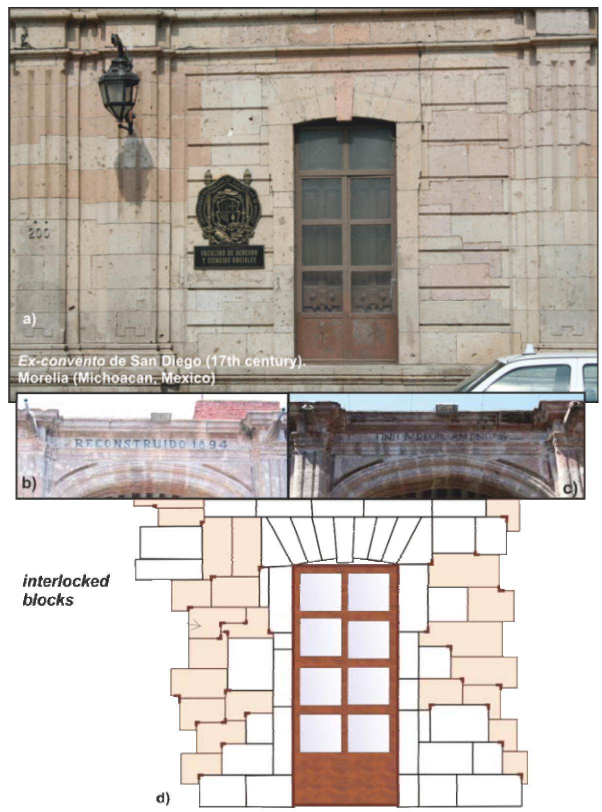

Fig. 3: a) Detail of the reconstruction (1884) of the façade of the former convent of San Diego using earthquake-resistant construction methods, (b) reconstruction also dated in the late 19th century (1895) (c) following the great Patzcuaro earthquake of 1858 that devastated the towns of Morelia and Patzcuaro. The reconstruction of the façade shows the systematic use of interlocked blocks (d).

It is worthy to recall that such construction measures are common in many former cultures, as for instance in the buildings' remains (Yacatas) of the Tarascan culture (pre-Columbian culture, 14th century) in the state of Michoacan (Mexico) (Fig. 6).

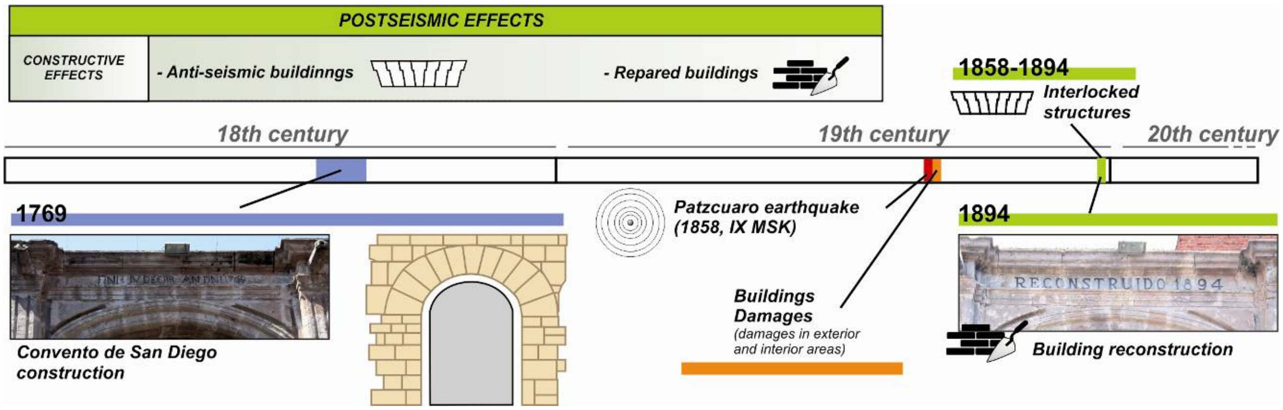

Fig.4 : Diagram of the chronology of the construction and subsequent reconstruction of the former convent of San Diego (Morelia, Mexico (see text for explanation).

PATZCUARO CITY

Effects of the 1858 earthquake can also be found around the city of Patzcuaro, such as the use of recycled imitation elements in the reconstruction of a church affected by the earthquake.

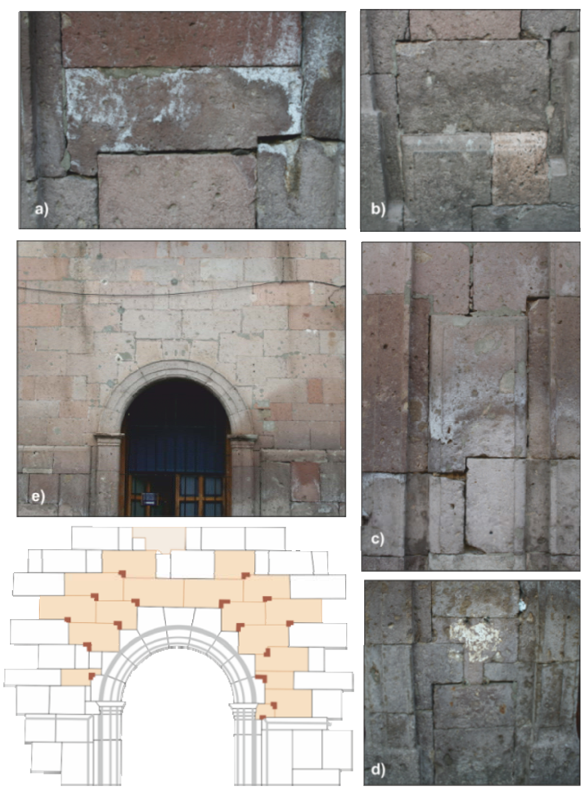

Fig. 5: Examples (a, b, c and d) of the complex design of some of the interlocking inventoried in the city of Morelia (Mexico) in the old St. Augustine inn (17th century). e) Photo and drawing of one of the doors in the building.

The city of Patzcuaro shows both post-seismic (Fig. 7) and co-seismic effects of this event and although most of its buildings are made of adobe, numerous marks of the 1858 earthquake have been recorded in the city.

Especially significant is the use of earthquake-resistant construction techniques in adobe, including a layer formed by reeds to provide the structure with greater strength against horizontal loads (Fig. 7b).

Some co-seismic structures can also be seen, although the material type (adobe structures) and the lack of unequivocal dating do not allow for a more comprehensive analysis.

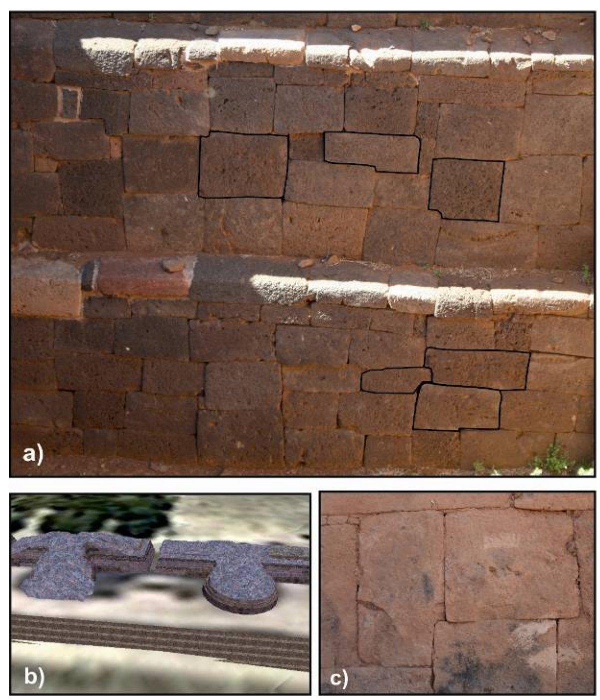

Fig. 6: Yacatas in Tzintzuntzan, Tarascan settlement (16th century) in the state of Michoacan (Mexico). a) Outer walls of older yacatas, which show numerous examples of interlocking construction in the pyramids. b) 3-D model showing the shape of these structures, with some collapses possibly caused by seismic events. c) Interlocked structures in the blocks that make up the roof of later yácatas.

Fig. 7: Post-seismic structures in the town of Paztcuaro. a) Arch reconstruction structure in one of the houses in the principal square. The top left corner of the arch shows the date the structure was rebuilt (1859), one year after the earthquake struck. b) Earthquake-resistant building structure in an adobe wall to reinforce these walls against horizontal strain, which included a layer of cane that gave greater consistency against deformation parallel to the plane of the wall. Note that one part has been replaced with wire mesh. c) Repair of a lintel on one of the doors in the town museum.

DISCUSSION AND CONCLUSIONS

A systematic use of earthquake resistant building measurements is observed in the cities of Morelia and Patzcuaro. Although in some cases these structures can not be directly related to reparations after the occurrence of an earthquake (Giner-Robles et al., 2011), many of these reparation and/or reconstruction works have a direct chronological relation with the destructive effects of the 1858 Patzcuaro earthquake. Systematic use of interlocking blocks is observed, for instance, in many reconstructed buildings of Morelia that were damaged by this seismic event. The simple dating by the inscriptions included in the same building allows to clearly identifying the earthquake resistant origin to these structures.

Nevertheless, there are many examples in the area where this kind of building structures do not have a clear relation with specific earthquakes, mainly in colonial buildings of the ancient quarter of both cities (16th and 17th centuries) and in Tarascas buildings (pre-columbian culture, 14th to 16th centuries). This fact allows confirming that seismic activity in the area has been sufficiently continuous to justify the adoption of this kind of building procedures by the different cultures, always directed to the mitigation of earthquake effects

Extended use of these structures in time, mainly the interlocked stones that reduce the horizontal seismic movements, allow us to develop a qualitative analysis of seismic hazard in the area, improving the prevention and mitigation of its effects.

On the other hand, the analysis of the post-seismic effects allows fixing chronologies and repetitions of damages in time (Rodríguez-Pascua et al., 2012), being possible to improve the activities directed to protect the cultural heritage from seismic activity. In the precise case of Morelia this kind of activities becomes extremely important given the fact that its historical centre was declared World Heritage by UNESCO in 1991.

Finally, we believe that the multidisciplinary integration of post-seismic effects in the analysis of poorly documented historical earthquakes can improve the historical earthquakes catalogues and consequently the analysis of seismic hazard.

Acknowledgements: This work has been supported by Spanish research projects EDASI (Fundación MAPFRE), RESCATELO (CGL2011-14925-E) and it is a contribution to INQUA Project 1229 (EEE Metrics) and IGCP-567.

References

Giner-Robles, J.L.; Rodríguez-Pascua, M.A.; Pérez-López, R.; Silva, P.G.; Bardají, T.; Grützner C. y Reicherter, K. 2009. *Structural analysis of Earthquake Archaeological Effects (EAE) Baelo Claudia Examples (Cádiz, South Spain)*, 137 pp.

Giner-Robles, J.L., Silva Barroso, P.G., Pérez-López, R., Rodríguez-Pascua, M.A., Bardají Azcárate, T.; Garduño-Monroy, V.H. y Lario Gómez, J. 2011. *Evaluación del daño sísmico en edificios históricos y yacimientos arqueológicos. Aplicación al estudio del riesgo sísmico*. Proyecto EDASI". Serie Investigación. Fundación MAPFRE, 96 pp.

Rodríguez-Pascua, M.A., Pérez-López, R., Silva, P.G., Giner-Robles, J.L., Garduño-Monroy, V.H. and Reicherter, K. 2011. A Comprehensive Classification of Earthquake Archaeological Effects (EAE) for Archaeoseismology, *Quaternary International*, 242: 20-30.

Rodríguez-Pascua, M.A., Pérez-López, R., Giner-Robles, J.L., Silva, P.G., Garduño-Monroy, V.H., y Reicherter, K. 2012. Efectos Arqueológicos del terremoto de Lorca del 11 de mayo de 2011 en su Patrimonio Cultural. Nuevas estructuras de deformación y reactivación de estructuras anteriores pertenecientes al terremoto de 1674. *Geo-Temas*,13: 465.

Silva, P.G., Borja, F., Zazo, C., Goy, J.L., Bardají, T., De Luque, L., Lario J., Dabrio, C.J. 2005. Archaeoseismic record at the ancient Roman City of Baelo Claudia (Cádiz, south Spain). *Tectonophysics*, 408 (1-4): 129-146.

PALEOSEISMOLOGY & ARCHAEOSEISMOLOGY
MORELIA • MEXICO 2012
INQUA-TERPRO PALEOSEISMOLOGY
EARTHQUAKE ARCHAEOLOGY

GEOLOGICAL STRUCTURAL ANALYSIS OF SURFACE DEFORMATIONS OF MORELIA SYSTEM FAULTS

Giner-Robles, Jorge L. (1), Garduño-Monroy, Victor H. (2), Díaz Salmeron, José E. (2); Hernández-Madrigal, Victor M. (2), Pérez-López, Raúl (3), Rodríguez-Pascua, Miguel A. (3), Silva, Pablo G. (4), Avila Olivera, J. (2)

(1) Dpto. Geología y Geoquímica, Facultad de Ciencias, Universidad Autónoma de Madrid. Madrid. SPAIN. jorge.giner@uam.es
(2) Instituto de Investigaciones Metalúrgicas. Universidad Michoacana de San Nicolás de Hidalgo. Morelia. MEXICO. vhgardunom@gmail.com, edmundods@hotmail.com, vitorio_manuel@yahoo.it
(3) Instituto Geológico y Minero de España. Madrid. SPAIN. ma.rodriguez@igme.es, r.perez@igme.es
(4) Dpto. Geología, Escuela Politécnica Superior de Ávila, Universidad Salamanca. Ávila. SPAIN. pgsilva@usal.es

Abstract (Structural analysis of the superficial deformations of Morelia system faults): *The city of Morelia, state of Michoacan, Mexico, presents a series of several kilometer long normal faults. Since the 80s, these faults have been presenting creep movement, thereby causing important damage to the city's infrastructures. The deformation is associated to subsidence due to aquifer overexploitation. The characteristics and orientation of these faults are coherent with the regional tectonics, which points out to a tectonic control of this subsidence. This paper explains the analysis of the faults' superficial planes and the displacement vectors of the different damaged infrastructures, systematically obtaining displacement vectors orientations which indicate a normal movement, notwithstanding an important left lateral component. This normal left lateral tendency is in line with the construction of the focal mechanism of the earthquake occurred in Morelia in 2007, with epicenter in the city itself. All these results allow to infer that the fault activity in Morelia is characterized by tectonic creep which is included and amplified by aquifer overexploitation.*

Key words*: Morelia faults system, normal fault, tectonic crepp, México,*

INTRODUCCIÓN

In numerous cities of Mexico, subsidence has been described as a process linked to aquifer exploitation deprived of structural or tectonic control. In the 80s, however, observations in the cities affected by this subsidence associated to older basins, showed that it developed along regional faults controlling lacustrine sedimentation (Aguirre-Diaz et al., 2000). In Morelia, subsidence corresponds to NE-SW and E-W structures which are part of the Mexican volcanic belt (Garduño-Monroy et al., 2001).
The city of Morelia is located in Mexico's east-central area, at an approximate distance of 280 km from Mexico City (Fig. 1a and b). Since 1983, subsidence has been reported in the centre of the city. The latter is oriented along the regional fault system, ENE-WSW (Garduño-Monroy et al., 1998 and 1999), and with moderate associated seismic incidence (e.g. Acambay earthquakes, 1568 and 1912). Cartographic traces of these faults present mediate N65ºE (Fig. 1d) orientation, and dip mostly NW, matching the general tectonic semigraben structure of the area (Fig. 1b).
The activity of these faults provokes numerous deformations in the urban buildings and infrastructure. These deformations seem to present an important lateral component. The scope of this paper is to characterize the geometrics and kinematics of the Morelia faults on the base of the analysis of the superficial deformations which have been observed. Furthermore, an attempt will be made to quantify the lateral component of the movement, in order to relate this data with the seismotectonic activity in the area.

ANALYSIS OF STRAIN STRUCTURES

In an attempt at quantifying the lateral component of the faults, the superficial deformations caused by these faults in Morelia have been closely observed. The orientation of the superficial deformation planes and displacement vectors associated with the deformation visible in several infrastructures (buildings, sidewalks, roads, etc) have also been measured.
The orientation of the displacement vectors obtained are compared with the orientation of the displacement vector on the fault plane in the direction of the dipping, that is the azimuth of a vector respondent to a vertical movement, without lateral movements.
All in all, 50 superficial fault planes and more than 63 displacement vector orientations have been measured in different structures, mainly in buildings, roads and sidewalks of the most affected streets. The orientation of the superficial fault plane is an important indicator, for assuming it maintains its direction in depth, it allows us to establish the control parameter in the analysis, as the dipping direction of the plane defines the orientation of the displacement vector with normal pure movement (slipping in the dipping sense).

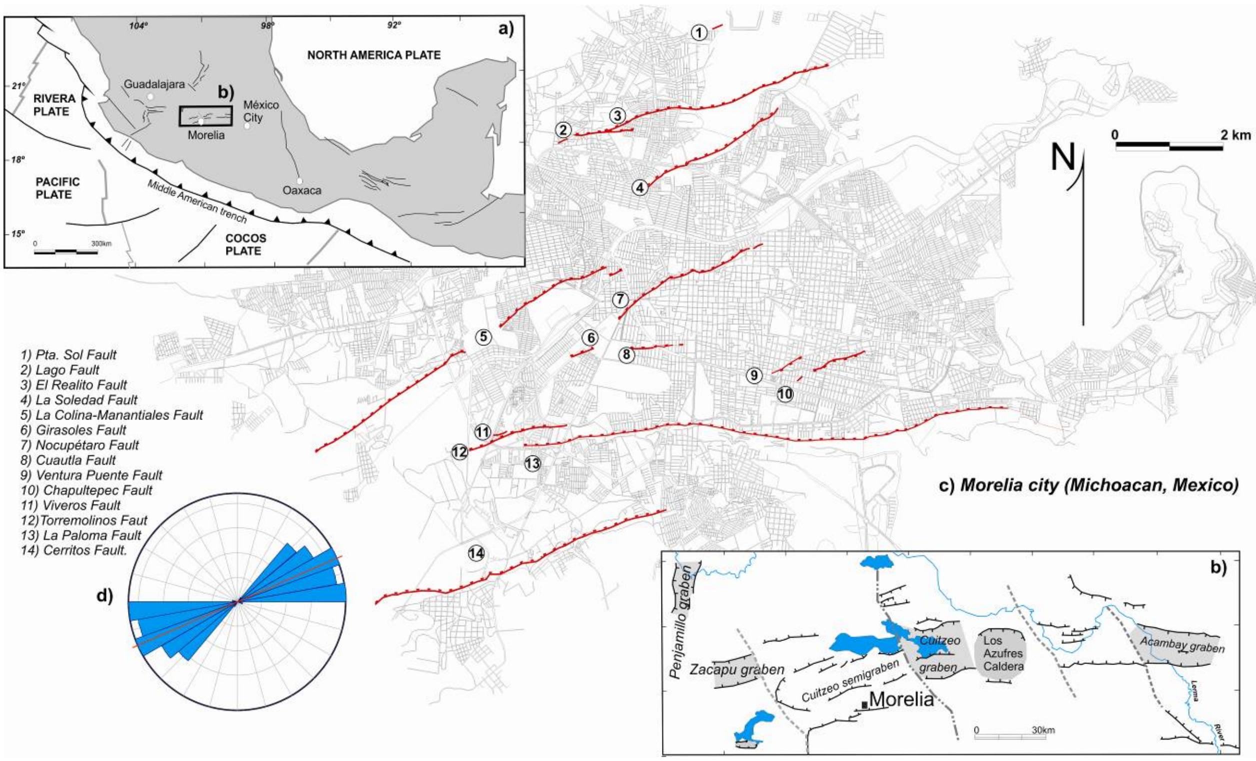

Fig.1: a) Regional geology of the fault system in Morelia Acambay. b) situation of Morelia in the tectonic context which affects the central part of the Mexican Volcanic Belt (lakes in blue and the main grabens in grey). c) cartography of Morelia and of the normal-sinistral fault system which affects the city (modified by Hernández-Madrigal et al., 2012): 1) Pta. Sol Fault, 2) Lago Fault, 3) El Realito Fault,4) La Soledad Fault, 5) La Colina-Manantiales Fault, 6) Girasoles Fault, 7) Nocupétaro Fault, 8) Cuautla Fault, 9) Ventura Puente Fault, 10) Chapultepec Fault, 11) Viveros Fault, 12)Torremolinos Faut, 13) La Paloma Fault and 14) Cerritos Fault. d) Rose diagram of trace orientations of Morelia's fault system.

The figure 2 explicates the analysis methodology in two of the analyzed sectors: the Nocupetaro fault (sector Avenida Nocupetaro), dipping NW; and the Chapultepec fault (sector Calle Batalla), dipping SE. In both cases the fault planes cyclographics and the measured displacement vectors are highlighted in red; the average orientation of the planes with the displacement vectors are drawn in grey, supposing a normal pure slipping (in the same sense of the dip).

In both cases we can observe the deviation between the average orientation of the measured vectors (red arrow) and the normal pure shifting vector (grey arrow).

This deviation, of more than 15° in the case of the Nocupetaro fault, defines the lateral component of this fault's movement. This fact is systematically present in all sectors of the analyzed faults, reaching at some points 30° of difference between both vectors (figs. 3 and 4). In aerial photographs of the 60's it is possible to see the trace of some of the faults, as in the case of the Colina fault (Garduño-Monroy et al., 2001).

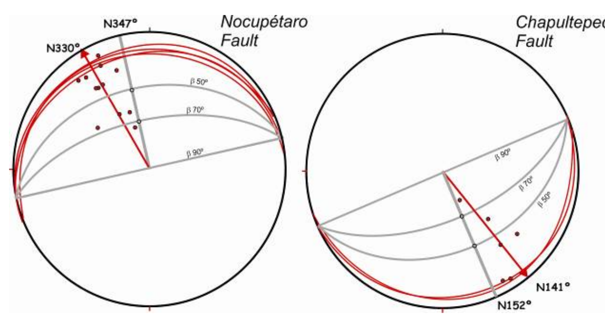

Fig.2: results obtained for the Nocupetaro fault and the Chapultepec fault; the latter is one of the few faults in Morelia dipping South (see fig 1c). The superficial displacement planes and vectors obtained by the analysis are in red; the average orientations with different dipping points are in grey, as the displacement vectors for the fault traces, supposing only vertical movement.

Some areas show the relatively recent nature of the creep activity of the faults. In the Campestre sector of the la Paloma fault, the fault runs through a 17th century colonial building (fig. 4). This construction, which does not present important deformations associated to the activity of the fault in the last 300years, has suffered important damage due to creep movement in the last few years. This fact proves that this slow fault movement has begun in the last decades, as pointed by Garduño-Monroy et al. (1999 and 2001).

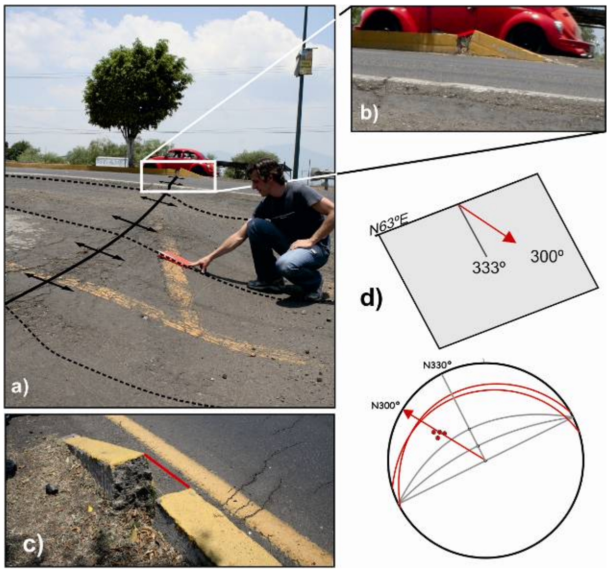

Fig. 3: Results obtained for the Colina Fault (sector W-Libramiento). a) street deformations as a consequence of the fault movement, which at some points fractures the cement blocks of the brims (b, c). Stereographic projection of data recollected in the zone. Variations of more than 30° between the real vector (red) and the normal pure sliding vector are observable (see figure 2 caption).

In order to make a comparison of the results obtained with the fault geometrics and kinematics, which define the current tectonic of the zone, we retained the earthquake of Morelia (17/10/2007), with a magnitude of 3.5 and epicenter in the city itself (Red Sismológica Nacional, UNAM). The construction of the focal mechanism of this earthquake shows a sub-parallel fault plane in comparison to the large normal faults of the area (N85°E 65NW) (fig 5a and 6a2). The slipping on the fault plane shows a normal fault with left lateral component, which would present a N284° dip direction.

The final results (fig 5b) show that the orientation of the fault planes measured on the surface (N72°E) present sub-parallel orientations as to the cartographic traces of the faults (N65°E, see Fig 1) and to the fault plane of the focal mechanism of the Morelia earthquake (Fig 5a1).

The slipping vectors obtained show an average orientation following N321°, which presents a 21°angle with the orientation of the theoretical slipping vector for a normal pure fault (N342°, slipping in the sense of dipping). The same rotation is to be observed in the slipping vector of the fault plane of the Morelia earthquake (fig. 5a2).

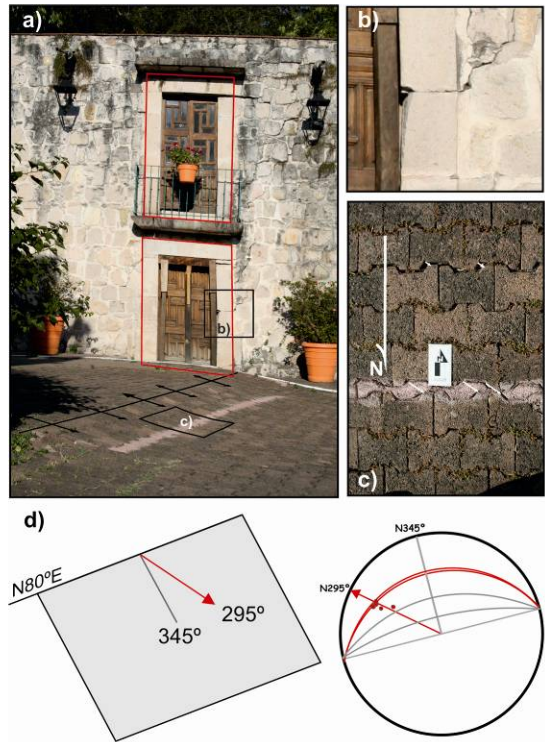

Fig. 4: Results obtained for the la Paloma fault (Campestre sector). a) deformations on the front of a colonial 17th century building, due to shear. Detail of the displacements measured on the façade (b) and on the ground (c). d) representation of the fault plane with the measured displacement (red) and the displacement supposing only vertical movement (grey). Stereographic projection of the data measured upon this structure, the angular difference between both vectors is 50° (see figure 2 caption).

In order to establish coherence between the kinematics of the faults and the regional tectonics, we must define some theoretical planes. These present the real average orientation data of the fault plane and the slipping vector obtained upon the field. The real dipping values cannot be used because of the correspondence with the superficial adjustment to the fault movement. Therefore, we have supposed and established dipping values between 50° and 80° (taken 5° by 5°).

If we apply deformation analysis methods to compare the kinematics of the theoretical planes and those of the Morelia earthquake fault plane, we obtain very coherent data. The maximum horizontal shortening orientations (ey) are sub parallel, following N60°E (fig. 6b1) for the theoretical planes and N50°E for the Morelia earthquake fault (fig. 6a1). The type of fault defined in the analysis is also coherent in both cases: the theoretical planes (right dihedral diagram) (fig. 6b2), and the focal mechanism of the Morelia earthquake (fig. 6a2) define normal faults with left lateral component.

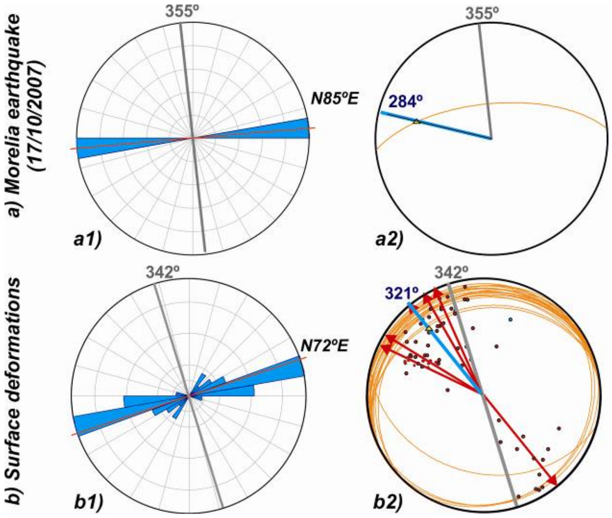

Fig. 5: Comparison between the 17/10/2007 (M3.5) Morelia earthquake fault plane and (a) the results obtained by means of the superficial deformation analysis; (b) fault plane orientation rose: (a1) of the Morelia earthquake, (b1) of all the planes measured in this paper (average plane dipping orientation in grey). Stereographic projection of the fault planes and the slipping vectors: (a2) Morelia earthquake fault plane, (b2) superficial deformation (blue line: average orientation of the slipping vectors; red arrow: average orientation of the slipping vectors for each fault).

DISCUSSION AND CONCLUSIONS

The data obtained with the analysis of superficial deformations produced by the Morelia fault system indicate a normal superficial movement with left lateral component. It seems that the activity of these faults started and thereby began to impact upon the infrastructure of the city of Morelia in the 80s, due to over-exploitation of the city's water resources (Garduño-Monroy et al., 2001).

The left lateral movement presented by the faults seems conditioned by the structural control of the active faults in the zone. We infer that the horizontal movement systematically observed in the superficial deformations produced by these faults does not exclusively correspond to subsidence induced by the soil compactation posterior to the over-exploitation of aquifers.

This movement is coherent with the 17/10/2007 Morelia earthquake fault kinematics (M 3.5), the epicenter of which lies very close to the city and with the regional stress state in the zone. This fact indicates that the activity of these faults is subject to the state of tectonic stress/deformation of the zone.
The geometric and kinematic coherence of the faults whose tectonic structures are active indicate that the current creep movement of the Morelia fault system has a clear coherent structural and kinematic control with the regional tectonic. It also seems obvious that the over exploitation of aquifers has been the initial factor and the amplifier of the process.

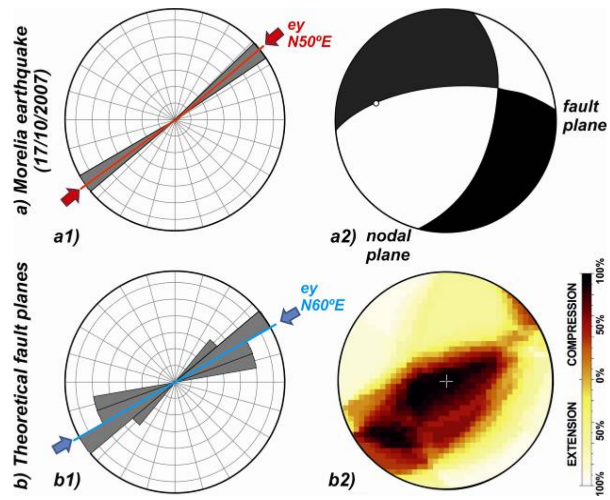

Fig. 6: deformation analysis by means of the Slip Model (De Vicente, 1987) (a1 and b1), and by means of the Right Dihedra Method (b2) (Angelier and Mechler, 1977). a2) construction of the focal mechanism of the Morelia earthquake.

Acknowledgements: This work has been supported by Spanish research project EDASI (Fundación MAPFRE), and it is a contribution to INQUA Project 1229 (EEE Metrics) and IGCP-567.

References

Angelier, J., Mechler, P. 1977. Sur une méthode graphique de recherche des contraintes principales également utilisables en tectonique et en sismologie: la méthode des dièdres droits. *Bulletin de la Société Géologique de la France*, 19, 1309-1318.

Aguirre-Díaz, G.J., Zúñiga Dávila-Madrid, R., Pacheco-Alvarado, F.J., Guzmán-Speziale, M., y Nieto-Obregón, J., 2000, El graben de Querétaro, México–Observaciones de fallamiento activo: *Geos, Unión Geofísica Mexicana*, 20 (1), p. 2-7.

De Vicente, G. 1987. The e/k' diagram. An application of the slip model to the population fault analysis. *Revista de la Sociedad Geológica de España* 1, 97–112.

Garduño, V.H., Arreygue, R.E., Chiesa, S., Israde, I., Rodríguez, G.M., Ayala, G. M., 1998. Las fallas geológicas y sísmicas de la Ciudad de Morelia y su influencia en la planificación del territorio. *Ingeniería Civil*, 1 (5), p. 3-12.

Garduño-Monroy, V.H., Rodríguez-Torres, G.M., Israde-Alcantara, I., Arreygue, E., Canuti, P. and Chiesa, S., 1999. "Efectos del clima (El Niño) en los fenómenos de Fluencia de las fallas geológicas de la Ciudad de Morelia". *Geos*, *Unión Geofísica Mexicana*, 19 (2), p.84-93.

Garduño-Monroy, V.H., Arreygue-Rocha, E., Israde-Alcántara, I. y Rodríguez-Torres, G.M. 2001. Efectos de las fallas asociadas a sobreexplotación de acuíferos y la presencia de fallas potencialmente sísmicas en Morelia, Michoacán, México. *Revista Mexicana de Ciencias Geológicas*,18 (1), p. 37-54.

Hernández-Madrigal V.M., Garduño-Monroy V.H. y Avila-Olivera J.A. 2012. *Atlas de peligros geológicos de la ciudad de Morelia*, Mich. SEDESOL-H. Ayuntamiento de Morelia, 82 p.

MEASURES OF ORIENTED DAMAGE AFFECTING BUILDINGS AND GENERATED BY THE LORCA EARTHQUAKE (MW 5.2, 11TH, MAY 2011): APPLICATION TO ARCHAEOSEISMOLOGY

Giner-Robles, Jorge L. (1), Pérez-López, Raúl (2), Rodríguez-Pascua, Miguel A. (2), Martín-González, Fidel (3), Silva, Pablo G. (4) y Cabañas, Luis (5)

(1) Dpto. Geología y Geoquímica, Facultad de Ciencias, Universidad Autónoma de Madrid. Madrid. SPAIN. jorge.giner@uam.es
(2) Instituto Geológico y Minero de España. Madrid. SPAIN. ma.rodriguez@igme.es, r.perez@igme.es
(3) Área de Geología, ESCET, Universidad Rey Juan Carlos. Móstoles (Madrid). SPAIN. fidel.martin@urjc.es
(4) Dpto. Geología, Escuela Politécnica Superior de Ávila, Universidad Salamanca. Ávila. SPAIN. pgsilva@usal.es
(5) Instituto Geográfico Nacional. Madrid. SPAIN. lcabanas@fomento.es

Abstract (Measures of oriented damage affecting buildings generated by the Lorca earthquake (Mw 5.2, 11th, may 2011): Application to archaeoseismology: *The analysis of the directionality of damage affecting buildings and generated by instrumental earthquakes allows the calibrating and to improving the archaeoseismic analysis methods. These methodologies are based on the analysis of the predominant damage directions in an archaeological site or in an historic building in such a way that allows us to analyze the possible seismic origin of deformations studied. The oriented damage analysis of the Lorca's earthquake on May 11th 2011 has allowed us to calibrate these methodologies. From the structures analysis an average of maximum strain very homogenous is deduced (NO-SE). This orientation is almost perpendicular to the fault orientation and, furthermore, it fits with the orientations of the displacement vectors into the horizontal as we can deduce from the accelerogram of the seismic station of the IGN placed at the city center of Lorca. The trajectories of maximum shortening show that the presence of different tectonic structures could induce to variations on to the damage orientations.*

Key words*: archaeoseismology, earthquake archaeological effects (EAEs), Lorca earthquake, oriented seismic damage*

INTRODUCTION

The analysis of the damage orientations affecting buildings on instrumental earthquakes allows the calibrating the archaeoseismic analysis methods. These methodologies are based on the analysis of the predominant damage directions in an archaeological site in such a way that allow us to analyze the possible seismic origin of deformations studied.

Main difficulties in this kind of study are: 1) to calibrate the analysis methodologies and 2) to establish a relation between damage orientation and seismic focal parameters (e.g. orientation and type of fault).

This is why it is interesting to analyze the damages caused by instrumental earthquakes into the archeological and architectonical heritage. The analysis in this type of earthquake allows us to prove and calibrate the methods used on the earthquake studies registered in the archaeological heritage. In this work it is shown the analysis of the oriented damage in the Lorca earthquake of 11th 2011.

METODOLOGY

The earthquake analysis methodology applied for the study in the archaeological sites (Giner-Robles et al., 2009, 2011) offers a multidisciplinary character as it is required the presence of various specialists. The analysis has different phases: (1) inventory and effects identification (earthquake archaeological effects, EAEs) (Rodríguez Pascua et al., 2011), (2) dating of the damages, quantification of the deformations in the observed structures, and (3) the analysis of the historic and archaeological documentation of the archaeological site (Fig. 1). In the case of an instrumental earthquake, as the one in Lorca (Mw 5.2) it is only essential to quantify the deformation focused principally on the coseismic effects in the fabric constructions (Fig. 1).

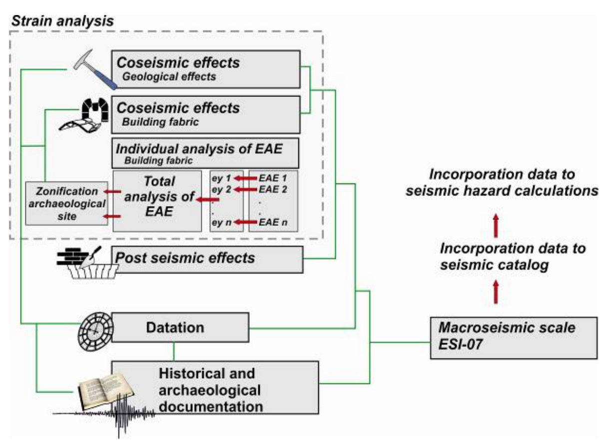

Fig. 1: Method diagram proposed by Giner-Robles et al. (2011) for the quantitative analysis of strain deformation present in structures on an archaeological site (EAE) (Rodriguez Pascua et al., 2011) (ey orientation of maximum horizontal shortening).

CUANTIFICATION OF STRAIN

To quantify correctly the deformation there are several phases to follow (Fig. 1): a) inventory and damage classification, b) individual structures analysis, c) joint data analysis, maximum horizontal shortening trajectories calculation, zoning of the city, to finally establish a connection between damage orientation and seismic parameters (e.g. fault orientation).

To inventory the seismic damages in the city of Lorca, it is used the classification of earthquake archaeological effects (EAEs) proposed by Rodríguez Pascua et al. (2011).

To make a correct analysis we just consider the historical buildings damages since as the type of materials and the construction methods of these buildings are comparable to those that could be present in an archaeological site.

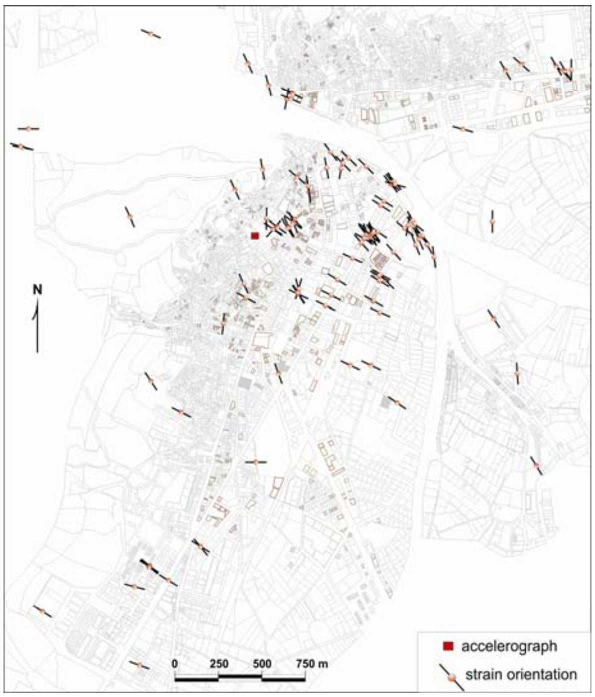

Figure 2: Map of the central part of the city of Lorca with the location of the analyzed structures and orientations of deformation derived for each.

Altogether, it have been inventoried more than 140 structures that could be analyze, being located, most of them, in Lorca's historic center (Fig. 2) (Rodríguez-Pascua et al., in this volumen).

The second phase of the analysis consisted of the determination of the maximum deformation observed in each one of the individual structures (Figure 2, 3 and 4), putting in practice the methodology proposed by Giner-Robles et al. (2011).

From kinematics deduced from the structures movements by seismic acceleration, we can define the orientation where the most important deformation has been occurred. Every one of EAEs types require specific consideration to study them in situ and to its subsequent analyze and interpretation.

In figure 3 it is possible to observe the analysis of one of such structures, in this case the tower of San Juan's Church, close to the Lorca's Castle. On this tower with an octagonal floor, the collapse of the central arch in the opposite windows oriented in N170E (windows 1 and 3) is observed; whereas in the windows oriented in N80ºE (windows 2 and 4) collapse does not occur.

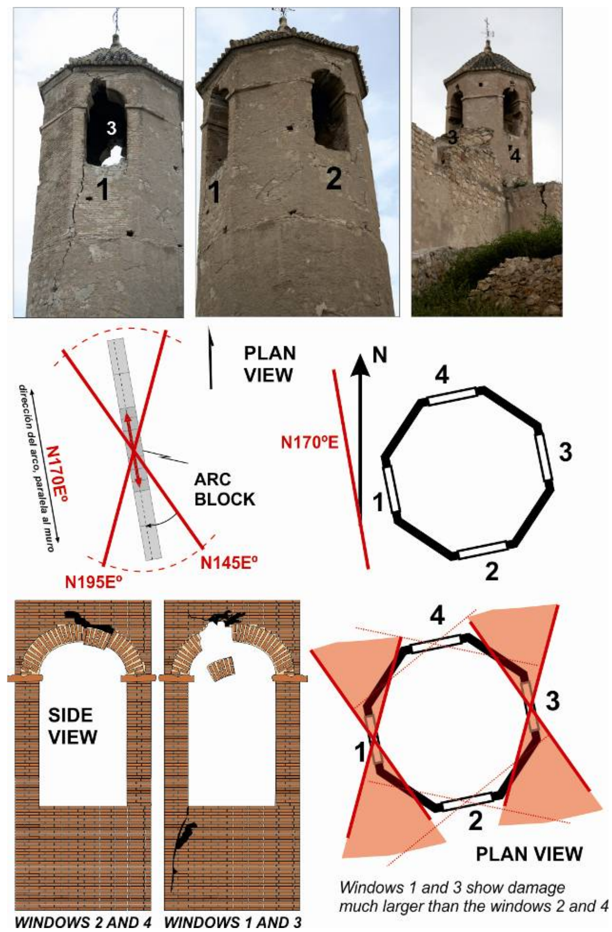

Fig. 3: Sample analysis and quantification of the deformation in the damage in the tower of San Juan's Church, in the city of Lorca. On the tower of this Church, with an octagonal floor, the collapse of the central arch in the opposite windows oriented in N170E (windows 1 and 3) is observed; in the windows oriented in N80ºE (windows 2 and 4) collapse does not occur. Based on the methodology developed by Giner-Robles et al. (2009, 2011) a maximum deformation directions range (red area) can be obtained.

This type of structures is systematically observed in almost every tower of the principal churches of Lorca that were affected by the earthquake.

In several occasions it has been possible to identify different EAE in the same building. In this case, the different EAE have been studied altogether and we have obtained a representative result of the building and, at the same time, coherent with individual data (Fig.4). To represent the effects on a map it is used the symbols proposed by Giner-Robles et al. (2011) that as well as represent the damage location, allow to symbolize the different elements which are necessary to analyze the deformation (e.g. wall orientation).

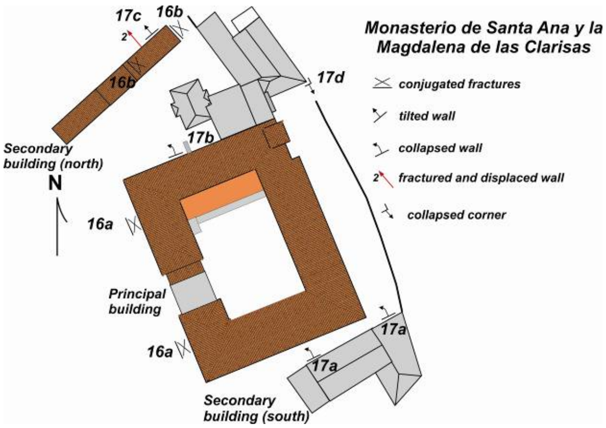

Figure 4: Example of structural mapping and analysis of damage to the Monastery of Santa Ana. The building had five different types of EAEs and the joint analysis allows to establish the consistency of the individual results

The total results obtained from the analysis according to the type of inventory effect (Figure 5) show homogeneous orientations with very few dispersion, with a media direction of maximum strain sub-parallel to the media orientation obtained for the whole city. These results show that the orientation average for the whole city is of the type inventory effect.

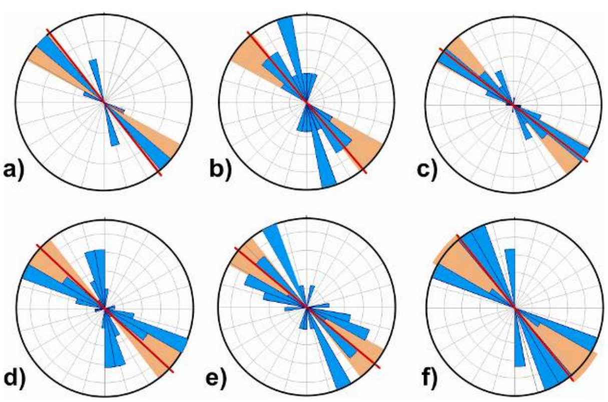

Figure 5. - Rose diagram of maximum deformation deduced on the basis of the type of effect (Rodríguez-Pascua et al., 2011; Giner-Robles et al., 2011). It represents the average orientation (red line) and the range of dispersion in the direction of maximum deformation obtained from the analysis of all data (N130 ° E ± 12º) (Figure 6a). a) walls tilted. b) marks of impact by collapse, c) falls oriented (e.g. chimneys, balustrades), d) walls collapsed, e) conjugate fractures, f) arc blocks displaced..

The results from the joint analysis of the whole data of the city (Fig. 6a) show an homogeneity in the direction of maximum strain according to NW-SE, which is perpendicular to the fault's orientation that caused the earthquake. In some EAEs concrete cases (collapsed walls, chimneys, impact marks, etc.) the results, apart from the direction, define the azimuth damage (Figure 6b). The azimuth of the damage is on the opposite orientation to seismic shock direction.

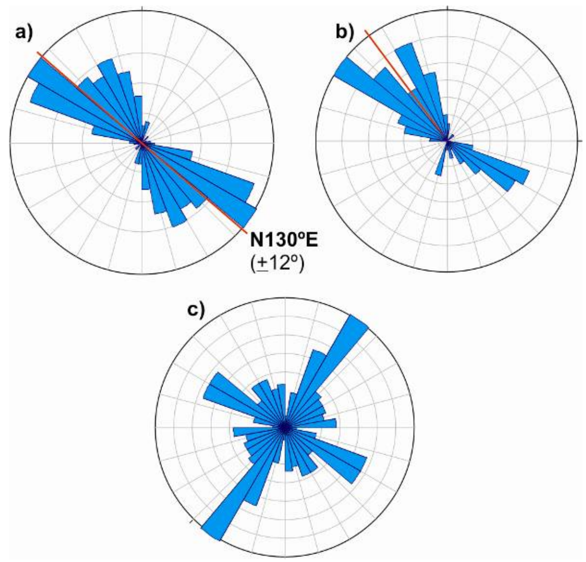

Fig. 6: Rose diagrams of orientations of maximum deformation obtained from the analysis of all inventory effects in the city of Lorca and surrounding areas: a) orientation of maximum deformation, b) azimuth of maximum deformation, c) orientation of the structures that are on damages.

In the city there is an accelerograh of the IGN (Instituto Geográfico Nacional) that registered the event (Fig.2). The 2D ground motion is obtained from the study of the accelerogram allowing defining the main orientations of the displacement vectors in the accelerograh site. These vectors orientations (Fig. 7b) appear more towards the north than deformation directions obtained from the whole inventory effects of the city (Figure 4a). However, if we compare them with the deformation directions obtained from the study of the area near accelerograph station is located (Fig. 7a), it is observed that displacement vectors orientation are parallel to the deformation orientations obtained in that area (Figure 9b).

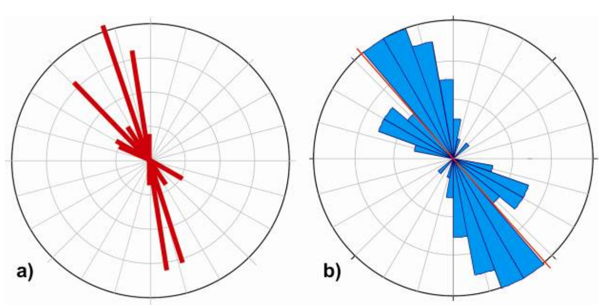

Figure 7.- a) Motion vectors obtained from the accelerogram analysis of the movement of the particle 2D of the IGN accelerograh registration. b) Rose diagram of maximum strain orientation in the area near accelerograph station is located.

From specific strain data it is possible to interpolate the trajectories by outlining the setting variations of the maximum strain orientations. In Lorca's city center the maximum horizontal shortening trajectories are oriented NNW-SSE whereas in the surrounding areas they are oriented NE-SW or even WNW-ESE. These orientation variations give to the trajectories drawing a clear form of sigmoid (Fig.8)

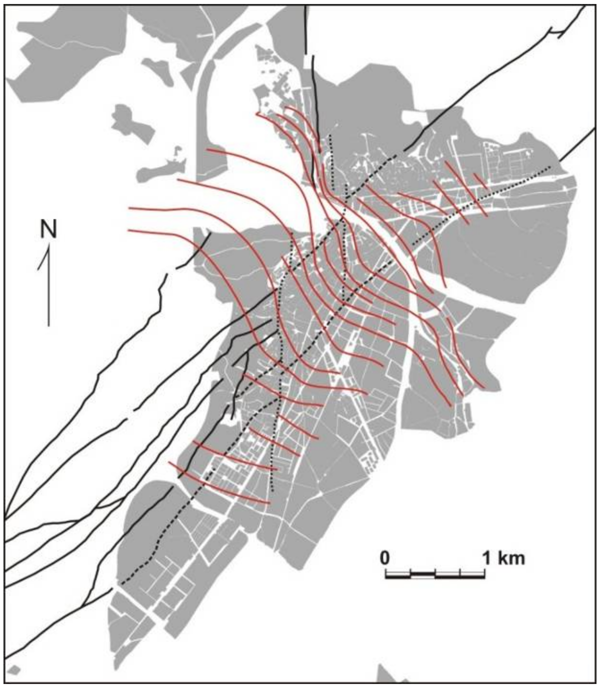

Fig. 8: Trajectories of maximum deformation (red lines) made from interpolating the point of maximum deformation results deduced from the individual analysis of the structures (EAE's). It is also represented the main tectonic structures present in the 1:25.000 scale geological mapping.

These changes in the direction of the trajectories do not seem to be interrelated neither with the orientation of the major streets and avenues of the city (Figure 6c) nor with the distance to the epicenter (nor even with its azimuth regarding the affected structures). The orientations of trajectories are determined by the major faults presents in the geological cartography: strike-slip faults with reverse component in NE-trending and normal faults oriented N-S (Figure 8).

DISCUSSION AND CONCLUSIONS

The focal mechanism of Lorca earthquake calculated by the IGN define a left lateral reverse fault with nodal planes oriented N127ºE 59ºSE and N040ºE 69NW. The nodal planes of focal mechanism construction have an angular fitting with the strain orientations obtained from the analysis of whole effects: one is perpendicular and the other one is parallel. However the nodal plan that better fit with the geological cartography (Fig. 8) is the oriented one according to N040ºE, it is to say, the plane perpendicular to the average orientation of damages observed in the city of Lorca (N130ºE). Moreover, this orientation is normal to directivity of the seismic waves propagation (N220º) obtained by López-Comino et al. (2012).

The near-field instrumental earthquakes can be analyzed from oriented damages. We have obtained similar results to the analysis of acelerogram in relationship with the fault plane orientation and the rupture directivity.

The use of this methodology permits to corroborate its utility when analyzing archaeological and historical buildings, presenting it as a very useful instrument to take advantage of the historical seismicity knowledge of a zone.

This type of analysis offers new research lines that could be apply to seismic hazard analysis and to the preservation of the historical heritage.

Acknowledgements: This work has been supported by Spanish research projects EDASI (Fundación MAPFRE), RESCATELO (CGL2011-14925-E) and it is a contribution to INQUA Project 1229 (EEE Metrics), IGCP-567 and QTECT (AEQUA spanish association).

References

Giner-Robles, J.L.; Rodríguez-Pascua, M.A.; Pérez-López, R.; Silva, P.G.; Bardají, T.; Grützner C. y Reicherter, K. 2009. *Structural analysis of Earthquake Archaeological Effects (EAE) Baelo Claudia Examples (Cádiz, South Spain)*, 137 pp.

Giner-Robles, J.L.; Silva Barroso, P.G.; Pérez-López, R.; Rodríguez-Pascua, M.A.; Bardají Azcárate, T.; Garduño-Monroy, V.H. y Lario Gómez, J. 2011. *Evaluación del daño sísmico en edificios históricos y yacimientos arqueológicos. Aplicación al estudio del riesgo sísmico*. Proyecto EDASI". Serie Investigación. Fundación MAPFRE, 96 pp.

Lopez-Comino, J.A.; Mancilla, F.; Morales, J. y Stich, D. 2012. Rupture directivity of the 2011, Mw 5.2 Lorca earthquake (Spain". *Geophysical Research Letters*, 39.

Rodríguez-Pascua, M.A., Pérez-López, R., Silva, P.G., Giner-Robles, J.L., Garduño-Monroy, V.H., y Reicherter, K. 2011. A Comprehensive Classification of Earthquake Archaeological Effects (EAE) for Archaeoseismology, *Quaternary International*, 242: 20-30.

Rodríguez-Pascua, M.A., Pérez-López, R., Giner-Robles, J.L., Silva, P.G., Garduño-Monroy, V.H., y Reicherter, K. 2012. (en este volumen): Efectos Arqueológicos del terremoto de Lorca del 11 de mayo de 2011 en su Patrimonio Cultural. Nuevas estructuras de deformación y reactivación de estructuras anteriores pertenecientes al terremoto de 1674.

PALEOSEISMOLOGY & ARCHAEOSEISMOLOGY
MORELIA • MEXICO 2012
INQUA-TERPRO PALEOSEISMOLOGY
EARTHQUAKE ARCHAEOLOGY

SOCIAL MEDIA AND WEB 2.0 IN EARTHQUAKE GEOLOGY

Grützner, Christoph (1), Schmidt, Martin (2), Klinger, Riccardo (3)

(1) RWTH Aachen University, Neotectonic and Natural Hazards Group, Lochnerstr. 4-20, 52064 Aachen, Germany. c.gruetzner@nug.rwth-aachen.de
(2) www.starteins.de, Reumontstr. 36, 52064 Aachen, Germany.
(3) www.digital-geography.com, Feldtmannstr. 132 B, 13088 Berlin, Germany

Abstract (Social media and web 2.0 in earthquake Geology): *This paper throws light on the manifold of Web2.0 sources and social media related to earthquake geology. We discuss special web mapping applications and databases, blogs, paper-related websites, video and photo services, social media networks and news services with regard to our research field. A website specially designed for paleoseismological topics is introduced and its visitor numbers presented. The statistics clearly reveal that the site is regarded as a news source in case of catastrophic earthquake events.*

Key words*: twitter, blog, facebook, paleoseismicity*

INTRODUCTION

Hundreds of new scientific applications have emerged during the last years and it is hard to imagine modern scientific work without internet access. This is not only true for communication purposes, but also for administrative work, organization of congresses, workshops and field trips, data storage and transfer, data bases and archives, online publications, literature search, data visualization, work crowd sourcing and online collaboration, polls, etc. In Geography, web-based applications have opened an entire new research field by using geographical information systems (GIS; Rhind, 1988; Walsh, 1988). Other map-based applications like GoogleEarth have become powerful tools for geoscientists (Butler, 2006). Recently, the so-called Web2.0 (a more collaborative, interactive and user-dependent world wide web) opened new horizons for researchers and teachers by easing discussions and using the power of many to solve tasks that were too laborious in the past. These techniques also include social media with its most prominent representatives being Facebook, Twitter, and YouTube among more specialized business networks like Xing or Academia and also photo services like Instagram and Flickr.

In earthquake geology, the advantages of internet-based techniques have been incorporated like in any other science discipline. A first Web2.0-like attempt could be seen in the mailing lists that were used to spread information in the field of earthquakes, tectonics, and tsunamis (e.g., EQ-GEO-NET, 2012). This paper aims on providing an overview about different approaches and possibilities without claiming to be complete. It throws light on a project especially designed for earthquake geologists, the webpage www.paleoseismicity.org.

WEB2.0 AND SOCIAL MEDIA IN EARTHQUAKE GEOLOGY

Mapping utilities

GIS-based or other web mapping applications are widely used for making all kinds of data available to a broader audience. In many cases, GoogleEarth imagery serves as a data base for terrain models, geospatial data and satellite views (GoogleEarth, 2012). Many applications are available for mobile devices. Not only are open source GIS programs available for all operating systems, but it is also possible to enhance the software's performance by using programming languages like Python, C++, Java, R, etc. (Etherington, 2011; Digital Geography, 2012). Numerous websites, mainly run by professional users, specialize on providing help with these techniques, discuss problems with users in forums, and publish tutorials (geo-affine, 2012) and video guides (ricckli, 2012).

In earthquake geology and related research fields, several databases and applications are available to be used by researchers. These include:

- The EEE catalogue documents Earthquake Environmental Effects worldwide and is based on the GoogleEarth API (Guerrieri, et al., 2011; EEE catalogue, 2012).
- The Archive of Historical Earthquake Data (AHEAD, 2012) is maintained by the SHARE project (SHARE, 2012) and collects information on historical events in Europe and the Mediterranean. Within the SHARE project, a European and Mediterranean database on active faults is currently being established, including the Greek Database of Seismogenic Sources (GreDaSS; Sboras, 2012).
- The European-Mediterranean Seismological Centre runs two databases. The EMSC database (EMSC, 2012) allows to access worldwide instrumental seismicity data from Oct 2004. SHERPA (2012) collects images from earthquake surface ruptures.
- QAFI is a database on the active faults on the Iberian Peninsula (QAFI, 2012) and run by the Spanish Institute for Geology and Mining (IGME).
- The Database of Potential Sources for Earthquakes Larger than M 5.5 in Europe was established at the Italian INGV, following the FAUST project (FAUST, 2012).

- Outcropedia (2012) is a map-based collection of outcrop locations and photographs, among them fault scarps and other earthquake related features.

What all these examples have in common is that they are easy to use and can be accessed worldwide. Some allow users to register and to add content.

Facebook and Twitter

Among other social networks like Google+ (Google+, 2012), Facebook (2012) has proven to be the most popular web service of its kind. A number of groups are specialized on earthquakes and related topics; some of them are private, and some are run by institutions like the INQUA or university departments (e.g., AGD-GIG, 2012; GIS-users, 2012). Group members use these platforms to share information on latest publications, to discuss meetings and scientific questions, to inform about job opportunities and to create public outreach. Institutions do not only inform about their current achievements, but also share information of broader interest to the community. Often, these pages are very specialized (e.g., paleoseismicity, 2012; INQUA_ECR, 2012; Geodynamics & Geofluids - KU Leuven, 2012). Especially after damaging earthquakes and tsunamis, Facebook is widely used to rapidly obtain information about the event's impact and consequences. Also, first aid and relief campaigns have subsequently been organized through this website.

One important thing always to be remembered when using Facebook, despite its obvious usefulness for spreading information, is the huge number of fake accounts, false information and pseudo-scientific quacks that are present due to the lack of any review process.

Twitter is a short message service that allows its users to publish messages that may not exceed 140 characters (Twitter, 2012). Those following an account are then notified about the new "tweet". Twitter is probably the fastest social media news site. Some research has already been done on the use of the spatial distribution of tweets in combination with certain keywords ("hashtags") like #earthquake to detect earthquakes (Earle et al., 2010; Sakaki et al., 2010). Fischer (2011) published a nice example of the tweet behaviour after the Virginia M5.5 earthquake from 23 Aug 2011. Twitter is often used to collect news streams, e.g., from earthquake detection websites and tsunami warning institutions (@ItalyQuakes, 2012; @tsunamiwatch, 2012; @USGS_EQ_CA, 2012). It can, therefore, be an important tool to spread earthquake and tsunami information quickly. False alarms, however, may also be spread fast. Additionally, notifications about recent publications, blog entries and other relevant data can be easily spread, very rapidly. One of the major disadvantages of Twitter is surely the sheer number of accounts and tweets sent every day. Important information may be drowned out by the huge volume of tweets, reducing Twitter's efficiency to spread valuable information. Also, it is a common phenomenon that pseudoscientific accounts like @quakeprediction (2012) have far more followers than reliable sources (@lastquake, 2012).

Photo and video services

Services like Panoramio (Panoramio, 2012) allow users upload photos, to tag and to geotag them, and to make them available to the public via GoogleEarth. While there are more specialized sources like Outcropedia, tags like "earthquake", "fault", "tsunami" etc. allow users to quickly access thousands of images that are related to natural disasters, environmental earthquake effects and other topics. Usually, there is either a minor review on the image quality or none at all. The lack of review can lead to location errors and/or wrong tagging. The aforementioned EMSC database (SHERPA, 2012) specializes on earthquake rupture images.

YouTube is the world's largest video platform and contains thousands of earthquake-related videos (YouTube, 2012). Among them are hundreds of unique documents on the primary and secondary effects of earthquakes, tsunamis, and related phenomena. It is, however, not always simple to verify the source. Several institutions like universities run their own YouTube channels and provide information on research projects and ongoing work (e.g., OregonGeology, 2012). Numerous channels also specialize on geoscience education and training. Again, there is a need to check the sources and to identify pseudo-scientific accounts.

Special cases are videos that are associated to scientific publications. One example to illustrate the use of this approach is by Garcia-Castellanos (2011). The video shows an animation of the "Geography of the Gibraltar Arc during the early stages of the Messinian Salinity Crisis" (Garcia-Castellanos, 2011) and was created to accompany a paper on the same topic by the same authors (Garcia-Castellanos & Villaseñor, 2011). Surprisingly, a scientific discussion was triggered in the video's comments. Animations prove very helpful to illustrate complex features in certain cases, and may result in a public outreach that can often not be created by scientific publications alone.

Papers with websites

There are several papers that have associated homepages. The reason for, in most cases, is that programs or source codes are published this way and made available to the (scientific) community. Three examples may illustrate this application of online services:

- A number of online plate motion calculators are freely available (see UNAVCO, 2012 for an overview). DeMets et al. (2010), for example, did not only publish this paper but also set up an online calculator based on the publication (MORVEL, 2012).
- Atakan et al. (2000) introduced a logic tree for calculating uncertainties in paleoseismologic investigations. The software that was created for that purpose can be downloaded from a special website at Bergen University (UNIPAS, 2012).

- Williams et al. (2011) published their research on a paleoearthquake that happened around the early first Century AD in the Dead Sea. Since the topic was likely to cause media coverage and a broader interest, Williams also set up a blog, explaining the science to non-professionals (Dead Sea Quake, 2012).

Blogs

A number of blogs related to earthquake geology can be found, although they share only a minor part of the geoblogosphere. The reasons for blogging about scientific topics are manifold, but one main reason seems to be the possibility to easily receive feedback. Some bloggers seek to inform or entertain the public

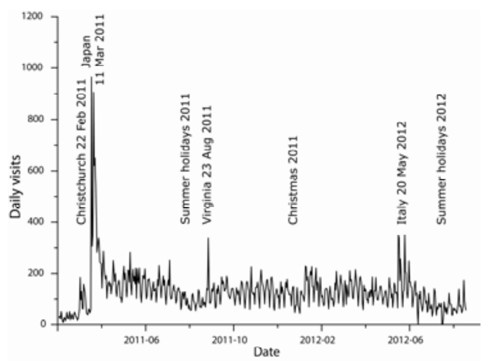

Fig. 1: The daily visits to paleoseismicity.org are clearly related to earthquake events which were covered by blog posts.

rather than to address colleagues from the scientific community, others prefer to discuss scientific topics with researchers worldwide. Blogging using the English language ensures a broad audience, however, many bloggers prefer to use their native tongue to address the local public and to keep an excellent style of writing (e.g., Mente et Malleo, 2012; Planeet Aarde, 2012). Some blogs are designed as multiple-author blogs (Earthquake Geology in Greece, 2012; Paleoseismicity.org, 2012). Besides the aforementioned ones, blogs related to earthquake geology and similar topics include: Active tectonics (2012); Groundswell (2012); History of Geology (2012); Paleotsunami travels (2012); Retos Terrícolas (2012); Salvatore Barba (2012); and The Trembling Earth (2012). The above list should not to be regarded as a complete and some of them only cover earthquakes occasionally. A good way to keep informed of the latest posts is Geobulletin (2012), which lists almost all known geoblogs.

PALEOSEISMICITY.ORG

Based on our experience with existing geoblogs, we felt a need for an online resource specially dedicated to paleoseismology, archaeoseismology, neotectonics and earthquake geology. Paleoseismicity.org (2012) is designed as a multi-author blog platform, where anyone interested in participating can register via e-mail and write posts. An event calendar is integrated to collect data on upcoming workshops and conferences. A specialty of the site is the directory, which is a list of the people who carry out research and work in paleoseismology thorough the world. This is a unique dataset, useful to anyone who needs to contact a paleoseismologist or to looks for collaborators. Statistics on the number of visits make clear that the popularity of the site strongly depends on blog posts on recent catastrophic earthquake events (Fig. 1). A fast response to those events increases the visitor numbers. Also, seasonal and weekly fluctuations are obvious. This illustrates how blogs run by scientists are regarded as an important news source by the interested public.

DISCUSSION

Social media and Web2.0 have already found their place in the field of earthquake geology, and it turns out that there is a special need for news, additional to the press coverage, on catastrophic earthquake and tsunami events. Also, social media are widely used to discuss scientific problems and news - a service that naturally cannot be covered by classic scientific journals. However, the advantages, such as the rapid spread of information and the ability to discuss and reach the public, do take their toll; the lack of review leads to a growing number of quacks and pseudoscientific members that may not easily be identified by non-professionals, despite scientists being able to recognize them immediately.

References

@ItalyQuakes 2012. Earthquakes in Italy, Latest earthquakes (terremoti) recorded by the INGV seismic network (italy). https://twitter.com/ItalyQuakes, Twitter account.

@lastquake 2012. EMSC, Not-for-profit scientific NGO and provider of rapid earthquake information which invites eyewitnesses to share their experience and pics. Tell us, it helps! https://twitter.com/LastQuake, Twitter account.

@Quakeprediction 2012. Earthquake forecasts. Earthquake forecasts for Los Angeles, San Francisco, San Diego California and Japan updated every 24 hours. Forecasts based on research since 2005, https://twitter.com/Quakeprediction, Twitter account.

@tsunamiwatch 2012. tsunami watch, A bounced feed from the Pacific Tsunami Warning Center. We proudly support Handle With Care International - who provide humanitarian aid to impoverished people, https://twitter.com/tsunamiwatch, Twitter account.

@USGS_EQ_CA 2012. USGS Earthquake CA, A Twitter feed of USGS Earthquake notifications for the State of California over M2.5, https://twitter.com/USGS_EQ_CA, Twitter account.

Active Tectonics 2012. Active tectonics blog, http://activetectonics.blogspot.de/, blog.

AGD-GIG 2012. Archaeological Geology Division (AGD) of the Geological Society of America (GSA) and the Geoarchaeology Interest Group (GIG) of the Society for American Archaeology (SAA), https://www.facebook.com/groups/33028214313/members/, Facebook group.

AHEAD 2012. Archive of Historical Earthquake Data, http://www.emidius.eu/AHEAD/main, web database.

Atakan, K., Midzi, V., Moreno Toiran, B., Vanneste, K., Camelbeeck, T., Meghraoui, M. 2000. Seismic hazard in regions of present day low seismic activity: uncertainties in the paleoseismic investigations along the Bree fault scarp

(Roer Graben, Belgium). *Soil. Dyn. Earthquake, Eng.*, 20, 415-427.

Butler, D. 2006. Virtual globes: The web-wide world. *Nature*, 439, 776-778.

Dead Sea Quake 2012. Geologic Research into an Earthquake that occured during the same time period as the crucifixion, http://www.deadseaquake.info/home/, website.

DeMets, C., Gordon, R.G., Argus, D.F. 2010. Geologically current plate motions, *Geophysical Journal International*, 181, 1, 1-80, doi: 10.1111/j.1365-246X.2009.04491.x.

Digital Geography 2012. http://digital-geography.com/, blogger community.

Earle, P., Guy, M., Buckmaster, R., Ostrum, C., Horvath, S., Vaughan, A. 2010. OMG earthquake! Can twitter improve earthquake response? *Seismological Research Letters*, 81, 2, 246-251.

Earthquake Geology in Greece 2012. http://eqgeogr.weebly.com/blog.html, blogger community.

EEE Catalogue 2012. Earthquake Environmental Effects, http://www.eeecatalog.sinanet.apat.it/terremoti/index.php, web database.

EMSC 2012. European Mediterranean Seismological Centre, http://www.emsc-csem.org/Earthquake/?filter=yes, web database.

EQ-GEO-NET 2012. eq-geo-net-ml@aist.go.jp, mailing list maintained by Takashi Azuma, Active Fault and Earthquake Research Center, AIST (Tsukuba, JAPAN).

Etherington, T.R. 2011. Python based GIS tools for landscape genetics: visualising genetic relatedness and measuring landscape connectivity. *Methods in Ecology & Evolution*, 2, 1, 52-55.

Facebook 2012. https://www.facebook.com, social network.

FAUST 2012. Faults as a Seismologists' Tool. The Database of Potential Sources for Earthquakes Larger than M 5.5 in Europe. http://faust.ingv.it/current_2.htm, web database.

Fischer, E. 2011. Animated map of earthquake Tweets, Aug 23, 2011. http://www.flickr.com/photos/walkingsf/6079677293, Flickr photo service website.

Garcia-Castellanos 2011. 3D animation - Mediterranean isolation and desiccation during the Messinian Salinity Crisis, http://youtu.be/bw-qf_zQMWs, YouTube video.

Garcia-Castellanos, D., Villaseñor, A., 2011. Messinian salinity crisis regulated by competing tectonics and erosion at the Gibraltar arc. *Nature*, 480, 359-363.

geo-affine 2012. http://www.geo-affine.org, blog.

Geobulletin 2012. http://www.geobulletin.org/, blog list and news service.

Geodynamics & Geofluids - KU Leuven 2012. University of Leuven, https://www.facebook.com/pages/Geodynamics-Geofluids-KU-Leuven/252767388103831, Facebook page.

GIS-users 2012. https://www.facebook.com/groups/gis.users/, Facebook group.

GoogleEarth 2012. http://www.google.com/earth/index.html, homepage.

Google+ 2012. https://plus.google.com, social network.

Groundswell 2012. Earthquake outreach, http://groundswell.azgs.az.gov/, blog.

Guerrieri, L., Blumetti, A.M., Brusita, E., Esposito, E., Lucarini, M., Michetti, A.M., Porfido, S., Serva, L., Vittori, E. & the INQUA TERPRO Project #0811 Working Group 2011. Earthquake environmental effects, intensity and seismic hazard assessment: The EEE Catalogue (INQUA Project #0418). In: **Grützner, C., Fernández Steeger, T., Papanikolaou, I., Reicherter, K., Silva, P.G., Pérez-López, R., Vött, A. (eds.): Proceedings 2nd INQUA-IGCP567 International Workshop on Active Tectonics, Earthquake Geology, Archaeology and Engineering 19-24 September 2011, Corinth (Greece), 62-65**.

History of Geology 2012. http://historyofgeology.fieldofscience.com/, blog.

INQUA_ECR 2012. INQUA Early Career Researchers, https://www.facebook.com/INQUAECR, Facebook page.

Mente et Malleo 2012. Mit Verstand und Hammer die Erde erkunden. http://www.scilogs.de/wblogs/blog/mente-et-malleo, blog (in German).

MORVEL 2012. MORVEL and NNR-MORVEL56 plate velocity estimates and information, http://geoscience.wisc.edu/~chuck/MORVEL/index.html, website.

OregonGeology 2012. Oregon Deptartment of Geology & Mining Industry http://www.youtube.com/user/OregonGeology, YouTube channel.

Outcropedia 2012. The online outcrop database project, http://www.outcropedia.org, web database.

Paleoseismicity 2012. Paleoseismicity.org, https://www.facebook.com/pages/Paleoseismicity/139495536098998, Facebook page.

Paleoseismicity.org 2012. Http://www.paleoseismicity.org, blogger community.

Paleotsunami travels 2012. http://paleotsunami.blogspot.de/, blog.

Panoramio 2012. www.panoramio.com, geotagged photo database.

Planeet Aarde 2012. Blogportaal voor wetenschap. http://weetlogs.scilogs.be/index.php?blogId=19, blog (in Dutch).

QAFI 2012. Quaternary Active Faults Database of Iberia v.2, http://www.igme.es/infoigme/aplicaciones/qafi, web database.

Retos terrícolas 2012. Earth Science Blog, http://retosterricolas.blogspot.de, blog.

Rhind, D. 1988. A GIS research agenda. *International Journal of Geographical Information Systems*, 2, 1, 23-28.

ricckli 2012. Riccardo Klinger, http://www.youtube.com/user/ricckli, YouTube channel.

Sakaki, T., Okazaki, M., Matsuo, Y. 2010. Earthquake shakes Twitter users: real-time event detection by social sensors. *Proceedings of the 19th international conference on World wide web, WWW '10,* 851-860, New York, NY, USA, April 2010. ACM.

Salvatore Barba 2012. http://salvatorebarba.blogspot.de/, blog

Sboras, S. 2012. The Greek Database of Seismogenic Sources: seismotectonic implications for North Greece, PhD Thesis, University of Ferrara, 252 p., http://www.scribd.com/doc/88588015/The-Greek-Database-of-Seismogenic-Sources-seismotectonic-implications-for-North-Greece.

SHARE 2012. Seismic Hazard Harmonization in Europe, http://www.share-eu.org, project website.

SHERPA 2012. Sharing of Earthquake Rupture Pictures Archive, http://sherpa.emsc-csem.org, web database.

The Trembling Earth 2012. Exploring the phenomenon of earthquakes, http://tremblingearth.wordpress.com/, blog.

Twitter 2012. http://www.twitter.com, social short message service.

UNAVCO 2012. Plate Motion Calculator, http://www.unavco.org/community_science/science-support/crustal_motion/dxdt/model.html, website.

UNIPAS 2012. Software for systematic treatment of uncertainties in paleoseismic investigations. http://www.uib.no/rg/geodyn/artikler/2010/02/software#unipas, website.

Walsh, S.J. 1988. Geographic Information Systems An Instructional Tool for Earth Science Educators. *Journal of Geography*, 87, 1, 17-25.

Williams, J.B., Schwab, M.J., Brauer, A. 2011. An early first-century earthquake in the Dead Sea. *International Geology Review*, 54, 10, 1219-1228.

YouTube 2012. Broadcast yourself, http://www.youtube.com, video platform.

EARTHQUAKE ENVIRONMENTAL EFFECTS INDUCED BY THE 2012 SEISMIC SEQUENCE IN EMILIA: IMPLICATIONS FOR SEISMIC HAZARD ASSESSMENT IN NORTHERN ITALY

Guerrieri Luca (1), Vittori Eutizio (1), Di Manna Pio (1), Piccardi Luigi (2), Castaldini Doriano (3), Berlusconi Andrea (4), Blumetti Anna Maria (1), Comerci Valerio (1), Livio Franz (4), Michetti Alessandro Maria (4)

(1) ISPRA, Servizio Geologico d'Italia, Via Vitaliano Brancati 48, 00144 Roma, ITALY
(2) CNR, Istituto di Geoscienze e Georisorse, Via La Pira, 4, 50121 Firenze, ITALY
(3) Dipartimento di Scienze Chimiche e Geologiche, Università degli Studi di Modena e Reggio Emilia, Largo S. Eufemia, 19. 41100 Modena, ITALY
(4) Dipartimento di Scienza e Alta Tecnologia, Università dell'Insubria, Via Valleggio, 11, 22100 Como

Abstract (Earthquake Environmental Effects induced by the 2012 seismic sequence in Emilia: implications for seismic hazard assessment in Northern Italy): *The field characterization of Earthquake Environmental Effects occurred in the epicentral area of the 2012 Emilia seismic sequence (mainly liquefaction-type phenomena, ground fractures and hydrological anomalies) has allowed i) to identify in the affected area the zones more susceptible to local geological instability and ii) to make an independent intensity assessment through the ESI 2007 intensity scale.*

The distribution of ground effects is suggestive of two events of Intensity VIII, even if the maximum intensity might have been even higher (IX?) in San Carlo and Mirabello. Nevertheless, the estimated intensity of the 2012 Emilia earthquake is sensibly less than that recorded in the Po Plain area in historical times (I_0 IX to X), and therefore should not be considered the "reference earthquake" for this area.

Key words*: Earthquake Environmental Effects, liquefaction, ESI 2007, seismic hazard.*

INTRODUCTION

This note aims at characterizing Earthquake Environmental Effects induced by the seismic sequence that affected a portion of Emilia region (Northern Italy) since May 20, 2012.

The sequence has been characterized by two main shocks (Fig. 1) occurred on May 20 (Ml = 5.9; epicenter near Finale Emilia; focal depth about 6 km) and May 29 (Ml = 5.8; epicentre about 12 km west of the first shock; focal depth about 10 km). Furthermore, five more Ml ≥ 5 shocks and thousands of aftershocks of lower magnitude, have distributed on an about 40 km long WNW-ESE trending zone. Most of these events have been characterized by NNE-SSW nearly pure compression.

The detailed characterization of the geological effects caused by the main shocks (mainly ground cracks, liquefaction-type phenomena and hydrological anomalies) has allowed i) to identify in the affected area the zones more susceptible to local geological instability in case of earthquake occurrence and ii) to make an independent intensity assessment through the ESI 2007 intensity scale (Guerrieri and Vittori, eds., 2007), which is based only on coseismic effects on the natural environment.

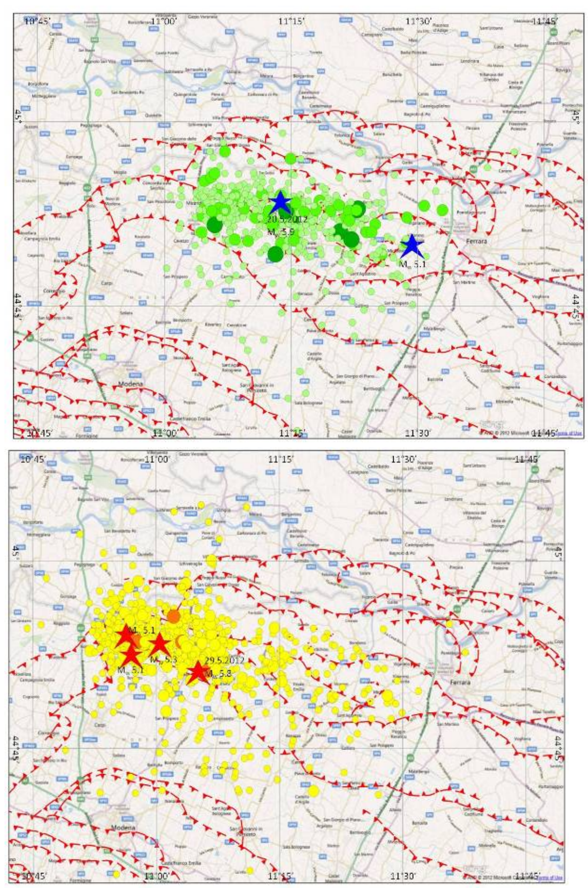

Fig. 1 - The 2012 Emilia seismic sequence is characterized by a first main shock occurred on May 20 and associated aftershocks (in green, see above) and a second main shock occurred in May 29, and associated aftershocks (in yellow, see below). Red lines are buried thrusts, many of them judged capable of causing coseismic surface deformation (source: ITHACA).

GEOLOGICAL FRAMEWORK

In the subsoil of the 2012 Emilia earthquake epicentral area are located compressive structures of the Apennines' orogenic belt overlain by marine and continental deposits of the Po River plain. Active convergence of northeast-verging Apennines and south-verging Southern Alps structures is clearly indicated by stratigraphic, morphologic, geodetic and seismic evidence (e.g. Serva, 1990; Castiglioni, 1997; Boccaletti et al., 2004; Toscani et al., 2009; Boccaletti et al., 2011; Comerci et al., 2012; Michetti et al., 2012, and references therein).

Active tectonics strongly controls the complex drainage and paleo-drainage pattern of the local rivers (Po, Secchia, Panaro and Reno), together with climatic conditions and human activities. Several localities in the epicentral region are located on the ancient (last two millennia) abandoned channels of these rivers (Castaldini et al., 1979; Castiglioni and Pellegrini, 2001).

Some active fault-related folds (e.g. the Mirandola structure, Fig. 2) are very close to the ground surface, even deforming the topographic surface. Several other thrusts, also supposed to be capable of producing surface deformation are shown in the ITHACA database (http://sgi1.isprambiente.it/GMV2/index.html?config=config_sismaMO.xml).

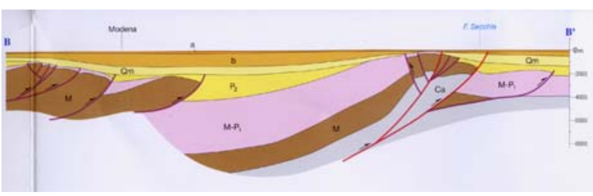

Fig. 2 - The Mirandola compressive structure, with faults cutting Upper Pleistocene deposits (Boccaletti et al., 2004).

The epicentral zone corresponds to the so-called Novi-Poggio Renatico seismogenic source (DISS, 2010), made by the individual sources Mirandola, Canalazzo di Finale Emilia and Concordia (expected Mw 5.9). According to Serva (1990), these structures are associated to a potential Intensity VIII (MCS) earthquake. Historical catalogues point out that a seismic sequence comparable to the present one occurred in 1570-1574 (Guidoboni et al., 2007, Castelli et al., 2012).

CHARACTERIZATION OF GROUND EFFECTS

More than five hundred ground effects have been recognized, spread over an area of about 700 km^2 (Fig. 3), mainly liquefaction-type phenomena, ground ruptures and hydrogeological anomalies (strong water-table fluctuations). About four hundred effects were mostly located in the eastern and northern sectors, induced by the first main shock (May 20), while more than one hundred ground effects followed the second main shock (May 29). The collected data have been progressively added to the EEE Catalogue, on-line in the portal (http://www.eeecatalog.sinanet.apat.it/emilia/earthquake/index.php).

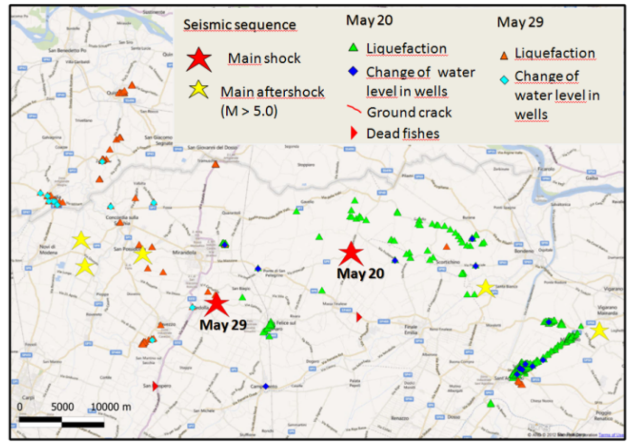

Fig. 3 – Earthquake Environmental Effects induced by the 2012 Emilia earthquake.

Liquefaction-type effects and ground cracks

Liquefaction-type effects have been the most relevant type of Earthquake Environmental Effect. In general, ejection of sand has occurred along ground cracks, often made evident by alignments of emission points.

The zone with the most evident and widespread effects induced by the first main shock (May 20) is unquestionably located at San Carlo (Fig. 3 and 4), in the municipality of Sant'Agostino. Here, large ground cracks and widespread liquefaction-type phenomena affected paved roads, buildings and farmed land.

These effects were concentrated on a relatively narrow NE-SW trending elongated area, about 6.5 km long, running from San Carlo to Mirabello (Fig. 4). The ground ruptures were almost continuous, damaging all the constructions above them, especially the houses in San Carlo) and the industrial settlements between San Carlo and Mirabello.

This area is entirely located in correspondence to the right embankment of a paleo-channel of the river Reno, active till the end of the XVIII century, mostly characterized by sands, interbedded by finer layers (clays and silts). These local conditions have undoubtedly promoted the occurrence of ground open cracks and liquefactions and significantly enhanced their size.

Ground ruptures were very often characterized by a significant vertical offset (generally lowering to the NW side) that locally reached 50 cm already on the day after the first main shock (Fig. 5a). This offset was apparent especially in the area between San Carlo and the cemetery of Sant'Agostino, where opening of cracks was generally in the order of tens of centimeters, and occasionally in excess of half a meter. Repeated surveys have shown a clear post-seismic evolution of ground cracks in terms of their increase of throw and opening.

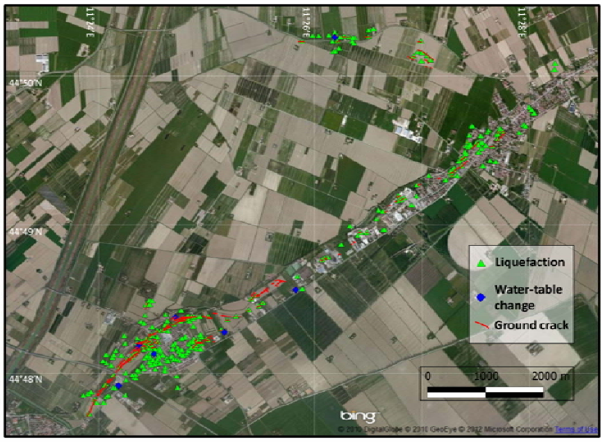

Fig. 4. Liquefaction-type phenomena and ground ruptures between Sant'Agostino and Mirabello. These effects, distributed on a NE-SW trending elongated area on an ancient embankment of the river Reno, have heavily damaged private buildings and industrial settlements located above them. Other effects have been mapped in a WNW-ESE trending narrow area located some km northwest of the Mirabello village. These effects were found on a very flat portion of the floodplain, not directly linked to any ancient embankment.

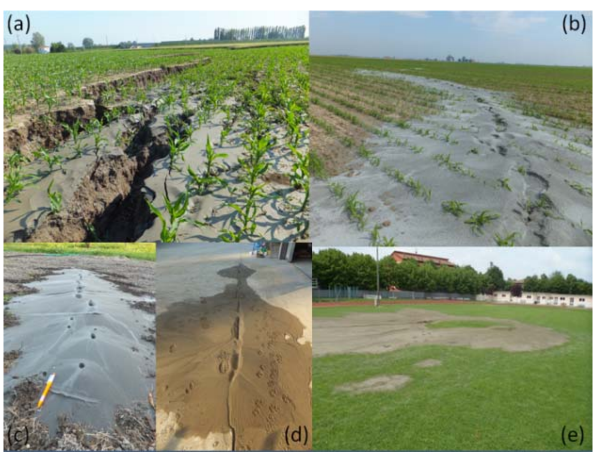

Fig. 5. Ground ruptures and associated liquefaction-type phenomena at San Carlo (a), Scortichino (b), Cavezzo (c, d) and San Felice sul Panaro (e).

Ground cracks were typically associated to liquefactions. The areal extension of ejected material was very different, ranging from a few square meters up to many hundreds of square meters. Commonly, grain size of sand gets finer, up to clayey silt, moving upwards in emission cones.
It must be noted that similar effects were found in other areas of the Po River flood plain that were not related to ancient embankments (northwest of Mirabello and Obici (Fig. 5b).

The second main shock induced the occurrence of analogous effects; in particular, large ground ruptures with emission of sand have been documented mainly in the Cavezzo, San Possidonio, Moglia and Quistello territorial municipalities (Figs. 3c and 3d).

Hydrological anomalies
A relevant increasing of water-table level (from 3-4 up to 8-9 m) was measured in the water wells. Sometimes liquefied sand was ejected out of wells, or often following paths on the outer face of the casing, most likely associated to liquefaction. In some cases, the water outflow, associated or not to sand ejection, has continued for hours after the earthquake. Increasing in water temperature as well as an anomalous concentration of H_2S were also reported.
Concerning the May 29 main shocks, hot water from ground cracks and water wells has been noted at San Possidonio and Moglia.
Furthermore, beginning a few days before the onset of the seismic sequence, an anomalous activity was noted in some mud volcanoes (locally named "Salse"), located at the margin of the Modena and Reggio Emilia Apennines, about 40 km far from the epicentral area.

ESI intensity assessment
Although some liquefaction-type and hydrogeological effects may have escaped recording in more remote areas or hidden by grown crops, the scenario of Earthquake Environmental Effects is certainly fully representative of the most significant ground effects. Therefore, it is adequate to define a preliminary macroseismic intensity field (Fig. 6) based on the ESI 2007 scale (Guerrieri and Vittori, eds., 2007), the seismic intensity scale entirely based on the characteristics and size of earthquake-induced environmental effects, already applied to several modern, historical and paleoearthquakes (e.g. Reicherter et al., eds., 2009 and bibliography therein).
The total area where ground effects were mapped is in the order of 300-400 km^2 for each event: this indicates that the ESI epicentral intensity of the two main shocks is VIII.
ESI local intensity values in excess of VIII, possibly reaching the IX degree have been recorded in two localities (San Carlo and Mirabello), based on the size and length of ground ruptures and areal distribution of liquefaction, showing a specific vulnerability of the natural environment at the local scale.
Comparing the ESI local intensity values with the macroseismic intensity evaluations (MCS, Galli et al., 2012) based on the pattern of damages to buildings, it is evident that: i) epicentral intensity evaluations are comparable; ii) where available, Earthquake Environmental Effects can be a better tool for local intensity assessment, since they are independent from the type of construction, but are governed directly by the true geological site conditions.

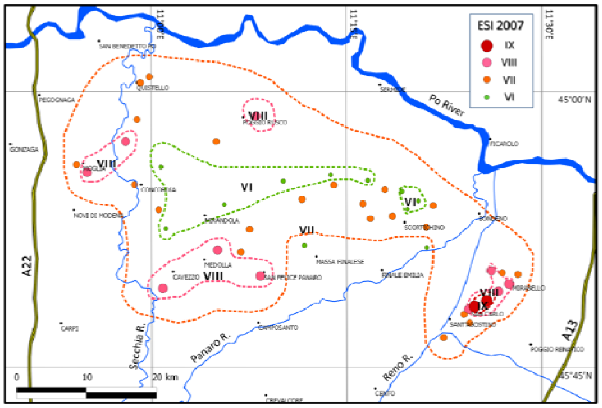

Fig. 6. ESI local intensities (based on the characteristics of the surveyed ground effects) and inferred isoseismals.

For these reasons, a macroseismic intensity field which integrates ESI and MCS intensity evaluations represents a better tool to characterize this event in the frame of the seismic hazard assessment of the Po Plain area. In this perspective, the 2012 Emilia event should be regarded as a relatively minor event when compared to the "reference earthquake" of the Po Plain, which, as demonstrated by the 1117 Verona and 1222 Brescia earthquakes (e.g., Serva 1990; Michetti et al., 2012), should be expected characterized by an intensity I_0 of IX to X degrees, both in the macroseismic scales and the ESI 2007.

FINAL REMARKS

The most common type of Earthquake Environmental Effect occurred in the epicentral area of the 2012 Emilia seismic sequence has been the liquefaction-type phenomenon, characterized by the ejection of sand from ground fractures and wells.
Such phenomena are not randomly distributed, but appear to concentrate along alignments which can be followed even for kilometers. This is the case of the impressive set of SW-NE aligned fractures, widely connected to lateral spread, between San Carlo and Mirabello, which follows the right margin of an abandoned and suspended river bed relative to a former course of the river Reno. All the effects along this alignment can be interpreted as secondary effects driven not only by the local stratigraphic characteristics of the subsoil, but also by the local recent geomorphological evolution, dominated by a complex network of palaeo-drainages and abandoned meanders. A less evident alignment is observable also in the distribution of the effects induced by the May 29 event near Cavezzo, related to an ancient bed of the river Secchia.
Other roughly east-west oriented alignments have been identified in completely flat areas of the Po flood plain (e.g., northwest of Mirabello and west of Bondeno). These alignments cannot be directly explained with the local influence of a palaeo-drainage. Instead, their origin might be linked to the presence of east-west trending tectonic discontinuities that characterize the very shallow subsoil of the area. The coseismic reactivation of these tectonic structures could have facilitated the occurrence of sand ejection up to the surface.
The distribution of ground effects is suggestive of two events of Intensity VIII on the ESI 2007 scale, even if the maximum intensity might have been higher (IX?) in San Carlo and Mirabello. Nevertheless, the estimated intensity of the 2012 Emilia earthquakes is sensibly less than that recorded in the Po Plain area in historical times (I_0 IX to X), and therefore the 2012 event should not be considered the "reference earthquake" for this area.

References

Boccaletti M., Bonini M., Corti G., Gasperini P., Martelli L., Piccardi L., Severi P., Vannucci G., 2004, Carta sismotettonica della Regione Emilia Romagna. Scala 1:250000. SELCA, Firenze.

Boccaletti, M., G. Corti and L. Martelli (2011). Recent and active tectonics of the external zone of the Northern Apennines (Italy), Int. J. Earth Sci. (Geol. Rundsch), 100(6), 1331-1348, DOI: 10.1007/s00531-010-0545-y

Castaldini, D., G. Gasperi, M. Panizza and M. Pellegrini (1979). Neotettonica dei Fogli 74 (Reggio nell'Emilia) (p.p.) e 75 (Mirandola) nell'intervallo da 18.000 B.P. all'Attuale (interv. V), CNR Progetto Finalizzato Geodinamica, Nuovi contributi alla realizzazione della Carta Neotettonica di Italia, Pubbl. 251, 317-332.

Castiglioni, G.B. (Coord.) (1997). Carta geomorfologica della Pianura Padana alla scala 1:250.000. SELCA, Firenze.

Castiglioni, G.B. and G.B. Pellegrini (2001). Note Illustrative della Carta Geomorfologica della Pianura Padana - Illustrative Notes of the Geomorphological Map of Po Plain, Suppl. Geogr. Fis. Dinam. Quat., IV.

Comerci, V., A.M. Blumetti, P. Di Manna, D. Fiorenza, L. Guerrieri, M. Lucarini, L. Serva and E. Vittori (2012). Il Progetto ITHACA e le Faglie Capaci della Pianura Padana, Ingegneria Sismica, Vol. Speciale "Rischio Sismico in Pianura Padana", in press.

DISS Working Group (2010). Database of Individual Seismogenic Sources (DISS), Version 3.1.1: A compilation of potential sources for earthquakes larger than M 5.5 in Italy and surrounding areas, http://diss.rm.ingv.it/diss/, © INGV 2010 - Istituto Nazionale di Geofisica e Vulcanologia.

Galli, P., Castenetto, S. and Peronace, E., (2012). Terremoto dell'Emilia, Maggio 2012. Rilievo macrosismico speditivo. Dipartimento della Protezione Civile Nazionale, Roma, 26 pp., http://www.protezionecivile.gov.it/resources/cms/documents/TerremotoEmiliaMCS.pdf

Guidoboni, E., G. Ferrari, D. Mariotti, A. Comastri, G. Tarabusi and G. Valensise (2007). Catalogue of Strong Earthquakes in Italy from 461 BC to 1997 and in the Mediterranean area, from 760 BC to 1500, An Advanced Laboratory of Historical Seismology, http://storing.ingv.it/cfti4med/.

Guerrieri, L. and E. Vittori, eds. (2007). Intensity Scale ESI 2007, Memorie Descrittive Carta Geologica. d'Italia, vol. 74, Servizio Geologico d'Italia – Dipartimento Difesa del Suolo, APAT, Roma, 53 pp.

Michetti, A.M., F. Giardina, F. Livio, K. Mueller, L. Serva, G. Sileo, E. Vittori, R. Devoti, F. Riguzzi, C. Carcano, S. Rogledi, L. Bonadeo, F. Brunamonte, and G. Fioraso (2012). Active compressional tectonics, Quaternary capable faults and the seismic landscape of the Po Plain (N Italy), Annals of Geophysics, accepted.

Reicherter, K., Michetti A.M. & P. G. Silva Barroso, 2009, Palaeoseismology: historical and prehistorical records of earthquake ground effects for seismic hazard assessment –

introduction. In Reicherter, K., Michetti, A.M. & Silva, P.G. (eds) Palaeoseismology: Historical and Prehistorical Records of Earthquake Ground Effects for Seismic Hazard Assessment. The Geological Society, London, Special Publications, 316, 1-10. DOI: 10.1144/SP316.9 0305-8719/09/ # The Geological Society of London 2009

Serva, L. (1990). Il ruolo delle Scienze della Terra nelle analisi di sicurezza di un sito per alcune tipologie di impianti industriali: il terremoto di riferimento per il sito di Viadana (Mn), Boll. Soc. Geol. It., 109, 375-411.

Toscani, G., P. Burrato, D. Di Bucci, S. Seno and G. Valensise (2009). Plio-Quaternary tectonic evolution of the Northern Apennines thrust fronts (Bologna-Ferrara section, Italy): seismotectonic implications, Ital. J. Geosci. (Boll. Soc. Geol. It.), 128, 2, 605-613, doi: 10.3301.IJG2009.128.2.605.

PALEOSEISMOLOGY & ARCHAEOSEISMOLOGY
MORELIA • MEXICO 2012
INQUA-TERPRO PALEOSEISMOLOGY
EARTHQUAKE ARCHAEOLOGY

Paleoseismic record in the recent deposits of Urao Lake (Merida Andes, Venezuela)

Huerta, Pedro (1), Audemard, Franck. (2), Guerrero, Omar (3), Cuevas, Rómulo (3) Alvarado, Miguel (3), Silva, Pablo, G (1).

(1) Dpto. Geología, Escuela Politécnica Superior de Ávila, Universidad de Salamanca. Ávila. SPAIN. phuerta@usal.es
(2) Fundación Venezolana de Investigaciones Simológicas, FUNVISIS, Final Prolongación Calle Mara, Quinta Funvisis, El Llanito, Caracas 1073, Venezuela. faudemard@funvisis.gob.ve
(3) Dpto. Geología General, Escuela de Ingeniería, Universidad de los Andes, Campus de La Hechicera, Mérida (Venezuela). oguerre@ula.ve

Abstract (Paleoseismic record in the recent deposits of Urao Lake (Merida Andes, Venezuela): *The Urao lake locates in the Merida Andes where the Boconó fault is the main fault system, a large dextral strike-slip fault system, in the area. This lake occurs in a pull apart basin developed between two branches of the above mentioned fault system. In this paper we describe the paleoseismic record found in 5 cores extrated in the lake. The paleoseismic evidences are faulted laminae, convoluted lamination, sand injections, and pillar structures. The proximity of these structures with active faults belonging to the Boconó fault system suggest that the mentioned structures record seismic events in this area of the Venezuelan Andes. The paleoseismic structures appear in two levels, approximately at 40-60 cm and 100-120 cm from the lake bottom. The ^{14}C cal. age of a bed situated at 238 cm is 300 years BP (Mazzarino, 2000). So the two levels with paleoseismic structures could correspond to two events later to 1650 AD. Assuming a sedimentation rate of 0.73 cm/year (0.68+ 0.05 cm/year), the bed at 120 cm depth corresponds with the event of 1812 AD (VIII intensity in the area), and the bed at 60 cm depth corresponds with the event of 1894 AD (VIII intensity in the area).*

***Key words**: Urao lake, Lagunillas, Merida, Santa Cruz de Mora, earthquake.*

INTRODUCTION

This paper describes the paleoseismic evidences in the Urao lake deposits. This lake is known by the alkaline carbonates (trona and gaylussite) which have been traditionally extracted by the locals to produce "Chimó" something like chewing tobacco.

The Urao lake occurs in the Venezuelan or Merida Andes which is a mountain range with NE-SW trend related to the Late Miocene collisional event between the Maracaibo block and the Guyana Shield (Audemard and Audemard, 2002) (Fig. 1). The Boconó fault is a large (500 km long) dextral strike-slip which separates, in the Merida area, the Sierra de La Culata in the northern block and the Sierra Nevada in the southern block.

In the central sector of the Merida Andes, the Boconó fault bifurcates and produces a pull-apart basin known as La González basin in which the Lagunillas pull apart basin is developed (Schubert, 1980; Alvarado, 2008).

The Lagunillas basin, and the Urao lake (1020 m, absl) locate in the lower block of two faults that bound the basin by the north and south. The northern basin margin has high relief (2200 m, absl) and the Jurassic siliciclastic rocks of La Quinta Fm. nourish the alluvial fans that fringe this margin (Fig.1). The fault in the

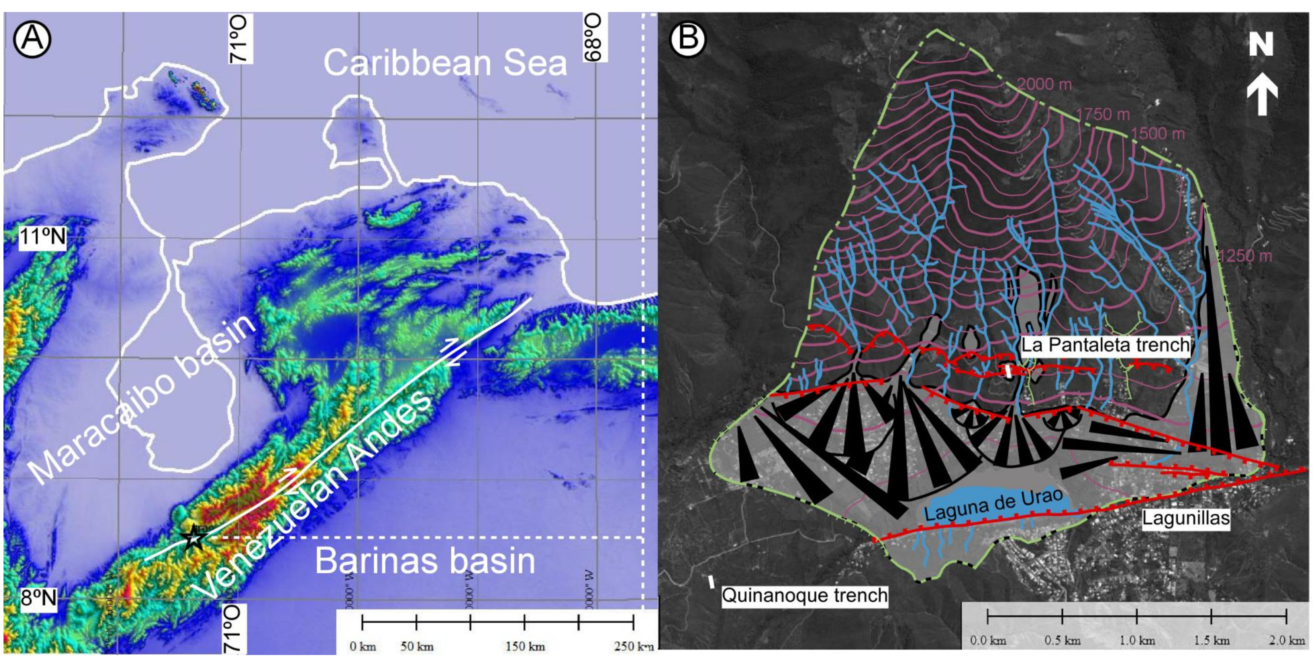

Fig. 1: Situation of the Urao lake. A) Regional geological sketch. A star marks the situation of the Urao lake. B) Geomorphological map of the Urao lake watershed. The red line are faults, the drainage is in blue.

southern basin margin produces a 20 m high shutter ridge, with E-W trend developed on Quaternary alluvial deposits.

FAULTS BOUNDING THE LAKE

The Urao lake is a shallow lake enlarged in E-W direction, 200 m wide and 1000 m long, parallel and close to the fault that bounds the Lagunillas pull apart basin by the south. This fault is a strike slip fault with normal component and is considered active because forms a shutter ridge that maintains the drainage and the lake closed and elevated with respect to the local base level situated in the Chama river.

The Lagunillas pull apart basin is also bounded by faults at the north. The northern margin is elevated and the Jurassic rocks are cut by several old faults which show milonites, and younger ones which have geomorphologic expression. In this area, La Pantaleta trench was excavated, in elevated alluvial deposits and a wide set of paleoearthquakes was recognized, since 2470-2200 AD to present, and an important surface rupture was created since 1610 (Alvarado, 2008). The recurrence interval for the events found in this trench is about 300 years (Alvarado, 2008).
In the knick point that connects the alluvial fan deposits of the Lagunillas pull apart basin and the Jurassic basement there is probably another fault that in some parts is covered by alluvial fan deposits, and no rupture evidences have been detected, probably because is covered by houses.
The fault in the southern part of the basin, continues laterally outside of the watershed of the Urao lake, towards the west the Quinanoque trench was excavated by a Funvisis-ULA team (Alvarado, 2008). In these trench the same range of events than in the Pantaleta trench was found. The recurrence interval of the events found in this trench is about 400-450 years (Alvarado, 2008).

THE LAKE DEPOSITS

The Urao lake shows a transition from the alluvial fan deposits in the northern margin of the basin towards the fine clay deposits of the lake centre. The palustrine areas are characterized by floating vegetation that extends into the lake several tens of meters.
Six cores were extracted in the lake bottom sediment reaching from 50 cm to 212 cm depth (all core depths are referred to the lake bottom). All the sediment analyzed is constituted by chlorite, muscovite, quartz, calcite and analcime (Huerta, et al., 2012) (Fig. 2).
The sediment is mainly dark grey to white mud with some intercalations of sand. The lamination is only well preserved in some beds and there are at least to levels with disrupted lamination and sand dykes which are interpreted as paleoseismites.
The paleoseismites occur at two depths in the most of the cores studied, 40-60 cm (SGL-01; SGL-03; SGL-05; SGL-06) and at 100-120 cm (SGL-03; SGL-05; SGL-06) (Fig. 3). In E99 core extracted by a team from the University of Massachusetts Amherst (Mazzarino, 2000) dated a bed with a depth of 238 cm by the ^{14}C cal. as 300 years BP.

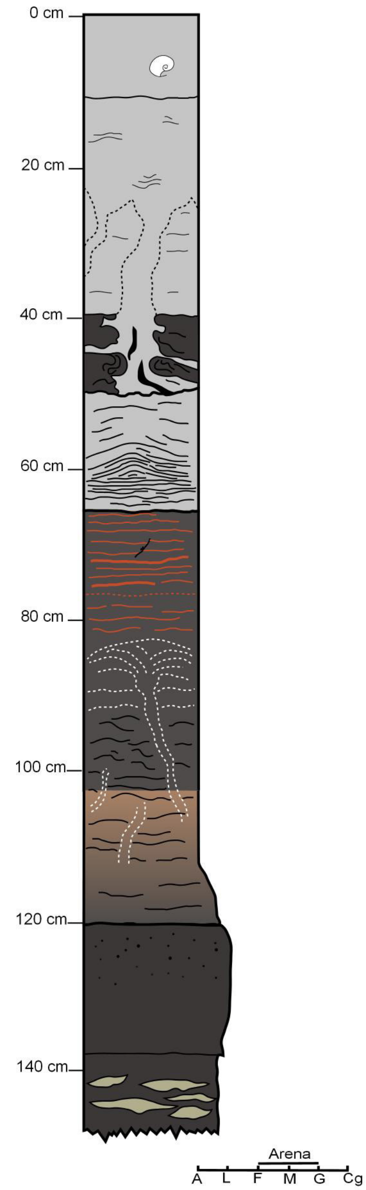

Fig. 2: Detailed log of the Core SLG-06.

DISCUSSION

The two levels with faulted beds, convoluted and disrupted lamination, sand injections and pillar structures are interpreted as two paleoseismic events recorded in the most of the lake as liquefaction processes. Similar examples have been described in lacustrine and other sedimentary environments (Sims, 1975, Audemard and Santis, 1991; Rodríguez-Pascua*,* et al., 2000, Alfaro*,* et al., 2010).

Considering that this two levels with paleoseismites appear at the same depth range (40-60 and 100-120) along all the lake centre and that each one records the same seismic event, it is possible interpret that the sedimentation rate is constant all along the lake centre during the last centuries.

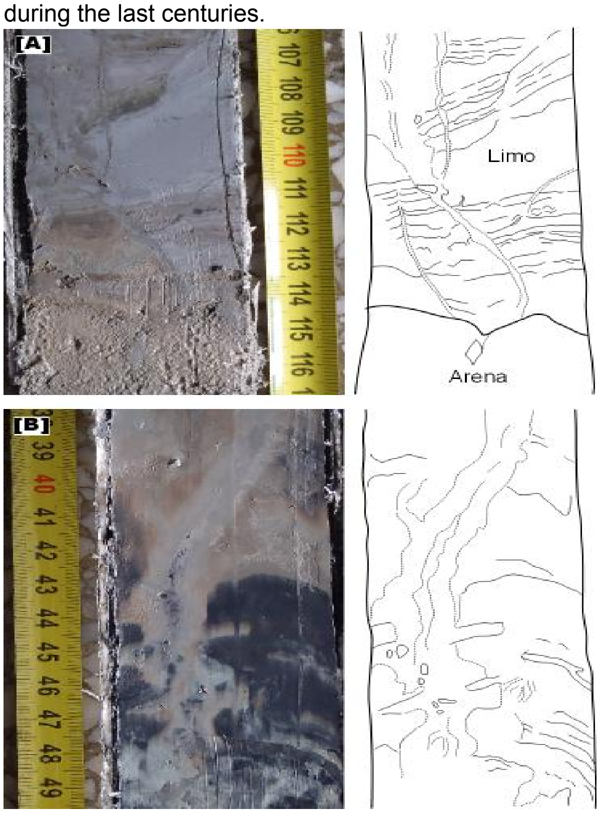

Fig. 3: Fluid escape structures and fractures in the Urao lake cores. A) Core SLG-03, B) Core SLG-06 with fluid escape structures marked by organic matter oxidation.

The age of the core E99 at 238 cm depth is 300 years BP (^{14}C cal), what is the year 1650 AD. So the sedimentation rate till this core was extracted is about 0.68 cm/year. If we assume that this sedimentation rate is constant during this period the event at 120 cm depth occurred in 1823 AD and the event recorded at 60 cm depth was produced in 1911 AD. But if the sedimentation rate is increased in 0.05 cm/year (0.73 cm/year), the event at 120 cm depth corresponds with the year 1811 AD and the event at 60 cm depth is equivalent to the year 1894 AD. So we conclude that the event recorded at 120 cm depth represents the Merida earthquake of 1812 AD recorded with an VIII Intensity in the area (Soulas et al, 1987; Audemard, 1997, 1998), and the event at 60 cm depth corresponds with the Santa Cruz de Mora earthquake, also with VIII intensity in the area (Soulas et al, 1987; Audemard, 1997, 1998).

Acknowledgements

The first author acknowledges the travel grant that received from the University of Salamanca for a research stay in the University of Los Andes (Venezuela), and the help received from INPARQUES.

References

Alfaro, P., Gibert, L., Moretti, M., García-Tortosa, F. J., Sanz de Galdeano, C., Galindo-Zaldívar, J., López-Garrido, T. C. 2010, The significance of giant seismites in the Plio-Pleistocene Baza palaeo-lake (Spain). *Terra Nova*, 22 (3), 172-179.

Alvarado, M. 2008, *Caracterización Neotectónica de la cuenca de tracción La González, Mérida Venezuela*. Tesis de Maestría, Universidad Central de Venezuela, 89 p.

Audemard F.A. 1997, Holocene and historical earthquakes on the Boconó Fault System, southern Venezuelan Andes: Trench Confirmation. *Journal of Geodynamics 24 (1-4), 155-167.*

Audemard, F. 1998, Contribución de la paleosismología a la sismicidad histórica: los terremotos de 1610 y de 1894 en los Andes venezolanos meridionales. *Revista Geográfica Venezolana*, 39 (1-2), 87-105.

Audemard, F. E., Audemard, F. A. 2002, Structure of the Mérida Andes, Venezuela: relations with the South America-Caribbean geodynamic interaction. *Tectonophysics*, 345 (1-4), 299-327.

Huerta, P., Guerrero, O., Cuevas, R., Armenteros, I., F. A. Audemard, F. A., Paredes, J., 2012, Caracterización sedimentológica de la laguna de Urao (Andes de Mérida, Venezuela). *Geo-Temas*, 13, 73 p.

Mazzarino, M. 2000, *Clay and evaporite-mineralogy in the lago de Urao basin: clues to environmental fluctuations in the Holocene of Venezuela*. Master thesis, University of Massachusetts Amherst, 82 p.

Rodríguez-Pascua, M. A., Calvo, J. P., De Vicente, G., Gómez-Gras, D. 2000, Soft-sediment deformation structures interpreted as seismites in lacustrine sediments of the Prebetic Zone, SE Spain, and their potential use as indicators of earthquake magnitudes during the Late Miocene. *Sedimentary Geology*, 135 (1-4), 117-135.

Schubert, C., 1980, Late Cenozoic pull-apart basins, Boconó Fault Zone, Venezuela Andes. *Journal of Structural Geology 2, 463-468.*

Sims, J. 1975, Determining earthquake recurrence intervals from deformational structures in young lacustrine sediments. *Tectonophysics*, 29, 41-152.

Soulas, J. P., Giraldo, C., Bonnot, D. 1987, Actividad cuaternaria y características sismogénicas del sistema de fallas de Oca-Ancón y de las fallas de Lagarto, Urumaco, Río Seco y Pedregal. Afinamiento de las características sismogénicas de las fallas de Mene Grande y Valera. FUNVISIS para INTEVEP, S.A. 65 p + anexos. Inédito.

PALEOSEISMOLOGY & ARCHAEOSEISMOLOGY
MORELIA • MEXICO 2012
INQUA-TERPRO PALEOSEISMOLOGY
EARTHQUAKE ARCHAEOLOGY

PRELIMINARY STUDY ON AIRBORNE LIDAR PROCESSING AND INTERPRETATION FOR LOCATING POSSIBLE ACTIVE FAULTS IN SOUTH KOREA

HyunTae Kim (1), Young-Seog Kim (1), J Ramón Arrowsmith (2), Kwang-Jae We (3)

(1) Dept. of Earth Environmental Sciences, Pukyong National University. S. KOREA.
(2) School of Earth and Space Exploration, Arizona State University. USA
(3) Hanjin information Systems & Telecommunication Co. S. KOREA.

Abstract: *Earthquakes can cause a serious loss of life and a significant amount of property damage. Many huge earthquake related hazards are responsible for the reactivation of active faults.. Thus, the study of active faults is very important for predicting future fault activity and hazards caused by future earthquake events. Furthermore, recurrence interval, displacement and magnitude are also important subjects in active fault study. Structural mapping and the tracing of faults are the primary steps for active fault study. Active faults have been mapped in South Korea, using aerial photography, satellite images and low quality DEM until now. Lineament analysis for active faults in Korea was ineffective due to local geological characteristics (weak tectonic activity) and a high degree of vegetation cover. In this study, therefore, we introduce and apply an Airborne LiDAR technique to help to overcome these problems in Korea. The preliminary results show that Korean LiDAR data might be very useful for tracing new active faults in Korea, if enough data is collected.*

Key words: *GIS, Airborne LiDAR, Removed vegetation, Active fault.*

INTRODUCTION

Damage caused by earthquakes has been widely reported all over the world. Most earthquakes above a magnitude of 6 produce surface ruptures. Most huge earthquakes occur as a result of reactivation of pre-existing active faults. Therefore, active fault research is an important step for forecasting earthquakes and studying their characteristics. Active fault research is progressing in many different ways. Many researchers are studying several subjects related with active faults, such as fault activity, recurrence interval , displacement and earthquake size (e.g. Kim et al., 2011). However, in order to understand the characteristics of fault activity, we have to first define the existence of active faults. In previous studies, we commonly analysed fault related lineaments using aerial photos or satellite images (e.g. Kyung, 1997). More recently, a new remote sensing technique has been developed, called LiDAR (e.g., Krabillet al., 1995; Carter and Shrestha, 1997; Ridgeway et al., 1997; Burnman, 2000). This method brings about a great improvement in active fault recognition. The main difference between previous methods and this technique is resolution (Fig 1);

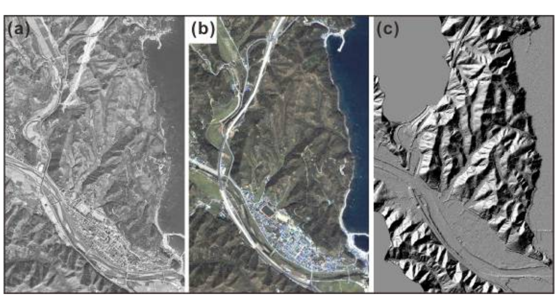

Fig. 1: Samchuck area (a) Arial photograph (b) Satellite image (c) Airborne LiDAR image.

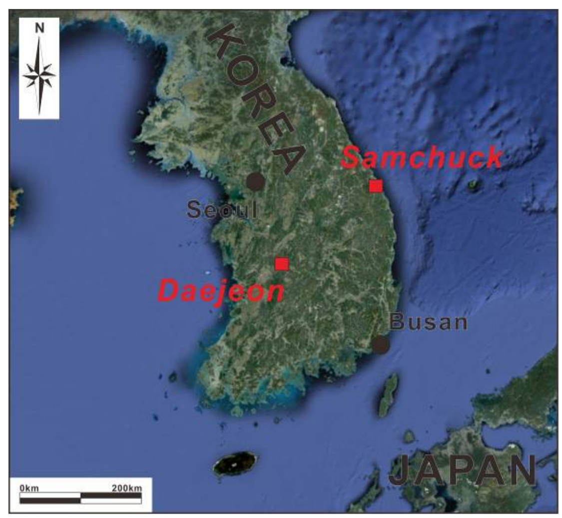

Fig. 2: Study area (red boxes) in Korea

especially new LiDAR processing methods can completely remove vegetation or buildings that obstruct the recognition of lineaments. Thus, active faults could be easily defined as clear lineaments on these images. This is the first and most basic, yet crucial, information for active fault mapping (e.g. Arrowsmith et al., 2009).
Airborne LiDAR methods use lasers to scan the ground to produce visual images. The obstructing vegetation and buildings on the ground can be removed using filtering techniques. This method is very useful in Korea because most areas are covered with thick vegetation, which is difficult to penetrate.
In this study, we selected a few examples of Korean LiDAR data acquired by Hanjin information Systems & Telecommunication Company, that is from the

Samchuck and Bomun mountain regions near Daejon(Fig. 2). One of the main purposes of this study is also using new processing and interpretation tools to re-process old data to make it more useful and accurate.

BACKGROUND OF AIRBORNE LIDAR TECHNIQUE

Aircrafts equipped with a laser scanner are also equipped with GPS (Global Positioning System) and INS (Inertial Navigation System) to give the true location. When the data is processed, a topographic map, based on 3-dimensional coordinates, can be produced (Lee, 2006). Airborne Light Detection and Ranging, or LiDAR (Fig.3) uses return points filtered using various algorithms after changing the files to an ASCII format (Yoon et al., 2006). This can produce ground only data. Many researchers are carrying out studies in filtering techniques from LiDAR binary data (Kraus and Pfeifer, 1998; Haugerud and Harding, 2001; Zhang et al., 2003). In Korea, recently some researchers are also studying new filtering methods (Lee, 2006; Chung et al., 2005; Kim et al., 2006; Yoon et al., 2006; Hwang and Lee 2011).

If we use newly developed software, we can convert images to a different format and increase their applicability. When working with LiDAR data, most people use different programs rather than one for their own research (e.g. Arrowsmith et al., 2008).

Recently, a lot of researches on surface ruptures use ground image data acquired through Airborne LiDAR. Active faults often show strong lineaments, and so we can recognize them with remote sensing data; we are able to identify these structures more easily from LiDAR. Also, it could give us basic information for faults and help with detailed field-work plans (e.g. Arrowsmith et al., 2009).

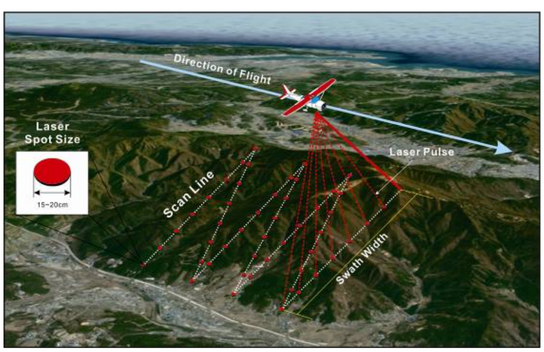

Fig. 3: LiDAR data collection.

APPLICATIONS OF LIDAR TECHNIQUE TO SOUTH KOREA

Recently, many countries have collected LiDAR data from various areas and have conducted many research projects using this data (e.g. Blair et al., 1999; Haugerud et al., 2003). South Korea has also started to collect LiDAR data and have used this method in some research. However, these studies have generally been used in city planning projects (Lee and Yu, 2003), natural hazards (Han et al., 2009), etc. So far, LiDAR hasn't been used in geological studies to the degree that it has in other leading countries. Because this method can remove vegetation or buildings using filtering methods, it must be very useful for geological interpretations in Korea. After filtering, we are able to classify two kinds of point; obstructions (vegetation, building) and ground. For this study, two samples of data were selected from the Samchuck area and the Bomun Mountain area in Daejon, South Korea. These areas are mostly covered with thick vegetation and are in tectonically stable areas. The data was acquired with Optech ALTM 30/70 laser scanner, and the aircraft altitude was between 1,200 and 1,400m, the point spacing was 3.5 point per 2m.

Removing Vegetation

South Korea has a high vegetation density in mountainous areas and non-urban areas. Although filtering was not easy, the filtering method greatly improved the data during this work and we got high resolution ground data. First, we processed the Samchuck area. We removed the vegetation (bare earth) and it shows clear topography and lineaments on the image, which are clearer than in all other images. Thus, we can now clearly recognize previously unclear streams (Fig. 4). If we apply this analysis to other topographic features (e.g.: streams and ridges), we can easily recognize tectonically deformed topography.

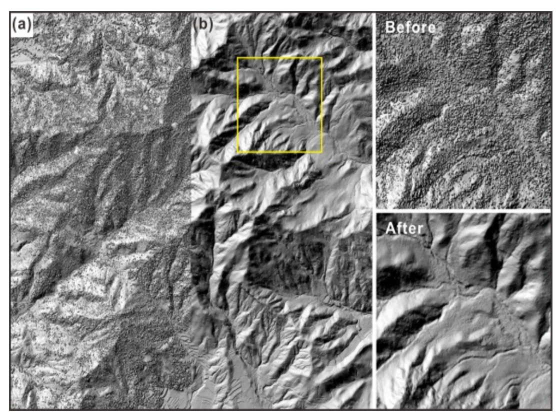

Fig. 4: Bomun MT. in Daejon. (a) Full feature (b) Bare earth. Yellow box area show LiDAR data advantage.

Recognition of Lineaments

Bomun Mountain in Daejon has much more vegetation than the Samchuck area. The density of vegetation of this area is typical in Korean mountains which are often covered with thick impenetrable vegetation. After filtering with the new software applications, we are able to get much more information than we did from the previous LiDAR image. Fig.4 shows an image that has been filtered using the software. The image is quite clear and weak lineaments have become stronger, rivers are easily visible. Therefore, it is also quite useful to recognize the displacement of rivers along strong lineaments (Fig 5).

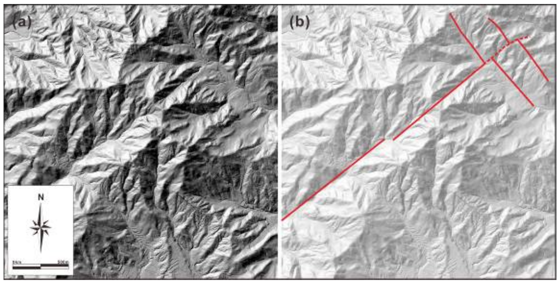

Fig. 5: Bomun MT. in Daejon. (a) Bare earth image (b) Recognized lineaments.

Discussion: application to Korean active faults and environmental characteristics

Active faults on the Korea Peninsula have been reported since the 1990s (Okada et al., 1994). Since then active fault studies have been carried out using aerial photos based on marine terrace levels. Marine terrace uplift indicates geological events caused by isostasy or tectonic events. The uplift events of Korea peninsula might be caused by tectonic events rather than isostasy due to the tectonic setting of the Korean Peninsula. Previous studies show that the uplift ratings were between 0.19m/ky~0.88m/ky. This study shows discontinuity between uplift rates in several study areas and is useful for active fault study (Chwae and Choi, 2007). The main difficulty in locating active faults inland is interference due to vegetation and building cover. The LiDAR technique is very useful to mitigate these problems.

One of the most difficult issues in LiDAR data acquisition is the high vegetation cover in South Korea. The transmission of Airborne LiDAR changes throughout the year; with 20-40% transmissivity in the summer which results in poor imagery and a huge increase to around 70% in the winter (Yoon and Lee, 2006).It is quite obvious that if we collect data at a suitable time of year, when the level of transmissivity is highest, we could be able to get far superior images to work with.

CONCLUSION

Globally, many kinds of research methods were suggested using LiDAR analysis. They give excellent results, especially; filtering methods for removing obstacles (building, vegetation) which is a very important method for active fault research.

South Korea has now introduced modern LiDAR data collection and processing methods and we can now use this for active fault studies.

In this study, we analysed already collected data in two inactive areas and we examined the possibility of filtering in Korea where a high percentage of vegetative cover exists. As software applications are improved, we will be able to produce higher quality images useful for active fault research in Korea, a relatively inactive area.

Acknowledgements: We thank David E. Haddad, Barrett Salisbury, Gayatri Marliyani, Tsurue Sato for their great cooperation in Tempe, AZ, USA. We also thank Paul Edwards for his constructive review.

References

Arrowsmith, J R., Glenn, N., Crosby, C.J., Cowgill, E., 2008. Current capabilities and community needs for software tools and educational resources for use with LiDAR high resolution topography data, Studying Earth Surface Processes with High-Resolution Topographic Data Workshop..

Arrowsmith, J R, Zielke, O., 2009. Tectonic geomorphology of the San Andreas Fault zone from high resolution topography: An example from the Cholame segment, Geomorphology Vol. 113 pp.70-81.

Blair, J.B., Rabine, D.L., and Hofton, M.A., 1999. The Laser Vegetation Imaging Sensor: a medium-altitude, digitisation-only, airborne laser altimeter for mapping vegetation and topography, ISPRS Journal of Photogrammetry and Remote sensing, Vol.54, p. 115-122.

Burnman, H. (2000).Calibration and Orientation of Airborne Image andLaser Scanner Data Using GPS and INS,Royal Institute of Tech-nology, Stockholm.

Carter, W. E., and R. L. Shrestha (1997). Airborne laser swath mapping: instant snapshots of our changing beaches, In Proceedings of the Fourth International Conference: Remote Sensing for Marine and

Coastal Environments,Environmental Research Institute of Michi-gan, Ann Arbor,I,298–307.

Chung, D.K., Goo, S.H., Eo, J.H., Yoo, H.H., 2005, DTM Extraction from LiDAR Data by Filtering Method, GIS/RS Joint Spring Symposium, pp.355-361.

Chwae, U-C., Choi, S-J., 2007. Active fault study of Korea: the past, present and future, Quaternary Tectonics of Southeastern Korea, p1~31

Han, J-G., Kim, S-P., Chang, D-H., Chang, T-S., 2009. Estimation of Inundation Damages of urban area Around Haeundae Beach Induced by Super Storm Surge Using Airborne LiDAR Data, The Journal of GIS Association of Korea, Vol.17, No.3, pp.341-350.

Haugerud, R.A., and Harding, D.J., 2001. Some algorithms for virtual deforestation (vdf) of lidar topographic survey data, International Archives of Photogrammetry and Remote Sensing, XXXIV-3/W4, pp.211-217.

Haugerud, R.A., Harding, D.J., Johnson, S.Y., Harless, J.L., Weaver, C.S., Sherrod, B.L., 2003. High-resolution Lidar topography of the Puget Lowland, Washington-a bonanza for earth science. GSA Today, Geological Society of America 13 (6), 4-10.

Hwang, S. and Lee, I., 2011. Current Status of Tree Height Estimation form Airborne LiDAR Data, Korean Journal of Remote Sensing., Vol. 27, No. 3, pp.389-401.

Kim, H-I., Park, E-K., Park, K-D., 2006. Analysis of LiDAR data processing algorithms for wooded areas, Korean Journal of Remote Sensing, pp.131-134.

Kim, Y-S., Kihm, J-H. and Jin, K.,, 2011. Interpretation of the rupture history of a low slip-rate active fault by analysis of progressive displacement accumulation: an example from the Quaternary Eupcheon Fault, SE Korea, Journal of the Geological Society, Vol. 168, pp.273-288.

Kim, Y-S., Jin, K., Choi, W-H., Kee, W-S., Understanding of active faults: A review for recent researches, Journal of the Geological Society of Korea, Vol. 47, No. 6, P.723-752.

Krabill, W. B., R. H. Thomas, C. F. Martin, R. N. Swift, and E. B. Frederick(1995). Accuracy of airborne laser altimetry over the Greenland ice sheet, Int. J. Remote Sensing,16,no. 7, 1211–1222.

Kraus, K., and Pfeifer, N., 1998. Determination of terrain models in wooded areas with airborne laser scanner data, ISPRS Journal of Photogrammetry and Remote Sensing, Vol. 53, pp.193-203.

Kyung, J.B., 1997. Paleoseismological Study on the Mid-northern Part of Ulsan Fault by Trench Method, The Journal of Engineering Geology, Vol.7, No.1, pp.81-90

Lee, I., 2006. A Feature Based Approach to Extracting Ground Points from LiDAR Data, Korean Journal of Remote Sensing, Vol.22, No.4, pp.265-274.

Okada, A., Watanabe, M., Sato, H., Jun, M.S., Jo, W.R., Kim, S.K., Jeon, J.S., Chi, H.C. and Oike, K., 1994, Active fault topography and trench survey in the central part of the Yangsan fault, southeast Korea. Journal of Geography, 103, 111-126(in Japanese).

Ridgeway, J. R., J.-B. Minster, N. Williams, J. L. Bufton, and W. B. Krabill(1997). Airborne laser altimeter survey of Long Valley, California, Geophys. J. Int.131,no. 2, 267–280.

Yoon, J-S.. and Lee, K-S., 2006. Prospects for Understanding Forest Structure using LiDAR, Korean Journal of Remote Sensing, pp149-152.

Yoon, J-S.. and Lee, K-S., Shin, J-I., Woo, C-S, 2006. Characteristics of Airborne Lidar Data and Ground Points separation in Forested Area, Korean Journal of Remote Sensing, Vol.22, No.6, pp.533-542.

Zhang, K., Chen, S.-C., Whitman, D., Shyu, M.-L., Yan, J. and Zhang, C., 2003. Aprogressive morphological filter for removing nonground measurements form airborne LiDAR data, IEEE Transactions on Geoscience and Remote Sensing, Vol. 41, No. 4, pp.872-882.

LACUSTRINE EVOLUTION OF THE EASTERN SECTOR OF THE ACAMBAY GRABEN BASED ON THE DIATOM RECORD

Israde-Alcántara Isabel (1), Hernández-Olivares Rene (1), Garduño-Monroy Víctor H. (2), Rodríguez-Pascua Miguel A. (3), Pérez López Raúl (3), Macías-Vázquez José L. (4)

(1) Isabel Israde Alcántara. Dpto de Geología y Mineralogía, Universidad Michoacana San Nicolás de Hidalgo, Instituto de Investigaciones Metalúrgicas. MÉXICO. isaisrade@gmail.com
(1) Rene Hernández Olivares. Dpto de Geología y Mineralogía, Universidad Michoacana San Nicolás de Hidalgo, Instituto de Investigaciones Metalúrgicas. MÉXICO. hero_8585@hotmail.com
(2) Víctor Hugo Garduño Monroy. Dpto de Geología y Mineralogía, Universidad Michoacana San Nicolás de Hidalgo, Instituto de Investigaciones Metalúrgicas. MÉXICO.vhgarduno@gmail.com
(3) Miguel Angel Rodriguez Pascua. Dpto. de Investigación y Prospectiva, Área de Peligrosidad y Riesgos Geológicos, Instituto Geológico y Minero de España (IGME), ESPAÑA. ma.rodriguez@igme.es
(3)Raúl Pérez López. Dpto. de Investigación y Prospectiva, Área de Peligrosidad y Riesgos Geológicos, Instituto Geológico y Minero de España (IGME), ESPAÑA. r.perez@igme.es
(4) José Luis Macías Vázquez. Instituto de Geofísica, UNAM. Campus Morelia. MEXICO. macias@geofísica.unam.mx

Abstract (Lacustrine evolution of the eastern sector of the acambay graben based on the diatom record): *A biostratigraphic study of two paleolacutrine sequences west of the Acambay graben was made from 21 stratigraphic columns. It was observed that the Tierras Blancas paleolake maintained its maximum extension during the Pleistocene, ending at 1.2+-0.13 Ma (Mercer; et al. 2010). The limiting paleolake (Valle de los Espejos) developed during the Upper Pleistocene Holocene, its disappearance being accelerated by human settlements. Volcanic-tectonic events in these periods caused regressions-transgressions, liquefaction and landslides that fractured diatom valves in both paleolakes. The detailed description of sedimentary facies allows for distinguishing the more distal sectors of the paleolake where algal production was most concentrated, with diatomites of a deep lake reaching up to 400x10^7 valves per gram of dry sediment intercalating with fine clays. Proximal facies show fine slimy sand sediments suggesting a lake with low energy drainages.*

Key words: Acambay, diatoms, Pleistocene, Holocene.

Introduction

The Acambay graben is located within the Morelia-Acambay fault system in the states of Mexico and Michoacán (Aguirre-Díaz. 1995). The more important faults in the eastern zone are Pastores and Acambay-Tixmadejé, both limiting the Acambay graben, the latter one with recent seismic activity (Urbina and Camacho.1913, Langridge *et al.* 2000, Quintero-Legorreta. 2002, Rodríguez-Pascua; *et al*. 2010).
The study area is located at 19° 50' and 20° 06' N and 99° 42' and 100° 05' W; it comprises two lacustrine areas: the Tierras Blancas (characterizing the Pleistocene) and the Valle de los Espejos (representing the Holocene) paleolakes.
The study consisted in the analysis of 21 columns distributed in nine sectors of the paleolake. Based on sedimentary and biogenic facies and on volcanic events the marker levels were determined, the paleoenvironments and the possible causes of its desiccation.

Tierras Blancas Paleolake

The evolution of the graben dates to the Miocene, starting with the formation of the Pastores and Acambay-Tixmadejé faults (Aguirre-Díaz. 1995), followed by the eruption of the San Pedro stratovolcano in the Pliocene and the Santa Lucía dome during the Upper Pliocene-Pleistocene (Norato-Cortes 1998), which products made up of volcanic deposits formed the basement of the Tierras Blancas Paleolake.
After these events, a shallow lake originates with diatomite forming an index level for the region. Figure 1 shows this lacustrine sequence for the Pleistocene, in which the basal diatomite represents a marker level. The 10 cm maximum thickness of the diatomite indicates that this paleolake remained active during several hundred thousand years.
The sedimentation of the Mio-Pliocene paleolake can be summarized in three sectors: a) Lagunita de Cantashi (GALC), b) El Fresno (EF) and c) Tierras Blancas (TB).
a) The base of the Lagunita de Cantashi marks the beginning of the lake with intercalated tephras and silts bearing abundant well-preserved *Cyclotella meneghiniana*, which indicates a shallow lake with concentration of ions.
In stratigraphically ascending order, presence of *Stephanodiscus subtransilvanicus var. minutula* suggests an increase in lake level that is maintained for a short time, given that silty facies with common carbonate concretions successively appear. Associated are *Campylodiscus clypeus* and *Cyclotella meneghiniana* indicating dry phases.
In this same sector, activation of the faults delimiting the paleolake is observed that deformed the lacustrine sediments and fracturing diatom valves.

b) In the El Fresno (GAEF) zone to the southwest of the paleolake, proximal zones of fluvial-lacustrine facies having abundant primary structures form the base. Above these, clayey deposits dominated by exclusively deep-water diatoms occur such as *Stephanodiscus excentricus*, *S. niagarae and Aulacoseira granulata*. The lake maintains a transgression with mesotrophic conditions and some turbidity. Pyroclastic fall deposits and flows cover these deposits.

c) Tierras Blancas (TB) is the zone having more lacustrine development and conforms the more distal zone of the paleolake, dominated by planktonic diatoms living in a deep lake. Characterized by ca. 10 m of pure diatomite intercalated with clayey facies interrupted by short episodes of volcanic fall deposits.

The basal diatomite is dominated by the planktonic species *Stephanodiscus excentricus* and *S. niagarae*, accompanied by the shallower, more turbid and colder water diatoms *Aulacoseira granulata* aff. *angustissima and A.* aff. *ambigua*. The diatomite in the central zone corresponds to a planktonic environments alternating with more silty phases with shallow water diatoms (*Cocconeis placentula*, *Nitzschia amphibia*).

The increased presence of *Stephanodiscus* indicates a return to deeper conditions. At the summit of the sequence, a stratum of compacted volcanic sand conforms a detachment level, on which lays a deformed and fragmented fine diatom deposit, in turn overlaid by a liquefied fine sand stratum; which was previously identified by Rodriguez-Pascua et al., (2010) as Paleoevent 4.

On top of the fine sand, a cream color, compact clayey silt layer is observed, in which remains of *Equus* sp. molars characterized by Mercer et al., (2003) have been collected,

The lacustrine sequence is topped by fall deposits dated at 1.2±0.13 Ma (Mercer, et al. 2010). In a phase after 1.2 Ma, andesitic domes were constructed to the east and west that charred the diatomite and obstructed the drainage. During the final phase of the Pleistocenic lake extinction alluvial deposits covered the paleolake. All the succession is afterwards affected by tectonic lifting of the basin.

Tectonics plays a relevant role in the region, given that faulting generates a last depression during the late Pleistocene and early Holocene.

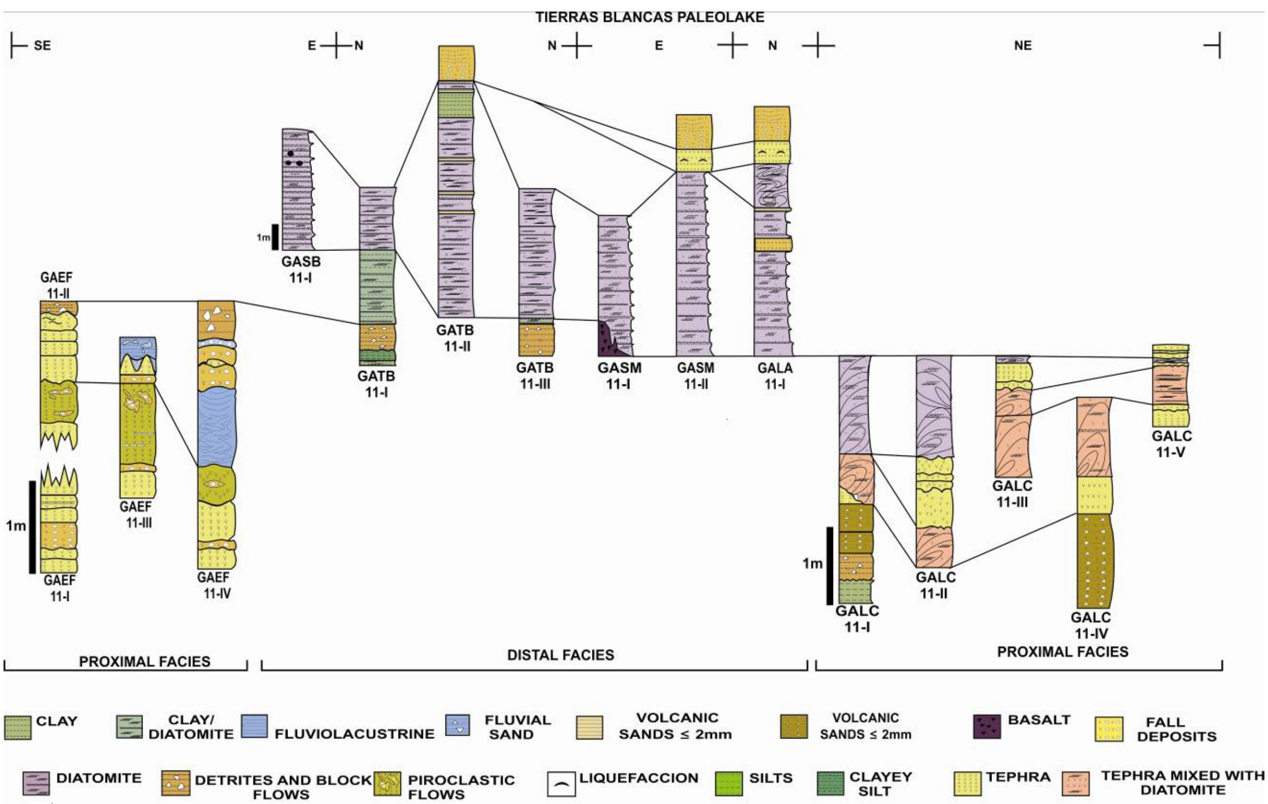

Fig. 1: Stratigraphic columns of lacustrine and fluviolacustrine succession during the Pleistocene in the Tierras Blancas paleolake.

Valle de los Espejos Paleolake

During the Pleistocene-Holocene limit, tectonic activity is so intense that it hampers a lacustrine development with a sufficiently deep water level for clayey sedimentation. In the Valle de los Espejos paleolake, the facies are limited to clayey silt deposits together with silt loams and epiclastites. Diatom development is minimal and sponge spicules are evident. Figure 2 shows the sedimentary evolution in Acambay of the Los Espejos paleolake.

The La Soledad sector (GALS) corresponds to the depocenter of the paleolake with clay deposits containing *Cyclotella meneghiniana* indicator of an increase in the salt concentration.

Seismicity is again present in the strata, causing two liquefaction events that are more clearly recorded in the distal zone of the paleolake, with the posterior fracturing of diatoms. Meanwhile, fluvial inputs are generated to the northeast.

In the Dongu sector to the northeast of the graben, a 1 m thick volcanic breccia is deposited overlying the fluviolacustrine deposits. The lake attempts to keep its expansion but is reduced to unstable pools allowing for the development of *Tabellaria fenestrata*, characteristic of fluvial currents.

On top of the fluvial sequences, a massive tephra deposit is generated in the southwest of the paleolake, corresponding to the last deposit on top of the paleolake. Finally, the historical geography of the lake ends in its reduction to marshes with development of up to 80 cm deep paleosoils.

These marshes persist until the draining of the Los Espejos Lake, which destabilized the lake's hydrology. At present, the Los Espejos Lake has been reduced to shallow pools.
The extraction of groundwater from this basin is forbidden to communities within the graben, given it is channeled to Mexico City, thus limiting the productivity of these fertile soils to rainfed cropping.

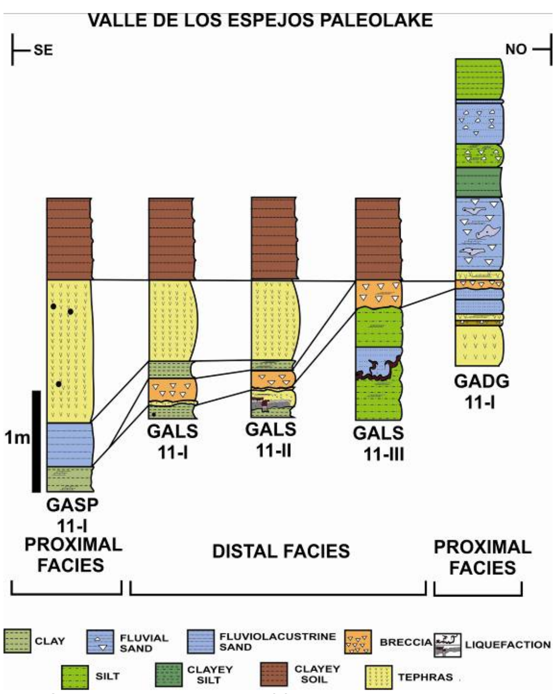

Figure. 2: Stratigraphic columns of fluviolacustrine succession during the Holocene in the Valle de los Espejos paleolake.

DISCUSSION

The lacustrine sequence of the oldest paleolake in the zone (Tierras Blancas) begins and ends with volcanism, obstructing the drainage system (Israde; *et al*. 2004) after 1.2±0.13 Ma (Mercer; *et al*. 2010).

In particular, activity of the Temascalcingo and Jocotitlán volcanoes, with eruptions during the Pleistocene and Holocene (Siebe and Macías, 2006, Roldán–Quintana, *et al*. 2011), could have emitted their products on both paleolakes favoring the constant development and precipitation of diatoms.

In the diatomites of the Tierras Blancas Lake the seismic events reported by Rodríguez-Pascua; et al. (2010) are clearly seen in the figure 3. The first event caused the regression of the paleolake reducing it to a shallow lake. During events three and four, the diatomites of deep environments experiment extensive fragmentation, which is absent in the subjacent and overlying levels.

Fig. 3: Landscape of the uplifted diatomites in Acambay graben.

In the Valle de los Espejos paleolake two liquefaction events occurred, accompanied by microfaulting. The detrital flows are associated with destabilization of the graben's faults (Norini, et al. 2010, Sarochi. 2010).

Through the results of the present study and the examination of cores from later studies in the region (c.f., Carranza et al. in the proceedings of this Congress), it is suggested that seismicity was intense during the Plio-Pleistocene, becoming less frequent during the Holocene.

In other lakes limiting the Trans Mexican Volcanic Arc during the Pleistocene deep phases occurred due to high precipitations in lakes Pátzcuaro (Bradbury. 2000), Zirahuén (Ortega et al. 2010), Cuitzeo (Israde et al. 2010), Zacapu (Ortega et al. 2002) and the Tierras Blancas paleolake (Israde et al. 2004, Mercer et al., 2010, Andrade and Israde. 2009).

Shallow conditions were present in other studied Mexican lakes, such as Cuitzeo (Israde et al. 2010), Upper Lerma (Chignahuapan) (Metcalfe 1984, Lozano-García et al. 2005), Zacapu (Arnauld et al. 1997, Ortega et al., 2002) and Chalco (Watts y Bradbury 1982, Caballero 1997), characteristics that are similar in the Valle de los Espejos paleolake as evidenced by *C. meneghiniana* and *T. fenestrata*.

The latter paleolake disappeared due to anthropogenic effects during recent years. Lakes affected by draining are Zacapu (Arnauld; *et al.* 1997) and the Upper Lerma (Chignahuapan) (Metcalfe. 1984), and by other anthropic influences, lakes Pátzcuaro (O´Hara, 1993; Fisher et al. 2003; Israde et al. 2005) and Cuitzeo (Israde et al., 2010b).

During humid periods in the Pleistocene, several lacustrine sequences are recognized in central Mexico with development of several meters thick diatomites (Israde et al 2010a). Diatomites are restricted to tectonically active zones where interpolate earthquakes inhibit stable sedimentation, deforming the sublacustrine sequence.

Synsedimentary landslides are common in the development of diatomites from deep waters in the Miocene in Chapala (Israde et al, 2010), the Pliocene in Acambay (Rodríguez Pascua et al., 2010), the Pleistocene in Pátzcuaro (Israde-Alcántara et al., 2005) and also in Holocene lakes limited by faults where age inversions are common. These age inversions must be accounted for when interpreting paleoenvironments.

Much remains to do in other regions with intra continental seismicity and diatomite producing lakes such as in Peru, Colombia, Spain and Africa among other regions (Gasse. 1988, Tiercelín et al., 1988). The potential of diatomites has been demonstrated in zones affected by earthquakes (Nelson et al., 1998).

Acknowledgements: The present work was elaborated due to funding from the Coordinación de la Investigación Científica de la UMSNH, through project 1.22 "*Paleoambientes Holocenicos del Graben de Acambay*" 2011.

References.

Aguirre-Díaz. (1995). La toba Amealco y su correlación con la formación las americas a través del graben de Acambay, estados de México, Michoacán y Querétaro, México. Revista Mexicana de Ciencias Geológicas. Vol. 12(1): 17-2.

Andrade, A. G. e Israde, I. (2009). Variaciones del Pleistoceno en la fase lacustre de la localidad de San Bartolo Lanzados (Atlacomulco, México), evaluadas mediante estratigrafía de diatomeas. Ciencia Ergo Sum. Vol.16 (3): 273-277.

Arnauld, C; Metcalfe S y Petrequin P. (1997). Holocene climatic change in the Zacapu lake basin, Michoacan synthesis of results. Quaternary international. Vol 43(44): 173-179.

Bradbury, J. P. (2000). Limnologic history of lago de Patzcuaro, Michoacán, Mexico for the past 48 000 years: impacts impacts of climate and man. Paleogeography, Paleoclimatology, Paleoecology. Vol. 163: 69-95.

Caballero-Miranda. (1997). Reconstrucción Paleolimnológica del lago de Chalco, México durante el último glaciar-el registró de diatomeas entre 34,000 y 15,000 A.P. Revista Mexicana de Ciencias Geológicas. Vol. 14(1): 91-100.

Fisher, C., Pollard, P; Israde-Alcántara; Garduño-Monroy and Banerjee. (2003). A Reexamination of Human-induced environmental change within the Lake Patzcuaro Basin, Michoacan, Mexico. Proceedings of the National Academy of Sciences, 100(8): 4957–4962.

Gasse, F: (1980). Les diatomées lacustres Plio-Pléistocénes du Gadeb (Ethiopie), systematique, paléoécoligie, biostratigraphie.

Israde, I; Andrade, A. G; Monroy, V. H; Rodríguez, M. A y Mercer, L. 2004. Fluctuaciones ambientales del Pleistoceno en la localidad de San Bartolo Lanzados, municipio de Atlacomulco, con base en la información micropaleontológica. Ciencia Nicolaita. No. 39: 95-108.

Israde-Alcántara, W.E Miller, V.H. Garduño- Monroy, J. Barron,M.A.Rodriguez-Pascua (2010a). Palaeoenvironmental significance of Diatom and Vertebrate fossils from Late Cenozoic Tectonic Basins in west-central México: A review. Quaternary International.Vol.219. 79-94.

Israde, I; Velázquez-Duran; Lozano, M. A; Bischoff, J; Domínguez G y Garduño, V. H. (2010b). Evolución Paleolimnológica del Lago Cuitzeo, Michoacán durante el Pleistoceno-Holoceno. Boletín de la Sociedad Geológica Mexicana. Vol. 62(3): 345-357.

Israde-Alcántara, I; Garduño-Monroy, V.H; Fisher C.T; Pollard, H.P; Rodríguez-Pascua, M.A. 2005. Lake level change, climate, and the impact of natural events: the role of seismic and volcanic events in the formation of the Lake Patzcuaro Basin, Michoacan, Mexico. Quaternary International. Vol. 135: 35-46.

Langridge, R. M., R. J. Weldon, J. C. Moya, G. Suárez, (2000). Paleoseismology of the 1912 Acambay earthquake and the Acambay–Tixmadejé fault, Trans–Mexican Volcanic Belt. J. Geophys. Res. Vol.105: 3019–3037.

Lozano-García, S., Sosa-Nájera S. Sugiura Y., Caballero M. (2005). 23,000 yr of vegetation history of the Upper Lerma, a tropical high-altitude basin in Central Mexico.. Quaternary Research 64 (2005) 70– 82.

Metcalfe, S; Street-Perrott; Perrott, R. A y Harkness, D. (1984). Enviromental changes during the late quaternary in the upper Lerma basin, estado de Mexico, Mexico. 8th. Diatom-symposium.471-264.

Mercer, L.T; Kowallis, B. J; Chistiansen, E; Miller; W. E; Carranza-Castañeda e Israde-Alcántara (2010). Geology of the Tierras Blancas area in the Southeastern Acambay Graben, Central Mexico.BYU Geology studies. Vol. 48: 1-36.

Nelson.A.R.,Yoko Ota, Masatomo Umitsu, Kaoru Kashima and Yoshiaki Matsushima, 1998. Seismic or hydrodynamic control of rapid late-Holocene sea-level rises in southern coastal Oregon, USA?. The Holocene 8,3 (1998). 287–299

Norato-Cortez, T. A; (1998). Estudio estratigráfico-vulcanológico estructural de los volcanes San Pedro y Altamirano (estados de México Y Michoacán) y su relación con la evolución tectónica del sector central del Cinturón Volcánico Mexicano. Tesis de maestría. Universidad Autónoma de Nuevo León. Linares, Nuevo León. 73 pp.

Norini, G; Capra. L; Borselli, L; Zuniga, F. R; Solari, L; Sarochi. D. (2010). Large scale landslides triggered by quaternary tectonics in the Acambay graben, Mexico. Earth Surfaces and Landforms. Vol. 35: 12(1445-1455).

O'Hara, S. L; Alayne, S.P y Bart, T. P. (1993). Accelerated soil erosion around a Mexican Highland lake caused by prehispanic agriculture. Nature. Vol. 362: 43-46.

Ortega, B; Caballero, C; Lozano, S; Israde, I y Vilaclara, G. (2002). 52000 years of environmental history in Zacapu basin, Michoacan, Mexico: the magnetic record. Earth and Planetary Science Letters.Vol. 202(3-4): 663-675.

Quintero-Legorreta, O. 2002. Análisis estructural de fallas potencialmente activas: Boletín de la Sociedad Geológica Mexicana: Tomo LI. (1): 1-11

Rodríguez-Pascua, M. A; Garduño-Monroy V. H; Israde-Alcántara, I y Pérez-López, R. 2010. Estimation of the paleoepicentral area from the spatial gradient of deformation in lacustrine seismites (Tierras Blancas Basin, Mexico). Quaternary International. 1-27.

Roldán-Quintana, J; Aguirre-Díaz, G. J; Rodríguez-Castañeda, J.L. (2011): Deposito de avalancha de escombros del volcán Temascalcingo en el graben de Acambay, Estado de México. Revista Mexicana de Ciencias Geológicas. Vol. 28: 1(118-131).

Siebe C., and Macias J.L. 2006. Volcanic hazards in the Mexico City metropolitan area from eruptions at Popocatepetl, Nevado de Toluca, and Jocotitlan stratovolcanoes and monogenetic scoria cones in the Sierra Chichinautzin Volcanic Field Geological Society of America Special Papers, 402, 253-329

Tiercelín J.J., Chorowics, Bellon H., Richert J.P.,MWanbene J.T.,Walgenwittz F.,(1988). East African rift system, offset, age and tectonic significance of the Tanganyika-Ruwka-Malawi intracontinental fault zone. Tectonophysics, 148. 241-252.

Urbina, F., Camacho, H., (1913), La zona megasísmica Acambay-Tixmadejé, Estado de México, conmovida el 19 de noviembre de 1912: Boletín del Instituto Geológico de México, 32, 125 pp.

Watts, W y Bradbury, J. (1982). Paleoecological estudies at lake Patzcuaro on the west-central Mexican plateau and the Chalco in the basin of Mexic. Quaternary research. Vol. 17: 56-70

PALEOSEISMOLOGY & ARCHAEOSEISMOLOGY
MORELIA • MEXICO 2012
TERPRO
IUGS UNESCO 567
I PALEOSEISMOLOGY
EARTHQUAKE ARCHAEOLOGY

ESTRATIGRAFIA Y PALEOAMBIENTES DELPALEOLAGO DE ACAMBAY EN BASE A UN NUCLEO DE 2.5 M DEL DEPOCENTRO DE LA CUENCA

STRATIGRAPHY AND PALEOENVIROMENTS OF THE ACAMBAY PALEOLAKE BASED ON A 21.5 M CORE FROM THE DEPOCENTER OF THE BASIN

Ana Gabriela Carranza Rivera (1); Isabel Israde Alcántara (2), Bertha Oliva Aguilar Reyes (3), Avto Gogichiasvili (4).

(1) Posgrado en Geociencias y Planificación del Territorio. Universidad Michoacana San Nicolás de Hidalgo, Instituto de Investigaciones Metalúrgicas. MÉXICO. gabs_any@hotmail.com
(2) Dpto de Geología y Mineralogía, Universidad Michoacana San Nicolás de Hidalgo, Instituto de Investigaciones Metalúrgicas. MÉXICO.isaisrade@gmail.com
(3) (4). Instituto de Geofísica de la UNAM. Campus Morelia. baguilar@geofisica.unam.mx
avto.gogichai@gmail.com

Resumen: *En base análisis multiproxy (Carbono orgánico total (TOC), Carbono inorgánico total, geoquímica y susceptibilidad magnética) de un núcleo de 21 m extraído en el depocentro del lago de Acambay es posible inferir que del Pleistoceno superior al Holoceno el paleolago de Acambay fue un cuerpo de aguas bajas pero estable al menos durante los últimos 100 ky. Fases secas se observaron entre 21.48 y 10 metros, mostrando fluctuaciones húmedas particularmente entre 18 y 20 metros en donde altos niveles de TOC asociados a Ferrihidrita están indicando las condiciones más húmedas de todo el registro. De 10 m hasta la cima del núcleo (0m), el lago muestra un cambio a condiciones ligeramente mas húmedas, particularmente de 6.50 a 7.50 m en los que la asociación de Stephanodiscus aff.medius-Aulacoseira granulata sugiere una estabilidad hacia una profundización del lago. .Evidencias de fenómenos de deformación se observan de 4.50 to 4.70 m,14 to 15m , 16,17 and 19 m y pueden estar asociados a eventos sísmicos.*

Abstract: *Based in TOC (Total organic carbon), Total inorganic carbon (TIC), geochemical and magnetic susceptibility multiproxy analysis of a 21m core of the depocenter of Acambay paleolake it is possible to infer that from Upper Pleistocene to Holocene Acambay paleolake was a stable low lacustrine water body at least during the last 100 ky. Dry phases, were observed between 21.48-10 m, showing short humid fluctuations particulary between 18 and 20 m in which high TOC and Ferrihidrita, are indicating the more humid period of all the record. From 10 m to the final of the record (0m), the lake shows a sudden change to a little more humid particularly from 6.50 to 7.50 m in which the Stephanodiscus aff.medius-Aulacoseira granulata ensamblage suggest stable conditions . Evidences of deformation phenomena are recorded from 4.50 to 4.70 m,14 to 15m, 16,17 and 19 m and can be associated to seismicity phenomena.*

Key words: *Acambay graben, paleolake, multiproxies.*

INTRODUCTION

The Valle de los Espejos is located within the central sector of the Trans Mexican Volcanic Belt in the mountainous zone of the municipality of Acambay, State of Mexico It conforms the northern portion of the Acambay Graben limiting to the Acambay-Tixmadeje fault. It has a circular structure of over 90 km^2, its plain showing it was an extensive lake.

The purpose of this work was to document climatic and environmental variability in the lacustrine sediments during the Upper Pleistocene-Holocene by the interpretation of paleoclimatic indicators (proxies) through the analysis of a 21.48 m lacustrine sediment core (ACA I-11).

The sedimentary column was sampled every 10 cm or where sedimentation changes were appreciated, obtaining a total of 160 samples. Samples were analyzed by means of the paleoclimatic indicators of organic (TOC) and inorganic (TIC) carbon contents, magnetic susceptibility, mass spectrometry and diatoms. Dating of the core is in process. Seven zones were discerned based on the lithology, characterized by the dominance of clayey, silty and limey sand facies. Peat strata are present at 1.14 and 3.85 m, besides the presence of four strata of volcanic material at depths of 8.70, 8.90, 10.50 and 10.60 m.

The concentrations (in ppm or in % by weight) in sediments of chemical elements were determined by means of mass spectrometry as a basis for paleoenvironmental interpretation, and for defining the provenance of the minerals present in the sediments of the basin.

In this study Fe, Ti, Al, K and Fe/Al were used as proxies of the terrigenous contribution; other elements such as Na, Ca and Mg indicating salt enrichment. These elements, associated with TIC and TOC allowed for identification of wet and dry phases, transgressions and regressions, volcanic events and other synsedimentary phenomena. A trend for dryer conditions was observed during the late Pleistocene, while in the Holocene the stability of the lake is maintained with shallow marshes dominating the landscape.

From the base to the top of the core, the TIC and TOC values reveal more stable wet and dry periods between 18 and 21 meters, beginning with a drought period between 20 and 21 m followed by a wet phase between 18 and 20 meters. This wet phase is again present in the final 5 meters of the lake deposits.

ZONE 1- During the drought period between 20 and 21 m, although the content of Fe is low relative to the remaining profile, two maximums of this element are present coinciding with the peaks of □$_{lf}$, the most intense one being registered at 2090 cm, reflecting the predominance of ferromagnetic minerals due to a source of detritus. The minimum values of □$_{lf}$ within this range are coincident with high TIC. It is worth noticing that carbonates and alkaline salts are diamagnetic and decrease the □$_{lf}$ values. During this episode *Campylodiscus clypeous* and *Surirella* spp. are common, species that live in environments having high ionic concentrations.

ZONE 2-Between 18 and 20 m the highest TOC values in the record are observed in coincidence with high Fe values, probably present as a mixture of Ti-magnetite minerals and as ferrihydrite, mostly associated with humid environments. A short drought period is noticeable at 19.40 m (where *Campildiscus* and *Surirella* are common), however the trend in the record is towards humidity consistent with associations of *Epithemia*, *Rhopalodia* and scarce *Stephanodiscus*, all present in stable alkaline lake environments with moderate oxygenation.

ZONE 3-From 1800 to 1250 cm values of TIC and concentrations of Ti and Al are increased. The TOC decreases, contrariwise to the previous phase. Environments with high salt concentration are evidenced in saline environment diatom associations (*Campylodiscus* and *Navicula*). Very low values of □$_{lf}$ are observed, probably due to part of the Fe being present as paramagnetic minerals, besides the presence of large amounts of diamagnetic minerals (decreasing □$_{lf}$ values).

This trend decreases towards the summit (12.50 to 12.70) where erosion declines and deep water inhabiting taxa are more abundant (*Stephanodiscus* and *Aulacoseira*).

ZONE 4-In the next zone, from 1250 to 850 m, two volcanic events alter the stability of the lake, the TOC fluctuates giving place to associations of *Aulacoseira* and *Stephanodiscus* indicating turbidity and a certain trend to deepening. However, the silty facies with abundant concretions of carbonates and reworked clays reveal a shallow lake with sudden decreases in water level with the contribution of volcanic activity. Diatom populations continue to show associations from saline, shallow lake environments in which *Surirella* and *Campylodiscus* are common. High values of TIC are coincident with the increase in □$_{lf}$

values, with a maximum at 1180 cm, because of which the magnetic phase corresponds to Ti-magnetite with variables amounts of Ti due to volcanic input.

ZONE 5-From 850 to 600 cm, an ascending stability of strata is recorded interrupted by a short high ionic concentration phase. However, diatoms in this interval are characteristic of more diluted environments than in the previous phase (*Aulacoseria*, *Staurosira* and *Stephanodiscus*). Above these strata, a noticeable decrease in TIC and the lowest χ_{lf} values are observed. Despite a slight drop in Fe content, this is present as non-magnetic minerals, the low amounts of magnetic mineral probably being present as a Ti-maghemite highly enriched in Ti. TOC values remain constant.

ZONE 6-From 600 to 400 cm, course detrital facies confer relatively high χ_{lf} values peaking at 475 cm. This maximum value is clearly due to the presence of Ti-magnetite, the remaining sector of the core containing the same mineral but with a higher substitution of Ti and the magnetic fraction also probably having a higher percentage of superparamagnetic grains. Diatoms are characterized by coexisting in shallow lacustrine, marshy (*Eunotia*) and diluted (*Cymbella cistula*) environments.

ZONE 7-Towards the core's summit (400-0 cm) the TOC values increase, peat facies dominated by *Eunotia* and *Nitzschia* being noticeable at 3.85 and 1.14 m. This humid phase with shallow ponds is interrupted by a slight increase in χ_{lf} peaking at 200 cm with presence of Ti-magnetite, the remaining sector probably containing ferrihydrite as the magnetic phase, suggesting a rise in humidity. No diatoms were preserved in this top segment, possibly due to a rise in alkalinity of the lake.

FINAL REMARKS

The multi-proxy analysis of the depocenter of the Upper Pleistocene to Holocene Acambay paleolake reveals dry phases, generally observed between 21.48-10 m and showing short humid fluctuations, while from 10 m to the summit the lake shows a sudden change to more humid and stable conditions.
Evidences of the seismic activity in this basin are recorded in several depths of the core, mainly from 4.50 to 4.70m, 14-15, 16-17 and 19m. Dating in process will give more evidences of the seismic phenomena in the zone covering the Pleistocene-Holocene record.

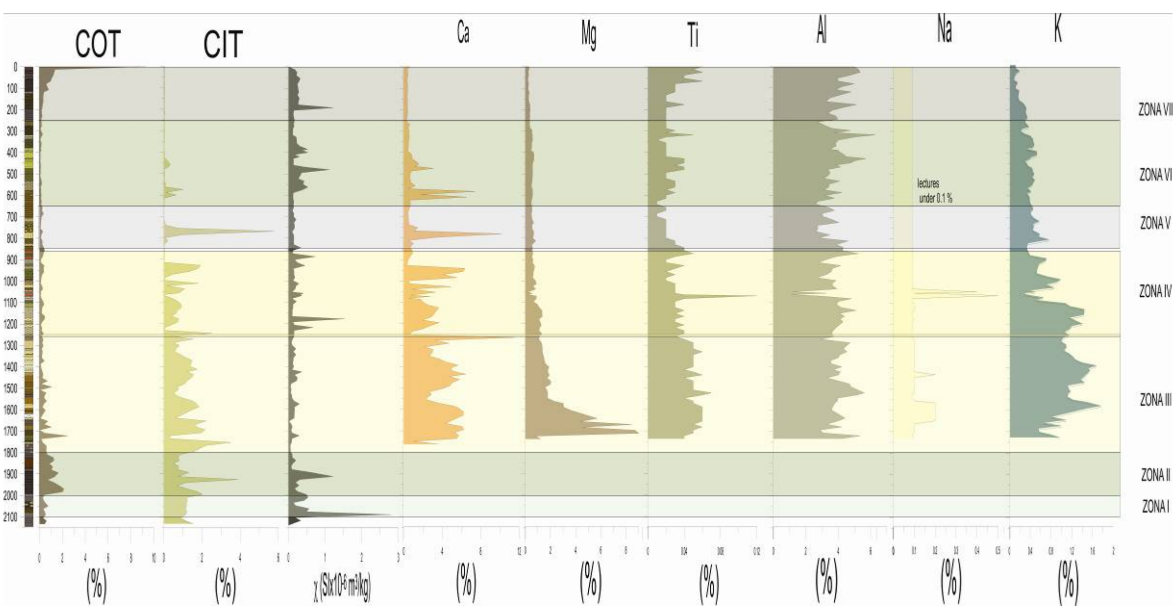

FAULT AND FRACTURE ANALYSIS OF CHICHONAL VOLCANO AND ITS RELATIONSHIP WITH SEISMIC HAZARDS

Jiménez Haro Adrián. (1), Garduño-Monroy Víctor H. (2)

(1) Escuela Superior de Ingeniería y Arquitectura U. Ticomán. Instituto Politécnico Nacional. D.F. MEXICO.
adrianjharo@hotmail.com

(2) Instituto de Investigaciones Metalúrgicas. Universidad Michoacana de San Nicolás de Hidalgo. Morelia. MEXICO.
vhgardunom@gmail.com

Abstract: *The Chichonal Volcano is located at the SE portion of Mexico, where three great tectonic domains converge (North American, Caribbean and Cocos Plates) and had been active from Miocene to Recent time, generating seismic activity and producing several damages in some Chiapanecan communities. The structural geology survey shows that the left lateral system fault with E-W direction has presented recent movement and seismic activity, generating a scrolling on N-S oriented rivers. One of the secondary structures of these left lateral faults is the Chichón-Catedral fault, a structure which controls the volcanic activity, landslides and hydrothermal activity of Chichonal.*

Keywords*: Left lateral faults, Chichón-Cateral Fault, seismicity, volcanic activity*

Till now, the neotectonic studies in Chichonal Volcano had been made only to understand and describe the origin, arrangement and geometry of the structures affecting the rocks of the area. The direct relation between the activity of these structures and the seismic hazards had not been taken into account; nevertheless, there is a clear evidence of potential geological hazards related to these structures originated by active tectonics, such as landslides and volcanic activity.

The Chichón Volcano is located at the southeastern portion of the country, in Chiapas State. It belongs to a volcanic complex that mainly consists on domes and craters with traqui-andesitic composition and Holocene ages (Layer *et al*., 2009). The volcanic complex was emplaced over the Buena Vista synclinal, a folded sedimentary sequence where the axes of these folds show a NW-SE direction.

The Chichonal Volcano is settled at the NW of the Chiapanecan Volcanic Arc (CHVA) in a complex structural zone, where three great tectonic domains converge (North American, Caribbean and Cocos Plates) and suffer great deformations due to the rotation of Caribbean Plateo over the North American Plate (Adreani *et al*., 2008), generating a migration of southeastern Mexico towards the Caribe since middle Miocene (Guzmán-Speziale and Meneses-Rocha, 2000) (Fig.1). Therefore this region is related to a tectonic transpression, which can be reflected on the structures of the Chichonal Volcano.

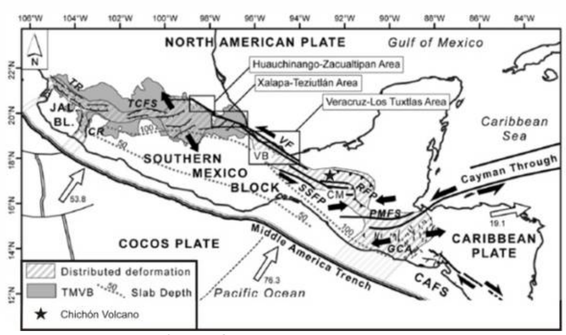

Fig 1. Location of the Chichonal Volcano, the mega-structure suggested by Andreani et al. (2008), and its relationship with the Chiapas lateral fault system; modified from Adreani et al., 2008.

The Chichonal Volcano is located near the zone of left lateral faults of Chiapas, where some major segments of these faults have presented recent movements (Guzmán-Speziale and Meneses-Rocha, 2000). Last century they generated high magnitude seismicity which produced serious damages; like the 1902 event in San Bartolomé de los Llanos (now called Venustiano Carranza), the 1914 event in Altamirano, Ocosingo and Huixtán communities (Figueroa, 1973); all of them were shallow movements, where their focal mechanisms suggest a relation with left lateral faults (Fig 2).

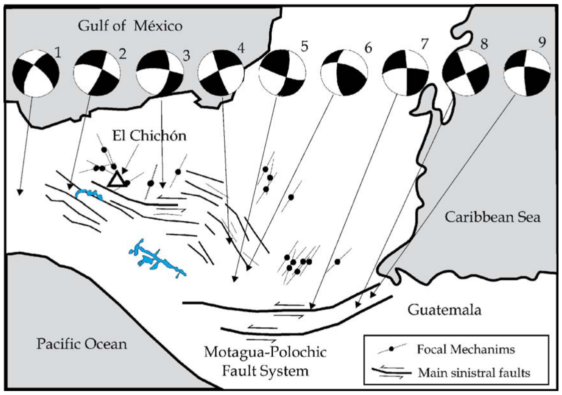

Fig 2. Seismic data analysis and focal mechanisms for the Chichonal Volcano; from García Palomo, 2004 and modified from Guzmán-Speziale and Meneses-Rocha, 2000.

Fig. 3. Picture that shows a segment of the Chichón-Catedral Fault, which perpendicularly cuts the Susnubac river; the vertical displacement and the intense fracturing can be seen.

The tectonic context has led to a N-S to NW-SE oriented folded range, with NW axes slopes (García-Palomo *et al*. 2004). The basement consists of a Mesozoic-Tertiary carbonate formation, where the fractures show four different main directions: the more common are NE-SW and NW-SE oriented, meanwhile the least common show a NNE-SSW and ENE-WSW direction (Fig. 3). Although the structural analysis shows that the fractures are defined by tension fractures, shear fractures and hybrid fractures related to a plicative deformation with a NE-SW oriented horizontal S1, some of them are also related with grater left lateral faults.

One of the structures that suggest the active tectonic effects on the Chichonal Volcano is the Chichón-Catedral Fault. This fault has a NW-SE direction and it can be seen from the southeastern part of the ranges, passing through the Chichonal volcanic crater to the eastern part of it.

Another important structure is the Catedral Fault, NE from Chichonal Volcano, a normal fault with left lateral component, it measures 18 km and presents a 200 m scarp. This structure controls the drainage network direction and has an important effect on regional landslides and hydrothermal activity. On the geomorphology we can observe an angular geometry, obeying the E-W left lateral faults. It can be said that the Catedral Fault is a secondary structure that works as a Riedel fault relative to the NW-SE regional lateral system fault (Fig. 3).

Although some authors consider that the Chichón volcano is not within the Chiapas lateral fault zone, like the Copainala-Ocosingo, Malpaso-Chicoasen and la Venta system faults, García Palomo *et al.* (2004) found strong evidence of left lateral structures affecting some units of the studied area; some of them are the San Juan Fault, the Arroyo de Cal Fault and the Ixtacomitán Fault with E-W direction (Fig. 4).

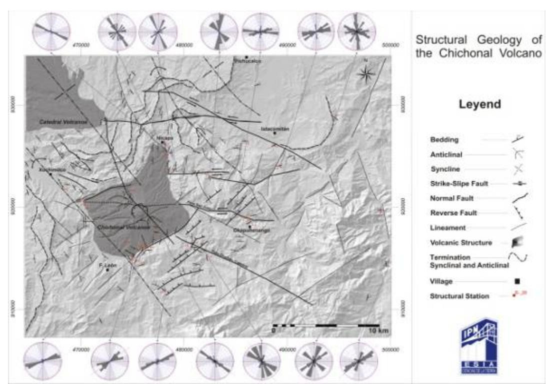

Fig. 4. Geological and structural map of Chichonal Volcano, which shows the main structures, structural stations, some communities and the fracture analysis of the most representative sites, represented by the rose diagrams.

The faults and fractures found in this region are related with geological hazards and represent a major risk for the population and the infrastructure near them because they can trigger regional seismic movements, landslides or volcanic activity.

In general, this work shows that the tectonic ambience near Chichonal Volcano has been active since Miocene to recent times, and although we didn't find clear coseismic ruptures there are three relevant aspects that can assure an active tectonic activity on this area;

1. The morphological analysis shows the displacement of some rivers with recent sedimentation, which present a preferred N-S

orientation and which are cut by E-W left lateral structures.

2. The recent seismic activity related to shallow movements originated by left lateral faults, causing great damages on some Chiapanecan communities, and is congruent relation with the actual stress system.
3. The hydrothermal activity observed along the Chichón-Catedral Fault, which controls the volcanic activity of Chichonal Volcano.

References

Andreani L., Rangin C., Marinez-Reyes J., Le Roy CH., Arandas-Garcia M., Le Pichon X., Peterson-Rodriguez R., 2008**.** The Neogene Veracruz fault: evidence for left-lateral slip along the southern Mexico block. Bull. Soc. Géol. Fr., t. 179, no. 2, p 195-208.

García Palomo, A., Macías J.L. and. Espindola J.M. Strike-slip faults and K-Alkaline volcanism at El Chichón volcano, southeastern Mexico. Journal of Volcanology and Geothermal Research, 136: 247-268, 2004.

Guzman-Speziale M. y Meneses-Rocha J.J., 2000. The Noth America-Caribbean plate boundary best of the Motagua-Polochic fault system: a fault jog in Southeastern Mexico. Journal of South American Earth Sciences, 13, p. 459-468.

SLIP COMPENSATION AND STRUCTURAL MATURITY OF LINKED FAULT SYSTEMS: A CASE STUDY FROM THE BOGD RUPTURE ASSOCIATED WITH THE 1957 GOBI-ALTAY EARTHQUAKE, MONGOLIA

Jin-Hyuck Choi, Young-Seog Kim

GSGR, Dept. of Earth Environmental Sciences, Pukyong National University, Busan 608-737, KOREA. cjh0421@pknu.ac.kr

Abstract: *It is recently proposed that structural maturity of the inter-segment zones are closely related to surface rupture propagation associated with large earthquake. The aim of this study is to understand the relationship between structural maturities and slip compensation, transferring of slip amounts between horizontal and vertical displacements, at inter-segment zones. For this purpose, we carried out slip analyses along the surface rupture, which shows unilateral propagation, associated with the M_W=8.1 1957 Gobi-Altay earthquakes. Segmentation and propagation scenario of the surface rupture are firstly examined based on damage patterns and abrupt slip changes. We then plotted two slip components (horizontal and vertical) at mostly inter-segment zones. The results show that inverse relationship between two slip components, here called as* ***slip compensation****, is considered as a common characteristic of inter-segment zones. However, both slip components decrease coincidentally at some inter-segment zones, where the linkage acts as a barrier to rupture propagation. Moreover, slip compensation is remarked at only one side tip, which arrest main propagation of coseismic rupturing, of the surface rupture. It means that the patterns of slip compensation can be a criterion to identify structural maturity of inter-segment zones and can be an important factor, controlling rupture propagation. Therefore, detailed analysis of slip compensation may provide important information for characteristics of earthquake rupture propagation as well as fault growth and evolution.*

Key words*: Fault damage zone, earthquake surface rupture, inter-segment zones, structural maturity, slip compensation.*

Introduction

Understanding what can controls earthquake rupture propagation and/or arrest, particularly along strike-slip faults, is important in modern earthquake hazard studies. Although it is well known that connectivity between neighbouring fault segments is a key controlling factor (e.g. Scholz, 2002; Manighetti et al., 2005; Kim et al., 2005), it is difficult to define the structural maturity of the inter-segment zones. We carried out detailed mapping of the surface rupture associated with the 1957 Gobi-Altay earthquake (M_W 8.1), that occurred along the Bogd left-lateral strike-slip fault in Mongolia, to find the controlling factors, allowing or arresting surface rupture propagation. For this purpose, we first classified rupture patterns based on the well-defined "fault damage model" along natural faults by Kim et al. (2003, 2004). We then defined segmentation of the surface rupture based on slip distribution combined with the location of damage zones. A scenario of rupture propagation and termination was then proposed based on the barrier concept (e.g. Aki, 1979; Klinger et al., 2006; Manighetti et al., 2007) with asymmetric slip distribution and tip damage patterns. Finally, we examined whether slip compensation at inter-segment zones occurs or not and looked at the relationships between slip compensation and the propagation of earthquake ruptures.

FAULT DAMAGE ZONES AND EARTHQUAKE

Fault damage zones are defined as deformed zones where secondary structures have developed around faults to accommodate displacement along the faults (e.g. McGrath and Davison, 1995; Shipton and Cowie, 2003; Kim et al., 2003, 2004; Myers and Aydin, 2004; Fig.1a). They can be mainly classified as wall-, linking- and tip-damage zones depends on their location along segmented faults. Linking damage zone, a main focus of this study, can be defined as the area with a high intensity of secondary structures between two fault segments. Tip damage zone develops as a result of stress concentration at fault tips where slip terminates. These damage structures including their slip variations might be closely related to primary earthquake rupturing (e.g. Sibson, 1989; King, 1986; Scholz, 1990; Schultz, 1999). Interestingly, Kim and Sanderson (2008) attributes the reason for the formation of an asymmetric slip profile and tip damages to the main direction of rupture propagation (Fig.1b).

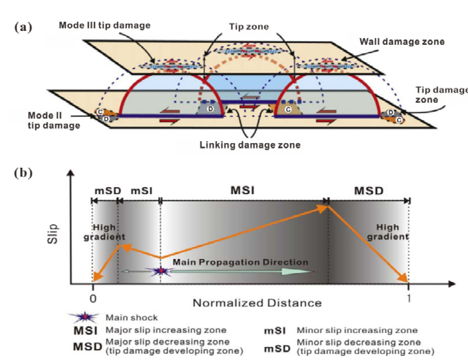

Fig. 1: (a) Conceptual model of fault damage zones (modified from Kim et al., 2004). (b) Unilateral earthquake propagation model (from Kim and Sanderson, 2008)

OVERVIEW: THE 1957 EARTHQUAKE SURFACE RUPTURE

The surface rupture associated with the 1957 Gobi-Altay earthquake in Mongolia occurred along the eastern Bogd fault system (Fig.2a, 2b). This fault system is considered as a main mature intra-continental fault related to the Indian plate's northward moving into the Eurasian plate (e.g. Molnar and Tapponnier, 1975). Although the rupture patterns are various, they depend obviously on their location along the segmented rupture trace. Various complex patterns, such as branch, splay and pull-apart, including minor vertical slip components are represented at linking and tip damage zones along the segmented faults (Fig.2e~2i), although a straight-line pattern dominates in the central parts of each fault segments (Fig. 2c, 2d).

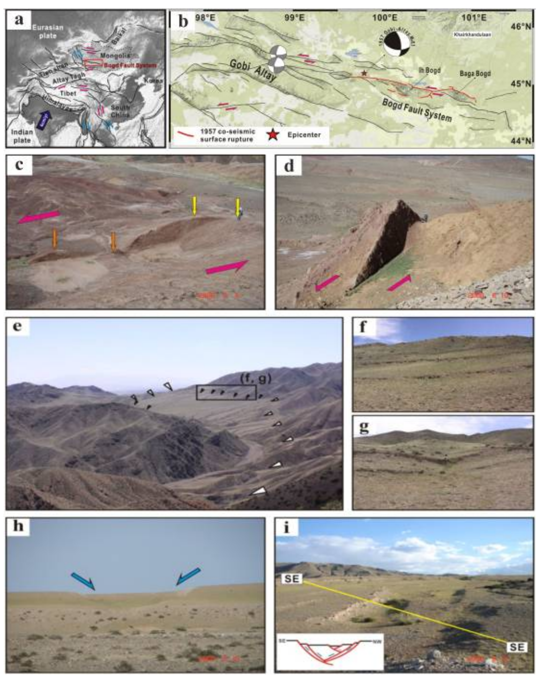

Fig. 2: (a, b) Simplified tectonic and structural maps around the Bogd fault system, Mongolia. Geomorphic offsets showing straight-line pattern (c, d) and damage patterns (e~i) along the 1957 coseismic surface rupture.

The surface rupture shows a dominant left-lateral strike-slip sense, with an average slip of about 3.5 to 4.0 m (e.g. Kurushin et al., 1997) with an increase or decrease at damage zones (Choi et al., *in revision*; Fig.3b, 3c). Vertical slip occur ranging from 1.0 to 1.5 m (e.g. Kurushin et al., 1997) and shows abrupt changes at damage zones (Choi et al., *in revision*; Fig.3b, 3c). Slip changes at linking and tip damage zones may indicate that damage patterns are closely related to rupture propagation and termination. A notable point is that a decrease of both horizontal and vertical slip has been observed at only three releasing linking damage zones, even though there are more than ten geometrical step-over zones, and both tip zones (Fig.3b~3d).

We identified three major segments and a widely deformed eastern tip damage zone along the surface rupture based on the following criteria: 1) considerable changes of rupture patterns, 2) abrupt changes in slip amount, and 3) locations of fault step-overs (Choi and Kim, 2011). Each segment was named using previous designation from Rizza et al. (2011) moving from west to east as follows: North Ih Bogd (NIB), East Ih Bogd (EIB), and North Baga Bogd (NBB) segments (Fig.3a).

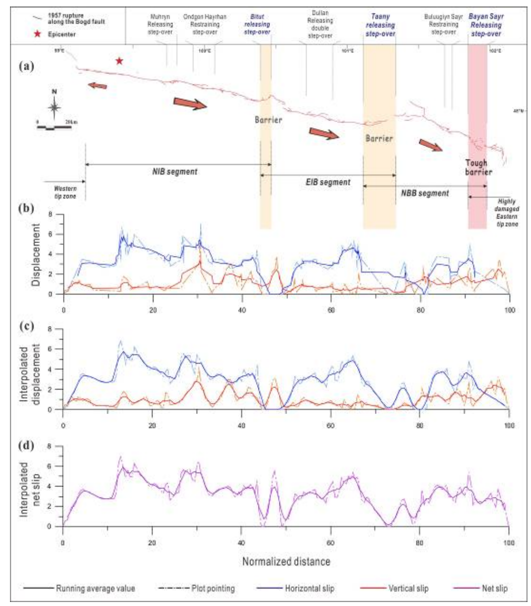

Fig. 3: Fault geometry (a) and slip distribution (b~d) along the 1957 coseismic surface rupture. These patterns can be used as criteria of fault segmentation and dynamic rupture propagation.

RUPTURE PROPAGATION

Choi and Kim (2011) pointed out that the epicenter of the 1957 event is located at the western end rather than central part of the coseismic surface rupture and that a highly damaged tip zone has developed at the eastern end. The tip zone is bounded on one side by the easternmost inter-segment zone at which both horizontal and vertical slip decrease. It reminds an above mensioned unilateral propagation concept (Kim and Sanderson, 2008; Fig.1b).

Another approach to rupture dynamics is the barrier concept (Klinger et al., 2006; Manighetti et al., 2007), which states that fault discontinuities such as inter-segment zone can act as barriers, arresting or stopping ruptures as stress concentrators. Some inter-segment zones acting as barriers are expressed as slip trough on slip distributions along earthquake ruptures (Ellis and Dunlap, 1988; Peacock and Sanderson, 1991; Walsh et al., 2003; Manighetti et al., 2009). For this perspective, the structural maturity of inter-segment zone is a major controlling factor for allowing propagation or arresting it (e.g. Manighetti et al., 2007). A mature linkage can behave as a through-going fault, and rupture will propagate through the fault linkage. In contrast, immature fault linkage will act as a resistant barrier and can terminate rupture.

Based on the unilateral propagation model and the barrier concept, along with detailed damage patterns and slip distribution along the 1957 Bogd surface rupture, we propose a possible scenario for the surface rupture propagation. Firstly, the main shock occurred at the western NIB segment which ruptured. The rupturing then propagated mainly eastward, while westward propagation terminated. Subsequently, an eastward unilateral propagation through two barriers occurred and was finally arrested at a tough barrier (easternmost step-over). A highly damaged tip zone developed to accommodate the remaining stress (Fig.3a).

SLIP COMPENSATION

The segmentation and propagation of the Bogd surface rupture show that they are clearly controlled by the structural maturity of inter-segments zones. Lettis et al. (2002) proposed that fault step-overs with a width greater than 4 to 5 km, perpendicular to fault strike between two fault segments, can arrest up to 5.0 m or more of fault displacement, but a narrow step-over 1 to 2 km wide would allow propagation. However, our observations do not seem to show that dimension of the step-over can be a main criteria that necessarily defines the structural maturity at inter-segment zones. Kim and Sanderson (2005) suggests that whether displacement is decreased or not at linkage zones can be a key to identify the degree of connectivity being described, as hard-linked or soft-linked. However, they mentioned only the changes of horizontal displacements along strike-slip faults.

Horizontal and vertical slip distributions along the rupture, when plotted comparatively, show that they are commonly in inverse relationship at fault damage zones (Fig.3b, 3c). This means the transfer between two slip components, defined here as slip compensation, are common and act as a bridge during earthquake rupture propagation, but not always.

To exam, in more detail, the relationship between slip compensation and surface rupture propagation and/or termination, we plotted the horizontal slip against vertical slip at each geometrically separated sections such as linking and tip damage zones (Fig.4a). The results indicate that individual step-over or tip zones display different compensation patterns. Firstly, both tip zones show different results – slip compensation occur only at the highly damaged eastern tip zone (Fig.4b). Different patterns are also seen between step-overs that act as barriers and others: no slip compensation occurring at barrier-related inter-segment zones, while both slip components compensate each other at other step-overs (Fig.4c). In the latter case, compensation ratio between two slip components are higher at restraining step-overs rather than realesing step-overs.

The greatest amount of slip compensation is visible at the easternmost step-over zone where unilateral rupturing terminates (Fig.4d). Although this zone acts as a barrier during rupturing, the compensation pattern is different from the other two inter-segment barriers. The characteristics of this slip compensation is closely related to fault damage zones and their roles during rupture propagation. This means that detailed analysis of slip compensation can be a major criteria to identify structural maturity of linking damage zones and can be a importnat factor in the control of rupture propagation.

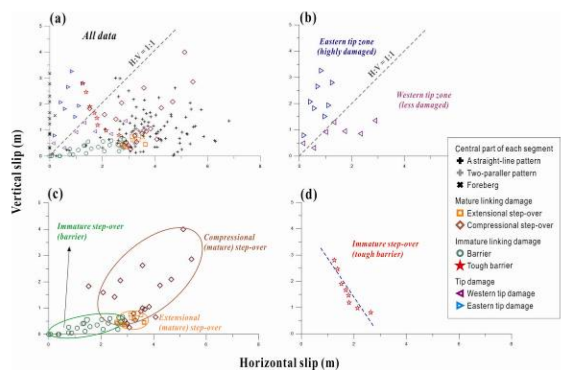

Fig. 4: Plots of horizontal versus vertical slip along the 1957 coseismic surface rupture. (a) All data, (b~d) data for each fault damage zones.

DISCUSSION

Individual step-overs or tip damage zones display different patterns of slip compensation which is related to its maturity along the coseismic surface rupture. At step-overs acting as inter-segments barrier, less or no slip compensation occur probably due to the immature (soft-linked) inter-segments. In contrast, other step-overs, which lead to slip compensation, allows continual rupturing, and it may be the result of mature (hard-linked) step-overs. In other words, two segmented faults act as almost a single fault. Furthermore, another factor for different compensation ratio could be considered, which might depend on whether it belongs to a releasing or restraining linkages zone. This is probably related to stress accomodation associated with kinematic characteristics in linking damage structures with different slip and step senses. In fact, we observed more secondary surface ruptures within releasing step-overs, such as branchs, splays and pull-aparts, rather than at restraining step-overs.

For this perspective, the remarked slip compensation at a tough barrier and connected tip zone is probabaly translated as numerious secondary ruptures. On the assumption that unilateral rupture propagation causes asymmetric tip damage between both ends of a coseismic surface rupture, the different slip compensation is attributed to the unilateral rupture propagation. These results indicate that evolutional characteristics as well as geometry and kinematics of damage zones along the surface ruptrue can improve our understanding for mechanism of coseismic surface rupturing.

CONCLUSIONS

We analyzed rupture pattern, slip distribution and compensation, mostly at fault damage zones, along the Bogd surface rupture associated with the 1957 Gobi-Altay earthquake. This coseismic rupture is composed of three major segments (NIB, EIB and NBB) with a highly damaged eastern tip zone. Asymmetric damage pattern and slip compensation at both tips may result from an eastward unilateral rupture propagation. Detailed analysis of slip compensation at step-overs shows that it is closely related to structural maturity of linked fault segments and surface rupture propagation. Detailed compensation patterns, between two slip components, can help us to better understand rupture behaviors and earthquake hazards.

Acknowledgements: We thank Amagalan Bayasgalan, Dandar Enkhbayar and Battogtokh Davvasambuu for their positive cooperation in Gobi-Altay, Mongolia. We also thank Paul Edwards, Tae-Seob Kang, Carol Prentice and Aiming Lin for their very constructive comments.

References

Aki, K. 1979. Characterization of barriers on an earthquake fault, J. Geophys. Res., 84, 6140-6148.

Choi, J.-H., Y.-S. Kim. 2011. Propagation of coseismic surface ruptures based on damage patterns, slip distribution, and fault segmentation: A case study of the Bogd rupture associated with the 1957 Gobi-Altay earthquake, Mongolia. 2011 AGU Fall Meeting.

Choi, J.-H., K. Jin, D. Enkhbayar, B. Davvasambuu, A. Bayasgalan, Y.-S. Kim, *in revision*, Rupture propagation based on damage patterns, slip distribution, and fault segmentation of the 1957 M_W 8.1 Gobi-Altay earthquake rupture along the Bogd fault, Mongolia. J. Geophys. Res.

Ellis, M. A., W. J. Dunlap.1988. Displacement variation along thrust faults: implications for the development of large faults, J. Struct. Geol., 10, 183–192.

Kim, Y.-S., D. C. P. Peacock, D. J. Sanderson. 2003. Mesoscale strike-slip faults and damage zones at Marsalforn, Gozo Island, Malta, J. Struct. Geol., 25, 793-812.

Kim, Y.-S., D. C. P. Peacock, D. J. Sanderson. 2004, Fault damage zones, J. Struct. Geol., 26, 503-517.

Kim, Y.-S., D. J. Sanderson. 2005. The relationship between displacement and length of faults: a review, Earth Sci. Rev., 68, 317-334.

Kim, Y.-S., D. J. Sanderson. 2008. Earthquake and fault propagation, displacement and damage zones, in Structural Geology: New Research, edited by S. J. Landowe and G. M. Hammler, pp. 99-117, Nova Science Publishers, Hauppauge, New York.

King, G.C.P. 1986. Speculations on the geometry of the initiation and termination processes of earthquake rupture and its relation to morphology and geological structure, Pure Appl. Geophys., 124, 567-585.

Klinger, Y., R. Michel, G. C. P. King. 2006. Evidence for an earthquake barrier model from Mw ~7.8 Kokoxili (Tibet) earthquake slip-distribution, Earth. Planet. Sci. Lett, 242, 354-364.

Kurushin, R.A., A. Bayasgalan, M. Olziybat, B. Enhtuvshin, P. Molnar, C. Bayarsayhan, K. W. Hudnut, J. Lin .1997. The surface rupture of the 1957 Gobi-Altay, Mongolia, earthquake, GSA Special Paper, 320.

Lettis, W., J. Bachhuber, R. Witter, C. Brankman, C. E. Randolph, A. Barka, W. D. Page, A. Kaya. 2002. Influence of releasing step-overs on surface fault rupture and fault segmentation: examples from the 17 August 1999 Izmit earthquake on the North Anatolian Fault, Turkey, Bull. Seism. Soc. Am., 92(1), 19-42.

Manighetti, I., M. Campillo, C. Sammis, P. M. Mai, G. King. 2005. Evidence for self-similar, triangular slip distributions on earthquakes: Implications for earthquake and fault mechanics, J. Geophys. Res., 110, B05302.

Manighetti, I., M. Campillo, S. Bouley, F. Cotton. 2007. Earthquake scaling, fault segmentation, and structural maturity, Earth. Planet. Sci. Lett., 253, 429-438.

Manighetti, I., D. Zigone, M. Campillo, F. Cotton. 2009. Self-similarity of the largest-scale segmentation of the faults: implications for earthquake behavior, Earth. Planet. Sci. Lett., 288, 370-381.

McGrath, A. G., I. Davison .1995. Damage zone geometry around fault tips, J. Struct. Geol., 17, 1011–1024.

Molnar, P., P. Tapponnier. 1975. Cenozoic tectonics of Asia: effects of a continental collision, Science, 189, 419-426.

Myers, R., A. Aydin .2004. The evolution of faults formed by shearing across joint zones in sandstone, J. Struct. Geol., 26, 947-966.

Peacock, D. C. P., D. J. Sanderson .1991. Displacement and segment linkage and relay ramps in normal fault zones, J. Struct. Geol., 13, 721-733.

Rizza, M., J.-F. Ritz, R. Braucher, R. Vassallo, C. Prentice, S. Mahan, S. McGill, A. Chauvet, S. Marco, M. Todbileg, S. Demberel, D. Bourles .2011. Slip rate and slip magnitudes of past earthquakes along the Bogd left-lateral strike-slip fault (Mongolia), Geophys. J. Int., 186, 897-927.

Scholz, C. H. 1990. The Mechanics of Earthquakes and Faulting, 1st ed., pp. 461, Cambridge Univ. Press, New York.

Scholz, C. H. 2002. The Mechanics of Earthquakes and Faulting, 2nd ed., pp. 471, Cambridge Univ. Press, New York.

Schultz, R. A. 1999. Understanding the process of faulting: selected challenges and opportunities at the edge of the 21st century, J. Struct. Geol., 21, 985-993.

Shipton, Z. K., P. A. Cowie .2003. A conceptual model for the origin of fault damage zone structures in high-porosity sandstone. J. Struct. Geol., 25, 333-344.

Sibson, R. H. 1989. Earthquake faulting as a structural process, J. Struct. Geol., 11, 1-14.

Walsh, J. J., W. R. Bailey, C. Childs, A. Nicol, C. G. Bonson. 2003. Formation of segmented normal faults: a 3-D perspective, J. Struct. Geol., 25, 1251-1262.

PALEOSEISMOLOGY & ARCHAEOSEISMOLOGY MORELIA • MEXICO 2012
INQUA-TERPRO PALEOSEISMOLOGY
EARTHQUAKE ARCHAEOLOGY

PALEOSEISMOLOGICAL INVESTIGATIONS IN THE NORTHERN TIEN SHAN NEAR BISHKEK (KYRGYZSTAN)

Landgraf, A. (1), Abdrakhmatov, K. (2), Djumabaeva, A. (2), Strecker, M.R. (1), Arrowsmith, J.R. (3)

(1) Inst. für Erd- und Umweltwissenschaften, Universität Potsdam, Potsdam, GERMANY. landgraf@geo.uni-potsdam.de
(2) Kyrgyz Institute of Seismology, Bishkek, KYRGYZSTAN.
(3) School of Earth and Space Exploration, Arizona State University,Tempe, USA.

Abstract *The northern Tien Shan was affected by a series of major earthquakes in the late 19th and earliest 20th centuries, which are amongst the largest known intraplate earthquakes worldwide: 1885 (Ms 6.9), 1887 (Ms 7.3), 1889 (Ms 8.3), and 1911 (Ms 8.1). We started paleoseismological investigations near Panfilovkoe, about 75 km west of the Kyrgyz capital Bishkek, where youthful scarps in alluvial-fan deposits attest to sub-recent ground deformation. The alluvial fan has been active since Late Pleistocene time and comprises distinguished lobes with vertical offsets between about 0.6 m and 3.8 m, respectively. Three trenches, excavated in the main scarp, have revealed that this offset distribution reflects repeated surface rupturing earthquakes with predominant dip-slip motion. The ultimate event was characterized by an offset between 1.2 and 1.4 m, corresponding to a possible magnitude between 6.8 and 7.2, emphasizing the seismogenic nature of the Tien Shan with infrequent, large magnitude earthquakes.*

Key words*: Intracontinental paleoearthquakes, Tien Shan, Kyrgyzstan*

INTRODUCTION

The Kyrgyz Tien Shan is an intracontinental orogen, characterized by reverse-fault bounded ranges, ubiquitous evidence for active tectonism and mainly moderate earthquake magnitudes (Kalmetieva et al., 2009). Although about 22 mm/a of shortening, which constitutes about half of the total convergence between India and Eurasia, are accommodated in the Tien Shan (Zubovich et al., 2010), Quaternary deformation phenomena, including decadal time scales, show that this rate is widely distributed across the entire belt, leading to slip rates of 1-2 mm/a for individual faults (Thompson et al., 2002; Zubovich et al., 2010). The historic earthquake in Kyrgyzstan (Fig. 1) reaches back to 250+/-100 yrs BP (e.g., Abdrakhmatov et al., 2002; Kalmetieva et al., 2009). From reported damage, magnitudes > 6 have been inferred for many of these events. However, such reports are often incomplete and biased for instance by the population distribution as well as cultural or political transitions, accompanied by widespread destruction and loss of documentation. The location of the Tien Shan and present-day Kyrgyzstan between the northern and southern branches of the silk route (e.g., Korjenkov et al., 2003) might have resulted in higher population density along the former trade routes and thus a higher probability that earthquakes affecting these areas got reported. Indeed, the distribution of significant events (M > 6.5) seems to be concentrated along the northern and southern sectors of the Tien Shan, respectively (Fig. 1). At the turn of the 19th century, a series of large-magnitude earthquakes, exceeding magnitude 7, affected the northern Tien Shan in 1885 (Ms 6.9), 1887 (Ms 7.3), 1889 (Ms 8.3), and 1911 (Ms 8.1) (e.g., Abdrakhmatov et al., 2002). This corresponds to a large amount of energy released in such a short period of time in an intraplate setting. Furthermore, the epicentral areas of these events were located near the present-day Kyrgyz capital (Bishkek) and the previous Kazakh capital Almaty (formerly Alma-Ata or Verny), which were severely damaged.

The spatiotemporal clustering of these events might show a synchronization of the associated faults (e.g., Scholz, 2010), possibly promoting fault (segment)-wise triggering or alternating of subsequent shocks or events, as observed in other areas such as along the Denali fault (Eberhart-Phillips et al., 2003), the North Anatolian fault (Stein et al., 1997; Hubert Ferrari et al., 2000), or along the eastern Californian shearzone (Rockwell et al., 2000).

For a better mechanistic understanding of these events it is crucial to document the exact historic rupture patterns, to increase the time span of observation concerning previous events along the ruptured fault systems, and to analyze their paleo-seismic history. This will help to better understand, if the observed seismic behavior is unique or recurrent, and if any kind of pattern can be distinguished from these records. In this study, we have started paleo-seismological investigations near Bishkek, Kyrgyzstan, in the vicinity of the 1885 event epicentral area.

PALEO-EARTHQUAKES AT PANFILOVKOE

The study area is located north of the Kyrgyz range, thus along the northern margin of the Tien Shan (Fig. 1). The main structures that bound the Kyrgyz range to the north, are the en échelon arranged Chonkurchak and Shamsi-Tunduk faults (e.g., Thompson et al., 2002). The Chonkurchak fault marks the boundary between pre-Cenozoic basement and late Cenozoic deposits at the western range front. In the central part of the Kyrgyz range, where the deformation front has migrated northwards, Neogene sediments are thrusted over foreland deposits along the approximately 120 km long Issyk-Ata fault, a splay of the Chonkurchak and Shamsi-Tunduk fault system. Thompson et al. (2002) have estimated a Quaternary slip rate of 2.1 +1.7/-0.3 mm/yr for its central part.

We present paleoseismic data from a site, located about 35 km west of Belovodskoie, the epicenter of the 1885 (Ms 6.9) earthquake, about 75 km west of Bishkek in the immediate foreland of the Kyrgyz range. The site (Panfilovkoie) is comprises youthful, north-facing scarps, probably related to activity of the Chonkurchak fault. The scarps cut through an alluvial fan, whose former transport surface is inclined about 3-4° to the north; this surface is nested inside a late Pleistocene loess terrace (Fig. 2). The northern, more prominent and approximately E-W striking scarp can be followed for about 4 km across the alluvial fan. This scarp is aligned with a cumulative break in topography of about 13 m in the loess-covered surface to the west. The trace of the scarp suggests a dominant reverse-faulting mechanism. The subordinate southern scarp trends ENE-WSW and mainly comprises left-stepping segments, suggesting a minor left-lateral component of motion due to oblique shortening. The alluvial fan is composed of different lobes of boulder-rich alluvial deposits with distinct offsets between about 0.6 m and 3.8 m. Three trenches (PT1 to PT3, marked as stars in Fig. 2) were excavated by us at the main scarp in order to better document the offset distribution and associated earthquake history.

PT1 was excavated in a scarp segment showing 1.5 to 2 m offsets. During the excavation the trench walls repeatedly collapsed at the position of the fault trace, producing an overhang and a change in orientation of the trench wall. The penultimate event can only indirectly and not unambiguously be recognized by the occurrence of a clay-rich deposit which lacks a counterpart in the hanging wall. We interpret this deposit as the wash part of the colluvial wedge, following the penultimate seismic event and sealing the rupture trace below. This deposit, in turn was cut by faulting during the most recent seismic event. Rupture at this location had occurred along an irregular plane, dipping approximately 40° to the south. The rupture zone is marked by rotated boulders and patches of grus, aligned below large boulders and passively transported along the fault trace. This layer of grus, probably originated from the same clast, has been logged for the length of approximately 1.20 m along the fault trace, corresponding to a vertical offset of about 77 cm.

PT2 reveals a succession of two alluvial deposits (units 1 and 2), covered by an organic-rich soil horizon (unit 3). These three units are faulted by one event. The offset units show a clear drag towards the fault zone. Two parallel associated fault planes dip approximately 36° to the south. The identified paleo-earthquake resulted in a hanging-wall collapse scarp. The associated colluvial wedge, with a maximum thickness of about 65 cm, seals the fault traces. A fine-grained wash deposit covers the wedge and the footwall units. Both, hanging wall and footwall are capped by a thin veneer of recent organic-rich soil. Similar to PT1, granite clasts along the fault lines were cataclasized to grus, which was transported or trapped below larger boulders, but could not attributed to the same source clast and thus did not serve as an offset marker. Furthermore, because the deposits were dragged towards the fault, the offset estimate involves a larger uncertainty. We determined the vertical offset to be approximately 80 cm, based on extrapolation of the contact between units 2 and 3 between meters -1.0 and 1.0 and between meters 3.5 and 5.5, respectively. An offset of 80 cm is in agreement with the vertical offset of the scarp profile, revealed near the trench location (Fig. 2C), resulting in approximately 136 cm of total slip during this event.

Trench PT3, which is located near PT2, but at a higher-offset location associated with a compound scarp segment (2.60 m in the nearest profile, Fig. 2), reveals the evidence for at least two paleo-earthquakes. Unfortunately, the stratigraphic base recording earlier events could not be excavated due to technical limitations. The excavation exposed a southeast-dipping fault zone with two sub-parallel branches. The northern branch ruptured during the penultimate, the southern during the ultimate event, respectively. The fault zone cuts two footwall units and an older colluvial wedge. The northern, older rupture trace contains sheared grus. Along this fault line, the lowest exposed footwall unit is vertically offset by approximately 50 cm, which corresponds to total dip-slip of about 89 cm, assuming a 34° dip of the fault. Above that, a colluvial wedge is recognizable by cataclasized clasts. The younger, southern fault trace extends below the large boulders that limit the excavation of the hanging wall. These boulders have no counterpart in the footwall. The fault plane strikes obliquely to the scarp and is traceable for about 1.20 m inside the trench. It cuts the lower colluvial wedge. The upper colluvial wedge comprises toppled boulders, with carbonate coatings, which are not everywhere on undersides. The vertical offset, when measured at the location of the fault, is on the order of 50 cm, resulting in approximately 76 cm of dip-slip along a 41° dipping fault. However, this is probably underestimated because the offset hanging-wall unit was clearly dragged towards the fault. If measuring the base between meters 6.0 and 7.0, however, which is parallel to the top of the unit and rather horizontal, the vertical offset amounts to approximately 90 cm, or about 1.37 m dip-slip, comparable to the slip observed in PT1 and PT2 for the ultimate event.

DISCUSSION AND CONCLUSION

In all investigated trenches, dip-slip motion was the dominant faulting process, resulting in hanging-wall collapse scarps and the deposition of colluvial wedges. However, the meter-size boulders in the hanging wall of PT3 which abut against the fault trace and which lack a counterpart in the footwall could either reflect a much higher dip-slip offset (i.e., buried boulders) or a lateral component of slip. Overall, we find that the observed offset distribution along the scarp reflects the interplay between surface faulting and alluvial fan dynamics. We find one event in the low-offset segment, which corresponds to alluvial deposits, apparently only marginally incised by ephemeral streams. The other two trenches, which correspond to alluvial-fan lobes that are more dissected and thus possibly more mature, reveal evidence for at least two rupture events, respectively. Unfortunately, the stratigraphic base to further decipher earlier events could not be excavated due to technical issues. Nevertheless, the scarp profile and trenching data show that this area has been repeatedly affected by surface rupturing events, when the fans were active. Preliminary ^{10}Be-surface exposure ages indicate that the faulted alluvial fan must have been active since late Pleistocene time. The different fan lobes, however, could not be further temporally distinguished. Ongoing age determination of offset strata and colluvial wedges are expected to provide additional data to unravel the faulting history. Besides reported Quaternary activity along the mountain-bounding Chonkurchak fault, the Panfilovkoe scarps indicate ongoing propagation of faulting into the foreland. If this activity, however, superseded activity along the mountain front or if both branches compete in a partitioning of slip, is not yet known. Nevertheless, our new trenching data suggest that the ultimate event recorded in all three trenches was characterized by an offset between 1.2 and 1.4 m, thus recording a major earthquake. Using probabilistic magnitude estimates (after Biasi and Weldon, 2006), this may correspond to a magnitude between 6.8 and 7.2, emphasizing the seismic activity of the northern Tien Shan with infrequent, large magnitude earthquakes.

Acknowledgements: This work was partially supported by the initiative Potsdam Research Cluster for Georisk Analysis, Environmental Change and Sustainability (PROGRESS) and the initiative TIPTIMON (support code 03G0809), by the German Federal Ministry of Education and Research.

References

Abdrakhmatov, K.E., Delvaux, D., & Djanuzakov, K.D., 2002. Active tectonics and seismic hazard of the Issyk-Kul basin in the Kyrgyz Tian-Shan, in Klerx, J., and Imanackunov, B., eds., *Lake Issyk-Kul: Its natural environment*, Vol. IV. Earth and Environmental Sciences, v. 13, 147-160.

Biasi, G.P. & Weldon II, R.J., 2006. Estimating Surface Rupture Length and Magnitude of Paleoearthquakes from Point Measurements of Rupture Displacement, Bulletin Seism. Soc. America, 96(5), 1612-1623.

Eberhart-Phillips, D., Haeussler, P.J., Freymueller, J.T., Frankel, A.D., Rubin, C.M., Craw, P., Ratchkovski, N.A., Anderson, G., Carver, G.A., Crone, J.A., Dawson, T.E., Fletcher, H., Hansen, R., Harp, E.L., Harris, R.A., Hill, D.P., Hreinsdottir, S., Jibson, R.W., Jones, L.M., Kayen, R., Keefer, D.K., Larsen, C.F., Moran, S.C., Personius, S.F., Plafker, G., Sherrod, B., Sieh, K., Sitar, N. & Wallace, W.K., 2003. The 2002 Denali Fault Earthquake, Alaska: A large magnitude, slip-partitioned event, *Science*, 300, 1113-1118.

Hubert-Ferrari, A., Barka, A., Jaques, E., Nalbant, S., Meyer, B., Armijo, R., Tapponier, P. & King, G.C.P., 2000. Seismic hazard in the Marmara Sea region following the 17 August 1999 Izmit earthquake, Nature, 404, 269-273.

Kalmetieva, Z.A., Mikolaichuk, A.V., Moldobekov, B.D., Meleshko, A.V., Jantaev, M.M., & Zubovich, A.V., 2009. Atlas of Earthquakes in Kyrgyzstan, ECHO, UNISDR, and CAIAG, pg. 233.

Korjenkov, A., Baipakov, K., Chang, C., Peshkov, Y., & Savelieva, T., 2003. Traces of Ancient Earthquakes in Medieval Cities Along the Silk Road, Northern Tien Shan and Dzhungaria, *Turkish J.Earth Sci*., 12, 241-261.

Rockwell, T.K., Lindvall, S., Herzberg, D., Murbach, D., Dawson, T. & G. Berger, 2000. Paleoseismology of the Johnson Valley, Kickapoo, and Homestead Valley faults: clustering of earthquakes in the eastern California shear zone, *Bulletin Seism. Soc. America*, 90, 1200-1236.

Scholz, Ch.H., 2010. Large Earthquake Triggering, Clustering, and the Synchronization of Faults, *Bulletin Seism. Soc. America*, 100(3), 901-909.

Stein, R.S., Barka, A.A., and Dieterich, J.H., 1997. Progressive failure on the North Anatolian fault since 1939 by earthquake stress triggering*, Geophys. J. Int*.,128, 594-604.

Thompson, S.C., Weldon, R.J., Rubin, C.M., Abdrakhmatov, K., Molnar, P., & Berger, G.W., 2002. Late Quaternary slip rates across the central Tien Shan, Kyrgyzstan, Central Asia, *J. Geophys. Research*, 107

Zubovich, A.V., Wang, X.q., Scherba, Y.G., Schelochkov, G.G., Reilinger, R., Reigber, C., Mosienko, O.I., Molnar, P., Michajljow, W., Makarov, V.I., Li, J., Kuzikov, S.I., Herring, T.A., Hamburger, M.W., Hager, B.H., Dang, Y.m., Bragin, V.D., & Beisenbaev, R.T., 2010. GPS velocity field for the Tien Shan and surrounding regions, *Tectonics*, 29, p. 23, TC6014

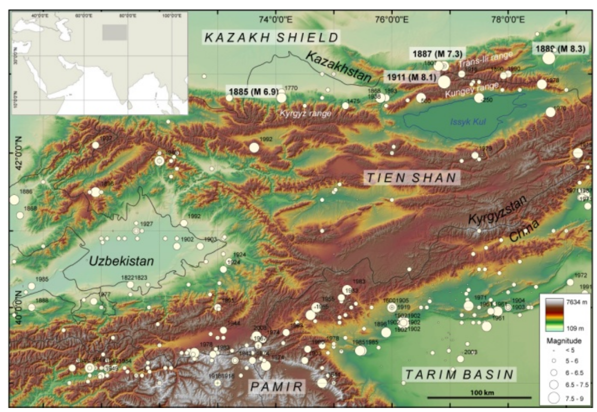

Figure 1: Digital Elevation model (SRTM) of Kyrgyzstan and bordering countries. Major geographic features are labeled. Overlain are historical earthquakes (Kalmetieva et al., 2009), events with magnitudes >6 are labeled with the year of occurrence. Note the series of strong events along the northern rim of the Tien Shan at the turn of the penultimate century. Inset shows position of figure (shaded area) in an Asian-Eurasian framework.

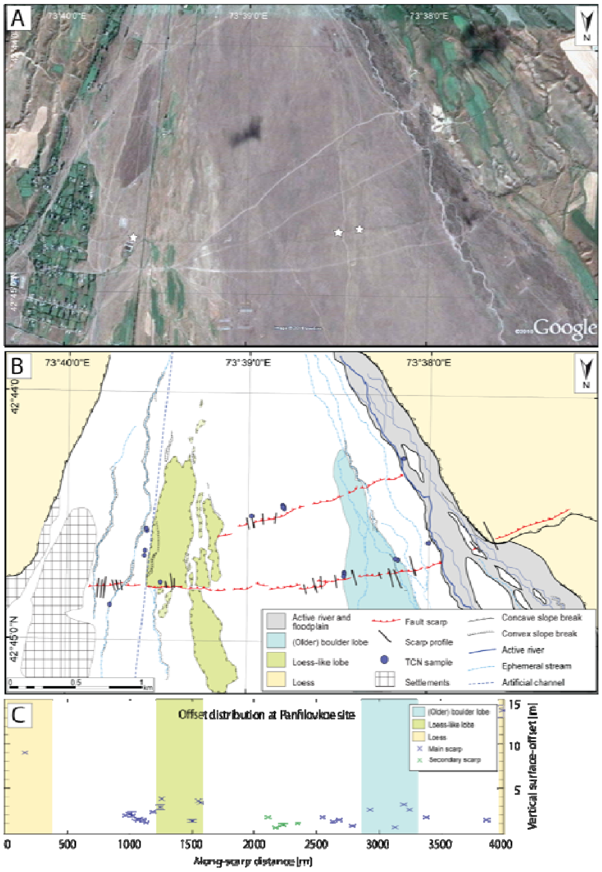

Figure 2: Google Earth satellite image (A) of the Panfilovkoe site showing sub-parallel, linear scarps in the alluvial fan and bordering Loess terrace and the geomorphic interpretation (B). White stars in (A) depict the trench locations (from left to right: PT1, PT2, PT3).

.

PALEOSEISMIC PARAMETER DETERMINATION USING THE METHOD OF TRENCHES

Lechuga-Valderrábano, Florencio. (1), Miranda-Rojas, María del Carmen. (2), González-Mellado, María Dolores. (3)

(1) Federal Commission of Electricity, Construction Subdivision, Management of Civil Engineering Studies, Department of Geology. florencio.lechuga@cfe.gob.mx
(2) Federal Commission of Electricity, Construction Subdivision, Management of Civil Engineering Studies, Department of Geology. carmen.miranda@cfe.gob.mx
(3) Federal Commission of Electricity, Construction Subdivision, Management of Civil Engineering Studies, Department of Seismotectonics and Geophysical Exploration. dolores.gonzalez@cfe.gob.mx

Abstract.
The study area is located to the NW of Mexico at the site of the Cerro Prieto Geothermal Central property. Here are localized active tectonic structures related to the opening of the Gulf of California associated to the migration of the Baja California Peninsula. Some of the parameters obtained in seismic hazard studies applying the technique of Paleoseismology trough trenching on active faults are: recorded of displacement during earthquake, velocity or displacement rate average, segmentation faults; evolution morphological landscape in the short or long term, the magnitude and recurrence of historic and prehistoric earthquakes as a result of tectonics.

Keywords: *Paleoseismology, Trenches, Holocene and Morphology.*

Introduction

Studies fault in trench excavations, provide elements to quantify processes of recent tectonic activity in a region, understand their influence on the local geomorphology, obtain structural and seismological models of the behavior and development of discontinuities. Previously performed structural geological mapping area Cerro Prieto Geothermal Central.

Activities for Paleoseismic Analysis.

Revision of ownership, use and possession of the land, establish location, size, method of excavation, initial conditions and final delivery of the affected area. Perform procedures to obtain permits dig sites where the trenches and deforestation. You should consider the water level, runoff near the proposed site of excavation, time of year; you will run the stage of excavation and subsequent study to use machinery and work efficiency, ground conditions for dry or wet materials and preservation of organic matter needed in collecting samples for radiocarbon of methods. Determine that surface materials and excavation stability condition. This design allows the final geometry of the trench, define the method of washing and scraping walls.

Geological Conditions for the Study paleoseismic

The discontinuity (fault) must affect the stratigraphic record with no evidence of erosion and be related to sedimentary environment or placed in interphase, where tectonic shows a block and the other accumulation erosion, in order to analyze the seismic record as associated deformations at the time of an earthquake can introduce vertical slopes slightly modify the erosive balance / scale sedimentary very precisely indicates that the local occurrence of paleoearthquakes. However, the erosion rate of sedimentation as not to be very fast, because events can be found sedimentary mass covering much of the exposed wall, which reduces the number of cycles to determine seismic. You should consider digging a trench in the present fault depth and lateral lithological changes that are not necessarily associated with a paleoearthquake therefore, we should analyze the occurrence of well marked lateral changes or abrupt such as; laminar stratification, parallel, cross, gradual or rhythmic, the age of the material, origin and sedimentary environment of deposition, to there by determine the deformations associated with a seismic event. In trench walls and continuous core recovery paleoliquefaction analyzes are performed, data contributors historic and prehistoric seismic events that help determine the surface area affected by this phenomenon. (Picture1).

Picture1. Excavation of trench T1 on the trace of the Cerro Prieto Fault, located within the geothermal field, in the area adjacent to the Laguna Vulcano.

Site Seismotectonic Conditions

It is necessary to identify and characterize the "seismogenic sources" to perform seismic risk studies. The surface seismogenic sources are classified into zones and large faults. The first projection surface representing a volume of cortex, where it is recognized that seismic occurrence is controlled by the set of fault systems that are located inside the cortical volume. The latter are unique tectonic deformation is concentrated and, therefore, the occurrence of large earthquakes effective measurable displacement surface (Butler, 2006), which can be estimated maximum recurrence within 10 000 years. It is considered as "active fault" (according to California Division of Mines and Geology), one that has offset within this time period. The "power failure", defined by the U.S. nuclear industry, is presenting evidence of at least one surface movement in the last 35 ka, or recurrent movements in the last 500 years. From a geological point of view is preferred classify faults based on their rate or sliding speed. The "Research Group for Active Faults in Japan", classifies the activity of faults in three groups named by the letters A, B and C. Failures in group A are those with a slip rate greater than 1 m/ka (1 mm / year), group B between 1 and 0.1 m/ka, and C below 0.1 m/ka. For the case of Cerro Prieto slip rate is considered 50 mm/year, which corresponds with faults "A". The sliding velocity of failure allows a preliminary estimate of the maximum credible magnitude range of earthquakes that can generate, and the average period of recurrence of these. A higher rate of fault slip, higher frequency of small magnitude earthquakes or intermediate stress state in a heterogeneous. Slip faults low rates major earthquakes occur with less frequency periods, and relates to a concentrated stress state. Identification of active faults in surface depend on the balance established between the slip rate of the fault and the rate of change of the landscape (erosion), mainly controlled by climate. In intraplate areas or margins of plate (as in the case of the Geothermal Cerro Prieto, BC) show active faults important slip rates, surface faults such place is easier than in wet arid . There are no active faults are observed on the surface, these cases are used for geophysical prospecting techniques.

Digging of trenches

For interest and review paleoseismic data measured directly on the trace of faults affecting the area of Cerro Prieto geothermal field, we conducted a field survey to locate sites with active faulting, four sites had this feature, so it was just digging trenches and mapping of its walls, was established stratigraphic column and associated structures, to analyze the pattern of ground deformation affecting also sampled for dating sediments. Three trenches are located on segments of the trace of the Cerro Prieto Fault and Failure more about Morelia. The excavation should expose young soft Quaternary sediments towards to detect deformations. It provides a grid reference on the walls of 0.50 meters and marked side reference levels and structures, detailed survey is made of the geometry and the horizons exposed identify seismic events recorded in the section studied and quantified the deformation; samples are deformed datable horizons, e.g. ground volcanic ash or organic matter. The average rate of displacement is obtained from displacement of the horizons dated. The evaluation of the magnitude of the paleoearthquakes is by empirical relations between magnitude and displacement jump or fault scarps and from the appearance of different signs on the ground. The recurrence evaluation period for the previously calculated displacement rate. The oldest horizons accumulate a greater leap than newer, and can eventually be undistorted levels. It should be located topographically the site where the trench was excavated in order to relate these works to a topographic and geologic basis of the area of interest.

Trench Sampling

To define the age of the soil horizons that are affected or deformed by seismic type geodynamic processes associated with tectonic activity in a given region is carried out sampling strata lithology of previously selected, which can provide important information from the point of paleoseismic view. Then proceed to drive a PVC pipe with dark opaque color 4" diameter, schedule 80 and length of 0.50 m. sampled on the horizon, approaching the material recovered four kg. The central part of the sample has the best conditions for analysis in the laboratory. When removing the tube, the orifice is installed generated gamma ray spectrometer that records the natural ground radioactivity. This procedure is based on determining the effects caused by the ionizing radiation of the radioactive isotopes of decomposition product of the elements uranium, thorium, potassium and cosmic radiation on a crystal lattice structure can be achieved very recent relative ages, with a range between 100 and 800 000 years. These radioisotopes data obtained in this stage are regarded as basis for the calculation and interpretation of the results obtained in the laboratory. Dating methods known and used are conventional C^{14}, Thermoluminescence (TL) and more rarely by Stimulated Luminescence Optical-Optical Stimulated Luminisence-(OSL), cosmogenic isotopes-BE^{10}, Al^{26}, He^{3}, amino acid racemization and uranium series (U / Th) and sometimes it is possible to require paleomagnetic dating. The geological environment of the study area, sediment composition showed quartz-feldspar materials sampled in the trenches. Was applied in this case the thermoluminescence (TL), which is to know the property of certain minerals (quartz, glass, and feldspar, etc.) to emit light if the temperature rises to a sufficient value, but below incandescence. This method can date samples up to 500 000 years old.

Structural-geological survey trenches

Trench T1 (Cerro Prieto Fault). Was excavated perpendicular to the trace of the Cerro Prieto fault in one direction NE35°SW, in the cartesian coordinates (UTM) E= 665 253.233 m, N= 3 582 474.442 and Elevation=

11,539 msnm, with a depth of 3.00 m and a length of 4.50 m. There were six horizons stratigraphically those affected by a failure of direction and cast N70°W/85°NE displacement of 0.49 m and the detection of an event paleoseismic. The top of the section T1 corresponds to the horizon "A" consisting of laminations yellow ocher to greyish, with fragments of quartz, feldspar and mica, their sizes ranging from medium to coarse sands, merging with fragments of clay, which fill a cone colluvial type that sits on the fault plane Cerro Prieto. 9.5 And 8.5 m, is lagoon-type deposits have formed on the horizons "C" and "E" respectively, formed of laminar clay material, with high organic matter content of dark gray to black color. 10.0, 9.0 and 8.0 m horizons "B", "D" and "F" respectively with cross bedding and ripples that indicate a depositional environment farm, consisting of medium-grained sands and interbedded fine clay, evidence that the area has presented over time periods of seasonal flooding and drought. Picture 2.

Trench T2 (Cerro Prieto Fault). It is located northwest of the evaporation pond in the cartesian coordinates (UTM) E= 660 024.669 m, N= 3 588 034.619 and Elevation= 21.040 msnm; SW11°NE direction perpendicular to the Cerro Prieto Fault, with 3.00 m deep and 8.75 m in length. Six recognized stratigraphic units affected by four fault planes associated to the same number of events with displacements paleoseismic 0.05 to 0.39 m. The horizons "T2-1" and "T2-2" correspond to slope deposits, combined with black and volcanic lithic eolian sands representing two periods of sedimentation red sands overlie horizontal stratification surfaces in cutting the ditch as "T2-3", the latter is likely to be correlated with an event effusive volcano Cerro Prieto. A depth horizons shows "T2-4" and "T2-6" made up of fine-grained sand medium with cross-bedding and ripples. The stratum "T2-5" is made up of sand medium to coarse grained volcanic rock fragments associated with events of volcanic or tectonic instability, influenced by slope deposits that came from the Cerro Prieto volcano wall.

Trench T3 (Cerro Prieto Fault). Located northwest of the evaporation pond in the cartesian coordinates (UTM) E= 659 986.663 m, N= 3 588 038.589 m and Elevation= 16.696 msnm, on the trace of the Cerro Prieto fault. The cut of the trench was a NE25°SW direction, perpendicular to the trace of the fault, at a depth of 3.00 m and length of 9.25 m. There were five stratigraphic units, which are affected by the fault whose orientation varies from N68° -75°W and inclination of 66-75°NE and six paleoseismic events. It breaks are 0.11 to 0.62 m**.** The horizon "T3-1" corresponds to the cutting layer is associated with slope deposit composed of black volcanic rock fragments and eolian sands. The slope deposits overlie the horizon "T3-2" consisting of stratified sand light gray to brown, correlates with the unit "T2-3" trench T2, whose origin is probably effusive volcano Cerro events Prieto.

Trench T4 (Morelia Fault). Was performed to the evaporation pond with cartesian coordinates (UTM) E= 665 502.217 m, N= 3 588 510.392 m and Elevation= 11.539 msnm, normal to the trace of the fault orientation Morelia NE73°SW**.** The excavation depth was limited to the water level to 2.20 m and length 2.50 m. Six stratigraphic units were recognized, affected by fault planes that show four paleoseismic events, movements vary from 0.11 to 0.26 m. At the top of the section is located the horizon "T4-1" to grayish yellow ocher, fragments consisting of quartz, feldspars, micas and organic matter, the size of fine sand suggesting a lake reservoir. Underlying it unity "T4-2" consists of dark gray to black clay, with a high content of organic matter and reddish, associated with a reducing environment lake. This unit overlying strata "T4-3" and "T4-6" with depths of 11.10 and 9.50 m, respectively, comprising a thin medium sands and ripples with cross reflect half of tank farm type. The horizon "T4-4" to 10.50 m depth consists of clays with a high organic content, is associated with lake environment. The stratum "T4-5" overlaps the "T4-6", composed of fine-grained sand, with the presence of organic matter, this unit shows injected into the Morelia fault plane associated with liquefaction due to seismic event. The stratigraphic arrangement presents the trench T4 has been subject to seasonal periods of flood and drought.

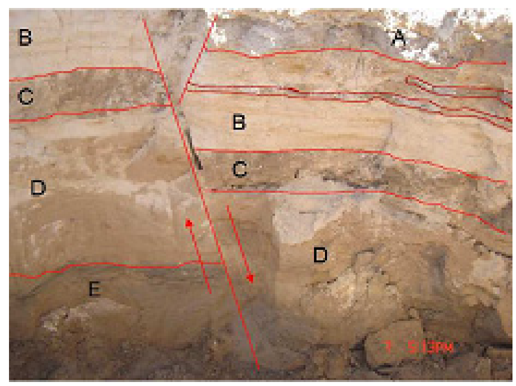

Picture 2. Stratigraphic Court of trench T1, excavated on the trace of the Cerro Prieto Fault, the picture was taken when not yet discovered the horizon "F".

Seismic Hazard Determination observed in the trenches

Displacements measured empirically excavations magnitude was calculated for these events, which gives us an idea of possible earthquakes expected in the Cerro Prieto Geothermal Central. Once the magnitude, we calculated the expected peak ground acceleration for these earthquakes. To calculate the magnitudes of the events recorded in the excavation of the trenches, we used the ratio obtained by Lettuce *et al*. (2008 and 2009), which used data from a compilation by Donald *et al*. (1994). The calculation of peak ground acceleration for the Cerro Prieto area used the empirical relationship of Boore *et al*., (1994). In seismic risk calculations assume an average value of recurrence within the lower and upper limits that characterize their uncertainty.

Assuming that the events have a frequency characteristic constant mean, the recurrence interval or half period was calculated from (Singh and Ordaz, 1994) Table 1.

Conclusions

It was identified eleven tectonic events on the trace of the Cerro Prieto fault and four in Morelia failure, which are associated with earthquakes of magnitudes from 6.8° to 7.6 ° Richter. A magnitude within the range found (7.2° Richter) was recorded on April 4, 2010; however they did not originate in any of the above failures, but on the Laguna Salada fault, located approximately 20 kilometers the Central, and caused considerable damage to the infrastructure of the same. Seismic network currently operating in the plant, there has been no event greater than 6.8° on the Cerro Prieto fault but in May 2006 was also presented an earthquake of 5.6° Richter Morelia associated with failure, which caused damage cooling tower Generation Unit III. This helps to visualize the Cerro Prieto Geothermal Central is a condition vulnerable to a seismic event greater than 6.8° Richter, under these conditions would have serious consequences on the structure of the Central.

Falla	No. Trinchera	Evento Tectónico	Desplazamiento (m)	Desplazamiento Acumulado (m)	Magnitud (M)	Recurrencia (años) (Singh y Ordaz, 1994)	Recurrencia (años) (Slemmons, 1982)
C.P.	T1	1	0,49	0,49	7,2	891	600
C.P.	T2	1	0,22	0,73	6,9	400	380
		2	0,05		6,8	91	220
		3	0,07		6,8	127	220
		4	0,39		7,1	709	400
C.P.	T3	1	0,11	2,45	6,8	200	220
		2	0,35		7,1	636	400
		3	0,24		7,0	436	330
		4	0,93		7,6	1691	1030
		5	0,20		6,9	364	380
		6	0,62		7,3	1127	690
Mor.	T4	1	0,11	0,69	6,8	200	220
		2	0,26		7,0	473	330
		3	0,08		6,8	145	220
		4	0,24		7,0	436	330

Table1. Calculating magnitudes and recurrence periods based on data obtained in paleoseismic trenches excavated.

We recognize the support for the realization of this study to the Subgerencia de Estudios Geológicos y Geofísicos de la Gerencia de Estudios de Ingeniería Civil, to the Gerencia de Proyectos Geotermoeléctricos, Residencia General de Cerro Prieto, Departamento de Geología y Geofísica de la Residencia General de Cerro Prieto and to the Residencia de Estudios de la Central Cerro Prieto.

References

Boore, D. M. (1994). Algunas notas sobre la determinación de la velocidad de ondas de corte y la atenuación, Actas del taller sobre "Técnicas geofísicas para el sitio y Material Caracterización ", Atlanta, GA, 1993, 129 – 134 pp.

Donald L. Wells, Kevin J. Coppersmith (1994). New Empirical Relationships among Magnitude, Rupture Length, Rupture Width, Rupture Area, and Surface Displacement, Bulletin of the Seismological Society of America, Vol. 84, No. 4, 974-1002 pp.

García-Mayordomo J, Giner-Robles J.L. (2006). Definición de zonas sismogenéticas en base al gradiente geotérmico, resistencia y profundidad del límite frágil-dúctil en la corteza superior. Aplicación metodológica para el cálculo de la peligrosidad sísmica en el Sureste de España. Geogaceta, 39pp

Lechuga et al. (2008 y 2009). Estudio de paleosismicidad para Tres sitios de interés para CFE. Proyecto Tecnológico, Comisión Federal de Electricidad. 82 p.

McCalpin, James P. 1996. Paleoseismology. Academic Press, USA. International Geophysics Series, Vol 62, 588 pp.

Singh S. K., Ordaz M. (1994) Seismic energy release in Mexican subduction zone earthquakes. Seismological Society of America. Bulletin of the Seismological Society of America, Vol. 84, 1533-1550 pp.

Slemmons, D. B. (1982). Determination of design earthquake magnitudes for microzonation, Proc. Of the Third International Earthquake Microzonation Conf. Vol. 1, U.S. National Science Foundation, Washington, D.C., 119-130 pp.

PALEOSEISMOLOGY & ARCHAEOSEISMOLOGY
MORELIA • MEXICO 2012
INQUA-TERPRO PALEOSEISMOLOGY
EARTHQUAKE ARCHAEOLOGY

COMPARATIVE STUDY OF ENVIRONMENTAL EFFECTS DURING TWO LARGE EARTHQUAKES: TOHOKU, JAPAN (Mw 9.0, MARCH 11TH, 2011) AND SOUTH ISLAND, NEW ZEALAND (Mw 7.0, SEPTEMBER 3RD, 2010)

Maldonado, Rafael F. and Sánchez, Jhon J.

(1) Departamento de Geociencias, Universidad Nacional de Colombia-Sede Bogotá, Cra 30 45-03, Edif. Manuel Ancízar, Bogotá, Colombia. rfmaldonado@unal.edu.co, jjsancheza@unal.edu.co

Resumen (*ESTUDIO COMPARATIVO DE EFECTOS AMBIENTALES ASOCIADOS A DOS GRANDES TERREMOTOS: TOHOKU, JAPON (Mw 9.0, MARZO 11, 2011) Y SOUTH ISLAND, NUEVA ZELANDA (Mw 7.0, SEPTIEMBRE 3, 2010)*):

La escala ESI 2007 permite complementar los resultados obtenidos con otras escalas a partir de parámetros ambientales y geológicos. En este trabajo se utiliza esta escala para comparar los efectos ambientales de la sacudida sísmica durante los terremotos de South Island, Nueva Zelanda (M_w=7.0, 2010) y Tohoku, Japón (M_w=9.0, 2011), con el fin de construir mapas de intensidad ambiental según la escala ESI 2007 para estos eventos. Resultados preliminares indican intensidades en el rango VIII - XII para el sismo de Tohoku y en el rango V - X para el sismo de South Island.

Palabras Clave: *Intensidad Sísmica Medio- Ambiental, Tohoku (Japón), South Island (Nueva Zelanda), Sacudida Sísmica.*

Abstract (*COMPARATIVE STUDY OF ENVIRONMENTAL EFFECTS DURING TWO LARGE EARTHQUAKES: TOHOKU, JAPAN (Mw 9.0, MARCH 11TH, 2011) AND SOUTH ISLAND, NEW ZEALAND (Mw 7.0, SEPTEMBER 3RD, 2010)*):

The ESI 2007 scale allows complementing the results obtained with other intensities scales from environmental and geologic parameters. Here we use this scale to compare the environmental effects of shaking during the South Island, New Zealand (M_w=7.0, 2010) and Tohoku, Japan (M_w=9.0, 2011) earthquakes, with the objective of constructing an intensity map in the ESI 2007 scale for this events. Preliminary results indicate intensities in the range VIII – XII for the Tohoku earthquake and V-X for the South Island earthquake.

Key words*: Environmental Seismic Intensities, Tohoku (Japan), South Island (New Zealand), Earthquake Shaking.*

Introduction

This work shows two examples of application of the Environmental Seismic Intensity Scale-ESI 2007 (Michetti et al., 2007) which is based on the environmental and geological surface effects of earthquakes. The assessment of seismic shaking by means of the ESI scale includes twelve degrees of incremental severity and considers not only the different effects of shaking that are used in traditional scales (such as MCS, MSK, MM, etc.) but also other effects that complement macroseismic assessment. Such effects include ground rupture, uplifting, subsidence, and tipping of terrain and secondary effects like landslides, liquefaction, shaking of trees and vegetation, dust clouds generation, displacement and movement of rocks, tsunami generation as well as hydrological anomalies all of which are associated wit shaking and thus to the size and location of the earthquake. The effects as well as the scale itself do not exhibit saturation for large magnitudes.

Application of ESI scale is implemented by compilation and quantification of the surface effects of shaking (i.e. length and width of ground fractures, landslides volumes) of two large recent earthquakes: South Island, New Zealand (3 September, 2010) M_w = 7.0 and Tohoku, Japan (11 March, 2011) M_w = 9.0. These two earthquakes took place on different geological and tectonic settings: 1) Along a strike-slip fault that is part of the tectonics between the Australian and Pacific plates which involves compressional regime and dextral componnet of motion in the case of the South Island Earthquake and 2) along the contact in the subduction zone between the Pacific and North American Plates at the latitude of the Japan trench in the case of the Tohoku earthquake. From secondary information mined from various sources such as 1) reports of reconnaissance campaigns, 2) published papers, 3) satellite imagery and photographs, and 4) local reports from the affected areas, we compiled a database with surface environmental effects of the two earthquakes to determine intensity levels and to construct preliminary maps of intensities of shaking.

Data: Environmental effects in the region of study

In the case of the South Island Earthquake we compiled information on the following effects: mud volcanoes and ejections of sand and gravel with diameters in the range 60 cm – 10 m; liquefaction areas with thicknesses between 20 cm and 60 cm (in some areas diameters were measured up to 500 m); ground cracks with lengths between some cm and 450 m and openings up to 120 cm and vertical displacements up to 33 cm. We also found information on ground sinking with a maximum of 40 cm in urban areas and 120cm in the field.

In the case of the Tohoku earthquake we collected information of landslides with a maximum volume of 70,000 m^3, sand ejections (a common grain size) with diameters between 50 cm and 140 cm; ground cracks with lengths of up to 800 m and vertical displacements up to 2 m; sinking of the ground in the range of some dm to 2 m; increase in the water level (Fujinuma Dam) of 3 m; damaged trees (uprooting, tipping, falling) near a fault that was reactivated during the main shock, and as one of the most important characteristics we note the temporal change in sea waves and tsunami generation with maximum height of various tens of meters.

Discussion

The different data sets of environmental effects during the two earthquakes were classified following Michetti et al., (2007) and a value of intensity was assigned to each type of effect according to their dimensions and their characteristics. For each earthquake we collected 73 reports on surface effects and constructed the maps shown in Figures 1 and 2.

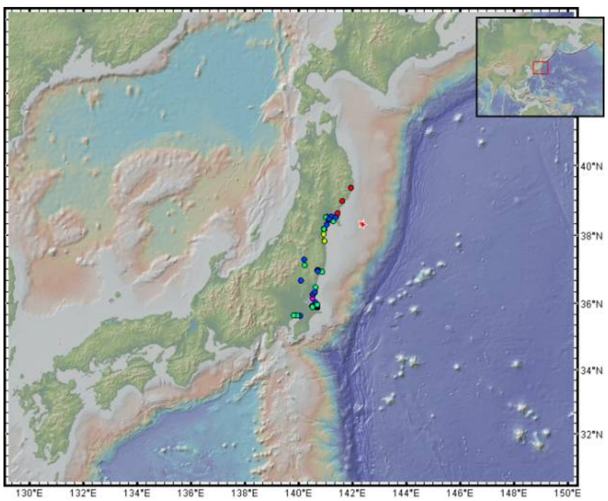

Figure 1. Location and classification of environmental effects and their intensities for the Tohoku earthquake.

Surface effects for the Tohoku earthquake locate primarily along the northern coast of the Honshu Island roughly parallel to the Japan Trench (Figure 1). Most of effects and their sizes suggest ESI intensities of at least VIII and are mainly associated to uplifting and subsidence usually accompanied with ground rupture and expulsion of sediments (mostly sand). Maximum values of ESI intensities ranked XII and were associated to the tsunami that swept northern Honshu (wave heights > 10 m). We suggest that the reported effects allow classification of the Tohoku earthquake in the VIII-XII ESI intensity range. Because the Tohoku shock was a great earthquake, the effects are distributed over large areas, and it is quite plausible that minor effects are not reported because researchers and campaign crews are focused in noticeable effects.

In the case of the South Island earthquake the more representative effects were documented in the Canterbury province (Figure 2), with tendency to locate near the city of Christchurch, perhaps because of a larger population density. Surface effects in this area indicate ESI intensities in the range V-X, with the largest value reached near the epicenter and corresponding to a series of ground cracks with lengths of 450 m and gravel expulsions with diameters exceeding 6 m. Clearly, we observe a decrease in severity with the distance to the East of the epicenter, roughly parallel to the causative fault.

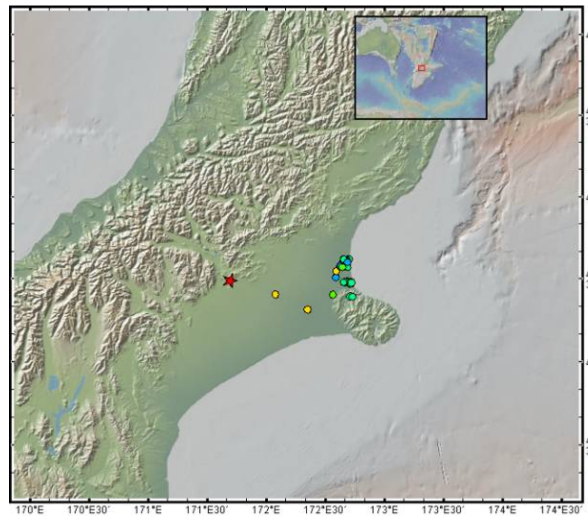

Figure 2. Location and classification of environmental effects and their intensities for the South Island earthquake.

For this earthquake the intensity with most reporting was VIII, with a tendency to level VII and with effects mostly associated to ground cracks and ejection of clays and sands. We suggest a V-X preliminary classification in the ESI intensity scale.
The procedure followed in this study allowed associating intensity values to surface effects based solely on documented cases. For completeness, it would be quite beneficial to corroborate some values of intensities based on field inspection (Mosquera-Machado et al., 2009), but given the time elapsed since the two earthquakes this may be not so fruitful.

Acknowledgements: We thank C. Lalinde for help with information and valuable suggestions and to the various agencies, researchers and workers that made their reports available.

References

Barrell D.J.A., Litchfield N.J., Townsend D.B., et al. Strike-slip ground-surface rupture (Greendale Fault) associated with the 4 September 2010 Darfield earthquake, Canterbury, New Zealand. 2011. In: *Quarterly Journal of Engineering Geology and Hydrogeology* 2011; v. 44; p. 283-291.

Geotechnical Extreme Events Reconnaissance, 2011, Geotechnical Reconnaissance of the 2011 Christchurch, New Zealand Earthquake. In: Report of the National Science Foundation-Sponsored Geotechnical Extreme Events Reconnaissance (GEER) Team.

Harder L.F., Kelson K.I., Kishida T. 2011. Preliminary Observations of Levee Performance and Damage following the March 11, 2011 Tohoku Offshore Earthquake, Japan.

Geotechnical Extreme Events Reconnaissance (GEER) Association Report No. GEER-025b.

Harder L., Kelson K.I., Kishida T, Kayen R. 2011. Preliminary Observations of the Fujinuma Dam Failure Following the March 11, 2011 Tohoku Offshore Earthquake, Japan. *Geotechnical Extreme Events Reconnaissance (GEER) Association Report No. GEER-025e –Preliminary-.*

Kayen R., Tanaka Y.,Tanaka H., Sugano T., Estevez I.A., Cullenward S.S., Yeh W., Thomas D. 2011. LiDAR and Field Investigation Of the March 11, 2011 M9.0 Great Tohoku Offshore Earthquake, and April 7, 2011 M7.4 Aftershock. *Geotechnical Extreme Events Reconnaissance (GEER) Association Report No. GEER-025f –Preliminary-.*

Kelson K.I., Harder L.F., Kishida T., Ryder I. 2011. Preliminary Observations of Surface Fault Rupture from the April 11, 2011 Mw6.6 Hamadoori Earthquake, Japan (an aftershock of the March 11, 2011 Tohoku Offshore Earthquake, Japan). *Geotechnical Extreme Events Reconnaissance (GEER) Association Report No. GEER-025d –Preliminary-.*

Michetti A.M et al., 2007, Intensity Scale ESI2007. Mem. Descr. *Carta Geologica d'Italia, 74. Servizio Geológico d'Italia – Dipartamento Difensa del Suolo*. APAT, Rome, Italy. Traduction to Spanish by P.G. Silva et al. 2010.

Mosquera S., Lalinde C., Salcedo E., Michetti A. M., 2009. Ground effects of the 18 October 1992, Murindo earthquake (NW Colombia), using the Environmental Seismic Intensity Scale (ESI 2007) for the assessment of intensity. In: *Geological Society, London, Special Publications* 2009; v. 316; p. 123-144.

Massey C., Petley D., Rosser N. 2010. Harper Hills Landslides, Canterbury -GeoNet Landslide Response-, *Institute of Geological and Nuclear Sciences Limited.* New Zealand.

Meneses J., Arduino P. 2011. Preliminary Observations of the Effects of Ground Failure and Tsunami on the Major Ports of Ibaraki Prefecture. *Geotechnical Extreme Events Reconnaissance (GEER) Association Report No. GEER-025c.*

Scott A. Ashford, Ross W. Boulanger, Jennifer L. Donahue, and Jonathan P. Stewart. 2011 Geotechnical Quick Report on the Kanto Plain Region during the March 11, 2011, Off Pacific Coast of Tohoku Earthquake, Japan. *Geotechnical Extreme Events Reconnaissance (GEER) Association Report No. GEER-025a.*

U.S Geological Survey National Earthquake Information Center. 2010. M7.0 South Island, New Zaeland Eartquake of 3 September 2010. Available in World Wide Web: *http://earthquake.usgs.gov/earthquakes/eqarchives/poster/2010/20100903.php*, Last review: 3/5/2012.

U.S Geological Survey National Earthquake Information Center. 2011. The M9.0 Great Tohoku Earthquake (northeast Honsu, Japan) of March 11, 2011. Available in World Wide Web: *http://earthquake.usgs.gov/earthquakes/eqarchives/poster/2011/20110311.php*, Last review: 14/8/2012.

"Searching for the continuation of the fault in the Northeast Frontier in Sonora; by morphostructural analysis"

Martínez-Marmolejo, Yasmín Gudalupe. (1), Ortega-Rivera, María Amabel. (2).

(1) Departamento del área Física, Fac. de Geografía, Universidad Autónoma del estado de México. Cerro de Coatepec s/n Ciudad Universitaria, código postal 50110, Toluca, México. dractiger_43@hotmail.com

(2) Instituto de Geología, Universidad Nacional Autónoma de México, Estación Regional del Noroeste, Apartado Postal 1039, Hermosillo, Sonora, 83000, México. amabel@unam.mx

Abstract

Structural geomorphology, is one of the main branches of geomorphology, which studies the structure and discusses the fundamentals that define lithologic and tectonic relief on Earth, and large morphostructural units, contacts, and relationships of hydrography with the geological structure.
The sector-Esqueda Borders, located in northeastern Sonora, geomorphologically is part of the Basin and Range Province, which is characterized by a system of intermontane valleys, formed by a set of normal faults, which directly influence the northeastern part of Sonora, which form numerous structures that comprise a system of horsts and grabens that have a NNW-SSE.
Within the segment Borders-Esqueda, there is the influence of the fault Borders, where you can see directly into the form, orientation and distribution and related structures have associated with it, and with the help of other agents such as exogenous (water , wind, weather, among others.) and endogenous (regional tectonics), resulting in the morphology of the area. Their orientation along with the accumulation of efforts serves to interpret the possible magnitude of earthquake activity, hence the importance of continuing to see where the fault and the direction it has, since very near the south towns are located of Esqueda and Nacozari, which implies a large seismic risk to these communities.

To address the research methodology was necessary to use geographic (location, distribution, time correlation and relationship with other agents), geomorphological (landform identification, qualitative analysis, where hiso a description of the characteristics of each structure that makes up the area and quantitative study, which were held conducted measurements, calculations, and description or recognition processes that are influencing to get the forms that occur). And finally carried out geological analysis (age, period, material type and identification of structures), which helped in the description of the various events online status and to analyze geological geomorphological evolution of the area, which finally allowed to decide Once confirmed all this in the field, if the fault is active, and the risks that exist for development (urban, road, tourism, spatial planning, among others.) in the area.

Within the geomorphological-structural analysis, which was addressed in this issue were taken 3 main factors control the evolution of land forms, according to the teachings of WM Davis, which are: structure, process and status. Where we clarify that the term structure in geomorphology has no sense of character of rocks such as folds, faults and unconformities, but includes all those peculiarities by which earth materials that are sculpted in the shapes of relief, differ from one another in their attributes.
The above was supplemented by thematic mapping, which currently is a tool that visually expresses analytical aspects, not only as a graphical representation of processes in the Geographic space, since from the point of view is partly to express the geomorphology of an area.

For this work, which is supported at an early stage in the morphologic and morphometric studies were obtained as a result the following thematic maps:
-Hypsometric map. -Geological map. Hydrological network-map.
-Dissection density map. Energy-relief map. -Map of earrings.
Morfolineamientos-map. -Morphostructural map.
It was supplemented in a second phase with geological and geomorphological profiles, horizontal and vertical were drawn at certain points of the area by reference to the main orographic axis.

In this study, we obtained the expected results, which were confirmed in a field trip to the area of study, results that were raised and were hypothesized in the approach of this research. Which yielded the following:
He found fault transect Borders to the south, passing through the mountains Pinitos.
-The geomorphology of the relief, shows that there are structures such as triangular facets, fractures, alternating blocks which have different orientation, trending faults, normal and thrust and folds indicate that the fault is active.
-The type of hydrological network is another indicator in the path of failure and morphology of the structures.
And finally confirmed the continuation of the fault Borders to the south.

These elements came to the conclusion that the failure Borders has recently presented earthquakes is geologically active, although some of the evidence is covered by recent sediment and further studies are planned to obtain paleoseismic recurrence times and possible magnitudes.

Key words: Boundary Fault, NW Sonora, Borders-Esqueda, landforms.

PALEOSEISMOLOGY & ARCHAEOSEISMOLOGY
MORELIA • MEXICO 2012
INQUA-TERPRO PALEOSEISMOLOGY
IUGS UNESCO 567
EARTHQUAKE ARCHAEOLOGY

"Buscando la continuación de la falla Fronteras en el Noreste del estado de Sonora; mediante un análisis morfoestructural "

Martínez-Marmolejo, Yasmín Gudalupe. (1), Ortega-Rivera, María Amabel. (2).

(1) Departamento del área Física, Fac. de Geografía, Universidad Autónoma del estado de México. Cerro de Coatepec s/n Ciudad Universitaria, código postal 50110, Toluca, México. dractiger_43@hotmail.com

(2) Instituto de Geología, Universidad Nacional Autónoma de México, Estación Regional del Noroeste, Apartado Postal 1039, Hermosillo, Sonora, 83000, México. amabel@unam.mx

Abstract

La Geomorfología Estructural, es una de las ramas fundamentales de la geomorfología; la cual estudia la estructura y trata de los fundamentos litológicos y tectónicos que definen el relieve en la Tierra, y las grandes unidades morfoestructurales, sus contactos, y de las relaciones de la hidrografía con la estructura geológica.
El sector Fronteras-Esqueda, localizado en el Noreste del estado de Sonora; geomorfológicamente forma parte de la Provincia del Basin and Range, que se caracteriza por ser un sistema de valles intermontanos; formados por un conjunto de fallas normales, que influyen directamente en la parte nororiental del Estado de Sonora, las cuales conforman numerosas estructuras que integran un sistema de horsts y grabens que presentan una orientación NNW-SSE.
Dentro del segmento Fronteras-Esqueda, se tiene la influencia de la falla Fronteras, donde se puede apreciar directamente en la forma, orientación y distribución que presentan las estructuras relacionadas y asociadas a ella, y con la ayuda de otros agentes como los exógenos (agua, viento, clima, entre otros.) y endógenos (tectónica regional), dan como resultado la morfología del área. Su orientación junto con la acumulación de esfuerzos sirve para interpretar la posible magnitud de la actividad sísmica, de aquí la importancia de ver hacia donde continúa la falla y la dirección que tiene, ya que muy cerca de la zona hacia el sur se localizan los poblados de Esqueda y Nacozari, lo que implica un gran riesgo sísmico para estas comunidades.
Para abordar la investigación, fue necesario utilizar metodologías geográficas (localización, distribución, tiempo, correlación y relación con otros agentes), geomorfológicas (identificación de geoformas, análisis cualitativo, donde se hiso una descripción de las características de cada estructura que conforma la zona de estudio y uno cuantitativo, donde se realizaran realizaron mediciones, cálculos, y descripción o reconocimiento de los procesos que están influyendo para obtener las formas que se presentan). Y por último se llevaron a cabo los análisis geológicos (edad, periodo, tipo de material e identificación de estructuras), que ayudaron en la descripción de los diferentes eventos identificados y poder analizar la evolución geológico-geomorfológica de la zona; que finalmente permitió decidir una vez corroborado todo esto en el campo, si la falla es activa, y los riesgos que existen para el desarrollo (urbano, carreteros, turísticos, ordenación territorial, entre otros.) de la zona.
Dentro del análisis geomorfológico-estructural, que se abordó en esta temática, se tomaron 3 factores principales de control en la evolución de las formas del relieve, de acuerdo a las enseñanzas de W.M. Davis, los cuales son: estructura, proceso y estado. Donde se nos aclara que el término estructura en geomorfología no tiene el sentido estricto de caracteres de rocas tales como: pliegues, fallas y discordancias, sino que incluye todas esas peculiaridades por las cuales los materiales de la tierra en los que se esculpen las formas del relieve, difieren unos de otros en sus atributos.
Lo antes mencionado fue complementado con cartografía temática, que en la actualidad es una herramienta que expresa de forma visual aspectos analíticos, no sólo como una representación gráfica de procesos ocurrentes en el espacio Geográfico; ya que desde el punto de vista anterior se parte para expresar las características geomorfológicas de un territorio.
Para este trabajo, que se apoyó en una primera fase en el estudio morfológico y morfométrico, se obtuvieron como resultado los siguientes mapas temáticos:
-Mapa hipsométrico. -Mapa geológico. -Mapa de red hidrológica.
-Mapa de densidad de disección. -Mapa de energía del relieve. -Mapa de pendientes.
-Mapa de morfolineamientos. -Mapa morfoestructural.
Y fue complementado en una segunda fase con perfiles geológico-geomorfológicos, horizontales y verticales que se trazaron en ciertos puntos de la zona tomando como referencia el eje orográfico principal.

Con este estudio, se obtuvieron los resultados esperados, que fueron confirmados en una salida de campo a la zona de estudio; resultados que se plantearon y se tenían como hipótesis en el planteamiento de esta investigación. Donde se obtuvo lo siguiente:
-Se encontró el transecto que de la falla Fronteras hacia el sur, que pasa por la sierra Pinitos.
-La geomorfología del relieve, muestra que se tienen estructuras como: facetas triangulares, fracturas, bloques alternados que presentan diferente orientación, fallas de rumbo, normales e inversas y pliegues que indican que la falla se encuentra activa.
-El tipo de red hidrológica es otro indicador en la trayectoria de las fallas y morfología de las estructuras.
Y finalmente, se corroboró la continuación de la falla Fronteras hacia el sur.

Con estos elementos se llegó a la conclusión de que la falla Fronteras, recientemente no ha presentado movimientos sísmicos, es geológicamente activa, aunque parte de las evidencias está cubiertas por material sedimentario reciente y se planean hacer más estudios paleosísmicos para poder obtener tiempos de recurrencia y posibles magnitudes.

***Key words**: Falla Fronteras, NW Sonora, Fronteras-Esqueda, morfoestructuras.*

Bibliography:

Aranda-Gómez,J.J., Christopher, H.D., LUHR, J.F., (2000). "*Evolución tectonomagmática post-paleocénica de la Sierra Madre Occidental y de la porción meridional de la provincia tectónica de Cuencas y Sierras, México".* Boletín de la Sociedad Geológica Mexicana, vol. LIII, p. 59-71.

Barragán R., Campos M. Emiliano (2010). "Código Estratigráfico Norteamericano". Instituto de Geología. UNAM. D.F.

Cárdenas Monroy Caridad. (2007). "Historia de la Tectónica de Placas". Servicio Sismológico Nacional. Instituto de Geofísica Universidad Nacional Autónoma de México.
Coque, Roger. (1984). "Geomorfología". Ed. Alianza Editorial, España, pp. 475.
Coque Roger. (1997). "Geomorfología". Alianza Universidad Textos. 79. Ed. Alianza.

Davis, G.H., y Reynolds, S.J. (1996). "*Structural geology of rocks and regions".* Wiley, N. Y., 776 p.

Derrau Max. 1983. "Geomorfología". Ed. Ariel.

De Miró I. Orell Manuel y Montserrat Doming. (1985). "Breviorio de Geomorfología". Ed. Oikos-Tau, Barcelona.

DiBiase Roman. "*Landscape form and millenial erosion rates in the San Gabriel Mountains, CA." School of Earth and Space Exploration. Arizona State University.*

Espinoza Maldonado, I.G., (1989). "Los fundamentos teóricos de los sensores remotos y la interpretación geológica de una imagen Landsat path 36-row 39". Universidad de Sonora, Tesis de Licenciatura, nov.1989.

García Palomo Armando; Zamorano José J., López Miguel Celia. (2008). "El arreglo morfoestructural de la Sierra de las Cruces, México central". Revista Mexicana de Ciencias Geológicas, v. 25, núm. 1. p. 158-178.

Griem Wolfgang, Griem Susanne. (2006). "Geología General Apuntes". Universidad de Atacama, Chile.

Hernández José R., Blanco Pedro, Díaz Jorge L. (1988). "Rasgos estructuro-geomorfológicos del fondo de los mares y océanos circundantes en Cuba". Editorial Academia de Ciencias de Cuba. Instituto de Geografía.

Hernández José R., Ortiz Pérez Mario A., Figueroa Mah Eng Manuel. "Análisis morfoestructural del Estado de Oaxaca, México un enfoque de clasificación tipológica del relieve". I nvestigaciones Geográficas, Boletín del Instituto de Geografía, UNAM
ISSN 0188-4611, Num. 68, 2009, pp. 7-24.

"Introducción a la Geología-Fundamentos de Geología". (2008). Escuela de Geología y Biología. Universidad Autónoma de México.

Kostenko, Natalia (1991). Aspectos "Teóricos del Análisis Geomorfológico Estructural". UAEM. 1ª Edición.

Kostenko Natalia Petrovna. (1975). "Geomorfología Estructural Aplicada". UNAM. Instituto de Geografía. Resumen del curso dictado en Sep-Oct. 1995. 113 p.

Leet y Judson (1980). "Fundamentos de la Geografía Física". Limusa.
Lugo Hubp José. (1995). "La Geomorfología en México". En Ciencia ERGO, SUM, Vol. 2 Número. Uno Febrero. UAEM.

Lugo Hubp Jose. (1986). "Las estructuras mayores del relieve Terrestre". Facultad de Ingeniería. UNAM.

Lugo Hubp José. (1988). "Elementos de Geomorfología Aplicada" (Métodos Cartográficos). Instituto de Geografía. UNAM.
Lugo Hubp José. (1989). "Diccionario Geomorfológico". Instituto de Geografía. UNAM.

Fig. 1.- Sector de sur de la falla Fronteras en Esqueda, Noreste del estado de Sonora.

STUDY OF THE STABILITY OF b-VALUE TO SEISMOTECTONICS REGIONS OF MEXICO.

Mendoza-Ponce, Avith del R. (1), Zúñiga, Ramón. (1)

(1) Centro de Geociencias, UNAM, Campus Juriquilla, Queretaro, Mexico. avith3@gmail.com
(1) Centro de Geociencias, UNAM, Campus Juriquilla, Queretaro, Mexico. ramon@geociencias.unam.mx

Abstract (Study of the stability of b-value for seismotectonics regions of Mexico): *In order to find reliable parameters for the evaluation of seismic hazard, which forms the basis for seismic risk calculations and therefore the recommendations made in the construction manuals, b values were calculated from the Gutenberg-Richter relation. b value estimations were made for the 19 regions in which Mexico was divided according to seismotectonic regionalization of Zúñiga et al. (1997). Thus, the fundamental aim of the developed research in this work was to obtain a more precise knowledge of the b value for different regions of Mexico using a new method of statistical seismology. Based on the findings, we observed that the methodology employed in this study worked properly, especially in zones with large quantity of seismic events, showing that this new technique is suitable. With our results, we hope to provide an additional strategy, which help to improve the quality of construction manuals, as well as provide some basis for future research.*

Key words: *Mexico, b-value, regionalization, seismic risk.*

INTRODUCTION

The problem of seismic risk evaluations in Mexico is of utmost importance due to the frequency with which destructive earthquakes affect most of its territory. The terrible losses suffered during the September 19 and 21, 1985 events underline the priority imposed on studies that can shed light on the seismic vulnerability of those zones exposed to seismic phenomena.

Thus, the principal mobile that drives the development of this work is to have better assessment of seismic risk in different parts of Mexico, in order to have greater knowledge of how much damage can occur in a particular site.

One of the parameters that directly influence the seismic risk assessment is the seismic hazard. Seismic hazard determination is based on recurrence interval, that is an estimate of the interval of time between events of a certain magnitude, also known as return period, or its inverse, the exceedance rates (number of times that an event of a type occurs, or which exceeds an acceleration value at a given time). It is seldom possible to make a direct quantification of the number of times exceeds a value, since the catalogs are not complete enough because of the short story instrumental. It is therefore necessary to make assessments using available information and probabilistic estimates that complement the missing data (usually related to the occurrence of earthquakes of great magnitude). This parameter is closely related to the b value of the Gutenberg-Richter relationship, the centerpiece of this research.

Therefore, the backbone of the analysis of seismic hazard is the Gutenberg-Richter relationship or G-R relationship (log (N) = a-bm). This is a statistical model and simply tells us that the logarithm of the cumulative number of earthquakes (N) is related to the magnitude (m) linearly through the a-constant and b-constant (better known as b value). The importance of the b value is that this value corresponds to the slope of the straight line that best fits the linear part of the G-R relationship, besides that it is a parameter which describes the distribution tectonic relative sizes of events.

As mentioned above, to calculate the hazard at a site of interest, you need to evaluate the rate of activity produced by all sources that may affect the site or calculate the return period. The return period (RP) for a specific magnitude is calculated by the equation:

$$RP = Pt / 10^{\wedge} (a-bM)$$

where Pt is the time period used in the estimate, while the denominator is the number of events in this time window. M is the magnitude of interest for which you want to calculate the RP (typically M> 7).

This fact motivates us to calculate the b value more accurately across the territory of Mexico, allowing us to know the return period of destructive earthquakes.

The Seismotectonic Regionalization of Mexico.
The seismic catalogue used in this research is taken from Zúñiga *et al.* (personal communication, 2011), corresponding to earthquakes that have occurred in Mexico between 1899 and 2007. Furthermore, it was homogenized in the surface wave magnitude (MS). We also use the first order seismotectonic regionalization proposed by Zúñiga *et al.* (1997). The territory of Mexico was subdivided into 19 regions. This regionalization is not unique, but provides a consistent and systematic division that incorporates most of the knowledge of general characteristics of earthquakes in different parts of the country. Also consider the destructive potential of major events that have occurred in the past.

The main zones (*Fig. 1*) are described below:

SUBR.- Interplate shallow (h < 15 km) events zone. Rivera-NOAM weak coupling convergence.

SUB1.- Shallow (h < 40 km) intermediate coupling subduction events zone. Transitional zone between Rivera - NOAM (North-American Plate) convergence and Cocos - NOAM convergence.

SUB2.- Shallow (h < 40 km) strong coupling subduction events zone. Cocos - NOAM convergence.

SUB3.- Shallow (h < 40 km) strong coupling subduction events zone. Transitional zone, Cocos - NOAM convergence.

SUB4.- Shallow (h < 40 km) strong coupling subduction events zone. Cocos - Caribe convergence.

IN1.- Intermediate depth (40 km < h < 180 km) intra-plate events zone. Cocos plate. Extension in depth of zone SUB2.

IN2.- Intermediate depth (40 km < h < 260 km) intra-plate events zone. Transitional zone, Cocos Plate.

IN3.- Intermediate depth (40 km < h < 300 km) intra-plate (Cocos) events zone. Extension in depth of zone SUB4.

MVB.- Intra-plate (NOAM) shallow (h < 15 km) events zone in Central Mexico. Mexican Volcanic Belt tectonic province.

NAM.- Intra-plate (NOAM) shallow (h < 15 km) events zone, South-East Mexico. Not related to the volcanic regime of the MVB.

BC1.- Intra-plate (Pacific) shallow (h < 20 km) events zone. Baja California.

BC2.- Interplate (Pacific-NOAM) shallow (h < 15 km) events zone. Baja California-Gulf of California region.

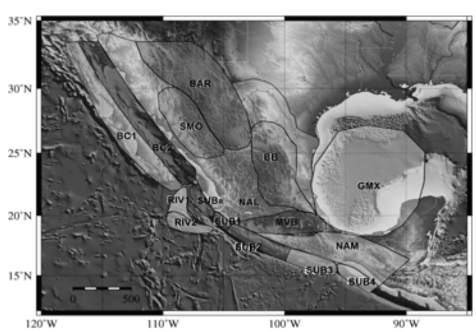

Fig. 1: Seismotectonic zones of Mexico according to the regionalization proposed by Zúñiga et al. (1997). These regions correspond to earthquakes of shallow depth.

SMO.- Intraplate (NOAM) shallow (h < 20 km) events zone. Sierra Madre stress province.

BAR.- Intraplate (NOAM) shallow (h < 15 km) events zone. Possible extension of Basin and Range-Río Grande Rift provinces.

BB.- Intraplate (NOAM) shallow (h < 15 km) events zone. Burgos Basin stress province.

RIV1.- Interplate shallow (h < 15 km) events zone. Normal faulting Pacific-Rivera interface.

RIV2.- Interplate shallow (h < 15 km) events zone. Strike-slip faulting Pacific-Rivera interface.

GMX.- Intraplate (NOAM) shallow (h < 20 km) events zone. Gulf of Mexico province.

NAL.- Scarce seismicity, shallow faulting events zone.

The methodology used to obtain the b value for each region firstly consisted to estimate the magnitude of completeness Mc with maximum curvature (MAXC) and best combination (BC) methods. Then, the b value was estimated by maximum likelihood. The b value against time was plotted to study the variability that it presents. These graphs were constructed by increasing the catalogue in a year from the most recent date, in order to ensure the lowest uncertainty in estimating the b value in each zone. The variability is used to find periods of stabilization over time and to have more confidence in the assessment of that value. The obtained results are: for most subduction zones (SUBR, SUB2, SUB3 and SUB4) we have very good estimates of b values, as well as to shallow (BC1, RIV1, MVB, BB and GMX) and intermediate (IN3) depth events zones. However, for the intraplate (BAR, NAM, NAL, IN1 and IN2) and interplate (SUB1, RIV2 and BC2) events zones we do not found

Región	Núm. de eventos	$\overline{b}$	$\overline{a}$	$\overline{M_c}$
SUB1-*MAXC*	105	0.73 ± 0.39	2.92 ± 1.62	3.16 ± 0.56
SUB1-*MC*		0.70 ± 0.40	2.84 ± 1.66	3.06 ± 0.55
SUB2-*MAXC*	3,900	0.74 ± 0.07	3.94 ± 0.21	2.57 ± 0.16
SUB2-*MC*		0.74 ± 0.04	3.87 ± 0.11	2.62 ± 0.07
SUB3-*MAXC*	4,197	0.76 ± 0.04	4.15 ± 0.13	2.70 ± 0.07
SUB3-*MC*		0.80 ± 0.05	4.17 ± 0.18	2.83 ± 0.12
SUB4-*MAXC*	1,515	0.72 ± 0.03	3.92 ± 0.11	3.18 ± 0.05
SUB4-*MC*		0.72 ± 0.05	3.93 ± 0.22	3.19 ± 0.10
SUBR-*MAXC*	20	0.73 ±	2.15 ±	3.34 ± 0.63
SUBR-*MC*		0.75 ±	2.19 ±	3.36 ± 0.64

Fig. 2: Results of the values a, b and Mc with their uncertainties for the 5 subduction regions of Mexico.

reliable estimates of b value (see *Fig. 2*).

Based on the above findings, we observed that the methodology employed in this study worked properly, especially in zones with large quantity of seismic events, showing that this new technique is suitable.

DISCUSSION

The b value gives us information on certain physical properties such as effort and the average size of tectonic fractures in a volume. The b value is inversely proportional to the accumulation of efforts, which would be expected to have lower b values in areas of strong coupling, such as subduction zones considered in this study. Indeed, the areas with lower b values (b <0.78) are the regions SUBR, SUB1, SUB2, SUB3, SUB4, IN1, BC1 and BC2, which correspond to areas of increased accumulation of effort. However, we also have the areas RIV1, RIV2 and BAR with low b values, and these are not considered areas of strong coupling. We attribute these results to the scarcity of data in the zones and this aspect clearly impairs the statistical calculation.

The remaining regions have higher b values (b <0.78), indicating that the zones are of lesser accumulation of effort. These regions are IN2, IN3, NAM, GMX, MVB, BB and NAL.

b values obtained (0.70 - 0.80) in this study are consistent with the average values found by Zuñiga and Wyss (2001) for the subduction zone. As expected, the interpretations of these results, both studies show a high level of effort in these regions. b values obtained in these regions also have very similar values, this indicates that there are similar stress conditions along the entire trench. At the same time, implies that the average size of rupture for each subduction region is also similar. These results agree with those obtained by Ávila (2007), which also found that the average sizes of rupture zones of SUB2, and SUB4 SUB3 regions are not significantly different.

These results are important because b values not exist in the literature for each of the different areas that make up the regionalization proposed by Zúñiga et al. (1997).

Finally, in this work we estimate the recurrence time o return period for each of the areas involved in the study, because we consider it a good technical comparison between our calculated values and the observed data. In this case, we use Hypothesis testing to decide whether the calculated and observed return period are or not significantly different. Fig. 3 shows the results of return periods for the subduction zones. We can see that for most areas, we obtain acceptable b values, based on insignificant differences between the calculated and observed RP.

CONCLUSIONS

The presentation of these results provides an important part of the basis for determining areas under high seismic risk, such as the seismic hazard. That coupled with the knowledge of local conditions, such as closeness to active faults, local effects of soil structure, etc., to define a seismic zoning of first order of our country.

The impact of this analysis is concentrated on engineering area, because for them is of vital importance to have risk estimates for a given area. The role of the b

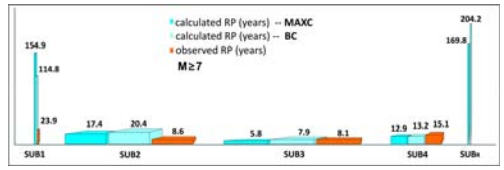

Fig. 3: Graph of the return periods calculated and observed in years for M>7, on the Pacific coast of Mexico in the period 1970-2007. The results of the return periods calculated for Mc, calculated by the MAXC method is presented in deep blue color, while the return periods for Mc calculated by the BC method is presented in light blue. The return period observed is presented in orange. The size of the boxes represents the density of events corresponding to each zone.

value is of utmost importance because it is used to determine the exceedance rates of acceleration. In addition, these parameters are important because if you know more precisely for each area of Mexico can better estimate the recurrence periods for events of a specific magnitude (e.g., greater than 7.0) and can be extrapolated in areas with low frequency of occurrence of major seismic events.

We also present the estimated return periods for all regions, compared with the observed return periods of the catalog used. Based on these results, we conclude that the correspondence between the observed and calculated PR in most regions is very good, especially in cases of good instrumental density, demonstrating that the estimates are reliable.

The lack of correspondence in some regions may be due to seismicity data are incomplete; in areas with low frequency of occurrence is possible that not have a catalog sufficiently representative; to scarce or null occurrences of earthquakes of medium magnitude (can not compare extrapolations with return periods observed) and/or problems with the method.

It is noteworthy that it is still necessary to carry out further research on where to get the b value as stable and define the selection criteria more precisely. However, the results of this study provide a foundation and precedent for future studies to corroborate the method postulated here. The results obtained may be considered for purposes of review and/or modification of the building codes in the country, in order to provide a higher quality design and construction of earthquake resistant structures, in order to mitigate damages.

In conclusion, this research provides guidelines to make more detailed studies in the future, in order to assess more accurate the seismic hazard in each of the seismotectonic zones of Mexico used here.

Acknowledgements: I would like to thank the Centro de Geociencias, UNAM Campus Juriquilla for providing me all the necessary to develop this work. I also want to thank Ramón Zúñiga for providing me with catalog data and share his knowledge with me. The research has been partly supported by CONACyT (CB-2009-01-129010) and DGAPA-PAPIIT-UNAM No. IN112110.

References

Aki, K. 1965. *Maximum likelihood estimate of b in the formula logN=a – bM and its confidence limits. Bull. Earthquake Res. Inst.*, 43, 237-239.

Avila, B.L. 1997. *Hacia una regionalización del peligro sísmico ocasionado por réplicas, para sismos en la costa del pacífico mexicano.* Tesis de Maestría. Universidad Nacional Autónoma de México.

Wiemer, S. y Wyss, M. 2000. *Minimum Magnitude of Completeness in Earthquake Catalogs: Examples from Alaska, the Western United States, and Japan, Bull. Seismol. Soc. Am.,* 90, 4, 859-869.

Zúñiga, F.R., Suárez, G., Ordaz, M. y García-Acosta, V. 1997. *Proyecto: Peligro Sísmico en Latinoamérica y el Caribe, Instituto Panamericano de Geografía e Historia, proyecto 89-0190.*

Zúñiga, F.R. y Wyss, M. 2001. *Most- and Least-Likely Locations of Large to Great Earthquakes along the Pacific Coast of Mexico Estimated from Local Recurrence Times Based on b-Values. Bull. Seismol. Soc. Am.,* 91, 6, 1717-1728.

APPLICATION FOR STRUCTURAL ANALYSIS TECHNIQUE IN THE CENTRAL PALEOSEISMICITY CERRO PRIETO GEOTHERMAL, MEXICALI, BAJA CALIFORNIA

Miranda-Rojas, María del Carmen. (1), Lechuga-Valderrábano, Florencio. (2), González-Mellado, María Dolores. (3)

(1) Federal Commission of Electricity, Construction Subdivision, Management of Civil Engineering Studies, Department of Geology. carmen.miranda@cfe.gob.mx
(2) Federal Commission of Electricity, Construction Subdivision, Management of Civil Engineering Studies, Department of Geology. florencio.lechuga@cfe.gob.mx
(3) Federal Commission of Electricity, Construction Subdivision, Management of Civil Engineering Studies, Department of Seismotectonics and Geophysical Exploration. dolores.gonzalez@cfe.gob.mx

Abstract
The Central is located to 37 km south of Mexicali, between 9 and 12 meters above sea level. With excellent sedimentary record of the Colorado River Delta, affected by the fault systems Cerro Prieto - Imperial associated with the San Andreas fault that stretches from the Pacific back to the Imperial Valley (Mexicali) oriented NW-SE, displacement speed these systems range from 1 to 60 mm per year, and a secondary system of extensional type with orientation NE-SW, represented by Morelia and Oaxaca failures. The earthquake on May 24, 2006 in Morelia failure reached 5.2° in the Richter scale. This event damage important Central Geothermal facilities and confirm the high seismic activity and instability in the area.

***Keywords**: Fault, sedimentary, Dorsal and Richter scale.*

Introduction

The north of Mexico is one of the largest regions where earthquakes are recorded each year since the establishment of the National Seismological Service in early 1900 to date has logged more than 15,000 events. Fortunately none of them has been devastating, but some have caused great economic losses, citing for example the November 29, 1852 with 6.5 ° (MI), on February 23, 1892 with 7 ° (Mw), 18 May 1940 with 7.2 ° (Ms), the August 7, 1966 with 6.3 ° (Ms), the October 15, 1979 with 6.9 ° (Ms), that of June 9, 1980 with 6.4 ° (Ms), the most recent on May 23, 2006 of 5.4 ° (Ms) and April 4, 2010 7.2 (MI) caused damage structural to the installations of the Cerro Prieto CG , B.C.

Regional Tectonic Framework

The Gulf of California is located in the margin of the Pacific and North American plates. In this region, the limit varies from oceanic to continental. In the southern portion of the peninsula, the lithosphere is fully opened facilitating the expansion of ocean floor and creating a rift zone, while in the northern half, still has not formed new oceanic crust and the displacement of the plates occurs along a zone of continental extensional deformation.

An important feature of this rift system is its complex tectonics occurred in western North America. Before the opening of the Gulf, was developed a subduction zone convergent between the now extinct Farallon oceanic plate and the North American continental plate. When the Pacific Plate oceanic contacted with the North American continental plate, the subduction ceased along the Baja California Peninsula. The Gulf of California extension appears to have occurred in two stages. During the first, the Baja Peninsula acted as a microplate confined between the Pacific and North America, so that the early opening of the Gulf adds to overall motion between these two plates. This early stage due rift have a movement orthogonal to the displacement direction and located outside the protogulf possibly along the Pacific edge continental. During the second phase, the Peninsula must be adhered to the plate so that the Pacific after 6 Ma displacements during opening Gulf represents the North Pacific oblique movement.

Paleoseismicity

For interest and review paleoseismicity data measured directly on the trace of faults affecting the area of Cerro Prieto geothermal field, we conducted a field survey to locate sites active faulting. The discontinuity (fault) must affect the stratigraphic record with no evidence of erosion and be related to sedimentary environment or placed in interphase, where tectonic shows a block and the other accumulation erosion, in order to analyze the seismic record as associated deformations at the time of an earthquake can introduce vertical slopes slightly modify the erosive balance / scale sedimentary very precisely indicates that the local occurrence of paleoearthquakes. However, when rates of erosion or sedimentation are very high, cannot be found sedimentary mass episodes covering much of the exposed wall, which reduces the number of seismic cycles to determine. Intraplate areas or plate edges in the case of the Cerro Prieto Geothermal Station, BC), show large active faults slip rates on the surface, this type of failure is easier to place in arid than in wet. Furthermore, there are active faults which no shown surface sliding, in these cases geophysical prospecting techniques are used to reveal the structure.

Local Geology

The area where is located the Cerro Prieto Geothermal Power Station consists of a package of sediments semiconsolidated to unconsolidated, ranging from 2 000 to 6 000 m thick. Lithostratigraphic reconstruction from the analysis of the response of geophysical records as vertical electrical sounding, acoustic and radioactive (Pacheco Romero, M., *et al*., 2006), allow the stratigraphic sequence split into three main units: The first is related to marine mudstones (LC and LG) of possible Late Miocene directly overlying crystalline basement. The second consists of alternating mudstones and sandstones (Ar) are interpreted as delta front deposits and sea plain, therefore, it is possible that this unit is in two parts interdigitated with one unit sequence. While the third stratigraphic unit consists of sandstones and conglomerates, with subordinate silts and muds typical facies defined channels interlinked systems, most abundant near the apex of the delta and are associated with alluvial deposits (SCNC).

The configuration of the top of the basement indicates that thinner levels of the sequences may coincide with a structural high that is oriented in the same direction of the evaporation pond (NW-SE) and to its sides the thickness may vary from 5400 to 6000 m. It is possible that this structural high to match the high level block of Cerro Prieto fault.

Structural Geology

In the area significantly reflected the activity of recent tectonic processes fault system in the Imperial Valley, evidenced by the Cerro Prieto and Imperial faults of dextral transcurrent type and both associated with the record of seismic activity in the area. The general orientation of this fault system is NW-SE. However, it develops other system structural secondary with a preferential direction NE-SW represented locally by the faults Oaxaca and Morelia (Figure 1).

Imperial fault

This fault is located northeast of the geothermal field, can be considered as the main connection between the San Andreas fault system and the Gulf of California. The Imperial fault has an approximate length of 75 km, the route goes through the south of the city of Brawley, California, USA, to the Cerro Prieto spreading center and presents an orientation general N42 ° W. It is estimated that the travel speed for this structure is 47 mm / year and are associated tremors El Centro and Imperial Valley, occurred on May 18, 1940 and October 15, 1979, respectively.

Cerro Prieto fault

Its type dextral transcurrent, with approximate length of 80 km, from the Cerro Prieto spreading center to the Wagner Basin, is seen as the continuation of a displaced segment of the Imperial fault. The moving average for the Cerro Prieto fault is considered greater than 50 mm / year and major earthquakes are associated with an average size of 6-7 ° Richter. The general orientation (Picture 1) of this structure is N50-60°W with dip of 85°NE.

Michoacan fault

This system is located northwest of the Central Geothermal has a preferential orientation N35-45 ° W and is more or less parallel to the Cerro Prieto fault, has apparently normal displacement vertical to the NE with right lateral component. You can see its influence on the walls of the canal that runs next to the Ejido Michoacan, on the premises of the geothermal field and the road that runs next to the town of El Chimi. Various traces observed within the geothermal field, which include: high humidity areas, subsidence, liquefaction presence of structures, deformation and dip of the train tracks, fracturing and tilting of the concrete walls that control the channel. This structure is part of the Cerro Prieto fault system, which affects the Channel Delta One and therefore if this were to suffer significant harm, impact on the campus of the geothermal field, causing considerable damage to the premises of the Central Geothermal Cerro Prieto.

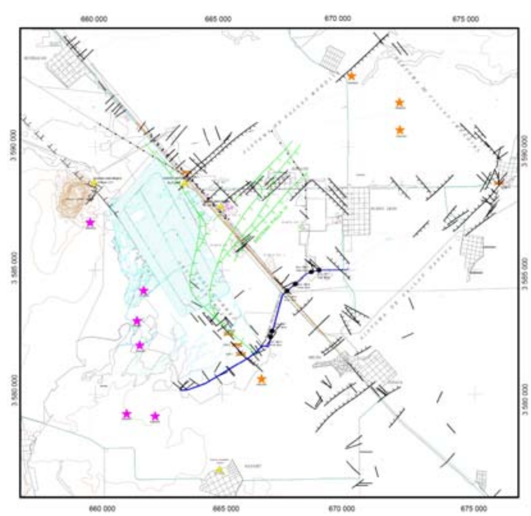

Figure 1: First stage of study evidenced the activity of recent neotectonic processes of Cerro Prieto fault system, Imperial, Morelia and Oaxaca. The fault system in green H was identified in surveys, and magenta and orange symbols represent earthquakes of September and December 2009 respectively.

Graben Cerro Prieto

The area located between the trace of the Cerro Prieto and Imperial faults is known by the name of Cerro Prieto spreading center. Based on the configuration of the basement by Lira and Arellano 2006, we can see that this scattering center can be associated with a graven of type tectonic affecting the basement and is bounded by the two afore mentioned faults. The reflection of the structural arrangement of the basement is present at the surface level, and affects the entire sequence of sediments by a normal fault system of NE-SW preferred orientation, as in the case of failures Morelia and Oaxaca.

Morelia fault

It is approximately four miles and is bounded by the trace of the Cerro Prieto and Imperial faults. It presents a strike that varies of N28-50 ° E and a dip of 88°SE, whose slip planes ranging from 18 to 38 cm.

The trace of the fault Morelia is located about 400 m away to the north with respect to the Cerro Prieto Generation Unit III and extends into the central portion of the evaporation pond. Such failure may stop below the pond in the western portion of the site indicated.

Regarding seismic activity reported for Morelia fault, is estimated as the geological structure responsible for the quake May 24, 2006 at 04:20 hours Universal Time (21:20 local time on May 23) and produced a earthquake with a magnitude of 5.2 degrees on the Richter scale, which caused damage to the facilities of the Geothermal.

Oaxaca fault

It is located at southeast of the Cerro Prieto Geothermal Central, this structure has an approximate length of 12 km, can be seen on the canals that surround the Ejido Nuevo Leon, the trace continues in a northeasterly direction toward Ejido Vicente Guerrero, where their effects are reflected in the concrete walls of the New Delta Canal. This regional geological structure type, have normal faulting with strike N20-45°E, where the block moved down to NW.

Seismicity

Geothermal energy production is closely linked to the seismicity, arguably not given one without the other. The heat required for steam is generated in the subsoil is related to active tectonic processes whose latency is evidenced by the generation of tremor. For this reason in 1978 installed a monitoring network in the area of Cerro Prieto, whose basic activities were two: The first one was to conduct a seismic record at regional level, through the installation of a network that covered ranging from the Sierra of Cucapáh to the northwestern state of Sonora. The management and control of the telemetric network was held jointly between the CFE and CICESE. The second activity was local in the geothermal field.

It is necessary to identify and characterize the "seismogenic sources" to perform seismic risk studies. The surface seismogenic sources are classified into zones and large faults. The first projection surface representing a volume of crust, where it is recognized that seismic occurrence is controlled by the set of fault systems that are located inside the cortical volume. The second are special tectonic structures which concentrate deformation and the occurrence of large earthquakes with displacement effective measurable in surface (Mayordomo, 2006), which can be estimated maximum recurrence within 10 000 years. It is considered as "active fault" (according to California Division of Mines and Geology), one that has displacement within this time period. The "capacity of failure", defined by the U.S. A. nuclear industry, is the presenting evidence of at least one surface movement in the last 35 ka, or recurrent movements in the last 500 years. From a geological point of view is preferred classify faults based on their rate or sliding speed. The "Research Group for Active Faults in Japan", classifies the activity of faults in three groups named by the letters A, B and C. Failures in group A are those with a slip rate greater than 1 m / ka (1 mm / year), group B between 1 and 0.1 m / ka, and C below 0.1 m / ka. For the case of Cerro Prieto slip rate is considered 50 mm / year, which corresponds with faults "A". The sliding velocity of failure allows a preliminary estimate of the maximum credible magnitude range of earthquakes that can generate, and the average period of recurrence of these. A higher rate of fault slip, higher frequency of small magnitude earthquakes or intermediate in a heterogeneous stress state. Slip faults low rates major earthquakes occur with less frequency periods, and relates to a concentrated stress state. Identification of active faults in surface depend on the balance established between the slip rate of the fault and the rate of change of the landscape (erosion), mainly controlled by climate. In intraplate areas or edges of plate (as in the case of the Geothermal Cerro Prieto, BC) show active faults important slip rates in surface, this type of faults is easier located in wet arid than in weather.

Picture 1.Overview of the trace of the Cerro Prieto fault. In the picture we see that the fault does not behave as a straight line, as it breaks into segments ranging from N60°W to N50°W and dip of 85° to the NE, similar to the "pull-apart" that manifested in the Gulf of California.

Conclusions

These studies have focused primarily on research of active faults at the regional level that have direct influence on the Cerro Prieto Geothermal Central; the structures found in recent river sediments are associated with tectonic processes such historical earthquakes linked to being the basis for making analysis of paleoseismic Central. The occurrence of major earthquakes in the region as a result of the tectonic activity will facilitate the continuous movement of faults in the region.

Defined two active transcurrent fault systems with strike NW-SE and NE-SW, these systems give rise to an open area respectively leading to a depression of type "pull-apart" capable of being filled by sedimentary materials. Within these systems there are five geological structures (faults), affecting the stratigraphic record where this Central Geothermal. The Cerro Prieto, Imperial, Morelia and Oaxaca faults shows a big slip rate in the surface, on the other hand, the Michoacan fault has not superficial scarp, however, you can see features as: seismites, collapse, cracking and high humidity as result of the activity of this structure. Geophysical techniques are demanded in future studies to define the area of influence of the discontinuity. For subsequents paleoseismic analysis, four sites were chosen for excavation of seismic hazard analysis trenches three of them were located in the Cerro Prieto fault and the fourth in Morelia fault.

We recognize the support for the realization of this study to the Subgerencia de Estudios Geológicos y Geofísicos de la Gerencia de Estudios de Ingeniería Civil, to the Gerencia de Proyectos Geotermoeléctricos, Residencia General de Cerro Prieto, Departamento de Geología y Geofísica de la Residencia General de Cerro Prieto and to the Residencia de Estudios de la Central Cerro Prieto.

REFERENCES

Albores A., Reyes A., Brune, J., González J., Garcilazo L. y Suárez F., 1980, "Seismic studies in the region of the Cerro Prieto geothermal field", Geothermics, Vol. 9, p. 65-77.

Cruz Castillo M., 2002, "Catálogo de fallas regionales activas en el norte de Baja California, México", GEOS, Unión Geofísica Mexicana A. C.

INEGI, 2001, Carta Topográfica Mexicali I11D65.
Escala 1:50 000.

Lira y Arellano (2006), Geología de la Central Geotermoeléctrica Cerro Prieto, Informe inédito Comisión Federal de Electricidad. 22p

Martín Barajas M., Steckler Mike y Stock Joann., 2001, Ruptura de la litósfera continental en la región del Golfo de California y Salton Trough. Reporte del Taller Margins de Puerto Vallarta. GEOS, Unión Geofísica Mexicana, A.C.

Pacheco Romero M, Martín Barajas A., Elders Wilfred, Espinoza Cardeña J.M., Belenes Javier and Segura Alberto., 2006, Stratigraphy and structure of the Altar basin of NW Sonora: Implicationes for the history of the Colorado River delta and the Salton Trou. Revista Mexicana de Ciencias Geológicas v.23, No. 1, p. 1-22.

Rebollar *et al*., (2003), Stress heterogeneity in the Cerro Prieto Geothermal Field, Baja California Mexico. Bulletin of the Seismological Soc. Of America, vol. 93, pp 783-794

Suárez Vidal F., González Mario, Murguía Orozco L., Wong Ortega V., Vidal Antonio y González García., 2001, Distribución de daños materiales en el Valle de Mexicali, B.C., ocasionados por los sismos del 1 de junio y 10 de septiembre de 1999, Mv=4,8. GEOS, Unión Geofísica Mexicana, A.C.

PALEOSEISMOLOGY & ARCHAEOSEISMOLOGY
MORELIA • MEXICO 2012
INQUA-TERPRO PALEOSEISMOLOGY
EARTHQUAKE ARCHAEOLOGY

PALEOSEISMIC FRACTURING OF ROCK CARVINGS 1000 BC IN SE SWEDEN

Nils-Axel Mörner (1)

(1) Paleogeophysics & Geodynamics, Rösundavägen 17, 13336 Saltsjöbaden, Sweden. morner@pog.nu

Abstract (Paleoseismic fracturing of rock carvings 1000 BC in SE Sweden): At about 1000 BC, a major (M>6) earthquake struck SE Sweden. This event fractured several rock carvings from the Bronze Age in a radius of, at least, 5 km from the centre of fracturing. At the centre, the Cambrian quartzite was heavily deformed and fractured-up in loose blocks and deep fractures, dominated by a strong extensional force. This fractured bedrock was, by the local people, converted into a quarry used to obtain flat blocks for the nearby grave known as "Brantarör" (which had, at least, 60 curb-stones and 12 blocks for the central sarcophagus) and for the huge bow and stern stones in the large stone-ship of Ales Stones, 30 km away. The quarrying seems to have in operation around 800 BC.

Key words: Earthquake 1000 BC, fracturing Bronze Age rock carvings, quartsite quarry, the Brantarör grave, Ales Stones, SE Sweden

INTRODUCTION

A total of 61 major (M >6) earthquakes have been identified in Sweden (e.g. Mörner 2003); 3 during the pre-LGM interstadial (32-28 ka), 46 during the period 13,000–5000 BP, and 12 during the last 5000 years. The latest event documented was found in 2012. It has number 61 in the Swedish Paleoseimic Catalogue and it occurred 1000 BC. It fractured several rock carvings from the Bronze Age in SE Sweden (Fig. 1).

Fig. 1. The 1000 BC earthquake had its centre at Brantevik where the Cambrian quartzite was fractured-up in blocks, used by the locals as a quarry for archaeological monuments. The earthquake fractured many rock carvings within a radius of, at least, 5 km (e.g. Järrestad).

The Bronze Age in SE Sweden is characterized partly by the early influence of visitors arriving by big ships from the East Mediterranean trading bronze for amber and partly by a strong Sun-cult (Mörner et al., 2009; Lind & Mörner, 2010; Mörner & Lind, 2010; 2012; Mörner, 2012).

There are large astronomical calendars; one in the form of a stone circle named Heimdall's Stones (Mörner et al., 2009) and one in the form of a 67 m long stone-ship named Ales Stones (Lind & Mörner, 2010; Mörner & Lind, 2012). The bow and stern stones of Ales Stones consist of two large blocks of quartzite (about 5 tons each), which must have been brought from Brantevik, 30 km to the NE (Lind & Mörner, 2010).

At Järrestad, there is a flat bedrock surface of quartzite, which is covered by rock carvings from the Bronze Age. The pictures have a very strict alignment with respect to the solar motions of the year (Mörner, 2012).

Already a decade ago, it was observed that the surface was fractured in postglacial time (Mörner, 2003, p. 267). In 2012, new data emerged (this paper) indicating that, indeed, an earthquake had fractured the surface after the carvings were made.

THE BRANTEVIK EARTHQUAKE 1000 BC

In connection with studies at Brantevik (Lind, 2012), I came to visit a swampy depression in the quartzite, later named "Brante Träsk" (the Brante Swamp).

After much cleaning, digging and coring, a new picture emerged: the bedrock surface was cut-up in large blocks by a network of fractures (Fig. 2) indicating strong extensional forces by a large earthquake (M >6). Later, people had used this "pre-fractured" bedrock as a quarry, removing loose blocks and breaking-up flat blocks into a 1 m deep quarry (now overgrown by peat as recorded by coring at 21 points).

The quartzite is a sandstone from the Cambrian time. Its extension is limited to the Simrishamn–Brantevik region. The lithology differs along the coast. Only at Brantevik itself (including the area around Brante Träsk), the bedding structures are clear, exhibiting the irregular building up of a sandstone bed (of quartz grains). These bedding characteristics, like the weathered glacially polished rock surface, are identical to those of the bow and stern stones at Ales Stones (Mörner, in Lind, 2012).

Fig. 2. The fractured bedrock of quartzite at Brante Träsk. It is traversed by fractures, all recording multi-directional extension generated by earthquake forces (cf. Fig. 5). Then, the broken-up surface was used by Bronze Age people for collecting loose blocks and for breaking up new ones; i.e. the seismically "pre-fractured" bedrock was turned into a quarry. Flat stones were needed for the building of the Brantarör grave (which, on a drawing from 1777, had, at least 60 curb-stones, and 12 large block for the central sarcophagus). The bow and stern stones of Ales Stones seems also to originate from this area (Mörner, in Lind, 2012).

The Brante Trösk quarry and stone industry

On a drawing from 1777 (Fig. 3), the Brantarör grave is very well recorded; today, it is gone (Lind, 2012). The high number of curb-stones (flat and trimmed) and the sarcophagus blocks must have called for a place of "industrial" quarrying; and now, we have found it at Brante Träsk (Fig. 2).

From the sarcophagus in the Brantarör grave, an urn (Fig. 4) was taken (together with the hilt of a bronze sward) in 1767. This urn has been kept in the family all though the years, and was "refound" in 2012, when it was handed over to B.G. Lind (Lind, 2012). The urn has been professionally examined by E. Jonsson and assigned an age of 800-500 BC (Lind, 2012). Consequently, the Brantarör graves (there was at least 5 of them) were built in the Late Bronze Age.

Fig. 3. The Brantarör grave as drawn by Hilfeling in 1777 (from Lind, 2012).

Fig. 4. The urn taken from the sarcophagus of Brantarör in 1767 and kept in the family up to today (from Lind, 2012). The urn has been assigned an age of 800–500 BC.

In the period 1000-700 BC, sea level was 2.1 m higher than today in the Brantevik area. The land/sea line has been carefully reconstructed (Mörner, in Lind, 2012) and a natural harbour existed right in present-day Brantevik; with 50-60 m to the Brantarör grave and some 400 m to the quarry at Brante Träsk.

It seems highly reasonable that the shipping of the large blocks of quartzite, now as bow and stern stones in Ales Stones, were transported from the quarry to the harbour (400 m) and then by ship/raft to the shore at Kåseberga (30 km) and up to their present place (400 m). This happened prior to 600 BC, and probably around 800 BC.

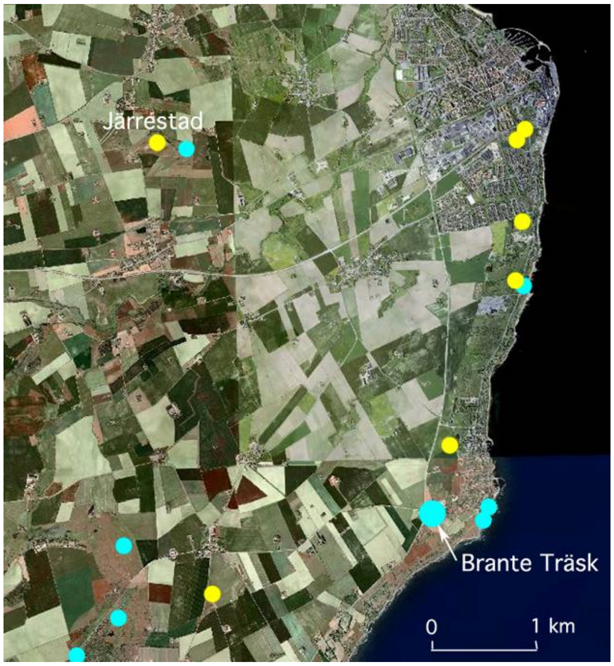

Fig. 5. Earthquake deformations in the Brantevik–Simrishamn area as recorded by deformed and tectonized bedrock (blue dots) and fractured pictures carved into the bedrock surfaces in the Bronze Age (yellow dots).

Fractured rock carvings

The Simrishamn–Brantevik–Järrestad area is full of rock carvings from the Bronze Age. Already a decade ago, I observed (Mörner, 2003) that the glacially well-polished quartzite surface had been fractured in postglacial time. After the finding of the Brante Träsk earthquake, seven sites were investigated (yellow dots in Fig. 5). At all sites, post-carving fracturing was recorded. The Järrestad site, 5 km from Brante Träsk, has a quite remarkable gallery of pictures (Mörner, 2012). Some examples of fractures crossing rock carvings in a manner that they must post-date the carvings are given in Figs. 6–10.

Fig. 6. The bedrock surface at Järrestad; a Cambrian quartzite, strongly polished by the glacial ice movements, leaving glacial striae and crescent-marks in the smooth surface. The fractures were induced in post-glacial time, even in post-carving time as evident from all the pictures now cut by fractures (Figs. 7-10).

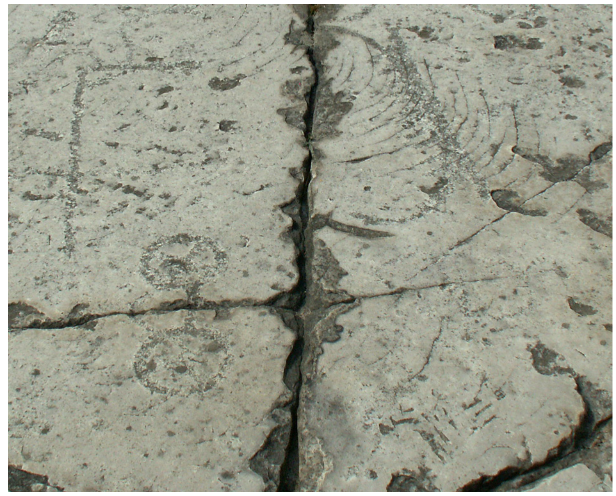

Fig. 9. Fractures cutting crescent-marks from the glacial time (seen in the central upper part) and a rock carving from the Bronze Age (two sun-symbols connected by a line).

Fig. 8. A pair of shoes cut by fractures in post-carving time. There are 19 pair of shoes and 45 single shoes on the rock surface at Järrestad; 95.3% of them point to the sunrise at winter-solstice (Mörner, 2012).

Fig. 9. A foot and 3 cup marks (circular depressions) cut by fractures, which must have been created after the foot and the marks were carved.

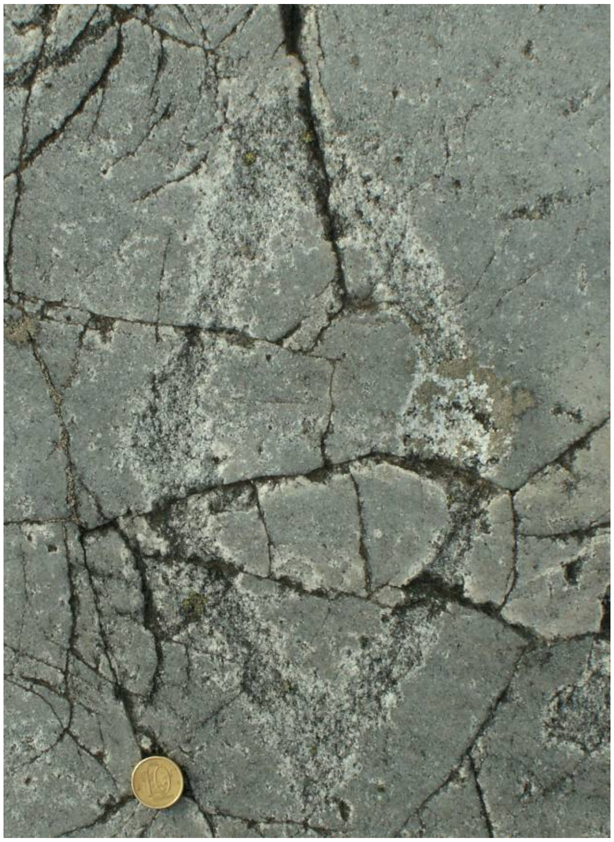

Fig. 10. The "sun boat" (Lind & Mörner, 2010; Mörner, 2012) at Järrestad. The bedrock surface is heavily fractured. This cannot have been the case when the carving was done. Hence the fracturing must post-date the carving.

These examples of fractured rock carvings (Figs. 6-10, and many more not shown) indicate that the bedrock must have become fractured after the carvings were done. The connection with the earthquake fracturing at Brante Träsk (Fig. 2) seems obvious. Whilst the fractures are fresh and sharp-edged at the inland sites (Figs. 2 and 11), they are wave-washed at the coast (Fig. 12).

Fig. 11. Strongly fractured bedrock at Järrestad consisting of sharp-edged individual blocks, which are likely to have been dislocated by the glacial shearing, if they had been in this stage at the deglacial time. This suggest a postglacial origin.

Fig. 12. At the shore, the fractures are smoothened by the wave action. At this site located about +2.5 m, only the waves of the +2.1 m shore dated 1000-700 BC have acted. This indicates that the earthquake pre-dates or co-insides with this sea level.

CONCLUSIONS

An earthquake struck the Brantevik–Simrishamn area in Mid-Bronze Age time. It post-dates the age of the rock carvings fractured, and it pre-dated or co-insides with the high sea level position 1000-700 BC. The strongest deformation occurred at Brante Träsk (Fig. 2). Fractured bedrock (e.g. Fig. 11) and fractured rock carvings (Figs. 6-10) occur in a radius of, at least, 5 km from Brante Träsk. At the shore, the fracturing seems to pre-date or co-inside with the high sea level at 1000-700 BC. The seismically fractured bedrock at Brante Träsk was turned into a quarry, delivering stones to the Brantarör graves (from 800-700 BC) and to the bow and stern stones in Ales Stones. The natural harbour at Brantevik only existed during the high sea level 1000-700 BC. The Ales Stone monument must have been build before the period of aridity and sand drift dated at 600-500 BC.

In conclusion, the earthquake must have occurred in the period 1000-800 BC (900±100 BC).

References

Lind, B.G. 2012. Från Brantarör till Brantevik. Stjärnljusets förlag. (with "Geologisk Rapport" by N.-A. Mörner, 29-32).

Lind, B.G., Mörner, N.-A. 2010. Mykenska och Fenisiska spår på Österlen. Stjärnljusets förlag.

Mörner, N.-A., 2003. Paleoseismicity of Sweden – a novel paradigm. A contribution to INQUA from its Sub-commission of Paleoseismology, Reno 2003, ISBN-91-631-4072-1, 1-320.

Mörner, N.-A., 2012. Strict solar alignment of Bronze Age rock carvings in SE Sweden. Journal of Archaeological Science 39, 3301-3305.

Mörner, N.-A., Lind, B .G., 2010. A Mediterranean trading centre in southeast Sweden. In: The Atlantis Hypothesis - Commentary 2008 (Paraminopoulos, S.P. Ed.), 685-699. Heliotopos Publications.

Mörner, N.-A., Lind, B.G., 2012. Stonehenge has got a younger sister. Ales Stones decoded. Journal of Astronomy and Astrophysics 2(1), 23-27.

Mörner, N.-A., Lind, B.G., Possnert, G. 2009. Heimdall's Stones at Vitemölla in SE Sweden and the chronology and. stratigraphy of the surroundings. Geogr. Ann. 91A, 205-213.

PALEOSEISMOLOGY & ARCHAEOSEISMOLOGY MORELIA • MEXICO 2012
INQUA-TERPRO PALEOSEISMOLOGY
EARTHQUAKE ARCHAEOLOGY

SEISMIC HAZARD ASSESSMENT ON A NUCLEAR WASTE TIME SCALE

Nils-Axel Mörner (1)

(1) Paleogeophysics & Geodynamics, Rösundavägen 17, 13336 Saltsjöbaden, Sweden. E-mail: morner@pog

Abstract (Seismic hazard assessment on a nuclear waste time scale): *Nuclear waste storage in the bedrock or sedimentary deposits calls for safety assessments over a time period of 100,000 years or even more. This may be to drive our assessments "in absurdum". Still, we have to do what we can, and this calls for sophisticated studies in paleoseismicity covering the deglacial period or preferably a full glacial/interglacial cycle. We investigate the situation in Sweden and Finland where repositories are in preparation. During the deglacial phase with a very high rate of glacial isostatic uplift, this region was a high-seismic area in magnitudes (M>8) as well as in frequency (6 events within 102 years). If this paleoseismological data base is not included in the hazards assessment, it will become meaningless and even directly misleading.*

Key words: *Hazard assessments, nuclear waste storage, paleoseismology, Sweden*

INTRODUCTION

For a proper handling of the future safety of buildings and constructions, we normally have to rely on careful seismic hazard assessments. In most cases, however, our seismological records are confined to measurements over some decades up to a century. This may do for short-term assessments. The instrumental records are far too short when it concerns longer-term assessments. Then we have to turn to paleoseismology and archaeo-seismology as illustrated in Fig. 1.

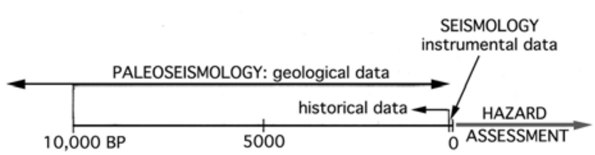

Fig. 1. A sound seismic hazard assessment must be founded on a combination of instrumental recording (seismology) and long-term recording by geological data (paleoseismology), archaeological data (archaeosiesmology) and historical documentation (from Mörner, 2011).

When it concerns the construction of nuclear waste repositories in the bedrock or in sedimentary deposits, the safety assessment has to be extended over at least 100,000 years. In such a case, the seismological records becomes meaningless and, maybe, even misleading. The only means of obtaining any guidance for some sort of meaningful assessment is via careful and extensive investigations of available geological data; i.e. paleo-seismology. This is especially important in areas like Sweden and Finland where the seismic activity has changed considerably over the last 12,000 years as a function of the change from deglacial to postglacial environment; at the time of deglaciation and high rates of glacial isostatic uplift, Fenoscandia was an area of very high seismic activity in magnitudes as well as in frequencies (Mörner, 2003, 2011), whilst it today is an area an area of moderate to low seismic activity.

To extend a seismic hazard assessment over such an immense time period as 100,000 years may, in fact, be to carry the predictions "in absurdum" (Mörner, 2001). Still this is what is now required both in Sweden in Finland where underground repositories for high-level nuclear waste are under final assessment in Sweden and partly already under construction in Finland. In both cases, the seismic hazard assessments are quite badly performed by the responsible firms (SKB and Posiva).

In Sweden, it is claimed that the maximum seismic event in 100,000 years is one M 6 event, despite the fact that 5 events are recorded in direct vicinity of the repository planned and 21 additional events are recorded with a radius of 150 km (Mörner, 2003, 2011). Their own study (Lagerbäck et al., 2005) includes extensive trenching (recording multiple deformational structures) but with a very weak (not to say incompetent) interpretation. This provides us with a concrete example of the necessity of focusing on paleoseismological data and to do this with a modern view of its recent achievements.

In Finland, the situation is even worse. Very little was done with respect to meaningful seismic hazard assessment. Important paleoseismic data (e.g. Koltilainen & Hutri, 2004) were ignored. In the close vicinity of the repository site, I was later able to document multiple paleoseismic events (Mörner, 2010).

In this paper I will focus on the paleoseismic records in Swedish with respect to dating, recurrence, frequency, magnitude and multiple expression in primary and secondary effects. The implication for a repository in the bedrock over a ten times longer period is assessed.

PALEOSEISMICITY OF SWEDEN

The paleoseismicity in Sweden has been discussed in numerous papers (where the more recent ones are: Mörner et al., 2000; Tröften 2000; Mörner 2001, 2003, 2004, 2005, 2007, 2008, 2009, 2011; Mörner & Sun, 2008; Mörner & Dawson, 2010; Mörner & Sjöberg, 2011). In total, 59 events have been recorded in Sweden up to 2012 (Fig. 2); 2 from the pre-LGM interstadial, 46 from deglacial to Mid Holocene time when glacial isostatic uplift was still strong, and 11 from the last 5000 years, where the uplift conditions were more or less the same as today.

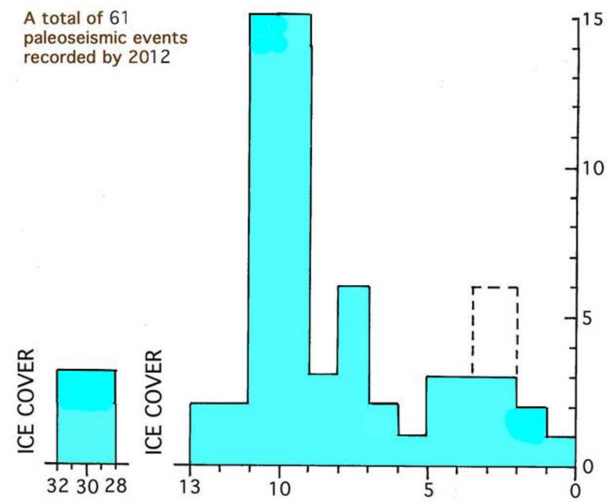

Fig. 2. Histogram of 58 paleoseismic events recorded and dated for every 1000 years over the past 13,000 years.

Fauls

The distribution of active faults and related secondary features in Sweden has been discussed elsewhere (Mörner, 2004). The Pärve and Lansjärv faults in northernmost Sweden are, indeed, spectacular features (Lagerbäck, 1990). The Falkberget Fault at Hudiksvall is impressive, too (Mörner, 2003). The Mälardalen area is traversed by an old E–W-trending fault, reactivated at in deglacial time with repeated events at high frequency and magnitude (Mörner, 2003, 2011, Fig. 10). The Kattegatt Sea is traversed by an active NW–SE-trending fault (Mörner, 2003, 2004).

Recurrence

Thanks to very sharp dating, it was possible to identify, date and establish the paleoseismic recurrence (Fig. 3).

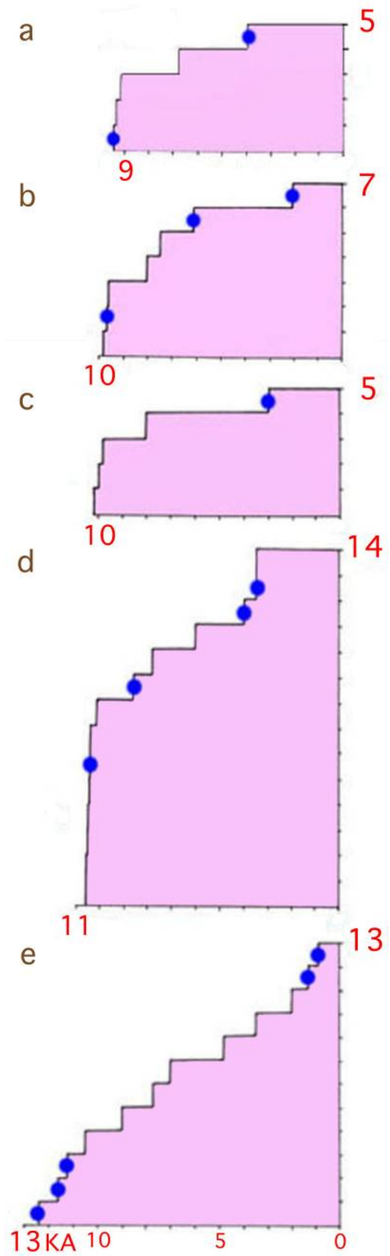

Fig. 3. Recurrence established at separate areas: (a) Umeå: 5 events in 9.5 KA, (b) Hudiksvall: 7 events in 10 KA, (c) northern Uppland (the Forsmark area): 5 events in 10.2 KA, (d) the Stockholm-Mälardalen area: 14 events in 10.6 KA, and (e) the West Coast area: 13 events in 13 KA. Blue dots mark tsunami events. A very high frequency of deglacial events was recorded in the Stockholm area (d): 6 events in 102 years. See Mörner (2003, 2009, 2011).

A high-sesmic region

The Bothnian Sea region with the proposed repositories for high-level nuclear waste in Sweden and Finland must be regarded as a high-seismic region in deglacial time as evident from the paleoseismic data recorded (Fig. 4).

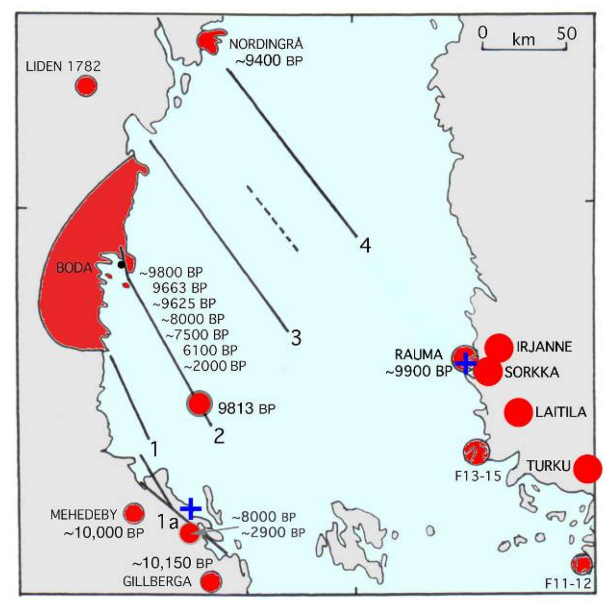

Fig. 4. The Bothnian Sea region with all the paleoseismic events recorded in Sweden (areas b-c in Fig. 3; Mörner, 2003, 2009) and Finland (Kuivamäki et al., 1998; Koltainen & Hutri, 2004; Mörner, 2010). Blue crosses mark the location of the proposed repositories of high-level nuclear waste at Forsmark (Sweden) and Olkiluoto (Finland).

The mere location of the repositories in this high-seismic region seems badly chosen, neglecting proper consideration of our science of paleoseismology. In view of all the observational facts available, it seems “remarkable” (to say the least) that the nuclear power agencies, in their so-called safety analyses, claimes that the maximum earthquake in 100,000 years will be one M6 event.

This is precisely why we have to insist that paleoseismology must play a central role in their safety and hazard assessments.

Magnitude estimates

It is, of course, not easy estimate magnitudes and/or intensities of paleoseismic events (Mörner, 2003, 2011). We use a combination of different available information:

fault criteria, spatial distribution of bedrock fracturing, spatial distribution of individual liquefaction events, material and character of liquefaction structures, number of phases of liquefaction at separate events, type and distribution of slides, heights of tsunami events, spatial distribution of turbidites and mode and distribution of magnetic grain re-orientation.

The multiple criteria of the 10,430 and 9663 vBP have been discussed separately (Mörner, 2011) and they must both represent events of M>8 (and intensity XII). The Pärve (~9000 vBP) and Landsjärv (~0150 vBP) Faults must also represent >8 magnitude events. An event dated 10,388 vBP (Mörner, 2008, 2011) exhibits violent large-scale liquefaction structures including the venting of coarse gravel. At the 2008 IGC excursion, X said *"this must be the largest liquefaction structures ever described"*. This merits the assignment of M>8. Similarly, the 6100 BP event represents venting of coarse gavel and a tsunami wave of at least 15 m suggesting M8->8.

The liquefaction structures representing the 10,430 and 9663 vBP events have a spatial distribution of 320x100 km and at least 80x40 km (probably 150x100 km), respectively. Furthermore, the 9663 vBP event contains 5 separate phases (Mörner, 2003, 2005).

In total 17 separate tsunami events have been identified (Mörner, 2003; Mörner & Dawson, 2010). Their time and height distribution is given in Fig. 5.

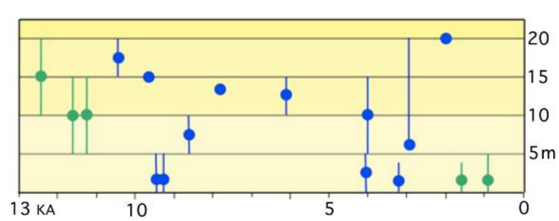

Fig. 5. Recorded heights of tsunami events in the Baltic (blue) and Kattegatt (green) coasts of Sweden.

The off-shore dynamics of the tsunami is given in Fig. 6 (from Mörner & Dawson, 2010).

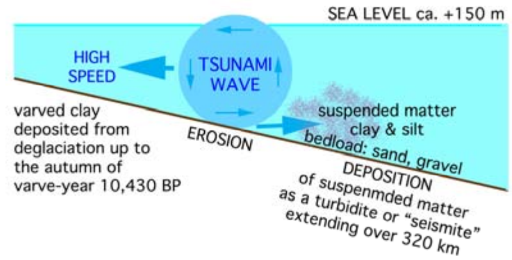

Fig. 6. Deformation, erosion and deposition in association with the 10,430 vBP event, generating a turbidite extending over an area of 200x320 km.

The varve 10,430 vBP turbidite is a marker varve of 10,430 BP identified in numerous sites with a spatial distribution of 320x200 km. It is always found at the same chronological level; varve 10,430 BP. In three sites, it has even been pinpointed at the autumn of this varve. The 9663 vBP event set up a similar marker bed with a turbidite extending over an area of 320x100 km.

The seismicity of Fennoscandia has changes considerably over the last 13,000 years (Fig. 1); 50% of the events occurred at the top rates of isostatic uplift (with M>8 and 6 events in 102 yarve years), 11 events are recorded over the last 5000 years (with M7, the youngest one at 900 BP), the historical events reached M5.4 in 1904 and the maximum present event M4.8 in 2008.

CONCLUSIONS

The safety analyses and seismic hazard assessments in association with the nuclear waste repositories at Forsmark in Sweden and at Olkiluoto in Finland are not adequately based on available paleoseismic data and geodynamical processes. Therefore, they should be regarded as insufficient and even misleading.

Though seismic hazard assessment over such immense time periods as 100,000 or more hardly is feasible and maybe even to drive predictions "in absurdum" (Mörner, 2001), we have – in view of our paleoseismological responsibility – to make the best estimates we can and to use all available facts and modern achievements.

In view of this, both the Forsmark area and the Olkiluoto area may over the next 100,000 years experience ~1000 M6 events, some ~100 M7 events and ~10 M8 events. In addition to this there is a threat of methane gas venting tectonics (Mörner, 2003, 2011).

In such an environment there can be no guarantees what so ever for a safe deposition of high-level nuclear waste in the bedrock; rather the opposite: it will not work.

Acknowledgements: The basic studies were undertaken at the department of Paleogeophysics & Geodynamics at Stock-holm University (which I headed 1991-2005). The 9663 vBP event was the target of a major international project including Franck Audemard, Sue Dawson, Douglas Grant, Andrej Nikonov, Dimitri Zykov, beside our own team of Christian Bronge, Ole Kvamsdal, Alf Sidén, Rabbe Sjöberg, Guangyu Sun, Per Erik Tröften, Hans Wigren. In 1999 and 2008, we run international excursions devoted to the process of land uplift and documented paleoseismic records in Sweden. The study in Finland was conducted in 2010.

References

Kotilainen, A., Hutri, K.-L. 2004. Submarine Holocene sedimentary disturbances in the Olkiluoto area of the Gulf of Bothnia: a case of postglacial paleoseismicity. *Quaternary Science Reviews* 23, 1125-1135.

Kuivamäki, A., Vuorela, P., Paananen, M. 1998. Indications of Postglacial and Recent Bedrock Movements in Finland and Russian Karelia. *Geol. Survey Finland*, Rep.,YST-99, 1-92.

Lagerbäck, R. 1990. Late quaternary faulting and paleoseismicity in northern Sweden, with particular reference to the Lansjärv area, northern Sweden. *Geol. Fören. Stockholm Förh.* 112, 333-354.

Lagerbäck, R., Sundh, M.,, Svedlund, J.O., Johansson, H. 2005. Forsmark site investigation. Searching for evidence of late- or postglacial faulting in the Forsmark region. *SKB*, R-05-51, 1-50.

Mörner, N.-A. 2001. In absurdum: long-term predictions and nuclear waste handling. *Engineering Geology* 61, 75-82.

Mörner, N.-A. 2003. *Paleoseismicity of Sweden - A Novel Paradigm*. A Contribution to INQUA from its Sub-commission of Paleoseismology. Reno 2003, ISBN 91-631-4072-1, 320 pp.

Mörner, N.-A. 2004. Active faults and paleoseismicity in Fennoscandia, especially Sweden: primary structures and secondary effects. *Tectonophysics* 380, 139-157.

Mörner, N.-A. 2005. An investigation and catalogue of paleoseismology in Sweden. *Tectonophysics* 408, 265-307.

Mörner, N.-A. 2008. Paleoseismicity and Uplift of Sweden, *Guidebook, Excursion 11 at 33rd IGC*, Oslo 2008, 107 pp. www.33IGC.org.

Mörner, N.-A. 2009. Late Holocene earthquake geology in Sweden. *Geological Society of London* Spec. Publ. 316, 179-188.

Mörner, N.-A. 2010. Seismotektoniska grottor i Finland. *Grottan* 45 (4), 6-14.

Mörner, N.-A., Dawson, S. 2011. Traces of tsunami events in off- and on-shore environments. Case studies in the Maldives, Scotland and Sweden. In: Mörner, N.-A. (Ed.), *The Tsunami Threat: Research and Technology*. InTech Publ. Co, pp. 371-388.

Mörner, N.-A., Sjöberg, R. 2011. Excursion Guide, 2nd International Conference on Granite Caves, Sweden June 2011, *Swedish. Speleological Soc.,* Speleo Publications 12, 1-28.

Mörner, N.-A., Sun, G., 2008. Paleoearthquake deformations recorded by magneticvariables. *Earth Planetary Science Letters* 267, 495-502.

Mörner, N.-A., Tröften, P.E., Sjöberg, R., Grant, D., Dawson, S., Bronge, C., Kvamsdal, O., Sidén, A. 2000. Deglacial paleoseismicity in Sweden: the 9663 BP: the Iggesund event. *Quaternary Science Reviews* 19, 1461e1468.

Tröften, P.E. 2000. The use of varved clay chronology as a means of recording paleoseismic events: the Erstaviken record in the Stockholm area, south Sweden. *Sedimentary Geology* 130, 167-181.

HOLOCENE EARTHQUAKES RECORDED AT THE TIP OF THE PASTORES FAULT SYSTEM (CENTRAL MEXICO)

Ortuño, María (1, 2), Zúñiga, Francisco Ramón (1), Aguirre, Gerardo (1), Carreón, Dora (1), Cerca, Mariano (1), Roverato, Matteo(1)

(1) Centro de Geociencias, Universidad Nacional Autónoma de México, Blvd. Juriquilla, 3001, 76230, Juriquilla, Querétaro, MEXICO
(2) Dept. deGeodinàmica i Geofísica, Universitat de Barcelona, C/ Martí i Franquès s/n, 08028, Barcelona, SPAIN.
ortuno.maria@gmail.com

Abstract (Holocene earthquakesrecorded at the tip of thePastores fault system (Central Mexico)):*The Pastores fault is one of the most active structures within the Intra-arc zone of the TransmexicanVolcanic Belt. It defines the southern margin of the Acambaygraben, extending E-W along near 30 km. this study, we mapped the fault western termination, which corresponds to a fault splay, and performed a paleoseismological researchon one of the fault branches. We relied on GPR data to properly locate the fault on depth. The trenches exposed an igimbritic deposit interbedded withfluvio- lacustrine and coluvial deposits. The deformation of this sequence suggests that this part of the Pastores fault moved at a maximum dip slip rate of 0.10 -0.15 mm/yr (three to four times greater than the rate previously estimated) and produced at least three (and possibly five) earthquakes during the last 2.4 – 3.67 kyr. Some of the deformation observed in the trenches could be triggered by seismic ruptures in nearby faults, as it is the Acambay-Tixmadejé fault rupture on 19th November 1912.*

Key words*: Acambay graben, slow faults, paleoearthquake chronology, Ground Penetration Radar*

INTRODUCTION

The Transmexican Volcanic Belt (TMVB) is a 900 km long and up to 200 km wide extensional zone that crosses continental Mexico from E to W, from the Mexican Gulf to the Pacific Coast (Fig. 1). This active deformational zone has been associated to the subduction of the Rivera and Cocos plates underneath the Northamerican plate. The deformation rate of the individual structures within the TMVB do not overpass 0.3 mm/a (Suter et al., 2001), which leads to consider the structures as slow faults. Among the main fault systems that comprise the TMVB are the Chapala, Morelia, Acambay and Queretaro grabens.

The historical seismic catalogue shows that the faults in this region are capable to produce earthquakes of up to M = 7. Some good examples of these intraplate earthquakes are the Chapala (1568, M ~ 7), Jalisco, 1875 (M ~ 7.1), Acambay, 1912 (mB = 6.9) and Jalapa, 1920 (mb = 6.9; Suarez, 1992) events.

This study focuses on the Pastores fault(Fig. 2), one of the most active faults in the intra-arc fault system(Suter et al. 1995, 2001). This fault is part of the Morelia-Acambay fault system (Martínez-Reyes and Nieto-Samaniego, 1990; Suter et al., 1992; 1995; 2001; Ramírez-Herrera et al. 1994; Garduño et al., 2009) and is the southern bounding fault of the Acambaygraben (Langridge et al. 2000). It dips 50-70º to the N and is characterized a by a very rectilinear trace, mainly developed on lava flows of different composition. The fault has a ~ 30 km trace length and an up to 250 m high scarp in its central part. Based on the age of lava flow deposits affected by the eastern prolongation of the fault, Sutter et al. (2001) approximated the vertical slip rate of the Pastores fault in 0.04 mm/yr.

Historical activity of the Pastores fault was reported by Urbina and Camacho (1913), who observed the formation of discrete scarps parallel to the fault main

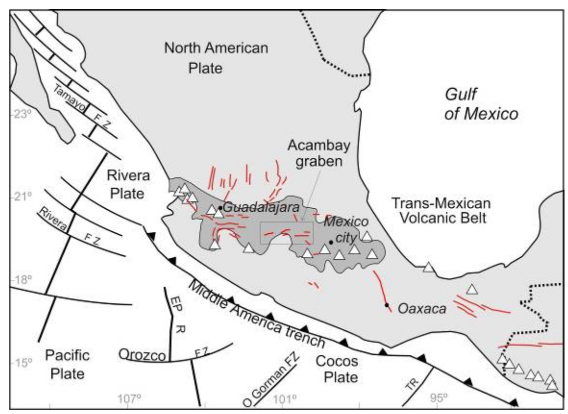

Fig. 1: Location of the Acambay graben within the Trans-Mexican volcanic belt (TMVB).

trace during the 19th November 1912 Acambay earthquake.

More recently, Persaud et al. (2006) performed a paleoseismic study in its eastern termination, concluding that the fault moved at 0.03 mm/yr during the Late-Pleistocene-Holocene and that it produced at least three earthquakes in the last 32 kyr. The study suggested that the fault segment did not move during the Acambay earthquake.

RESULTS

In this study, we search to evaluate the seismogenic activity of the Pastores fault in its westernmost termination. To do so, we performed an integrated study combining basic geomorphological and structural cartography to refine the location of the fault trace and to identify a site suitable for paleoseismological trenching. Then, we obtained subsurface GPR profiles across the fault (Fig. 3) using a SIR20 radar with a 200 MHz antenna, which helped us to locate the zones with greater deformation. The excavation of two trenches perpendicular to the fault trace permitted to study the most recent deformational history of the fault western end.

The Pastores fault western tip displays a fan-like termination array of 2 fault segments (a horse-tail structure composed of a southern and a northern fault). In this area, the main activity of the Pastores fault is transferred to the Venta the Bravo fault by a left-step over. The fault affects volcanic complexes of Miocene to Pleistocene age. In the down-thrown block, the fault affects lacustrine and fluvial Plesitocene sequences. The activity of the southern fault has been reported at two natural outcrops (Fig. 2 a and b), and that of the northern fault, by the study of two paleoseismic trenches in a sag pond structure, the Laguna Bañí site, formed by a step to the south inflexion of the fault trace (Fig. 2 c). The southern fault affects fluvial deposits located at the toe of the main scarp, which are displaced > 1 m by secondary faults showing SC structures and slicken-lines indicating a vertical with minor left-lateral component.

The study of the trenches revealed that the northern segmentof the western termination of the Pastoresfault is active and has produced at least three earthquakes (and possibly five) during the last 3.7 kyr. These earthquakes have produced small (< 30 cm) displacements, mainly vertical, on a fluvio-lacustrine and colluvial sequence interbedded with an ignimbrite deposited 2.4 – 3.67 kyr BP. Six fault zones were identified, which suggests that the fault westernmost tip splays in a fan of secondary faults. The maximum cumulated displacement was observed in C-6 colluvial unit, at the base of the trench, which is displaced vertically by 84 cm. By using the age of the ignimbrite as the minimum age for C6, we obtained a maximum slip rate of 0.10 -0.15 mm/yr.
The relationship between the seismic events and the volcanic deposits was analysed as recommended by Villamor et al. (2011). This analysis suggests that one (and possibly two) paleoearthquakes occurred at least some hundred years before the deposition of the ignimbrite. It also indicates that two paleoearthquakes took place immediately before and after the ignimbrite deposition. A fifth earthquake would have occurred after the 983 ± 36 yr, as deduced by the infill of a open crack.

Some of the deformation recorded on the trench could be due to secondary seismic effects triggered by the neotectonic movement on a nearby fault. This idea alerts about the interpretation of discrete deformational features, which can have a secondary origin (related to shacking or gravitational processes) and be produced by the seismogenic ruptures on nearby fault segments and not on the studied fault. Although this fact can be a handicap in the determination of the paleoearthquake chronology of a single fault, it can also be considered as the possibility of having a wider and concentrated record of the paleoseimic events affecting a given site.

Acknowledgements: This research was founded by the Mexican Government through CONACYT (Ciencia Básica-2009) and by the Universidad Nacional Autónoma de México-UNAM (PAPIIT-2009).

References

Ferrari, L., Orozco-Esquivel, T., Manea, V., Manea, M., 2011. The dynamic history of the Trans-Mexican Volcanic Belt and the Mexico subduction zone.Tectonophysics.
Garduño-Monroy, V. H., Pérez-Lopez, R., Israde-Alcantara, I. , Rodríguez-Pascua, M. A., Szynka-ruk, E., Hernández-Madrigal, V. M., García-Zepeda, M. L., Corona-Chávez, P., Ostroumov, M., Medina-Vega, V. H., García-Estrada, G., Carranza, O., Lopez-Granados, E., Mora Chaparro, J. C., 2009. Paleoseismology of the southwestern Morelia-Acambay fault system, central Mexico. Geofísica Internacional 48 (3), 319-335
Langridge, R., Weldon, R., Moya, J. and Suarez, G., 2000. Paleoseismology of the 1912 Acambya earthquake and the Acambay-Tixmadejé fault, Trans-Mexican Volcanic Belt. J. Geophys. Res., v. 105, p. 3019–3037
Martínez Reyes, J., Nieto-Samaniego, A. Efectos geológicos de la tectónica reciente en la parte cantral de México. Revista Instituto de Geología 9, 33 -50.
Persaud et al., 2006. Persaud, M., Zúñiga, F. R., Aguirre-Díaz, G., Villamor, P., Langridge, R., 2006. First Steps Towards the Paleoseismological History of the Pastores and Venta de Bravo Faults, Acambay Graben, Trans-Mexican Volcanic Belt, Central Mexico. American Geophysical Union, Fall Meeting, abstract #T13B-0501
Ramírez-Herrera, M. T. 1994. *Tectonic geomorphology of the Acambaygraben, Mexican Volcanic Belt*, PhD thesis, University of Edinburgh, 251 pp.
Suter, M., Quintero, O., and Johnson, C.A., 1992, Active faults and state of stress in the central part of the Trans-Mexican volcanic belt, 1—The Venta de Bravo fault: Journal of Geophysical Research, v. 97, 11983–11994.
Suter, M., Quintero, O, López-Martínez, M., Aguirre-Díaz, G. and Farrar, E. 1995. 'The Acambaygraben: Active intrarc extension in the Trans-Mexican Volcanic Belt, Mexico', Tectonics, 14(5), 1245–1262.
Suter, M., López-Martínez, M., Quintero O, and Carrillo-Martínez, M., 2001. Quaternary intra-arc extension in the central Trans-Mexican vol- canic belt.Geological Society of America Bulletin, v. 113, no. 6, p. 693– 703.
Urbina, F. and Camacho, H. 1913.La zona megaseismicaAcambay–Tixmadeje, Estado de México, conmovida el 19 de noviembre de 1912, Bol. Inst. Geol. Mex., 32, 125.
Villamor, P., Berryman, K.R., Nairn, I.A., Wilson, K., Litchfi eld, N., Ries, W, 2011. Associations between volcanic eruptions from Okataina volcanic center and surface rupture of nearby active faults, Taupo rift, New Zealand: Insights into the nature of volcano-tectonic interactions. GSA Bulletin, v. 123; no. 7/8; p. 1383–1405.

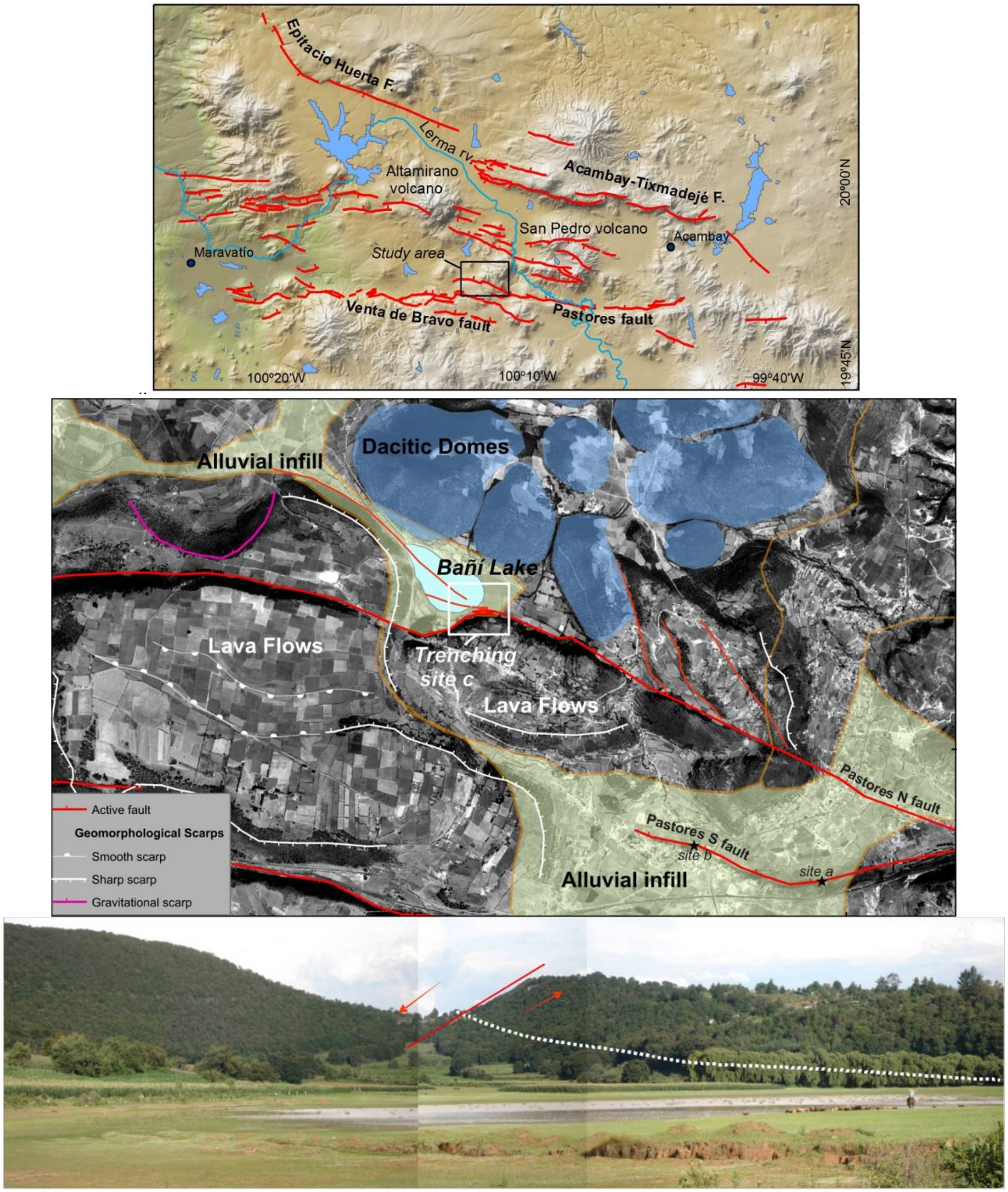

Fig. 2: Above: Location of the Acambaygraben within the Trans-Mexican volcanic belt (TMVB). Middle: Detailed neotectonic map of the westerntermination of the Pastores fault. Below: Field view of the Pastores North fault in the Bañí lake

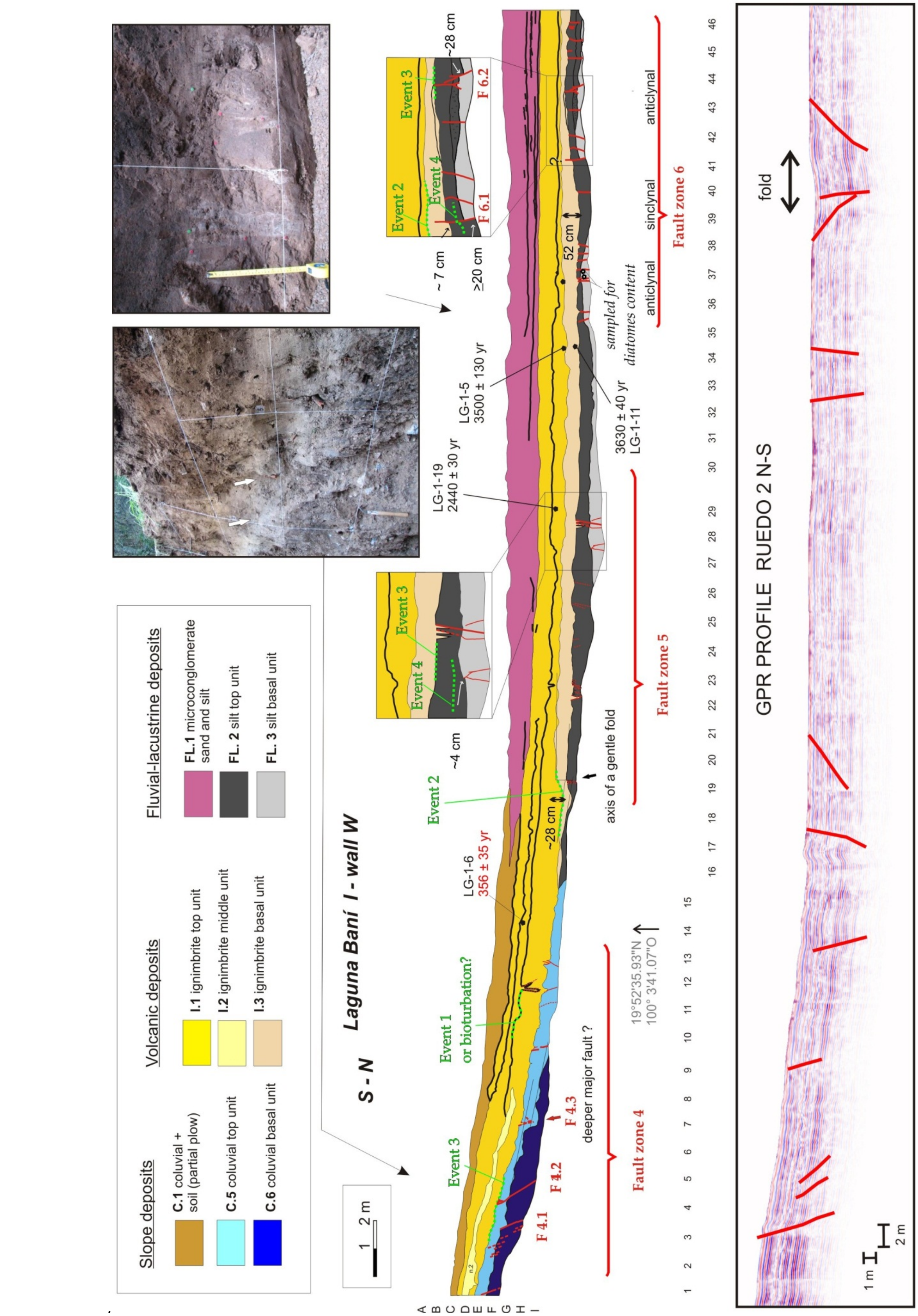

Fig 3: Above: Log of La Laguna Bañl trench-I. Below: GPR profile corresponding to the section of the trench

PALEOSEISMOLOGY & ARCHAEOSEISMOLOGY
MORELIA • MEXICO 2012
INQUA-TERPRO PALEOSEISMOLOGY
EARTHQUAKE ARCHAEOLOGY

SPATIAL AND TEMPORAL ANISOTROPY FOR THE QUATERNARY TECTONIC SLIP-RATE WITHIN THE TRANS MEXICAN VOLCANIC BELT (MEXICO)

Pérez-López Raúl (1), Garduño-Monroy Víctor H. (2), Giner-Robles, Jorge L. (3), Rodríguez-Pascua, Miguel A. (1), Menela Luca (2)

(1) IGME – Instituto Geológico y Minero de España. Madrid, 28003. SPAIN. r.perez@igme.es ; ma.rodriguez@igme.es
(2) UMSNH-IIM Departamento de Geología y Mineralogía, vhgardunom@gmail.com
(3) Departamento de Geología. UAM Universidad Autónoma de Madrid. jorge.giner@uam.es

Abstract (Spatial and Temporal Anisotropy for the Quaternary Tectonic Slip-Rate within the Trans Mexican Volcanic Belt, Mexico): *This paper addresses the spatial variation of the Quaternary slip-rates for active faults throughout the central part of the Trans-Mexican Volcanic Belt, located within the central part of Mexico. This landscape is determined by plenty of monogenetic volcanoes and graben structures defined by E-W and NE-SW normal faults with strike slip left-component. Hence, we have represented the slip rates obtained by different authors (e.g. Suter et al., 2001) by plotting the scalar value of the slip rate with the orientation of the fault. Results obtained from this polar plot suggest that there is a relationship between the maximum horizontal shortening (SHMax) with NE-SW trending and the orientation of the fault with maximum SR measured by paleoseismology. Furthermore, short-term SR values are related with the local orientation of SHMax whilst long-term vales with the regional SHMax.*

Key words*: slip-rate, anisotropy, maximum horizontal shortening, Mexico.*

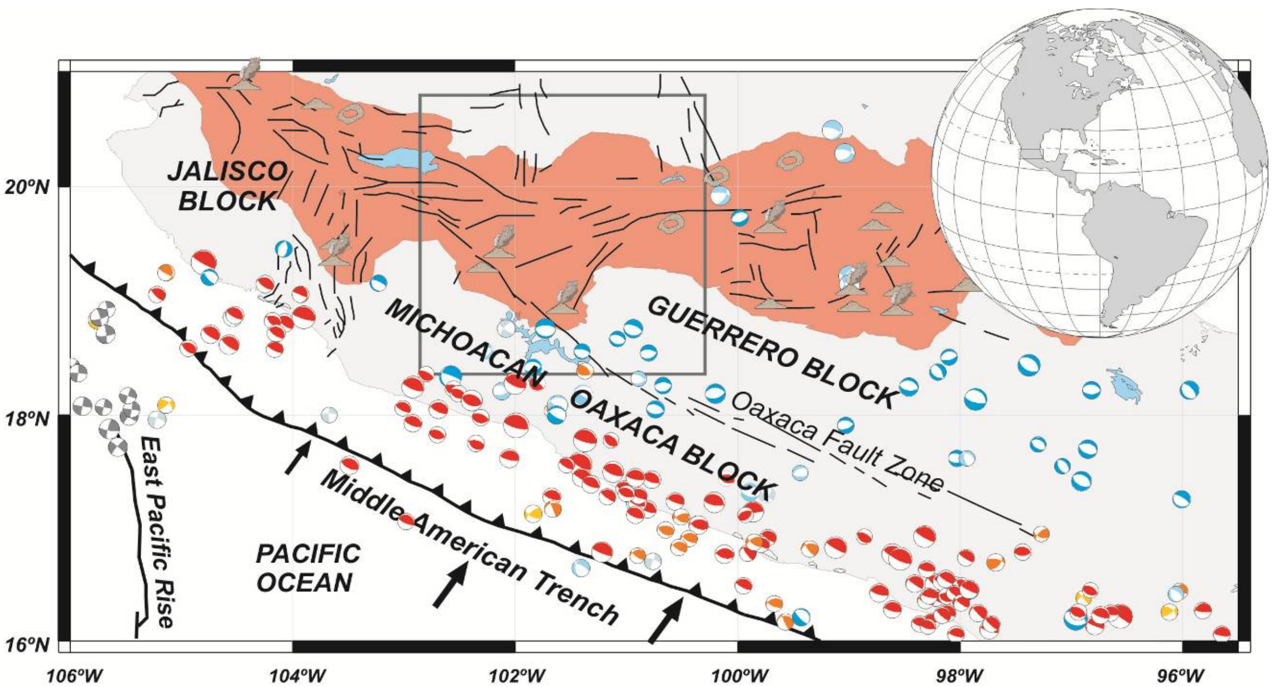

Fig. 1: Geographical location of the Trans-Mexican Volcanic Belt (orange area) and the Quaternary faults studied here (rectangle). Focal mechanism solutions beach balls are classified in: blue: extension, red compression and orange strike-slip. Tectonic plate convergence varies from 52 to 59 mm/yr.

INTRODUCTION

Active tectonics is often described by multiple parameters associated to active faulting: age of the last earthquake, maximum expected earthquake, recurrence interval and the tectonic slip-rate among others. The tectonic slip-rate is a physical parameter which describes the tectonic deformation accommodated by fault movement in a period of time. In general, the physical units are either mm per year or meters per kyr. Different discussions would address whether the slip-rate may include only coseismic deformation instead of coseismic and creep deformation.

In a general overview, plate tectonics is assumed as uniform motion with constant rates for the last 10 millions of years. Hence, active faults related to the tectonic activity should move at constant slip-rate for the temporal period of activity (Nichol et al., 1997). However, earthquakes triggered by active faults are arranged in temporal clusters showing gaps related to the seismic cycle (Scholz, 2002). These earthquake clusters related to active faulting suggests the opposite. Roberts et al., (2002) demonstrated an increment of the tectonic slip rates for active faulting in interplate conditions. Furthermore, the friction laws for the stick-slip fault movement (Burridge and Knopoff, 1967; Carlson and Langer, 1989), implies non-linearity and chaotic dynamical system defined by SOC (self organized criticality, Bak and Tang, 1989). In this physical condition, could local non-linear systems behave like continuous lineal dynamics is time?

Of course the scale observation of earthquake-fault phenomena is a relevant parameter to constrain the dynamical behaviour and the tectonic slip-rate for major faults. Hence the question is to establish the temporal window for earthquake-paleoearthquake observation phenomenon, (a) instrumental window for geodetic and seismological data, 100 years (b) geomorphic window in active lands 100-1,000 years and (c) geologic record , 1-100-1,000- 10,000-100,000 years. Geodetic estimations of slip-rates are usually faster than the geological record (i.e. Gourmelen et al., 2011). This fact suggests the question whether the fault offset represent the "complete" tectonic deformation of plate tectonics driving forces. Of course heat transfer and seismic waves transport energy involved in the plate tectonics scheme. Nevertheless, acceleration and deceleration of faults could be plausible if the final model is conservative, this means that the final summation state for the tectonic deformation is constant during a particular geological time interval, though the fault dynamic is defined by spatio-temporal clusters of earthquakes.

Other relevant parameter is the distance between the plate boundaries and the intraplate zones. Intraplates areas are determined by slow slip-rates (< 0.5 mm yr, Calais et al., 2010) and consequently, the seismic cycle for repeating events associated with an active fault segment are definitively longer in time. Recurrence periods for different slip rates can be consulted in Slemons, 1982.

Whatever the case, what is the time interval for earthquake-paleoearthquake completeness in a tectonic actively area? Is it correct the estimation of the tectonic slip-rate as a continuous displacement in time? Faults accelerate and decelerate in time and earthquakes gathered in spatio-temporal clusters around faults. With this aim, we have analysed the Plio-Quaternary tectonic slip-rate (hereafter SR) for the Acambay Graben System in central Mexico, obtaining eleven displacements of SR for 9 active segments, and plotting these values *versus* the segment orientation, age, type of faulting and strain axis orientation. Results suggest a spatio-temporal anisotropy of the SR related to the local strain tensor orientation.

THE TMVB QUATERNARY FAULT SYSTEM

The Trans-Mexican Volcanic Belt (hereafter TMVB) represents the largest volcanic intra arc field of Neogene ages with different types of volcanism from the Early Miocene (Polygenic, monogenetic, caldera collapse, etc.). This volcanic field is explained as a tectonic partitioning generated by the angle between the vector convergence of the Middle American Trench and the volcanic arc (Fig.1)(Pardo and Suarez, 1995; Ego and Ansan, 2002). The velocity of subduction between the Cocos and North America plates lies between 52 and 59 mm per yr., increasing form NW to SE, respectively. Pardo and Suarez (1995) explained this fact in relationship a variation of the dip angle of the slab decreasing to the southward.

The central part of the TMVB is tectonically active with historical large earthquakes like the Acambay earthquake of 1912 (6.9<Ms<7.1, Langridge et al., 2000). This active central part of the TMVB is also classified in three well-defined parts (Fig. 2)(Suter et al., 1992, 1995, 2001): (1) western zone, located between Morelia and Los Azufres, with the Cuitzeo Graben formed by NW- and E- trending normal faults with left-lateral strike-slip component, (2) central part, mainly determined by Venta del Bravo Fault System and (3) eastern zone, defined by the Acambay Graben System,

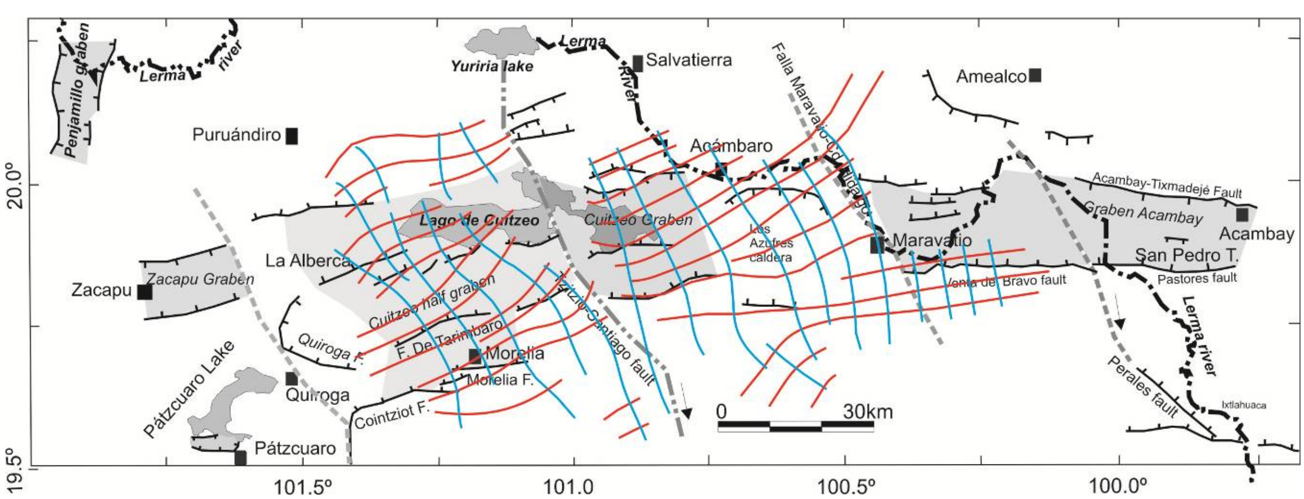

Fig. 2: Fault traces within the central part of the TMVB after Suter et al (2001) and Garduño-Monroy et al. (2009). Red lines are the orientation of SHMax () and blue ones the oriention of Shmin.

with the Acambay-Tixmadejé Fault and Los Pastores Fault, both activated during the 1912 earthquake (Langridge et al., 2000).

THE SLIP-RATE POLAR PLOT

We have collected the Quaternary slip rates for active faulting within the central part of the TMVB from bibliography and field work. In total we have compiled 22 active fault segments with enough quality for our purposes (Suter et al., 2001; Langridge et al., 2001; Ego and Ansan, 2002; Garduño-Monroy et al., 2009). Figure 2 encompasses the fault traces analysis in this work after Suter et al., (2001), Garduño Monroy et al. (2009), showing mainly normal faults with left-lateral component and E-W trending and secondary one NE-SW trending.

Figure 3 represents the polar plot of the SR with the orientation of the segment. Red arrow indicates the orientation of the stress/strain field in the area (Suter et al., 1995; Ego and Ansan, 2002; Garduño et al., 2009). Axis of the circle is scaled in logarithmic values from 0.001 to 10 mm/yr. Ego and Ansan (2002) pointed out that the maximum value for the tectonic SR lies between 2 and 7 mm/yr., for E-trending normal faults with left-lateral component. The red zone of Figure 3 shows the threshold zone, red zone for short-term E-trending faults and green area for NE-trending long-term faults. The radius of the dots includes the error for the SR estimation, the 10% of the value obtained by the authors.

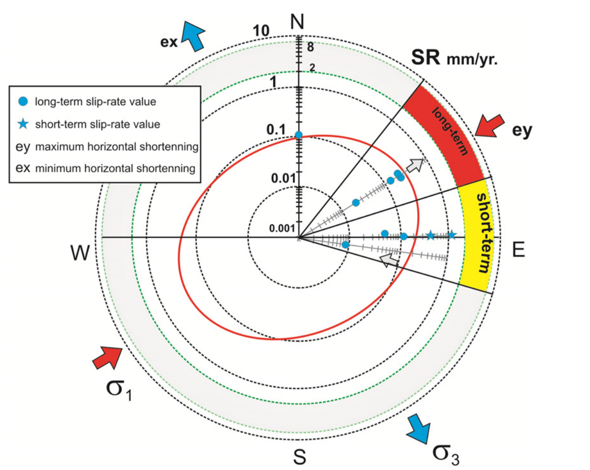

Fig. 3: Polar plot of the Quaternary slip-rates. We have plotted the orientation of the fault with the slip-rate value in a log axis. Red arrow indicates the orientation of the ey or maximum horizontal shortening. See text for further explanation.

Several SR data were obtained by simple division between the heights of the fault scarp divided buy the oldest age of deposits affected by the fault. This implies that whether fault creep movement or subsidence occurred, the SR value obtained is greater than the tectonic SR. Subsidence phenomenon was reported in Morelia city (Garduño et al., 200?). However, the values obtained here are congruent.

DISCUSSION

Tectonic SR measured for twenty two active segments within the central part of the TMVB oscillates between 0.002 and 0.2 mm/yr for Quaternary ages. SR estimated from earthquakes of the instrumental era (100 yrs.) is greater than SR for short-term (10,000 yrs.) and long-term (1,000,000 yrs).

The spatial distribution of SR with the segment orientation demonstrates that SR is higher for segment parallel to SHMax, ey. The NE-trending greater value of SR could be explained as the addition between the far-field tectonic convergence (NE-trending) and the near field into a transtensive zone with extensive grabens with E-W trending. Of course the partitioning between the far field convergence and the E-w trending of the TMVB implicates the addition of a tectonic deformation E-W and N-S. This could be the explanation for the similar values in both directions.

The relevance of this analysis suggests that the recurrence period of active faulting within the TMVB strongly depends on the fault type, orientation and age.

Acknowledgements: This work is a contribution of the QTECT – AEQUA (Asociación Española de Estudio del Cuaternario).

References

Bak, P. and Tang, C. 1989. Earthquakes as a self-organized critical phenomenon, *J. Geophys. Res*. 94, 15,635-15,637.

Burridge R. and L. Knopoff. 1967. Model and theoretical seismicity, *Bull. Seism. Soc. Am*. 57, 341–371.

Calais, E., A. M. Freed, R. Van Arsdale and S. Stein. 2010. Triggering of New Madrid seismicity by late-Pleistocene erosion. *Nature* 466, 608-611.

Carlson J. M. and J. S. Langer. 1989. Properties of earthquakes generated by fault dynamics. *Phys. Rev. Lett*. 62, 2632–2635.

Ego, F. and Ansan, V. 2002. Why is the Central Trans-Mexican Volcanic Belt (102º–99ºW) in transtensive deformation? *Tectonophysics*, 359, 189-208.

Garduño-Monroy, V. H., R. Pérez-Lopez, I. Israde-Alcantara, M. A. Rodríguez-Pascua *et al.* 2009. Paleoseismology of the southwestern Morelia-Acambay fault system, central Mexico. *Geofísica Internacional* 48(3), 319-335.

Gourmelen, N., T. H. Dixon, F. Amelung, G. Schmalzle. 2011. Acceleration and evolution of faults: An example from the Hunter Mountain–Panamint Valley fault zone, Eastern California. *Earth and Planetary Science Letters* 301, 337–344.

Langridge, R. M., R. J. Weldon, J. C. Moya, G. Suárez. 2000. Paleoseismology of the 1912 Acambay earthquake and the Acambay-Tixmadejé fault, Trans-Mexican Volcanic Belt. *J. Geophys. Res.*,10(105), 3019-3037.

Nicol, A., J. J. Walsh, J. Watterson, and J. Underhill.1997. Displacement rates of normal faults. *Nature*, 390, 157–159.

Pardo, M., Suárez, G., 1995. Shape of the subducted Rivera and Cocos plates in southern Mexico: seismic and tectonic implications. *J. Geophys. Res*. 100, 12,357–12,373.

Roberts, G. P., A. M. Michetti, P. Cowie, N. C. Morewood and I. Papanikolaou. 2002. Fault slip-rate variations during crustal-scale strain localisation, central Italy. *Geophysical Research Letters* 29(8), 1168, doi: 10.1029/2001GL013529.

Scholz, C.H. 2002. *The mechaniscs of Earthquakes and Faulting. 2nd Edition*. Cambridge University Press. Cambridge. 471 pp.(See the Chapter 5, The earthquake cycle).

Slemons, D. B. 1982. Determination of design earthquake magnitudes for microzonation. In: *Proceedings of the 3rd International Earthquake Microzonation Conference*. Seattle, Washington. 119-130.

Suter, M., O. Quintero, and C. A. Johnson. 1992. Active Faults and State of Stress in the Central Part of the Trans-Mexican Volcanic Belt, Mexico 1. The Venta de Bravo Fault. *Journal Geophysics Research*, 97(B8), 11,983–11,993, doi:10.1029/91JB00428.

Suter, M., O. Quintero-Legorreta, M. López-Martinez, G. Aguirre-Díaz, and E. Farrar. 1995. The Acambay graben: Active intraarc extension in the trans-Mexican volcanic belt, Mexico. *Tectonics*, 14(6), 1245–1262, doi:10.1029/95TC01930.

Suter, Max,. Margarita López Martínez, Odranoel Quintero Legorreta and Miguel Carrillo Martínez. 2001. Quaternary intra-arc extension in the central Trans-Mexican volcanic belt. *Geological Society of America Bulletin*, 113(6), 693-703.

ROCK-FALLS RELATED TO THE 1674 HISTORIC EARTHQUAKE IN LORCA (SPAIN): LICHENOMETRIC AGES

Raúl Pérez-López(1), Fidel Martín-González(2), José J. Martínez-Díaz(3), Miguel A. Rodríguez-Pascua(1)

1 Grupo de Eventos Extremos. Instituto Geológico y Minero de España. C/ Ríos Rosas 23. Madrid, 28003. ESPAÑA. Email: r.perez@igme.es y ma.rodriguez@igme.es .
2 Área de Geología. ESCET. Universidad Rey Juan Carlos I. Email: fidel.martin@urjc.es
3 Departamento de Geodinámica. Facultad de Ciencias Geológicas. Universidad Complutense de Madrid. Avda. Antonio Novais s/n. Madrid, 28004. Madrid. ESPAÑA. Email: jmdiaz@geo.ucm.es

Abstract (ROCK-FALLS RELATED TO THE 1674 HISTORIC EARTHQUAKE IN LORCA (SPAIN): LICHENOMETRIC AGES): *During the earthquake at Lorca (Murcia, SE Spain) in 2011 (5.2 Mw, 4km depth) several rock-falls occurred, mobilizing an estimated volume of close to 2,000 m^3. All these rock-falls took place within the Estancias and La Tercia mountain ranges. We have conducted a lichenometric study to obtain the age of the ancient rock-falls within the Las Estancias Range. We have assumed an annual growth rate of 0.24 mm for lichen species classified as calcicolous and related to warm climatic conditions. Our aim was to corroborate the hypothesis that historic seismic events triggered these rock-falls. The city of Lorca had experienced two near-field historic earthquakes (1674 EMS VIII and 1818 EMS VI) and one far-field tremor during the great Lisbon earthquake in 1755 (EMS VI). Results obtained here indicate that the earthquakes of 1674 and 2011 were quite similar, except that the 1674 one mobilised a greater quantity and twenty times the volume of blocks mobilised during the 2011 earthquake. Therefore, we conclude that the size of the earthquake of 1674 was possibly between 6.0<M<6.8, assuming similar focal and seismotectonic conditions to those of the instrumentally measured earthquake of 2011.*

Key words*: earthquake, rock-fall, lichenometry, Lorca.*

INTRODUCTION

On 11 May 2011 the city of Lorca (SE Spain) experienced a small earthquake (5.2 Mw, IGN, 2011), although 9 people were killed, more than 300 injured, several modern buildings collapsed and damage affected c.a. 1,000 other constructions,. The energy released during the quake was 5.62 x 10^{12} Jules, triggering various rock-falls across the La Tercia and Las Estancias mountain ranges to the north of the city. The shallow hypocentral depth (4 km approx.) and the alluvial infilling of the site probably played an important role in increasing the damage caused by the seismic event.

The major geological effects observed in association with this earthquake were the rock-falls located on the northern reliefs in the vicinity of the epicentral area (Fig. 1). Different authors have estimated the total volume mobilised during this earthquake to be close to 1,000 m^3 (cf. Pérez-López et al., 2011; Alfaro et al., 2012). A few hours after the earthquake a team of geologists made observations in the field within the affected zone to document the geological effects associated to the earthquake: ground cracking, liquefaction, rock-falls and landslides.

The main geological effect documented was rock-falls. Moreover, all these rock-fall areas showed evidence of ancient fallen blocks. Therefore, the aim of this work has been to obtain the ages of the ancient fallen blocks by resorting to lichenometric dating. The occurrence of historic seismicity within the zone, the well documented earthquake effects and the seismic intensity all suggest a potential relationship between the previous rock-falls and these historic earthquakes. Furthermore, it is possible to speculate about the size of the historic earthquake by direct comparison with focal parameters determined for the earthquake of 2011.

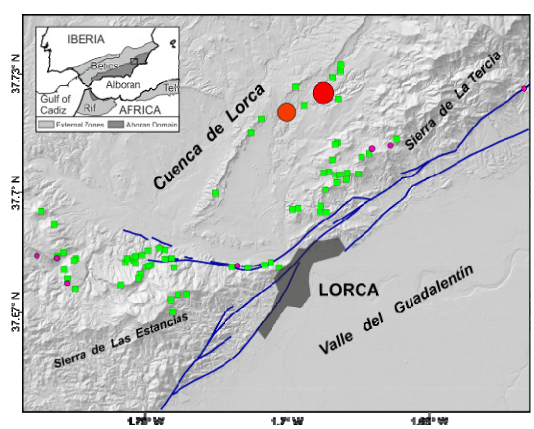

Fig. 1: Geographical location of the epicentre of the 2011 Lorca earthquake (red dot) and rock-fall locations (green dots) for rock blocks of a volume of more than 1 m^3.

HISTORICAL SEISMICITY AT LORCA

The city of Lorca dates from the Roman period in the Iberian Peninsula (AD 1st Century). At least three historic earthquakes of an intensity greater than VI (EMS98 scale, Martínez-Solares and Mezcua, 2002) have shaken the city (Muñoz-Clarés et al., 2012), in 1579 (VII EMS), 1674 (VII EMS) and 1818 (VI-VII EMS). Probably previous earthquakes affected the city during the Muslin and Roman cultural periods, though this part of the history in the city regarding the seismic occurrence is unclear so far.

LICHENOMETRIC METHOD

The lichenometry dating technique involves determining the age of rocks by studying the growth of lichens on their exposed surfaces. The principal premise is that lichen grows at a constant rate and so lichenometry can be used to calculate geomorphic ages for exposed rock surfaces related to rock-falls and landslides, among other geomorphic events. Proctor (1977) studied the method and practical use of lichenometry for dating purposes and reached a time interval of 5,000 yrs. The most used and powerful lichen species for dating is *Rhizocarpon geographicum*, a discoidal, crustose lichen with a constant growth rate (Innes, 1985). Jomelli et al. (2007) described the growth pattern over time of this lichen specie and reported its annual growth rate and various ways of measuring the *tallus* of the lichen: minimum diameter, maximum diameter etc. Bull (1996) demonstrated that lichen colonizes rock-falls soon after the event in patterns that indicate different mobilisations depending on previous earthquakes.

The first step for applying lichenometry is to obtain the annual growth rate of the lichen species by taking

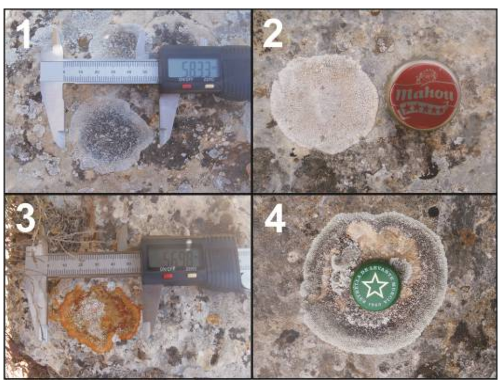

Fig. 2: Photos of the four main lichen species used in this study. Calcicolous and crustose lichen species recognised in this work were located at the Rambla de los 17 Arcos (R17A): 1. "Aspicilia radiosa", 2. "Aspicilia calcarea", 3. "Caloplaca aurantia" and 4. "Lecanora muralis".

measurements of the *tallus* diameter on the surface of rocks of known age. In general the best choice is to use tombstones in cemeteries. The growth curve can then be obtained by plotting the lichen diameter against the age of the tomb and then extrapolating the resulting curve to other exposed surfaces.

In this work we used the following lichen species: *Lecanora muralis* (Schreber), *Aspicilia calcarea* (L.), *Aspicilia radiosa* (Hoffm.) and *Caloplaca aurantia* (Hellb.) (Fig. 2), depending upon the type of Tortonian calcarenitic sandstone studied. We assumed an annual growth rate for *A. radiosa* of 0.24 mm/yr (Pérez-López et al., 2010b).

RESULTS

We have analysed two areas with rock-falls activated during the 2011 Lorca earthquake, both also showing evidence of ancient rock-falls (Fig. 1): (1) "El Cejo de los Enamorados" and (2) "La Rambla de los 17 Arcos". Zone (1) contains two huge blocks with an estimated volume of 30 m^3.

The second zone (R17A) is located one km from the first zone and the total affected area of rock-falls is greater than the previous one (0.02 km^2); its maximum block size is one of 350 m^3 (Fig.3). We estimated the age of 20 rock blocks in all and measured in the field a total volume for these blocks of 1,200 m^3. During the 2011 earthquake, however, the total volume mobilised in the same area barely reached 100 m^3. Bearing in mind the error in the estimation of the annual growth rate (4 yrs) (Pérez-López et al., 2010b) and the ecesis period of 5 yrs. (average time for colonization by the lichen species on a newly exposed rock surface; cf. Fink, 1917), we would suggest that the first rocks-falls affecting this hill (SW side) were activated during the 1674 earthquake.

CONCLUSIONS

As a preliminary result, the lichenometric dating of rock falls located within the Las Estancias range allowed us to distinguish the geological effects of historic earthquakes affecting the mountain range just to the north of Lorca. Thus we conclude:

1. The historic earthquake of 1674 triggered several rock falls located at the "Cejo de los Enamorados" and "Rambla de los 17 Arcos" hills in the sierra to the north of the city of Lorca.
2. Other historic seismic events such as the great Lisbon earthquake in 1755 remobilised several blocks, though smaller in size than those mobilised during the earthquake of 1674. The earthquake of 2011 also triggered rock-falls in similar zones.
3. The total volume of rocks mobilised by the 1674 earthquake at the "Rambla de los 17 Arcos" was 2,000 m^3, twenty times greater than the volume mobilised during the 2011 earthquake.

Therefore, we have estimated that the 1674 earthquake ranged in size between $6.0<M<6.1$ and M 6.8, depending upon whether its hypocenter was 5 km or deeper (from between 12-15 km). Furthermore, this earthquake was triggered by the Lorca-Totana segment of the Alhama de Murcia fault, bearing in mind the location of the rock-falls in relation to the epicentral location of the 2011 earthquake.

Acknowledgements: This work was funding by the Spanish projects: RESCATELO (CGL2011-14925-E) and TECTACT GR35/10-A-910368. Furthermore, this is a contribution of QTECT- Grupo de Tectónica Activa y Paleosismicidad de AEQUA – Active Tectonic and Paleoseismicity Group of the Spanish Association for Quaternary Research.

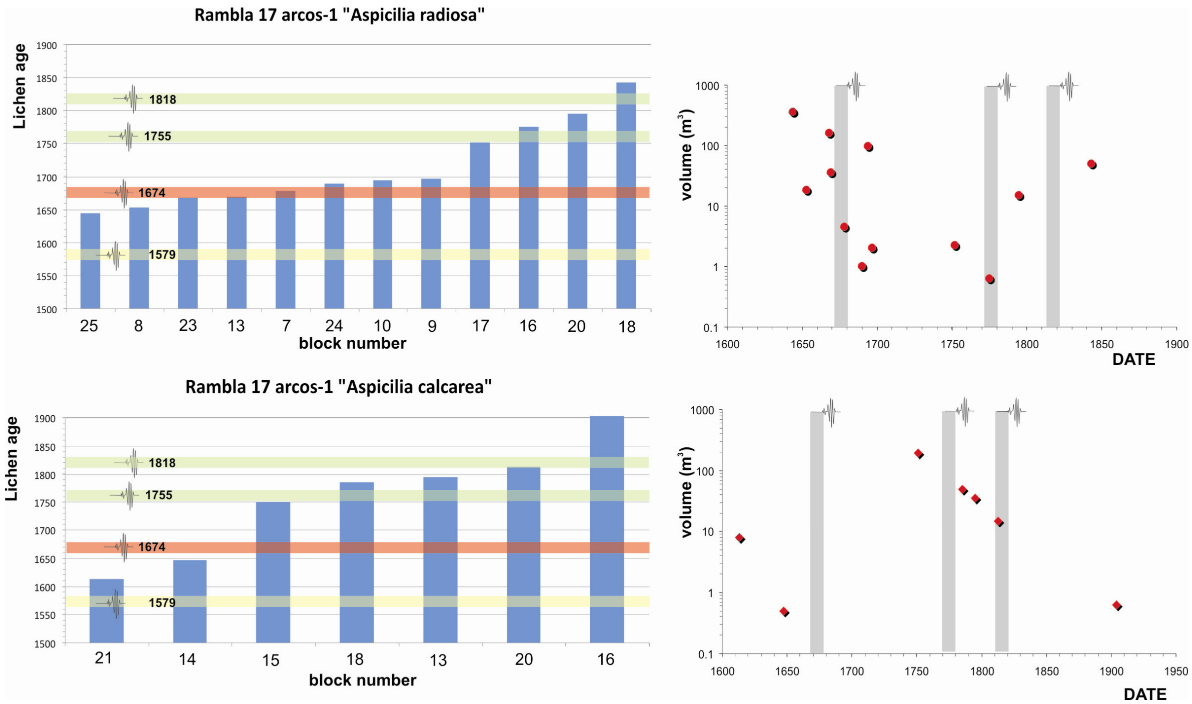

Fig. 3: Left: Lichenometric ages of several blocks in the Rambla de los 17 Arcos. Most of the blocks were mobilised around 1674, the date of the biggest earthquake ever recorded at Lorca. There is also evidence for the remobilisation of several blocks in 1755 (the great earthquake at Lisbon) and 1818. Right: Relationship between the volume of the block and the age of mobilisation. The 1674 earthquake mobilised the greatest number of rocks (1,000 m^3) and the 1755 and 1818 earthquakes lesser quantities. During the 2011 earthquake only 75 m^3 were mobilised. These volumes were obtained by direct measurement in the field.

References

Alfaro P., J. Delgado, F.J. García-Tortosa, L. Lenti, J.A. López, C. López-Casado, S. Martino. 2012. Widespread landslides induced by the Mw 5.1 earthquake of 11 May 2011 in Lorca, SE Spain. *Engineering Geology* 137-138, 40–52.

Bull, W.B. 1996. Dating San Andreas Fault earthquakes with lichenometry. *Geology* 24, 111-114.

Fink, B. 1917. The rate of growth and ecesis in lichens. *Mycologia* 9, 138–158.

Innes, J. L. 1985. Lichenometry. *Progress in Physical Geography* 9, 187-254.

Jomelli, V. Grancher, D. Naveau, P. Cooley, D. and Brunstein, D. 2007. Assessment study of lichenometric methods for dating surfaces. *Geomorphology* 86, 131-143.

Martínez-Solares, J.M. y Mezcua, J. 2002. *Catálogo sísmico de la Península Ibérica (880 a. C.-1900)*. Instituto Geográfico Nacional. Monografías nº 18. Madrid. 256p. in Spanish.

Muñoz-Clarés, M., M. Fernández-Carrascosa, M. O. Alcolea-López, M. C. Arcas-Navarro, N. Arcas-Ruiz, P. Caro del Vas, M. T. Cruz-López, M. García. 2012. Sismicidad histórica y documentación municipal: el caso de Lorca. *Boletín Geológico y Minero* 124, 415-429. In Spanish.

Pérez-López, R., M.A. Rodríguez-Pascua, P.G. Silva, J.L. Bischoff, L.A. Owen, J.L. Giner-Robles and Díez-Herrero, A. 2010a. Lichenometry dating of rock collapse related to the great Lisbon Earthquake (1755) at the SE part of Spain. *Geophysical Research Abstracts* 12, 2p.

Pérez-López, Raúl, Rodríguez-Pascua, Miguel A., Silva, Pablo G., Giner-Robles, Jorge L., Bischoff, James L. y Owen, Lewis A. 2010b. Determinación de la curva de crecimiento para “Aspicilia radiosa” aplicada en dataciones liquenométricas en caidas de bloques. In: Avances de la Geomorfología en España 2008-2010, XI Reunión Nacional de Geomorfología, libro de resúmenes. Solsona. In Spanish.

Pérez-López R., J.L. Giner-Robles, M.A. Rodríguez-Pascua, F. Martín-González, J. García Mayordomo, J.A. Álvarez-Gómez, M. Rodríguez-Peces, J.M. Insua-Álvarez, J. J. Martínez-Díaz and Silva, P.G. 2011. Testing Archaeoseismological techniques with instrumental seismic data caused by the Mw 5.1 Lorca Earthquake (11-5-2011, SE of Spain). In: *2nd INQUA-IGCP-567 International Workshop on Active Tectonics, Earthquake Geology, Archaeology and Engineering*. Abstract Volume 1, 10-14. Corinth, Greece.

Pérez-López, R., J.J. Martínez-Díaz, M.A. Rodríguez-Pascua y F. Martín-González. 2012. Análisis de sismicidad histórica en Lorca mediante liquenometría aplicada a caídas de bloques: los terremotos de 1579 AD, 1674AD y 2011. *Geotemas* 13 pp. 470.

Proctor, M. C. F. 1977. The growth curve of the crustose lichen Buellia canescens (Dicks.) de Not. *New Phytologist* 79, 659–663.

PALEOSEISMOLOGY & ARCHAEOSEISMOLOGY
MORELIA • MEXICO 2012
INQUA-TERPRO PALEOSEISMOLOGY
EARTHQUAKE ARCHAEOLOGY

APPLICATION OF THE ESI SCALE: : CASE STUDY OF THE FEBRUARY 4, 1976 GUATEMALA EARTHQUAKE

Porfido Sabina (1), Esposito, Eliana (2), Spiga, Efisio (3), Mazzola, Salvatore (4)

(1) IAMC – CNR, National Research Council, Napoli, ITALY. sabina.porfido@iamc.cnr.it
(2) IAMC – CNR, National Research Council, Napoli, ITALY. eliana.esposito@iamc.cnr.it
(3) Geologist, Avellino, ITALY. spiga.efisio@gmail.com
(4) IAMC – CNR, National Research Council, Napoli, ITALY. salvatore.mazzola@iamc.cnr.it

Abstract (Application of the ESI Scale: Case study of the February 4, 1976 Guatemala earthquake): *The ESI 2007 scale is applied to February 4,1976 disastrous earthquakes, which occurred in Guatemala along the boundary between the North American and Caribbean plates. For this earthquake, the available seismic, geological and macroseismic data have been reviewed and integrated through an updated interpretation of the original scientific papers written immediately after the event. A large number of ground seismic effects were catalogued including primary effects (surface faults) and secondary effects such as hydrological changes and tsunami, liquefaction features, ground cracks, ground settlements and landslides. The cataloguing and analysis of the seismically induced environmental effects has provided (a) a more detailed picture of the macroseismic fields, (b) I_0 estimates based on ESI 2007 scale (c) useful data for seismic zonation. These results have confirmed once more the essential role of ESI 2007 Scale in the process of seismic hazard assessment and risk reduction.*

Key words: *1976 Guatemala earthquake, ESI 2007, natural hazards, ground effect.*

INTRODUCTION

For the Guatemala 1976 earthquake, the original scientific descriptions have been reviewed in order to highlight effects on natural environment. This process has detected and localized coseismic environmental effects, and classifies them into six main types: surface faulting (SF), slope movements (SM), ground cracks (GC), ground settlements (GS), hydrological changes (HC) and tsunami (TS). The quantitative and qualitative information on environmental effects has been collected in a database in order to assess the epicentral intensity I_0 with the new macroseismic scale: the ESI 2007 scale (Michetti et al.2007), for a more accurate evaluation of the earthquake.

Tectonic setting

The tectonics of Central America are particularly complex, with the interaction of three major tectonic plates on their boundaries : the Cocos, the Caribbean and the North American plates. In this region relative plate motions vary between 2-9 cm=yr and are accompanied by active volcanism and shallow and intermediate seismicity. According to Benito et al. (2012), the seismicity has been associated with different zones: surface seismicity (h ≤ 25 km, 6≤M≤8) to crustal zones, intermediate seismicity (25 km < h ≤ 60 km, 6.8≤M≤8.2) to interface zones, and deep seismicity (h > 60 km, 6.2≤M≤8.2) to in-slab zones, taking into account tectonic, seismic criteria and regional seismogenic zonation.
The largest earthquakes are produced by the slab zone of the Cocos and Caribbean plates in the Middle America Trench situated in the Pacific Ocean. Large earthquakes are also produced along the boundary between the North American and the Caribbean plates, defined by a zone of large left lateral strike–slip faults that run through Guatemala from the Swan Fracture Zone in the Caribbean Sea. The earthquakes generated along these transcurrent faults, although less frequent, have a great importance to seismic hazard in Central America (Guatemala, Honduras, Belize, Mexico) more than the subduction earthquakes, because of their shallow ipocentre and the proximity of many cities and villages to these active faults. The most destructive event in this region was the earthquake associated with the Motagua fault, occurred on 4 February 1976, Ms = 7.5, causing 23 000 deaths in Guatemala.

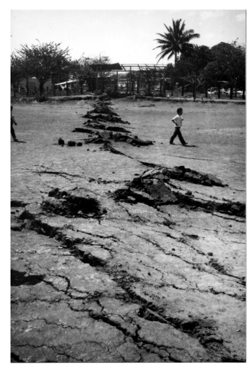

Fig. 1: The 1976 Guatemala earthquake : Gualan, football field: "mole tracks" along the left lateral Motagua fault (Earth. Inf. Bull. N.94, USGS)

Earthquakes and ground effects in Guatemala

For the Guatemala have been collected the macroseismic data of historical earthquakes that triggered large coseismic environmental effects since 1541 (Table 1). There are at least 18 events, with 5.6≤M≤7.9 that induced mostly slope movements (77,7%

of events), followed by ground cracks, ground settlements, hydrological changes, topographic changes, tsunamis and in some cases surface faults. The most damaging were the 1902 (M=7.5), 1942 (M=7.9) and 1976 (M=7.5) earthquakes.

1902-04-19 earthquakes.: Landslides and ground fractures reported within the epicentral area. Enormous slope movement dammed the Naranjo and Ixtacapa Rivers; in Ocos liquefaction and settlement phenomena. Landslides and ground fissures were in Sololà and on the Atitlàn, Agua and Cerro Quemado volcanoes (Ambraseys & Adams 1996; Bommer &. Rodrıguez 2002).

DATE	M	Effects
1541-09-09	-	SM
1585/1586	-	SM,GC
1773-07-29	-	SM,GC
1816	-	SM
1855-01-12	-	SM
1863-12-12	-	GC, HC
1874-03-09	-	TC
1885-12-18	-	GC,HC
1902-04-19	7.5	GS,GC,SM
1915-09-09	7.8	GC, SM
1917-12-26	5.9	SM,GS
1917-12-29	5.6	SM
1942-08-06	7.9	GC,GS, SM
1945-08-10	5.9	SM
1950-10-23	7.2	TS
1976-02-04	7.5	F, GC, GS, HC, SM, TS
1991-09-18	6.1	SM
1993-09-10	7.3	SM

Table 1. Characteristics of Guatemala effects-inducing earthquakes since 1541. F = Fault; GC =Ground Cracks; GS= Ground settlements; HC= Hydrological Changes; SM=slope Movement; TC = Topographic Changes; TS= Tsunami (Sources: Espinosa, (Ed.) 1976, Harp et al., 1981, Ambraseys & Adams 1996; Bommer &. Rodrıguez 2002.

1942-08-06 earthquakes: Many landslides and destruction along the west-central highlands in Guatemala. Slope movements affected also the Pan-American highway and secondary roads. Many settlements, especially in the western Pacific coast region (Ambraseys & Adams 1996; Bommer &. Rodrıguez 2002).

1976-02-04 earthquakes: A left-lateral surface break of the Motagua fault, 230 km long, with maximum horizontal slippage of 325 cm. Widespread landsliding within epicentral area, affecting roads and damming rivers. High concentration of slope movement was along Motagua, Pixcaya´, Las Vacas and Los Chocoyos Rivers. Lateral spreads and liquefaction in the Motagua valley along Atlantic coast of Guatemala and Honduras. The shock caused also a tsunami in the Gulf of Honduras with a maximum amplitude of 45 cm (Espinosa, (Ed.) 1976; Harp et al., 1981; Ambraseys & Adams 1996; Bommer &. Rodrıguez 2002)

The February 4, 1976 Guatemala earthquake

In the morning of February 4,1976 an earthquake of M 7.5, devastated a large areas of Guatemala. The epicentre was located near Los Amates about 157 km NE of Guatemala City. It was associated with a left-lateral slippage on the Motagua fault and was felt over an area of at least 100,000 km^2. The shock was strongly felt in Chiapas and in El Salvador, as well as in Honduras, Belize, and as far away as Mexico City, 1000 km from the epicentral area. Thousands of aftershocks followed the main event, delineating the Motagua fault and several secondary north-south faults (Mixco faults) near Guatemala City.

There were 22,870 deaths and 77 200 injuries. The total number of houses destroyed was 258 000, and 1.2 million people were left homeless. The maximum estimated Modified Mercalli (MM) intensity was IX in Gualan, in the Mixco area and in the centre of Guatemala City (Espinosa et al, 1976). The intensities were understimated despite there was high level of damages, infact several towns and villages were totally destroyed (100% of houses) such as Cabafias, Comalapa, Gualan, El Jicaro, Joybal Morazan, Parramos, Patzicia, El Progreso, Rabinal, San Andreas Itzapa, San Jose Poaquie, Progreso Cabecera, San Martin Jilotepeque, etc and although the earthquake triggered very large primary and secondary effects.

Main surface fault and secondary surface faults

Detailed studies indicate that the length of the main surface fault, a strike-slip, was 230 km and that the main break from relocated epicenter data was 270 km. The main fault was identified in the Motagua Valley and the mountainous area west of the valley, from Quebradas to Patzaj. Maximum horizontal displacement was 325 cm with an average value of about 100 cm.

The fault trace was a well-defined linear zone with strike from N.65° E. to N. 80° W. It was a right-stepping en echelon fractures and connecting low compressional ridges that locally formed the "mole tracks" that are characteristic of strike-slip faults, Fig. 1 (Plafker et al,1976). Secondary faults were observed in the Mixco area, in the western part of Guatemala City, and in the area between those cities, Fig.2. The total length of the Mixco faults was about 10 km. Maximum displacement was about 12 cm vertical slip combined with 5 cm of right slip, or about 13 cm of oblique slip (Plafker et al,1976).

Secondary effects

The1976 Guatemala earthquake triggered a very great number of secondary effects on the natural environment,

Locality	Rock type	Slide type	Volume (V), m^3	Notes
Los Chocoyos	Pumice/tefra	block slide/ rock-fall avalanche	$10^6 > V > 0{,}75*10^6$	7 victims
San José Poaquil	Dark tuff /pumice	Complex block slide/rotational slump/rock-fall/avalanche.	$V > 3.5*10^6$	Temporary lake
San Martin Jilotepeque	Pumice/tuff	Complex rotational slump/ earthflow	$V > 10^6$	17 victims ; 14 houses destroyed; temporary lake; lateral spread ;
Estancia de la Virgen	andesitic volcanic rocks	Rotational slump/rock-fall avalanche	$V > 6*10^6$	13 victims, temporary lake
Rio Polima	andesitic volcanic rocks/ pumice	Block slides	$V > 0{,}2*10^6$	temporary lake
Rio Naranjo	pumice	rotational slump	$V > 0{,}3*10^6$	
Rio Blanco	andesitic volcanic rocks/ pumice	Complex rock-fall/avalanche	$V > 0{,}2*10^6$	temporary lake
Rio Ruyalché	andesitic volcanic rocks / pumice	Rotational slump	$V > 0{,}5*10^6$	
Rio Cotzibal	andesitic volcanic rocks	Rotational slump	$V > 0{,}3*10^6$	temporary lake
Rio Teocinte	andesitic volcanic rocks	Rotational slump / rock-fall avalanche	$0{,}5*10^6 > V > 0{,}3*10^6$	temporary lake
Rio Los Cubes	Metamorphic rocks	rock-fall/avalanche	$V > 0{,}1*10^6$	temporary lake

Table 2.The eleven large landslides triggered by the Guatemala, 1976 earthquake (Modified from Harp et al.1981)

such as slope movements, ground cracks, ground settlements, hydrological changes and tsunami. The event induced over all landslides, thousands of slides throughout a broad region of central Guatemala parallel to the main fault Fig.2. The types of slope movements were mainly rock falls, debris slides, and flows involving thick pumiceous pyroclastic rocks, but they also included slides of consolidated bedrock, mostly from small to moderate-size (≤ 15,000 m^3) and in some cases large size (several million m^3 of material), (Harp et al. 1981).
They blocked many roads, damaged structures, and damming river. Eleven large landslides (V≥ 100,000 m^3) induced by the earthquake are described briefly in Table 2. According to Harp et al, 1981, the total area affected by landslides was 16.000 km^2 extends from Quebradas on the E to Quezaltenango on the W and from Lago Amatitlan on the S to Sacapulas on the N, Fig.2. Lateral spreads and liquefaction occurred in the Motagua valley, along Atlantic coast of Guatemala and Honduras, and along some lake shores in the highlands (Lake Amatitlan). Extension cracking and settlements accompanied the spreading of these areas. The shock caused a tsunami recorded in Puerto Cortes with a maximum amplitude of 45 cm, Fig.2. The earthquake caused some hydrological changes in hot-springs and according to Ambraseys and Adams, 1996 caused also fluctuations in well-water levels in Georgia, Idaho, Indiana and Wisconsin.

Conclusions

The review of the effects on the natural environment triggered by the 1976 Guatemala earthquake has allowed estimation of epicentral intensity I_0 values independently from the damage effects on the built area. According to the ESI scale 2007, the surface faulting parameter, MSF= 230 km and MD=325 cm and the total areal distribution of secondary effects equal to 18 000 km^2 , Fig.2, (area of slope movements=16 000 km^2, plus the area of ground cracks and ground settlements = 2 000 km^2) indicate I_0 = XI, a value more realistic respect the intensity IX MM assessed by Espinosa e al.1976.
In conclusion it is important underline the rule played by environmental effects on the seismic hazard evaluation, for the national and regional zonation. However, for a correct land planning is fundamental to keep in mind the active faults' role (Motagua and Mixco faults), and the total area of secondary effects) that affected large area of the territory (about 1/6 of the Guatemala territory). This event confirm once again the relevance of earthquake environmental effects as a major source of hazard, in addition to vibratory ground motion. Moreover, it has been clearly demonstrated that the implementation of geologically documented past earthquakes in the existing seismic catalogues is crucial for the improvement of the seismic and tsunami hazard knowledge, as well as for a more rational urban development and location of critical engineering facilities (Esposito et al. 2009; Lekkas et al. 2008 ;Porfido et al. 2007; Reicherter et al.(Eds) 2009; Serva et al.2007).

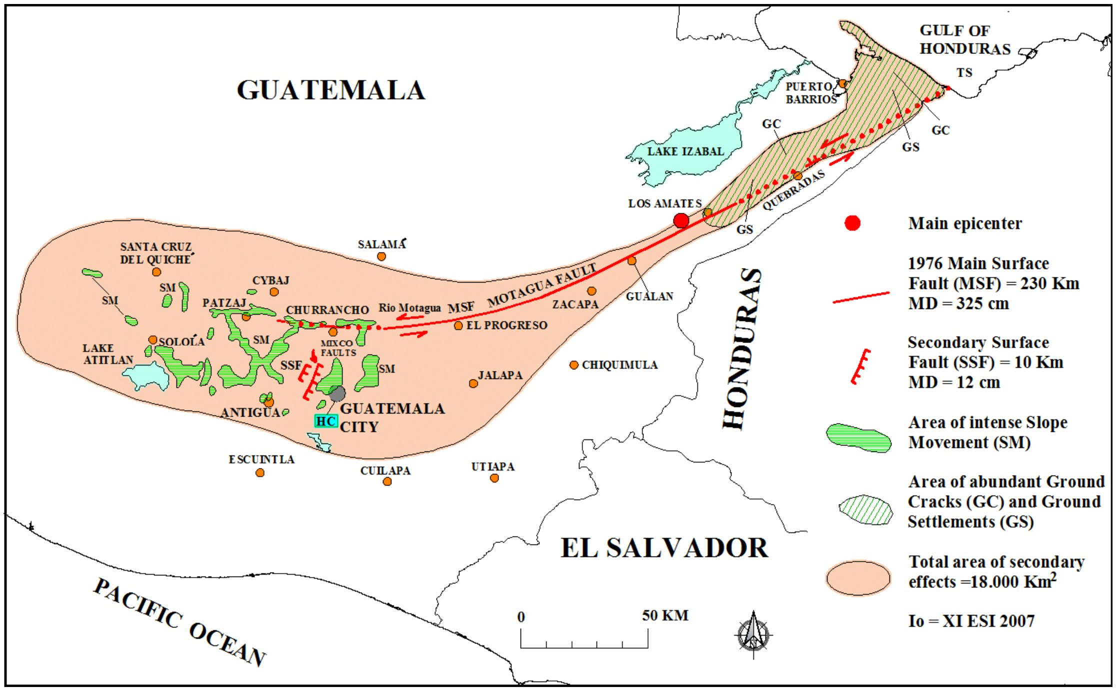

Fig.2 Map showing main epicenter, main surface fault (MSF), secondary surface faults (SSF), area of intense slope movement (SM), area of abundant ground cracks (GC),ground settlements (GS), hydrological changes(HC), tsunami (TS) and the total area of secondary effects of the 1976, Guatemala earthquake (Modified from Plafker et al. 1976 and from Harp et al. 1981).

References

Ambraseys, N.N., Adams, R.D., 1996. Large-magnitude Central American earthquakes, 1898– 1994. *Geophysical Journal International* 127, 665– 692.

Benito M. B., C. Lindholm E., Camacho et al,. 2112. A New Evaluation of Seismic Hazard for the Central America Region. Bull. Seismol. Soc. of America, Vol. 102, No. 2, pp. 504–523

Espinosa A.F. (Ed.), 1976. The Guatemala Earthquake of February4, 1976: A Preliminary Report. *USGS P. P. 1002.*

Espinosa A.F., Husid R., Quesada A., 1976. Intensity and source parameters from filed observations. The Guatemalan Earthquake of February 4, 1976. *USGS P. P. 1002, 52– 66.*

Esposito E., Pece R., Porfido S., Tranfaglia G., 2009. Ground effects and hydrological changes in the Southern Apennines (Italy) in response to the 23 July 1930 earthquake (MS=6.7). *Nat. Hazards Earth Syst. Sci.,9, 539-550.*

Harp E.L., Wilson R.C., Wieczorek G.F., 1981. Landslides from the February 4, 1976, Guatemala earthquake. *USGS Professional Paper, 1204 A.*

Lekkas E.L., I. D. Papanikolaou, D.I. Papanikolaouand Danamos G., 2008. Correlating the damage pattern and the geological structure. Local site effects from the 2006 MW=6.7 KYTHIRA island intermediate depth event, SW Greece. The 14th World Conf. Earth. Eng. October, 2008, Beijing, China

Michetti A.M., Esposito E., Guerrieri L., Porfido S., Serva L., Tatevossian R., Vittori E., Audemard F., Azuma T., Clague J., Comerci V., Gurpinar A., Mc Calpin J., Mohammadioun B., Morner N.A., Ota Y. & Roghozin E., 2007. Intensity Scale ESI 2007. *Memorie Descrittive Carta Geologica. d'Italia*, vol. 74, Servizio Geologico d'Italia –APAT, Roma, 53 pp.

Plafker G., Bonilla M.G., Bonis S.B., 1976. Geologic effects. The Guatemalan Earthquake of February 4, 1976. *USGS Professional Paper 1002, 38– 51.*

Porfido S., Esposito E., Vittori E., Tranfaglia G., Guerrieri L., Pece R. (2007). Seismically induced ground effects of the 1805, 1930 and 1980 earthquakes in the Southern Apennines (Italy). *Boll.Soc.Geol.It. (Ital .J. Geosci.), 126, 2* , pp. 333-346.

Reicherter K., Michetti A., P.G. Silva (eds.), 2009. Palaeoseismology: Historical and Prehistorical Records of Earthquake Ground Effects for Seismic Hazard Assessment. *Geological Society of London, Special Publications, 316. London, U.K. Publ., 316, 55-71.*

Serva L., Esposito E., Guerrieri L., Porfido S., Vittori E., Comerci V. 2007. Environmental effects from five hystorical earthquakes in Southern Apennines (Italy) and macroseismic intensity assessment: Contribution to INQUA EEE Scale Project. *Quaternary Int., 173-174, 30-44.*

PALEOSEISMOLOGY & ARCHAEOSEISMOLOGY
MORELIA • MEXICO 2012
INQUA-TERPRO PALAEOSEISMOLOGY
EARTHQUAKE ARCHAEOLOGY

FROM THE PRESENT TO THE PAST: DAMAGED BUILDINGS AND STRUCTURES AS SEISMOSCOPES

Reicherter, Klaus (1)

(1) RWTH Aachen University, Inst. of Neotectonics and Natural Hazards, Lochnerstr. 4-20, 52056 Aachen, Germany.
k.reicherter@nug.rwth-aachen.de

Abstract (From the present to the past: damaged buildings and structures as seismoscopes): *In this preliminary study structural damage is described including several examples from recent earthquakes all over the world, and is compared to damage caused by slow processes like creep and subsidence. Earthquake archaeological effects (EAE) are presently used widely to delineate ancient or pre-historical earthquakes, especially in areas of recent seismic quiescence or lack of historically documented earthquake shocks. However, it is absolutely necessary to analyze the finite deformation image in terms of multi-event destruction, where "event" may also cover and include other processes. Furthermore, because structural damages are confined to human settlings, which are probably wide spread in Europe since at least Roman times, other information like earthquake environmental effects have to be regarded and carefully related to earthquake geology and palaeoseismicity. The last earthquakes in central Europe and Iran of M ≤ 6 in 2012 showed that the deformation pattern observed in buildings and other structures almost show identical patterns as observed in slow deformation processes. This finding complicates the evaluation of EAE in terms of assigning a palaeo-magnitude or palaeo-intensity to the observed building damage due to moderate earthquakes (M ≤ 6.5), post-seismic changes and modification may lead to an overestimation.*

Key words*: archaeoseismology, palaeoseismicity, deformation of building structures, final deformation image*

INTRODUCTION

Pre-historic and historic damage in man-made structures and buildings are often used in archaeology, history and archaeoseismology to delineate the causes of damage. The causes are manifold and are partly of anthropogenic origin or the consequence of anthropogenic action. The other portions are made up of geological, geophysical and climatic causative processes, including extremes and long-term changes, and site-dependent side effects. Deciphering a finite damage image in terms of individual events causing deformation and the temporal consecutive sequence of those are of major interest, especially this is important in areas, where the earthquake catalogues or climate registrations are not complete with respect to covering at least one seismic cycle of the fault or fault system (e.g., the last two seismic events).

The finite damage image gets even more complex, when subsequent events are closely followed by each other or in cascading hazards. Examples for this are provided by the two Christchurch earthquakes in 2010 and 2011, the two shocks in northern Italy in May 2012, or by cascading hazards, like earthquake, flooding or fires, and anthropogenic modification, which may be not separable or overestimated (following e.g., the EAE scale after Rodriguez-Pascua et al., 2011).

Also in areas with little population density during ancient times, or unfortified low-quality buildings EAE have to be applied with great caution.

The backstripping or retrodeformation and the accurate dating and deformation determination of the single steps of the finite damage image may yield clues on the participation of damaging earthquakes. We are still in the beginning of distinguishing different types of deformation and relate them to single events.

Fig. 1: Cracks in the town hall of the medieval city of Staufen/Breisgau, Germany. Note the cracks is following the rock.framed window.

CASE STUDIES

For a first but incomplete assessment of deformation related to slow creep and subsidence, several deformed structures in Staufen/Germany and in Venice/Italy have been studied. These are compared to damage caused by recent earthquakes in Italy (Pianura Padana earthquakes in May, 2012) and Iran (August, 12th, 2012), and evaluated with respect to archaeoseismological studies in Spain and Greece.

Staufen/Breisgau (Upper Rhine Graben, Germany)
Staufen is a little medieval town in southern Germany located on the eastern margin of the tectonically active southern Upper Rhine Graben. Staufen is situated on Mesozoic rocks, which are fault-bound and tilted in a domino-style. Mesozoic rocks include claystones, sandstones and anhydrite/gypsum of Triassic age (Keuper). During geothermal drilling (7 wells of around 140 m depth) in 2007 and later exploitation water intruded in anhydrite layers, which changed to gypsum, and into expanding clays. Partly, a volumetric gain of these layers of up to 60% occurred during this. As a result differential uplift happened under the town centre near the town hall on the order of 11 mm/month. Today, uplift is slowing down but still ongoing. Technical improvements stopped more or less the expansion, rates in March 2012 were still 4 mm/month. In total, locally uplift is larger than 260 mm since 2007 (Sass and Burbaum, 2010).
The damage observed in Staufen is regarded as slow and ongoing "creeping" damage and not fault-related but confined to the area of the wells. It lead to extensional and rotational cracks (Fig. 1), most of the cracks follow mortar joints or cut stone around windows and doors (mainly of the Buntsandstein or Bunter of Triassic age). Partly arch-like structures are compressed and shortened.

Venice (Italy)
The lagoon of Venice has been settled since Medieval times, and since then subject to subsidence. Another factor is provided by sea level rise in the last centuries,

Fig. 2: Bell tower of San Pietro Apostolo, Venice, Italy

both account for approx. 25 cm relative sea level rise only in the 20th century (50% subsidence, 50% sea level rise). The differential subsidence leads to structural damage, especially when the construction is relatively heavy (churches, towers, large buildings). Subsidence leads to cracks, tilted towers (Fig. 2), and other peculiar deformation.

Recent earthquake damage: Italy, Iran, China and others
Examples of structural damage from recent earthquakes are manifold and strongly dependent on the type of material used (economic and historical values) and ground amplification. All those earthquakes have in common that the magnitude did not exceed 6. Damage observed in the structures partly resembles that of "slow" deformation. Other damages are complete collapses of structures, including new constructions. However, the effects of afterslip or postseismic modifications have not been taken into account. As in the May, 20th and 29th, 2012 earthquake in Northern Italy (Finale Emilia), sackungen and liquefaction led to differential ground

Fig. 3: Damaged family house in San Antonio in Mercadello, Roverto, Italy, Pianura Padana May, 2012 (from: INGV, 2012)

settling (Fig. 3), the resulting cracks point to mortar-joint parallel deformation patterns.

Olympia, Dionysus and Samicum (Greece)
The ancient Olympia on the western Peloponnese/Greece is worldwide known as the place of the classical Olympic Games. The domino-like toppled column drums of the Zeus temple are famous and widely accepted as earthquake-related structural damage of an unknown not precisely dated event(s) of the 6th cent. AD. However, there are more indicators as already outlined by Reicherter (2011), however, we have no exact map or dates for the destruction(s).
The fortified village of Samicum (Reicherter, 2011) is situated in the southern part of the Elis region, on top of the Lapithas mountain ridge, south of mouth of the Alfeios river. Most probably Samicum was founded in the last 5th cent. BC and was occupied until the 2nd cent. AD and later abandoned. The city wall and its blocks show various indicators of seismic damage. Among them are moved and rotated blocks, corner break-outs, and collapsed watch towers. Again, here we have no age for the deformation, but we attribute it preliminarily to one single deformation.

DISCUSSION

The evaluation of EAE in terms of assigning a palaeo-magnitude or palaeo-intensity to the observed building damage due to moderate earthquakes (M ≤ 6.5), post-seismic changes and modification may lead to an overestimation, and therefore needs and claims for other flanking methods and parameters to assign a better constrained assessment of the historical earthquakes, e.g. like the ESI-scale provides.

References

Carbognin, L., Teatini, P., Tomasin, A., Tosi, L., 2010. Global change and relative sea level rise at Venice: what impact in term of flooding. Clim. Dyn., 35, 1039-1047; doi: 10.1007/s00382-009-0617-5.

Grützner, C., Reicherter, K., Silva, P.G., 2010. Comparing semiquantitative logic trees for archeoseismology and paleoseismology: the Baelo Claudia (southern Spain) case study. GSA Spec. Vol. 471: 129-144.

Hinzen, K.-G., Schreiber, S., Fleischer, C., Reamer, S.K., Wiosna I., 21012. Archeoseismic study of damage in Roman and Medieval structures in the center of Cologne, Germany. J. Seismol., DOI 10.1007/s10950-012-9327-2.

INGV, 2012, last visited on 09/19/2012; foto of Fig. 3: http://www.flickr.com/photos/75528623@N07/7375116752

Jusseret, S., Sintubin, M., 2012 All That Rubble Leads to Trouble: Reassessing the Seismological Value of Archaeological Destruction Layers in Minoan Crete and Beyond. Seismol. Res. Lett., 83, 4, 736-742; doi: 10.1785/0220120011.

Reicherter, K., 2011. Frontiers of earthquake archaeology: The Olympia and Samicum cases (Peloponnese, Greece). 2nd INQUA-IGCP-567 International Workshop on Active Tectonics, Earthquake Geology, Archaeology and Engineering, Corinth, Greece (2011). pp. 194-197.

Reicherter, K., Schaub, A., Fernández-Steeger, T., Grützner, C., Kohlberger-Schaub, T., 2011. Aquisgrani terrae motus factus est (part 2): Evidence for medieval earthquake damage in the Aachen Cathedral (Germany). Quaternary International, doi:10.1016/j.quaint.2011.05.006.

Rodríguez-Pascua, M.A., Pérez-López, R., Giner-Robles, J.L., Silva, P.G., Garduño-Monroy, V.H., Reicherter, K., 2011. A comprehensive classification of Earthquake Archaeological Effects (EAE) in archaeoseismology: Application to ancient remains of Roman and Mesoamerican cultures. Quaternary International, doi:10.1016/j.quaint.2011.04.044.

Sass, I., Burbaum, U., 2010. Damage to the historic town of Staufen (Germany) caused by geothermal drillings through anhydrite-bearing formations. Acta Carsologica 39/2, 233–245, Postojna.

Silva, P.G., Reicherter, K., Grützner, C., Bardají, T., Lario, J., Goy, J.L., Zazo, C., Becker-Heidmann, P., 2009. Surface and subsurface paleoseismic records at the ancient Roman City of Baelo Claudia and the Bolonia Bay area, Cádiz (South Spain). In: Reicherter, K., Michetti, A.M., Silva, P.G. (eds.), 2009. Paleoseismology: Historical and prehistorical records of earthquake ground effects for seismic hazard assessment. J. Geol. Soc. London, Spec. Publ., 316: 93-121.

Tama, Y.S., 2012. Structural damages observed in state buildings after Simav/Tiurkey earthquake occurred on 19 May 2011. NHESS, 12, 2709-2718.

THE ACAMBAY EARTHQUAKE OF 1912, REVISITED 100 YEARS AFTER

Rodríguez-Pascua, Miguel A. (1), Garduño-Monroy, V.H.(2), Pérez-López, R. (1), Perucha-Atienza, M.A. (1), Israde-Alcántara, I.(2)

(1) Instituto Geológico y Minero de España. Madrid. SPAIN. ma.rodriguez@igme.es, r.perez@igme.es, ma.perucha@igme.es
(2) Instituto de Investigaciones Metalúrgicas. Universidad Michoacana de San Nicolás de Hidalgo. Morelia. MEXICO. vhgardunom@gmail.com; aisrade@gmail.com

Abstract: *The Acambay earthquake of 1912 was one of the most destructive intraplate earthquakes in the XX Century located in central Mexico. Urbina and Camacho, geologist and seismologist respectively, researchers of the Mexican Geological Survey made one of the most complete and interesting field reports about destructive earthquakes. These authors reported the geological and archaeoseismological effects in the macroseismic zone. All of these data are useful so far and this paper revisited the macroseismic zone 100 years after and apply modern structural analysis in order to obtain new vision of the real consequences and the spatial distribution of the effects.*

INTRODUCTION

The historical record of seismic events occurring in Mexico extends back, with major gaps, to the 16th century, whilst the instrumental record of seismicity beginning in 1910 (García-Acosta and Suárez-Reynoso, 1996). Due to these historical gaps, the paleoseismological study of numerous faults and lake systems in the Trans-Mexican Volcanic Belt (TMVB) has become an essential tool to improve the seismic catalogue.

The central part of the TMVB contains one of the most seismic active faults of Mexico: the E-W trending Morelia-Acambay Fault System (MAFS) (Suter et al., 1992, 2001). The tectonic activity of this fault determines the landscape (Ramírez-Herrera, 1998) and sedimentary evolution of several lacustrine basins in the surroundings, such as the Tierras Blancas Basin (TBB) (Rodríguez-Pascua et al., 2010). One of the most active faults of MAFS is the Acambay-Tixmadeje Fault (ATF), consisting of several E-W normal fault active segments, located in the northern region of the area (Fig. 1). This fault (ATF) exhibits geological evidence of recent seismic activity. For example, close to Acambay City (Fig.1), the northern zone of the area registered a destructive earthquake in 1912 (Ms = 6.9).

Urbina y Camacho (1913) located the epicenter and surface rupture caused by the first earthquake. Later, Langridge et al. (2000) mapped the active segment associated to this earthquake by using paleoseismological trenching techniques. This fault activity has generated soft-sediment deformation structures during the Quaternary: sand, silt and gravel dikes, pillows, mushrooms structures and decametric slumps disturbing the sedimentary infilling of the Tierras Blancas Basin in Acambay. From these seismites and their stratigraphic spatial correlation, five strong-moderate paleoearthquakes (E1-E5) have been established in the basin. The spatial distribution of these seismites exhibits a gradient of deformation defined by the intensity of deformation (Rodríguez-Pascua et al., 2010).

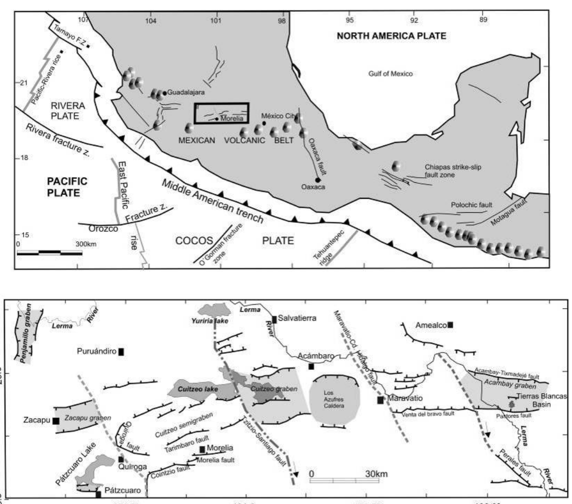

Fig. 1. A). Geographical and tectonic setting of the Morelia-Acambay fault system (black rectangle), located at the central part of the Mexican Volcanic Belt, Michoacan. B). Detailed location of the macroseismic zone of the 1912 Acambay earthquake (Acambay-Tixmadeje and Pastores faults). Several great E-W trending faults are observed bounding graben basins. All of these segments represent the Morelia Acambay Fault System.

MACROSEISMIC ZONE

The report of Urbina and Camacho (1913) of the 1912 Acambay earthquake includes a very interesting and complete information about seismic intensity (Calcany Scale), earthquake geological effects and oriented damages in the buildings. The original cartographical information of 1913 about the fault scarps was plotted over a topographical sketch. We have re-mapped the

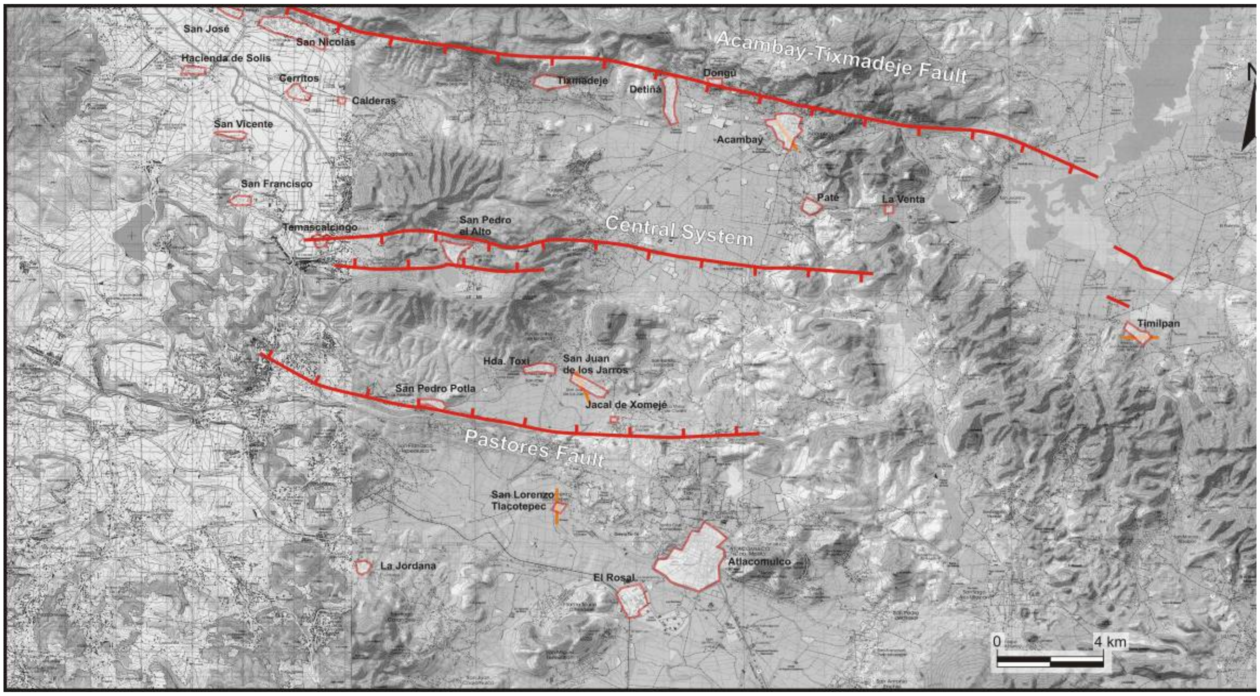

Fig. 2. Structural maping of the normal fault scarps created during the 1912 Acambay Earthquake mapped after Urbina y Camacho (1913).

fault scarps generated during the earthquake using the new official maps of Mexico (Fig. 2). For this objective we used the schematic map of Urbina and Camacho (1912), field work and geomorphologic criteria. In this map is possible distinguish the three main zones of fault scarps:

- Acambay-Tixmadeje Fault (north limit of the graben)
- The Central System (axial zone of the graben)
- Pastores Fault (south limit of the graben)

The macroseismic information compiled by Urbina and Camacho (1913) are synthesized in the figure 3 (Calcani Intensity). We drew the isoseismal areas using these data and the result (Fig. 3) sow two main areas. The north of the macroseismic zone has an area of intensity X parallel to the Acambay-Tixmadeje fault . The other area with intensity X is located between the Central System and the Pastores faults and conditioned by the direction NW-SE of the Lerma river and the soft sediments of the flood plain. This fact can imply that the Acambay earthquake was a composite earthquake associated with two normal faults of the composite graben of Acambay.

GEOLOGICAL EFFECTS, THE ESI07 SCALE

The descriptions of earthquake geological effects realized by Urbina and Camacho (1913) include a complete catalogue of structures. We applied the macroseismic scale ESI07 (Michetti et al., 2007) in order to obtain the spatial distribution of the earthquake geological effects and calculate de intensity ESI 07. The most important earthquake geological effects mapped in the figure 4 are: surface ruptures, soil cracking and fissures, permanently uplifted zones, liquefactions, rock falls and minor landslides, river-bank collapses, temporal changes of temperature and quality of springs and changes of location, water level and flow rate at springs and wells. The area affected by the earthquake was 750 km^2. All of these data and the extension and dimensions of the structures can assign to this earthquake a magnitude ESI07 of VIII-X.

Earthquake Archaeological Effects and geological structural analysis

Urbina and Camacho (1913) compiled an important amount of oriented damages in buildings. Several city maps with oriented deformation were publicised in the 1913 report: Acambay, Temascalcingo and San Andrés de Timilpan. Moreover, the complete photographical report has allowed us to oriented different Earthquake Archaeological Effects (EAEs, using the classification proposed by Rodríguez-Pascua et al., 2011) and revisited on the field these buildings after 100 years. Applying geological structural analysis to the EAEs (Giner et al., 2009) the result are trajectories of ground movement direction. These trajectories are perpendicular to the main faults and there are deviations in the NW and in the east of the macroseismic zone (Fig. 5).

The fault scarps mapped by Urbina and Camacho (1913) were revisited on the field in order to obtain structural

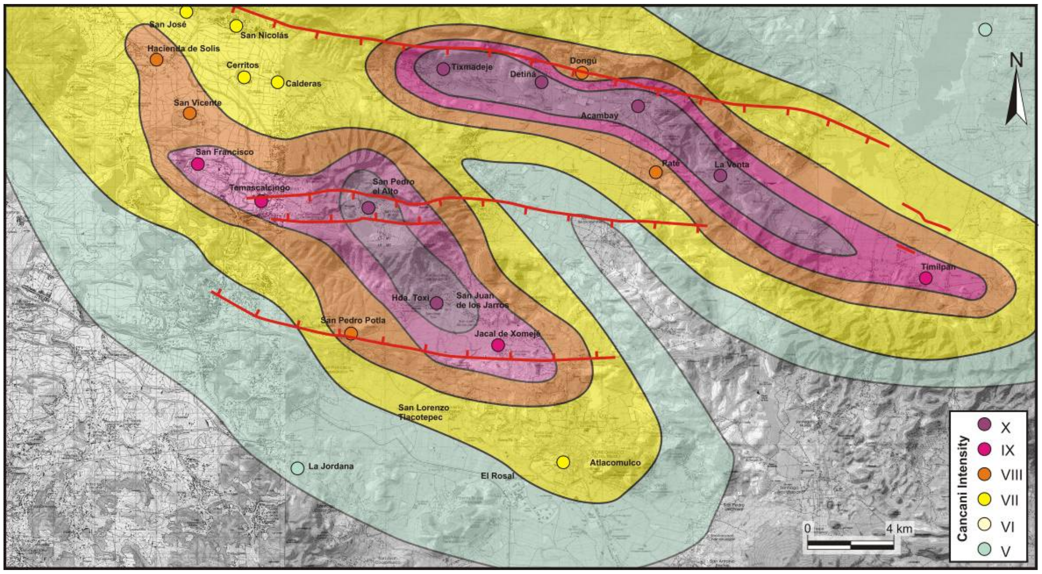

Fig. 3. Isoseismal map calculated using the intensity data (Calcani Intensity) of Urbina and Camacho (1913).

data of fault planes with slickenside. All of these data were analysed by techniques of fault population analysis, using the Right Diedra method for graphical representation. The results are that the interference figures of right diedra are normal fault with strike-slip component and a direction of extension N-S, parallel to the mean trajectories of ground movement generated by the Acambay earthquake of 1912.

Discussion and conclusions

The Acambay of 1912 earthquake was one of the more important intraplate earthquakes in Central Mexico (M =6.9). The distribution of the macroseismic intensities, the geological mapping of the fault scarps generated during the earthquake, the geological intensities ESI07 and the structural data show the characteristics of a composite earthquake. This event was generated by the complex graben of Acabay, composed by three different fault zones (Acambay-Tixmadeje, Central System and Pastores faults) with superficial fault scarps. The most important effects were generated by the Acambay-Tixmadeje fault and the Central System fault zone. The intensity of the ESI07 scale was VIII-X with important and destructive consequences in the towns of the macroseismic area. The archaeoseismological data show a direction of ground movement N-S, parallel to the maximum direction of extension, obtained by fault population analysis of the fault scarps.

Acknowledgements: This work was supported by the Mexican CONACYT Project: *Estudio Tectónico, de Paleosismología y de efectos sísmicos Arqueológicos en lagos del Holoceno y Actuales del Cinturón Volcánico Trasmexicano y del Bloque Jalisco*. This paper is a contribution of the Spanish working group on paleoseismology and archaeoseismology (QTEC) of AEQUA.

References

García-Acosta V., Suárez-Reynoso G., 1996. *Los sismos en la historia de México. Vol. Y: 450 años de documentos*. México FCE/CIESASUNAM. 718p.

Giner-Robles, J.L., Rodríguez-Pascua, M.A., Pérez-López, R., Silva, P.G., Bardají, T., Grützner, C. and Reicherter, K. 2009. *Structural Analysis of Earthquake Archaeological Effects (EAE): Baelo Claudia Examples (Cádiz, South Spain)*. Instituto Geológico y Minero de España. 130 pp.

Langridge, R.M., Weldon, R.J., Moya, J.C., Suárez, G., 2000. Paleoseismology of the 1912 Acambay earthquake and the Acambay-Tixmadejé fault, Trans-Mexican Volcanic Belt. *J. Geophys. Res*. 105 (B2), 3019-3037.

Michetti A.M., Esposito E., Guerrieri L., Porfido S., Serva L., Tatevossian R., Vittori E., Audemard F., Azuma T., Clague J., Comerci V., Gurpinar A., Mc Calpin J., Mohammadioun B., Morner N.A., Ota Y. and Roghozin E. 2007. Intensity Scale ESI 2007. En: Guerrieri L. & Vittori E. (Eds.): Memorie Descrittive Carta Geologica d'Italia., 74, Servizio Geologico d'Italia – Dipartimento Difesa del Suolo, APAT, Roma, 53 pp.

Ramírez-Herrera, M.T. 1998. Geomorphic assessment of active tectonics in the Acambay Graben, Mexican Volcanic Belt. *Earth Surface Processes and Landforms* 23, 317–332.

Rodríguez-Pascua, M.A., , Garduño-Monroy, V. H., Israde-Alcántara, I. and Pérez-López, R. 2010. Estimation of the paleoepicentral area from the spatial gradient of deformationin lacustrine seismites (Tierras Blancas Basin, Mexico). *Quaternary International* 219, 66–78.

Rodríguez-Pascua, M.A., Pérez-López, R., Silva, P.G., Giner-Robles, J.L., Garduño-Monroy, V.H., y Reicherter, K. 2011: A Comprehensive Classification of Earthquake Archaeological Effects (EAE) for Archaeoseismology, *Quaternary International* 242: 20-30.

Suter, M., López Martínez, M., Quintero Legorreta, O., Carrillo Martínez, M., 2001. Quaternary intra-arc in the central Trans-Mexican volcanic belt. *GSA Bulleting*. 113 (6), 693-703.

Urbina, F. y Camacho, H., 1913. La zona megaseismica Acambay – Tixmadege, estado de México, movida el 19 de noviembre de 1912. *Boletín del Instituto Geológico de México*. 32, 125 p.

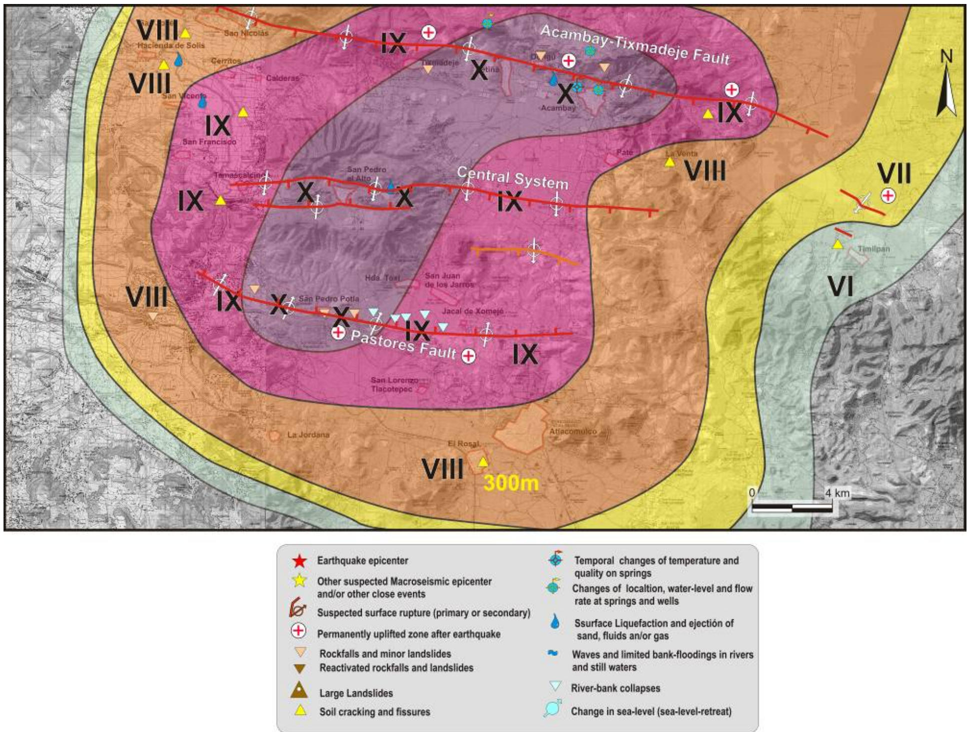

Fig. 4. Geological effects of the 1912 Acambay earthquake compiled from the report of Urbina and Camacho

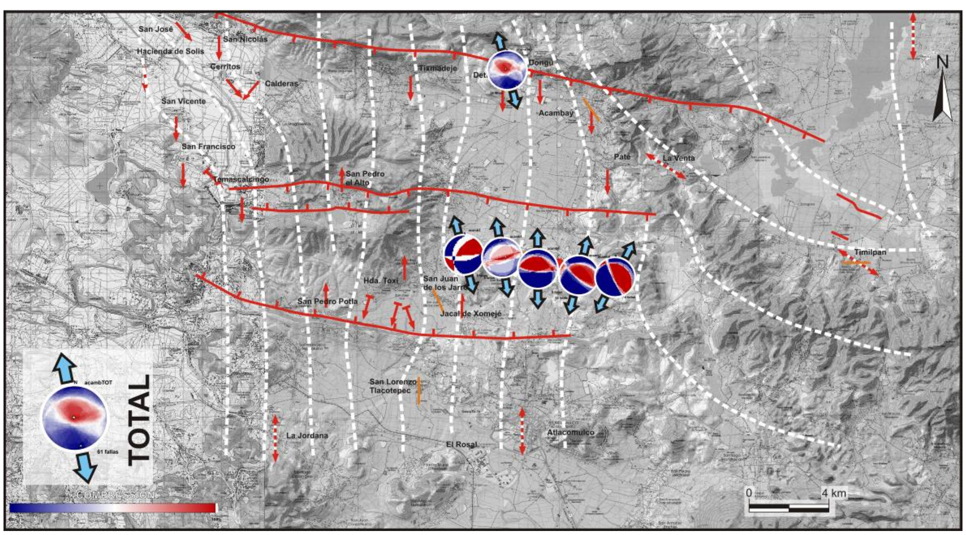

Fig. 5. Directions of ground movement generated by the 1912 Acambay earthquake. The red arrows are data take from Urbina and Camacho (1913) and the orange ones are field data revisited after 100 years. The white lines represents the mean trajenctories of ground movement generated during the 1912 earthquake. The right diedra representation are obtained from fault planes with slikensides.

PALEOSEISMOLOGY & ARCHAEOSEISMOLOGY
MORELIA • MEXICO 2012
INQUA-TERPRO PALEOSEISMOLOGY
EARTHQUAKE ARCHAEOLOGY

NEW AND REACTIVATED EFFECTS ON THE ARCHITECTURAL HERITAGE OF LORCA CAUSED BY THE EARTHQUAKE OF MAY 2011

Rodríguez-Pascua, Miguel A. (1), Pérez-López, Raúl (1), Martín-González, Fidel (2), Giner-Robles, Jorge L. (3), Silva, Pablo G. (4)

(1) Instituto Geológico y Minero de España. Madrid. SPAIN. ma.rodriguez@igme.es, r.perez@igme.es Dpto. Geología y Geoquímica,
(2) Área de Geología, ESCET, Universidad Rey Juan Carlos. Móstoles (Madrid). SPAIN. fidel.martin@urjc.es
(3) Facultad de Ciencias, Universidad Autónoma de Madrid. Madrid. SPAIN. jorge.giner@uam.es
(4) Dpto. Geología, Escuela Politécnica Superior de Ávila, Universidad Salamanca. Ávila. SPAIN. pgsilva@usal.es

***Abstract:** The earthquake of 11 May 2011 caused a series of structural deformations which affected the architectural heritage of the city of Lorca. We have classified and studied all these earthquake architectural effects (EAEs) according to the tenets of geological structural analysis to ascertain the direction of the movements responsible. We have furthermore identified two new EAEs which complete the previous classification. Accordingly, we were able to estimate the orientation of the maximum horizontal movement of the ground, which turned out to trend NW-SE on average. It was also clear that the deformations generated by the present earthquake shared very similar characteristics and even the same orientation of the maximum horizontal movement with those of the recorded earthquake of 1674. Most of these structures moved in a similar direction again during the 2011 earthquake, indicating that the Lorca-Totana segment of the Alhama de Murcia fault (FAM) triggered both and that both had similar values of seismic intensity, affected a very similar area and resulted in the same type of building damage and EAE orientation.*

***Key words:** earthquake architectural effects (EAEs); Lorca earthquake; reactivated EAEs; structural geological analysis; oriented seismic deformations.*

INTRODUCTION

The seismic series of Lorca on 11 May 2011 began at 15:05 UTC (local time 17:05) with an earthquake of Mw = 4.6 at 2 km in depth. At 16:47 UTC the main earthquake of Mw = 5.2 took place at a depth of 3 km and 0.41 g of ground peak acceleration (http//www.ign.es), which caused serious damage in Lorca. The second earthquake resulted in the death of 9 people and injuries to 324 as well as leaving 20,000 homeless. The epicentre was located at the NE of the city of Lorca, very close to the Alhama de Murcia fault (FAM) (Martínez-Díaz et al., 2011, 2012). This trace of the FAM is known as the Lorca-Totana segment fault and was responsible for this earthquake. The earthquake generated different deformations affecting the architectural heritage of the city. In consequence we have collected the data concerning the earthquake architectural effects (EAEs) to the historic buildings using the classification proposed by Rodríguez-Pascua et al. (2011). This classification was created for use in archaeological sites and historic buildings to distinguish seismic effects from other causes. The geological tool used for this purpose was the analysis of seismic strain structures. All of these deformational structures have been classified and studied according to the tenets of geological structural analysis to estimate the orientation of the maximum horizontal movement of the ground. The initial hypothesis requires that most of the seismic damage must be oriented in relation to the seismic ground movement, and this allows us to compare oriented seismic data with unoriented non-seismic damage (Fig. 1).

THE 2011 LORCA EAES

We recorded and compiled 127 EAEs obtained in 64 buildings affected by the earthquake in the historic centre of Lorca (Giner-Robles et al., 2012), where the streets still follow the same unoriented winding pattern as they did in Islamic times, unlike that of the Roman grid system. This lack of ordered orientation does in fact help our geological structural analysis in that it is not conditioned by the previous orientation of the streets. EAEs are classified on the basis of co-seismic, or primary, effects, which can be divided into geological effects (i.e. rock falls) and damage to the building fabric (i.e. collapsed walls). This classification contains strain structures that are susceptible to analysis by classical techniques in structural geology. Therefore, it is possible to study both the kinematic and dynamic seismic

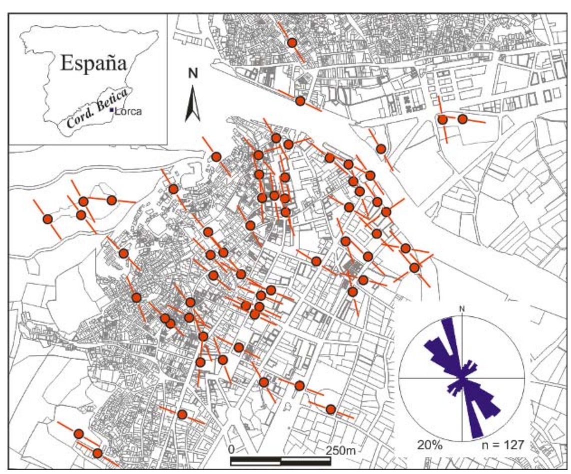

Fig. 1: Geographical setting of the epicentral area of the Lorca Earthquake (Mw=5.2), Spain (2011/05/11). Map of Lorca city centre, showing the sites of 64 buildings with EAEs (red dots) used to calculate the direction of the substrate movement. Red lines mark the general direction of movement for each building. The rose of directions shows the total values for the directions of motion calculated for the EAEs (upper left). This direction is parallel to the motion of a theoretical particle removed from the accelerogram located in Lorca by IGN.

behaviour of historic buildings. The EAEs work as a control group of seismic strength structures in that they indicate the present and future seismic behaviour of a historic building. The geological EAEs summarized in this work are: rock fall; fractures, folds and pop-ups on regular pavements and substratum compacting of artificial detrital infill (Fig. 2). The effects to the building fabric in Lorca were: shock breakout in flagstones; folded and tilted walls; penetrative fractures in masonry blocks; conjugated fractures in brick walls; fallen and oriented columns and impact marks; rotated and displaced masonry blocks in walls and drums in columns; displaced masonry blocks; fallen and pop up key stones in arches or lintels in windows and doors (Fig. 3); folded steps and kerbs; collapsed walls; collapsed vaults and dipping broken corners. After the geological structural analysis of these strain structures, we arrived at a congruent solution for all the EAEs. The average direction of ground movement generated by the 2011 earthquake was NW-SE (Fig. 1). Therefore, the seismic effects in buildings were oriented in this direction and this criterion can be used in archaeological sites to identify ancient earthquakes and distinguish them from non-seismic effects in the ruins. The 2011 Lorca earthquake has corroborated this approach, developed in archaeological sites damaged by earthquakes with no seismological data (Giner-Robles, et al., 2009 and 2012).

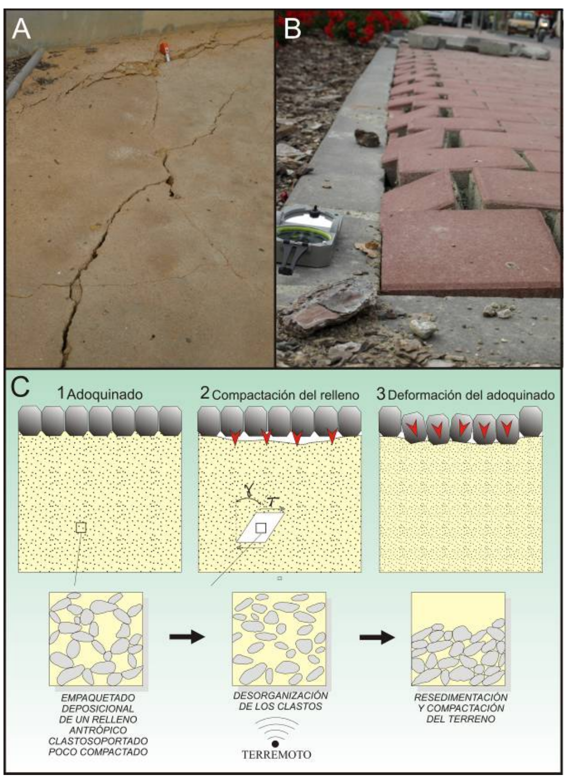

Fig. 2: Seismic compaction of anthropic infillings in dry conditions: A) subsidence of 16 cm in artificial infillings in Santa Clara Street at its junction with Juan Carlos I Street; B) fold in paving stones related to seismic compaction in the Las Clarisas monastery; C) sketch of the origin of seismic compaction in dry conditions.

Fig. 3: Pop up of the key stones generated by cyclic shear stress without vertical load of the roof; the direction of the arch is N155ºE. Consolidated ruins of the Santa Maria church.

EAES GENERATED BY THE 1674 EARTHQUAKE AND REACTIVATED BY THE 2011 EARTHQUAKE

The EAEs produced by the historic earthquake of 1674 (Martínez Guevara, 1984) are still visible in Lorca, in the Collegiate Church and City Hall, for example. Our work has been focused upon the effects in the Collegiate Church because information concerning the earlier earthquake is available in the municipal historic archives. The 1674 earthquake (N055ºE) displaced masonry blocks in the walls of the main nave; the shear direction of this movement was perpendicular to these walls, the same direction as that revealed by the 2011 earthquake data (Fig. 4). One of the most important EAEs observed in the Collegiate Church are the reactivated structures and anomalous recycled elements (Fig. 5) and dipping corners broken by the 1674 earthquake, which were reactivated by the 2011 earthquake (Fig. 6). The orientation of the maximum horizontal movement obtained from the analyses trended NW-SE on average in both earthquakes. This maximum horizontal movement was used to calculate trajectories of movement/strength in the Collegiate Church. These trajectories showed an overall NW-SE direction, congruent with the average values of N150ºE calculated for the EAEs in Lorca city centre, parallel to the seismic ground peak acceleration calculated by Alfaro et al. (2012) . The rose diagram calculated from the accelerometer located in the City Hall in the city centre showed the same direction of movement (Fig. 1). Therefore, the direction of movement calculated from the EAEs by geological structural analysis was the same as that recorded by the accelerometer located at Lorca city centre.

Fig. 4: EAEs reactivated by the 2011 earthquake. Horizontal displacements of masonry blocks in the SE wall (direction of the wall: N055ºE) of the San Patricio collegiate church generated by: A) the 1674 earthquake and B) the 2011 earthquake.

DISCUSSION AND CONCLUSIONS

We have observed that the deformations generated during the 1674 earthquake were very similar in character and even showed the same orientation of maximum horizontal movement (NW-SE) as the 2011 quake and thus most of the earlier deformations had been renewed by the recent seismic event (Figs. 4, 5 and 6) (Giner Robles et al., 2012; Pérez-López et al., 2012; Rodríguez-Pascua et al., 2012). This may well indicate that the Lorca-Totana segment of the Alhama de Murcia fault (FAM) triggered both earthquakes as the seismic intensity of both was similar, they affected the same area to great degree, and caused a similar type of building damage and EAE direction. The EAE data close a seismic cycle of 337 years in the Lorca-Totana segment fault. This kind of analysis complements the information obtained from palaeo-seismological data, particularly when the earthquakes did not produce surface ruptures (M<6) as in this case. The EAEs and the geological structural analysis of these deformations proves to be a useful tool for studying the behaviour of historic buildings during seismic events and can help in the restoration and prevention of such effects in our cultural heritage. It is more than likely that the next earthquake in the Lorca-Totana segment will lead to similarly oriented damage. If we suppose a theoretical church oriented NE-SW, perpendicular to the main ground direction of movement, and this church is affected by a similar earthquake generated by the same fault the effects will be much the same. The most significant damage will be produced in the walls running parallel (NW-SE) to the main movement. The EAEs that appear in these walls will be conjugated fractures, fallen key stones in arches and so on. In the walls running NE-SW the damage will be less than in the NW-SE walls. The EAEs in these walls will be horizontal fractures, and their tilting and complete collapse if they are unconnected to the main body of the building. This kind of method and the data it affords could be integrated into the national preventive plans to prevent seismic damage to architectural heritage.

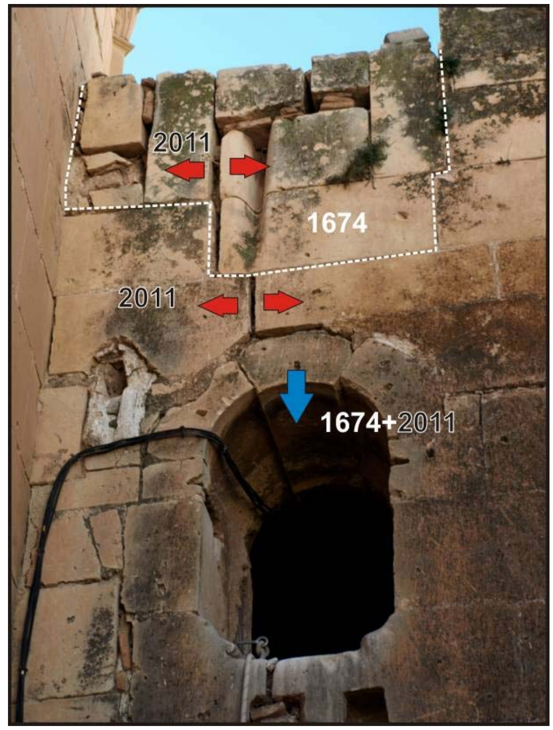

Fig. 5: Seismic deformations in the buttresses of the main nave of the collegiate church (direction of the buttresses: N055ºE). The dotted line marks the reparation with abnormal constructive elements after the earthquake of 1674. Cracks can be seen to affect these repairs and the reactivation of the fallen voussoirs in the arch by the earthquake of 2011.

Acknowledgements: This work was supported by the Spanish Project: RESCATELO (CGL2011-14925-E). This paper is a contribution of the Spanish working group on paleoseismology and archaeoseismology (QTEC) of AEQUA.

References

Alfaro, P., Delgado, J., García-Tortosa, F.J., Lenti, L., López, J.A., López-Casado, C. and Martino, S. 2012. Widespread landslides induced by the Mw 5.1 earthquake of 11 May 2011 in Lorca, SE Spain. Engineering Geology, 137-138, 40–52.

Giner-Robles, J.L., Rodríguez-Pascua, M.A., Pérez-López, R., Silva, P.G., Bardají, T., Grützner, C. and Reicherter, K. 2009. Structural Analysis of Earthquake Archaeological Effects (EAE): Baelo Claudia Examples (Cádiz, South Spain). Instituto Geológico y Minero de España. 130 pp.

Giner-Robles, J.L., Pérez López, R., Silva P.G., Rodríguez Pascua, M.A., Martín González, F., y Cabañas L. (2012): Direccionalidad de los daños del Terremoto de Lorca de mayo de 2011: Aplicaciones a estudios arqueosismológicos. *Boletín Geológico y Minero*. 123(4), 503-513.

I.G.N. (2011): http//www.ign.es/ign/layout/sismo.do

Martínez Guevara, J. B. (1984). Temblores de tierra del núcleo sísmico de Lorca-Totana (Murcia). Estudio de sismicidad histórica I.G.N. Original nº 51.

Martínez-Díaz, J.J., Rodríguez-Pascua, M.A., Pérez López, R., García Mayordomo, J., Giner Robles, J.L., Martín-González, F., Rodríguez Peces, M., Álvarez Gómez, J.A., e Insua Arévalo, J.M. (2011): Informe Geológico Preliminar del Terremoto de Lorca del 11 de mayo del año 2011, 5.1 Mw, Instituto Geológico y Minero de España, Madrid. 35 pp.

Martínez-Díaz, J.J., Bejar-Pizarro, M., Álvarez-Gómez, J.A., Mancilla, F.L., Stich, D., Herrera, G. and Morales, J. 2012. Tectonic and seismic implications of an intersegment rupture. The damaging May 11th 2011 Mw 5.2 Lorca, Spain, earthquake. Tectonophysics. In press. doi: 10.1016/j.tecto.2012.04.010

Pérez-López,R., F. Martín-González, Martínez-Díaz, J.J. and Rodríguez-Pascua, M.A. (2012): Datación mediante liquenometría de los desprendimientos rocosos asociados a la sismicidad histórica en Lorca (Murcia, España). *Boletín Geológico y Minero*. 123(4), 473-485.

Rodríguez-Pascua, M.A., Pérez-López, R., Silva, P.G., Giner-Robles, J.L., Garduño-Monroy, V.H., y Reicherter, K. (2011): A Comprehensive Classification of Earthquake Archaeological Effects (EAE) for Archaeoseismology, Quaternary International, 242: 20-30.

Rodríguez-Pascua, M.A., Pérez-López, R., Silva, P.G., Giner-Robles, J.L., Garduño-Monroy, V.H., y Reicherter, K. (2012): Efectos arquitectónicos del terremoto de Lorca del 11 de mayo de 2011. Neoformación y reactivación de efectos en el Patrimonio Cultural. *Boletín Geológico y Minero*. 123(4), 487-502.

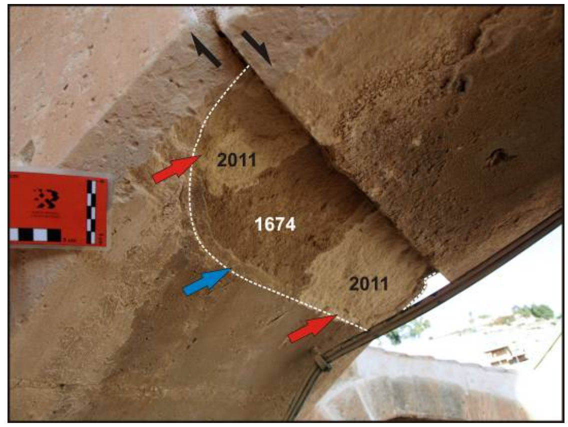

Fig. 6: Reactivated EAEs in the collegiate church of San Patricio. Broken corner in one of the buttresses of the apse; the dotted line marks the boundary of the fracture zone of the missing wedge of rock; the fracture covered with carbonate is associated with the earthquake of 1674 and fresh fissures have been generated by the earthquake of 2011.

PALEOSEISMOLOGY & ARCHAEOSEISMOLOGY MORELIA • MEXICO 2012
INQUA-TERPRO PALEOSEISMOLOGY
EARTHQUAKE ARCHAEOLOGY

POLIGENETIC SAND VOLCANOES GENERATED BY A SINGLE EVENT: THE EARTHQUAKE OF THE EMILIA ROMAGNA (2012/05/20; M_W=5.9) (ITALY)

Rodríguez-Pascua, Miguel A. (1), Pérez-López, Raúl (1), Giner-Robles, Jorge L. (2), Martín-González, Fidel (2), Silva, Pablo G. (4)

(1) Instituto Geológico y Minero de España. Madrid. SPAIN. ma.rodriguez@igme.es, r.perez@igme.es Dpto. Geología y Geoquímica,
(2) Facultad de Ciencias, Universidad Autónoma de Madrid. Madrid. SPAIN. jorge.giner@uam.es
(3) Área de Geología, ESCET, Universidad Rey Juan Carlos. Móstoles (Madrid). SPAIN. fidel.martin@urjc.es
(4) Dpto. Geología, Escuela Politécnica Superior de Ávila, Universidad Salamanca. Ávila. SPAIN. pgsilva@usal.es

Abstract (title of contribution): *One of the most important geological effects generated by the seismic series of Emilia Romagna (2012) were the liquefactions. The first earthquake took place in 20th of May (M_w = 5.9) and generated important liquefaction phenomena in San Carlo. These liquefactions generated fissures sand volcanoes. The sedimentary sections made across the sand volcanoes show the superposition of several normal graded beds. This fact is interpreted like polygenetic sand "eruptions" generated by a single earthquake.*

Key words*: seismic liquefaction, polygenetic sand volcano, Emilia Romagna earthquake*

INTRODUCTION

Earthquakes with minimum magnitudes between 5-5.5 are capable to generate liquefactions in water saturated clastic sediments (Atkinson, 1984; Audemard and De Santis; 1991; Obermeier, et al., 1993; McCalpin, 2009). A very common seismic liquefaction structure is the sand volcano. The trigger mechanism of this structure can be seismic or sedimentary. The seismic sand volcanoes are "fissure eruptions". Sedimentary trigger mechanism of sand volcanoes (i.e. overloading) produces tubular volcanoes without any structuring or alignments (Li et al., 1996; Rodriguez-Pascua et al., 2000).The Emilia Romagna earthquake on May 20, 2012 (Mw=5.9) (fig. 1) generated liquefaction processes with very important sand volcanoes in some towns of the epicentral area (ISPRA, 2012), specially in San Carlo, where this job is focused. These authors relate the sand volcanoes to lateral spreading (Youd, 1984), but in other cases affirm that it will be necessary another interpretation. Previous jobs in seismic sand volcanoes describe the granulometry, geometry, sedimentary conditions and laboratory experiments (Owen 1996; Nichols et al., 1994; Moretti et al., 1999). The detailed stratigraphy of sand volcanoes is not extensively studied. The objective of this job is study the stratigraphy of the sand volcanoes´ cones and proposes a genetic hypothesis.

Fig. 1: Geographical setting of the epicentral area of the Emilia Romagna Earthquake (Mw=5.9), Italy (2012/20/05).

SAND VOLCANOES IN SAN CARLO

The town of San Carlo was seriously damaged by liquefaction processes. The main external expressions of these liquefactions processes were the sand volcanoes. A detailed description of the liquefaction processes is reported by the Italian Geological Survey (ISPRA, 2012). In some places the sand volcanoes are fissure extrusion of more than 100 m (fig. 2). The grain size was between fine sand to coarse sand. In order to made observation about sedimentary structures in the cones of the sand volcanoes, we made some sections across the cones (figs. 3 and 4). In some cases the stratigraphic log of the cone was a single section with a normal graded bed, that we consider "monogenetic" extrusions (fig. 3). But in other cases we could find several overlapped positive graded sets, which we define like "polygenetic" extrusions (fig. 4). The coarse sand in the bottom of the log has an erosive contact and cross bedding upwards (fig. 3). At the top of the log the grain size was decreasing until fine sand with parallel lamination (Fig. 3). These normal graded beds are consequence of a high energy at the beginning of the eruption and the energy was decreasing at the end of the extrusion of the sediments. The overlapping of different normal graded beds (fig. 4) indicates that they were generated by several pulses during the extrusion.

In every place in San Carlo were possible find cones with both cases, monogenetic and polygenetic sand volcanoes. The maximum number of sets is 3 in the studied sand volcanoes in this zone.

Fig. 2: Fisural sand volcanos in San Carlo (Emilia Romagna, Italy).

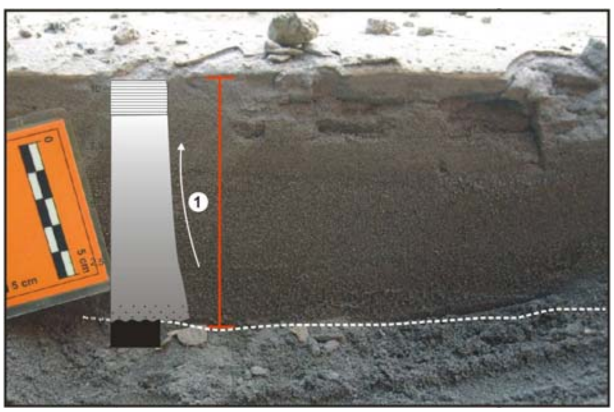

Fig. 3: Cross section of the cone of a monogenetic sand volcano generated by the earthquake of the Emilia Romagna in San Carlo, Italy (2012/05/20) (Mw= 5.9).

GENETIC HYPOTHESIS OF POLYGENETIC SAND VOLCANOES

Japan earthquake of 2011/03/11 generated sand volcanoes in the Chiba city (http//:www.youtuve.com videos: http://www.youtube.com/watch?v=DlhIHhadTqc; http://www.youtube.com/watch?v=I3hJK1BoRak http://www.youtube.com/watch?v=JG4stumV9EQ&feature=related). In video sequences is possible appreciate liquefied sand extrusions in pulses. Every pulse is an "eruption" and generated a new layer in de cone of the sand volcano. It is possible observe that the substratum is unstable and it has a ductile behaviour. This fact generates in the substratum mobile folds like waves. Unfortunately we do not have movies of the sand volcanoes in San Carlo during de earthquake, but the sediments of the sand volcanoes cones show different extrusions for a single earthquake.

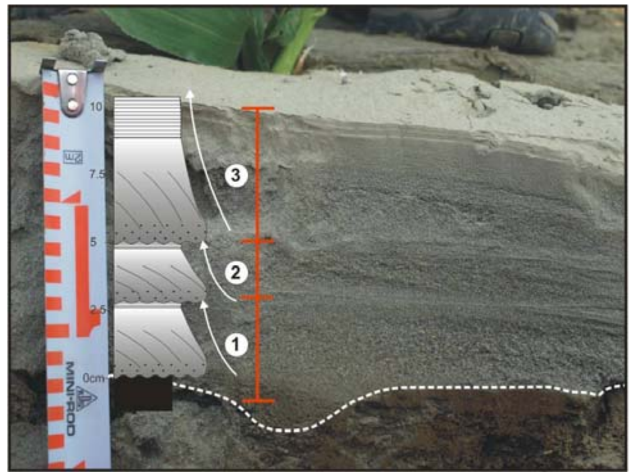

Fig. 4: Cross section of the cone of a polygenetic sand volcano generated by the earthquake of the Emilia Romagna in San Carlo, Italy (2012/05/20) (Mw= 5.9).

When the liquefaction affect to the liquefiable layer the water is accumulated in the inter-phase between the non liquefiable layer and the sand layer. The hydrostatic pressure increase until de hydrostatic fracture of the non liquefiable layer occurs and the fluidization of the sand generates the sand extrusion (fig.5). The extrusions generate a lack of sediment in the underlying sand layer and a synclinal fold in the overlying non liquefiable layer. The plastic behaviour of the non liquefiable layer produces a wave movement at the surface. This phenomena combined with lateral spreading generates alternated fissure eruptions of sand. When the hydrostatic pressure was equilibrated the liquefaction process ended. In every fissure eruption the extruded sediment is recorded by a normal graded bed. The grain size distribution fines upward, the coarse sand in the bottom implies high energy at the beginning of the eruption and the fine sediments with parallel stratification is due to low energy in the liquefied sediment.

CONCLUSIONS

The fissure sand volcanoes generated during the Emilia Romagna earthquake (2012/05/20; Mw=5.9) was generated mainly by lateral spreading. But in other cases the plastic behavior of the confining layer in the surface generated wave movement at the surface. When a synclinal fold was located in a fissure the extrusion took place and in the anticline folds the eruptions stopped. An alternating movement generated eruptional pulses. Every pulse was recorded by a normal graded bed overlapping each other. In conclusion a single earthquake can generate different eruptional pulses in sand volcanoes and this fact should not be confused with several earthquakes or aftershocks in the fossil record.

Acknowledgements: Thanks are given to Salvatore Barba, Eutizio Vittori and the Italian firefighters (Vigili del Fuoco) for their assistance during our field trip. This work was supported by the Spanish Project: RESCATELO (CGL2011-14925-E).

References

Atkinson, G. 1984. Simple computation of liquefaction probability for seismic hazard applications. Earthquake Spectra, 1 (1): 107-123.

Audemard, A. y De Santis, F. 1991. Survey of liquefaction structures induced by recent moderate earthquakes. Bull. Inter. Assoc. Eng. Geol., 44: 5-16.

ISPRA. 2012. Geological effects induced by the seismic sequence started on may 20, 2012, in Emilia (Mw=5.9). Prelyminary Report. Open file report. Servizo Geologico d´Italia. 10pp.

Li, Y., Craven, J., Schweig, E.S. and Obermeier, S.F. 1996. Sand boils induced by the 1993 Mississippi River flood: Could they one day be misinterpreted as earthquake-induced liquefaction?. *Geology*, 24, 2: 171-174.

McCalpin, J.P., 2006. *Paleoseismology*. 2nd Edition. Academic Press, San Diego. 613pp.

Moreti, M., Alfaro, P., Caselles, O., and Canas, J.A., 1999. Modelling seismites with a digital shaking table. *Tectonophysics*. 304, 369-383.

Nichols, R.J., Sparks, R.S.J. and Wilson, C.J.N., 1994.
Experimental studies of the fluidization of layered sediments and the formation of fluid escape structures. *Sedimentology*.

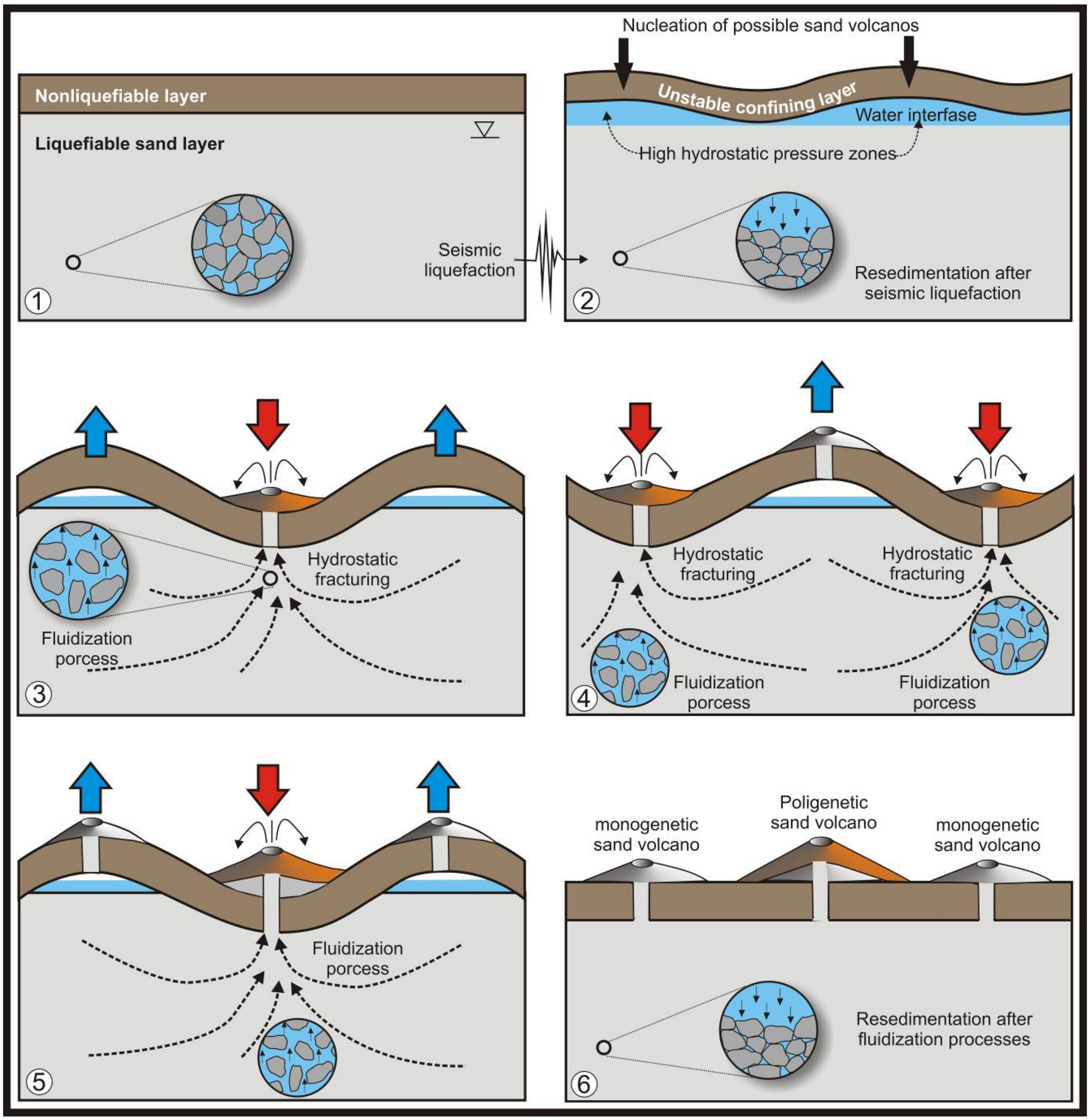

Fig. 5: Synthetic evolutionary scheme of polygenetic sand volcanoes generated by the earthquake of the Emilia Romagna in San Carlo, Italy (2012/05/20) (Mw= 5.9).

41, 233-253.

Obermeier, S.F., Martin, J.R., Frankel, A.D., Youd, T.L., Munson, P.J., Munson, C.A. y Pond, E.C. 1993. Liquefaction evidence for one or more strong Holocene earthquakes in the Wabash Valley of southern indiana and Illinois, which a preliminary estimate of magnitude. *U.S. Geol. Surv. Prof. Pap.*, 1536.

Rodríguez-Pascua, M.A., Calvo, J.P., De Vicente, G. and Gómez Gras, D., 2000. Soft-sediment deformation structures interpreted as seismites in lacustrine sediments of the Prebetic Zone, SE Spain, and their potential use as indicators of earthquake magnitudes during the Late Miocene. Sedimentary Geology, 135, 117 – 135.

Youd, T.L. 1978. Major cause of earthquake damage in ground failure. *Civil Engineering*, April: 47-51.

THE ZANCLEAN FLOODING IN THE GIBRALTAR ARC (SOUTH SPAIN): PROXY DATA ON PLIOCENE INDUCED SEISMICITY BY THE MEDITERRANEAN SEA REFILLING

Pablo G. Silva (1), Pedro Huerta (1), Javier Elez (1), Jorge Civis (2), M. Ángeles Perucha (3), Cari Zazo (4), Jose L. Goy (2), Cristino J. Dabrio (5), Teresa Bardají (6)

(1) Dpto. Geología, Escuela Politécnica Superior de Ávila, Universidad de Salamanca. Avda. Hornos Caleros, 50. 05003-Ávila. SPAIN. pgsilva@usal.es, jelez@usal.es, phuerta@usal.es,
(2) Dpto. Geología, Facultad de Ciencias, Universidad de Salamanca, Salamanca, Spain. civis@usal.es, joselgoy@usal.es
(3) Instituto Geológico y Minero de España. Ríos Rosas, 23. 28003-Madrid. SPAIN. ma.perucha @igme.es
(4) Dpto. Geología, Museo Nacional de Ciencias Naturales (CSIC), 28006-Madrid SPAIN
(5) Dpto. Estratigrafía. Facultad CC. Geológicas. Universidad Complutense de Madrid. 28040-Madrid. SPAIN.
(6) Dpto. Geología, Universidad de Alcalá de Henares, 28871- Alcalá de Henares, Madrid SPAIN

Abstract (The Zanclean Flooding in the Gibraltar Strait (South Spain): Proxy data on Pliocene induced seismicity by the Mediterranean Sea Refilling) *The refilling of the Mediterranean after the Messinian Salinity Crisis allows to consider the Gibraltar Strait as a giant kilometric dam separating the Atlantic waters from the adjacent desiccated Mediterranean Basin. The available evaluations on associated drawdown (-1000 m), time of refilling (3 years) and associated rates of loading (10 m/week) coming from recent models (García-Castellanos et al., 2009) allow to infer the occurrence of a mega-case of reservoir-induced seismicity (RIS) during or soon after the Zanclean Flooding. Preliminary data presented here evidence the occurrence of outsized slumps and large tsunami events during the Lower Pliocene – Zanclean Period, age indicated by the foraminifera content of the analysed littoral sediments. The dimensions of slumps, related liquefaction structures and subsequent tsunami-transported blocks indicate the occurrence of strong seismic event(s) up to IX ESI Intensity and Mw ≥ 9.0. Evaluations on the equivalent column of water (204.8 m) and associated overloading (2.08 MPa) excess in several orders those related with common RIS (0.3 - 0.5 MPa)*

Key words*: Zanclean Flooding, Induced seismicity, Algeciras Basin, Gibraltar Strait.*

INTRODUCTION

The "Messinian Salinity Crisis" is one of the rare and unique large-scale events illustrating the nearly desiccation of an entire sea-basin during the recent geological record. This event occurred during a relatively short time span of 630 kyr from 5.96 and 5.33 Myr ago and triggered the disconnection of the Mediterranean Sea from the Atlantic Ocean in response to the final stages of build-up of the Gibraltar Arc (e.g. Blanc, 2006). Different approaches (e.g. Ryan, 2009) consider the Mediterranean basin desiccation occurred in two steps. The first step involves a minor sea-level drawdown (< 200 m) with multiple cycles of re-flooding from the Atlantic Ocean giving place to the early salt precipitation and massive gypsums in almost 14-17 successive cycles.

The second step implies a kilometric-scale sea-level drop (c.a. 1000 m) allowing the sedimentation of thick evaporite series, lago-mare deposits and the occurrence of large Messinian erosion surfaces. The duration of these two stages has been estimated in ca. 360 and 270 kyr respectively on the basis of cyclic precipitation during the first stage interpreted as the result of Milankovitch precessional cycles (i.e Briend, 2008; García-Castellanos and Villaseñor, 2011).

This Messinian sea-level drop generated a unique topographic scenario along the growing emerged tectonic wedge of the Gibraltar Arc, with an oceanic (Atlantic) foreland basin to the West and a large desiccated sea to the East. This situation gave place to an abrupt asymmetry in the base-level at both sides of the uplifting Gibraltar Arc, and therefore triggered asymmetric fluvial erosion, backfeeding differential uplift in mountain building (Silva et al., 2011). In this scenario, the Gibraltar Arc worked as a gigantic dam that impeded the Atlantic waters to enter into the desiccated Mediterranean basin.

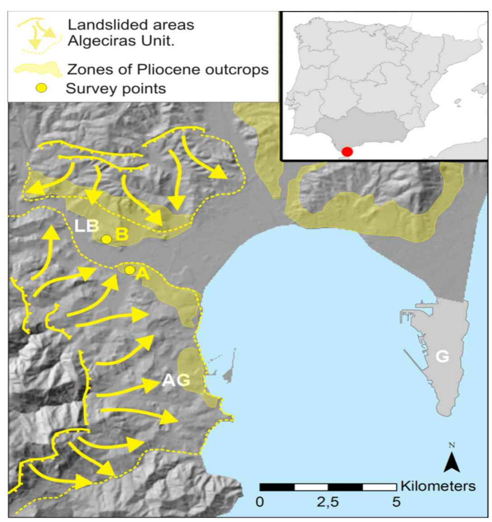

Fig. 1: Location of the Algeciras Bay and studied sections in relation to the slumped/landslided areas corresponding to the Algeciras Flysch Unit.

In detail, the processes involved in the opening of the Gibraltar Strait are largely unknown (Blanc, 2002), but the subsequent Zanclean Flooding inundated the entire Mediterranean basin balancing again base-levels at both sides of the Gibraltar Arc. Recent models indicate that it took place in a nearly instantaneous time-span of about 3 years dissipating a gravitational potential energy of about 1.63×10^{22} J (García-Castellanos et al., 2009). This energy is three orders of magnitude greater than the largest earthquake instrumentally recorded (Mw 9.5).

Considering the Gibraltar Arc as a huge dam located on an active plate boundary, the cyclic re-flooding events during the first stage (± 200 m) and the eventual outsized Zanclean Flooding will necessarily generate induced seismicity. Reservoir-induced seismicity (RIS) is a known process able to produce moderate seismic events (> Mw 6.0) even in no-seismic regions (Simpson et al., 1992; Gupta, 2002). Basic requirements are not properly related to the size of the reservoir, but basically with the height of the column of water (> 100m) and the existence of faults properly oriented in relation with the additional load induced by the stored reservoir-water. However, the review of Gupta (2002) points to other critical factors on RIS, such as rapid cyclic changes of the water-level, temporal duration of the loading process and the rates of variation of the water-level, indicating that rates of loading > 10 m/week are sufficient to generate induced earthquakes (Mw > 5.0).

The Mediterranean Sea was subject to cyclic variations (ca. ± 200m) over about 360 kyr and to an eventual giant water-refilling of about 1000 m during the Zanclean Flooding in a very short time-span of only 3 years inducing loading rates of about 10-12m/week (García-Castellanos et al., 2009). This work introduces to preliminary evidences of large-scale mass movements; rapid Lower Pliocene catastrophic water-refilling; outsized liquefaction structures and apparent large tsunami events witnessed in the geologic record of two key-sections located in the southernmost Pliocene outcrops the Algeciras Bay at the Gibraltar Strait area.

THE ALGECIRAS BAY BASIN

The Algeciras Bay basin constitutes a N-S trending graben orthogonal to the NNW-SSE compressive stress linked to the Africa-Europe collision (Goy et al., 1995) located in the Mediterranean side of the Gibraltar Strait (Fig. 1). Its development is related to post-orogenic E-W extension and is mainly filled by transgressive Pliocene littoral deposits (Benkhelil, 1977; Goy et al., 1995) prograding about 20 km landwards. The typical Pliocene deposits are constituted by Upper Pliocene littoral conglomerates, sands and calcarenites with minor interbedded marly layers. No Lower Pliocene deposits have been described in the Mediterranean side of the Gibraltar Strait area up to now. On the contrary, good Lower to Upper Pliocene sequences are fully described for the adjacent Atlantic side (e.g. Rico-García et al., 2006).
The margins of the basin are mainly carved on synorogenic flysch formations, such as the Aljibe and the Algeciras units (González-Lastras et al., 1991). The substratum over which the Pliocene deposits prograded is mainly constituted by the Algeciras flysch unit, Eocene-Lower Miocene in age, but outcrops of Lower Miocene (Aquitanian-Burdigalian) olisthostrome also occur at the basin centre. The Algeciras unit is complexly deformed and slumped displaying a variety of sub-vertical folding styles and overturning across the basin (Fig. 1). The timing of deformation of this unit is considered to be post-Burdigalian (< 16 Myr) and the opening of the Algeciras Graben as Pliocene s.l., since no other Neogene sediments are present within this basin (González-Lastras et al., 1991). Elevations of Pliocene deposits range from 30-35 m in the south to about 120 m in the northernmost locations. The N-S normal faults bounding the Algeciras basin are weakly defined, and most of them coincided with near vertical contacts within the Aljibe flysch unit. However these faults display evidence of recent moderate seismicity (Silva et al, 2006).

Fig. 2: Slumped Lower Pliocene marls and sands and related metric-size liquefaction structures in the San Bernabé Quarry. North Algeciras

MASS-MOVEMENTS AND LIQUEFACTIONS

The main evidence of large-scale mass movements in the Gibraltar Strait area is provided by the thick breccias filling the submarine paleochannels carved in the so-called Camarinal Sill during the Zanclean Flooding. This is the main submarine threshold actually separating the Atlantic and Mediterranean basins at a depth of -220 m. These paleochannels (1.5 km width and 650 m depth) are partially filled up to a depth of -300 m by slumped breccias incorporating large angular boulders of the adjacent Algeciras and Bolonia flysch units (Esteras et al., 2000). These authors suggest that the involved minimum mobilized volume of materials was about 6.5 km^3 produced by large scale avalanches at both sides of the Gibraltar Strait after the termination of the Zanclean Flooding suggesting its probable seismic origin. In fact, the occurrence of interstratified breccias and slumped materials in the evaporite and subsequent Pliocene succession of the Mediterranean basin is a common feature. Many authors have hypothesised about their probable seismic origin in relation to the large-scale slope instability generated by the desiccation of the Mediterranean (e.g. Blanc, 2002; Ryan, 2009).

The evidences presented in this study come from the San Bernabé Quarry located in the locality of Los Barrios (A: Fig. 1) near Algeciras. This Quarry was investigated by Benknelil (1977) offering outcrops of the Upper Pliocene littoral calcarenitic series with evidence of E-W extension in the Gibraltar Strait area.

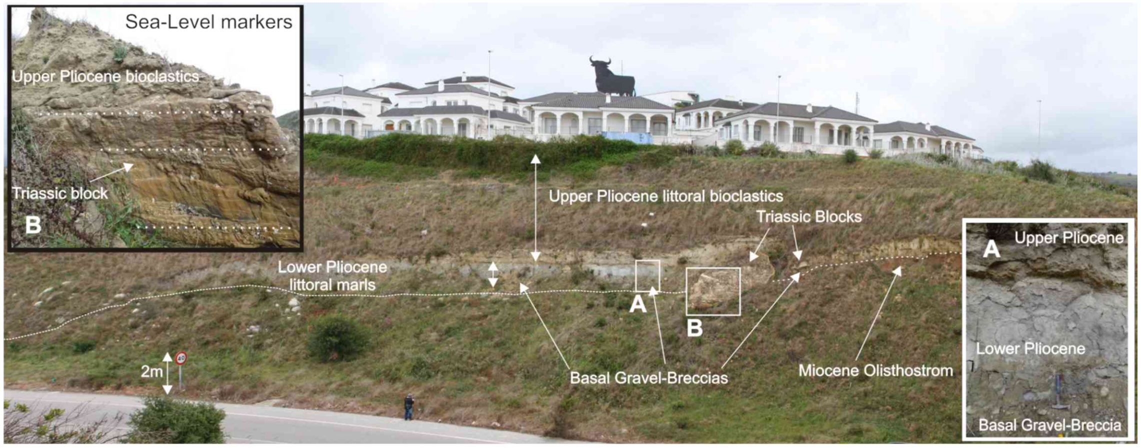

Fig.3: Panoramic view of the Los Barrios Motorway Pliocene outcrop. A: Basal Pliocene section displaying the basal breccias, marl and sands (intermediate unit) and the upper bioclastic littoral calcarenites. B: metric block (1.6 x 2.2 m) of Triassic sandstone displaying three levels of boring littoral organisms (lithophaga). The block is toped by the upper bioclastic calcarenites

Field surveys since the year 2000 revealed that the basal beds of the Pliocene series contained sandy and marly levels affected by soft-sediment deformation structures several meters size (2x5 m), displaying metric injection structures and large angular blocks of the flysch units (Fig.2). The sequence (6 m thick) contain 1.2-1.8 m thick green clayey marls, rich in terrestrial gastropods (entire and fragmented), organic matter, root traces and fenestral porosity with flasher thin cm-size beds of silty fine mica-sands displaying symmetric oscillation ripples. Remains of organic matter include small mm to cm-sized fossil wood fragments (i.e. lignites) with characteristic reduction halos, but also 15-10 cm size well preserved fossil tree trunks. Sandy bodies (< 1m thick) are pervasively liquefied and injected in the overlying clayey marls. Several fossil tree-trunks lignites are typically placed within the metric-scale vertical sand injection columns. The sequence can be interpreted as a vegetated marshland area subject to tidal influence. The marshland sequence overlays (erosive unconformity) the complexly deformed (slumped, folded and overturned) Algeciras flysch unit, which is constituted in this area by interbedded red clays and grey limestones of Eocene-Oligocene age (González Lastras et al., 1991). However, a basal intervening bed (0.8 – 1.0 m thick) occurs locally, in which the red clays of the flysch are injected in the overlying clayey marls, which also contain embedded pillow-like bodies or mud-blocks (20-60 cm in size) of the underlying red clays giving place to a mixture layer. This deformational assemblage strongly suggests that the Lower Pliocene marshland sequence and the Algeciras flysch substratum slumped together or almost coeval.

The slumped materials are overlain in erosive and angular unconformity by the transgressive upper Pliocene littoral calcarenites (8-9 m thick in this zone), which filled the complex topography resulting from the slump event(s). The slumped sequence is affected by a complex set of N90-130ºE reverse and normal faults congruent with a NNE directed mass-movement (Fig. 1). However, a more recent set of N350-N10ºE normal faults cut the whole Pliocene succession, displaying metric (1.5 – 3.0 m) offsets and illustrating Plio-Quaternary extensional tectonics in the Algeciras graben basin (Goy et al., 1995). All these data allow us to consider that the complexly deformed Algeciras flysch unit was mass-wasted during the Lower Pliocene, at least along the entire western border of the Algeciras Bay basin (Fig. 1). Several approaches to the complex structure of the flysch units in the Gibraltar area consider the occurrence of large gravitational processes during the tectonic emplacement of the betic units (I,e, Martín Serrano, 1985; Durand-Delgá, 2007; and references therein)), but these models show a relevant disagreement about the precise structural arrangement of the flysch units in the zone. This is mainly due to the fact that any previous approach considered the occurrence of large-scale post-tectonic mass-wasting in relation with the initial development of the Algeciras Bay Pliocene graben. In fact the Graben margins are defined by subvertical contacts between the Aljibe (Marginal reliefs) and the Algeciras (depressed and slumped zone) flysch units. Taking into account the distribution of the outcrops of the slumped Algeciras unit, the slump event(s) affected a minimum area about 47 km^2 along the western border of the Algeciras Bay graben (Fig. 1), but around more than 130 km^2 within the entire Basin.

PROBABLE TSUNAMI EVENTS

One km north of the San Bernabé Quarry a few new roadcuts expose outcrops at the locality of Los Barrios (Fig. 1). These outcrops record the almost complete Pliocene succession prograding into the Algeciras Basin. The outcrops display undeformed Pliocene materials inset within the underlying lower Miocene clayey olisthostrom. Survey of the available outcrops around Los Barrios strongly suggests that the preserved materials belong to the infilling of a flat paleovalley inundated during the Zanclean Flooding. The preserved sediments grade from basal clayey marls, thin interbedded marls and sands to upper bioclastic calcarenites and littoral conglomerates, these last typical of the upper Pliocene in the Gibraltar Strait Area (González-Lastra et al., 1991; Goy et al., 1995; Rico-Garcia et al., 2008).

The intermediate unit of interbedded marls and sands (1.6 m thick) is very rich in littoral macrofauna (molluscs and gastropods), and embeds large blocks (2x1 m) of Triassic sandstones detached from the underlying Miocene olisthostromic unit. The large blocks rest on a 10-12 cm thick breccia of marly sands which includes a variety of reworked clasts of Triassic sandstones and limestones, Lower Miocene red clays (rip-up mud clasts) and large fragments of littoral fauna.

and "*Lithophaga"* 15-40 cm apart (Fig.3b). The preservation of this kind of sea-level markers is common in areas affected by coseismic uplift, Therefore these markers may indicate the occurrence of repeated local coseismic uplift during the end of the Zanclean Flooding. The boulders are eventually embedded and buried by the trangressive Upper Pliocene bioclastic calcarenites.

All these preliminary data indicate the occurrence of a tsunami-type energetic event during the earlier phases of the Zanclean Flooding that inundated the existing subaerially-incised valleys carved within the Algeciras basin. The boulders and the basal breccia layer found in the Lower Pliocene sequence may have a near source zone, but a high-energy event is required to mobilize these elements within an otherwise not particularly energetic sedimentary sequence, as also supported by the mixture of benthonic and placktonic species in the basal Zanclean deposits.

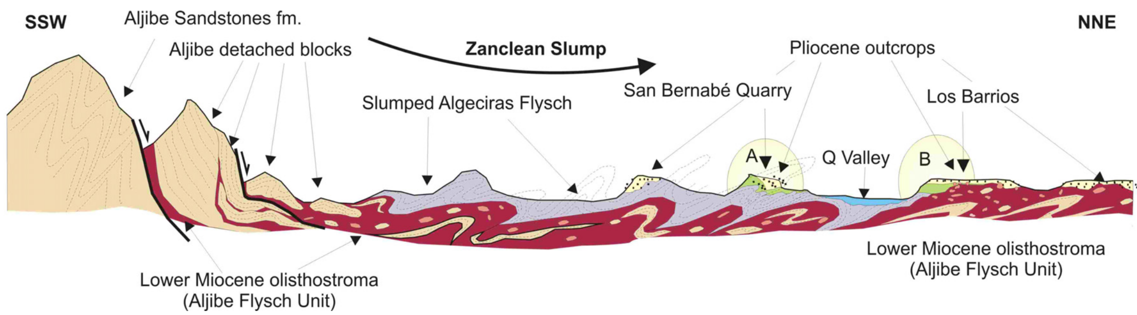

Fig.4: Schematic cross-section throughout the Algeciras Bay graben-basin displaying the overall features and structural relationships of the slumped units of the Algeciras Flysch in relation to the Zanclean Pliocene outcrops reported in this stuffy. A: San Bernabé Quarry; B. Los Barrios Motorway section.

The breccia layer is continuous, but thins away from the boulders constituting the erosive base of this intermediate unit over the underlying basal massive clayey marls, but also directly rest on the Lower Miocene materials (Fig. 3). This breccia is rich in foraminifera, and preliminary sampling indicates an outstanding mixture of benthonic and planktonic groups with an unexpectable dominance of planktonic species (68–81%). These data indicate an unusually-high percentage of planktonic species (19-20) unlikely for a littoral sequence, resulting in a pelagic index (IP) between 0.7 and 0.8. Of special interest are the absence of *G. puncticulata* (Middle Pliocene), the presence of *Globorotalia margaritae* and *Sphaeroidinellopsis seminulina* (Lower Pliocene) and the occurrence of *Globoturborotalita nepenthes. This last plancktonic foraminifera is of special interest because become extinct in the* basal Zanclean biozene MPL-1 (Iaccarino et al., 2007). Therefore this preliminary reported foraminifera assemblage allow to place the basal breccia layer and the base of the overlying intermediate sand-marly in the basal Lower Pliocene - Zanclea Biozone (MPL-1) between 5.33 to 4.50 Myr (Iaccarino et al., 2007). On the other hand the mixture of benthonic and planktonic foraminifera, as well as the dominance of the last ones strongly suggest the occurrence of an intervening energetic event pushing oceanic waters in the littoral environment.

The large boulders embedded in the fossiliferous littoral sands and marls zanclean deposits indicate a subsequent rapid inundation of the zone. These display three different paleosea-level markers represented by encrusted intertidal boring molluscs

CONCLUSIONS

Preliminary data presented here indicate the occurrence of large-scale slump events, affecting littoral vegetated marshland sediments, the rapid inundation of the zone and intervening tsunami-like events during the Zanclean period as determined by foraminifer's biozonation. The features of these anomalous sedimentary records and deformations suggest that they can be linked with strong seismic events occurring during, or soon after, the so-called Zanclean Flooding. Considering the Gibraltar Arc a "Mega-Dam" that impeded the Atlantic waters to enter the desiccated Mediterranean, the eventual refilling of the Mediterranean should produce a period of increasing seismicity in analogy to reservoir-induced seismicity (RIS). Data reported here point to the occurrence of strong seismic events, up to intensity IX following the standards of the ESI-2007 Scale (Michetti et al., 2007), capable to produce large-size slumps and relevant tsunamis.

Digital data processed in the TOPOMED Project indicate that the dimensions of the Mediterranean slope in the Gibraltar strait area down to a depth of -1000 m (presumed drawdown) are of 11,733 km^2 capable to store a volume of water of 2403.0 km^3. The resulting average equivalent water column

(EQWC: km^3/km^2) is 204.8 m, following the standards for the calculation of the geophysical relief in drainage basins (i.e. Silva et al., 2011). This average column of water resulting from a complete Zanclean flooding will induce an extra load of 204,803 kg/m^2 (2.008 MPa). For comparison, we have calculated the equivalent average column of water (km^3/km^2) related to the more relevant cases of RIS ≥Mw 6.0 (Xsinfengjiang, Koyna, Kariba, and Kremasta dams; e.g. Gupta, 2002) resulting in values between 30 – 50 m (extra load of 0.3-0.5 MPa). In other words, the normal RIS EQWC values obtained here are about four times lower than the calculated for the Mediterranean refilling after the Messinian. Following the model of García-Castellanos et al. (2009), the refilling of the Mediterranean was completed in about 3 years, with related peak rates of load of 10m/week, similar to the more relevant cases of RIS (Gupta, 2002). Recently, the devastating 2008 Sichuan earthquake (Mw 7.9) has been related with the filling of the 156 m height Zipingpu Dam (Keer and Stone, 2009). Since this dam is located in a narrow gorge (<1.2 km wide), its height is relatively one half of the equivalent column of water (71.9 m) but about the 34% of that resulting from the Zanclean Flooding in the Gibraltar Strait area (208.4 m). Preliminary simple lineal regression of EQWC vs Earthquake Magnitude for selected cases of RIS indicate a relatively good correlation, better than only considering water height or stored volume of water developed by other authors. This preliminary regression indicate a that the EQWC of the Zanclean Flooding would produce at least one strong earthquake of minimum magnitude 9.4 Mw. However the reported data needs to be fully analysed and implemented in a model in order to consider the occurrence of several strong seismic events releasing this enormous energy for this outsized RIS-like case. From this point of view the opening of the Algeciras Bay graben is a consequence of large-scale mass wasting (Fig. 4) related to induced strong seismicity (≥Mw 9.0) during the Mediterranean refilling after the Messinian salinity crisis.

Acknowledgements: This work has been supported by the EUROCORES-TOPOMED PROGRAM through the Spanish research project CGL2008-03474-E/BTE (CSIC) produced by the USAL TopoMed-Spain Onshore Research Group. Also financial support has been obtained from the research projects CGL08-03998BTE, CGL08-04000BTE. UCM Research Group 910198.

References

Benkhelil, J. (1977). Etude néotectonique de la terminasion occidentale des Cordillères Bètiques (Espagne). Thése d'Etat, Univ. Nice, France.

Blanc, P. L. (2002). The opening of the Plio-Quaternary Gibraltar Strait: assessing the size of a cataclysm. Geodin. Acta, 15, 303–317.

Blanc, P. L. (2006). Improved modelling of the Messinian Salinity Crisis and conceptual implications. *Pal. Pal. Pal.,* 238, 349–372.

Briend, F. (ed.) (2008). The Messinian Salinity Crisis from Mega-Deposits to Microbiology – A Consensus Report. CIESM Workshop Monographs 30, CIESM.

Durand-Delga, M., Esteras, M. & Olivier, P. (2007), Los «Taríquides» (Arco de Gibraltar): Problemas estructurales, paleogeográficos y consideración histórica. Revi. Soci. Geol. España, 20 , 119-134.

Esteras, M. Izquierdo, J. Sandoval, N. G. & Bahmad, A. (2000) Evolucio´n morfologica y estratigrafıca Plio-Cuaternaria del Umbral de Camarinal (Estrecho de Gibraltar) basada en sondeos marinos. Rev. Soc. Geol. Esp. 13, 539–550.

Garcia-Castellanos, D., Estrada, F., Jiménez-Munt, I., Gorini,C., Fernández, M., Vergés, J. & De Vicente, R. (2009). Catastrophic flood of the Mediterranean after the Messinian salinity crisis. *Nature,* 462, 778-782.

Garcia-Castellanos, D. & Villaseñor A. (2011). Messinian salinity crisis regulated by competing tectonics and erosion at the Gibraltar arc. Nature, 480, 359-363.

González Lastras, J., García de Domingo, A., Hernaiz, P.P., Zazo, C. & Goy, J.L., 1991. Cartografía geológica y memoria de la hoja 13-47 (Tarifa). Mapa Geológico de España, Escala 1:50.000. Plan MAGNA, 2ª Serie. IGME, Madrid, Spain.

Goy, J.L., Zazo, C., Silva, P.G., Lario, J., Bardají, T. & Somoza, L., (1995). Evaluación geomorfológica del comportamiento neotectónico del Estrecho de Gibraltar (Zona Norte) durante el Cuaternario. In: M. Esteras, (ed.), El Enlace Fijo del Estrecho de Gibraltar, SECEGSA, Madrid, Vol. 2, 51-69.

Gupta, H. K. (2002). A review of recent studies of triggered earthquakes by artificial water reservoirs with special emphasis on earthquakes in Koyna, India. Earth-Science Reviews 58, 279–310.

Iaccarino, S.M., Premoli-Silva, I., Biolzi, M., Foresi, L.M., Lireer, F., Turco, E. & Petrizzo, M.R. (2007). Practical manual of Neogene planktonic foraminifera. 6th course. Università degli Studi di Perugia, Perugia, Italy.140 pp.

Martín Serrano, A. (1985). La estructura de los flyschs del Campo de Gibraltar: consecuencias tectónicas y paleogeográficas. Boletín Geológico y Minero, 161, 117-140.

Michetti, A.M. et al. (2007): Intensity Scale ESI-2007. Memorie Descriptive Della Carta Geologica D'Italia, 74. APAT, SystemCart Srl, Roma, Italia.

Keer, R.A. & Stone, R. (2009). A Human Trigger for the Great Quake of Sichuan? Sicience, 323 (5912), p. 322.

Rico-García, H., Aguirre, A.J. & González-Delgado, J.A. (2008). Taphonomy and taphofacies models of the Pliocene deposits of Vejer de la Frontera (Cádiz, SW Spain). Pal, Pal, Pa., 285 (3-4): 264-276

Ryan, B. W. F. (2009). Decoding the Mediterranean salinity crisis. Sedimentology, 56, 95–136

Silva, P.G., Goy, J.L., Zazo, C., Bardají, T., Lario, J. & Somoza, L. (2006). Neotectonic fault mapping at the Gibraltar Strait Tunnel area, Bolonia Bay (South Spain). Eng. Geology, 84, 31–47.

Silva, P.G., Ribó, A., Martin-Betancour, M., Huerta, P., Perucha, M.A., Zazo, C., Goy, J.L., Dabrio, C.J. & Bardají, T. (2011). Relief production, uplift and active tectonics in the Gibraltar arc (South Spain) from the Late Tortonian to the present. In: Proceedings 2nd INQUA-IGCP Workshop. Corinth, Greece. 139-142.

Simpson, D.W., Leith, W.S. & Scholz, C.H. (1988). Two types of reservoir-induced seismicity. Bull. Seismol. Soc. Am. 78 (6), 2025–2040.

INITIAL RESULTS OF PALEOSEISMIC RESEARCH IN THE SOUTHERN END OF DE BOCONÓ FAULT (VENEZUELA)

Rodríguez-Luz y Audemard-Franck (1)

(1) Dpto. Ciencias de la Tierra, Fundación Venezolana de Investigaciones Sismológicas. VENEZUELA. lrodriguez@funvisis.gob.ve.

Abstract: *The southern end of the Boconó fault competes with other important faults as relevant seismogenic source. This is due to the regional tectonic complexity that characterizes the frontier region south of the Andes. Given the unknown effective role of the Boconó fault in the large and destructive earthquakes known to us through seismic history in the Andes of Táchira, Venezuela and northern Santander, Colombia, it is of particular importance to increase paleoseismic research in the aforementioned tectonic accident region. To this effect, two paleoseismic trenches were excavated in the southern end of the Boconó fault that revealed various paleoseismic events that await dating.*

Key words: *Paleoseismology, Boconó fault, populations, seismic risk*

PREVIOUS RESEARCH

In the Andes of southeastern Venezuela, the active trace of the Boconó fault progressively looses the position of axis that it maintains in the central portion of the range up to La Grita. The fault obliquely crosses Táchira state and opens up in the shape of a horse's tail towards Colombia. The southern Andean frontier region between La Grita and Pamplona features a telling concentration of destructive earthquakes that make up a remarkable history of events: 02/03/1610, 01/16/1644, 02/15/1796, 06/24/1827, 02/26/1849, 05/18/1875, 05/28/1894, 07/10/1919, 03/14/1932, 07/08/1950, 04/21/1957, 10/17/1981, 06/15/1983. (Singer et al. 1991, Grases et. al. 1999; Ramírez, 2004). These events reflect the structural complexity of the region.

The first paleoseismic events that were detected in the southern portion of the Boconó fault correspond to the research carried out by FUNVISIS in the 1980s, when the La Grita trench was excavated. This work established a seismotectonic association between this fault and the historical destructive earthquakes of 1610, 1894 (and possibly of 1932) and determined the magnitude of the first two events to have been 7,1 - 7,3 Ms (Soulas et. al. 1987; Singer et. al. 1991, Singer y Beltrán 1996). Additionally, the Cordero trench, located north of San Cristóbal, determined two paleoseismic events between 3795± 100 and 3760 ±90 years BP and of magnitude greater than 7 Ms (Soulas et. al. 1987). However, a more recent interpretation of the paleoseismic data from this trench leads us to extend the period of return of an earthquake of 7 Ms to 3000 and 3500 years in this fault (Audemard, F. 1997). Still, much more paleoseismic data from this fault are needed due to the structural complexity of the southern portion and the difficulties involved in its segmentation.

PRELIMINARY DATA OF ONGOING PALEOSEISMIC RESEARCH

Two trenches were excavated along the southern portion of the Boconó fault during the months of April and May of this year. The first excavation was done near Libertad (Capacho Viejo), near the frontier with Colombia, in an environment of fine sedimentation of lake origin very favorable for paleoseismic investigation. From this excavation we obtained evidence of two to three paleoseismic events. The second trench, in the Páramo El Zumbador, between San Cristobal and La Grita, was excavated in a sequence of lake sediments deposited in a sag-pond and flexural in fault propagation fold, with a remarkable normal component. From this trench we learned of at least 3 to 4 paleoseismic events. Their dating is pending.

Acknowledgements: To the work team of the Department of Earth and Geophysical Sciences (FUNVISIS), who supported all of the fieldwork. Likewise with the personnel of the regional and local Civil Protection units, who showed interest in supporting and learning about the research carried out in their region. A special thank you to the local authorities of Michelena and Libertad, in Táchira State.

References

Audemard, F.A., 1997. Holocene and historical earthquakes on the Boconó fault system, southern Venezuela Andes: trench confirmation. Journal of Geodynamics 24 (1-4), 155-167.

Grases, J., Altez, R. y Lugo, M., 1999. Catálogo de sismos sentidos o destructores de Venezuela 1530-1998. Facultad de Ingeniería, Universidad Central de Venezuela. Edición. Innovación Tecnológica. Vol. XXXVII. 654 p.

Ramírez, E. 2004. Actualización de la historia de los terremotos en Colombia, Instituto Geofísico Universidad Javeriana. Editorial pontificia pág. 186.

Soulas J., Singer A. y Lugo M. 1987. Tectónica cuaternaria, características sismogénicas de las fallas de Boconó, San Simón y piedemonte occidental andino y efectos geológicos asociados a la sismicidad histórica. Funvisis para Maraven. S.A. 90 p + anexos. Inédito. (Informe confidencial).

Singer A. Beltrán, C, Lugo M. (1991). Características neotectónicas y parámetros sismogénicos de las fallas activas cuaternarias, y efectos geológicos de la actividad sísmica en la región de proyecto y en las obras proyectadas. Proyecto Sumandes II. Funvisis para Maraven, S.A. 2 volumen. 239 p. Inédito

PALEOSEISMIC EVIDENCE IN LAS LOMAS, ZACAPU MICHOACÁN, MEXICO.

Soria-Caballero D.C.(1), Garduño-Monroy V.H.(2), Rodríguez-Pascua M.A.(3), Velázquez-Bucio M.M.(4).

(1) Posgrado en Ciencias de la Tierra, Instituto de Geología, UNAM. dianscc@hotmail.com
(2) Departamento de Geología y Mineralogía. Instituto de Investigaciones Metalúrgicas. UMSNH.vhgardunom@gmail.com
(3) Instituto Geológico y Minero de España.ma.rodriguez@igme.es
(4) Posgrado en Geografía, Centro de Investigaciones Geográficas y Ambientales, UNAM. magda_vb@yahoo.com.mx

Abstract. (Paleoseismic evidence in Las Lomas, Zacapu Michoacan, Mexico) *The Zacapu basin has a potentially important sedimentary record for paleoseismic studies, because of its location and development. Previous paleoenvironmental studies have faced challenges in the interpretation of such record, such as inverted ages or hiatus in the record. The present work suggests that these difficulties are due to seismic effects in the sedimentary sequence identified from liquefaction structures, deformation of sediments and underwater landslides (slumps) observed in the open trenches, and the fossilization of seismic waves observed in the landscape. Geomorphological analysis suggests that the tectonic structures affecting the basin belonging to the Morelia-Acambay Fault System (MAFS),which has a preferential ENE-WSW direction and is affecting lithological units from the Miocene until recent ages. The evolution of the Zacapu basin has been influenced by the activity of MAFS, who also controlled the location and deposition of volcanic products at different periods of activity.*

Key words*: Zacapu, paleoseismicity, synsedimentary deformation.*

INTRODUCTION

The Zacapu basin (19°51'N, 101°40' O) is located at the boundary between the Pliocene Volcanic Zone and the Trans Mexican Volcanic Belt (TMVB) *sensu stricto.* it is part of a group of volcanic highlands formed during Quaternary ages (Álvarez, 1972; Watts *et al.*, 1982; Street-Perrott *et al.*, 1989; O´Hara *et al.*, 1993; Metcalfe *et al.*, 1994; Israde *et al.*, 1999; Fisher *et al.*, 2003; Davies *et al.*, 2004; Rodríguez-Pascua *et al.*, 2004; Israde *et al*., 2005; Park *et al*., 2010). The basin, which has an area of 261 km² and a total drainage of 335 km², was formed by trans-arc extensional tectonics from the Late Pliocene to the Pleistocene (3 – 1 Ma) and uprisings due to faults near Villa Jiménez during the Quaternary. The regional volcanism influenced its formation reactivating some faults and causing local subsidence. Until Hispanic periods, the basin harbored a marsh which was drained in the nineteenth century for agricultural purposes (Demant *et al.*, 1992; Medina, 1993; Petrequin, 1994; Gómez–Tuena *et al.*, 2005). The stratigraphy of the area is summarized in Table 1.

The Zacapu basin has an important record for paleo-seismicity in the TMVB because it shows evidence of faulting in N-S, E-W and SW-NE directions, faults which were active until recently. This activity is expressed as deformation and uplift of the lacustrine sequence, contact between sediments and the volcanic basement, modification of the paleolake drainage, underwater landslides, slipped lavas tilted by faulting, fall of resistant blocks, masked faults, alignment of structures, building of recent pyroclastic volcanoes on active faults, lavas cut and underwater lava flows. The most recent of these (28000 yr) mixed old and young material and was fossilized by deep-water lake sediments. Apparently, the lacustrine sequence in Zacapu moved into a mosaic of faulted blocks and reached high altitudes, with a maximum difference of 70m, indicating recent deformation. In some places the former lake is 20m above the marsh, which is explained by tectonic deformation in opposite directions.

The area of Las Lomas records clay formations produced by alteration of diatomite in submerged conditions, interspersed with layers of volcanic ash. Its

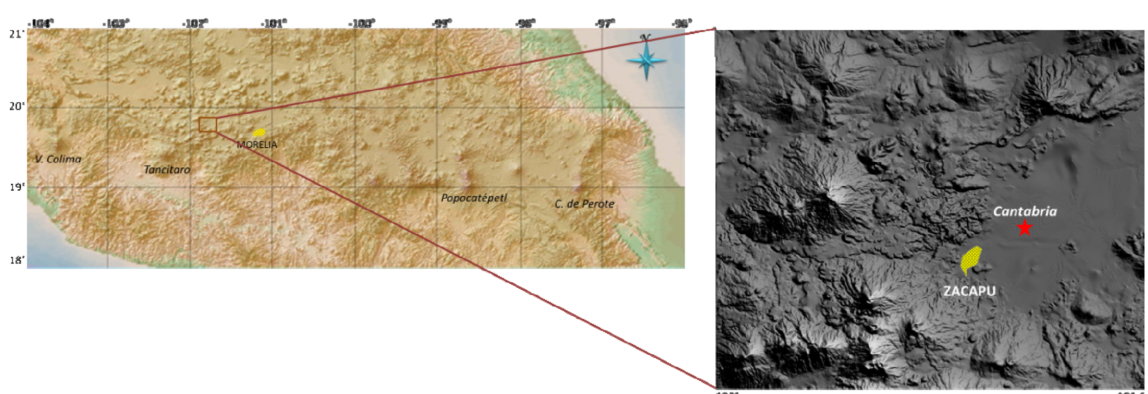

Fig. 1: Location of the paleobasin of Zacapu within the TMVB and location of the study area: Las Lomas (marked with a star).

origin was related to large radius tectonic uplift, with a minimum age of 28,000 years, which continued until recently. This was followed by the drying up of the former lake during regression prior to the recent arrangement, forming broad, shallow valleys and wind deflation depressions. Tricart nonetheless located its formation between 8000 and 7000 yr BP due to a series of volcanic eruptions followed by tectonic activity. In this area, episodes were reconstructed of high and low lake level prior to the historic marsh conditions. The sedimentary record suggests humid conditions between 52000-39000 yr. At 28000 yr a discontinuous record, poorly developed, with an elevated sedimentation rate, hiatus, and deformed layers, suggests a deep changing from lake to a shallow marsh from 24000 yr BP. The drying conditions occurred during the Last Glacial and Middle Holocene, to worsen between 14000 and 4800 years BP. Lowest lake levels were reached in 2800-2400 yr BP and 1100 yr BP due to both climate change and tectonics. Currently, the smooth topography hides the strong tectonic deformation (Metcalfe *et al.,* 1988, 1989 y 1994; Demant *et al.*, 1992; Tricart, 1992; Petrequin, 1994; Xelhuantzi,1994; Arnauld *et al.*, 1997; Ortega *et al.,* 2002).

<table>
<tr><td rowspan="5">QUATERNARY</td><td colspan="2">HOLOCENE</td><td colspan="2">Holocene lacustrine sequence from marshy environment 8100 BP</td></tr>
<tr><td rowspan="4">PLEISTOCENE</td><td rowspan="2">LATE</td><td colspan="2">Ancient lacustrine sequence between 35,000 and 30,000 years BP</td></tr>
<tr><td colspan="2">Recent volcanism <40,000 years BP</td></tr>
<tr><td rowspan="2">EARLY</td><td colspan="2">Quaternary volcanism between 500,000 and 40,000 years BP</td></tr>
<tr><td colspan="2">Lacustrine deposits</td></tr>
<tr><td rowspan="5">NEOGENE</td><td rowspan="3">PLIOCENE</td><td rowspan="2">LATE</td><td colspan="2">Dacites</td></tr>
<tr><td colspan="2">Large volcanic buildings (basalts and basaltic andesites)</td></tr>
<tr><td>EARLY</td><td colspan="2">Lacustrine deposits</td></tr>
<tr><td colspan="2" rowspan="2">MIOCENE</td><td rowspan="2">Succession of Mil cumbres</td><td>Ignimbrites</td></tr>
<tr><td>Calc-alkaline andesites</td></tr>
</table>

Table 1: Stratigraphy of the Zacapu region (Israde 1999).

METHODOLOGY

A microtopographic survey was conducted in the area of Las Lomas using a Leyca accuracy GPS, which were acquired 4822 points used to generate a contour map at 20 cm of equidistance to describe the geometry of this zone. Stratigraphy was performed upon 13 trenches dug in Las Lomas at 2-3m and 3m depth pit used for storage of fodder.

RESULTS

Geomorphological analysis: North of the basin stand high, straight reliefs with natural and artificial drains. To the south there is a transition zone with uncertain hydrology and terrain undulations with archaeological sites. At the center lies a swamp area with elevations from 1973 to 1978 m asl, which joins long and wide digitations, penetrating the hills and the lacustrine formations passing to alluvial accumulations and valleys. To the west there is a raised area (10 m) called Las Lomas and lavas called Malpais bordered by Holocene volcanic buildings up to 3365 m elevation. The most recent lava flows closed the NW part of the basin and are cut by faults. 7 geochronological units were delineated in the Zacapu basin (Fig. 2):

1. Miocene sequence with large polygenetic buildings of andesite composition, with colors from green to gray, and highly weathered. The entire sequence is strongly affected by faulting and fracturing.
2. Early Pliocene sequence formed by volcanic buildings of lavas and breccias with andesite composition and grayish coloration. This sequence has well development drainage and is also affected by severe faulting. At this stage, the basin is formed and begins to deposit the lacustrine sequences.
3. Late Pliocene sequence with semi-shields volcanoes formed by lavas and breccias of gray andesites. Such buildings are visibly affected by faulting.
4. Early Pleistocene sequence formed by emplacement of semi-shields volcanoes of andesite composition and poorly development drainage. During this stage there is also the formation of a caldera structure.
5. Middle Pleistocene sequence formed by largest semi-shields volcanoes composed for andesitic lavas and breccias.
6. Late Pleistocene sequence formed by emplacement of smaller semi-shield volcanoes composed by andesitic lavas and breccias.
7. Holocene sequence formed by small volcanic buildings such as cinder and ash cones and domes, and lava flows. This is the result of major episodes of effusive volcanism, sometimes interacting with groundwater to generate hydromagmatic structures. The emplacement of volcanoes and the deposition of their lava flows follows an orientation controlled by NE-SW and ENE-WSW faulting. The lacustrine sequences become more important, but in recent times lacustrine bodies tend to disappear.

The most important faulting affects Miocene to Holocene units, following a mainly ENE-WSW direction with normal movement. The activity of these faults played a significant role in shaping the lake basins in the area. Later, in Pleistocene and Holocene times occurred the first and second reactivation of the structures, now changing the type of faulting to normal movement with a left lateral component.

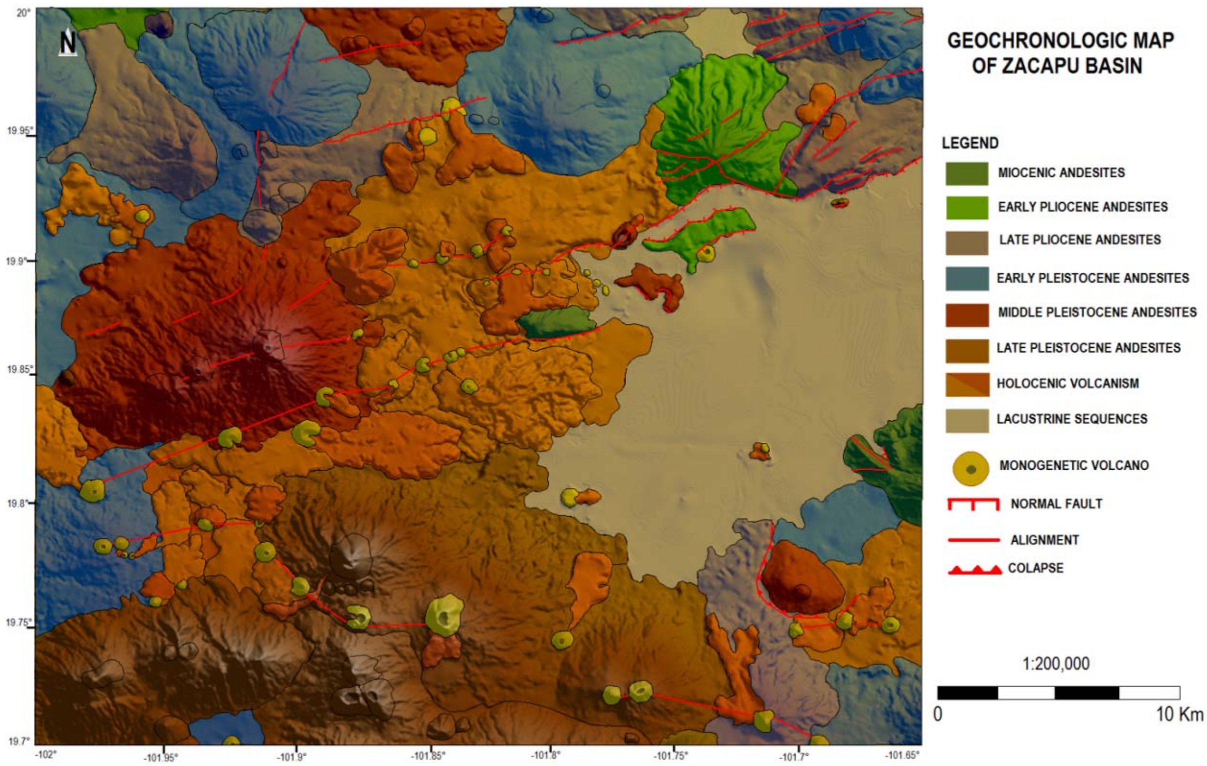

Fig. 2: Geochronologic map of the Zacapu basin.

Microtopography: The elevation model (Fig. 3) shows a series of hills from 2 to 10m high, almost parallel to each other and with preferential NNW-SSE direction, reaching a maximum elevation of 1982m and a minimum of 1972m; they have gentle slopes, are elongated, and their largest axis stands in N-S direction, the shortest E-W . To the south there is a depression corresponding to the old drain for the Laguna of Zacapu. In general, the topography is higher in the northwest portion and lower in the south. The morphology suggests that the formation of Lomas may be related to a folding in NNW-SSE direction, generated by the fossilized seismic waves that rose and deformed lacustrine sediments deposited in the ancient marsh. Only Loma Alta and Point 1 of CEMCA show a roughly circular morphology which is inconsistent with the rest of the hills. This is probably due to anthropogenic modification. There are some previous studies by Demant *et al.* 1992, Petrequin1994 and Ortega *et al.* 2002.

Stratigraphy: the general column for the Las Lomas area consisted of 6 units, from base to top (Fig. 4):
U1: A series of laminate layers of cream to light brown diatomite with 2m thick (base unseen) contains remains of fishes, vegetation and moderate oxidation. It interspersed 5 layers of black and gray volcanic ashes, with maximum of 10cm and minimum 3cm thickness, high content of volcanic glass, cinders and pumice. This unit shows liquefaction structures associated with collapse, where the volcanic ash intrudes the diatomite layers (Fig. 4A). The age obtained for this unit by C^{14} was 39200 years BP.
U2: Non-laminar layers of 1m thick light brown diatomite, sometimes with cross-bedding, with remains of fishes, vegetation, and abundant oxidation, bioturbations and scattered pulmonate gastropods. Interleaving is a layer of white volcanic ash 2cm thick, in lenticular structures and two of 5 and 10 cm thick layers of black volcanic ash, with fragments of cinders, glass and quartz. Its lower contact is slightly erosive.
U3: 0.9m thick gray silt clay layers result of mixing black volcanic ash, diatomite and carbonate aggregates, with high content of pulmonate gastropods, bivalves and ostracods (near 80% of the components of the sediments). Ostracod species observed belonging to 4 families *(Candonidae, Cyprididae, Limnocytheridae* and *Darwinulidae)* who prefer relatively deep water bodies and aquatic vegetation. The most abundant gastropod is *Physa*, associated with perennial water bodies. The unit shows synsedimentary structures such as current ripples, and its lower contact is transitional
U4: a 0.9 m thick layer of black volcanic ash, sometimes appearing as a fallen block, with many fragments of glass, obsidian, bones of fish and oxidation. Its lower contact is an erosive discordance.
U5: brown silt-clayed 1m thick layers, mixed with lenticular structures of black volcanic ash, aggregates of diatomite and carbonates, with moderate oxidation, fish remains, volcanic glass, dispersed coal and bioturbations. Calcified organisms have disappeared.

Towards the top, four layers of black volcanic ash from 2 to 5 cm thick are interspersed and affected by micro-faulting, fallen blocks of black volcanic ash and laminated diatomite appears (Fig. 4C-D). Its lower contact is transitional. The age obtained by C ^{14} to 10 cm from the top was 34500 years BP, the accuracy of this age remains uncertain due to slumps processes in this unit.

U6: A series of dark brown 1.1m thick silt and sandy loam layers, with traces of oxidized, black volcanic ash and aggregates of carbonates, intercalated with white volcanic ash forming liquefaction structures within the silts. Contains abundant diatoms at the base, their number diminishing towards the top, increasing organic material content, and fragments of Purepecha pottery.

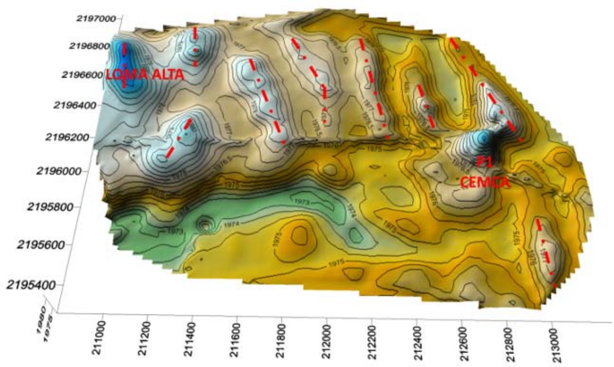

Fig. 3: Digital elevation model for the Las Lomas area showing the geometry and the points taken for previous studies.

Paleoseismic structures

At least 4 of the 6 units described have some kind of structure related to ancient seismic activity. The main types of structures belong to indirect indicators of A-type seismicity, such as liquefaction processes, deformation, landslides (slumps) and micro-faulting (Audemard *et al.*, 2011). Liquefaction structures are found in U1 and U6. A light gray ash in U1 is liquefied within diatomite layers. The average length of these structures is 5 cm and its maximum is 7 cm, with a probable age >39 000 years (Fig. 4A). In U6 we find liquefaction of light gray volcanic ash in silt-clay sediments with fragments of prehispanic pottery, prior to the reworked layers. According to literature on the zone, these events must have a magnitude M ≥ 5 (Obermeier, 1996; Rodríguez-Pascua, 1997). The deformation of the layers is registered in U2 and U5. U2 shows layers of dark gray volcanic ash of 13cm thick deformed-like rhythmic waves, the height of these waves is ~ 4 cm and the wavelength is ~ 10 cm (Fig. 4C). U5 has layers affected first by micro-faulting and then by deformation associated to load (Fig. 4D). Additionally we recorded fallen blocks (slumps) that mix U4, U5 and U6, possibly associated with other seismic events. We inferred at least four earthquakes, two of magnitude M ≥ 5 (liquefaction), and another that caused the deformation of sediments, is associated with the formation of Las Lomas and is also the last that generated the slumps and micro-faulting.

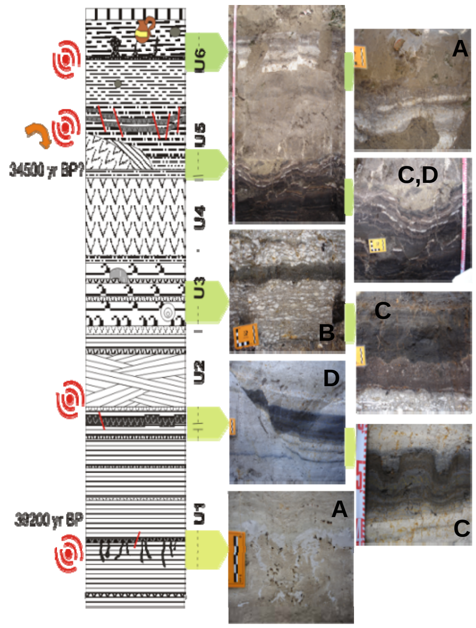

Fig. 4: Stratigraphic column and details of synsedimentary structures observed in the sedimentary record. A: Liquefaction, B: Ripples, C: Deformation, D: Micro-faulting.

DISCUSSIONS

At regional scale, the landscape shows evidence of active faulting characterized by scarps, emplacement of monogenetic volcanoes at different times and influencing the deposition of their lava flows. The microtopography of the area of Las Lomas suggests that its origin is related to a seismic event, whose wave could cause folding in NNW-SSE direction, which also lifted and deformed the sediments, creating enabling environments for human settlements, which in turn gradually changed the morphology of the hills, adding fillers and flats at several stages (Petrequin, 1994). The stratigraphic column has its oldest sediments of 39 200 yr BP ^{14} C and is made up of 6 lithological units in total, of which at least four have A-type structures that may be indirectly related to ancient seismic activity. The sedimentary record suggests at least 16 different volcanic episodes during the last 40 000 years, identified through fall deposits. The most influential event in the record corresponds to U4, which should be a local event, due to the thickness of the deposit. The obvious deformation of the lake sediments suggests the existence of at least four seismic events, the oldest around 40 000 years BP and the most recent set in a period of occupation by Purepecha culture. The main evidence recorded was generated by the side effects of such events and have been divided into: liquefaction structures, deformation, micro-faulting and landslides (slumps). For 2 of the 4 events a minimum magnitude of 5 was inferred, based on earlier works. These results reinforce the idea that the sedimentary record of Zacapu is controlled by both ancient and recent tectonics.

Acknowledgements: this project has been development thanks to CONACyT founds.

REFERENCES

Álvarez J. (1972). Ictiología Michoacana V. Origen y distribución de la Ictiofauna Dulceacuícola de Michoacán. *An.Esc.Nac.Cienc.Biol.Mex. 19.* 155 – 161.

Antaramián HE, G Correa. (2003). Fisiografía. In: *Correa G. 2003. Capítulo II: Geografía Física. Atlas Geográfico del estado de Michoacán.* UMSNH Colmich. SEP, Michoacán EDDISA S.A. 2 ed. 454 pp.

Arnauld C, SE Metcalfe, P Petrequin. (1997). Holocene climatic change in the Zacapu lake basin, Michoacán: Synthesis of Results. *Quaternary International*. 43/44. 173 – 179.

Audemard M FA, Michetti AM, McCalpin JP. (2011). Geological Criteria for Evaluating Seismicity Revisited. Forty Years of Paleoseismic Investigations and the Natural Records of Past Earthquakes. The Geological Society of America. Special Paper 479 .U.S.A.

Davies SJ, SE Metcalfe, AB MacKenzie, AJ Newton, GH Endfield, JG Farmer. (2004). Environmental changes in the Zirahuen Basin, Michoacan, Mexico, during the last 1000 years. *Journal of Paleolimnology* 31: 77 – 98.

Demant A, JN Labat, D Michelet, J Tricart. (1992). El Proyecto Michoacán 1983 – 1987. Medio ambiente e Introducción a los trabajos arqueológicos. *Cuadernos de Estudios Michoacanos 4*. 197 pp.

Fisher CT, HP Pollard, I Israde Alcántara, VH Garduño Monroy, S Banerjee. (2003). A reexamination of human induced environmental change within the Lake Patzcuaro Basin, Michoacan, Mexico. *Proceedings of the National Academy of Sciences.* 100 (8): 4957-4962.

Gómez-Tuena A, T Orozco-Esquivel, L Ferrari. (2005). Petrogénesis Ígnea de la Faja Volcánica Transmexicana. *Bol. Soc. Geol. Mex.* Volumen Conmemorativo del Centenario. Selected issues of mexican geology. LVII (3): 227-285.

Israde-Alcántara I, VH Garduño – Monroy. (1999). Lacustrine record in a volcanic intra arc setting: the evolution of the late Neogene Cuitzeo basin system (central – western Mexico, Michoacan). *Palaeo* 151: 209 – 227.

Israde-Alcántara I, VH Garduño Monroy, CT Fisher, HP Pollard, MA Rodríguez Pascua. (2005). Lake level change, climate, and the impact of natural events: the role of seismic and volcanic events in the formation of the lake Patzcuaro Basin, Michoacán, Mexico. *Quaternary International* 135: 35 – 46.

Medina Nava M. (1993). Ictiofauna de la subcuenca del río Angulo, cuenca Lerma. Professional *Thesis.* Fac. Biología. UMSNH. México. 146 pp.

Metcalfe SE, RB Brown, PE Hales, RA Perrott, FM Steininger, FA Strett – Perrott. (1989). Late Holocene Human Impact on Lake Basins in Central Mexico. *Geoarchaeology International Journal.* 4(2): 119 – 141.

Metcalfe SE, FA Street – Perrott, SL O´Hara, PE Hales, RA Perrott. (1994). The Paleolimnological Record of Environmental Change: Examples from the Arid Frontier of Mesoamerica. In: *Environmental Change in Drylands: Biogeographical and Geomorphological Perspectives.* Edit. AC Millington, K Pye. 131 – 145.

Metcalfe SE. Changing Environments of the Zacapu basin, Central Mexico: a diatom – based history spanning the last 30 000 years. School of Geography and Earth Resources, University of Hull, Hull HU6 7RX.

Obermeier SF. (1996). Use of liquefaction-induced features for paleoseismic analysis: An overview of how seismic liquefaction features can be distinguished from other features and how their regional distribution and properties of source sediment can be used to infer the location and strength of Holocene paleoearthquakes. *Engineering Geology.* 44. 1 – 76.

O'Hara SL, F Alayne SP y TP Burt. (1993). Accelerated soil erosion around a Mexican highland lake caused by prehispanic agriculture. *Letters to Nature.* 362: 43 – 46.

Ortega B, C Caballero, S Lozano, I Israde, G Vilaclara. (2002). 52 000 years of environmental history in Zacapu basin, Michoacan, Mexico: the magnetic record. *Earth and Planetary Science Letters.* 202. 663 – 675.

Park J, R Byrne, H Böhnel, R Molina-Garza, M Conserva. (2010). Holocene climate change and human impact, central Mexico: a record based on maar lake pollen and sediment chemistry. *Quaternary Science Reviews.* 29. 618 – 632.

Petrequin P. (1994). 8000 años de la Cuenca de Zacapu. Evolución de los paisajes y primeros desmontes. *Cuadernos de Estudios Michoacanos 6*. 144 pp.

Rodríguez-Pascua MA. (1997). Paleosismicidad en emplazamientos nucleares. Estudio en relación con el cálculo de peligrosidad sísmica. *Consejo de Seguridad Nuclear.* Colección Otros Documentos. 286 pp.

Rodríguez-Pascua MA, VH Garduño-Monroy, I Israde-Alcántara. (2004). Evidencias paleosísmicas en fallas activas y sedimentos deformados del Lago de Pátzcuaro, Jarácuaro, Michoacán, México. *Geotermas* 6 (3): 151-154.

Street – Perrott FA, RA Perrott, DD Harkness. (1989). Anthropogenic soil erosion around lake Pátzcuaro, Michoacán, México, during the Preclassic and Late Postclassic – Hispanic periods. *American Antiquity.* 54(4): 759 – 765.

Tricart J. (1992). La Cuenca Lacustre de Zacapu: Un acercamiento geomorfológico. En: *El Proyecto Michoacán 1983 – 1987. Medio ambiente e Introducción a los trabajos arqueológicos. CEMCA 4*. 115 – 197.

Watts AW y JL Bradbury. (1982). Paleoecological studies at Lake Pátzcuaro on the West-Central Mexican Plateau and at Chalco in the Basin of Mexico. *Quaternary Research* 17: 56-70.

Xelhuantzi López MS. (1994). Estudio palinológico de cuatro sitios ubicados en la cuenca de Zacapu: Fondo de la ciénega, Contacto loma – ciénega, Pantano interno y Loma alta. *Cuadernos de Estudios Michoacanos,* CEMCA. Vol. 6: 81 – 94.

PALEOSEISMOLOGY & ARCHAEOSEISMOLOGY
MORELIA • MEXICO 2012
INQUA-TERPRO PALEOSEISMOLOGY
EARTHQUAKE ARCHAEOLOGY
IUGS UNESCO IGCP 567

QUANTITATIVE EVALUATION OF HISTORICAL EARTHQUAKES ON THE MEXICAN VOLCANIC BELT

Gerardo Suárez (1), Gema V. Caballero-Jiménez (2)

(1) Instituto de Geofísica, Universidad Nacional Autónoma de México (UNAM), México D.F., gerardo@geofisica.unam.mx
(2) Posgrado en Geofísica, Instituto de Geofísica, UNAM, Mexico D.F., gingin1883@yahoo.com.mx

***Abstract* (Quantitative Evaluation of Historical Earthquakes on the Mexican Volcanic Belt):** *The historical record of earthquakes in Mexico for the past 450 years shows that several large earthquakes have occurred along the Trans Mexican Volcanic Belt. During the instrumental period, two large earthquakes produced severe damage and a high number of casualties: the 1912 Acambay (M_w6.9) and the 1920 Jalapa (M_w6.4) earthquakes. The latter caused over 700 casualties; the victims mostly perished under the mud landslides triggered by the strong shaking. Other important examples of large, crustal earthquakes exist in the historical record. Notable examples of these are the earthquakes in 1569 to the west of Lake Chapala and the 1875 event, which apparently took place to the northwest of the city of Guadalajara. Paleoseismological studies have shown that some of the faults mapped on the volcanic belt are seismically capable. The Acambay fault, for example, shows a recurrence period of approximately 3,600 years (Langridge et al, 2000). Using the method developed by Bakun and Wentworth (1997) we estimated attenuation curves for intensity values on the Modified Mercalli Intensity scale (MMI). The curves of attenuation of Mercalli intensity as a function of distance of the epicenter were estimated using the Acambay and the Jalapa earthquakes as calibration events, considering that the magnitude of both events is instrumentally determined. A catalog of intensity data points (IDP) was obtained for the more important historical earthquakes on the Mexican Volcanic Belt based on the historical reports of earthquakes published by García Acosta and Suárez (1996). The data were geo-referenced and an intensity value was assigned to each IDP. In the inversion process, the calibration curves of intensity as a function of distance were used to determine the epicentral location and the magnitude of the more important events on the Mexican Volcanic Belt. Our results indicate that in the past 450 years there has been a considerable seismic moment release produced by this type of crustal earthquakes, which should be taken into account in seismic hazard and seismic risk estimates.*

***Key words**: TMVB, historical earthquakes, magnitude estimation*

EVALUATION OF MAGNITUDE USING MACROSEISMIC DATA OF HISTORICAL EARTHQUAKES.

The need to compile homogeneous and complete earthquake catalogs and to evaluate the seismic hazard of seismically active areas has lead to quantitatively estimate the magnitude and epicentral location of earthquakes occurring prior to the instrumental record. The estimation of magnitude for these historical earthquakes for which only macroseismic data exists, allows extending the seismic record for several centuries. In the case of Mexico, historical accounts of earthquakes exist since the XV century (García Acosta and Suárez, 1996).

Traditionally, magnitude has been estimated from macroseismic data in a qualitative manner, comparing the intensity data with that of recent earthquakes for which the magnitude is known. In other cases, the magnitude has been estimated measuring the area of isoseismal curves and calibrating them with earthquakes of known magnitude. The drawback of this method is that often the intensity data is of insufficient coverage to accurately draw isoseismal curves with a good degree of accuracy.

Several methods have been proposed to assess in a quantitative manner the location and magnitude of historical events. Among these contributions are those of Sibol et al. (1987), Bakun and Wentworth (1997), Gasperini et al. (1999) and Musson et al. (2008). Bakun et al. (2011) have compared these various methods in estimating the magnitude and location of earthquakes in Italy. In this paper, we propose to use a quantitative approach developed by Bakun and Wentworth (1997), which has been applied successfully by various authors in different regions of the world.

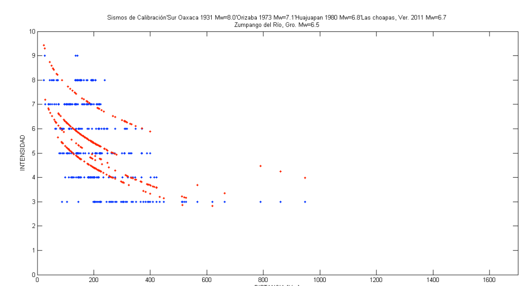

Fig. 1: Plots of modified Mercalli intensity as a function of distance for in-slab events in Central Mexico. The earthquakes used are the 1931 event in Oaxaca, 1973 Orizaba, 1980 Huajuapan, 2011 Las Choapas and Zumpango del Río.

The methodology suggested by Bakun and Wentworth (1997) consists in estimating the attenuation of intensity as a function of distance for earthquakes of various magnitudes. The magnitude used is the Modified Mercalli Intensity (MMI). These attenuation results are then used in a formal inversion to estimate, in a grid search, the magnitude and location of historical earthquakes, minimizing the errors in a least squares sense. The main advantage of this method is that each individual intensity data point (IDP) is used individually.

In the case of Mexico, the seismicity in the southern part of the country was divided into three different families: earthquakes associated with the subduction zone along the Pacific coast of Mexico; in-slab events which occur within the subducting Cocos or Rivera plates at depths that range from 40 to 180 km; and crustal earthquakes that take place along the Trans Mexican Volcanic Belt (TMVB).

For each of these three seismic regions an attenuation of intensity as a function of distance was constructed using earthquakes with known instrumental magnitude and location, for which the intensity data was obtained. Figure 1 shows the intensity attenuation as a function of distance for the selected family of calibration earthquakes of in-slab events.

Crustal events in the TMVB are less frequent. Figure 2 shows the calibration of intensity versus magntide using the 1912 Acambay and 1920 Xalapa earthquakes. Currently, we are collecting data form other earthquakes on or near the TMVB, in order to improve the quality of the calibration of intensity *vs*. distance.

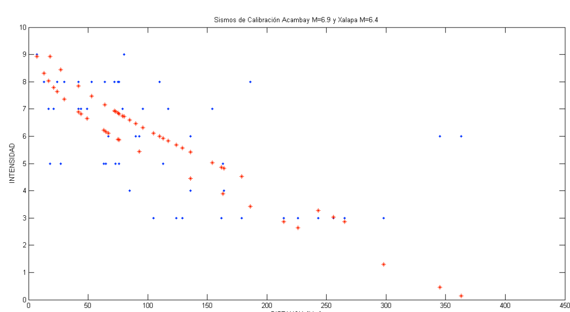

Fig. 2: Plots of modified Mercalli intensity as a function of distance crustal earthquakes along the TMVB. In this case, the 1912 Acambay and 1920 Xalapa earthquakes were used as calibration events.

HISTORICAL EARTHQUAKES ALONG THE TMVB

The most significant earthquakes on the TMVB were selected from the catalog of García Acosta and Suárez (1996). The macroseismic information for each individual earthquake was analyzed and intensity in the MMI scale was assigned for each city or location. All locations indicating that the earthquake was felt or where damage is reported were geo-referenced using the information provided by INEGI. In many cases, the name of locations has changed over the years. An investigation was conducted to locate these older names in the current almanac of towns and cities of Mexico.

Each location for which intensity data was assigned is called an IDP. The resulting list of IDP's was analyzed and the most significant events were used to conduct this first study.

Among the earthquakes selected are the event that caused widespread damage in western Mexico in 1569. Suárez et al. (1994) estimated the magnitude of this earthquake in a qualitative manner as $M_w 7.1$. This would make it the largest event recorded to date in the TMVB. Thus the interest in defining the magnitude and location in a more quantitative manner using the relatively well distributed intensity data. Other significant earthquakes studied are the event of 1875 that took place to the west of the city of Guadalajara, for which adequate intensity data exists also.

One of the more puzzling events in the historical record is the earthquake of 19 June 1858. Singh et al. (1996) interpreted this event as an in-slab event beneath the central part of Mexico, similar to the earthquakes that regularly take place in this part of Mexico. Nonetheless, the location selected by Singh et al. (1996) does not explain the very large intensities observed in the central part of the state of Michoacán, México. Our preliminary results suggest that this earthquake was a crustal event that took place along the TMVB, causing severe damage in the towns and cities of northern Michoacán.

The final objective of this work is to compile a list of earthquakes for which a reasonable number of well-distributed IDP's exist for historical Mexican earthquakes, putting emphasis on events located on the TMVB. The goal is to complete the seismic catalog of Mexico with recalibrated magnitudes and locations, extending it as far back as possible. Results obtained for the more significant earthquakes on the TMVB will serve to improve our knowledge of the seismic history in this part of the country where the largest concentration of population is established today.

It is possible that our lack of knowledge of the historical record has hampered an adequate estimation and evaluation of the seismic hazard that exists in this part of the country.

Acknowledgements: This project has been supported by a grant from the Consejo Nacional de Ciencia y Tecnología (CONACYT) number 082821 and with partial support by the Instituto de Geofísica, UNAM.

References

Bakun, W. H. and C. M. Wentworth, Estimating Earthquake location and magnitude from seismic intensity data, *Bulletin of the Seismological Society of America,* 87 (6), 1502-1521.

Bakun, W. H. A.A. Gómez Capera and M. Stucchi. 2011. Epistemic uncertainty in the location and magnitude of earthquakes in Italy from macroseismic data, *Bull. Seismol. Soc. Am.*, 100, doi:10.1785/01200110118.

García Acosta, V. and G. Suárez, 1996. Los sismos en la historia de México, Vol. 1, FCE-UNAM-CIESAS, Mexico, 718 pp,.

Gasperini, P., F. Bernardini, G. Valensise and E. Boschi. 1999. Defining seismogenic sources from historical earthquakes felt reports, *Bull. Seismol. Soc. Am. Bull.,* 89, 94-110.

Langridge R., Weldon R.J.II Moya J.C. and Suárez G. 2000., Paleoseismology of the 1912 Acambay earthquake and the Acambay-Tixmadejé fault, Trans-Mexican Volcanic Belt., *J. Geophys. Res.*, Vol. 105 No. B2, 3019-3037, 2000.

Sibol, M.S., G. A. Bollinger, and J.B. Birch. 2007 Estimation of magnitudes in central and eastern North America using intensity and felt area, *Bull. Seism. Soc. Am.*, 77, 1635-1654.

Singh, S.K., M. Ordaz and L.E. Pérez-Rocha. 1996. The great Mexican earthquake of June 19 1858: Expected ground motion and damage in Mexico City from a similar future event, *Bull. Seismol. Soc. Am.,* 86, 6, 1655-1666.

Suárez G., García-Acosta V. and Gaulon R. 1994. Active Crustal Deformation in the Jalisco Block, Mexico: Evidence of a Great Historical Earthquake in the XVI Century, *Tectonophysics*, 234, 117 - 127, 1994.

PALEOSEISMOLOGY & ARCHAEOSEISMOLOGY
MORELIA • MEXICO 2012
INQUA-TERPRO PALEOSEISMOLOGY
EARTHQUAKE ARCHAEOLOGY

ANALOGUE MODEL OF THE SAN PEDRO VOLCANO IN THE ACAMBAY GRABEN (MÉXICO)

Suñé Puchol, Ivan (1), Lacan, Pierre (1), Zuñiga, Ramón (1), Cerca, Mariano (1), Aguirre-Díaz, Gerardo (1) y Ortuño, Maria (2)

(1) Centro de Geociencias (CGEO), Campus Juriquilla, Querétaro de la Universidad Autónoma de México, UNAM.
ivanbatea@gmail.com; placan@geociencias.unam.mx ; ramon@geociencias.unam.mx ; mcerca@geociendias.unam.mx
(2) RISKNAT group: Dept. Geodinàmica i Geofísica. Universitat de Barcelona (Spain) C/Martí i Franquès s/n. 08028-Barcelona
maria.ortuno@ub.edu

Abstract (Analogue model of the San Pedro volcano in the Acambay Graben): We present here preliminary results of analogue modeling of the structural evolution of the San Pedro Volcano within the Acambay Graben. Most of the growth of the volcano took place at the beginning of the opening of the graben. Accordingly, the volcano is traversed by various faults that are considered active. The preliminary results of the analogue modeling are promising and give us a better understanding of (1) the influence of the volcanic edifice on the geometry of the faults, (2) reciprocal influence between the location of the faults and the volcanic structure, and (3) the location of the regional collapse of the volcano flanks.

Key words: *Analogue Modelling, Acambay Graben, San Pedro Volcano and Collapse.*

INTRODUCTION

The Acambay Graben is located in the Trans Mexican Volcanic Belt. It is limited to the south and to the north respectively by the Pastores and Acambay-Tixmadejé active normal faults. In its central part, it is cut by a system of small faults and volcanic edifices partially affected by the faulting. The relation and the mutual influence between the faults and the volcanic edifices were unclear until now.

Considering the present-day tectonic activity in the graben, it is important to characterize the evolution of the faults within it. To do that, we propose to study the system faults/volcanoes in its entirety using analogical Modelling to test the interaction that occurred between the weight of the volcanic edifice, the location and distribution of the fault and their activity.

Analogue models were carry out in the LAMMG laboratory of the Centro de Geociencias (UNAM) which focus on testing the evolution of a graben and the influence of a volcanic edifice in the location of the faults and the faults development.

Analogue models are a good tool to study and characterize the evolution of geological structures in the laboratory. They can simulate in a few hours geological processes that take place over several million years. The analogue modelling allows us to investigate the influence of different parameters (such as strain rate, rheology, kinematics) as well as analyze the evolution in 4D in detail. These experiments are still ongoing and here we present some preliminary results that seem promising.

THE SAN PEDRO VOLCANO IN THE MEXICAN VOLCANIC BELT

The San Pedro Volcano (SPV, also known as Temascalcingo Volcano) is located between the towns of Temascalcingo and Acambay, in the State of México (**Fig. 1**). The SPV is an andesitic-dacitic stratovolcano, apparently of Pliocene Age (*Roldan-Quintana et, al. 2011*), with a summit caldera and affected by several normal faults of the Acambay Graben (Aguirre-Diaz & McDowell, 1999).

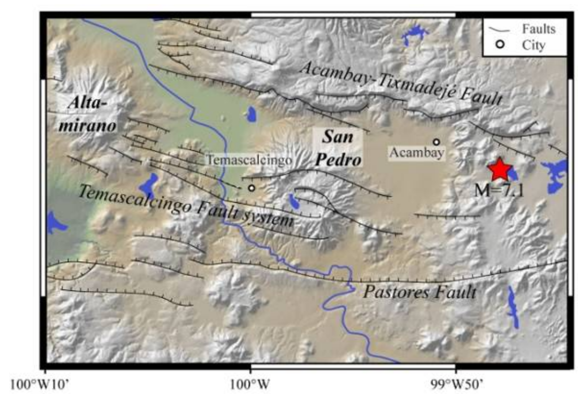

Fig. 1: Geologic and geographic context of San Pedro volcano within the Acambay graben and the boundary faults. The study area is in the eastern section of a several grabens along the MVB (Mexican Volcanic Belt). The red star represents the location of the Acambay 1912 earthquake.

The Acambay Graben is located in the Mexican Volcanic Belt (MVB), which is an E-W volcanic arc (Verma, 1996) associated to the subduction of the Cocos and Rivera plates under the Northamerican plate. The MVB traverses the central part of Mexico from the Pacific Coast to the Gulf of Mexico and is active since the Late Miocene (Ferrari et al., 1999a;b; Ferrari, 2000). Neotectonic activity along the MVB has led to a series of grabens and semigrabens, structure and kinematics of its faults have been studied by many authors (e.g. Urbina y Camacho 1912; Mooser y Ramírez-Herrera, 1989; Ramirez-Herrera 1994; Ferrari et al., 1994; Johnson y Harrison, 1990; Ramirez Herrera et al 1998; Alaniz-Álvarez et al., 1998; Langridge et al. 2000; Suter et al. (2001).

The faults near SPV (within the Acambay Graben) affect volcanic materials of Neogene and Quaternary Age, such a cinder cones, domes and lavas (basalt, andesite and rhyolite). Also fall deposits and ignimbrites (Aguirre et al., 2008; Garduño et al., 2009). The younger materials that have been cut by SAM (Acambay-Morelia system faults) are fluvial-lacustrine Plio-quaternary fillings sediments, and the older are cretaceous rocks metamorphosed (Suter et al., 1992; 1995; Ramírez-Herrera et al., 1994; Langridge et al., 2000).

Active faults

Many authors (like Suter, Langridge, Ortuño, etc.) can distinguish only 5 faults with activity during the late Quaternary-Holocene, Acambay-Tixmadeje, Temascalcingo and Pastores fault are included (Urbina and Camacho, 1913, Langridge et al 2000). These faults are delimiting the Acambay graben from the north to the south, respectively, and the Temascalcingo fault is in the middle and cutting the San Pedro volcano (**Fig. 2**). These are the only faults with evidences of historical rupture In Central Mexico. According to Urbina and Camacho (1913), both faults (Acambay and Pastores) broke up the surface during the earthquake of Acambay (1912). The interpretation of data led to Suter et al . (1995) to propose the length of the surface rupture as 41 km for the Acambay fault and around 20 km of length for the Temascalcingo fault.

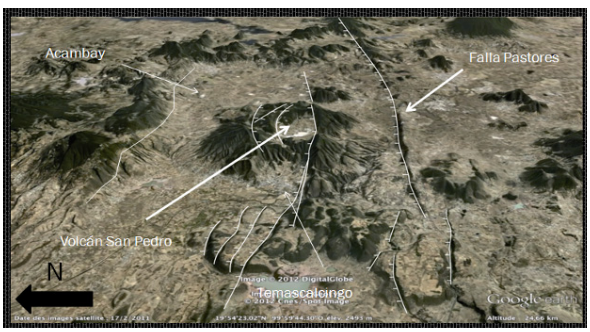

Fig. 2: Acambay graben seen from the west, bounded on the north by the Acambay-Tixmadeje fault, on the south by the Pastores fault and in the middle is placed the cone of San Pedro volcano, cut by the Temascalcingo fault.

Paleosismological studies allowed Langridge et al. (2000) to identify four Holocene ruptures with an average vertical displacement of 60 cm in Acambay-Tixmadeje fault, with a recurrence period of 3600 years and a vertical displacement rate of 0.17 mm/y. Urbina and Camacho, (1913), quantify the vertical displacements in Temascalcingo fault about 30 cm. Another study performed by Persaud et al. (2006) showed a seismic event in the Pastores fault with a minimum displacement of 35-50 cm occurred 21-28 ka ago, as a result of a vertical displacement rate of 0.02 mm/a.

ANALOGUE MODEL

To model the aperture of a tectonic depression (or graben) by extensional stress we use a table with two verticals walls, one of them is fixed and the other one is mobile. Between the walls, different layers of silicone and sand are employed to model the continental crust.

Different models of upper crust composition and deformation rates were performed to fit the lithologies and deformations observed on the field. Here we present two models that match the observed deformation and allow us to test various hypotheses of evolution of faults and the volcanic edifice.

Model 1

In the Model 1, we used 1 cm thickness layer of silicon to simulate the base of the crust which has a ductile behavior (1 in **Fig. 3**). Above the silicon we add 5 cm thick layer of quartz sand, in red and white interspersed layers, (2 in **Fig. 3**). Quartz sand is optimal to scale the cohesion of the upper brittle crust. The dimensions in surface are 30 x 35 cm (also properly scaled, 1km reality = 1 cm in the model).

The Model 1 is then subjected to an extension of ~0.9 cm/h concordant with the velocity, at scale, known in the region. In a couple of hours, the extensional stress start to generate several faults conforming a depression. At this moment a cone of silt is added to the model simulating the SPV (into the new tectonic basin and without interruption of the extension, 3 in **Fig. 3**). The extension carried on for 3 hours more so the resulting time to drive the Model 1 was 5' 15".

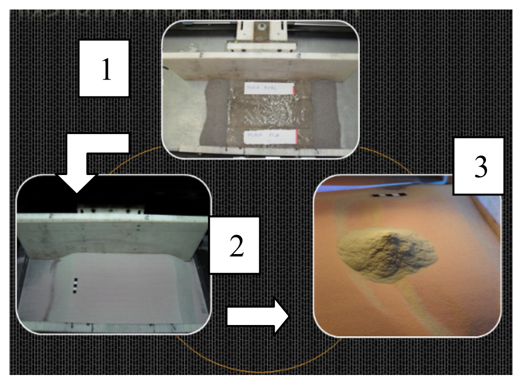

Fig. 3: Construction of the model 1 in three stages. A base ductile with silicon, quartz sand to the superior crust and a cone of silt simulating a volcano.

Model 2

The main differences in the second set up are the layer of quartz sand (now 4 cm thick and black and white colors'), also the dimensions of the Model 2 are quite different, the area now is 35 x 35 cm. The new velocity of extension is ~1 cm/h and the total time of extension is just 4 hours now. About the cone added to simulate the SPV, the new material is sand.

Videos of the different models have been performed to illustrate the structural evolution of the volcanic edifice during the extensive phase.

RESULTS

Figure 4 shows the final phase of the Model 1 in comparison to a DEM (Digital Elevation Model) of the Temascalcingo zone (below).
Look the similarities between the analogue model and the real structures:
- Parallel faults to define the graben.
- Regional collapse of a volcano flank (such is W flank, where is situated the city of Temascalcingo, *Roldan-Quintana et, al. 2011*).
- The traces of the faults are semi-circular in both, model and DEM.
- The silicone escapes through weak spots on the sides of the cone of the model (which coincides with the domes and Mount St, Lucia around the SPV, represented by yellow rings in **Fig. 4**).

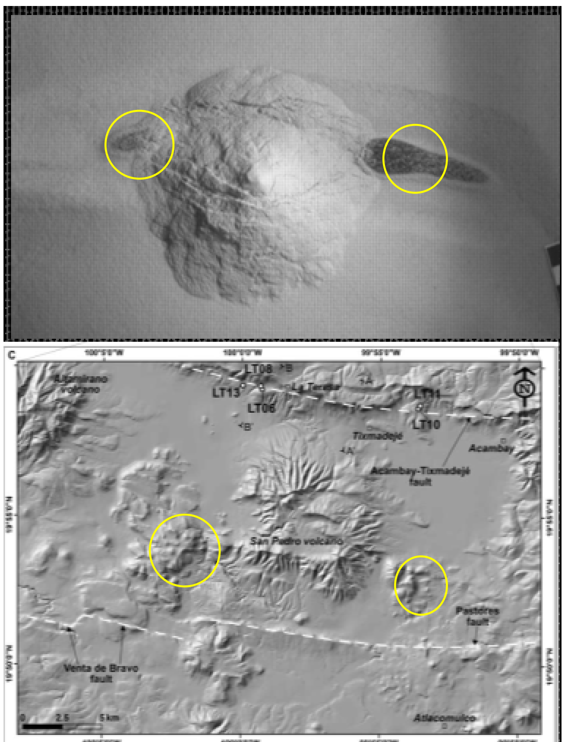

Figura 4: Superior photography shows the final results of the analogic model of the Acambay graben and San Pedro Volcano (Model 1), under that there is a DEM of the study area in Temascalcingo locality.

In the Model 2, the boundary faults of the graben are parallel as well, and the faults that cut the volcano are semi-circular like in the Model 1, but there is less number of cutter faults (just 2, one for each basement fault). White and black sand allowed us to better define the internal structure than in the model 1, and realize the continuity of basement faults along the volcano. Unlike the Model 1, in this second set up there is no sector collapse of a flank, however, the silicon escapes at the same points than in the model 1.

DISCUSSIONS AND CONCLUSIONS

Comparing the results of the two models, we conclude that there is a significant interaction between the faults of the graben and the volcanic edifice, since the semi-circulars traces of the faults cut along the volcano due the conic geometry of the volcano, while the graben faults are straight. Our interpretation about the structural geology of this area is due a deep fault at the basement (Temascalcingo fault) which is transmitted continuously on the flank of SPV, while others antithetical faults are cutting another flank.

Another observation to support a reciprocal influence between volcano and graben is given by the silicon, since it escapes on the sides of the volcano and just above the central fault, because those are weak spots created by the weight of the volcano and the discontinuity caused by the fault.

The results depend on the material that we use in the model. For example, the cone added in the model 2 was quartz sand (cohesion lower than silt used in the model 1) and didn't get any regional collapse and didn't break so many faults along the volcano like the first test. This collapse is produced by an instability caused during the extension.

This experiment help us to interpret the mechanics of faults that cut the volcano San Pedro, in Temascalcingo (Mexico), and we can verify our hypotheses regarding the evolution of deformation and geometry of the structures based on previous field work.

This work does not end here, and after seeing such interesting results obtained, we believe it is necessary to learn more about the relationship between active faults and volcanic environment. In the Acambay Graben there is a real seismic hazard, and these works and their dissemination assist in reducing the population vulnerability.

Acknowledgements: I am very grateful to my teachers in CGEO, who helped me to do this work (such R. Zuñiga, M. Marzo and P. Lacan), also I want to thank to my friend and student colleague Rodrigo Portillo. I dedicate this work to Maria Ortuño, because she trusted me since the first day.

References

Aguirre-Díaz, G.J., Labarthe-Hernández, G., Tristán-González, M., Nieto-Obregón, J., Gutiérrez-Palomares, I., " Ignimbrite Flare-up and graben-calderas of the Sierra Madre Occidental, Mexico: in J. Gottsmann and J. Martí, eds., "Caldera Volcanism: Analysis, Modelling and Response", Developments in Volcanology 10, Elsevier, Amsterdam, 492 p., (143-180 pp.), 2008.

Alaniz-Alvarez S.A, Nieto-Samaniego A. F., Tolson A., "A graphical technique to predict slip along a pre-existing plane of weakness" Engineering Geology 49 (1998) 53-60.

Ferrari L. "Avances en el conocimiento de la Faja Volcánica Transmexicana durante la última década". Boletin de la Sociedad Geológica Mexicana, V.LIII (2000) 84-92.

Garduño-Monroy V. H., Pérez-Lopez R., Israde-Alcantara I., Rodriguez-Pascua M.A., Szynkaruk E., Hernandez-Madrigal V. M., Garcia-Zepeda M. L., Corona-Chavez P., Ostroumov M., Medina-Veja V.H., Garcia-Estrada G., Carranza O., Lopez-Granados E. y Mora-Chaparros J.C., "Paleoseismology of the southwestern Morelia-Acambay fault system, central México." Geofísica Internacional 48 (3), 319-335 (2009).

Jonhson C. A. and Harris C. G. A., "Neotectonics in Central Mexico", Elsevier Science Publishers B.V., Amsterdam, Physics of the Earth and Planetary Interiors, 64 (1990) 187-210

Landgridge R.M., Weldon R. I., Moya J.C., and Suaréz G., "Paleoseismology of the 1912 Acambay earthquake and the Acambay-Tixmadejé fault. Trans-Mexican Volcanic Belt", Journal of Geophysical Research vol. 105, NO. B2, PAGES 3019-3037, February 10, 2000.

*Mooser, F. and Ramírez-Herrera, M. T., 'Faja Volcánica Transmexicana: Morfoestructura, tectónica y vulcanotectónica', Boletin Sociedad Geológica Mexicana (1989) T. XLVIII, **2**, 75–85.*

Norini G., Capra L., Borselli L., Zuñiga R., and Sarocchi D., "Large scale landslides triggered by Quaternary tectonics in the Acambay graben, Mexico" , Earth Surface processes and Landforms (2010).

Ortuño, C.M., Zúñiga, R., Aguirre-Díaz, G.J., Carreón-Freyre, D.,Cerca-Martínez, M., Mendoza-Ponce, A., López-Briseño, E.,2010, Avances en la paleosismología de las fallas del graben de Acambay (abstract), en Reunión Anual de la Unión Geofísica Mexicana 2010: GEOS, 30(1) p. 88.

Portillo-Pineda R., "Estructura y cinemática de la apertura del Golfo de California, por medio de experimentos Fisicos de extensión cortical y litosférica" UNAM, tesis de Maestria Centro de Geociencias (2012).

Ramírez-Herrera M. T., "Tectonic Geomorphology of the Acambay graben, Central Mexican Belt", tesis de Doctorado, University of Edimburgh, 1994.

Roldan-Quintana, J., Aguirre-Diaz, G. and Rodriguez-Castañeda J.L. " Depósito de avalancha de escombros del volcán Temascalcingo en el graben de Acambay, Estado de México, Revista Mexicana de Ciencias Geológicas, v. 28, núm. 1, 2011, p. 118-131

Sutter M., López-Martinez M., Quintero-Legorreta O. and Carrillo-Martinez M. "Quaternary intra-arc extension in the central Trans-Mexican volcanic belt" Geological Society of America, GSA Bulletin; June 2001; v. 113; no 6; p. 693-703.

*Verma, S. P.. 'Mexican Volcanic belt: Present state of knowledge and unsolved problems', Geof´ıs. Int., special volume on Mexican Volcanic Belt, 1987 **26**(3B), 309–340.*

Urbina F. y Camacho H., "Zona Megaseismica Acambay-Tixmadeje, estado de México". Instituto Geológico de México, Secretaria de Fomento, 1913.

PALEOSEISMOLOGY & ARCHAEOSEISMOLOGY
MORELIA • MEXICO 2012
INQUA-TERPRO PALEOSEISMOLOGY
EARTHQUAKE ARCHAEOLOGY

EVOLUTION OF THE PATTERN OF DRAINAGE IN THE ORIENTAL FOOTHILL OF ANDES AND HIS RELATIONS WITH THE QUATERNARY TECTONIC ACTIVITY (27º- 34º S AND 67°-70°W) ARGENTINA.

Suvires Graciela M. (1), Mon Ricardo (2), Gutiérrez Adolfo A. (3)

(1) National Council of Scientific and Technology Research, Argentina. National University of San Juan. Institute of Geology. San Juan. Argentina. Graciela_suvires@yahoo.com.ar
(2) National University of Tucumán. College of Natural Sciences and the Miguel Lillo Institute. Miguel Lillo 205, 4000 Tucumán, Argentina.ricardomon@arnet.com.ar
(3) National University of Tucumán. College of Natural Sciences and the Miguel Lillo Institute. Tucumán, Argentina.gutierrez.aa@hotmail.com

Abstract (EVOLUTION OF THE PATTERN of DRAINAGE IN THE ORIENTAL FOOTHILL OF ANDES And HIS RELATIONS WITH THE QUATERNARY TECTONIC ACTIVITY (27º- 34ºS AND 67°-70°W) ARGENTINA): *Neotectonic activity in the eastern Andean flank is found to the east of the magmatic arc of the Principal and Frontal Cordilleras, where a segment of around 1000 km has been studied in the western territories of the La Rioja, San Juan, and Mendoza provinces (Argentina). Spatial analysis of the drainage system facilitates the establishment of relationships between drainage pattern morphology and the presence of tectonic obstacles. The mains obstacles that have been recognized and that have also produced river diversions are magmatic bodies and structural highs.* Late Cenozoic structural features like High of *Médanos Grandes*, Mendoza Norte, and *Cerrilladas Pedemontanas*. They are main structures that were produced by the most recent Quaternary surface deformation. The ages of these controls of the drainage pattern decrease from N to S and from W to E.

Keywords: Quaternary tectonic activity; Evolution of drainage system; Central region of Argentina.

INTRODUCTION

This paper present a brief summary which focuses on the tectonic drivers of the spatial evolution of the drainage system of the central Andes between 27º S and 34º S. The Quaternary tectonism on the western edge of South America is reflected in the evolution of the drainage pattern of the eastern flank of the Andes and the adjacent foreland basin. As frequently occurs in the forelands of young, tectonically active orogens, the rivers that run along the mountain flank are diverted and concentrated by obstacles of tectonic origin into a smaller number of rivers (Gupta 1997; Mon 2005). In the central Andes, this process has special relevance. The geometry of the subduction of the Nazca plate below the South American plate controls the Quaternary deformations and the topography of the Andean Ranges, which extends for more than 8000 km along the edge of South America between 4° S and 46° 30´ S (Costa et al., 2006).The area considered is found on a subduction section of a very low angle between 5º and 10º, located between 27º S and 33º S. On the other hand it has an angle close to 30º between 18º S and 27º S similar to that of the southern region at 33º S (Ramos, 1996, Ramos *et al*., 2002, Lavenu, 2006, Alvarado *et al*., 2007). Neotectonic activity in the eastern Andean flank is found to the east of the magmatic arc of the Principal and Frontal Cordilleras, where a segment of around 1000 km has been studied in the western territories of the provinces of La Rioja, San Juan, and Mendoza (Argentina).Spatial analysis of the drainage system facilitates the establishment of relationships between drainage pattern morphology and the presence of tectonic obstacles. The most significant traits of this region are the Frontal and Principal Cordilleras. These ranges reach altitudes that exceed 6000 m, including the Aconcagua at 6959 m.a.s.l. (32° 39´S, 70°01´ W) in the Principal Cordillera and the Toro at 6168 m.a.s.l. (29º 08`38”, 69º47`50”) in the Frontal Cordillera. North of the 31º 15’ parallel, is the divide separating the drainage of the Pacific flank in the west from that of the Atlantic in the east. These high mountain ranges have a generally north-south orientation and are separated from the Precordillera by the Uspallata, Barreal, Calingasta, and, Iglesias valleys, a 350-km-long tectonic depression (Figs. 1a and 1b). The Bermejo valley separates the Precordillera from the Sierras Pampeanas. From north to south, the main river basins correspond to the Jáchal, San Juan, Mendoza, and Tunuyán rivers (Figs. 1a and 1b). Disconnected from the river valleys, there are small endorrheic basins represented by bogs, mud flat and salt pans that occupy tectonic depressions such as Gualilán, El Jumeal and Las Salinas mudflats. In large sectors the annual precipitation varies between 50 mm and 100 mm. Snowfall on the high peaks, toward the south constitutes the main water source and is the origin of the rivers in this region. As frequently occurs in the forelands of young, tectonically active orogens, the rivers that run through the mountain front are diverted and concentrated by obstacles of tectonic origin into a smaller number of rivers (Gupta op. cit,, Mon op.cit.). The central Andes of Argentina provide a particularly notable example of this phenomenon.This region experiences intense seismic and quaternary tectonic activity. Folds and faults that affect Pleistocene environment have been described by Cortés and Costa 1993, Cortés *et al.* 2006, and Martinez *et al.* 2008, among others. In addition, diversions and changes in the rivers have been observed even in historic times. The diversions of the rivers constitute an indirect indicator of tectonic activity, which is related to different young structures. The origin of this concentration is related to the progressive elevation of tectonic obstacles that have diverted, obstructed, and concentrated the rivers flowing through this part of the eastern Andean flank. Certain rivers must have run hundreds of kilometers from north to south before being able to open up to the east through weak zones of the mountain ranges that impeded their course. The obstacles that produce the diversions are of various kinds: cortical arching of long wavelength, steps related to exposed faults, flanks of regional scale folds, sheet edges raised by faults located on the opposite side of them or elevations of an undetermined origin that do not show visible relationships with faults. Along the edges of the mountain ranges, channels are controlled by back-thrust fault lines; for example, the western edge of the Precordillera (Damanti, 1993) controls the north-south course of the Blanco River and the Los Patos River (Fig.2). In other cases, the diversion is produced behind structures elevated by a fault, such as the north-south section of the San Juan River in the Tulum Valley. River diversion can be interpreted as the result of gradually rising mountainous barriers or the lateral growth of faulted belts or anticlines that propagate along blind faults like those observed in other sections of the Andes including northern Argentina (Mon *op.cit.).* Tectonic controls on the course orientations of large rivers have been recognized on all continents (Potter, 1978). Many obstacles are clearly related to visible structures on the surface but, in other cases, the uplift does not show an evident relationship with outcropping tectonic features like eastern foreland peaks. The headwaters of most of the rivers in the region are located in the high peaks of the Principal and Frontal Cordilleras, which divide the watersheds flowing to the Pacific and the Atlantic. Runoff is increasingly concentrated to the east of this divide on the Atlantic flank. In the westernmost strip, the Macho Muerto River, the Blanco River headwaters, the De La Sal River, and the Taguas River are blocked by a tectonic step (Falla El Cura) and concentrated into two courses: the Blanco River and El Cura River. Near the drainage divide to the south, the Falla Penitentes diverts various channels into the South Blanco River and the Los Patos River. Both faults El Cura and Penitentes have an elevated eastern block.

These tributaries feed major rivers; the Blanco River, Agua Negra stream and Iglesia stream flow into the Jáchal River, while the Castaño and Los Patos Rivers flow into the San Juan River. Both the Blanco and Los Patos Rivers represent examples of courses that must run hundreds of kilometers in the north-south direction before overcoming obstacles that impede their passage toward the east (Fig. 3).

The western border of the Precordillera), which is marked by the Uspallata - Barreal-Calingasta – Iglesia Valley represents a significant obstacle that has only been crossed by the largest collectors: the Jáchal, San Juan, and Mendoza rivers. The Jáchal River and the San Juan River are clearly antecedents. The Jáchal River crosses the Precordillera along a zone of weakness caused by a lateral ramp.

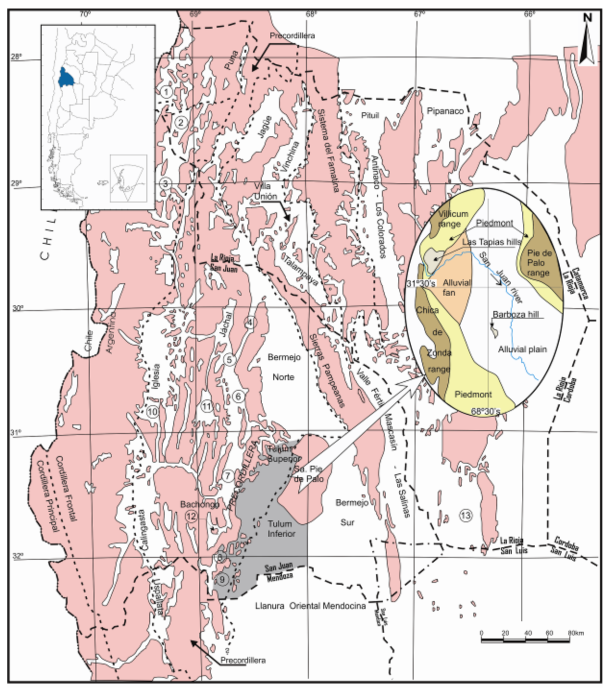

Fig. 1a.

QUATERNARY INTERMOUNTAIN DEPRESSIONS

1 Macizo del Potro
2 Río Blanco norte
3 Río Blanco
4 Huaco
5 Niquivil
6 Tucunuco - Matías Sanchez
7 Ullum - Zonda - Matagusanos
8 Pedernal
9 Acequión
10 Puchuzún
11 Gualilán
12 Bachongo
13 Chepes

Prequaternary outcrops
Tulum valley
Area with oval shape correspond to main oasis of San Juan city capital.

Finally, toward the east, the rivers that descend from the Frontal Cordillera and the Precordillera feed the Bermejo-Desagüadero system running parallel to the western front of the Sierras Pampeanas which, at these latitudes, constitute an insurmountable barrier for surface water. This system flows for more than 1000 km along this barrier before turning eastward and dumping its waters into the Colorado River.

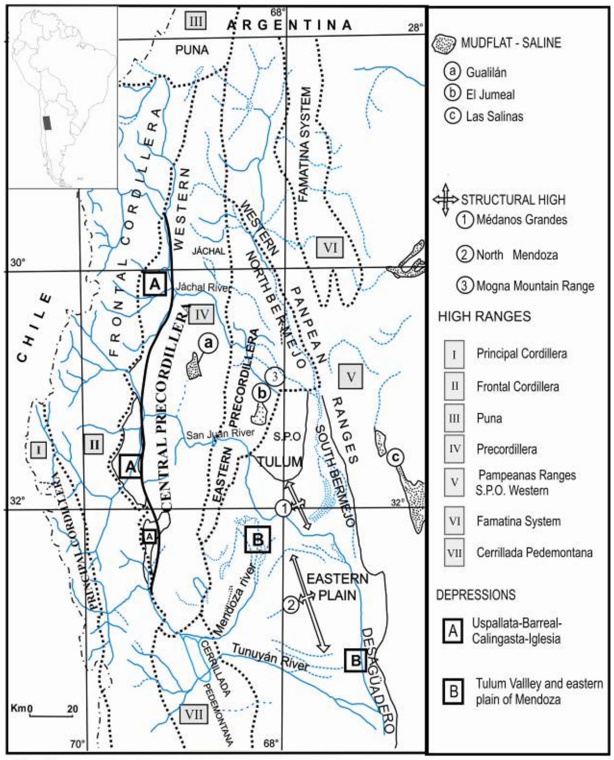

Fig. 1

The Bermejo Valley, the Tulum Depression and the eastern plain of Mendoza, which are situated between the Precordillera and the border of the Sierras Pampeanas, represent a current zone of high seismicity and pronounced tectonic activity. High rates of rise have been recorded for the surrounding mountains and confirmed by geodetic measurements. Rises of up to 1.2 meters have been recorded in the mountains of Pie de Palo range since the earthquake of 1977, which had a magnitude of 7.4 (Suvires *et al.*, 1995; Martínez *et al.*, 2008). In addition to the linear obstacles that have been described, there are positive buried structures that have also produced river diversions, including the high of Médanos Grandes and the structural high of Mendoza Norte – Tunuyán (Criado Roque *et al.*, 1981). These structures, along with the mountains of Pie de Palo, are probably recent obstacles associated with the ongoing deformation that is advancing towards the east. The Pie de Palo ranges are associated with a marked superficial seismic anomaly that is indicative of current activity and has been actively growing since 5-3 Ma (Siame *et al.*, 2006). This sector currently demonstrates the phenomena that have been operating throughout this section of the Andes during the last 20 Ma, diverting and concentrating the rivers that run towards the Atlantic.

The first obstacles to produce drainage concentration coincide with the steps related to the Penitentes and Cura Valley faults, which are located in a zone of high peaks in the westernmost edge of the area near the continental divide. These faults form part of a larger structure that is concavely curved toward the east and discontinuously exposed. The northern segment runs NNE (El Cura fault), and the southern segment runs NNW (Penitentes fault). Farther east, younger obstacles coincide with the faults that mark the back-thrust front of the western border of the Precordillera. These obstacles control the large, north-south-oriented rivers like the Blanco River, the main tributary of the Jáchal, and the Los Patos River, a tributary of the Juan River. Notably, these structures along the edge of the Precordillera efficiently divert major drainage rivers for the Andes like the Jáchal and San Juan Rivers, which subsequently flow to the east, crossing the mountains of the Precordillera as antecedent rivers. The Mendoza and Tunuyán rivers run toward the east, curving around the obstacles imposed by the highs of Mendoza Norte and Cerrillada Pedemontana until finally being retained and diverted by the Desagüadero – Bermejo fault on the western border of the Sierras Pampeanas to form the headwaters of the Colorado River.

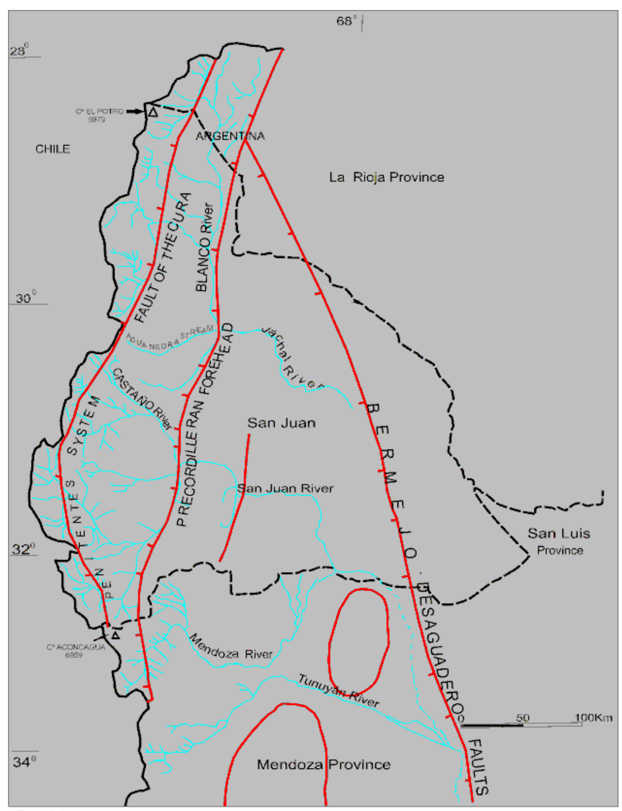

Fig.N° 2

The evolution of the drainage of the eastern Andean flank across 1000-km section between 27º S and 34º S is a powerful indicator of the tectonic phenomena that occurred between the Early Miocene and Late Quaternary Periods. This region has previously been identified as an area of intense seismic activity and Quaternary tectonics, and the current drainage pattern analysis confirms and reinforces this conclusion. Recent tectonics have produced a set of obstructions that divert rivers, culminating in an impressive final concentration of all of the runoff from this large Andean section reaches the Atlantic by a single collector trunk, the Colorado River. Structures along the western edge of the Precordillera and Desagüadero–Bermejo faults very effectively contain and divert the rivers that come from the west. Certain rivers must have run for hundreds of kilometers parallel to these structures before being able to follow their course toward the east. The morphostructural controls of the drainage pattern decrease in age from north to south and from west to east. Late Cenozoic structural features like the high of Médanos Grandes, Mendoza Norte, and Cerrilladas Pedemontanas, correspond to structures that were produced by the most recent Quaternary surface deformation (Suvires *et al*, 2012). All of these are situated in the Bermejo valley, which hosts intense seismic and neotectonic activity, as demonstrated by instrument measurements. Back-thrusts most efficiently control and divert rivers. From west to east, these structures correspond to the Penitentes system, El Cura fault, the back-thrust front of the Precordillera, and the Bermejo – Desaguadero faults (Fig. 2). The tectonic regime of the Andean Chain and in its foreland shifts significantly at 27º S, which is reflected in drainage behavior. North of 27º S, an endorrheic watershed is represented by La Puna, which acts as an intermediate area of surface water retention and blocks the rivers that begin in the high peaks from directly descending to the foreland. South of this section, the extreme north of the Sierras Pampenas is incorporated into the Andean Chain and does not represent an obstacle for surface runoff. To the south of 27º S, the rivers with headwaters in the high peaks of the continental divide flow directly toward the foreland. The western edge of the Sierras Pampeanas represents a very significant obstacle in this section that concentrates all of the channels that descend through the eastern Andean flank into the Colorado River, a primary artery flowing directly toward the Atlantic. The larger structures that regulate these changes are thought to represent features inherited from Paleozoic orogeny, especially the Ocloyicas Orogeny, which have been reactivated by recent tectonics (Mon 1993).

Acknowledgements: Thanks to Projects PIP 45 (2011-2013) supported by CONICET, Argentina and P 21- E of National University of San Juan.

References

Alvarado, P., Beck, S., and Zandt, G. 2007. Crustal structure of the south-central Andes Cordillera and backarcregion from regional waveform modelling. *Geophys. J. Int.* **170,** 858–875. doi: 10.1111/j.1365-246X.2007.03452.x

Cortés, J.M. y Costa, C.H. 1993. La deformación cuaternaria pedemontana al norte de la Pampa Yalguaraz, margen occidental de la Precordillera de San Juan y Mendoza. Actas XII Congreso Geológico Argentino y II Congreso de Exploración de Hidrocarburos III: 241- 245.Mendoza.

Costa, C., Audemard, F., Bezerra, F, Lavenu, A, Machette, M. and Paris, G. 2006. An Overview of the main Quaternary deformation of South America. Revista Asociación Geológica Argentina, 61 (4): 461-479. Buenos Aires.

Criado Roque, P., Mombrú, C. y Ramos, V.A. 1981. Estructura e interpretación tectónica. En M.R. Irigoyen (ed) Geología y Recursos Naturales de la provincia de San Luis. VIII Congreso Geológico Argentino.Relatorio: 155-192. Buenos Aires.

Gupta, S. 1997. Himalayan drainage patterns and the origin of fluvial megafans in the Ganges foreland basin. Geology 25 (1): 11-14.

Lavenu, A. 2006. Neotectónica de los Andes entre 1° N y 47° S (Ecuador, Bolivia y Chile): Una revisión. Revista de la Asociación Geológica Argentina 61(4): 504-524. Buenos Aires.

Martinez, M.P., Perucca, L.P., Giménez, M.E. y Ruiz, F. 2008. Manifestaciones geomorfológicas y geofísicas de una estructura geológica profunda al sur de la sierra de Pie de Palo, Sierras Pampeanas. Revista de la Asociación Geológica Argentina, 63(2):264-271.

Mon, R. 1993. Influencia de la Orogénesis Oclóyica en la segmentación andina en el norte argentino. XII Congreso Geológico Argentino, .3: 65-71.

Mon, R. 2005. Control tectónico de la red de drenaje de los Andes del norte argentino. Revista de la Asociación Geológica Argentina. 60 (3): 461-466. Buenos Aires.

Potter, P. E. 1978. Significance and origin of big rivers. Journal of geology 86: 13-33.

Ramos, V. A. 1996. Evolución tectónica de la alta cordillera de San Juan y Mendoza. Subsecretaría de Minería de la Nación. Dirección Nacional del Servicio Geológico. Anales 24 (16): 447-460. Buenos Aires.

Ramos, V.A., Cristallini, E.O. y Perez, D. 2002. The Pampean flat-slab of the Central Andes. Journal South American Earth Sciences, 15: 59-78. Pergamon.

Siame, L.L., Bellier, O., Sebrier, M. 2006. Active tectonics in the Argentine Precordillera and western Sierras Pampeanas. Revista de la Asociación Geológica Argentina, 61 (4):604-619. Buenos Aires.

Suvires, G., Sisterna, J., Quiroga, M y Robles, A. 1995. Generación de relieve cuaternario por efectos pre, co y pos-sísmicos en la intersección del paralelo de 31 30' de latitud sur y el meridiano de 68 00' de longitud oeste de Greenwich. Argentina. IX Congreso Latinoamericano de Geología.Actas, p:5-15. Caracas. Venezuela.

Suvires, G., Mon, R y Gutiérrez, A. 2012. Tectonic effects on the drainage disposition in mountain slopes and orogen forelands of the Central Andes, Argentina. Revista Brasileira de Geociencias. *Revista Brasileira de Geociências 42(1): 229-239. www.sbgeo.org.br* 229.

PALEOSEISMOLOGY & ARCHAEOSEISMOLOGY MORELIA • MEXICO 2012
INQUA-TERPRO PALEOSEISMOLOGY
EARTHQUAKE ARCHAEOLOGY

COSEISMIC STRATIGRAPHY IN HOLOCENE LACUSTRIAN SEQUENCES OF SAN PEDRO EL ALTO, ESTADO DE MÉXICO

Velázquez-Bucio M. Magdalena (1), Garduño-Monroy Victor H. (2), Soria-Caballero D. C. (3), Israde-Alcántara I. (2). Rodríguez-Pascua M.A. (4), Pérez-López R. (4)

(1) Centro de Investigaciones en Geografía Ambiental. Universidad Nacional Autónoma de México. Magda_vb@yahoo.com.mx
(2) Departamento de Geología. Instituto de Investigaciones Metalúrgicas. Universidad Michoacana de San Nicolás de Hidalgo.
(3) Posgrado en Ciencias de la Tierra. Universidad Nacional Autónoma de México
(4) Instituto Geológico y Minero de España (IGME)

Abstract (Coseismic stratigraphy in Holocene lacustrian sequences of the San Pedro El Alto, Estado de Mexico)
The Mexican Volcanic Belt contains a series of coseismic registers in lacustrian sequences in which the consequence of seismic collisions due to fault movements left deformed structures. The scope of this paper is to define the geological and biological evolution of the lacustrian depression of San Pedro el Alto, immersed in the Acambay graben. The area presents morphological evidence of current coseismic ruptures such as vertical height differences, fault edges, structural drainage control and counterslopes. The natural conditions, as well as the time and space relations in which seismic events took place will be demonstrated, underpinned by a detailed study of the area's stratigraphy and fossil diatoms. Furthermore, the fluctuations in the level of the lake can provide guidelines to understand the environmental factors linked to coseismal ruptures occurred during the Miocene (coseismal stratigraphy).

***Key words**: coseismic stratigraphy, lacustrian sequences, diatoms*

Introduction

The Trans Mexican Volcanic Belt (TMVB) is, geologically speaking, one of the most actives and representative zones of Mexico. Research carried out in this area gives stratigraphic, seismologic and historical evidence of its recent activity during the quaternary (Martinez and Nieto, 1990). The TMVB harbors some of Mexico's most important lakes and basins, all linked to the Tula-Chapala Fault system (Garduño –Monroy *et al*., 2010). The zone is characterized by large lake depressions (fig. 1) which have received and stored sedimentary series which register important paleoenvironmental geological events. The Acambay graben has raised particular interest among researchers due to the activity along the Morelia-Acambay fault system (MAFS), which according to Garduño Monroy *et al*. (2009), is associated with the birth of lacustrian depressions such as Chapala, Cuitzeo, Zacapu, Maravatio and Acambay, in which the 1912, 1979 and 2007 earthquakes formed.

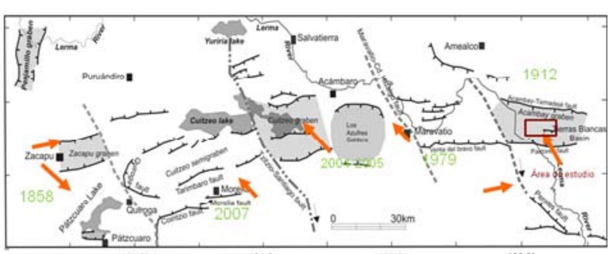

Figure 1. Area of study in the Morelia-Acambay fault system context. From Garduño Monroy et al.(2010).

The study of the many lacustrian systems in the area has been an essential tool in the seismic catalogue. Nonetheless, despite the zone's important seismic activity, the consequential deformations in recent

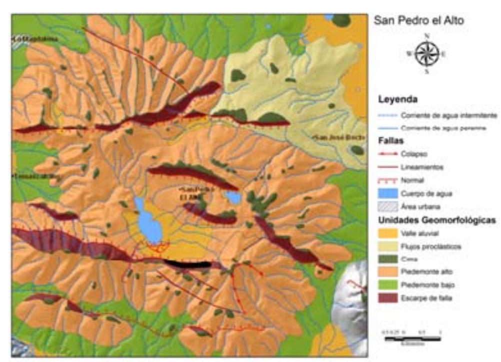

Figure 2. Geomorphological map of the San Pedro El Alto zone. The different geomorphological units are highlighted. The fault structures and their edges, with preferential E-W direction are obvious.

structures have been understudied (Garduno Monroy et al., 2003, 2009; Rodriguez Pascua et al., 2003, 2009). Neither are there studies systematically recording the ages of the sedimentary sequences for the San Pedro el Alto zone. The scope here is therefore to define the geological evolution of the area based on a detailed study of the stratigraphy and the identification of paleoseism (coseismic stratigraphy). Furthermore, the contribution of diatoms will indicate the natural conditions and the space and time relationships in which the events took place, as well as the fluctuations at the lake level, in order to yield guides to the understanding of environmental factors linked to coseismic ruptures which occurred during the Miocene.

The San Pedro el Alto lake depression corresponds to a MAFS fault segment. The artificial basin was constructed in a morphological depression in which the bowl-shape aspects and E-W segments of the MAFS were combined. Secondary effects of the Acambay 1912 seism (M6.9) and Maravatio seism in 1979 (M5.3) could have remained registered in this depression. In the same way, the morphology of the zone is defined by the fault activity of the MAFS. Seismic events in the area can be identified by means of secondary liquefaction structures with sediment deformation and sand dikes intrusion, all associated with events of more than M5.

Study area
The study area is immersed in the Acambay graben between coordinates 99°57’ 46’’ N y 19° 54’ 37’’ W. San Pedro el Alto is located at an average altitude of 2640 m ASL in the dacitic caldera of the Temascalcingo volcano (TV) (fig. 2). The TV is in his turn situated in the north eastern portion of the Estado de México state, in the Temascalcingo-Tuxtepec-Acambaro fault system, with E-W orientation and fault planes inclination up to 80° north and south. The stratigraphic column shows rocks ranging from the Oligocene to the Quaternary (Martínez and Nieto, 1990, Ramírez_Herrera, 1998, Roldán-Quintana *et al.*, 2011). According to Roldán Quintana *et al.*, 2011, this is a region which presents an abrupt topography, distinguished by the 800 m height at its base, and its 3000 and 3100 m ASL summits. The TV is a volcanic structure presenting a rectangular-shaped crater of 2x3 km, oriented E-W. It is distinguished by two main phases: 1) the construction of a stratovolcano of dacitic composition and 2) an explosive phase of rhyolitic composition which formed the summit of the caldera. The rhyolitic phase is apparently associated to deposits of ash fall located on the SE flank of the TV, dating back to 1.2+- 0.13 My (Mercer *et al*., 2002 in Roldan Quintana, 2012). The basaltic flows are exposed SE of the study area and are 0.4 +- 0.1 by A K/Ar old (Suter *et al*., 1995).

Geomorphological analysis
The geomorphological analysis carried out in the zone exposes the essential elements for the physical evaluation of the San Pedro el Alto landscape. This analysis suggests that the relief was constructed after the volcanic activity due to tectonic movements related the Morelia-Acambay Fault System activity and active tectonic activity. The morphological map (fig. 2) highlights the fault structures and their relevant edges in preferential E-W direction, with clear structural control of drainage, which modifies the radial drainage of a volcanic structure.

The southern edge of the dam shows a series of evenly E-W oriented escarpments. These yielded a lacustrian sequence of laminar dark-colored clays (fig. 3). According to the indirect effect classification made by Audemar *et al* (2011), this is considered a secondary effect, which corresponds to C- type tectonic uplift. The break modified the basin’s geometry, changing the sedimentological conditions of the water body, a fact which remained reflected in the analysis of diatom populations realized in a sample extracted from the sequence, pertaining to lacustrian sediments which contained abundant organic material and diatomaceous earth. The changes in the stratigraphical sequences of the fossilized diatoms are closely related to the tectonic evolution of the region. The species of diatoms as yet observed (fig. 3) correspond to *Navicula, Cymbella, Amphora, Cellaphora* genres, all of which indicate shallow swamp waters.

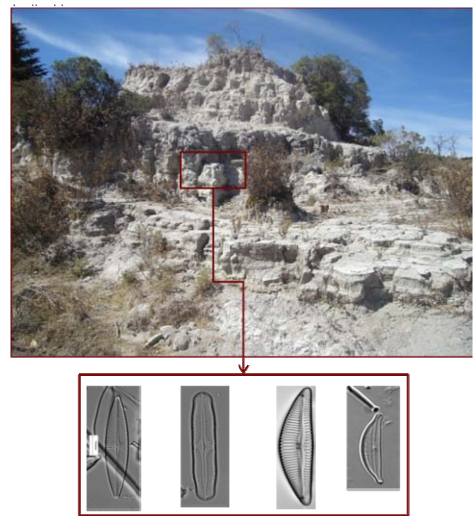

Figure 3. Localization of the deformed lacustrian sediment sample extraction with organic material and diatoms.

Extraction and nuclei analysis
By means of a gravity corer, 3 sediment cores were extracted from northern, central and southern parts of the dam (fig. 4a). Two of them are shown here, demonstrating that, as in the outcrops mentioned before, the planar structure of the sediments is affected. The nuclei are composed of layers and sheets intercalated by fine silty clay presenting a certain regularity similar to varves. Important structures and deformation are visible: a small slump structure is observable between centimeters 14 and 17. This notwithstanding, the strata at the base and at the summit are perfectly horizontal.

Nucleus 2 (fig. 4b) is 41.5 cm long, and was extracted from the central part of the dam, at 1.4m depth. It is similar to the previous, as it presents silty clay intercalations, of which the darkest sheets are the finest, and contain small carbon granules. This nucleus presents evidence of planar structure, from the summit to approximately 25 cm towards the base, where the strata begin to incline towards the base. The nuclei were sampled every 3 cm for later content analysis of organic and inorganic carbon (TOC and TIC), x-ray diffraction, magnetic susceptibility and diatoms. The results will yield information about the environmental conditions in the water body and its relationship with the 1912 and 1979 earthquakes. These analyses are being processed in various IMM laboratories of the Universidad Michoacan de San Nicolas de Hidalgo and the Universidad Nacional Autonoma de México. Another part remains refrigerated as evidence.

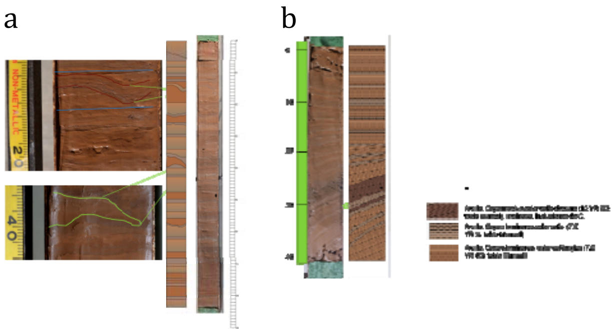

NÚCLEO SPA 0711-1
85 Cm Norte
14Q 0398747
2201518
Profundidad 3.5 m

NÚCLEO SPA 0711-2
41.5 Cm Centro
14Q 0398955
2201079
Profundidad 1.4 m

Fig 4. Sedimental nuclei extracted from the northern and central part of the San Pedro el Alto dam for stratigraphic and diatom analysis.

Coseismic structures

Following the geomorphological and the topographic uplift analysis, a trench was digged in the southeastern zone of the dam for subsuperficial analysis. The analized evidence of seismic activity corresponds in the Audemar *et al.* (2011) classification, to A-type (liquefaction, slumps) or B type (remobilization and sediment redeposition) secondary structures or indirect effects. According to Rodriguez-Pascua *et al.* (2000), and based on studies carried out in other lake areas subject to the effects of active faults, the shaping of such structures in lacustrian environments requires seismic events of a magnitude M>5 Rodriguez-Pascua *et al.* 2000).

The presence of secondary structures interpreted as seismites, was recognized by means of a detailed stratigraphic analysis. This allows to see several types of these seismites (fig. 5) and to relate them to recent seismic events, for the trench presents numerous crevices with material intrusion, in most cases from the surface to the base. Some of the structures identified in the trenches include: inconformity and sediment displacement, failed sediments, crevasses and material intrusion, variations in thickness of certain affected stratigraphic unities, slumps, pseudonodules and more material liquefaction structures. With current data and in the expectation of the results of the laboratory analysis (dating, magnetic susceptibility), as the digging of future trenches, we can already identify at least two seismic events which affect recent material and which have influenced the evolution of the basin.

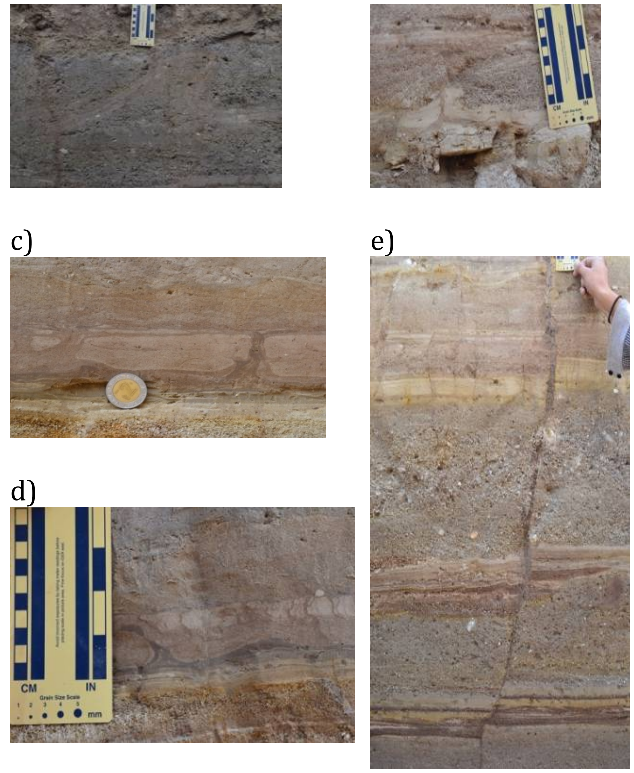

Figure 5. Different structures identified in the stratigraphic unities of the San Pedro el Alto trench. a) slump in the E-wall of the trench. b) small volcano in fine volcanic ash. c) pillow basalts. d) fine clay and sand liquefaction. e) failed sediment displacement, variation in thickness of failed stratigraphic units and crevice filling with recent material.

Preliminary conclusions

The segment of the San Pedro el Alto fault shows a well-preserved sedimentary register, in which it is possible to identify deformation structures related to recent seismic activity. The geomorphological analysis of San Pedro el Alto suggests that the relief was constructed after the volcanic activity, due to tectonic movements related to the Morelia-Acambay Fault System activity. It also suggests functioning tectonic activity.
Seismic events in the area can be identified by means of secondary liquefaction structures with sedimental deformation, crevices and recent material intrusion, all of which associated to events >M5.

With current data and in the expectation of the results of the laboratory analysis (dating, magnetic susceptibility), as the digging of future trenches, we can already identify at least two seismic events which affect recent material and which have influenced the evolution of the basin.

a) b)

Referencias

Audemard M. F.A., Michetti A. M., McCalpin J.P. 2011. Geological Criteria for Evaluating Seismicity Revisited. Forty Years of Paleoseismic Investigations and the Natural Records of Past Earthquakes. The Geological Society of America. Special Paper 479.U.S.A.

Garduño-Monroy, V.H., Rodríguez-Pascua, M.A. y Israde-Alcántara, I. 2003. La deformación de las secuencias lacustres del Pleistoceno – Holoceno: evidencias de actividad sísmica importante en las cuencas de Pátzcuaro y Zacapu, Michoacán, México. *GEOS*. 23 (2): 121-122.

Garduño M. V. H., Pérez L. R., Israde A. I., Rodríguez P. M. A., Szynkaruk E., Hernández M. V. M., García Z. M. L., Corona C. P., Ostroumov M., Medina V. V. H., García E. G., Carranza O., López G. E., Mora C. J. C. 2009. Paleoseismology of the southwestern Morelia-Acambay fault system, central Mexico. Geofísica Internacional. No. 48 Vol. 3. pp. 319-335

Garduño-Monroy, V.H., Pérez-Lopez R., Israde-Alcantara, I., Rodríguez-Pascua M.A., Szynkaruk E., Hernández-Madrigal V.M., García-Zepeda M.L., Corona-Chávez P., Ostroumov M., Medina-Vega V.H., García-Estrada G, Carranza O., López-Granados E. 2010. Paleoseismology Of The Southwestern Morelia-Acambay Fault System, Central Mexico. Geofisica Internacional 48(3): 319-335.

Garduño-Monroy V.H., D.C. Soria-Caballero, I. Israde-Alcántara, A. Rodríguez-Ramírez, V.M. Hernández-Madrigal, M. Ostroumov, M.A. Rodríguez-Pascua, A. Chacón-Torres y J.C. Mora-Chaparro. 2010. Evidence of Tsunami events in the paleolimnological record of Patzcuaro lake, Michoacan, Mexico. Geofísica Internacional. 50(2): 147 – 161.

Martínez R. J., Nieto S. A. F. 1990. Efectos geológicos de la tectónica reciente en la parte central de México. UNAM. Instituto de Geología. Vol. 9 No. 1. pp. 33-50

Ramírez H. M. T. 1998. Geomorphic assessment of active tectonics in the Acambay graben, Mexican Volcanic Belt. Earth Surface Processes and Landforms. Vol. 23. pp. 317-332.

Rodríguez-Pascua, M.A., Calvo, J.P., De Vicente, G., Gómez-Gras, D. 2000. Soft-sediment deformation structures interpreted as seismites in lacustrine sediments of the Prebetic Zone, SE Spain, and their potential use as indicators of earthquake magnitudes during the Late Miocene. Sedimentary Geology. 135: 117 – 135.

Rodríguez-Pascua, M.A., Garduño-Monroy, V.H., y Alcántara-Israde, I. 2003. Paleosismología y efectos de licuefacción en la región de Acambay, México. GEOS. 23 (2): 121-122.

Rodríguez-Pascua, M.A., V.H. Garduño-Monroy, I. Alcántara-Israde y R. Pérez-Lopéz. 2009. Estimation of the epicentral area from the spatial gradient of deformation in lacustrine seismites (Tierras Blancas Basin, Mexico). Quaternary International doi:10.1016/j.quaint.2009.11.006. 1-13.

Roldán Q. J., Aguirre D. G. de J., Rodríguez C. J. L. 2011. Depósito de avalancha de escombros del volcán Temascalcingo en el Graben de Acambay, Estado de México. Revista Mexicana de Ciencias Geológicas. Vol. 28. Núm. 1: 118-131

Roldán Q. J., Aguirre D.G. de J. 2012. The San Pedro Summit Caldera, Temascalcingo, Mexico.Cordilleran Section. 108th Annual Meeting. México.

Suter, M., Quintero-Legorreta, O., López-Martínez, M., Aguirre-Díaz, G., Farrar, E. 1995. The Acambay graben: Active intra-arc extensión in the trans-Mexican Volcanic Belt, Mexico. Tectonics. 14 (5): 1245-1262.

PALEOSEISMOLOGY & ARCHAEOSEISMOLOGY MORELIA • MEXICO 2012
INQUA-TERPRO PALEOSEISMOLOGY
EARTHQUAKE ARCHAEOLOGY

PILOT STUDY OF TECTONIC ACTIVE BEHAVIOR IN AREA OF XIAN SINCE LATE-QUATERNARY *

YAO Da-quan, CHEN An-guo, ZHENG Hai-gang

Seismological Administration of Anhui Province,Hefei,Anhui, P.R.China,230031

Abstract *Combining with macro-microscopical analyze, seismic archaeological and other synthesize methods, the author made cast back in an attempt to the seismic active behavior in the area of Xian and adjacent area since Late-Quaternary. The initial result indicated most of this faults of the area in the late Quaternary had even repeatedly activity occurred, there were multi times stronger earthquakes had been taken place in the research area since Late-Quaternary. Partial rupture of the latest activity is to sudden stick-slip and intermittent steady slide way. Weihe fault and Lintong ~ Changan fracture on a considerable scale of sand liquefaction events and coarse sand as main liquefied material layer phenomenon showed considerable period earthquake intensity is very large.*

Key words: *Xian, Late- Quaternary, Seismic vestige, Active fault.*

INTRODUCTION

Recently, accompanied by Prof. Feng Xijie, the researcher of the Seismological Administration of Shanxi Province, we have made a key observation of the piedmont fault of Mountain Hua and Mountain Li, the fault of Wei River and Lingtong – Chang'an fault zone, whose location and distribution are all around Xi'an city. Additionally, we also traced the investigation of the Huaxian earthquake and prehistoric earthquake as the main thread to finish the exploration record. Based on the comprehensive method which includes macro and micro analysis and archaeoseismology, we tried to trace this area's seismic active behaviors back to the Late-Quaternary period. The initial result suggests that there are several strong earthquakes in this zone since the Late-Quaternary period.

PIEDMONT FAULT OF MOUNTAIN HUA

The analysed profiles are located at Lipo village, Huaxian County. Two events with fast deformation have been identified in the observed profiles. Firstly, the forepart diluvium collapsed and formed the tensile colluvial wedge, which was covered with the newer gravel stratum horizontaly. Then the stratum the basin side fallen again which exposed the latest active fault plane. We noted the ruins of the AD 1556 Huaxian earthquake. This fault plane is (358°/64°) in trending and dip, and the dislocation is up to 8-9 m(Fig.1).

PLATEAU BEFORE FAULT OF MOUNTAIN HUA

These profiles are situated at Caiguo village, in Weinan City. We observed the extended parts of the plateau evidenced in the exposed Late Quaternary sediments on the river reconstruction site and natural river slope. This fault plane is flat and stably extends along the near north west - south east direction. The 3 profiles along the fault are as following.

(1) The fault plane is (045°/45°) in striking and dip, measured on the river reconstruction site. This large fault

Fig.1 Profile of piedmont fault of Mountain Hua, Lipo village (mirror to S)

plane consisting of early Holocene green materials . That is the earlier fault reacted and which generated large dislocation along the fault plane. Therefore, the foot wall with old materials are uplifted to the surface and the hanging wall is the upper gravel layer, with the flood plain deposits covered this sequence on the flat plane.

(2) The fault plane is (045°/50°) in striking and dip, respectively and it is exposed on the northwestern bank of the river. We observed different degrees of consolidation of the gauge on the fault plane, the inner gauge has been consolidated completely while the outside is still muddy. This observation indicates that the fault activity happened in different periods.

(3) The fault plane is (050°/30°) in trending and dip, and it is exposed on the southeastern bank of the river. There are shear rubbing belts can be seen on the profile, the inner part has been consolidated to oriented linear materials while the outside containing ambient debris is not. we want to note that the Eastern extension of this fault plane part is just the Huashan Piedmont fault.

WEIHE RIVER FAULT

The profile of Weihe River Fault is situated in a kiln of the western of Yangcun village, Xingping city. The fault plane trending towards NW, steep inclination to SE. (Fig. 2A).

Fig.2A Prehistoric earthquake relics on profile of the Weihe fault, Yangcun village(section view,mirror to NW)

There are rich prehistoric earthquake relics that have been revealed on the trench trending south-north, including colluvial wedge, sand liquefaction, faulted etc. Multi period activity chronological traces are as following:

Fig.2B Prehistoric earthquake relics on profile of the Weihe fault, Yangcun village,seismic sand liquefaction(mirror to NW).

Fig.2C Prehistoric earthquake relics on profile of the Weihe fault, Yangcun village,mixed with mud strip in the parent sand bed,(mirror to NW).

The first stage has the following features: mainly section as tensile dislocated sand bed, the sand bed of upper wall hidden underground, stagger unknown, the up to 8-9m extensional dislocation of S1 ancient soil layer, the extensional wedge formed as the mixture of the red soil and light grey soil in the upper wall; The second stage displays the directional band which is formed by the shear activities on the fault plane and cuts the tensile crack upwards. However the third stage with tension as the main feature shows the cleavage belt parallel to the fracture plane, the belt is partially filled with sludge-like materials and cut the composition or the fabric layer; The fourth stage has the sand vein of seismic liquefaction which is generated by the saturated sand layer originated from the parent sand bed and running up along the tensile cracks. Three liquefied sand veins with width 3-9cm are revealed in the exploratory trench (Fig. 2 B), and the sand vein extends upwardly to the top along the cracks. The rarer observation is the mud strip mixed in the parent sand bed (Fig. 2 C), we speculated that this mud filling was generated by the secondary seismic rupture in the coseismic rupture. In addition, a large number of ancient screws were found in the profile which means the events of later stages happened later.

Among the above four deformation stages,the first and fourth stages represent the significant prehistoric earthquake events ,while the second and third stages are to the relics of intermittent adjustment of deformation (stable slip).

Lintong ~Changan fault

In the profile on the west side of the second middle school of Changan, sand liquefaction veins have been found in the Holocene soil on the gouge wall of excavation pipeline.These eastern dipping veins with windth abourt 20cm cantain medium coarse sand (Fig. 3),the parent material layer can also be seen, it is

Fig.3 Seismic sand liquefaction on the profile of Lintong ~Changan fault , the second middle school of Changan (mirror to S)

confirmed that the sand bed formed in Qin dynasty according to Feng Xijie earlier works. So coarse sand in liquefaction process indicates the strong intensity of earthquake event in this period.

INITIAL UNDERSTANDING

According to common cognition in existence in the research field prehistory earthquake, the sand liquefaction is one of representative indicate of prehistoric earthquake(Bartholomew M J and Stickney M C,2002;Moretti M, Brodie B M, et al.,2002;Moretti M, Brodie B M,et al.,2006;Sukhija, B. S., Rao, M. N.,,et al.,1999; Susan Olig, Martha Eppes. 2004 YAO Da-quan.2004),based on the above observation,the following preliminary conclusions can be put forward:
Piedmont fault of Mountain Hua (plateau before fracture), Weihe fault and Lintong~Changan fault structure are Xi'an and adjacent area important active faults, most of them had acted once or even many times since the late Quaternary.

Partial faults' latest activities are acted by the way of sudden stick-slip and intermittent steady slide, which was supported by the observations in Weihe fracture Yang Village profile.

Considerable amounts of sand liquefaction events have been found in the Weihe fault and Lintong ~ Changan fracture, and coarse sand as main liquefied material layer phenomenon, these observations indicated that the earthquakes in the corresponding period are very strong.

Because of lots of the earthquake relics found near Xi'an and its adjacent area, we must strength the research of prehistoric earthquake characteristics and the sequence of the events, although few records about the large or huge earthquakes. Here we just briefly reported some new discoveries and initial conclusions, sample observation,testing and further analysis are under way.

Acknowledgements

Thanks to Mr.Fengxijie ,Seismological administration of Shanxi Province.

REFERENCES

Bartholomew M J, Stickney M C, Wilde E M, et al. 2002. Late Quaternary paleoseismites: Syndepositional features and section restoration used to indicate paleoseismicity, Atlantic Coastal Plain, South Carolina and Georgia. In: *Ettensohn F R, Rast N, Brett C.(eds). Ancient Seismites. Geol Soc Amer Special Paper* 369. Boulder, Colorado, USA. 63—74.

Moretti M, Brodie B M, Willoughby R H, et al. 2002. Late Pleistocene soft-sediment deformation structures interpreted as seismites in paralic deposits in the City of Bari (Apulian foreland, southern Italy). In: *Ettensohn F R, Rast N, Brett C.(eds). Ancient Seismites. Geol Soc Amer Special Paper* 369. Boulder, Colorado, U S A. 75—86.

Michael Strasser, Flavio S. Anselmetti, Donat Fäh, Domenico Giardini and Michael Schnellmann. 2006. Magnitudes and source areas of large prehistoric northern Alpine earthquakes revealed by slope failures in lakes. *Geology* 34(12),1005-1008.

Sukhija, B. S., Rao, M. N., Reddy, D. V., Nagabhushanam, P., Hussain, S., Chadha, R. K. and Gupta, H. K. 1999.Paleoliquefaction evidence and periodicity of large prehistoric earthquakes in Shillong Plateau, India. *Earth and Planetary Science Letters* 167(3), 269-282.

Susan Olig, Martha Eppes, Steven Forman, David Love and Bruce Allen.,2004.Gallery of Geology—Prehistoric earthquake ruptures on the Hubbell Spring fault and implications for seismic hazards south of Albuquerque on the Hubbell Spring fault, New Mexico. *Geology* 26(1), 34-36.

YAO, Da-quan. 2004. Macroscopic and Microscopic Evidence of Periodical Stick-Slip Deformation in an Active Fault[. *Recent Developments in World Seismology*,(4), 6-10. In Chinese.

SEISMOTECTONIC AND GEODYNAMIC DATA FOR TSUNAMI MODELING IN CENTRAL AMERICA. A FIRST STEP FOR PROBABILISTIC TSUNAMI HAZARD ASSESSMENT (PTHA).

Zamora, N. (1), Molina, E. (2) and Rojas, W. (3)

(1) Geodynamic Modeling Section, German Research Centre for Geosciences (GFZ), Potsdam, Germany. zamora@gfz-potsdam.de
(2) Instituto de Sismología, Vulcanología, Meteorología e Hidrología de Guatemala.
(3) Red Sismológica Nacional, Universidad de Costa Rica.

Abstract: *Bounded between the subducting Cocos plate at the west and Caribbean plate at the east, Central America represents a region of high seismic and tsunami hazard. Historical data indicate that almost 50 tsunamis have occurred in Central America since last 500 years. The main historical tsunamis have been generated at the Cocos-Caribbean subduction zone and the Nazca-Caribbean (Pacific margin), and Northern Panama Deformation Zone (Caribbean). Despite extensive geophysical and geodetic studies over last decades, not many works have been developed to determine tsunamigenic sources. Probabilistic Tsunami Hazard Assessment (PTHA) is needed to understand the sources that are posing the highest hazard along the coast as well as to provide scientific basis for risk quantification and mitigation. As part of this extensive work we present the seismic and tectonic zones that are considered for the tsunamigenic sources characterization. We have made use of the seismic catalog (CAT2011) compilation recently employed for the regional Probabilistic Seismic Hazard Assessment study for Central America. This catalog is considered to be the most complete data set currently available for the whole region according to its completeness, magnitude homogeneity (with Mw > 3.5) and the 500 year time-window. The first step of PTHA consists of seismotectonic zones determination: geometry and activity based on seismicity, geophysical data and focal mechanisms. The CAT2011 has been essential to calculate seismicity rates. However, due to its extensive data volume, no focal mechanism information is available in CAT2011. Therefore we have used several sources that provide this information to integrate the regional Focal Mechanism Catalog (FMcat) that will be open for use. We intend to have a catalog as revised as possible that could be used to improve characterization of Central America seismogenic zones and in our particular case carried out the probabilistic tsunami hazard assessment for this region.*

Key words*: seismic catalog, seismic sources, tsunami hazard, Central America.*

INTRODUCTION

Central America lies in the western side of the Caribbean plate (Fig 1). In this section of the Pacific margin the Cocos plate is subducting beaneath the Caribbean plate at a speed range of 8.5 – 9.0 cm/a generating a highly seismic region. These seismic sources have generated tsunamis in the past. Central American Pacific aand Caribbean coast are exposed to distant, regional and mainly local tsunamis (Fernández et al. 2000).

During the last five centuries ~50 tsunamis occurred along both coasts of Central America (Molina, 1997; Fernández et al. 2000 and references therein). And according to historical records the highest frequency and the strongest tsunamis occurred at the Pacific margin (Fig. 2). The latest strongest tsunami in the region occurred in 1992 along the coast of Nicaragua (Kanamori and Kikuchi, 1993; Bourgeois et al, 1992).

The hazard posed by specific seismic sources to generate tsunami still unknown, hence Probabilistic Tsunami Hazard Assessment (PTHA) is needed to quantify the sources that are posing the highest hazard along the coast. The first step of this PTHA consists of seismotectonic zones determination for which focal mechanisms are necessary. We present here first results

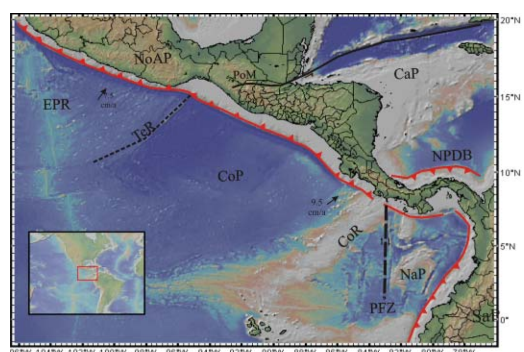

Fig. 1: Central America tectonic setting.

of revised catalog (FMcat) for Central America and the seismo-tectonic zones that will be used for PTHA model.

Method

The first step of this PTHA consists of seismotectonic zones determination: geometry and activity based on seismicity, geophysical data and focal mechanisms. The Central American Seismic Catalog (CAT2011) has been essential to calculate seismicity rates. However, due to its extensive data volume, no focal mechanism information is available in CAT2011. Consequently we have used several sources that provide this information to integrate the regional Focal Mechanism Catalog (FMcat).

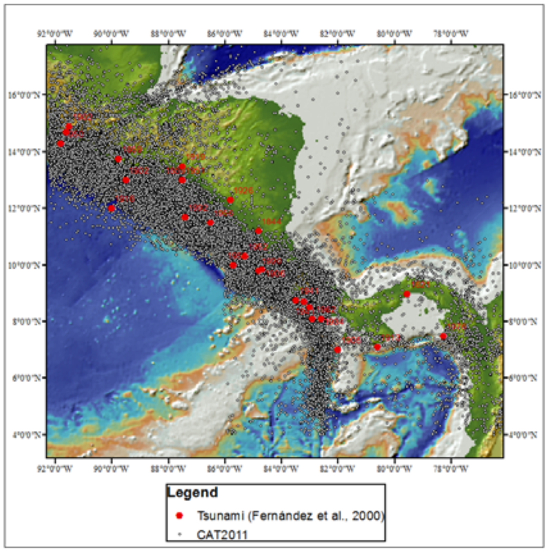

Fig. 2: Seismicity Mw> 3.5 and tsunami events.

In the following figure (Fig. 3) focal mechanisms from gCMT catalog with hypocenter relocations mainly by Engdahl and Villaseñor (2002) are presented. We have integrated the Centennial, the ISC and gCMT bulletins as well as data in publications available with earthquake relocations and high quality hypocenters of local networks, used in some tomography studies. Moreover we are trying to characterize which ones are aftershocks. This catalog contains earthquakes Mw>5.0 from 1972-09/2012 for Central America. This revision is important because it considers several source of weighted information, resulted in more precise data used for characterization tectonic segments of the region.

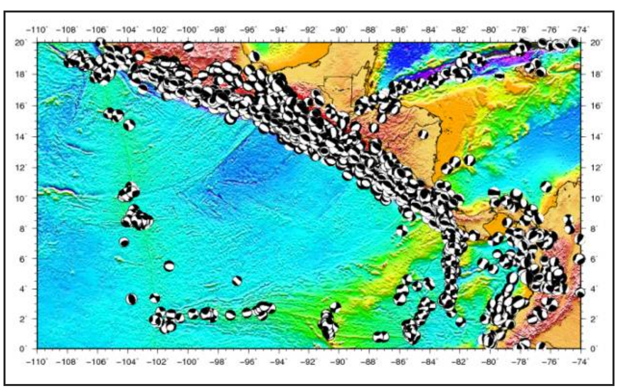

Fig. 3: Focal mechanism Mw >5.5.

As mentioned above using seismicity, geodetic and geophysical data the seismo-tectonic zones have been determined. Mainly 5 zones have to be considered for tsunami studies: the seismogenic zone (CO-CA), Panamá Fracture Zone, Cocos-Nazca (CO-NA), crustal Caribbean and outer rise region. These have been delimited as subregions according to seismo-tectonic characteristics (Fig. 4).

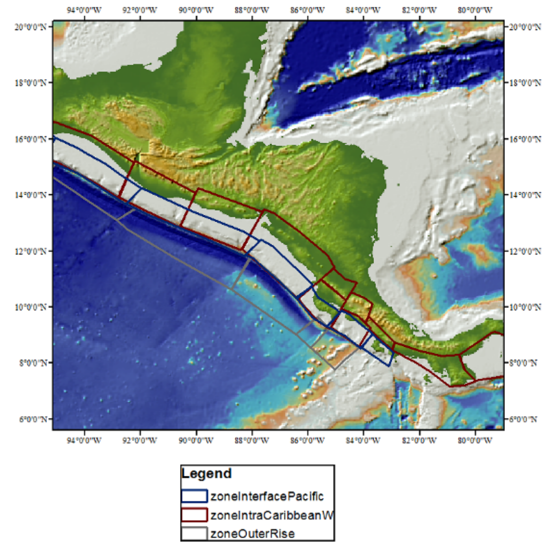

Fig.4: Example of seismo-tectonic zones

The segmentation is essential for both calculate seismicity rates and characterized tsunamigenic sources using fault models (e.g Okada, 1985) to determine ground deformation. The latter are input data to determine water column displacement and therefore tsunami generation.

Further work

Use focal mechanisms to describe deformation limits along south Middle America. , these data will be used to quantify the (seismic) tsunamigenic potential of along pacific coast of Central America.

Acknowledgements: N.Z thanks to Helmholtz Association for providing funding to conduct PhD studies through the GeoSim School. Thanks to Dr. Belén Benito that host N.Z at the Polytechnic University of Madrid. Also thanks to all the team from Central America that worked on the seismic hazard assessment for Central America (PSHA) for providing me the CAT2011 and fruitful discussions.

References

Engdahl, E.R., and Villaseñor, A. 2002. Global Seismicity: 1900-1999, in W.H.K. Lee, H. Kanamori, P.C. Jennings, and C. Kisslinger (editors). *International Handbook of Earthquake and Engineering Seismology*, Academic Press. Part A-41, 665-690.

Fernández, M., Molina, E., Havskov, J. & Atakan, K. 2000. Tsunamis and Tsunami Hazards in Central America. *Natural Hazards* 22 (2), 91-116.

GCMT-*The Global Moment Tensor*. www. globalcmt.org

International Seismological Centre, EHB *Bulletin, http://www.isc.ac.uk, International Seismogenic Cent*., Thatcham, United Kingdom, 2009.

Kanamori, H., and Kikuchi, M., 1993, The 1992 Nicaragua Earthquake -a slow tsunami earthquake associated with subducted sediments. *Nature*, 361: 714-716.

Molina, E. 1997. Tsunami catalogue for Central America 1539-1996. Reduction of natural disasters in Central America. *Earthquakes Preparedness and Hazard Mitigation*, Phase II, Technical Report No. II 1-04 Institute of Solid Earth Physics, University of Bergen, Norway.

Okada, Y. 1985. Surface deformation due to shear and tensile faults in a half-space. *Bulletin of the Seismological Society of America*. 75. 1135–1154.

TSUNAMI NUMERICAL MODELING ALONG NICOYA PENINSULA, NW COSTA RICA

Zamora, N. (1), Babeyko, A. (1)

(1) Geodynamic Modeling Section, German Research Centre for Geosciences (GFZ), Potsdam, Germany. zamora@gfz-potsdam.de

Abstract: *Most tsunamis occurring worldwide are generated along subduction zones. The Middle America megathrust fault is capable of generating destructive tsunamis as portrayed through historical data. Most of the strongest earthquakes in the last century have occurred inland, however historical records reveal that Central America lies in a tsunami prone area where further hazard assessment is required in order to evaluate the threat posed by seismic sources along this seismic active region. Developing studies to assess tsunamigenic sources potential could profit from available GPS and geophysical data. Such is the case of Nicoya Segment on the NW Costa Rica Pacific margin, where extensively geodetic data and new insights about seismogenic zone is recently available. This region is known to have a fifty-year inter-seismic period capable of generating a Mw 7.8. On Sept. 5th, 2012 a Mw 7.6 earthquake occurred in the estimated high coupling patches generating a small tsunami of 10 cm. Five main earthquakes have occurred between the years 1850-2012. The largest earthquake registered occurred in Nicoya in October 1950 (Mw 7.7) generating a small tsunami despite most deformation occurred inland. We present numerical simulations considering several earthquake models in order to determine tsunamigenic sources that can pose highest threat along surrounding coastal communities. We have used geophysical and historical data to define possible scenarios. Geodetic data has been very valuable to estimate possible sources based on slip deficient and using a plate rigidity characteristic to better estimate possible surface deformation. Finally, despite strong tsunamis have not occurred lately along Costa Rican coasts, we consider that local authorities along Nicoya and Central Pacific should prepare to reduce possible impacts of tsunami, especially if such an event is generated during high tides increasing inundation threat along coastal communities.*

Key words*: tsunami hazard, numerical modeling, tsunami earthquake, Nicoya Segment.*

INTRODUCTION

Costa Rica lies in the western side of the Caribbean plate (Fig 1) where the Cocos plate is subducting beaneath the Caribbean plate at a speed range of ~8.3-9.0 cm/a (DeMets et al., 2010) generating a highly seismic region. This region is prone to sources that have generated tsunamis in the past.

Tsunamigenic source assessment could profit from available GPS and geophysical data. Such is the case of Nicoya Seismic Gap (or Nicoya Segment) on the NW Costa Rica Pacific margin, where extensively geodetic data and new insights about seismogenic zone is recently available (Norabuena et al. 2004; LaFemina et al., 2009; Feng et al., 2012). This region is known to have a fifty-year inter-seismic period capable of generating earthquake (Mw 7.8). Four main earthquakes have occurred between the years 1850-2012. The largest earthquake registered occurred in Nicoya in October 1950 (Mw 7.7) generating a small tsunami despite most deformation occurred inland. Moreover, Nicoya lies on the southern limit of the Mw 7.6 tsunami-earthquake that occurred in Nicaragua.

Along Costa Rican Pacific margin 10 tsunamis have been registered. Their wave heights are in the order of centimeters. However, most of the known tsunamis come from historical records where unfortunately no wave height data is available. Nevertheless destruction of small villages has been described.

The aim of this research is to assess the tsunami

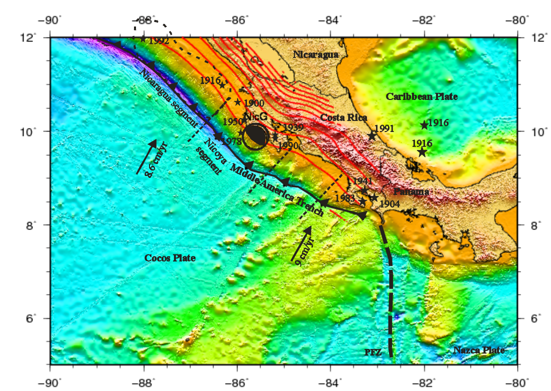

Figure 1. Tectonic setting of Costa Rica. Red contoures are slab depth every 20 m. Major earthquakes (stars). Hypothetical focal mechanism. PFZ:Panama Fracture Zone.

tsunami potential along the Costa Rican Pacific coast. Several scenario-based (deterministic) simulations have been performed using different fault models based on geodetic data and previous events.

Tsunami simulations have been performed using EasyWave (A. Babeyko) numerical code using a bathymetry grid of 900 m resolution. The input data is based on earthquakes that occurred on 1950, 1978, model by Chacón and Protti (2011) and geodetic models (Norabuena et al., 2008; Feng et al., 2012) and Sámara earthquake of 2012. We present three selected scenarios.

Discussion

The first step of tsunami simulation is to obtain surface deformation to assess if water displacement might occur. The resulted maximum surface deformation according to Okada (1985) model ranges between 0.7 m and 1.4 m. In figure 2 slip models are presented.

As expected it was identified the effect of different dip and slip distributions on the wave heights. The maximum surface deformations range from 1.1 - 1.4 m for Mod1 and Mod2 (Fig 2a; 2b). If an earthquake with focal mechanism similar to scenario Mod1 occurs, localities such as Nosara to Sámara and in general the central and southern coast of Nicoya Peninsula are exposed to high and moderate wave heights (2-3 m).

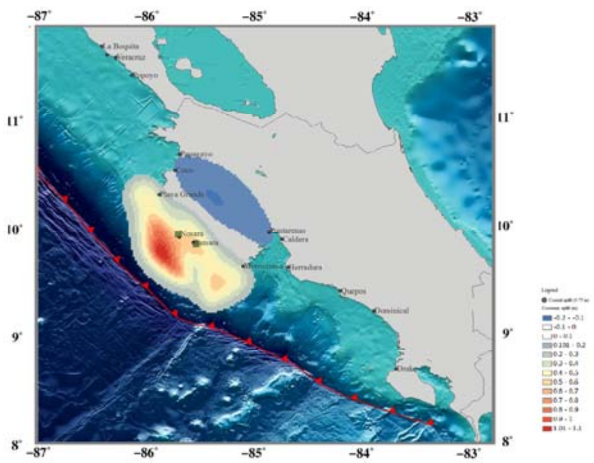

a. **Mod1** slip distribution modified from on Feng et al (2012). Magnitude Mw 7.8.

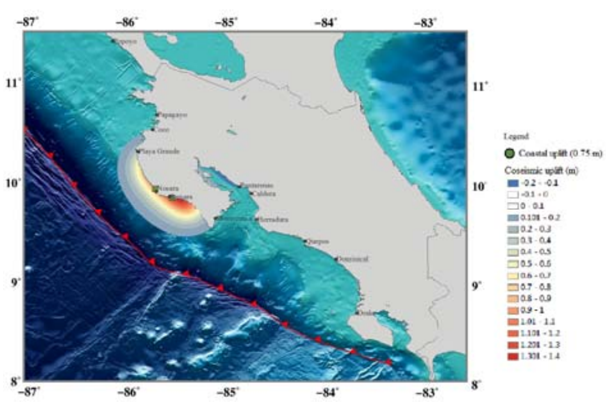

b. **Mod2** surface deformation resulted using fault mechanism with strike 315°, dip 18°, rake 90° and magnitude Mw 7.8.

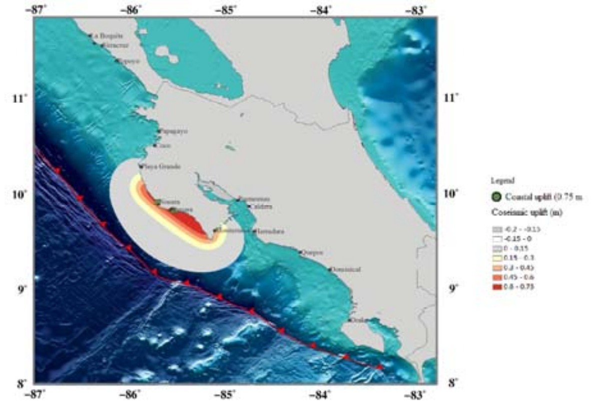

c. **Mod3** surface deformation using fault mechanism with strike 307°, dip 21°, rake 93° USGS CMT solution for Samara 2012 Mw 7.6 earthquake.

Fig. 2. Surface deformation based on Okada (1985) a. Based on slip deficient model of 435 subfaults (Feng et al., 2012) b. One finite rectangular source. c. Focal mechanism given by USGS CMT.

The calculations show that with an earthquake similar to Mod1 the highest wave will arrive in Garza and Nosara beach (Fig. 3). The maximum wave height at this site could range between 2.5-2.6 m according these scenarios. Lowest wave heights are simulated towards southern Nicoya Peninsula where wave heights could be up to ~ 1 m. In Coco beach the maximum wave height is 0.6 m and for Puntarenas is 0.3 m.

On Sept. 5th, 2012 an earthquake magnitude Mw 7.6 occurred offshore at 15 km depth (Arroyo et al., 2012) and most of deformation occurred close to shoreline where 0.7 m coastal uplift was determined (W. Rojas, pers. com.). Thus, if deformation occurs landwards, a possible surface uplift on the shoreline will work as buffer to tsunami inundation (Fig. 2c, 3). However this has to be tested with higher resolution bathymetry.

Hypocenter and earthquake characteristics from different seismological centers have been assessed; however in most of the cases there is an overestimation of tsunami inundation that we have to analyze with new models. Therefore inversion and tsunami modeling are a good complement to understand rupture extension.

Finally, the mean tidal for this region is around 3 m. Most of these coastal communities are not so exposed (mainly toward north) in the case a tsunami arrives in lower tides as was the case during Sept. 5th, 2012; however a tsunami arriving at high tide is the worst scenario to be considered within the aims of coastal planning and risk assessment.

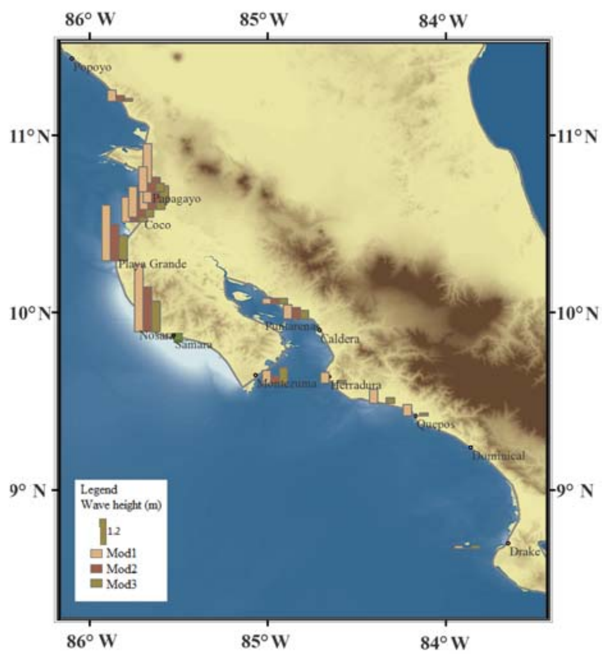

Fig. 3. Bars along coast show wave heights. Most exposed communities along Southern Samara.

Conclusions

Geodetic data has been very valuable to estimate possible sources based on slip deficient models using Okada model.

Despite strong tsunamis have not occurred lately along Costa Rican coasts, we consider that local authorities should prepare to reduce possible impacts of tsunami, especially if such events are generated during high tides increasing inundation threat along coastal communities.

Further work

These are preliminary results and more scenarios will be tested using bathymetry of higher spatial resolution and HyFlux2 finite volume numerical code (Franchello, 2008).

Stochastic slip distribution will be an important asset to better assess fault parameters implications on inundation along this region. in addition tsunami modeling considering events occurring at high tides will be performed.

Acknowledgements: Thanks to Dr. Lujia Feng and Dr. Andrew Newman for providing the interseismic coupling model of Nicoya Peninsula (Feng et al., 2012). We acknowledge Dr. Marino Protti for discussions related to Nicoya earthquake potential, and MSc. Silvia Chacón for providing her simulations of Sept. 5th event to compare with EasyWase results. Figures 1 and 2 were generated using GMT software (Wessel and Smith 1991) and ARCGIS10.1. N.Z thanks to Helmholtz Association for providing funding to conduct PhD studies through the GeoSim School.

References

Chacón, S. and Protti, M. 2011. Modeling a Tsunami from the Nicoya, Costa Rica, seismic gap and its potential impact in Puntarenas. Journal South America Earth Science 1, (4), 372-382.

DeMets, C.,. Gordon, R. G. and Argus, D. F. 2010. Geologically current plate motions, Geophysic Journal International 181, 1-80, doi:10.1111/j.1365-246X.2009.04491.x.

Feng, L., Newman, A., Protti, M., González, V., Jiang, Y., Dixon, T. 2012. Active deformation near the Nicoya Peninsula, northwestern Costa Rica, between 1996 and 2010: Interseismic megathrust coupling. Journal Geophysical Research 117, B06407.

Fernández, M., Molina, E., Havskov, J. and Atakan, K. 2000. Tsunamis and Tsunami Hazards in Central America. Natural Hazards 22(2), 91-116.

Franchello, G. 2008. Modelling shallow water flows by a High Resolution Riemann Solver. 2008. JRC Scientific and Technical Reports. EUR 23307 EN.

LaFemina, P., Dixon, T. H. Govers, R., Norabuena, Turner, E. H., Saballos, A., Mattioli, G., Protti, M. and Strauch, W. 2009. Fore-arc motion and Cocos Ridge collision in Central America, Geochemestry, Geophysics and Geosystems 10, Q05S14.

Arroyo, I., Mora, M. and Linkimer, L. Localización del evento principal. In Linkimer, L. and Soto, G. (eds). El terremoto de Sámara del 5 de setiembre del 2012. Red Sismológica Nacional, Costa Rica, 136 p.

Norabuena, E., Dixon, T.H., Schwartz, S., DeShon, H., Newman, A., Protti, M., González, V., Flueh, E., Lundgren, P., Pollitz, F. and Sampson, D. 2004. Geodetic and seismic constraints on some seismogenic zone processes in Costa Rica, J. Geophys. Res., 109, B11403,doi:10.1029/2003JB002931.

USGS CMT. USGS Centroid Moment Tensor http://earthquake.usgs.gov/earthquakes/eqinthenews/2012/usc000cfsd/neic_c000cfsd_cmt.php-

INCORPORATION OF PALEOSEISMOLOGICAL DATA IN THE CALCULATION OF THE SEISMIC HAZARD: AN EXAMPLE IN CENTRAL MEXICO

Zúñiga, F. Ramón (1), Ortuño, María (1,2), Figueroa-Soto, Angel (3)

(1) Centro de Geociencias, Universidad Nacional Autónoma de Mexico (UNAM), Juriquilla, Queretaro. ramon@geociencias.unam.mx
(2) Dept. de Geodinàmica i Geofísica, Universitat de Barcelona
(3) Posgrado en Ciencias de la Tierra, Universidad Nacional Autónoma de Mexico (UNAM).

Abstract (Incorporation Of Paleoseismological Data In The Calculation Of The Seismic Hazard): *There are many crustal faulting regimes in the world where not enough instrumentally recorded seismicity is available in order to make inferences on the exceedence rate of damaging ground motions exerted by earthquakes at a given location. For most of these cases, the only information which can be used towards this goal, at best, is that derived from paleoseismic studies, structural geology, deformation analysis and geomorphology. However, the implementation of a scheme which makes use of these data in order to estimate an average recurrence time for damaging events is not readily available.*
A procedure is presented for estimating the expected average interevent time for damaging events at a location which is surrounded by potentially hazardous known active faults for which deformation rates and paleoseismic data have been obtained or can be inferred. The estimates result from modeling the expected occurrence of events at every one of the proposed faults which may affect the site, based on attenuation and maximum magnitude relations, as well as suitable probability distributions. The procedure allows for a quick estimate of hazard which is susceptible of refinement as more data is gathered. If used under similar conditions in a larger region, relative estimates of average recurrence of damaging events allow for preliminary hazard mapping in this type of environment.

Key words: *Paleoseismology, seismic hazard, crustal faults, earthquake geology*

INTRODUCTION

One of the main challenges for the community working on seismic risk reduction is the incorporation of geologic data (i.e. paleoseismological) into the seismic hazard calculations, such as probabilistic data or recurrence contour maps. In the last decades, the number of studies that focus on acquiring geologic data to characterise seismogenic faults has increased dramatically.
However, the seismic hazard maps are still confectioned in most countries by considering only the historical and instrumental seismicity. In this work we propose a methodology for a preliminary systematic assessment of the average recurrence of damaging events affecting a location and the probability of exceedance of damaging ground motion in a given time period. The method allows for further refinements as more and better information about the neighbouring faults is gathered, but, as a first stage, offers the possibility of making relative estimates in regions which otherwise lack information. By using this simple approach, better constraints can be introduced for construction practices in this type of tectonic environments.
We illustrate the use of this program with Atlacomulco, as a focus of calculations, which is an industrial town of nearly 80,000 inhabitants, located ~ 40 km NW of Mexico city. This town is in the easternmost part of the Acambay Graben (Central part of the TransmexicanVolcanic belt), one of the few tectonic regions of Mexico for which paleoseismological data are available.

Discussion
Much research has been carried out to provide meaningful estimates of seismic hazard in tectonically active regions which generate a significant amount of

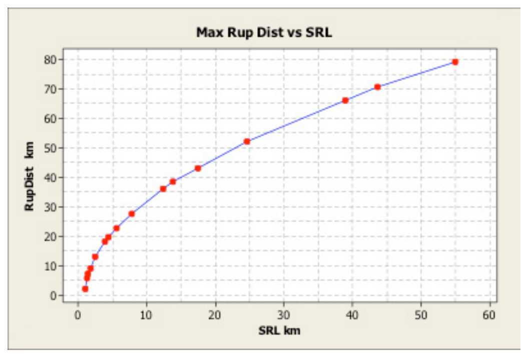

Fig. 1: Relation between minimum affectation distance (e.g. acceleration of 10%g) and surface rupture length (SRL).

seismicity be it of moderate or even low magnitude level. Most of these regions are related to plate boundary tectonics and thus, the frequency of occurrence of large events is far more than that at, so called, “stable regimes”. These stable regimes, however, are most of the time susceptible of generating large enough events to produce damage at nearby urban locations, even if their frequency of occurrence might exceed a human life’s span. There are many cases where such a type of situation has taken the lives of people and caused large economic losses, such as the Acambay, earthquake of November 1912 (Ms~7.0, Suter et al., 1992) which was responsible for at least 500 deaths. The scarce density of population in the past for that area, in any case, may have precluded the knowledge of previous events so we can not be certain of the past historical seismicity record.

When dealing with the estimation of occurrence of damaging events, if no recorded seismicity is available or if data is not enough given the time span of recording,

211

the only possibility is the use of paleoseismic studies, structural geology data, deformation rate estimates and geomorphological assessments. However, even if the researcher has the best data set available for all the faults that may be affecting a region, uncertainties due to factors such as the direct or indirect influence that an event occurring in one fault may have on another, relation between surface faulting to in-depth rupture, misidentification of paleoevents, etc. have to be taken into account. Furthermore, we can not state that a fault will behave in the same way as that observed in a speck of a time, which is what we always have access to. Thus, probabilistic estimates are a necessity.

As a first step, we select a location for which we want to come up with an estimate of recurrence of potentially damaging events. The idea is similar to that employed in most seismic hazard schemes (i.e. Cornell, 1968) where one needs to identify the seismogenic sources affecting a location. The difference is that in our case, few or no recorded seismicity is available and we can not make use of Gutenberg-Richter *b* values, or their counterpart *beta* values in engineering relations, in order to provide exceedance estimates.

To select the faults which pose a hazard for a given locality, an empirical relationship between the minimum affectation distance (a distance to which an acceleration of 10%g or more is induced by a fault of certain size) and the length of the fault trace is obtained by taking into account attenuation laws for continental earthquakes and empirical relations between magnitude and surface fault length (e.g. Toro et al., 1997; Wells and Coppersmith, 1994) (*Fig. 1*). Then, the recurrence time of these faults, derived from paleoseismological studies and/or geological and geomorphological studies is used to determine the mean recurrence time of the largest events and its standard deviation for the selected group of faults. With these values, a sequence of occurrences of seismic events is generated for a particular time period using a Weibull distribution and iterating in a Monte Carlo fashion in order to produce a sequence of 1 million years or more (*Fig. 2*). The mean interevent time at the site is then used to estimate the Poisson probability of one or more damaging earthquakes in the next 50 years.

We implemented a mathematical code (Trec) written in Matlab® programming language which allows us to calculate the probability of occurrence of one or more seismic events that could cause damage to the population: 1) for a given geographical site (i.e., an urban area or a town) and 2) in a given time spam.

Geological data recently acquired for the seismogenic faults in Central Mexico (Ortuño et al., 2011), and data from Persaud et al., (2006) and Langride et al. (2000) are used in the example test.

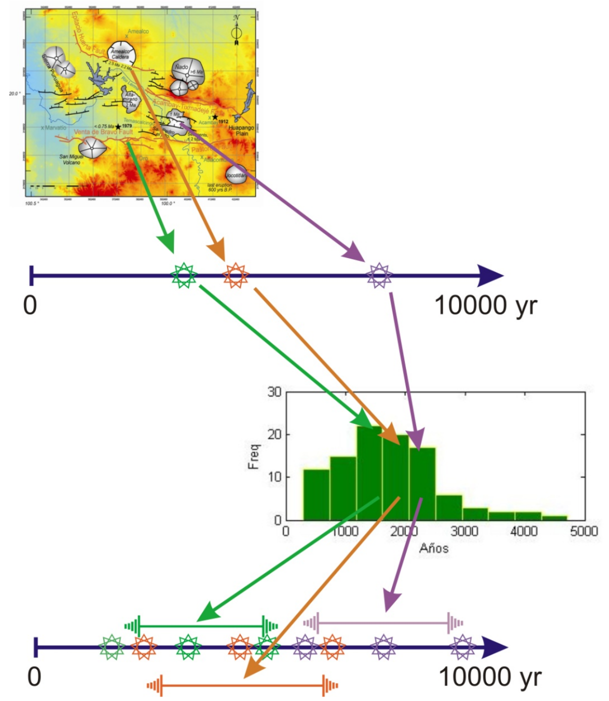

Fig. 2. Monte Carlo simulation of ruptures after Weibull distributions of recurrence times and uncertainties.

In our example, we use the known return periods for Acambay-Tixmadejé, Venta de Bravo, Pastores, Temascalcingo and Tepuxtepec faults which collectively give a mean recurrence time (MRec) of 3600 ka. Including all potentially hazardous faults near the site would comprise a total of 11 to 15, including those which lack paleoseismic information. Our results indicate that for a total of 15 faults, a mean recurrence time of damaging events of 243 +/- 24 yrs is likely, giving a Poisson probability of one or more events in 50 yrs of 19%. For 11 faults, our calculations give a mean recurrence time of damaging events of 331 +/- 30 yrs and a Poisson probability of one or more events in 50 yrs of 14%.

Acknowledgements: This research was sponsored by CONACyT (under grant CB-2009-01-129010) and UNAM (under grant DGAPA-PAPIIT-IN112110).

References

Cornell, A., 1968. Engineering seismic risk analysis, *Bulletin of the Seismological Society of America*, 58(5) , 1583-1606.

Langridge, R.M., Weldon, R.J., Moya, J.C.and Suarez, G. 2000. Paleoseismology of the 1912 Acambay earthquake and the Acambay-Tixmadeje fault, Trans-Mexican Volcanic Belt. *Journal of geophysical research*. Solid earth, 105(B2): 3019-3037.

Ortuño, M., Zúñiga, F.R., Corominas, O., Perea, H., Ramírez-Herrera, M.T., Štepancíková, Villamor, P., Aguirre, G. y Norini, G., 2011. Caracterización de fallas sismogenéticas en el centro del Cinturón Volcánico Trans – mexicano. Resultados Preliminares. *Abstracts of the XIV Latinoamerican Conference of Geology*, Medellín. 29-Agosto – 2 Septiembre, 165 -166.

Persaud, M., Zúñiga, F.R., Aguirre-Diaz , G., Villamor, P., Langdridge, R., 2006. First Step Towards the

212

Paleoseismological History of the Pastores and Venta de Bravo Faults, Acambay Graben, Trans-Mexican Volcanic Belt, Central México. *Eos*, *Transactions, American Geophysical Union,* 87(52:supplement), F1967-F1968.

Suter, M., Quintero, O., and Johnson, C.A., 1992. Active faults and state of stress in the central part of the Trans-Mexican volcanic belt, 1—The Venta de Bravo fault: *Journal of Geophysical Research*, v. 97, p. 11983–11994.

Toro, G.R., N.A. Abrahamson and Schneider, J.F., 1997. Model of Strong Ground Motions from Earthquakes in Central and Eastern North America: Best Estimates and Uncertainties, *Seismological Research Letters*, 68(1),41-57.

Wells, D.L., Coppersmith, K.J., 1994. New empirical relationships among magnitude, rupture length, rupture area and surface displacement. *Bulletin of the Seismological Society of America,* 84, 974–1002.

213

214

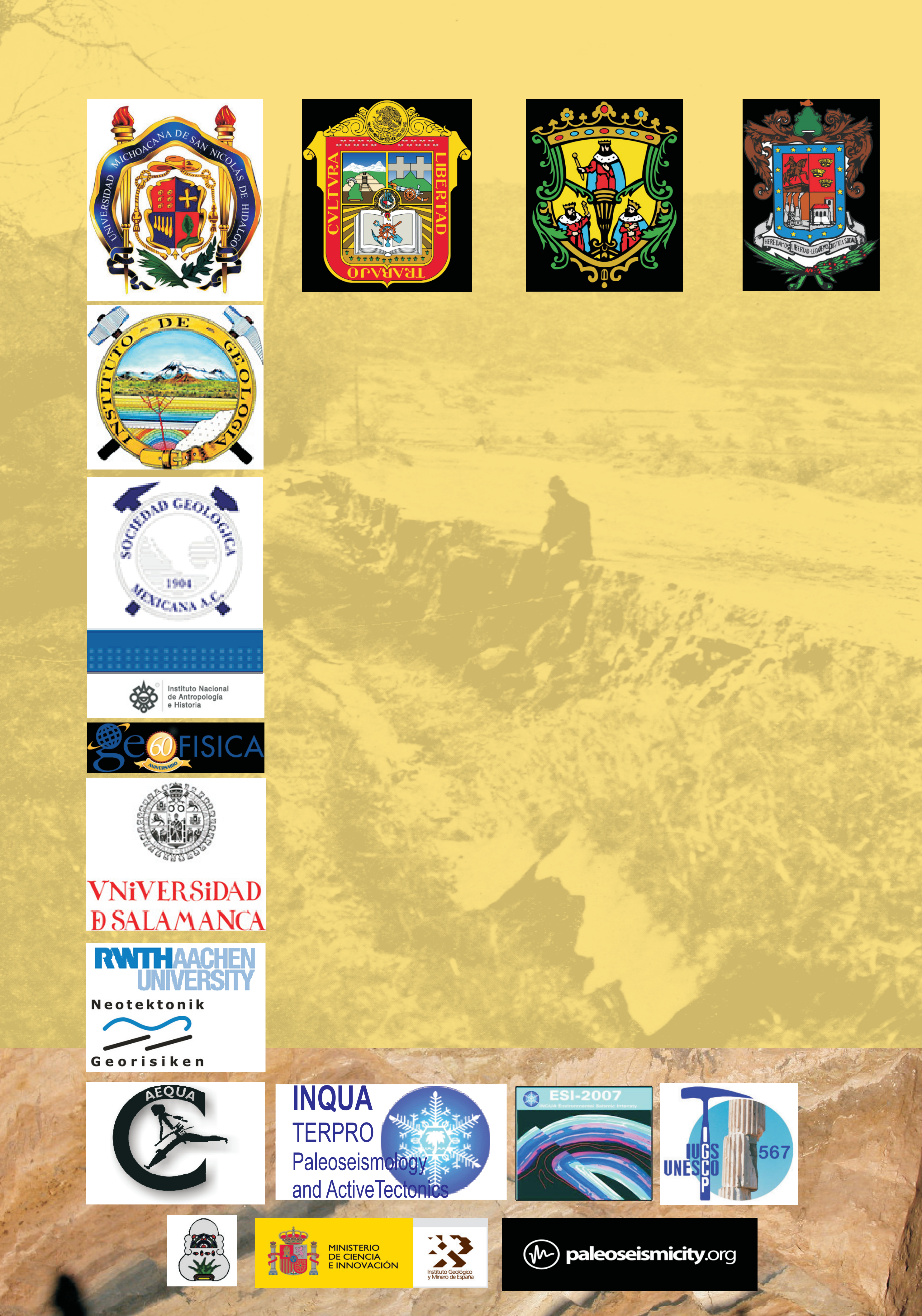

Proceedings

INQUA - IGCP 567 MORELIA (MEXICO), 2012